Nomination form for the 2021 Nishina Asia Award

Candidate (name, affiliation, curriculum vitae including the date of the degree of Ph.D., nationality, address, email and telephone)
Name : Hee-Cheol Kim Affiliation : POSTECH Nationality : South Korea Address : 77 Cheongam-Ro, Nam-Gu, Pohang, Gyeongbuk, Korea, 37673 E-mail : heecheol@postech.ac.kr Telephone : 054-279-2071 Academic Employment ● 2011.09 - 2013.08 : Research Fellow at Korea Institute for Advanced Study ● 2013.09 - 2016.08 : Postdoctoral Researcher at Perimeter Institute ● 2016.09 - 2017.12 : Postdoctoral Researcher at Harvard University ● 2018.01 - present : Assistant Professor at POSTECH Education ● Ph. D. in Physics (2011/08), Seoul National University, Seoul, Korea Advisor: Prof. Seok Kim (SNU) ● B. S. in Physics (2006/02), Yonsei University, Seoul, Korea ● B. S. in Computer Science (2006/02), Yonsei University, Seoul, Korea Research Interests ● Gauge/Gravity duality ● Supersymmetric gauge theories in various dimensions ●Non-perturbative dynamics in quantum field theories
Citation for the Award (within 30 words)
For his contributions to uncovering new physical phenomena and geometric structure of higher dimensional field theories.

Description of the work

One of the most surprising findings of string theory is the existence of consistent five- and six-dimensional conformal field theories (CFTs). The study of these higher dimensional theories reveals new structures hidden in supersymmetric field theories and underlies many recent developments in mathematical physics. For example, compactifications of the 5d and 6d theories lead to a rich class of supersymmetric theories in lower dimensions and provide remarkable predictions of new dualities and enhanced symmetries in the lower dimensional theories. Moreover, the higher dimensional field theories have a deep connection with mathematical structure of local Calabi-Yau geometries via string compactifications, which allows us to reformulate and investigate quantum phenomena of physical systems in a geometric fashion.

Higher dimensional field theories are intrinsically strongly-coupled and thus cannot be described by the conventional Lagrangian approach, making the study of this topic a challenging task. In recent years, classification programs have opened up a new avenue for studying the 5d and 6d supersymmetric field theories. Prof. Kim has made pioneering contributions to these subjects.

Prof. Hee-Cheol Kim with his collaborators has launched two new classification schemes for 5d supersymmetric field theories by means of both the gauge theoretic approach and the geometric engineering method. In late 1997, Intriligator, Morrison, and Seiberg attempted to classify 5d supersymmetric CFTs by examining the unitarity on the Coulomb branch moduli spaces of associated gauge theories. The first article [1] generalized this attempt and achieved the full classification of admissible 5d gauge theories with a simple gauge group. This work also solved the long-standing puzzle that certain 5d gauge theories apparently violating the unitarity condition somewhere on their moduli space, such as quiver gauge theories, can be consistently built in string compactifications by showing that the region violating unitarity is in fact outside the physical moduli space.

In the second article [2], Prof. Kim and his collaborators developed a new geometric technique to construct and classify 5d supersymmetric field theories based on M-theory compactifications on local Calabi-Yau threefolds. They established a systematic framework to realize local Calabi-Yau threefolds by gluing a number of compact complex surfaces and formulated geometric conditions necessary for engineering consistent 5d field theories. Using this framework, they completed geometric classification of all rank 2 5d supersymmetric CFTs. The framework was extended in [3] to develop the complete landscape of local Calabi-Yau threefolds engineering (twisted) compactifications of 6d superconformal theories. This result has led to a dramatic upturn in the recent advances in the geometric understanding of the supersymmetric field theories.

The effort to understand the higher dimensional quantum field theories and their compactifications to lower dimensions has led to newer understanding of strongly interacting quantum field theories in lower dimensional spacetime, with many exciting implications in high energy pheonomology and condensed matter physics. Prof. Kim is one of very standing out leading figure in this exciting development of geometric engineering for quantum field theory and has been making many breakthroughs. Prof. Kim brings enthusiasm, imagination, and precision to his research works and has put a higher intellectual standard. For this reason, I recommend Prof. Hee-Cheol Kim to the Nishina Asia Award in the strongest term.

Key references (up to 3 key publications*)

[1] P. Jefferson, Hee-Cheol Kim, C. Vafa and G. Zafrir, Towards Classification of 5d SCFTs: Single Gauge Node, arXiv:1705.05836.

[2] P. Jefferson, S. Katz, Hee-Cheol Kim and C. Vafa, On Geometric Classification of 5d SCFTs, JHEP 04 (2018) 103 [1801.04036].

[3] L. Bhardwaj, P. Jefferson, Hee-Cheol Kim, H.-C. Tarazi and C. Vafa, Twisted Circle Compactifications of 6d SCFTs, JHEP12(202)151, arXiv:1909.11666.

Nominator (name, affiliation, email, telephone and relation to the candidate)

Kimyeong Lee
Professor in the School of Physics
Korea Institute for Advanced Study
klee@kias.re.kr
82-2-958-3729
82-10-9917-9753
Collaborator and Postdoctoral Mentor

Signature Date March 30, 2021

Hee-Cheol Kim

Academic Employment

- 2011.09 - 2013.08 : Research Fellow at Korea Institute for Advanced Study
- 2013.09 - 2016.08 : Postdoctoral Researcher at Perimeter Institute
- 2016.09 - 2017.12 : Postdoctoral Researcher at Harvard University
- 2018.01 - present : Assistant Professor at POSTECH

Education

- **Ph. D.** in Physics August 2011
  Seoul National University, Seoul, Korea
  Advisor: Prof. Seok Kim (SNU)

- **B. S.** in Physics February 2006
  Yonsei University, Seoul, Korea

- **B. S.** in Computer Science February 2006
  Yonsei University, Seoul, Korea

Research Interests

- Gauge/Gravity duality
- Supersymmetric gauge theories in various dimensions
- Non-perturbative dynamics in quantum field theories

Publication List

1. Hirotaka Hayashi, Hee-Cheol Kim, Kantaro Ohmori
"*6d/5d exceptional gauge theories from web diagrams*"
arXiv: 2103.02799 [hep-th].

2. Hee-Cheol Kim, Minsung Kim, Sung-Soo Kim
"*Topological vertex for 6d SCFTs with Z2-twist*"
JHEP **03** (2021) 132 arXiv: 2101.01030 [hep-th].

3. Hee-Cheol Kim, Minsung Kim, Sung-Soo Kim, Ki-Hong Lee
"*Bootstrapping BPS spectra of 5d/6d field theories*"
arXiv: 2101.00023 [hep-th].

4. Jin Chen, Babak Haghighat, Hee-Cheol Kim, Marcus Sperling
"*Elliptic Quantum Curves of Class Sk*"
JHEP **03** (2021) 028 arXiv: 2008.05155 [hep-th].

5. Gil Young Cho, Dongmin Gang, Hee-Cheol Kim
"*M-theoretic Genesis of Topological Phases*"
JHEP **11** (2020) 115 arXiv: 2007.01532 [hep-th].

6. Sheldon Katz, Hee-Cheol Kim, Houri-Christina Tarazi, Cumrun Vafa
"*Swampland Constraints on 5d N=1 Supergravity*"
JHEP **07** (2020) 080 arXiv: 2004.14401 [hep-th].

7. Pietro Benetti Genolini, Masazumi Honda, Hee-Cheol Kim, David Tong
"*Evidence for a Non-Supersymmetric 5d CFT from Deformations of 5d SU(2) SYM*"
JHEP **05** (2020) 058 arXiv: 2001.00023 [hep-th].

8. Hee-Cheol Kim, Houri-Christina Tarazi, Cumrun Vafa
"*Four-dimensional N=4 SYM theory and the swampland*"
Phys. Rev. D **102** (2020) 2, 026003 arXiv: 1912.06144 [hep-th].

9. Lakshya Bhardwaj, Patrick Jefferson(MIT), Hee-Cheol Kim, Houri-Christina Tarazi, Cumrun Vafa
"*Twisted Circle Compactifications of 6d SCFTs*"
JHEP **12** (2020) 151 arXiv: 1909.11666 [hep-th].

10. Hee-Cheol Kim, Sung-Soo Kim, Kimyeong Lee
"*Higgsing and twisting of 6d DN gauge theories*"
JHEP **10** (2020) 014 arXiv:1908.04704 [hep-th].

11. Hee-Cheol Kim, Gary Shiu, Cumrun Vafa
"*Branes and the Swampland* ,"
Phys. Rev. D **100** (2019) 6, 066006 arXiv:1905.08261 [hep-th].

12. Hirotaka Hayashi, Patrick Jefferson, Hee-Cheol Kim, Kantaro Ohmori, Cumrun Vafa
"*SCFTs, Holography, and Topological Strings* ,"
arXiv:1905.00116 [hep-th].

13. Hee-Cheol Kim, Shlomo S. Razamat, Cumrun Vafa, Gabi Zafrir
"*Compactifications of ADE conformal matter on a torus* ,"
JHEP **09** (2018) 110 arXiv:1806.07620 [hep-th].

14. Hee-Cheol Kim, Shlomo S. Razamat, Cumrun Vafa, Gabi Zafrir
"*D-type Conformal Matter and SU/USp Quivers* ,"
JHEP **1806** (2018) 058 arXiv:1802.00620 [hep-th].

15. Patrick Jefferson, Sheldon Katz, Hee-Cheol Kim, Cumrun Vafa
"*On Geometric Classification of 5d SCFTs* ,"
JHEP **1804** (2018) 103 arXiv:1801.04036 [hep-th].

16. Hee-Cheol Kim, Joonho Kim, Seok Kim, Ki-Hong Lee, Jaemo Park
"*6d strings and exceptional instantons* ,"
Phys.Rev.D **103** (2021) 2, 025012 arXiv:1801.03579 [hep-th].

17. Hee-Cheol Kim, Shlomo S. Razamat, Cumrun Vafa, Gabi Zafrir
"*E-String Theory on Riemann Surfaces* ,"
Fortsch.Phys. 66 (2018) no.1, 1700074 arXiv:1709.02496 [hep-th].

18. Mathew Bullimore, Hee-Cheol Kim, Tomasz Lukowski
"*Expanding the Bethe/Gauge Dictionary* ,"
JHEP **1711** (2017) 055 arXiv:1708.00445 [hep-th].

19. Patrick Jefferson, Hee-Cheol Kim, Cumrun Vafa, Gabi Zafrir
"*Towards Classification of 5d SCFTs: Single Gauge Node* ,"
arXiv:1705.05836 [hep-th].

20. Mathew Bullimore, Tudor Dimofte, Davide Gaiotto, Justin Hilburn, Hee-Cheol Kim
"*Vortices and Vermas* ,"
arXiv:1609.04406 [hep-th].

21. Hee-Cheol Kim, Seok Kim, Jaemo Park
"*6d strings from new chiral gauge theories* ,"
arXiv:1608.03919 [hep-th].

22. Hee-Cheol Kim,
"*Line defects and 5d instanton partition functions* ,"
JHEP **1603** (2016) 199 arXiv:1507.08553 [hep-th].

23. Nikolay Bobev, Mathew Bullimore, Hee-Cheol Kim,
"*Supersymmetric Casimir Energy and the Anomaly Polynomial* ,"
JHEP **1509** (2015) 142 arXiv:1507.08553 [hep-th].

24. Davide Gaiotto, Hee-Cheol Kim,
"*Duality walls and defects in 5d N=1 theories,*"
JHEP **1701** (2017) 019 arXiv:1506.03871 [hep-th].

25. Mathew Bullimore, Hee-Cheol Kim, Peter Koroteev,
"*Defects and Quantum Seiberg-Witten Geometry,*"
JHEP **1505** (2015) 095 arXiv:1412.6081 [hep-th].

26. Mathew Bullimore, Hee-Cheol Kim,
"*The Superconformal Index of the (2,0) Theory with Defects,*"
JHEP **1505** (2015) 048 arXiv:1412.3872 [hep-th].

27. Davide Gaiotto, Hee-Cheol Kim,
"*Surface defects and instanton partition functions,*"
JHEP **1610** (2016) 012 arXiv:1412.2781 [hep-th].

28. Hirotaka Hayashi, Hee-Cheol Kim, Takahiro Nishinaka,
"*Topological strings and 5d T_N partition functions,*"
JHEP **1406** (2014) 014 arXiv:1310.3854 [hep-th].

29. Hee-Cheol Kim, Seok Kim, Sung-Soo Kim and Kimyeong Lee,
"*The general M5-brane superconformal index,*"
arXiv:1307.7660 [hep-th].

30. Chiung Hwang, Hee-Cheol Kim and Jaemo Park,
"*Factorization of the 3d superconformal index,*"
JHEP **1408** (2014) 018 arXiv:1211.6023 [hep-th].

31. Hee-Cheol Kim, Joonho Kim and Seok Kim,
"*Instantons on the 5-sphere and M5-branes,*"
arXiv:1211.0144 [hep-th].

32. Hee-Cheol Kim and Kimyeong Lee,
"*Supersymmetric M5 Brane Theories on $R \times \mathrm{CP}^2$,*"
JHEP **1307**, 072 (2013) arXiv:1210.0853 [hep-th].

33. Hee-Cheol Kim, Sung-Soo Kim and Kimyeong Lee,
“*5-dim Superconformal Index with Enhanced E_n Global Symmetry,*”
JHEP **1210**, 142 (2012) [arXiv:1206.6781 [hep-th]].

34. Hee-Cheol Kim and Seok Kim,
“*M5-branes from gauge theories on the 5-sphere,*”
JHEP **1305**, 144 (2013) arXiv:1206.6339 [hep-th].

35. Hee-Cheol Kim, Jungmin Kim, Seok Kim, Kanghoon Lee,
“*Vortices and 3 dimensional dualities,*”
arXiv:1204.3895 [hep-th].

36. Hee-Cheol Kim, Seok Kim, Eunkyung Koh, Kimyeong Lee and Sungjay Lee,
“*On instantons as Kaluza-Klein modes of M5-branes,*”
JHEP **1112**, 031 (2011) [arXiv:1110.2175 [hep-th]].

37. Hee-Cheol Kim, Seok Kim, Kimyeong Lee and Jaemo Park,
“*Emergent Schrodinger geometries from mass-deformed CFT,*”
JHEP **1108**, 111 (2011) [arXiv:1106.4309 [hep-th]].

38. Sangmo Cheon, Hee-Cheol Kim and Seok Kim,
“*Holography of mass-deformed M2-branes,*”
arXiv:1101.1101 [hep-th].

39. Hee-Cheol Kim and Seok Kim,
“*Semi-classical monopole operators in Chern-Simons-matter theories,*”
J.Korean Phys.Soc. 71 (2017) no.10, 608-627 arXiv:1007.4560 [hep-th].

40. Hee-Cheol Kim and Seok Kim,
“*Supersymmetric vacua of mass-deformed M2-brane theory,*”
Nucl. Phys. B **839**, 96 (2010) [arXiv:1001.3153 [hep-th]].

41. Jaehoon Jeong, Hee-Cheol Kim, Sangmin Lee, Eoin O Colgain, Hossein Yavartanoo,
“*Schrodinger invariant solutions of M-theory with enhanced supersymmetry,*”
JHEP **1003**, 034 (2010) [arXiv:0911.5281 [hep-th]].

Prepared for submission to JHEP

Towards Classification of 5d SCFTs: Single Gauge Node

Patrick Jefferson [a] **Hee-Cheol Kim** [a] **Cumrun Vafa** [a] **and Gabi Zafrir** [b]

[a] *Jefferson Physical Laboratory, Harvard University, Cambridge, MA 02138, USA*

[b] *Kavli IPMU (WPI), UTIAS, the University of Tokyo, Kashiwa, Chiba 277-8583, Japan*

Abstract: We propose a number of apparently equivalent criteria necessary for the consistency of a 5d SCFT in its Coulomb phase and use these criteria to classify 5d SCFTs arising from a gauge theory with simple gauge group. These criteria include the convergence of the 5-sphere partition function; the positivity of particle masses and monopole string tensions; and the positive definiteness of the metric in some region in the Coulomb branch. We find that for large rank classical groups simple classes of SCFTs emerge where the bounds on the matter content and the Chern-Simons level grow linearly with rank. For classical groups of rank less than or equal to 8, our classification leads to additional cases which do not fit in the large rank analysis. We also classify the allowed matter content for all exceptional groups.

Contents

1 Introduction

One of the main achievements of string theory has been a deeper understanding of quantum field theories. We have learned, in particular, of the existence of non-trivial superconformal field theories, not only in dimensions $d \leq 4$ but also in $d = 5, 6$. Studying the cases with $d > 4$ is interesting for a number of reasons: These theories turn out to involve, not only interactions of massless particles, but also of tensionless strings, which are quite novel. Higher dimensional SCFTs also seem to be simpler and in particular classifiable—in particular, the $(2, 0)$ SCFTs in $d = 6$ are believed to be classified by ADE [1] and a classification for the $d = 6$, $(1, 0)$ SCFTs has been proposed [2–4]. Another motivation for studying cases with $d > 4$ is that higher dimensional theories can lead to lower dimensional ones by compactifications and flowing to the IR. This relationship between lower dimensional theories and their higher dimensional 'parents' also leads to the emergence of dualities in lower dimensional theories as a manifestation of the different possible ways of assembling the intermediate manifold from elementary pieces.

It is thus natural to ask if we can also classify the $d = 5$ SCFTs. String theory suggests that this class of theories can be obtained geometrically as M-theory on non-compact Calabi-Yau 3-folds (CY_3) where some compact 4-cycles have shrunk to a point. Unfortunately at present these singularities are not fully classified, although some progress has been made in this regard [5]. Rather than attempting to classify these theories in terms of singularities, we instead take a clue from the classification of 6d (1,0) theories, for which various geometric conditions were ultimately distilled into constraints on gauge theoretic data. It was found that the allowed 6d (1,0) theories can be viewed as generalized quiver theories. In that case, the classification was split into two parts: first, a classification of the quiver node types (i.e. the single node case), followed by a specification of the rules according to which the quiver nodes can be connected. There are a few exceptional cases where the quiver nodes had no gauge theory associated with them, which were nevertheless reachable by Higgs branch deformations of some gauge theory. One may hope that a similar story can play out in the case of 5d SCFTs. An example of this structure is the class of $SU(2)$ gauge theories coupled to matter studied in [6–10], where it was found that $SU(2)$ gauge theories with up to 7 fundamental hypermultiplets can arise in a SCFT and are related to del Pezzo surfaces shrinking inside a CY_3. The case of $\mathbb{P}^2$ is the only case which is not realizable directly in terms of gauge theory (formally, this theory could be interpreted as '$SU(2)$ with -1 fundamental hypermultiplets'). But even this case can be obtained from gauge theory by starting from $SU(2)$ without matter and theta angle $\theta = \pi$, and passing through a strong coupling point where some massless modes emerge, are given mass, and integrated out [7, 11]. In a sense, this is similar to the exceptional cases in the 6d (1,0) classification.

Motivated by this analogy, we thus take seriously the idea of using gauge theoretic constructions as a window into the classification all 5d SCFTs. This approach was pioneered by Intriligator, Morrison, and Seiberg (IMS) in [8]. The idea in that work is that a weakly-coupled gauge system in its Coulomb phase can emerge in the IR as a deformation of an SCFT, so a classification of allowed IR theories would translate to a classification of UV fixed points, which correspond (in gauge theoretic terms) to the regime where the gauge coupling is infinite and all Coulomb branch parameters are set to zero. The assumption in [8] was that such an emergent IR gauge theory should be physically sensible for all values of the Coulomb branch parameters. More precisely, the condition that the vector multiplet scalars have a positive definite kinetic term on the entire Coulomb branch was imposed. This condition is equivalent to requiring that the matrix of effective couplings on the Coulomb branch is positive semi-definite. Using this criterion, quiver gauge theories were ruled out and theories with a simple gauge group coupled to matter were fully classified. However, it was found using geometric constructions [10] as well as brane constructions in Type IIB [12] that not only are quiver gauge theories allowed, but also that these quiver theories are sometimes dual to gauge theories with a simple gauge group. The loophole in the positivity condition of [8] ends up being the assumption that the gauge theoretic description should be valid for the entire Coulomb branch, since it could nevertheless be possible that for some values of the Coulomb branch parameters massless non-perturbative states emerge that introduce boundaries where the effective description breaks down. In some cases, these boundaries can be crossed at the expense of introducing a different description of the physics. Indeed, by using brane constructions and instanton analysis, new examples of gauge theories incompatible with the IMS criterion were found in [13–17], even in cases involving simple gauge group.

We propose a modification of the IMS criterion that only imposes the condition of positive definiteness of the metric to a subregion of Coulomb branch, rather than the entire Coulomb branch. However, it turns out that there are additional conditions that need to be checked: for example, 5d $\mathcal{N} = 1$ gauge theories theories have monopole strings, and the regions on the Coulomb branch where these strings become tensionless should be regarded as parts of a boundary where the effective gauge theory description breaks down. This is to say there may exist regions for which the metric is positive definite but some string tensions are nevertheless negative, which indicates that those regions are not physically sensible from the standpoint of a given effective description.

Therefore, the most natural criteria necessary for the consistency of allowed gauge theories are positive semi-definiteness of the metric on some subregion of the Coulomb branch, and furthermore positivity of masses and tensions of all physical degrees of freedom in that region. Even though this seems to be the most natural set of criteria, we find that there are three apparently simpler criteria, each of which we conjecture is equivalent to the previous statement: 1) the metric is positive-definite somewhere on the Coulomb branch, even if the string tensions are negative; 2) the tensions are positive in some region irrespective of metric positivity, as it seems that positivity of the metric in the same region automatically holds; and 3) the perturbative prepotential is positive on the *entire* Coulomb branch. The motivation for this last criterion is the convergence of the five-sphere partition function, which requires positivity of the perturbative prepotential. However, the surprise is that to get an equivalent condition to the other criteria, we need to check this positivity of the prepotential even in the excluded regions where the naive tensions or metric eigenvalues may be negative. Why all these criteria are equivalent to the existence of a region of Coulomb branch admitting positive definite metric and positive mass (and tension) degrees of freedom is unclear, but we have found no counterexamples to this assertion in the numerous examples we have explored.

The organization of this paper is as follows. In Section 2, we review some relevant facts concerning 5d $\mathcal{N}=1$ supersymmetric gauge theories. In particular, we explain in detail our assertion that the IMS criterion is incomplete. In Section 3, we propose our new (necessary) criteria for the existence of 5d SCFTs. We present our criteria in the form of a series of conjectures we believe to be equivalent. In Section 4, we classify non-trivial SCFTs with simple gauge group using our conjectures. We record the complete classification in a collection of several tables indicating the gauge group, matter content, classical Chern-Simons level (if applicable), and global symmetry groups. In Section 5, we discuss the connection between 6d SCFTs compactified on a circle and a class of 5d gauge theories we have identified. Finally, in Section 6, we conclude with a summary of our results and prospects for future research associated to this project. We summarize our conventions relevant to representation theoretic aspects of this paper in Appendix A; in Appendix B, we explain our rationale for excluding certain matter representations from our classification; and in Appendix C we discuss the five-sphere partition function along with its precise relation to the perturbative prepotential.

2 Effective Prepotentials on the Coulomb branch

We begin by presenting salient features of supersymmetric gauge theories in five-dimensions. The miminal SUSY algebra in 5d is the $\mathcal{N}=1$ algebra, which contains eight real supersymmetries. A large class of 5d $\mathcal{N}=1$ gauge theories can be engineered by (p,q) five-brane webs in Type IIB string theory [12, 18, 19] and also by M-theory compactified on Calabi-Yau threefolds [7–10].

A 5d gauge theory with a gauge group G has a Coulomb branch of moduli space where the real scalar field ϕ in the vector multiplet Φ takes nonzero vacuum expectation values in the Cartan subalgebra of the gauge group G. On a generic point of the Coulomb branch, therefore, the gauge symmetry is broken to its maximal torus $U(1)^{r_G}$ where $r_G = \mathrm{rank}(G)$, and therefore the Coulomb branch $\mathcal{C}$ is isomorphic to a fundamental Weyl chamber, $\mathcal{C} \cong \mathbb{R}^{r_G}/W(G)$, where $W(G)$ is the Weyl group of G. The low-energy abelian theory is governed by a prepotential $\mathcal{F}(\phi_i)$, which is a cubic polynomial in ϕ_i. The perturbative quantum correction to the prepotential is exactly determined by an explicit one-loop computation [20]. With matter hypermultiplets in generic representations $\mathbf{R}_f$, the exact prepotential of the low-energy abelian theory is given by [6, 8]

$$\mathcal{F}(\phi) = \frac{1}{2g_0^2}h_{ij}\phi_i\phi^j + \frac{\kappa}{6}d_{ijk}\phi_i\phi^j\phi^k + \frac{1}{12}\left(\sum_{e\in\mathrm{root}}|e\cdot\phi|^3 - \sum_f\sum_{w\in\mathbf{R}_f}|w\cdot\phi + m_f|^3\right) \tag{2.1}$$

where g_0 is the classical gauge coupling, $h_{ij} = \mathrm{Tr}(T_iT_j)$, m_f are the hypermultiplet masses, κ is the classical Chern-Simons level, and $d_{ijk} = \frac{1}{2}\mathrm{Tr}_{\mathbf{F}}(T_i\{T_j, T_k\})$, where $\mathbf{F}$ denotes the fundamental representation. Note that d_{ijk} is non-zero only for $G = SU(N \geq 3)$. Gauge invariance requires the classical Chern-Simons level to be quantized as $\kappa + \frac{1}{2}\sum_f c^{(3)}_{\mathbf{R}_f} \in \mathbb{Z}$ where $c^{(3)}_{\mathbf{R}_f}$ is the cubic Dynkin index of the representation $\mathbf{R}_f$ defined by the relation $\mathrm{Tr}_{\mathbf{R}_f}(T_i\{T_j, T_k\}) = 2c^{(3)}_{\mathbf{R}_f}d_{ijk}$. The last two terms in parentheses are one-loop contributions coming from, respectively, the massive vector multiplets and massive hypermultiplets on the Coulomb branch. Due to the absolute values in the prepotential, the Coulomb branch is divided into distinct sub-chambers, and the prepotential takes different expression in each sub-chamber.

The effective gauge coupling is given by a second derivative of the prepotential, and the metric on the Coulomb branch is set by the effecitve gauge coupling:

$$(\tau_{\mathrm{eff}})_{ij} = \left(g_{\mathrm{eff}}^{-2}\right)_{ij} = \partial_i\partial_j\mathcal{F} \ , \quad ds^2 = (\tau_{\mathrm{eff}})_{ij}\, d\phi_i d\phi^j \ . \tag{2.2}$$

The BPS spectrum for 5d $\mathcal{N} = 1$ theories includes gauge instantons, electric particles and magnetic monopole strings. The central charges of the electric particles and monopole strings are, respectively

$$Z_e = \sum_{i=1}^{r_G} n_e^{(i)}\phi_i + m_0 I \quad , \quad Z_m = \sum_{i=1}^{r_G} n_m^{(i)}\phi_{Di} \tag{2.3}$$

where $n_e^{(i)}, n_m^{(i)} \in \mathbb{Z}$, I is the instanton number, and the dual coordinates ϕ_{Di} are defined by way of the prepotential:

$$\phi_{Di} = \partial_i \mathcal{F}(\phi). \tag{2.4}$$

Bearing in mind that not every choice of integer coefficients $n_e^{(i)}, n_m^{(j)}$ in (2.3) corresponds to the central charge of a physical BPS state, we note that for any physical choice of coefficients $n_e^{(i)}, n_m^{(j)}$ the corresponding particle masses and monopole string tensions should be positive. Geometrically, because the tension of a monopole string is proportional to the volume of a 4-cycle, we can expect that there are at least as many independent monopole strings as there are 4-cycles. The number of independent monopole strings is therefore bounded below by r_G. At low energies, we expect that the number of independent strings is equal to the number of independent normalizable Kähler classes, implying that there are precisely r_G independent monopole tensions. We note that it is always possible to choose a coordinate basis for which the independent physical string tensions are

$$T_i(\phi) \equiv \partial_i \mathcal{F}(\phi) = \phi_{Di} \quad , \quad i = 1, \ldots, r_G. \tag{2.5}$$

In this paper, we will use the Dynkin basis (i.e. the basis of fundamental weights), in which we expect the tensions of r_G independent monopole strings are captured by the above expression. The rationale for this choice is that a classical string tension in the Dynkin basis is a root associated to gauge algebra and can thus be taken to have positive projection on the Weyl chamber. (In the gauge theory description, these correspond to monopole solutions.) We therefore expect that the quantum-corrected string tensions are also positive in this basis.

It was argued in [8] that when the quantum part of the metric is non-negative on entire Coulomb branch, a gauge theory can have non-trivial renormalization group fixed point at UV. Otherwise, the kinetic term may become negative at some point on the Coulomb branch, thereby preventing the existence of a UV fixed point. This necessary condition for the existence of 5d interacting quantum field theories is equivalent to the condition that $\mathcal{F}(\phi)$ be convex on all of $\mathcal{C}$ and, viewed in this fashion, imposes interesting constraints on the list of possible gauge theories. For example, quiver gauge theories are ruled out, since for such theories there is always a region on $\mathcal{C}$ for which the metric is negative. Thus, it was concluded in [8] that only gauge theories with simple gauge groups can have non-trivial UV fixed points. The Coulomb branch metrics of gauge theories with simple gauge groups were studied in relation to this condition and a full classfication was given in [8]. All the theories in this classification are expected to have interacting fixed points in either 5d or 6d.

However, string dualities relate some theories predicted by the criterion in [8] to theories (such as quiver gauge theories) excluded by the same criterion. For example, an $SU(3)$ gauge theory with $\kappa = 0$ and $N_{\mathbf{F}} = 2$ is dual to an $SU(2) \times SU(2)$ gauge theory, as explained in [12]. The metric of the former theory is positive definite on the entire Coulomb branch, while the latter theory has negative metric somewhere on the Coulomb branch. We discuss the details of this example below.

In fact, the existence of many interesting 5d field theories beyond the IMS bounds was argued by studying the dynamics of branes in string theory [13, 14, 17, 21, 22], CY_3-compactifications in M-theory [23–25], and also instanton analysis in 5d gauge theories [15, 16, 26]. For example, the authors in [8] predict that an $SU(N)$ gauge theory can couple to $N_{\mathbf{F}}$ fundamental hypermultiplets within the bound $N_{\mathbf{F}} \leq 2(N-|\kappa|)$. However, recently, the existence of the interacting fixed points for $SU(N)$ gauge theories with $N_{\mathbf{F}} \leq 2(N-|\kappa|)+4$ was argued in various literature [13–16]. These theories are obviously beyond the bound in [8]. See also [13–17, 21–26] for many other examples.

This tells us that the condition of the metric being positive semi-definite on the entire Coulomb branch is too strong, and therefore we may be able to relax the resulting constraints on the matter content and find a new classification which involves all known consistent 5d field theories.

Indeed, we find that the previous constraint on the metric on the Coulomb branch is too strong. This was already noticed for the simplest $SU(2) \times SU(2)$ quiver gauge theory, for instance, in [12]. The $SU(2)\times SU(2)$ gauge theory has real two-dimensional Coulomb branch of the moduli space. The scalar fields ϕ_1, ϕ_2 in the respective vector multiplets of each gauge group parametrize the Coulomb branch of the moduli space. In the chamber with $\phi_1 > \phi_2 > 0$, the quantum prepotential of this theory is given by

$$\mathcal{F}(\phi) = \frac{1}{2g_1^2}\phi_1^2 + \frac{1}{2g_2^2}\phi_2^2 + \frac{1}{6}\left(8\phi_1^3 + 8\phi_2^3 - (\phi_1+\phi_2)^3 - (\phi_1-\phi_2)^3\right) \ , \tag{2.6}$$

where g_1, g_2 are the respective gauge couplings for the two $SU(2)$ gauge groups. Here we have set the mass parameters of the bi-fundamental hypermultiplet to zero for convenience.

Let us examine if the metric is negative somewhere in the Weyl chamber. The matrix of effective couplings is

$$\tau_{\rm eff}(\phi) = \begin{pmatrix} 1/g_1^2 + 6\phi_1 & -2\phi_2 \\ -2\phi_2 & 1/g_2^2 - 2\phi_1 + 8\phi_2 \end{pmatrix} \ . \tag{2.7}$$

One can easily check that one of the eigenvalues of the metric becomes negative near $\phi_2 \sim 0.255\phi_1$ when the inverse couplings are small, $1/g_{1,2}^2 \ll 1$. Naively, this quiver theory cannot have an interacting fixed point according to the criterion of [8]. However, it turns out that this theory has a nice brane engineering in Type IIB string theory [12] as well as a geometric construction via compactification of M-theory on a CY_3 [10]. The five-brane web in Figure 1 will give rise to the 5d $SU(2)\times SU(2)$ gauge theory at low-energy.

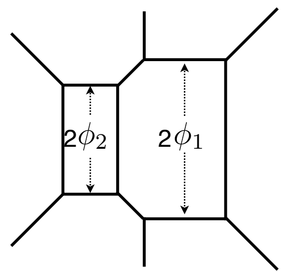

Figure 1. Five-brane web for the $SU(2)\times SU(2)$ gauge theory.

It was pointed out in [12] that this theory has a singularity in the Coulomb branch owing to the appearance of massless instanton particles and tensionless monopole strings. Thus the $SU(2)\times SU(2)$ gauge theory description breaks down beyond the singularity. This singularity can be detected by computing the monopole string tensions explicitly. The tensions of the monopole strings are given by

$$T_1 = \partial_1\mathcal{F} = \phi_1/g_1^2 + 3\phi_1^2 - \phi_2^2\ , \quad T_2 = \partial_2\mathcal{F} = \phi_2/g_2^2 - 2\phi_1\phi_2 + 4\phi_2^2\ . \tag{2.8}$$

In the brane configuration in Figure 1 monopole strings correspond to D3-branes wrapping two compact faces. Their tensions are proportional to the areas of two faces. We find that T_1 and T_2 are the same as the areas of the right and the left compact face respectively. As ϕ_2 decreases, the monopole string coming from the D3-brane wrapping the left square of ϕ_2 tends to be lighter and eventually becomes massless near $\phi_2 \sim \phi_1/2$ with $1/g_{1,2}^2 \ll 1$. It is clear that this point on the Coulomb branch where we meet the new light degrees of freedom is far away from the region where we encounter the negative metric. The prepotential in (2.6) cannot describe the dynamics of the system beyond the singularity due to the new light objects. The interior of the physical Coulomb branch of the $SU(2)\times SU(2)$ gauge theory is therefore specified by the bounds $\phi_1 > \phi_2 > \phi_1/2$. Notice, in particular, that this region is narrower than the naive Coulomb branch $\phi_1 > \phi_2 > 0$. The $SU(2)\times SU(2)$ gauge theory is an effective description of the system in Figure 1 only within the sub-region $\phi_1 > \phi_2 > \phi_1/2$.

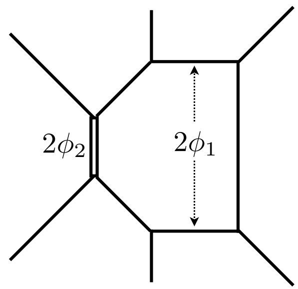

Figure 2. Appearance of massless degrees of freedom in the $SU(2) \times SU(2)$ gauge theory.

If we want to study the precise physics around $\phi_2 = \phi_1/2$ we should use another effective description which has the light particles in its perturbative spectrum. In this

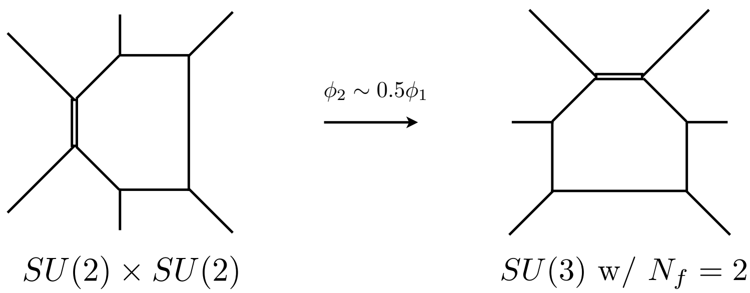

Figure 3. Duality of $SU(2) \times SU(2)$ theory and $SU(3)$ theory with two fundamental hypermultiplets, $N_{\mathbf{F}} = 2$.

case, the relevant description is the $SU(3)$ gauge theory with $N_{\mathbf{F}} = 2$. The duality between the $SU(2) \times SU(2)$ gauge theory and the $SU(3)$ gauge theory was studied in [12, 27]. Therefore, based on this duality, since the $SU(3)$ gauge theory is a non-tivial quantum theory with 5d CFT fixed point, which is predicted already in [8], we can also expect that the $SU(2) \times SU(2)$ gauge theory is a non-trivial quantum theory. These two gauge theories are good low-energy effective descriptions in different parameter regimes of the same theory.

In this example, by exploiting the S-duality of Type IIB, we can clearly understand what happens when some non-perturbative degrees of freedom becomes massless. While the $SU(2) \times SU(2)$ gauge theory description breaks down near the point $\phi_2 = \phi_1/2$ due to the emergence of light instanton particles, the perturbative description of the $SU(3)$ gauge theory is reliable at the point. The light instantons at $\phi_2 = \phi_1/2$ give rise to non-abelian $SU(2)$ gauge symmetry enhancement in the dual $SU(3)$ gauge theory. It follows that the Coulomb branch of the $SU(3)$ gauge theory beyond the point $\phi_2 = \phi_1/2$ is merely a Weyl copy of the enhanced $SU(2)$ gauge symmetry. This means that the correct prepotential on the chamber $\phi_2 < 2\phi_1$ after the transition is a copy of the original prepotential on the Weyl chamber $\phi_2 > 2\phi_1$ obtained by exchanging $\phi_1 \leftrightarrow \phi_2 - \phi_1$. Therefore we expect a discontinuity of the prepotential in the $SU(2)\times SU(2)$ gauge theory at the transition point $\phi_2 = \phi_1/2$ detectable by a non-perturbative quantum correction to the prepotential despite the fact that the perturbative prepotential cannot capture this. With the prepotential corrected by non-perturbative effects, the metric of the $SU(2) \times SU(2)$ theory is always positive definite on the entire (physical) Coulomb branch.

The lesson from this simple example is that in general, the physical Coulomb branch may be smaller than the naive Coulomb branch identified in the perturbative description. Stated differently, the actual physical Coulomb branch cannot necessarily be identified with a fundamental Weyl chamber.

3 New Criteria

The above example shows that the IMS criterion is too restrictive. In view of the above discussion, we will relax the condition that the metric be positive everywhere on the perturbative Coulomb branch, since this condition imposes metric positivity even in unphysical regions. Our reasoning is as follows: in some regions of the perturbative Coulomb branch, there may exist boundaries where the non-perturbative degrees of freedom become massless or tensionless. Beyond these boundaries, these masses and tensions appear to become negative, which signals that the perturbative computation can no longer be trusted. We therefore restrict our attention to the physical regions in the Coulomb branch where all degrees of freedom have positive masses or tensions.

3.1 Main conjecture

We claim that if the metric is positive definite on the physical Coulomb branch the gauge theory has non-trivial interacting fixed point. For these theories we can reach their fixed points by taking the infinite coupling limit $g_0^2 \to \infty$. It is therefore crucial to determine the exact physical Coulomb branch that we will investigate. We claim that the physical Coulomb branch is the subset $\mathcal{C}_{\rm phys} \subseteq \mathcal{C}$ bounded by the set of hyperplanes where some non-perturbative degrees of freedom become massless and/or tensionless:

$$\mathcal{C}_{\rm phys} = \{\phi \in \mathcal{C} \,|\, T(\phi) > 0, m_I^2(\phi) > 0\} \ . \tag{3.1}$$

Here $m_I^2(\phi) > 0, T(\phi) > 0$ indicates that the masses and tensions of all non-perturbative degrees of freedom are positive at the point ϕ. Furthermore, the metric on the above physical Coulomb branch must be positive-definite. Namely,

$$\tau_{\rm eff}(\phi) > 0 \ , \quad \phi \in \mathcal{C}_{\rm phys} \ . \tag{3.2}$$

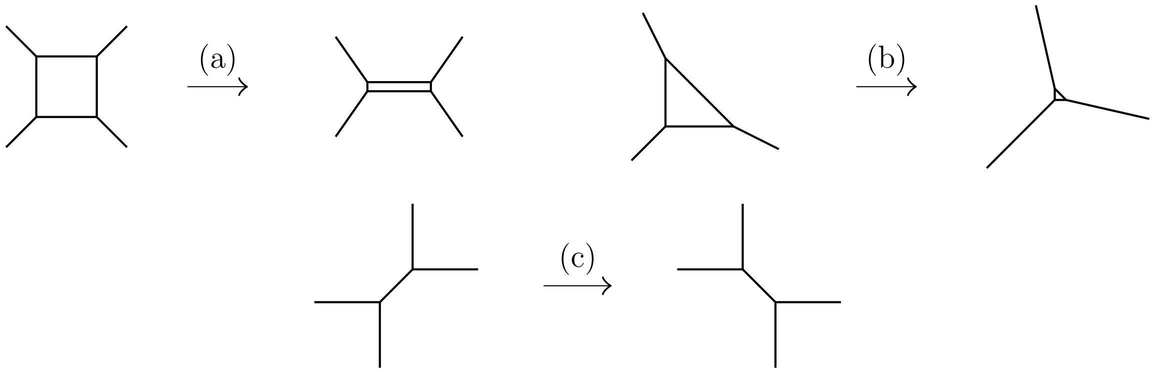

Figure 4. We illustrate the three types of geometric transitions occurring in Calabi-Yau threefolds using examples of (p, q) five brane webs. Transition (a) corresponds to a 4-cycle shrinking to a 2-cycle, (b) corresponds to a 4-cycle shrinking to a point, and (c) is a flop transition obtained by first shrinking a 2-cycle to a point and blowing up another 2-cycle.

This condition should be true for all physically-sensible 5d theories, including quiver theories.

It is crucial to our classification that we are able to identify the hyperplanes where massless degrees of freedom arise on the naive Coulomb branch. However, from a purely field-theoretic standpoint, the task of identifying such hyperplanes is somewhat subtle because it requires a non-perturbative analysis to identify exact instanton spectrum. On the other hand, from a geometric perspective, it is in principle a straightforward exercise to identify the hyperplanes bounding the physical Coulomb branch $\mathcal{C}_{\text{phys}}$—from a geometric point of view, these are regions where we encounter a geometric transition in the CY_3. Therefore, we embark on a short digression to explain how to characterize these hyperplanes, and moreover their relation to the BPS spectrum.

We remark that there are three possible geometric transitions[1] associated to particles or monopole strings becoming massless: (a) a 4-cycle shrinking to a 2-cycle, (b) a 4-cycle shrinking to a point, and (c) a 2-cycle shrinking to a point. Examples of these three types of transitions in the case of (p, q) five brane webs are depicted in Figure 4. We now describe these three types of transitions in more detail, and explain their relevance to our classification.

The first type of transition results in a local ADE singularity, as was argued in

[1]Note that 5d $\mathcal{N} = 1$ gauge theories can be constructed in string theory by compactifying M-theory on a CY_3 in which M2-branes wrap compact 2-cycles and M5-branes wrap compact 4-cycles in the CY_3. This setup leads to a 5d description in which BPS particle masses are controlled by the volumes of the 2-cycles, while monopole string tensions are controlled by the volumes of the 4-cycles.

[28], so that there is always a gauge symmetry enhancement due to the appearance of a collection of massless W-bosons arising from the shrinking 2-cycle. The low energy dynamics in the vicinity of the singularity can therefore be captured precisely by a gauge theory description involving a simply-laced gauge group. The region beyond this wall should be regarded as an image generated by the Weyl group associated to the enhanced nonabelian gauge group, and is therefore unphysical.

The second type of transition should be distinguished from the first in the sense that a 4-cycle shrinking to a point always results in the appearance of an infinite number of massless particles associated to 2-cycles inside the shrinking 4-cycle. In this case, the low energy dynamics is described by a CFT with tensionless monopole strings interacting with massless electric particles [20]. The classic example of such a phenomenon is the local $\mathbb{P}^2$ shrinking to a point. From a geometric point a view, continuing past this kind of wall is prohibited and therefore corresponds to an unphysical region of the moduli space.

The third type of transition corresponds to a 2-cycle shrinking to a point, while all 4-cycle volumes remain finite. This type of transition is typically described as a flop transition in a geometric setting. When the volume of the 2-cycle corresponds to the mass of some perturbative BPS particle, this transition can be captured by the one-loop prepotential (2.1) and manifests itself as a discontinuity of the cubic coefficients. However, when the volume of the 2-cycle corresponds to the mass of an instanton particle, the one-loop prepotential may not be able to detect this sort of transition at any point on the physical Coulomb branch. This sort of transition can in principle be captured by a careful analysis of the non-perturbative physics, such as a computation of the BPS partition function. Moreover, if a geometric description of the Calabi-Yau geometry is known, one can detect the presence of such a transition by computing the prepotential in terms of geometric data and carefully studying how the volumes of various 2-cycles change in the moduli space. An example of this is the geometric transition $\mathbb{F}_1 \to \mathbb{P}_2$ [7, 11].

The relationship between the volumes of 2-cycles (4-cycles) and the central charges Z_e (Z_m) described in (2.3) implies that some combination of central charges vanishes for each transition type discussed above. Moreover, restrictions on the "allowed" linear combinations of 2- and 4-cycle classes in the geometric setting translate into charge quantization conditions in the field theory setting that ensure the corresponding BPS states all lie within physical charge lattices. Such constraints, for example, imply that the vanishing of irrational linear combinations of ϕ_i (i.e. combinations $\sum n_e^{(i)} \phi_i$ where $n_e^{(i)} \in \mathbb{R} \backslash \mathbb{Q}$) cannot correspond to geometric transitions. We will thus need to be careful to distinguish between physical and unphysical boundary hyperplanes in our analysis.

In this paper, we conjecture that by turning off all of the mass parameters[2], we can identify $\mathcal{C}_{\text{phys}}$ by studying, in addition to flops by W-bosons, the first two types of transitions described above—namely those for which a 4-cycle shrinks. We expect that the one-loop prepotential can detect these types of transitions because the volumes of the string tensions are captured by partial derivatives with respect to the scalars ϕ_i. The above conjecture also implies that the third type of transition can arise only as a pertubative flop transition by some massless electric particle when the mass parameters are turned off. Therefore, we are led to the main statement of this paper, concerning the characterization of what we refer to as the 'physical' Coulomb branch:

Main Conjecture

The *physical Coulomb branch* $\mathcal{C}_{\text{phys}}$ is defined by

$$\mathcal{C}_{\text{phys}} = \mathcal{C}_{T\geq 0}, \tag{3.3}$$

where

$$\mathcal{C}_{T\geq 0} = \{\phi \in \mathcal{C} \,|\, T(\phi) \geq 0\} \quad \text{and} \quad \partial\mathcal{C}_{\text{phys}} \text{ is } \textit{rational.} \tag{3.4}$$

Moreover, non-trivial 5d gauge theories have positive definite metric on the physical Coulomb branch:

$$\tau_{\text{eff}}(\phi) > 0 \ , \quad \phi \in \mathcal{C}_{\text{phys}}. \tag{3.5}$$

Note that $\tau_{\text{eff}} > 0$ in the above equation indicates that τ_{eff} is a positive definite matrix, and *rational* means that the boundary $\partial\mathcal{C}_{\text{phys}}$ is specified by the setting some rational linear combinations of the Coulomb branch parameters equal to zero, i.e. $\sum_i n_i\phi_i = 0$, $n_i \in \mathbb{Z}$. In other words, we require that the boundary $\partial\mathcal{C}_{\text{phys}}$ is identified by the appearance of physical massless BPS particles, as discussed above. (Note that we find only five exceptional theories where our classification becomes subtle due to the rationality condition. These five exceptional theories will be discussed in Section 4.4.) For the remainder of the paper, we use $\mathcal{C}_{\text{phys}}$ to denote the subset of the Coulomb branch defined in (3.3), while we use $\mathcal{C}$ to denote the (naive) Coulomb branch isomorphic to a fundamental Weyl chamber. We will also use $\mathcal{C}_{T>0}$ to denote the interior of the physical Coulomb branch $\mathcal{C}_{\text{phys}}$.

[2]Note that 'mass parameters' refers collectively to both hypermultiplet mass parameters m_f and inverse gauge couplings $m_0 = 1/g_0^2$, which are treated on the same footing from the 5d perspective—they are mass parameters for the global symmetries of the 5d theory.

These new criteria can be used to classify all candidate non-trivial 5d QFTs with simple gauge groups. We emphasize that our main conjecture is a *necessary* (though perhaps not *sufficient*) set of criteria for the existence of a 5d interacting fixed point in the UV. Although brane configurations and geometric constructions can provide evidence confirming the existence of these theories, we will leave explicit realizations of the theories in our classification to future research. For the reason, it is important to bear in mind that our classification describes a maximal set of theories that can possibly exist, and the set of theories that actually exist may be a subset. For the remainder of this paper, we will be sloppy about the distinction between theories that satisfy the necessary set of conditions described by our conjectures and theories that have explicit realizations in string theory. In particular, we will refer to all candidates as 'non-trivial theories'.

We will classify these candidate non-trivial gauge theories below using our main conjecture for lower rank cases $r_G \leq 5$. For higher rank theories, our main conjecture appears to be rather inconvenient for the full classification of 5d QFTs. In the next sub-section, we will make three additional conjectures, each of which we believe is equivalent to the main conjecture described above, which make the problem of classification significantly more tractable. These additional conjectures impose constraints (involving at most one derivative of the prepotential), which are easier to implement in practice and thus enable us to make a full classification of arbitrary rank gauge theories with simple gauge groups. To our knowledge, our classification covers all known gauge theories with non-trivial fixed points and furthermore predicts large classes of new non-trivial 5d gauge theories that may exist. However, we would like to emphasize that only the main conjecture above is physically well-motivated at present. We do not have physical or mathematical arguments for the three additional conjectures described in the next sub-section.

Let us first demonstrate how to identify non-trivial QFTs and classify them using the Main Conjecture with simple examples. In this paper, we shall focus on the $\mathcal{N}=1$ gauge theories without adjoint hypermultiplets.[3] We will also turn off all mass parameters except the gauge coupling.

We begin with $SU(3)$ gauge theories. An $SU(3)$ gauge theory has a two-dimensional Coulomb branch parametrized by scalar fields ϕ_1, ϕ_2. We find that an $SU(3)$ gauge theory can have hypermultiplets only in the fundamental or the symmetric representation. The dimensions of other $SU(3)$ representations are so large that the prepotential be-

[3]Note that if we add a single adjoint hypermultiplet to a 5d theory with a simple gauge group, the theory will be promoted to a $\mathcal{N}=2$ gauge theory. All such 5d $\mathcal{N}=2$ theories can be obtained from 6d $\mathcal{N}=(2,0)$ SCFTs on a circle S^1 with or without outer automorphism twists [29]. Gauge theories with two or more adjoint hypermultiplets have negative prepotentials, so they are not renormalizable.

comes negative at large gauge coupling when such hypermultiplets are included, and hence those representations must be excluded.

For some purposes, we will find it convenient to use Dynkin basis for roots and weights, while in some other cases it will prove more convenient to use the orthogonal basis. In the Dynkin basis, W-boson masses are given by the inner products $\phi \cdot \alpha_i$ with simple roots $\{\alpha_i\} = \{(2,-1), (-1,2), (1,1)\}$. In the Weyl subchamber $\mathcal{C}^{(1)} = \{\phi_1 > \phi_2 > 0\}$, we find the prepotential of $SU(3)_\kappa + N_{\mathbf{F}}\mathbf{F} + N_{\mathbf{S}}\mathbf{S}$ is given by

$$\begin{aligned}\mathcal{F}_{SU(3)} = \frac{1}{g_0^2}(\phi_1^2 - \phi_1\phi_2 + \phi_2^2) + \frac{\kappa}{2}\left(\phi_1^2\phi_2 - \phi_1\phi_2^2\right) + \frac{1}{6}\left(8\phi_1^3 - 3\phi_1\phi_2^2 - 3\phi_1^2\phi_2 + 8\phi_2^3\right) \\ -\frac{N_{\mathbf{F}} - 9N_{\mathbf{S}}}{12}\left(2\phi_1^3 - 3\phi_1^2\phi_2 + 3\phi_1\phi_2^2\right) \ . \end{aligned} \tag{3.6}$$

The prepotential in the second Weyl chamber $\mathcal{C}^{(2)} = \{\phi_2 > \phi_1 > 0\}$ can be obtained by interchanging ϕ_1 and ϕ_2. The physical Coulomb branch is restricted to the sub-domain given by

$$\mathcal{C}^{(1)}_{\text{phys}} = \{\phi \in \mathcal{C}^{(1)} \,|\, T(\phi) > 0\} \ , \quad \mathcal{C}^{(2)}_{\text{phys}} = \{\phi \in \mathcal{C}^{(2)} \,|\, T(\phi) > 0\} \tag{3.7}$$

in the first and the second Weyl subchamber, respectively. The condition for the gauge theory being a non-trivial theory is that the metric on $\mathcal{C}^{(1)}_{\text{phys}}$ and $\mathcal{C}^{(2)}_{\text{phys}}$ is positive in the infinite coupling limit $g_0^2 \to \infty$.

First consider the cases of $\kappa = 0, N_{\mathbf{S}} = 0$. Since κ is an integer, we require $N_{\mathbf{F}}$ to be even. The theories with $N_{\mathbf{F}} \leq 6$ have a positive metric everywhere on the Coulomb branch, as discussed in [8], thus they are all non-trivial 5d QFTs. Therefore, we focus our attention on the cases with $N_{\mathbf{F}} > 6$. The eigenvalues of the metric and string tensions are drawn in Figure 5 for $N_{\mathbf{F}} = 6, 8, 10$. Unlike the case $N_{\mathbf{F}} = 6$ for which the metric always has positive eigenvalues, theories with $N_{\mathbf{F}} = 8, 10$ have a negative eigenvalue of the metric in certain sub-region of their Coulomb branches. However, one can easily check that their metrics are positive in the physical Coulomb branches defined by $T_1, T_2 > 0$. In other words, we encounter a singularity at $T_2 = 0$ in the naive Coulomb branch and the effective gauge theory description breaks down before we reach at the point where the metric becomes negative. Within the physical Coulomb branch $\mathcal{C}_{\text{phys}}$, the $SU(3)$ gauge theories with $N_{\mathbf{F}} = 8, 10$ have positive definite metrics. Thus we claim that they are good theories with non-trivial UV fixed points. They are good effective descriptions for the corresponding non-trivial theories at the fixed points in the parameter space $\mathcal{C}_{\text{phys}}$. We check that if we have $N_{\mathbf{F}} > 10$, the theories have no physical Coulomb branch, i.e. $\mathcal{C}_{\text{phys}} = \emptyset$, and thus these theories cannot have interacting fixed points. Indeed, it was conjectured in [14, 15] that the $SU(3)$ gauge theories with

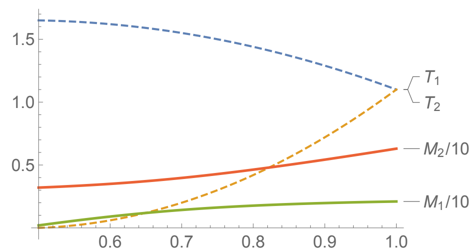

(a) $N_{\mathbf{F}} = 6$

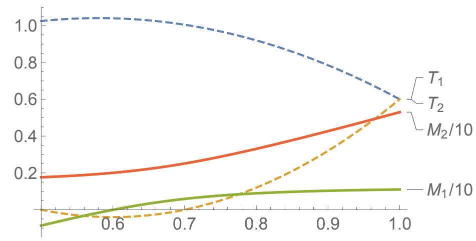

(b) $N_{\mathbf{F}} = 8$

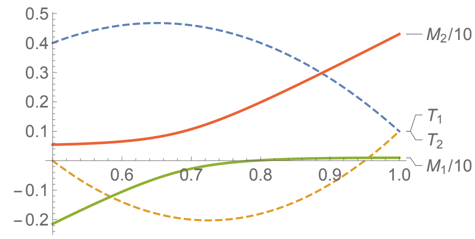

(c) $N_{\mathbf{F}} = 10$

Figure 5. Solid lines are eigenvalues $M_1/10$ and $M_2/10$ of the metric and dashed lines are two string tensions T_1 and T_2 at $g^{-2} = 0.1$ for $N_{\mathbf{F}} = 6, 8, 10$. The horizontal axis is the ratio ϕ_2/ϕ_1. The physical Coulomb branches are $\mathcal{C}_{\text{phys}}^{N_{\mathbf{F}}=6} = \phi_1 \geq \phi_2 \geq \phi_1/2$, $\mathcal{C}_{\text{phys}}^{N_{\mathbf{F}}=8} = \phi_1 \geq \phi_2 \geq 0.7\phi_1$, and $\mathcal{C}_{\text{phys}}^{N_{\mathbf{F}}=10} = \phi_1 \geq \phi_2 \geq 0.95\phi_1$, respectively, with $\phi_1 \geq 0$.

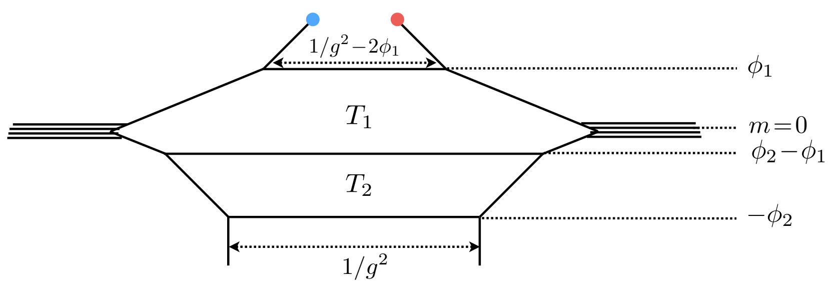

Figure 6. 5-brane web diagram for the theory $SU(3)_{-1} + 8N_{\mathbf{F}}$ at zero masses.

$N_{\mathbf{F}} \leq 10$ have non-trivial UV fixed points while the theories with $N_{\mathbf{F}} > 10$ may be inconsistent. Our computation provides concrete physical evidence for this conjecture.

Let us now turn on the Chern-Simons term at level κ. $SU(3)_{-1} + 8\mathbf{F}$ can be engineered in string theory by a (p, q) 5-brane web [14]. Figure 6 is the 5-brane web diagram for this theory at zero masses in the first Weyl chamber $\phi_1 > \phi_2 > 0$. The two 5-branes at the top of the diagram end on 7-branes. Since the length of the first D5-brane is given by $1/g_0^2 - 2\phi_1$, this brane picture is a good description for the theory only within the parameter regime $1/g_0^2 \geq 2\phi_1$. When $1/g_0^2 < 2\phi_1$, two 7-branes at the top of the diagram need to be pulled inside the 5-brane loop.

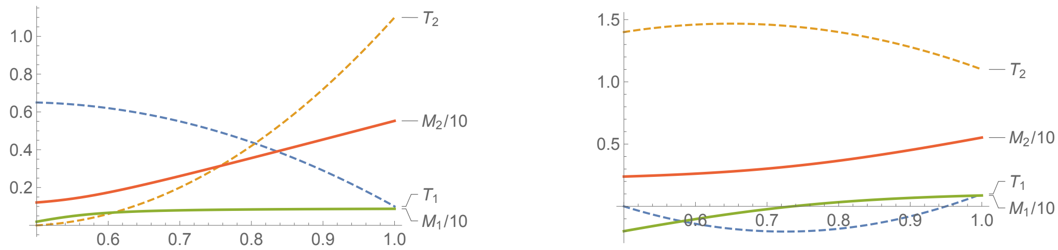

(a) $\mathcal{C}^{(1)}_{\text{phys}} : \phi_1 > \phi_2 > \phi_1/2$.

(b) $\mathcal{C}^{(2)}_{\text{phys}} : \phi_2 > \phi_1 > \phi_2/2$.

Figure 7. Eigenvalues of the metric (solid line) and string tensions (dashed lines) of $SU(3)_{-1} + 8\mathbf{F}$ fundamentals at $1/g_0^2 = 0.1$. The horizontal axes are ratios of scalar fields ϕ_2/ϕ_1 and ϕ_1/ϕ_2 respectively.

At small coupling $1/g_0^2 \gg \phi_1$, the brane description is reliable. The monopole strings correspond to D3-branes wrapping the compact faces and the tensions of these strings T_1, T_2 are given by areas of two compact faces. It is straightforward to read off the tensions from the diagram and the results are

$$T_1 = \frac{1}{g_0^2}(2\phi_1 - \phi_2) + 2\phi_2(\phi_1 - \phi_2) \ , \quad T_2 = \left(\frac{1}{g_0^2} + 2\phi_2 - \phi_1\right)(2\phi_2 - \phi_1) \ . \tag{3.8}$$

One can easily check that these string tensions agree with the tensions obtained from the first derivatives of the prepotential $\mathcal{F}_{SU(3)}$ in (3.6). Although the brane description breaks down at large coupling beyond $1/g_0^2 = 2\phi_1$, the gauge theory description is still good. Thus we can expect that the above tension formula for the monopole strings may give the correct tensions of wrapped D3-branes even after 7-branes are moved inside the 5-brane loop at large coupling. In Figure 6, the bottom face denoted by T_2 shrinks to zero area when the last two internal D5-branes are placed on top of each other, i.e. $2\phi_2 - \phi_1 = 0$. Then the D3-brane wrapping the bottom face contributes tensionless strings to the 5d gauge theory. The string tensions are non-negative on the entire Coulomb branch in the first chamber $\phi_1 > \phi_2 > \phi_1/2$ even in the infinite coupling limit $g_0^2 \to \infty$. The non-negativity of the string tensions thus implies that the $SU(3)$ gauge theory and the 5-brane web are both good descriptions for this theory in the first chamber. This is consistent with the fact that the $SU(3)$ gauge theory has a positive metric on the first chamber as depicted in Figure 7a. In the second chamber, the metric becomes negative around $\phi_1 < 0.74\phi_2$. However, this is fine because the physical Coulomb branch is restricted to $\phi_2 > \phi_1 > 0.95\phi_2$ due to the tensionless strings. Therefore, as expected, $SU(3)_{-1} + 8\mathbf{F}$ is a non-trivial 5d QFT according to our new criteria.

Another interesting example is $SU(3)_{-4} + 6\mathbf{F}$. This is a new non-trivial 5d theory

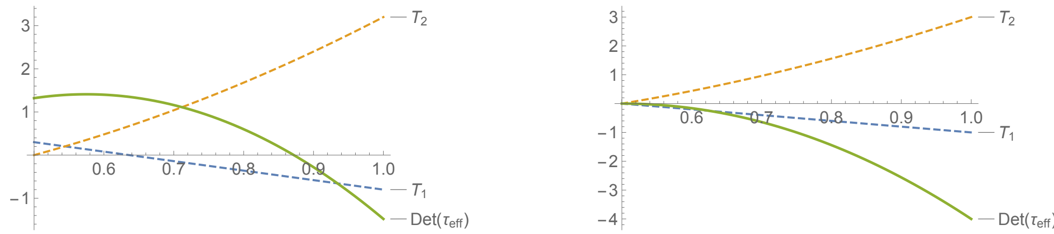

(a) $1/g_0^2 = 0.2$.

(b) $1/g_0^2 = 0$.

Figure 8. Det$(\tau_{\rm eff})$ (solid line) and string tensions (dashes lines) of $SU(3)_{-4} + 6\mathbf{F}$ in the first chamber.

we predict using our new criteria.[4] This theory has the physical Coulomb branch only in the first chamber and it becomes a one-dimensional real line ${\mathcal{C}_{\rm phys}}^{(1)} : 2\phi = \phi_2 \geq 0$ at infinite coupling. In the second chamber, there is no physical domain in the Coulomb branch. The metric on the physical Coulomb branch with $T \geq 0$ is non-negative as depicted in Figure 8.

Instanton operator analysis at 1-instanton level tells us that the global symmetry of this theory will be enhanced to $SO(12) \times U(1)$ at the fixed point. Following [15, 30], one can show that there is a conserved current multiplet in the antisymmetric representation of the classical $SU(6)$ flavor symmetry due to a 1-instanton operator which enhances the global symmetry $U(6) \times U(1)_I$ to $SO(12) \times U(1)$, where $U(1)_I$ is the instanton symmetry. It is not clear, however, whether or not this theory has a 6d uplift in the UV because the enhanced global symmetry is not of affine type.

3.2 Additional conjectures

In principle, we can classify all non-trivial 5d gauge theories for simple gauge groups of arbitrary rank using the criterion in (3.5). For low rank, this is a manageable problem and thus we classify all gauge theories with $r_G \leq 3$ using (3.5) in the next section. However, our method of classification in this case involves an analysis on the entire Coulomb branch, and thus becomes a difficult task for higher rank gauge theories.

To circumvent this issue, we propose the following three additional conjectures, each of which we have checked leads to the same classification of 5d theories obtained via our main conjecture, up to $r_G \leq 3$ analytically and up to $r_G \leq 5$ numerically:

More Conjectures

[4]This theory is a marginal theory whose fixed point theory is not a 5d SCFT. We discuss marginal theories in more detail in Section 4.

1. If $\tau_{\text{eff}}(\phi) > 0$ *somewhere* in the naive Coulomb branch $\mathcal{C}$ (possibly including unphysical regions), then there exists a physical Coulomb branch $\mathcal{C}_{\text{phys}}$.
2. If all $T(\phi) > 0$ in some region $\mathcal{C}_{T>0} \subseteq \mathcal{C}$, then $\tau_{\text{eff}}(\phi) > 0$ in $\mathcal{C}_{T>0}$.
3. If the prepotential $\mathcal{F}(\phi) > 0$ *everywhere* in the the Coulomb branch $\mathcal{C}$ (possibly including unphysical regions), there exists a physical Coulomb branch $\mathcal{C}_{\text{phys}}$.
4. Conjectures 1-3 above are equivalent to our main conjecture.

Physical or mathematical proofs for the additional conjectures above are currently lacking. However, the checks we did up to $r_G \leq 5$ are very compelling evidences for the above conjectures. So we believe that they also hold for arbitrary higher-rank gauge theories. We leave the proof of the equivalence of these conjectures to future study.

Each of the above three conjectures has its own interesting implications, which we now discuss briefly. Conjecture 1 can be viewed as an extension of the criterion previously discussed in [8]. There, the authors imposed that the constraint of metric positivity everywhere on the Weyl chamber $\mathcal{C}$, whereas Conjecture 1 merely requires that there exist *some* regions in $\mathcal{C}$ for which the metric is positive definite. Stated differently, we do not assume that the physical Coulomb branch $\mathcal{C}_{\text{phys}} = \mathcal{C}$.

Conjecture 2 is quite interesting because in all cases we have checked, the condition that the tensions be positive on some region $\mathcal{C}_{\text{phys}}$ guarantees that the metric is also positive definite on $\mathcal{C}_{\text{phys}}$. Therefore, according to our main conjecture, the existence of such a region $\mathcal{C}_{\text{phys}}$ is sufficient to imply the existence of a non-trivial fixed point. From a practical standpoint, Conjecture 2 is much easier to utilize for a systematic classification of 5d theories because the mathematical conditions we need to impose only involve the gradient of the prepotential, whereas metric positivity requires diagonalization of the Hessian of the prepotential. Moreover, the constraint of positive tension is convenient because we only need to apply it to a local region of the naive Coulomb branch (as opposed to the entire Coulomb branch) to identify a legitimate theory.

Conjecture 3 is essentially motivated by the convergence of the partition function on a compact five-manifold. More precisely, Conjecture 3 asserts that positivity of $\mathcal{F}$ on the entire Coulomb $\mathcal{C}$ branch guarantees the convergence of the naive perturbative partition function. However, it is not clear if Conjecture 3 can guarantee the convergence of the full partition function including non-perturabive contributions. We discuss the details of the partition function on S^5 and its connection to Conjecture 3 in Appendix C. One practical advantage of Conjecture 3 is that it only involves checking the prepotential itself, rather than its first or second derivatives. However, this advantage comes at the expense of having to analyze the prepotential on the entire Coulomb branch as opposed to a local region.

We remark that Conjectures 2 and 3 are complementary: Conjecture 2 can be used to argue the existence of non-trivial 5d gauge theories by locally identifying a physical Coulomb branch $\mathcal{C}_{\text{phys}}$, while Conjecture 3 can be used to exclude theories by again locally identifying a region of $\mathcal{C}$ that does not admit a positive prepotential. Therefore, a combination of these two conjectures gives us a powerful method to fully classify 5d SQFTs with simple gauge groups. In the following section we will explicitly describe the classification we obtained by using Conjectures 2 and 3.

4 Classification of 5d CFTs

4.1 Classification overview

Analysis on the Coulomb branch of the moduli space provides us a systematic way to classify non-trivial 5d gauge theories with interacting fixed points. For the first step toward this direction, we will classify all possible gauge theories with simple gauge group G.

An important and very useful assumption in our classification is the idea that the dimension of the largest matter representation must be less than the dimension of the adjoint representation. The reason for this assumption is the fact that the matter hypermultiplets contribute terms that "reduce" the convexity of the perturbative prepotential (2.1). In order to ensure the existence of a physical Coulomb branch for which the prepotential is convex, it is therefore necessary that the vector multiplet contributions to the prepotential "balance" against the hypermultiplet contributions. Building on an observation made in [8], we translate this requirement into the restriction that the lengths of the weights of a given representation be no larger than those of the adjoint representation. If this were not the case, then even for a single matter hypermultiplet it would be possible to locate a direction in the naive Coulomb branch for which the prepotential is negative[5] violating Conjecture 3.

[5]As described in Appendix A.3, the length $l(e)$ of a root e is defined to be the sum of the coefficients of e in a basis of simple roots, and similarly for a weight w. We note that it is always possible to locate a region $\phi^* \in \mathcal{C}$ for which $e \cdot \phi^* = l(e)$ and $w \cdot \phi^* = l(w)$, and hence at infinite coupling $1/g_0^2 = 0$, the prepotential is proportional to $6\mathcal{F}(\phi^*) = \sum_{e\in\text{roots}} |l(e)|^3 - \sum_{w\in\mathbf{R}_f} |l(w)|^3$, and the classical CS term $\sum_{w\in\mathbf{F}}(w\cdot\phi^*)^3 = \sum_{w\in\mathbf{F}} l(w)^3 = 0$. It is then evident that $\mathcal{F}(\phi^*)$ will be negative if the quadratic Dynkin index of $\mathbf{R}_f$ is larger than the quadratic Dynkin index of the adjoint representation—see Appendix B for further discussion.

In the following classification, we will distinguish between two types of theories—*standard* and *exceptional*. Standard theories are classes of 5d gauge theories with classical gauge groups for which the same specifications for the matter content (depending on the rank of the gauge group) applies for all rank r_G. The expressions bounding the matter content for standard theories are simple linear expressions involving r_G and the numbers of flavors. By contrast, exceptional theories exist only for some sporadic lower rank cases, where $r_G \leq 8$. For these theories, there is no simple formula constraining the matter content and therefore they must be studied on a case-by-case basis.

In the first sub-section, we will present the classification of all standard theories. We will first choose some particular subregions in the Weyl chamber (where the choices of subregions are motivated by data from lower rank studies) and examine these subregions using Conjecture 3. This will set upper bounds on the matter content for non-trivial QFTs. Note that this does not guarantee the existences of such theories, but merely exclude the theories beyond the bounds. Then we will apply Conjecture 2 along the same subregions to confirm the existence of the theories below these bounds. This will allow us to finish the full classification of non-trivial CFTs with single gauge nodes of higher ranks $r_G > 8$.

In the second sub-section, we will deal with exceptional cases at lower ranks $r_G \leq 8$. Our classification program involves both analytic and numerical search methods. By 'analytic', we mean that we have used a symbolic computing tool to derive precise inequalities describing the physical Coulomb branches with positive metric. By 'numerical', we mean that we have implemented a numerical search on the lattice discretization of a fundamental Weyl chamber to locate a region admitting physical Coulomb branch. Having determined such regions, we then analytically test whether or not such regions admit non-trivial theories using Conjectures 2 and 3.

For $r_G \leq 3$, we employ only our main conjecture to analytically perform the classification, without using the additional conjectures. For $3 < r_G \leq 5$, we employ a numerical search combined with our main conjecture to identify suitable theories, and then use Conjectures 2 and 3 to confirm the existence of these theories analytically. For $5 < r_G \leq 8$, we numerically perform the classification by using Conjectures 2 and 3.

Marginal theories vs. 5d CFTs One additional idea essential to our classification is the notion of a *marginal* theory. Marginal theories are those theories for which there exists a physical Coulomb branch $\mathcal{C}_{\text{phys}}$ with positive metric, but the strong coupling limit $1/g_0^2 \to 0$ is not a 5d SCFT fixed point. One distinguished characteristic of marginal theories is the vanishing of the some of the eigenvalues of τ_{eff} at infinite coupling limit, i.e. the metric is degenerate along $\mathcal{C}_{\text{phys}}$. In addition, the physical

Coulomb branch with positive string tensions collapses to a lower dimensional space at infinite coupling limit:

$$\dim \mathcal{C}_{\text{phys}}|_{g_0^2\to\infty} < r_G. \tag{4.1}$$

In order to preserve the full dimensionality of $\mathcal{C}_{\text{phys}}$, it is necessary to keep the gauge coupling finite, i.e. $g_0^2 < \infty$. Finite gauge coupling introduces a scale to such theories, implying that their UV completions cannot be 5d SCFTs. Some of these theories will have 6d UV completions instead of 5d SCFT completions. We will discuss such theories uplifted to 6d theories in Section 5. For other marginal theories, we do not have a clear understanding of their UV completions, or if they even exist.

We use the term *descendants* to refer to theories that can be obtained from some other theory with a larger number of matter hypermultiplets via RG flow after integrating out some massive matter hypermultiplets. All the descendants of the marginal theories flow to 5d SCFT fixed points at infinite coupling.

The reason for this, as explained in [8], is that the cubic deformations to the prepotential (coming from the terms $|w\cdot\phi + m_f|^3$) resulting from sending a mass parameter $m_f \to \pm\infty$ and integrating out the matter make the prepotential "more convex". The only other deformations to the prepotential arising from integrating out $N_{\mathbf{R}_f}$ massive matter hypermultiplets in the representation $\mathbf{R}_f$ with mass terms $\text{sgn}(m_f)|m_f|$ are terms of the form $-\text{sgn}(m_f)N_{\mathbf{R}_f}c^{(3)}_{\mathbf{R}_f}/2$ contributing to the classical CS level κ [8]. Therefore, for $SU(N\geq 3)$ theories, one can trade matter hypermultiplets for the CS level κ, and such theories will have interacting fixed points as demonstrated by our classification. On the other hand, if one increases κ or adds more matter to these marginal theories described above, the resulting theories have no physical Coulomb branch and consequently they are trivial.

Notational conventions In the following discussion, we adopt the condensed notation

$$G_\kappa + \sum_f N_{\mathbf{R}_f}\mathbf{R}_f \tag{4.2}$$

to refer to a gauge theory with simple gauge group G with CS level κ coupled to $N_{\mathbf{R}_f}$ matter hypermultiplets (or half-hypermultiplets) transforming in the representation $\mathbf{R}_f$. We encounter the following representations:

- **F**, fundamental
- **Sym**, rank two symmetric

- **AS**, rank-2 antisymmetric
- **TAS**, rank-3 antisymmetric
- **S**, spinor
- **C**, conjugate spinor.

4.2 Standard theories

A class of gauge theories with gauge groups $G = SU(N), Sp(N), SO(N)$ which exist even at large rank can be fully classified by employing our conjectures. We call such theories as *standard* theories as mentioned above. The results are summarized in Table 1. The theories in these tables are marginal theories. We expect that all of the standard have 6d uplifts at strong coupling, a point that we discuss further in Section 5. The descendants of these marginal theories are expected to have non-trivial 5d SCFT fixed points at UV. $\mathcal{C}_{\text{phys}}$ is the subregion in the Weyl chamber within which we have confirmed the metric and the string tensions of the corresponding theory are both positive.

F is the global symmetry at the UV fixed point which we obtain by using 1-instanton analysis in [15, 16, 26, 30][6]. Some lower rank theories have further symmetry enhancements which are listed in Table 2. The full global symmetry could be in general different from those listed in the table if the symmetry enhancement occurs at two or higher instanton level. In some cases, the global symmetry group is affinized by instanton operators. This may signal that the theory is uplifted to a 6d theory at the UV fixed point. Some of these global symmetries have already been confirmed by identifying brane constructions or explicit 6d uplifts of these theories [21, 22, 31].

In the following section we present an algorithm for the classification of the standard theories listed in Table 1.

4.2.1 $SU(N)$ gauge theories

Let us start with the classification of standard $SU(N)$ gauge theories with $N_{\mathbf{F}}$ fundamental, $N_{\mathbf{Sym}}$ symmetric, and $N_{\mathbf{AS}}$ antisymmetric hypermultiplets. Note that other representations are not allowed for higher rank theories $r_G > 8$. For lower rank theories

[6] In some cases, like $Sp(N)$ with fundamental matter, the 1-instanton analysis was supplemented by additional data. Also there are several subtleties and technical difficulties involved in the 1-instanton analysis, which in some cases prevent us from carrying the calculation. The cases of $SU(N)$ groups with symmetric matter hypermultiplets are particularly subtle. The symmetries written in these cases are the minimal ones we are sure of, but there may well be additional enhancements by 1-instanton states for low N cases.

$N_{\mathbf{Sym}}$	$N_{\mathbf{AS}}$	$N_{\mathbf{F}}$	$\lvert\kappa\rvert$	F	$\mathcal{C}_{\text{phys}}$
1	1	0	0	$A_1^{(1)} \times U(1)$	$\mathcal{S}^{(2)}_{SU(N)}$
1	0	$N-2$	0	$A_{N-2}^{(1)} \times U(1)$	$\mathcal{S}^{(2)}_{SU(N)}$
1	0	0	$\frac{N}{2}$	$U(1)^2$	$\mathcal{S}^{(1)}_{SU(N)}$
0	2	8	0	Even N : $E_7^{(1)} \times A_1^{(1)} \times A_1^{(1)} \times SU(2)$ Odd N : $D_8^{(1)} \times A_1^{(1)} \times SU(2)$	$\mathcal{S}^{(2)}_{SU(N)}$
0	2	7	$\frac{3}{2}$	Even N : $D_8^{(1)} \times SU(2)$ Odd N : $E_7^{(1)} \times SU(2) \times SU(2)$	$\mathcal{S}^{(3)}_{SU(N)}$
0	1	$N+6$	0	$A_{N+6}^{(1)} \times U(1)$	$\mathcal{S}^{(2)}_{SU(N)}$
0	1	8	$\frac{N}{2}$	$SO(16) \times U(1)^2$	$\mathcal{S}^{(1)}_{SU(N)}$
0	0	$2N+4$	0	$D_{2N+4}^{(1)}$	$\mathcal{S}^{(2)}_{SU(N)}$

(a) Marginal $SU(N)$ theories with CS level κ, $N_{\mathbf{Sym}}$ symmetric, $N_{\mathbf{AS}}$ antisymmetric, and $N_{\mathbf{F}}$ fundamental hypermultiplets. See (4.4) for an explicit description of the physical Coulomb branches described in the far right column.

$N_{\mathbf{AS}}$	$N_{\mathbf{F}}$	F	$\mathcal{C}_{\text{phys}}$
1	8	$E_8^{(1)} \times SU(2)$	$\mathcal{S}_{Sp(N)}$
0	$2N+6$	$D_{2N+6}^{(1)}$	$\mathcal{S}_{Sp(N)}$

(b) Marginal $Sp(N)$ theories with $N_{\mathbf{AS}}$ antisymmetric and $N_{\mathbf{F}}$ fundamental hypermultiplets. See (4.19) for a description of the physical Coulomb branches.

$N_{\mathbf{F}}$	F	$\mathcal{C}_{\text{phys}}$
$N-2$	$A_{2N-5}^{(2)}$	$\mathcal{S}_{SO(N)}$

(c) Marginal $SO(N>4)$ theories with $N_{\mathbf{F}}$ fundamental hypermultiplets. See (4.26) for a description of the physical Coulomb branch.

Table 1. Classes of standard gauge theories. Note that all of these theories are marginal and their descendants have 5d conformal fixed points in the UV. See (4.4), (4.19)

$r_G \leq 8$, we can also add $N_{\mathbf{TAS}}$ matters in the rank-3 antisymmetric representation. But theories with $N_{\mathbf{TAS}} > 0$ are exceptional theories that we will discuss separately below. Matter hypermultiplets in other representations are not allowed.

In the following discussion, we express the roots and weights in the orthogonal basis. The prepotential for $SU(N)_\kappa + N_{\mathbf{F}}\mathbf{F} + N_{\mathbf{AS}}\mathbf{AS}$ in the Weyl chamber $a_1 \geq a_2 \geq \cdots \geq a_{N-1} \geq 0$ is given by

$$\mathcal{F}_{SU(N)} = \frac{1}{2g_0^2}\sum_{i=1}^N a_i^2 + \frac{\kappa}{6}\sum_{i=1}^N a_i^3 + \frac{1}{6}\sum_{i<j}^N (a_i-a_j)^3 - \frac{N_{\mathbf{F}}}{12}\sum_{i=1}^N |a_i|^3 - \frac{N_{\mathbf{AS}}}{6}\sum_{i<j}^N |a_i+a_j|^3 \,, \quad (4.3)$$

with $a_N = -\sum_i a_i$. A symmetric matter hypermultiplet has the same contribution

N	$N_{\mathbf{AS}}$	$N_{\mathbf{F}}$	$\|\kappa\|$	F
4	2	8	0	$E_7^{(1)} \times B_3^{(1)}$
5	2	7	$\frac{3}{2}$	$E_7^{(1)} \times G_2$
4	2	7	$\frac{3}{2}$	$B_9^{(1)}$
5	1	11	0	$A_{11}^{(1)} \times A_1^{(1)}$
4	1	10	0	$A_{11}^{(1)}$
6	1	8	3	$SO(16) \times SU(2) \times U(1)$
5	1	8	$\frac{5}{2}$	$E_8^{(1)} \times U(1)$
4	1	8	2	$E_8^{(1)} \times U(1)$

Table 2. $SU(N)$ theories with further symmetry enhancement.

to the prepotential as the contribution from ($N_{\mathbf{AS}} = 1$, $N_{\mathbf{F}} = 8$) hypermultiplets. It follows that $(N_{\mathbf{AS}} = 1, N_{\mathbf{F}} = 8)$ hypermultiplets can be traded with $N_{\mathbf{Sym}} = 1$ at the level of the prepotential. So we will consider the cases $N_{\mathbf{Sym}} = 0$ and retrive the cases with $N_{\mathbf{Sym}} > 0$ by using the "equivalence" ($N_{\mathbf{AS}} = 1$, $N_{\mathbf{F}} = 8$) $\sim N_{\mathbf{Sym}} = 1$ as needed.

We will examine the following three regions of the Weyl chamber,

$$\mathcal{S}^{(1)}_{SU(N)} = (a, a, \cdots, a, -(N-1)a) \, , \quad \mathcal{S}^{(2)}_{SU(N)} = (a, 0, \cdots, 0, -a) \, , \quad \mathcal{S}^{(3)}_{SU(N)} = (a, a, 0, \cdots, 0, -2a) \, , \tag{4.4}$$

Firstly, Conjecture 3 imposes the condition for non-trivial $SU(N)$ theories that the prepotential should be positive $\mathcal{F}_{SU(N)} > 0$ along these three regions. Then each of three regions gives rise to the following three inequalities,

$$\begin{aligned} \mathcal{S}^{(1)}_{SU(N)} &: \; N_{\mathbf{F}}(N^2-2N+2) + 2|\kappa| N(N-2) + N_{\mathbf{AS}}(N-2)(N^2-4N+8) \leq 2N^3 \, , \\ \mathcal{S}^{(2)}_{SU(N)} &: \; N_{\mathbf{F}} + (N-2)N_{\mathbf{AS}} \leq 2N+4 \, , \\ \mathcal{S}^{(3)}_{SU(N)} &: \; 5N_{\mathbf{F}} + 5N_{\mathbf{AS}}(N-2) + 6|\kappa| \leq 10N + 24 \, . \end{aligned} \tag{4.5}$$

For a given N, these inequalities set some upper bounds on the matter content of the theories with non-trivial fixed points. We may be able to find other independent inequalities by examining other regions in the Weyl chamber. But we will show shortly that these inequalities are enough for higher rank theories. By analyzing these three inequalities, it can be shown that for $N > 6$ there are only five cases that saturate one of these inequalities while not violating the others:

$$(N_{\mathbf{AS}}, N_{\mathbf{F}}, |\kappa|) \; = \; (2, 8, 0) \, , \; (2, 7, \tfrac{3}{2}) \, , \; (1, N+6, 0) \, , \; (1, 8, \tfrac{N}{2}) \, , \; (0, 2N+4, 0) \, . \tag{4.6}$$

Other theories with $N > 6$ having more matter or higher Chern-Simons levels are all excluded by Conjecture 3 since they have negative prepotential along one of the above three regions.

We will now confirm that the upper boundary theories in (4.6) are indeed non-tivial theories having interacting UV fixed points by testing Conjecture 2 along the three subregions $\mathcal{S}^{(i=1,2,3)}_{SU(N)}$. First, we expand the Coulomb branch parameters around $\mathcal{S}^{(1)}_{SU(N)}$ as

$$a_i = a + \delta_i \ , \quad \delta_i \ll 1 \ , \tag{4.7}$$

with $\delta_i > \delta_{i+1}$. Then the string tensions can be approximated as

$$\begin{aligned} T_i &= (\partial_{a_i} - \partial_{a_{i+1}})\mathcal{F}_{SU(N)} \\ &= \left(\frac{1}{g_0^2} + \left(N + \kappa - \frac{N_{\mathbf{F}}}{2} - \frac{3}{2}NN_{\mathbf{AS}} + 4N_{\mathbf{AS}}\right)a\right)(\delta_i - \delta_{i+1}) + \mathcal{O}(\delta^2) \ , \\ T_{N-1} &= \partial_{a_{N-1}}\mathcal{F}_{SU(N)} \\ &= \frac{N}{g_0^2}a + \left(N^3 - \kappa N(N-2) - \frac{N_{\mathbf{F}}}{2}(N^2-2N+2) - \frac{N_{\mathbf{AS}}}{4}(N^3-6N^2+16N-16)\right)\frac{a^2}{2} + \mathcal{O}(\delta) \ . \end{aligned} \tag{4.8}$$

It is obvious that all the string tensions are positive at weak coupling $1/g_0^2 \gg 1$ since $\delta_i > \delta_{i+1}$. However, in the strong coupling limit $1/g_0^2 \to 0$, all of the string tensions are positive, i.e. $T > 0$, only if the matter content of the theory satisfies the following inequalities:

$$\begin{aligned} &2N + 2\kappa - N_{\mathbf{F}} - N_{\mathbf{AS}}(3N-8) \geq 0, \\ &N^3 - \kappa N(N-2) - \frac{N_{\mathbf{F}}}{2}(N^2-2N+2) - \frac{N_{\mathbf{AS}}}{4}(N^3-6N^2+16N-16) \geq 0 \ . \end{aligned} \tag{4.9}$$

When all the string tensions are positive, we identify the corresponding theory as a good theory with an interacting UV fixed point by using Conjecture 2.

Similarly, it is straightforward to show that the string tension analysis around $\mathcal{S}^{(2)}_{SU(N)}$ leads to the inequalities

$$2N + 4 - N_{\mathbf{F}} - N_{\mathbf{AS}}(N-2) \geq 0 \ , N_{\mathbf{AS}} \leq 2 \ . \tag{4.10}$$

Lastly, the string tensions near $\mathcal{S}^{(3)}_{SU(N)}$ are approximated as

$$\begin{aligned} T_1 &= \left(\frac{1}{g_0^2} + \left(N + k - \frac{1}{2}N_{\mathbf{F}} - \frac{1}{2}N_{\mathbf{AS}}(N-2)\right)a\right)(\delta_1 - \delta_2) + \mathcal{O}(\delta^2) \ , \\ T_2 &= \frac{a}{g_0^2} + \left(N + 4 + k - \frac{1}{2}N_{\mathbf{F}} - \frac{1}{2}N_{\mathbf{AS}}(N+2)\right)a^2/2 + \mathcal{O}(\delta) \ , \\ T_i &= \left(\frac{1}{g_0^2} + (4 - 2N_{\mathbf{AS}})a\right)(\delta_i - \delta_{i+1}) + \mathcal{O}(\delta) \ , \\ T_{N-1} &= \frac{2a}{g_0^2} + 2\left(N + 2 - k - \frac{1}{2}N_{\mathbf{F}} - \frac{1}{2}N_{\mathbf{AS}}(N-3)\right)a^2 + \mathcal{O}(\delta) \ , \end{aligned} \tag{4.11}$$

where $a_1 = a+\delta_1, a_2 = a+\delta_2$ and $a_i = \delta_i$ for $3 \leq i \leq N-1$ with infinitesimal parameters δ_i. Therefore the analysis $T > 0$ around $S^{(3)}_{SU(N)}$ gives the inequalities

$$N_{\mathbf{AS}} \leq 2 \ , \ 2N{+}2k{-}N_{\mathbf{F}}{-}N_{\mathbf{AS}}(N{-}2) \geq 0 \ , \ 2N{+}4{-}2\kappa{-}N_{\mathbf{F}}{-}N_{\mathbf{AS}}(N{-}3) \geq 0 \ . \quad (4.12)$$

We now have three sets of inequalities (4.9), (4.10), (4.10). Conjecture 2 tells us that if an $SU(N)$ theory on one of the three subregions $\mathcal{S}^{(i=1,2,3)}_{SU(N)}$ satisfies the corresponding inequality, the theory is a non-trivial theory having interacting fixed point at UV. With this criterion, one can easily show that all of the upper boundary theories in (4.6) are non-trivial theories. We will call these theories, and their descendants obtained by integrating out massive matter, standard $SU(N)$ gauge theories. The standard $SU(N)$ theories are summarized in Table 1a. Note that we obtained results for the theories with symmetric hypermultiplets by trading $(N_{\mathbf{AS}}, N_{\mathbf{F}}) = (1,8) \to N_{\mathbf{Sym}} = 1$. The theories (and their descendants) in Table 1a exist at any N and they are the only non-trivial theories at $N \geq 9$, which is proven above relying on Conjecture 2 and 3. This completes the full classification of standard $SU(N)$ gauge theories. In fact, all the theories listed in Table 1a lift to 6d SCFTs in the UV, and hence they are marginal theories. We discuss these theories and their 6d uplifts in more detail in Section 5.

4.2.2 $Sp(N)$ gauge theories

Let us turn to $Sp(N)$ gauge theories. $Sp(N)$ gauge theory can have $N_{\mathbf{F}}$ fundamental, $N_{\mathbf{AS}}$ antisymmetric, and $N_{\mathbf{TAS}}$ rank-3 antisymmetric representations of $Sp(N)$. We claim that no other representations are permitted, and furthermore $N_{\mathbf{TAS}} > 0$ only for theories with $N \leq 4$. The theories with $N_{\mathbf{TAS}} > 0$ are exceptional theories, and will be discussed separately below. In this section, we consider the standard theories $Sp(N) + N_{\mathbf{F}}\mathbf{F} + N_{\mathbf{AS}}\mathbf{AS}$. The $Sp(N)$ theory has a single Weyl subchamber $a_1 \geq a_2 \geq \cdots \geq a_N \geq 0$. The prepotential is given by

$$\mathcal{F}_{Sp(N)} = \frac{1}{2g_0^2}\sum_{i=1}^{N} a_i^2 + \frac{1}{6}\left(\sum_{i<j}^{N}\left((a_i-a_j)^3+(a_i+a_j)^3\right)(1-N_{\mathbf{AS}}) + (8-N_{\mathbf{F}})\sum_{i=1}^{N} a_i^3\right) \ . \quad (4.13)$$

Since the $Sp(N)$ theory has a single Weyl chamber, in sharp contrast to the $SU(N)$ cases with many distinct chambers, we can in fact examine every point on the Weyl chamber without restricting to particular subregions and thereby obtain a full classification using only Conjecture 2.

The string tensions are

$$\begin{aligned}
T_i &= (\partial_{a_i} - \partial_{a_{i+1}})\mathcal{F}_{Sp(N)} \\
&= (a_i - a_{i+1})\left(\frac{1}{g_0^2} + \sum_{j=1}^{i}(2a_j - a_i - a_{i+1})(1 - N_{\mathbf{AS}}) + \frac{1}{2}\left((2N-4)(1-N_{\mathbf{AS}}) + 8 - N_{\mathbf{F}}\right)(a_i + a_{i+1})\right) \\
T_N &= \partial_{a_N}\mathcal{F}_{Sp(N)} = a_N\left(\frac{1}{g_0^2} + \frac{8-N_{\mathbf{F}}}{2}a_N + 2(1-N_{\mathbf{AS}})a_T\right) \ ,
\end{aligned} \tag{4.14}$$

where $a_T = \sum_{i=1}^{N-1} a_i$. The condition on the last string tension $T_N > 0$ gives the inequality

$$N_{\mathbf{AS}} \leq \frac{8-N_{\mathbf{F}}}{4}\frac{a_N}{a_T} + 1 \ . \tag{4.15}$$

The right hand side of this equation is maximized near $a_1 = a_2 = \cdots = a_N$ and the result is

$$N_{\mathbf{AS}} \leq \frac{4N - N_{\mathbf{F}} + 4}{4(N-1)} \ . \tag{4.16}$$

For the theories with $N \geq 5$, this condition allows only the cases with $N_{\mathbf{AS}} = 0, 1$.

When $N_{\mathbf{AS}} = 1$, the tension positivity conditions reduce to the single condition

$$N_{\mathbf{F}} \leq 8 \quad (\text{when } N_{\mathbf{AS}} = 1)\,. \tag{4.17}$$

When $N_{\mathbf{AS}} = 0$, the string tensions can be written as

$$\begin{aligned}
T_i &= (a_i - a_{i+1})\left(\frac{1}{g_0^2} + 2\sum_{j=1}^{i-1} a_j + \frac{2N+8-N_{\mathbf{F}}-2i}{2}a_i^2 + \frac{2N+4-N_{\mathbf{F}}-2i}{2}a_{i+1}^2\right) \\
T_N &= a_N\left(\frac{1}{g_0^2} + \frac{8-N_{\mathbf{F}}}{2}a_N + 2a_T\right) \ .
\end{aligned} \tag{4.18}$$

The positive tension conditions $T > 0$ admit the maximum number of matter hypermultiplets near the subregion

$$\mathcal{S}_{Sp(N)} = (a, 0, \cdots, 0). \tag{4.19}$$

Around $\mathcal{S}_{Sp(N)}$, the only non-trivial condition is $T_1 > 0$ which gives rise to the bound

$$N_{\mathbf{F}} \leq 2N + 6 \ . \tag{4.20}$$

The standard $Sp(N)$ theories are those summarized in Table 1b along with their descendants. The theories in Table 1b have 6d uplifts at the UV fixed point, so they are marginal theories. Their descendants are expected to have 5d CFT fixed points in UV.

Note that, when $N_{\mathbf{F}} = 0$, the $Sp(N)$ gauge theory has a discrete theta angle $\theta = 0, \pi$ associated to $\pi(Sp(N)) \cong \mathbb{Z}_2$. Thus there are two more non-trivial $Sp(N)$ theories with $(N_{\mathbf{AS}} = 0, N_{\mathbf{F}} = 0)$ and $(N_{\mathbf{AS}} = 1, N_{\mathbf{F}} = 0)$.

One can immediately show that, for these standard theories, the prepotential (4.13) is always positive within the Weyl chamber. If we add more matter to these theories, their prepotential will become negative somewhere in the Weyl chamber. This confirms Conjecture 3 for the standard $Sp(N)$ gauge theories.

4.2.3 $SO(N)$ gauge theories

We consider the case of $SO(N)$ with $N_{\mathbf{F}}$ fundamental flavors. Spinor hypermultiplets can also be added when $N \leq 14$, but because such theories are not standard, we discuss them in the next subsection. In the case $N = 2r + 1$, there is only a single Weyl subchamber to consider, namely $a_1 \geq a_2 \geq \cdots \geq a_r \geq 0$. The prepotential for $SO(2r+1) + N_{\mathbf{F}}\mathbf{F}$ is

$$\mathcal{F}_{SO(2r+1)} = \frac{1}{g_0^2}\sum_{i=1}^{r} a_i^2 + \frac{1}{6}\sum_{i<j}^{r}[(a_i+a_j)^3 + (a_i-a_j)^3] + \frac{1-N_{\mathbf{F}}}{6}\sum_{i=1}^{r} a_i^3. \tag{4.21}$$

Using the above formula for the prepotential, we see that the tensions are given by:

$$\begin{aligned} T_{i<r} &= \left(\partial_{a_i} - \partial_{a_{i+1}}\right)\mathcal{F}_{SO(2r+1)} \\ &= \frac{2}{g_0^2}(a_i - a_{i+1}) + 2(a_i - a_{i+1})\sum_{j=1}^{i-1} a_j \\ &\quad + a_{i+1}^2\left(1 - \frac{1}{2}(N - N_{\mathbf{F}} - 2i - 2)\right) + \left(\frac{a_i}{2}(N - N_{\mathbf{F}} - 2i) - 2a_{i+1}\right) \end{aligned} \tag{4.22}$$

$$T_r = 2\partial_{a_r}\mathcal{F}_{SO(2r+1)} = \frac{2}{g_0^2}a_r + 4a_r\sum_{j=1}^{r-1} a_j + (1 - N_{\mathbf{F}})a_r^2. \tag{4.23}$$

Let us first focus on the expression for T_1:

$$T_1 = \frac{2}{g_0^2}(a_1 - a_2) + \frac{1}{2}(a_1 - a_2)((N - N_{\mathbf{F}} - 2)a_1 + (N - N_{\mathbf{F}} - 6)a_2). \tag{4.24}$$

It is possible to maximize the number of fundamental matters while keeping T_1 positive by setting $a_2 = 0$ in the infinite coupling regime $1/g_0^2 \ll 1$:

$$N_{\mathbf{F}} \leq N - 2. \tag{4.25}$$

Notice that when $a_2 = 0$, the remaining Coulomb branch parameters $a_j = 0$ for $j > 2$ according to the definition of the fundamental Weyl chamber. Therefore, we see that we can maximize $N_{\mathbf{F}}$ while keeping all tensions positive along the locus

$$\mathcal{S}_{SO(2n+1)} = (a, 0, \dots, 0). \tag{4.26}$$

For $N_{\mathbf{F}} = N - 2$, the only way to maintain positive tension is to keep the gauge coupling finite, $g_0^2 < \infty$. The resulting theory is a marginal theory with a 6d uplift at the UV fixed point. When the number of fundamental matters $N_{\mathbf{F}} > N - 2$, there is no physical Coulomb branch at infinite coupling $1/g_0^2 = 0$ with positive string tensions, and therefore such theories are trivial.

For $SO(2r)$ gauge theories with fundamental matter, the proof works identically to the above case, as we will now show. The prepotential for the $SO(2r)$ theory is

$$\mathcal{F}_{SO(2r)} = \frac{1}{g_0^2}\sum_{i=1}^{r} a_i^2 + \frac{1}{6}\sum_{i<j}^{r}[(a_i + a_j)^3 + (a_i - a_j)^3] - \frac{N_{\mathbf{F}}}{6}\sum_{i=1}^{r} a_i^3. \tag{4.27}$$

We again parametrize the fundamental Weyl chamber by the condition $a_1 \geq a_2 \geq \cdots \geq a_r \geq 0$. By computing derivatives of the above formula with respect to ϕ_i, we find that the monopole tensions are given by

$$\begin{aligned}
T_{i<r} &= \left(\partial_{a_i} - \partial_{a_{i+1}}\right)\mathcal{F}_{SO(2r)} \\
&= \frac{2}{g_0^2}(a_i - a_{i+1}) + 2(a_i - a_{i+1})\sum_{j=1}^{i-1} a_j \\
&\quad + a_{i+1}^2\left(1 - \frac{1}{2}(N - N_{\mathbf{F}} - 2i - 2)\right) + \left(\frac{a_i}{2}(N - N_{\mathbf{F}} - 2i) - 2a_{i+1}\right)
\end{aligned} \tag{4.28}$$

$$\begin{aligned}
T_r &= (\partial_{a_{r-1}} + \partial_{a_r})\mathcal{F}_{SO(2r)} \\
&= \frac{2}{g_0^2}(a_{r-1} + a_r) + 2(a_{r-1} + a_r)\sum_{j=1}^{r-2} a_j \\
&\quad + a_{r-1}\left(2a_r + \frac{a_{r-1}}{2}(N - N_{\mathbf{F}} - 2r + 2)\right) + a_r^2\left(1 - \frac{1}{2}N_{\mathbf{F}}\right).
\end{aligned} \tag{4.29}$$

From the above expressions, we see that the only difference with the tensions T_i associated to the $SO(2r+1)$ gauge theory is in the expression for T_r. By arguments identical to the above case $G = SO(2r+1)$, we find again that the bound on the number of fundamental flavors is $N_{\mathbf{F}} \leq N - 2$, with the case $N_{\mathbf{F}} = N - 2$ corresponding to a marginal theory.

4.3 Exceptional theories with rank ≤ 8

Rank 2

In the previous section, we confirmed that some 5d theories which go beyond the constraints introduced in [8] are in fact consistent theories with interacting fixed points.

We now turn our attention to the case of simple gauge groups G with $r_G = 2$, namely $G = SU(3), Sp(2), G_2$.

We begin by classifying non-trivial $SU(3)$ gauge theories. As discussed in the previous section, $SU(3)_\kappa + N_{\mathbf{F}}\mathbf{F} + N_{\mathbf{Sym}}\mathbf{Sym}$ has two Weyl subchambers, assuming the presence of fundamental hypermultiplets. Applying our main conjecture to the Coulomb branch, we find the list of marginal $SU(3)$ gauge theories displayed in Table 3. On the other hand, all the descendants of these theories obtained by integrating out matter hypermultiplets have non-trivial 5d conformal fixed points. This full list includes all known non-trivial 5d $SU(3)$ gauge theories, $SU(3)_0 + 1\mathbf{F} + 1\mathbf{Sym}$, and $SU(3)_0 + 10\mathbf{F}$, and their descendants. Other theories in the list are new non-trivial $SU(3)$ theories we predict based on new criteria.

$N_{\mathbf{Sym}}$	$N_{\mathbf{F}}$	κ	F	$\mathcal{C}_{\text{phys}}$
1	0	$\frac{3}{2}$	$SU(2) \times U(1)$	$2\phi_1 = \phi_2 \geq 0$
1	1	0	$A_1^{(1)} \times U(1)$	$\phi_1 = \phi_2 \geq 0$
0	10	0	$D_{10}^{(1)}$	$\phi_1 = \phi_2 \geq 0$
0	9	$\frac{3}{2}$	$E_8^{(1)} \times SU(2)$	$2\phi_1 = \phi_2 \geq 0$
0	6	4	$SO(12) \times U(1)$	$2\phi_1 = \phi_2 \geq 0$
0	3	$\frac{13}{2}$	$U(3) \times U(1)$	$2\phi_1 = \phi_2 \geq 0$
0	0	9	$U(1)$	$2\phi_1 = \phi_2 \geq 0$

Table 3. Marginal theories $SU(3)$ with CS level κ, $N_{\mathbf{Sym}}$ symmetric and $N_{\mathbf{F}}$ fundamental hypermultiplets. The theories with $\kappa < 0$ can be obtained by the interchange $\phi_1 \leftrightarrow \phi_2$.

We now turn to $Sp(2)$ gauge theories. $Sp(2)$ gauge theories can only have fundamental and antisymmetric matter, again because the dimensions of other representations are too large to admit a positive semi-definite metric on the physical Coulomb branch. There is a single Weyl chamber $\phi_2 \geq \phi_1 \geq \phi_2/2 \geq 0$ in the Dynkin basis. We find the marginal $Sp(2)$ gauge theories listed in the Table 4. The global symmetry algebras of these theories are all affine type [26]. Here $A_N^{(2)}$ denote the affine algebras with outer automorphism twists discussed in [29]. This means that all of them have 6d uplifts at their UV fixed points and their descendants have 5d CFT fixed points. This list completely agrees with matter bounds for $Sp(2)$ gauge theories given in [26]. $Sp(2) + 1\mathbf{AS} + 8\mathbf{F}$ has a two-dimensional Coulomb branch at infinite coupling. This implies that this theory has a two-dimensional tensor branch in 6d. Indeed, this theory is the 6d rank-2 E-string theory on a circle.

Lastly, the G_2 gauge theory can contain only fundamental hypermultiplets. This theory has a single Weyl subchamber $2\phi_1 \geq \phi_2 \geq 3\phi_1/2 \geq 0$ in the Dynkin basis.

$N_{\mathbf{AS}}$	$N_{\mathbf{F}}$	F	$\mathcal{C}_{\text{phys}}$
3	0	$A_5^{(2)}$ at $\theta=0$, $Sp(3)\times U(1)$ at $\theta=\pi$	$2\phi_1=\phi_2\geq 0$
2	4	$A_{11}^{(2)}$	$2\phi_1=\phi_2\geq 0$
1	8	$E_8^{(1)}\times SU(2)$	$\phi_1,\phi_2\geq 0$
0	10	$D_{10}^{(1)}$	$\phi_1=\phi_2\geq 0$

Table 4. Marginal $Sp(2)$ gauge theories with $N_{\mathbf{AS}}$ antisymmetric, $N_{\mathbf{F}}$ fundamental matters.

We find that these theories have a non-trivial physical Coulomb branch when $N_{\mathbf{F}}\leq 6$. The theory at $N_{\mathbf{F}}=6$ has an affine type global symmetry algebra and thus it will be uplifted to 6d at the UV fixed point [26].

$N_{\mathbf{F}}$	F	$\mathcal{C}_{\text{phys}}$
6	$A_{11}^{(2)}$	$2\phi_1=\phi_2\geq 0$

Table 5. A marginal G_2 gauge theory with $N_{\mathbf{F}}$ fundamental matters.

Rank 3

Let us start with the $SU(4)$ gauge theories. An $SU(4)$ gauge theory can have matter hypermultiplets in the fundamental, the antisymmetric, and the symmetric representations. When the theory contains symmetric or antisymmetric hypermultiplets, there are four distinguished Weyl chambers. We examine all these chambers and find the list of marginal $SU(4)$ theories in Table 6. Again, this list covers all previously known $SU(4)$ gauge theories in [8, 13–16, 21] and additionally it predicts many new interacting 5d gauge theories. The theories with $N_{\mathbf{AS}}=4, N_{\mathbf{Sym}}=N_{\mathbf{F}}=0$ and $\kappa=0,1,2,3,4$ are all marginal theories which cannot be obtained from other theories by integrating out massive matter.

Similarly, we can classify all non-trivial $Sp(3)$ gauge theories. The list of marginal $Sp(3)$ theories are given in Table 7. We can also have half-hypermultiplets in the rank-3 antisymmetric representation. However, due to the global anomaly described by Witten in [32], consistent $Sp(3)$ gauge theories with rank-3 antisymmetric matter must also have an odd number of half-hypermultiplets in the fundamental representation. The new criteria confirms that all previously known $Sp(3)$ gauge theories in [8, 26] are physical, with one exception. In [26], $Sp(3)+\frac{1}{2}\mathbf{TAS}+\frac{7}{2}\mathbf{F}+\mathbf{AS}$ may have a fixed point of 6d SCFT on a circle. However, we find that this theory has no physical Coulomb

$N_{\mathbf{Sym}}$	$N_{\mathbf{AS}}$	$N_{\mathbf{F}}$	κ	F	$\mathcal{C}_{\text{phys}}$
1	1	0	0	$A_1^{(1)} \times U(1)$	$2\phi_1 \geq \phi_2 \geq \phi_1 = \phi_3 \geq 0$
1	0	2	0	$A_2^{(1)} \times U(1)$	$\phi_1 = \phi_2 = \phi_3 \geq 0$
1	0	0	2	$U(1)^2$	$\phi_1 = \phi_2/2 = \phi_3/3 \geq 0$
0	4	0	4	$E_6^{(2)}$	$3\phi_1 \geq \phi_3 \geq \phi_1 = \phi_2/2 \geq 0$
0	4	0	$1,2,3$	$Sp(4) \times U(1)$	$\phi_1 = \phi_2/2 = \phi_3 \geq 0$
0	4	0	0	$A_7^{(2)}$	$\phi_1 = \phi_2/2 = \phi_3 \geq 0$
0	3	4	0	$A_{11}^{(2)} \times U(1)$	$\phi_1 = \phi_2/2 = \phi_3 \geq 0$
0	3	4	1	$Sp(7) \times U(1)$	$\phi_1 = \phi_2/2 = \phi_3 \geq 0$
0	3	4	2	$E_6^{(2)} \times SU(4)$	$\phi_1 = \phi_2/2 = \phi_3 \geq 0$
0	3	0	5	$Sp(3) \times U(1)$	$\phi_1 = \phi_2/2 = \phi_3/3 \geq 0$
0	2	8	0	$E_7^{(1)} \times B_3^{(1)}$	$2\phi_1 \geq \phi_2 \geq \phi_1 = \phi_3 \geq 0$
0	2	7	$\frac{3}{2}$	$B_9^{(1)}$	$\phi_1 = \phi_2/2 = \phi_3/2 \geq 0$
0	2	0	6	$Sp(2) \times U(1)$	$\phi_1 = \phi_2/2 = \phi_3/3 \geq 0$
0	1	10	0	$A_{11}^{(1)}$	$\phi_1 = \phi_2 = \phi_3 \geq 0$
0	1	8	2	$E_8^{(1)} \times U(1)$	$\phi_1 = \phi_2/2 = \phi_3/3 \geq 0$
0	1	0	7	$SU(2) \times U(1)$	$\phi_1 = \phi_2/2 = \phi_3/3 \geq 0$
0	0	12	0	$D_{12}^{(1)}$	$\phi_1 = \phi_2 = \phi_3 \geq 0$
0	0	8	3	$E_8 \times U(1)$	$\phi_1 = \phi_2/2 = \phi_3/3 \geq 0$
0	0	0	8	$U(1)$	$\phi_1 = \phi_2/2 = \phi_3/3 \geq 0$

Table 6. Marginal $SU(4)$ theories with CS level κ, $N_{\mathbf{Sym}}$ symmetric, $N_{\mathbf{AS}}$ antisymmetric, $N_{\mathbf{F}}$ fundamental matters. The theories with negative CS level are obtained by $\phi_1 \leftrightarrow \phi_3$.

branch. So our classification rules out this theory. It would be interesting to confirm this result using other arguments.

Finally, we come to the case of 5d $SO(7)$ gauge theories, which can have matter hypermultiplets in fundamental and spinor representations. The marginal theories $SO(7) + N_{\mathbf{F}}\mathbf{F} + N_{\mathbf{S}}\mathbf{S}$ are listed in Table 8.

Rank 4

In this section, we discuss exceptional 5d gauge theories, with gauge algebras $SO(8)$, $SO(9)$, F_4, and $SU(5)$. To begin, we consider $SO(8)$ gauge theories. An $SO(8)$ gauge theory can have $N_{\mathbf{F}}$ fundamental, $N_{\mathbf{S}}$ spinor, and $N_{\mathbf{C}}$ conjugate spinor representations. When there is matter in these three representations, the Weyl chamber splits into six distinct subchambers. We study each of these chambers and find the marginal theories

$N_{\mathbf{TAS}}$	$N_{\mathbf{AS}}$	$N_{\mathbf{F}}$	F	$\mathcal{C}_{\text{phys}}$
1	0	5	$E_6^{(1)}$	$3\phi_1 \geq \phi_3 \geq 2\phi_1 = \phi_2 \geq 0$
$\frac{1}{2}$	1	$\frac{5}{2}$	$Sp(4)$	$\phi_1 = \phi_2/2 = \phi_3/3 \geq 0$
$\frac{1}{2}$	0	$\frac{19}{2}$	$SO(19) \times U(1)$	$2\phi_1 \geq \phi_2 = \phi_3 \geq \phi_1 \geq 0$
0	2	0	$C_2^{(1)}$ at $\theta = 0$, $Sp(2) \times U(1)$ at $\theta = \pi$	$\phi_1 = \phi_2/2 = \phi_3/3 \geq 0$
0	1	8	$E_8^{(1)} \times SU(2)$	$\{2\phi_1 \geq \phi_3 \geq \phi_1 \cap \phi_3 \geq \phi_2 \geq (\phi_1+\phi_3)/2\} \cup$ $\{3\phi_1 \geq \phi_3 \geq 2\phi_1 \cap 2\phi_1 \geq \phi_2 \geq (\phi_1+\phi_3)/2\}, \phi_1 \geq 0$
0	0	12	$D_{12}^{(1)}$	$\phi_1 = \phi_2 = \phi_3 \geq 0$

Table 7. Marginal $Sp(3)$ gauge theories with $N_{\mathbf{TAS}}$ rank-3 antisymmetric, $N_{\mathbf{AS}}$ antisymmetric, $N_{\mathbf{F}}$ fundamental matters.

$N_{\mathbf{S}}$	$N_{\mathbf{F}}$	F	$\mathcal{C}_{\text{phys}}$
7	0	$Sp(7) \times U(1)$	$\phi_1 = \phi_2/2 = \phi_3 \geq 0$
6	1	$A_{11}^{(2)} \times SU(2)$	$\phi_1 = \phi_2/2 = \phi_3 \geq 0$
5	2	$C_7^{(1)}$	$\phi_1 = \phi_2/2 = \phi_3 \geq 0$
4	3	$E_6^{(2)} \times A_5^{(2)}$	$\phi_1 = \phi_2 \geq \phi_3 \geq \phi_1/2 \geq 0$
2	4	$A_{12}^{(2)}$	$\phi_1 = \phi_2 = 2\phi_3 \geq 0$

Table 8. Marginal $SO(7)$ gauge theories with $N_{\mathbf{S}}$ spinor and $N_{\mathbf{F}}$ fundamental matters.

summarized in Table 9d. Due to the triality of the D_4 Dynkin diagram, given such an $SO(8)$ gauge theory, there exists another $SO(8)$ gauge theory obtained by permuting $N_{\mathbf{F}}, N_{\mathbf{S}}, N_{\mathbf{C}}$. However, we stress that the physical Coulomb branches associated to different permutations are in general not identical. These results cover all known cases of $SO(8)$ gauge theories [26].

For $SO(9)$ gauge theories, there can be $N_{\mathbf{F}}$ fundamental and $N_{\mathbf{S}}$ spinors. When spinor matter is included, the fundamental Weyl chamber splits into three subchambers. We study each of these chambers and find the marginal theories summarized in Table 9e.

For $SU(5)$ gauge theories, we can consider hypermultiplets in the antisymmetric and the fundamental representations. We find four marignal theories as summarized in Table 9a. We would like to remark that our criteria for $SU(5)_{\frac{3}{2}} + 3\mathbf{AS} + 2\mathbf{F}$ is more involved. We find that this theory has a single sub-chamber which has a region $\mathcal{C}_{T>0}$ with positive string tensions and positive definite metric at infinite coupling. Therefore, naively, this theory is not marginal and it may have a 5d SCFT fixed point at UV. However, a careful analysis shows us that the boundary $\partial\mathcal{C}_{T>0}$ of the region is irrational. This indicates that this sub-chamber should not be a physical Coulomb branch. We expect that there exists a flop transition point where some non-perturbative instantons become massless so that we cannot reach the irrational boundary. We expect that, after taking into account the flop transition, this theory becomes marginal. The enhanced affine-type global symmetry of this theory in Table 9a supports this conjecture. The Coulomb branch with irrational boundaries and the geometric consideration associated to it will be discussed in Section 4.4.

Finally, we come to the case of $G = F_4$. Since the only representation with dimension smaller than the adjoint is the fundamental representation, an F_4 gauge theory can only have fundamental hypermultiplets. In this case, the Weyl chamber only consists of a single component, and therefore the task of determining a bound on the number $N_{\mathbf{F}}$ of fundamental half-hypers is straightforward. We find that $N_{\mathbf{F}} \leq 3$ and all these theories have 5d conformal fixed points at UV. So all the F_4 theories are non-marginal. The physical Coulomb branch of the theory with $N_{\mathbf{F}} = 3$ is given by

$$\mathcal{C}_{\text{phys}} = \{2\phi_1 > \phi_2, \phi_1 + 2\phi_3 > 2\phi_2, 2\phi_4 \geq \phi_3, 2\phi_3 > \phi_2 + \phi_4\}. \tag{4.30}$$

Rank 5,6,7,8

For $SU(6)$ theories, we can have $N_{\mathbf{TAS}}$ rank-3 antisymmetric hypermultiplets. Since **TAS** is pseudo-real, we can add half-hypermultiplets which we donote by $N_{\mathbf{TAS}} = 1/2$. The marginal $SU(6)$ theories are summarized in Table 10a. For $SU(7)$ theories, we can also have rank-3 antisymmetric hypermultiplets, but only a single full-hypermultiplet is allowed. All the exceptional cases have $N_{\mathbf{TAS}} = 1$. The $SU(7)$ theories are summarized in Table 11a. The first two of them are marginal. However, due to computational limits, we could not clearly identify the last theory whether it is non-marginal or exotic, which will be discussed in Section 4.4. For $SU(8)_\kappa + N_{\mathbf{TAS}}\mathbf{TAS}$ we find that there are no non-trivial exceptional $SU(8)$ theories for any value of $N_{\mathbf{TAS}}$.

For $SO(10)$ theories, we can have $N_{\mathbf{S}}$ spinor and $N_{\mathbf{F}}$ fundamental hypermultiplets. The marginal $SO(10)$ theories are summarized in Table 10b. For $SO(11)$ theories, we can have $2N_{\mathbf{S}}$ spinor half-hypermultiplets and $N_{\mathbf{F}}$ vector hypermultiplets. The marginal $SO(11)$ theories are summarized in Table 10c. For $SO(12)$ theories, we can have $N_{\mathbf{F}}$ fundamental hypermultiplets, along with $2N_{\mathbf{S}}$ spinor and $2N_{\mathbf{C}}$ conjugate spinor half-hypermultiplets. So we have a large number of exceptional theories as summarized in Table 11b. Note that the last theory in this table could either be non-marginal or exotic, as we are presently unable to verify its status due to computational limitations.

$N_{\mathbf{AS}}$	$N_{\mathbf{F}}$	$\lvert\kappa\rvert$	F
3	3	0	$C_3^{(1)} \times SU(3)$
3	1	3	$SU(4) \times SU(2) \times U(1)$
0	5	$\frac{11}{2}$	$SO(10) \times U(1)$
3	2	$\frac{3}{2}$	$E_6^{(2)} \times U(1)$

(a) Exceptional $SU(5)_\kappa$ gauge theories with $N_{\mathbf{AS}}$ antisymmetric, $N_{\mathbf{F}}$ fundamental matters. The first three are marginal theoriese and the last one is an exotic theory.

$N_{\mathbf{TAS}}$	$N_{\mathbf{F}}$	F
$\frac{1}{2}$	4	$SO(8) \times U(1)$

(b) Marginal $Sp(4)$ gauge theories with $N_{\mathbf{TAS}}$ rank-3 antisymmetric, $N_{\mathbf{F}}$ fundamental matters.

$N_{\mathbf{F}}$	F
3	$Sp(3) \times SU(2)$

(c) Exceptional F_4 gauge theories with $N_{\mathbf{F}}$ fundamental matters.

$N_{\mathbf{S}}$	$N_{\mathbf{C}}$	$N_{\mathbf{F}}$	F
5	2	0	$A_{14}^{(2)}$
5	1	1	$A_{13}^{(2)}$
4	4	0	$E_6^{(2)} \times E_6^{(2)}$
4	3	1	$F_4^{(1)} \times Sp(4)$
4	2	2	$A_7^{(2)} \times D_7^{(2)}$
3	3	2	$C_6^{(1)} \times Sp(2)$

(d) Marginal $SO(8)$ gauge theories with $N_{\mathbf{S}}$ spinor, $N_{\mathbf{C}}$ conjugate spinor, $N_{\mathbf{F}}$ fundamental matters. Due to triality of the D_4 Dynkin diagram, for each of the above theories there exists an entire family of theories obtained by permutation of the values $(N_{\mathbf{F}}, N_{\mathbf{S}}, N_{\mathbf{C}})$.

$N_{\mathbf{S}}$	$N_{\mathbf{F}}$	F
4	1	$E_6^{(2)} \times SU(2)$
3	3	$C_3^{(1)} \times Sp(3)$
2	5	$A_9^{(2)} \times A_4^{(2)}$
1	6	$A_{14}^{(2)}$

(e) Marginal $SO(9)$ gauge theories with $N_{\mathbf{S}}$ spinor, $N_{\mathbf{F}}$ fundamental matters.

Table 9. Rank 4 exceptional gauge theories.

All the other theories are marginal. For $SO(13)$ theories, we can have $2N_{\mathbf{S}}$ spinor half-hypermultiplets and the marginal theories are summarized in Table 11c. $SO(14)$ case has merely one exceptional theory with a $N_{\mathbf{S}} = 1$ spinor (or $N_{\mathbf{C}} = 1$ conjugate spinor) and $N_{\mathbf{F}} = 6$ fundamental hypermultiplets as listed in Table 11d. An E_6 gauge theory can have $N_{\mathbf{F}} \leq 4$ fundamental hypermultiplets and an E_7 gauge theory can have $2N_{\mathbf{F}} \leq 6$ fundamental half-hypermultilets. However, we are not sure whether or not the theories $E_6 + 4\mathbf{F}$ and $E_7 + 3\mathbf{F}$ are exotic. See Section 4.4 for more discussions about this. The $\mathcal{N} = 1$ E_8 gauge theory cannot have any hypermultiplets, and the E_8 theory without matter flows to a 5d SCFT at the UV fixed point.

$N_{\mathbf{TAS}}$	$N_{\mathbf{Sym}}$	$N_{\mathbf{AS}}$	$N_{\mathbf{F}}$	$\lvert\kappa\rvert$	F
2	0	0	0	0	$A_2^{(2)} \times A_2^{(2)}$
$\frac{3}{2}$	0	0	5	0	$SO(3)\times SU(5)\times U(1)^2$
$\frac{3}{2}$	0	0	3	2	$SO(3)\times SU(3)\times U(1)^2$
$\frac{3}{2}$	0	0	0	$\frac{9}{2}$	$SO(3) \times U(1)^2$
1	0	1	4	0	$D_4^{(1)} \times A_1^{(1)} \times U(1)$
1	0	1	3	$\frac{3}{2}$	$A_2^{(2)} \times A_2^{(2)} \times SU(4)$
1	0	1	0	4	$SU(2) \times U(1)^2$
1	0	0	10	0	$D_{10}^{(1)}$
1	0	0	9	$\frac{3}{2}$	$E_8^{(1)} \times A_2^{(1)}$
$\frac{1}{2}$	1	0	1	0	?
$\frac{1}{2}$	1	0	0	$\frac{3}{2}$	?
$\frac{1}{2}$	0	2	2	$\frac{3}{2}$	$D_4^{(3)} \times SU(2) \times U(1)$
$\frac{1}{2}$	0	2	2	$\frac{1}{2}$	$SU(5) \times U(1)$
$\frac{1}{2}$	0	2	0	$\frac{7}{2}$	$SU(3) \times U(1)$
$\frac{1}{2}$	0	1	9	0	$SU(11) \times U(1)$
$\frac{1}{2}$	0	1	8	$\frac{3}{2}$	$SO(16)\times SU(2)\times U(1)$
$\frac{1}{2}$	0	0	13	0	$SU(13) \times U(1)^2$
$\frac{1}{2}$	0	0	9	3	$SU(9) \times U(1)^2$
0	0	3	0	3	$D_4^{(3)} \times SU(2)$
0	0	3	0	1	$Sp(3) \times U(1)$
0	0	3	0	$0, 2$	$SU(3) \times U(1)^2$
0	0	0	0	9	$U(1)$

(a) Marginal $SU(6)_\kappa$ gauge theories with $N_{\mathbf{TAS}}$ rank-3 antisymmetric, $N_{\mathbf{Sym}}$ symmetric, $N_{\mathbf{AS}}$ antisymmetric, $N_{\mathbf{F}}$ fundamental matters.

$N_{\mathbf{S}}$	$N_{\mathbf{F}}$	F
4	2	$B_3^{(1)} \times SU(4)$
3	4	$C_3^{(1)} \times Sp(4)$
2	6	$A_{11}^{(2)} \times A_2^{(2)} \times A_1^{(1)}$
1	7	$A_{15}^{(2)}$

(b) Marginal $SO(10)$ gauge theories with $N_{\mathbf{S}}$ spinor, $N_{\mathbf{C}}$ conjugate spinor, $N_{\mathbf{F}}$ fundamental matters.

$N_{\mathbf{S}}$	$N_{\mathbf{F}}$	F
$\frac{5}{2}$	0	$Sp(2) \times U(1)$
2	3	$A_5^{(2)} \times A_2^{(2)} \times A_2^{(2)}$
$\frac{3}{2}$	5	$A_2^{(2)} \times Sp(5) \times U(1)^{(2)}$
1	7	$A_{13}^{(2)} \times A_1^{(1)} \times U(1)^{(2)}$
$\frac{1}{2}$	8	$Sp(9)$

(c) Marginal $SO(11)$ gauge theories with $N_{\mathbf{S}}$ spinor, $N_{\mathbf{F}}$ fundamental matters. We use $U(1)^{(2)}$ for a $U(1)$ compactified with an outer automorphism twist.

Table 10. Rank 5 exceptional gauge theories.

4.4 Exotic exceptional theories

In our main conjecture, we require that a physical Coulomb branch should have rational boundary. In geometry this means that a physical Coulomb branch must be determined as a subregion of the Weyl chamber bounded by hyperplanes where some of 4-cycles shrink to 2-cycles or contract to a point. In addition, it is necessary that when a 4-cycle shrinks to a 2-cycle, there must exist an associated shrinking 2-cycle. Such hyperplanes can be characterized by the condition that some of string tensions vanish, i.e. $T_i(\phi) = 0$

$N_{\mathbf{TAS}}$	$N_{\mathbf{F}}$	$\lvert\kappa\rvert$	F
1	6	0	$D_6^{(1)}$
1	5	$\frac{3}{2}$	$SO(10)\times SU(2)\times U(1)$
1	0	5	$U(1)^2$

(a) Exceptional $SU(7)_\kappa$ gauge theories with $N_{\mathbf{TAS}}$ rank-3 antisymmetric and $N_{\mathbf{F}}$ fundamental matters. The first two are marginal, while the last one could be non-marginal or exotic.

$N_{\mathbf{S}}$	$N_{\mathbf{C}}$	$N_{\mathbf{F}}$	F
$\frac{5}{2}$	0	0	$Sp(2)\times U(1)$
2	0	4	$E_6^{(2)}\times A_2^{(2)}\times A_2^{(2)}$
$\frac{3}{2}$	1	1	$SU(4)\times SU(2)$
$\frac{3}{2}$	$\frac{1}{2}$	4	$A_2^{(2)}\times Sp(4)$
$\frac{3}{2}$	0	6	$Sp(6)\times SU(2)\times U(1)$
1	1	4	$A_7^{(2)}\times A_1^{(1)}\times A_1^{(1)}\times U(1)^{(2)}$
1	$\frac{1}{2}$	6	$Sp(6)\times SU(2)^2$
1	0	8	$A_{15}^{(2)}\times A_1^{(1)}$
$\frac{1}{2}$	$\frac{1}{2}$	8	$A_{15}^{(2)}\times U(1)^{(2)}$
$\frac{1}{2}$	0	9	$Sp(9)\times U(1)$
2	$\frac{1}{2}$	0	$SU(4)$

(b) Exceptional $SO(12)$ gauge theories with $N_{\mathbf{S}}$ spinor, $N_{\mathbf{C}}$ conjugate spinor, $N_{\mathbf{F}}$ fundamental matters. The last theory could be non-marginal or exotic and the other theories are all marginal.

$N_{\mathbf{S}}$	$N_{\mathbf{F}}$	F
1	5	$A_9^{(2)}\times A_1^{(1)}$
$\frac{1}{2}$	9	$A_{17}^{(2)}$

(c) Marginal $SO(13)$ gauge theories with $N_{\mathbf{S}}$ spinor, $N_{\mathbf{F}}$ fundamental matters.

$N_{\mathbf{S}}$	$N_{\mathbf{F}}$	F
1	6	$A_{11}^{(2)}\times A_1^{(1)}$

(d) Marginal $SO(14)$ gauge theories with N_s spinor, $N_{\mathbf{F}}$ fundamental matters.

$N_{\mathbf{F}}$	F
4	$SU(4)\times SU(2)\times U(1)$

(e) Exceptional E_6 gauge theories with $N_{\mathbf{F}}$ fundamental matters. This theory can be non-marginal or exotic.

$N_{\mathbf{F}}$	F
3	?

(f) Exceptional E_7 gauge theories with $N_{\mathbf{F}}$ fundamental matters. This theory can be non-marginal or exotic.

$N_{\mathbf{F}}$	F
0	$\emptyset$

(g) E_8 gauge theory has no matters.

Table 11. Rank 6,7,8 exceptional gauge theories.

for some i. The rational boundary condition can therefore be recast as $\sum_j n_j\phi_j = 0$ with $n_j \in \mathbb{Z}$ for each hyperplane.

However, we notice that there are some cases where sub-chambers are bounded by irrational boundaries at $\sum_j n_j\phi_j = 0$ with $n_j \in \mathbb{R}\backslash\mathbb{Q}$. Such irrational boundaries are not allowed due to geometric considerations, as the class of the would-be 2-cycle that vanishes on such a boundary would have irrational coefficients and therefore be ill-defined. We also remark that the dictionary between geometry and field theory teaches us that these boundaries can equivalently be characterized by the vanishing of some BPS particle with irrational central charge, and therefore we find we must also dismiss such boundaries on physical grounds. This may imply that either we cannot enter such sub-chambers or that we will encounter a geometric transition such as a flop transition before we meet the irrational hyperplane, which cannot be captured by our perturbative analysis. When this happens, we admit that our perturbative analysis using the condition $T_i(\phi) = 0$ cannot determine the physical Coulomb branch in the sub-chamber exactly. If a theory has another sub-chamber with rational boundaries, we can apply our criteria for the sub-chamber and classify the theory accordingly. However, when all the sub-chambers are bounded by irrational hyperplanes, it turns out to be rather difficult to determine whether or not the theory has a 5d CFT fixed point. We find a handful of such *exotic* theories, which we describe in more detail below.

For example, $5\mathbf{F} + SU(2) \times SU(2) + 2\mathbf{F}$ has a single physical sub-chamber with irrational boundaries. The sub-chamber is given by

$$\frac{2}{3}\phi_1 < \phi_2 < \frac{1}{\sqrt{2}}\phi_1 \ , \tag{4.31}$$

where ϕ_1, ϕ_2 are scalar vevs of two $SU(2)$ gauge groups respectively. In the above sub-chamber, string tensions are positive and moreover the metric is positive definite at infinite coupling. However, it is clear from the above expression that one of the boundaries is defined by an irrational linear combination of Coulomb branch parameters,

$$\phi_1 + \sqrt{2}\phi_2 = 0. \tag{4.32}$$

From geometric considerations, we believe this boundary cannot correspond to the vanishing of a 4-cycle with rational divisor class, and hence the correspondence between BPS data and geometric data is invalid in this description. This is an indication that a flop transition of some sort—possibly due to the appearance of massless instantons—must occur before we meet this wall on the Coulomb branch. The presence of spurious boundaries of the above type is indicative of our inability to compute instanton masses and other non-perturbative data using only the perturbative expression for the prepotential.

It turns out that the $5\mathbf{F}+SU(2)\times SU(2)+2\mathbf{F}$ theory is dual to $SU(3)_{\frac{3}{2}}+9\mathbf{F}$. These two dual theories admit the same brane construction in Type IIB string theory. As we discussed in Section 4.3, the dual $SU(3)$ gauge theory has non-trivial 6d completion in the UV fixed point having a zero eigenvalue of the metric at infinite coupling. In fact, we can obtain the $SU(2)\times SU(2)$ gauge theory description from the $SU(3)$ gauge theory by turning on mass parameters such as $a_1 > m_{1,2,3,4,5,6,7} > a_2$, $a_2 > m_{8,9} > a_3$ where $a_{1,2,3}$ are Coulomb parameters of $SU(3)$ and m_i is the mass of the i-th hypermultiplet.

This corresponds to two consecutive flop transitions in the corresponding geometry. This supports our expectation that the geometry undergoes flop transitions before we meet the irrational boundary in the Coulomb branch. This example also shows that while we may not be able to reach the UV fixed point with the $SU(2) \times SU(2)$ gauge theory description, the 6d fixed point can nevertheless be attained by way of the $SU(3)$ gauge theory description after the flop transitions. Therefore, when we have only physical Coulomb branches bounded by irrational curves, then the naive application of our criteria cannot tell us whether or not the theory is marginal. We call such theory as *exotic*.

In our classification, we have encountered five possible cases of exotic theories, only one of which we have explicitly confirmed as such. They are:

1. $SU(5)_{\frac{3}{2}} + 3\mathbf{AS} + 2\mathbf{F}$ (confirmed)
2. $SU(7)_5 + 1\mathbf{TAS}$ (undetermined)
3. $SO(12) + 2\mathbf{S} + \frac{1}{2}\mathbf{C}$ (undetermined)
4. $E_6 + 4\mathbf{F}$ (undetermined)
5. $E_7 + 3\mathbf{F}$ (undetermined)

For the first case above, the $SU(5)$ theory, $\mathcal{C}_{\text{phys}}$ consists of a single component with irrational boundaries. Within this chamber, as expected, the string tensions are positive and the metric is positive definite. However, we expect that this theory has a 6d fixed point based on the affinization of the flavor symmetry $E_6^{(2)} \times U(1)$ according to a 1-instanton analysis. However, if this is case, it remains unclear what dual physical description we must introduce (as in the case of $5\mathbf{F} + SU(2) \times SU(2) + 2\mathbf{F}$) in order to reach the 6d fixed point through the Coulomb branch.

We have also numerically confirmed the existence of physical Coulomb branches $\mathcal{C}_{\text{phys}}$ for the other theories in the above list. Unfortunately, due to computational limitations, we have been unable to precisely test whether or not the boundaries of these regions are rational or irrational. For this reason, it is unclear whether or not these theories are exotic in the sense we have described above. However, we note the two exceptional theories in the above list each have two distinct candidates for their 6d lifts, namely 6d SCFTs corresponding to a single curve with self-intersection $-n$, where $n = 1, 2$. In the case of E_6, the $n = 1$ theory has $N_{\mathbf{F}} = 5$, while the $n = 2$ theory has $N_{\mathbf{F}} = 4$. In the case of E_7, the $n = 1$ theory has $N_{\mathbf{F}} = 7/2$, while the $n = 2$ theory has $N_{\mathbf{F}} = 3$.

5 6d Theories on a Circle

In this section we present some 6d SCFTs that are the lifts of some of the marginal 5d theories we found. We note that most of these theories have already been discussed elsewhere in the literature. We discuss the new theories in detail, while for the known theories we merely quote the results.

5.1 Generic $Sp(N)$ and $SU(N)$ with fundamental and antisymmetric matter

We start with the cases $Sp(N)$ and $SU(N)$, for generic N, with matter in the fundamental and antisymmetric representations. These theories can be constructed with ordinary brane web systems, where the $Sp(N)$ and $SU(N)$ theories with antisymmetric matter can be brought to this state by using an $O7^-$-plane and then decomposing it into a pair of 7-branes [17]. The 6d lifts of these types of theories were studied extensively in [14, 21, 31, 33], and we shall quote their results for the theories of interest.

The 6d SCFTs appearing in these cases can all be engineered by a brane system involving NS5-branes, D6-branes and D8-branes in the presence of an $O8^-$-plane. When compactified and T-dualized the system becomes a brane configuration of NS5-branes, D5-branes and D7-branes in the presence of two $O7^-$-planes. Upon decomposing the two $O7^-$-planes to a pair of 7-branes, one obtains the brane webs of the associated 5d gauge theories.

$\boldsymbol{SU(N)_0 + (2N+4)\mathbf{F}}$ and $\boldsymbol{Sp(N-1) + (2N+4)\mathbf{F}}$

The 5d gauge theory $SU(N)_0 + (2N+4)\mathbf{F}$ is known to lift to 6d [34]. The 6d lift was worked out in [15, 31], and is the so-called (D_{N+4}, D_{N+4}) conformal matter [35]. This theory has a low-energy description on the tensor branch as the 6d gauge theory $Sp(N-2) + (2N+4)\mathbf{F}$. In F-theoretic notation, this theory is denoted

$$\overset{\mathfrak{sp}_{N-2}}{\mathbf{1}} \quad [SO(4N+8)]$$

It is straightforward to see that the dimensions of the Coulomb branch in both descriptions agree. Also the 1-instanton spectrum of the 5d theory is consistent with an enhanced $D^{(1)}_{2N+4}$, agreeing with the spectrum expected from the compactification of the 6d theory on a circle.

The 5d gauge theory $Sp(N-1) + (2N+4)\mathbf{F}$ also lifts to 6d and is in fact dual to $SU(N)_0 + (2N+4)\mathbf{F}$ on account of both theories lifting to the same 6d SCFT [31].

$SU(N)_0 + 1\mathbf{AS} + (N+6)\mathbf{F}$

The 5d gauge theory $SU(N)_0 + 1\mathbf{AS} + (N+6)\mathbf{F}$ lifts to the 6d SCFT which has a low-energy description on the tensor branch as the 6d gauge theory $SU(N-1)+1\mathbf{AS}+(N+7)\mathbf{F}$ [21, 31]. In F-theoretic notation this 6d SCFT is denoted

$$\overset{\mathfrak{su}_{N-1}}{\mathbf{1}} \quad [SU(N+7)]$$

Again it is easy to see that the Coulomb branch dimensions agree. The 6d and 5d theories both have a Higgs branch, associated with giving a vev to the antisymmetric matter, upon which we reduce to the previous case.

We can also compare the global symmetries of these theories, which are summarized in Tables 1a and 2. For $N > 4$ The 1-instanton analysis suggests that the current spectrum of the 5d theory is consistent with $A^{(1)}_{N+6}$ which again agrees with the 6d theory on a circle. There are however additional currents when $N \leq 5$. For $N = 3$ an antisymmetric hypermultiplet is identical to an antifundamental hypermultiplet so in 5d this case is identical to the previous case. This feature is correctly captured by the 6d description, as for $SU(2)$ the antisymmetric representation is a singlet. For $N = 4$ the antisymmetric represenation is real and the $U(1)$ associated with this representation in the general case is perturbatively enhanced to $SU(2)$. There are then additional 1-instanton currents, and the spectrum of the 5d theory is consistent with a larger enhancement to $A^{(1)}_{11}$. This again agrees with the perturbative enhancement in 6d.

Finally when $N = 5$ we also get additional currents, and the spectrum is consistent with an enhancement to $A^{(1)}_{11} \times A^{(1)}_{1}$. This again agrees with the perturbative enhancement in 6d.

$SU(N)_0 + 2\mathbf{AS} + 8\mathbf{F}$

The 5d gauge theory $SU(N)_0 + 2\mathbf{AS} + 8\mathbf{F}$ has different 6d lifts depending on whether N is even or odd [21]. The 6d lift can be described on the tensor branch as a low-energy 6d semi-gauge theory. The description for these two cases is shown in Figure 9, where (a) is the $N = 2n$ case, and (b) is the $N = 2n+1$ case. Alternatively, we also provide an F-theoretic description of both cases,

$$[E_7] \quad \mathbf{1} \quad \underset{[SU(2)]}{\overset{\mathfrak{su}_2}{\mathbf{2}}} \quad \overset{\mathfrak{su}_2}{\mathbf{2}} \quad \cdots \quad \overset{\mathfrak{su}_2}{\mathbf{2}} \quad \overset{\mathfrak{su}_2}{\mathbf{2}} \quad [SU(2)]$$

$$[SO(16)] \quad \overset{\mathfrak{sp}_1}{\mathbf{1}} \quad \overset{\mathfrak{su}_2}{\mathbf{2}} \quad \overset{\mathfrak{su}_2}{\mathbf{2}} \quad \cdots \quad \overset{\mathfrak{su}_2}{\mathbf{2}} \quad \overset{\mathfrak{su}_2}{\mathbf{2}} \quad [SU(2)]$$

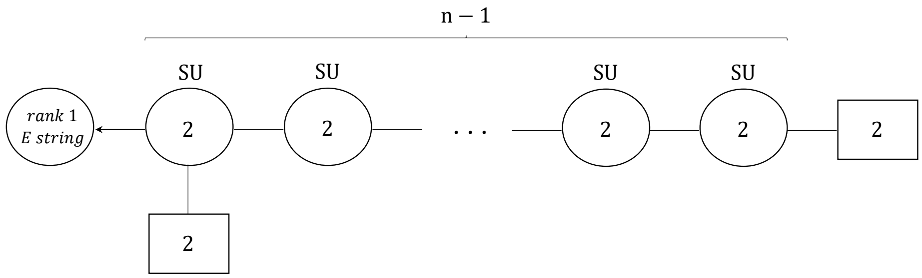

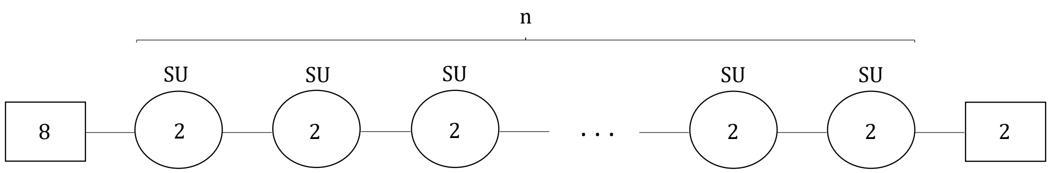

Figure 9. The low-energy description on the tensor branch of the 6d SCFTs which are the lifts of the 5d $SU(N)_0 + 2\mathbf{AS} + 8\mathbf{F}$ gauge theories. Quiver (a) describes the case $N = 2n$, while quiver (b) the case $N = 2n+1$. In quiver (a) the arrow into the rank 1 E-string theory represents gauging a subgroup $SU(2) \subset E_8$ of the global symmetry group of the E-string theory.

where the upper diagram is the $N = 2n$ case, the lower diagram is the $N = 2n + 1$ case. Note that there are $n - 1$ **2** curves in both diagrams above.

One can see that the Coulomb branch dimensions of the 5d theories and 6d theories on a circle agree. The global symmetries also agree, where instantons in the 5d gauge theory lead to additional conserved currents consistent with what is expected from the 6d theory on a circle. The results for the various cases are summarized in Tables 1a and 2.

$\boldsymbol{SU(N)_{\pm\frac{3}{2}} + 2\mathbf{AS} + 7\mathbf{F}}$

The 5d gauge theory $SU(N)_{\pm\frac{3}{2}}+2\mathbf{AS}+7\mathbf{F}$ is also known to lift to 6d, and again goes to different 6d theories depending on whether N is even or odd. The cases $N = 3, 4, 5$ were explicitly discussed in [21] and it is straightforward to generalize the construction to generic N. The 6d SCFTs can be again conveniently represented using the low-energy description on the tensor branch. Descriptions of the two cases are shown in Figure 9, where (a) is the $N = 2n$ case, and (b) is the $N = 2n + 1$ case. We also provide

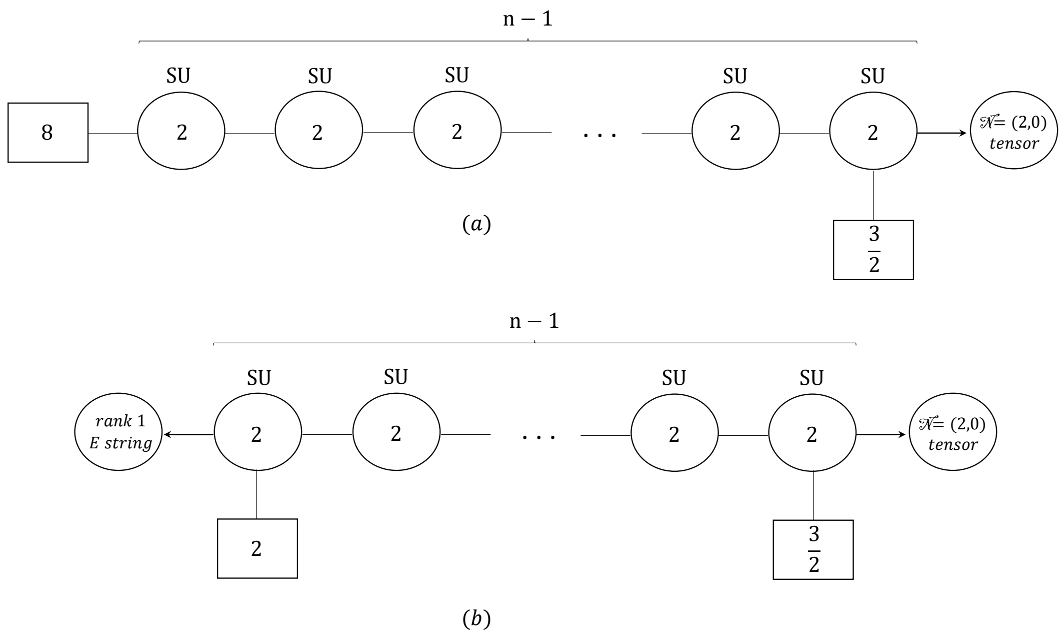

Figure 10. The low-energy description on the tensor branch of the 6d SCFTs which are the lifts of the 5d $SU(N)_{\pm\frac{3}{2}} + 2\mathbf{AS} + 7\mathbf{F}$ gauge theory. Quiver (a) describes the case $N = 2n$ while quiver (b) the case $N = 2n+1$. The arrow into the $\mathcal{N}= (2,0)$ tensor, which appears on the rightmost in both quivers, represents gauging the $SU(2)$ global symmetry of the tensor (this is part of its $Sp(2)$ R-symmetry that is seen as a global symmetry from the $\mathcal{N}= (1,0)$ point of view).

F-theoretic descriptions,

$$
\begin{array}{ccccccc}
[SO(16)] & \overset{\mathfrak{sp}_1}{\mathbf{1}} & \overset{\mathfrak{su}_2}{\mathbf{2}} & \overset{\mathfrak{su}_2}{\mathbf{2}} & \cdots & \overset{\mathfrak{su}_2}{\mathbf{2}} & \overset{\mathfrak{su}_2}{\mathbf{2}} & \overset{\mathrm{II}}{\mathbf{2}} \\
 & & & & & & [SU(2)] &
\end{array}
$$

$$
\begin{array}{cccccccc}
[E_7] & \mathbf{1} & \overset{\mathfrak{su}_2}{\mathbf{2}} & \overset{\mathfrak{su}_2}{\mathbf{2}} & \cdots & \overset{\mathfrak{su}_2}{\mathbf{2}} & \overset{\mathfrak{su}_2}{\mathbf{2}} & \overset{\mathrm{II}}{\mathbf{2}} \\
 & & [SU(2)] & & & & [SU(2)] &
\end{array}
$$

where the upper diagram is the $N = 2n$ case and the lower diagram is the $N = 2n+1$ case. Note that there are $n-1$ $\mathbf{2}$ curves in the upper diagram and n $\mathbf{2}$ curves in the lower diagram.

One can see that the Coulomb branch dimensions of the 5d theories and 6d theories on a circle agree. The global symmetries also appear to agree, at least as far as can be seen from the 1-instanton analysis. Again the results for the various cases are summarized in Tables 1a and 2.

$\boldsymbol{Sp(N-1)+1\mathbf{AS}+8\mathbf{F}}$ and $\boldsymbol{SU(N)_{\pm\frac{N}{2}}+1\mathbf{AS}+8\mathbf{F}}$

The case of $Sp(N-1)+1\mathbf{AS}+8\mathbf{F}$ is well known to lift to the rank $N-1$ E-string theory [36]. On the other hand, to our knowledge $SU(N)_{\pm\frac{N}{2}}+1\mathbf{AS}+8\mathbf{F}$, for $N>3$, has not been discussed in the literature. From brane webs we can argue that the 5d gauge theory $SU(N)_{\pm\frac{N}{2}}+1\mathbf{AS}+8\mathbf{F}$ should have a 6d lift.

To argue this we consider the brane web description of this theory, which can be engineered using an O7$^-$-plane and resolving it. The brane web looks slightly different depending on whether N is even or odd. For simplicity, we shall show here only the N even case, though most of the steps and results apply also to the N odd case.

Figure 11 shows the web for an $SU(N)_{\frac{N-N_{\mathbf{F}}+8}{2}}+1\mathbf{AS}+N_{\mathbf{F}}\mathbf{F}$ gauge theory. For simplicity we have only shown the external legs and not how these connect inside the web, as that is irrelevant for this discussion. By manipulating the web we arrive at the web on the bottom left of Figure 11. When $N>10$ one of the legs collides with another leg and further transitions ensue. We can calculate the monodromy "felt" by this leg when going around the entire web, and we find it to be the $SL(2,\mathbb{Z})$ transformation $T^{8-N_{\mathbf{F}}}$. Thus we see that if $N_{\mathbf{F}}<8$ and the transition does not terminate before going full circle, the brane will come back less divergent. Therefore this process will terminate after a finite number of rotations. In particular, for $N_{\mathbf{F}}=0$, this means that a fixed point exists for every N. For $N_{\mathbf{F}}=8$ the brane returns back to itself while for $N_{\mathbf{F}}>8$ the brane returns more divergent.

This suggests then that for $N_{\mathbf{F}}<8$ a 5d fixed point exists, while for $N_{\mathbf{F}}>8$ neither a 5d nor a 6d fixed point exists. The case $N_{\mathbf{F}}=8$ seems to be a 6d lift. For $N\leq 10$, the process already terminates at the step shown in the bottom left of Figure 11, and we can show this explicitly. Furthermore we can argue that this theory is dual to $Sp(N-1)+1\mathbf{AS}+N_{\mathbf{F}}\mathbf{F}$.

This follows from 7-brane manipulations. We have shown the relevant steps in Figure 12 for the simpler case of $N=6$. The manipulations for the other cases are similar, and we omit them for brevity. Therefore, in that range at least, the $SU(N)_{\frac{N-N_{\mathbf{F}}+8}{2}}+1\mathbf{AS}+N_{\mathbf{F}}\mathbf{F}$ class of theories go to a 5d fixed point for $N_{\mathbf{F}}<8$, and the $SU(N)_{\pm\frac{N}{2}}+1\mathbf{AS}+8\mathbf{F}$ theory should lift to the 6d rank $N-1$ E-string theory. We suspect this to be true for all N.

5.2 Generic $SO(N)$ and $SU(N)$ with symmetric matter

Next we examine the cases of $SO(N)$ and $SU(N)$ theories with matter in the symmetric representation for generic N. This class of theories can be engineered in string theory by brane webs in the presence of O7$^+$-planes[17]. The 6d lifts for $SO(N)$ with fundamental

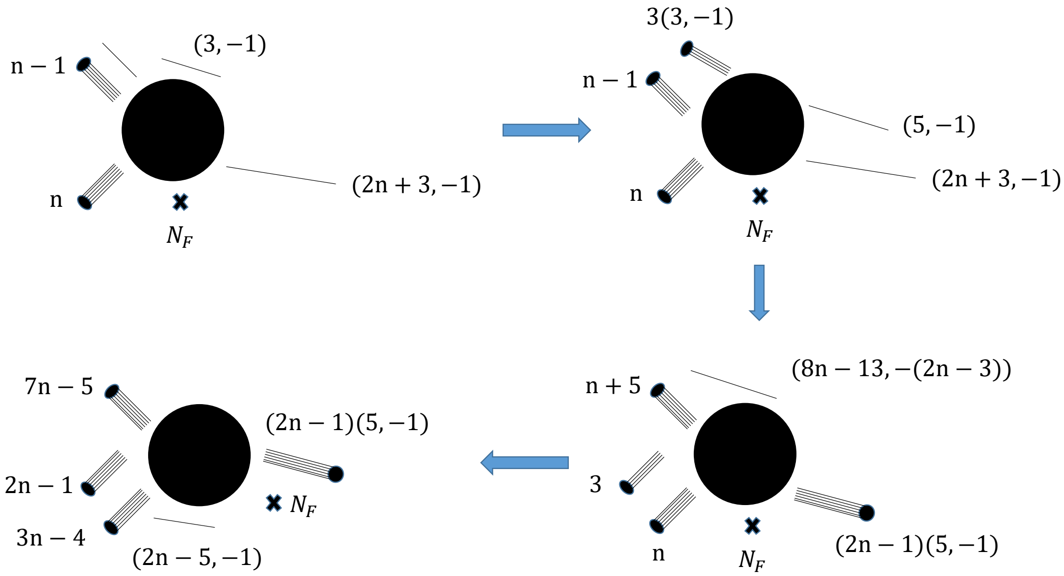

Figure 11. Brane web manipulation for $SU(N)_{\frac{N-N_{\mathbf{F}}+8}{2}} + 1\mathbf{AS} + N_{\mathbf{F}}\mathbf{F}$, in the case $N = 2n$. For ease of drawing, only the external legs are shown. We use a black '×' to represent the $N_{\mathbf{F}}$ 7-branes that give the flavors. The picture on the top left is for the initial web. Moving the $(3, -1)$ 7-brane through the single $(1, -1)$ 5-brane leads to the picture in the top right. Further moving the $(3, -1)$ 7-brane through the $n - 1$ $(1, -1)$ 5-branes leads to the picture in the bottom right, where we have also moved the $(5, -1)$ 7-brane through the $(2n + 3, -1)$ 5-brane. Finally, we move the $(8n - 13, -(2n - 3))$ 7-brane through all the $(1, -1)$ and $(1, 1)$ 5-branes leading to the picture at the bottom left. If $n \leq 5$ then no further transitions are required.

matter, and $SU(N)$ with symmetric and fundamental matter were studied in [22], and it is straightforward to extend these results to some of the other cases.

The 6d SCFTs in these cases can be engineered in string theory by a brane system involving NS5-branes, D6-branes and D8-branes, but the compactification is done with a $\mathbb{Z}_2$ twist in a discrete symmetry. In the brane system this discrete symmetry is manifested as worldsheet parity combined with a reflection in the direction orthogonal to the D8-branes. Performing T-duality, the authors of [22] mapped this system to a configuration involving NS5-branes and D5-branes in the presence of an $O7^+$ and $O7^-$-planes. Decomposing the $O7^-$-plane then leads to the brane webs for the 5d gauge theories.

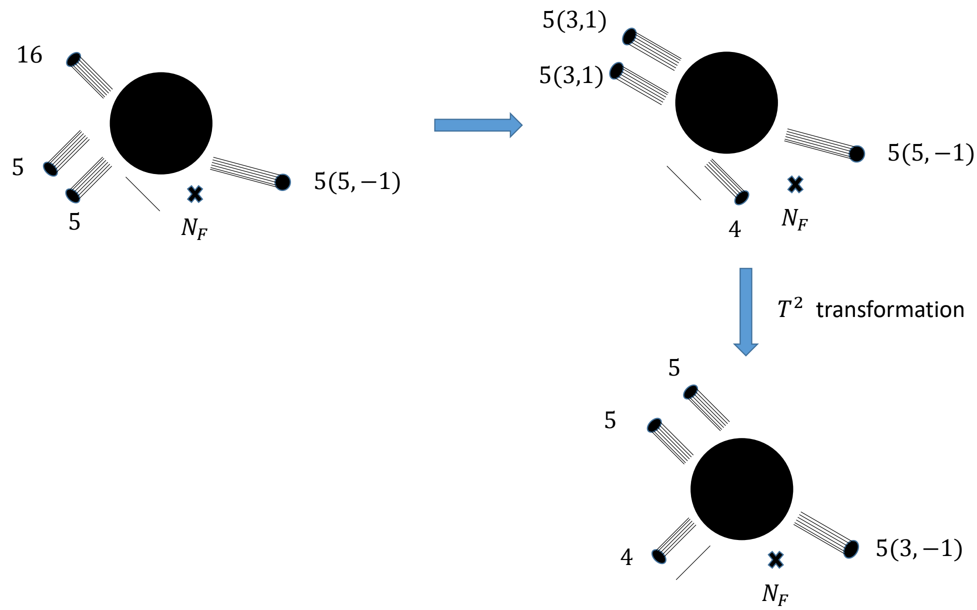

Figure 12. Brane web manipulation for $SU(6)_{\frac{14-N_{\mathbf{F}}}{2}} + 1\mathbf{AS} + N_{\mathbf{F}}\mathbf{F}$. The picture on the top left is just the web on the bottom left of Figure 11 for the case of $n = 3$. Moving the $(1,-1)$ 7-brane from top to bottom, we obtain the web on the top right. Performing an $SL(2,\mathbb{Z})$ transformation T^2, we end up with the web on the bottom right—this web is a known description of $Sp(5) + 1\mathbf{AS} + N_{\mathbf{F}}\mathbf{F}$, suggesting that these two theories are dual up to free hypermultiplets.

$SO(N) + (N-2)\mathbf{F}$

The case of 5d $SO(N) + (N-2)\mathbf{F}$ gauge theory is known to lift to a 6d SCFT. The 6d SCFT was worked out in [22] to be the one living on 2 M5-branes probing a $\mathbb{C}^2/\mathbb{Z}_{N-2}$ singularity. The compactification is done with a $\mathbb{Z}_2$ twist in a discrete symmetry of the 6d SCFT. Particularly, the 6d SCFT has a 1-dimensional tensor branch along which the theory has a low-energy description as an $SU(N-2) + (2N-4)\mathbf{F}$ gauge theory. In F-theory it is described by:

$$\overset{\mathfrak{su}_{N-2}}{\mathbf{2}} \quad [SU(2N-4)]$$

The discrete symmetry in question acts on the gauge theory as charge conjugation. It can also be thought of as the orbifold generalization of the outer automorphism twist compactifications of the A type $(2,0)$ theory.

The global symmetry of the 6d theory is consistent with the $A^{(2)}_{2N-5}$ found for $SO(N) + (N-2)\mathbf{F}$ using 1-instanton analysis. Additionally, the Coulomb branch dimension agrees between the two, after accounting for the fact that the twist projects out the odd dimension Coulomb branch generators that would have come from the $SU(N-2)$ vector upon reduction to 5d.

$\boldsymbol{SU(N)_0 + 1\mathbf{Sym} + (N-2)\mathbf{F}}$

This case was also covered in [22]. The 6d lift is the SCFT living on 3 M5-branes probing a $\mathbb{C}^2/\mathbb{Z}_{N-1}$ singularity, which has the F-theoretic description:

$$[SU(N-1)] \quad \overset{\mathfrak{su}_{N-1}}{\mathbf{2}} \quad \overset{\mathfrak{su}_{N-1}}{\mathbf{2}} \quad [SU(N-1)]$$

The compactification is again done with a twist, generalizing the outer automorphism twist now to the case of the A_2 $(2,0)$ theory, so the twist also acts non-trivially on the tensors. In the low-energy gauge theory description, $(N-1)\mathbf{F} + SU(N-1) \times SU(N-1) + (N-1)\mathbf{F}$, this discrete symmetry is manifested as a combination of quiver reflection and charge conjugation. As consistency checks, we note that the global symmetries and Coulomb branch dimensions agree.

$\boldsymbol{SU(N)_0 + 1\mathbf{Sym} + 1\mathbf{AS}}$

We can also consider the case of 5d $SU(N)_0 + 1\mathbf{Sym} + 1\mathbf{AS}$. This theory also lifts to 6d, and behaves differently depending on whether N is even or odd. For odd N we can find the 6d SCFT by generalizing the results of [22]. We find the 6d SCFT to be the one living on N M5-branes probing a $\mathbb{C}^2/\mathbb{Z}_2$ singularity, where again the compactification is done with a $\mathbb{Z}_2$ twist generalizing the outer automorphism twist for the A_{N-1} $(2,0)$ theory. The 6d SCFT has a low-energy gauge theory description as $2\mathbf{F} + SU(2) \times SU(2) \cdots SU(2) \times SU(2) + 2\mathbf{F}$, where there are $N-1$ $SU(2)$ groups. This theory also has the following F-theory description:

$$[SU(2)] \quad \overset{\mathfrak{su}_2}{\mathbf{2}} \quad \overset{\mathfrak{su}_2}{\mathbf{2}} \quad \cdots \quad \overset{\mathfrak{su}_2}{\mathbf{2}} \quad \overset{\mathfrak{su}_2}{\mathbf{2}} \quad [SU(2)]$$

where there are $N-1$ $\mathbf{2}$ curves in the above diagram. The $\mathbb{Z}_2$ discrete symmetry by which we twist acts on the gauge theory as quiver reflection. The web for the even N case has a different form, and appears to go to a different type of theory.

We can again perform several consistency checks for the odd N case. As indicated in Table 1a, the symmetry of the 5d theory is at least $A_1^{(1)} \times U(1)$. This is consistent with the global symmetry of the twisted theory. We also note that the Coulomb branch dimension agrees.

It is instructive to also consider Higgs branch flows. For instance, the 5d theory has a flow from $SU(N)_0 + 1\mathbf{Sym} + 1\mathbf{AS}$ to $SO(N) + 1\mathbf{AS}$ triggered by giving a vev to the symmetric matter, and one to $Sp(\frac{N-1}{2}) + 1\mathbf{S}$ triggered by giving a vev to the antisymmetric matter—these are just the maximally supersymmetric SO and Sp gauge theories. These flows should then also exist in the 6d theory. Indeed we can go on the Higgs branch of the 6d SCFT and flow to either the A_{N-1} or A_{N-2} $(2,0)$ theories. Compactification with a twist of the latter yields maximally supersymmetric $SO(N)$ while the same for the former yields maximally supersymmetric $Sp(\frac{N-1}{2})$ (with theta angle $\theta = \pi$) [29].

This leaves the case of even N, which seems to be of a different nature than the theories discussed so far. This is also apparent from the Higgs branch discussion. We again can flow to either the maximally supersymmetric $SO(N)$ or $Sp(\frac{N}{2})$ gauge theory. However the former when N is even lifts to the $D_{\frac{N}{2}}$ type $(2,0)$ theory with untwisted compactification. The latter, alternatively, lifts to twisted compactifications of either the $D_{\frac{N}{2}+1}$ type $(2,0)$ theory or the A_N type $(2,0)$ theory depending on the theta angle of the 5d theory [29]. It seems quite non-trivial to find a theory with this behavior, and therefore we reserve a determination of this case for future work.

$\boldsymbol{SU(N)_{\pm\frac{N}{2}} + 1\mathbf{Sym}}$

To our knowledge this class of theories has not been discussed in the literature. We can argue that this class should exist, at least as a 6d lift gauge theory, as follows. We can try to engineer this theory by using brane webs in the presence of an O7$^+$-plane. The existence of the theory is entirely determined by the asymptotic behavior of the 5-branes. Consider changing the O7$^+$-plane to an O7$^-$-plane with 8 D7-branes. This does not change the monodromy of the object and so does not change the asymptotic behavior of the 5-branes. However, this changes the gauge theory to the previously discussed $SU(N)_{\pm\frac{N}{2}} + 1\mathbf{AS} + 8\mathbf{F}$, which we have argued has a 6d lift. Therefore, it is reasonable to assume that $SU(N)_{\pm\frac{N}{2}} + 1\mathbf{Sym}$ also has a 6d lift. We note that the equivalence in monodromy between an O7$^+$-plane and an O7$^-$-plane with 8 D7-branes is the brane web manifestation of the invariance of the prepotential under exchanging a single symmetric hypermultiplet with a single antisymmetric and 8 fundamental hypermultiplets.

We can then ask what theory is the 6d lift. By examining the brane web in the case $N = 3$, we can reformulate the problem in a manner where we are in a position to apply the results of [22]. We then find that the 6d theory is the A_4 $(2,0)$ theory compactified with an outer automorphism twist. This implies that this theory is dual to maximally supersymmetric $Sp(2)_\pi$, and should thus have an enhancement of SUSY in the UV. Similarly, for $N > 3$, we suspect that the 6d theory is dual to maximally supersymmetric $Sp(N-1)_\pi$ and goes to the A_{2N-2} $(2,0)$ theory compactified with an outer automorphism twist.

6 Discussion and Future Directions

In this paper, we have given a clear physical explanation for why the naive Coulomb branch (i.e. the fundamental Weyl chamber) is not necessarily physical, and why it is therefore necessary to restrict a weakly-coupled gauge theory description to a subset of the Coulomb branch satisfying certain necessary physical criteria. It is necessary that the BPS spectrum consists of degrees of freedom with positive masses and tensions, and the metric be positive definite on this physical region of the Coulomb branch. By extending these ideas, we have proposed a set of conjectures in Section 3.1, 3.2 which we can use for the classification of 5d $\mathcal{N} = 1$ gauge theories with interacting fixed points.

By using these conjectures, we have given an exhaustive classification of 5d $\mathcal{N} = 1$ gauge theories with simple gauge group, which to our knowledge includes all known examples in the literature as a subset—for example, the theories described in [13–17, 21, 22, 26]. Our classification consists of two types of theories, namely standard theories (see Table 1) and exceptional theories (see Tables 3-11). Our strategy has been to identify extremal theories saturating the matter bounds imposed by our physical criteria and then use the fact that all descendants of such extremal theories will have non-trivial UV fixed points.

In practice, we used our main conjecture to test a number of low rank cases explicitly using a symbolic computing tool. Furthermore, we combined Conjectures 2 and 3 to circumvent the problem that a complete analysis of the naive Coulomb branch rapidly becomes intractable as the rank of the gauge group increases; the combination of our conjectures enabled us to make a full classification using a mixture of symbolic and numerical searches. The standard theories are particularly tractable and thus we were able to perform the classification by hand. Computational expense has only hindered our understanding of a few isolated cases of possible exotic theories, as discussed in Section 4.4.

There are a plethora of open questions that remain unresolved. The first question concerns our main conjecture, which asserts that the positivity of monopole string tensions can correctly identify the physical Coulomb branch when all of the mass parameters are switched off. As we explained in Section 3.1, the criterion of positive string tensions can in general miss flop transitions associated to the emergence of massless instantons without tensionless strings (note that the perturbative flop transitions are already captured by the gauge theory interpretation of the prepotential.) However, we remark that the massless instanton spectrum can be captured by an explicit computation of the BPS partition function as described in [37–42], and thus it would be interesting to see if we could test our main conjecture against an explicit computation of the instanton spectrum.

Another puzzle is why, as asserted by Conjecture 2, the positivity of the monopole string tensions guarantees the positivity of the metric. It is unclear from a mathematical perspective why this property should hold true for any gauge theoretic prepotential evaluated on the naive Coulomb branch, and moreover what properties of this function are essential for this phenomenon. Futhermore, Conjectures 1 and 3 seem to lack both mathematical proofs and physical explanations, given that these conjectures involve testing regions of the naive Coulomb branch that are obviously unphysical.

As explained in Section 4.4, there are four potentially exotic theories that we were not able to confirm due to computational limitations. With a better algorithm or more computational resources, it is possible to check explicitly whether or not these theories are indeed exotic. However, there is a more striking puzzle presented by the notion of exotic theories. From geometric considerations, we expect that truly exotic theories (such as $SU(5)_{\frac{3}{2}} + 3\mathbf{AS} + 2\mathbf{F}$) undergo some number of flop transitions before reaching the irrational boundaries of the putative physical Coulomb branch. If these theories could be constructed using geometry, this notion could tested explicitly. Alternatively, dual descriptions (as in the case of $5\mathbf{F} + SU(2) \times SU(2) + 2\mathbf{F}$, which has a dual description as $SU(3)_{\frac{3}{2}} + 9\mathbf{F}$) that are valid in the vicinity of the irrational components of the boundary could provide a clear indication that such theories are well-defined and have an interacting fixed point.

Lingering puzzles aside, there are also many future directions to be explored. For instance, many of the 5d theories appearing in our classification are still lacking a realization either in terms of brane configurations or local Calabi-Yau singularities, and it would be desirable to work out such descriptions in order to provide further evidence for the existence of these theories, as well as to capture the subtleties of the non-perturbative physics. It would be worthwhile to explore the possibility that all of the marginal theories we have identified can be obtained by compactifying some 6d SCFT; developing an understanding of the 6d compactifications, including a possible classification of the intermediary Kaluza-Klein theories, is critical for this purpose.

It would also be quite interesting to further develop a precise geometric understanding of the vanishing monopole string tensions and instanton masses that signal the breakdown of an effective gauge theory description. The field theoretic expression for $\mathcal{F}$ clearly encodes the appearance of massless electric particles in a collection of hyperplanes $w \cdot \phi + m_f = 0$ subdividing the fundamental Weyl chamber, across which the Chern-Simons levels jump discontinuously. Geometrically, these "jumps" are interpreted as the result of flops, which can be associated with the interchange of two nonisomorphic resolutions of the same singular Calabi-Yau geometry sharing a common blowdown. Both field theoretically and geometrically these transitions are rather transparent. However it is much more difficult to analyze the extremal transitions associated with the vanishing of monopole tensions or instanton masses away from the conformal point. This point is especially relevant for the distinction between rational and 'irrational' classes characterizing the exotic theories in our classification.

Finally, we would like to extend our classification of simple gauge groups to a full classification of 5d $\mathcal{N}=1$ SCFTs, including quiver gauge theories and non-Lagrangian theories. It is obvious that a physically sensible theory should have a positive definite metric on its physical Coulomb branch having only degrees of freedom with positive messes and tensions. In principle, we can classify general theories with gauge theory description by applying the same techniques we used for the present classification though it may be practically a tremendous task at the moment. A classification of non-Lagrangian theories in the same spirit as our current classification will require a better understanding of how geometric constraints translate into constraints on field theory, much as the case of the geometric description $\mathbb{P}^2$ in CY_3 translates to the (formal) field theory description $SU(2)$ with $N_{\mathbf{F}}=-1$.

Acknowledgements

We would like to thank Thomas T. Dumitrescu, Hirotaka Hayashi, Sheldon Katz, Seok Kim, Sung-Soo Kim, Kimyeong Lee, Kantaro Ohmori, Yuji Tachikawa, Masato Taki, Itamar Yaakov, Futoshi Yagi and Dan Xie for useful comments and discussions. The research of P.J. and H.K. and C.V. is supported in part by NSF grant PHY-1067976. H.K. would like to thank the Aspen Center for Physics Winter Conference on Superconformal Field Theories in $d \geq 4$, which is supported by NSF grant PHY-1066293, and also the Erwin Schrödinger Institute for its workshop on Elliptic hypergeometric functions in Combinatorics, Integrable systems and Physics for hospitality during the final stages of this work. G.Z. is supported by World Premier International Research Center Initiative (WPI), MEXT, Japan.

A Mathematical Conventions

Much of the notation and content of the following section is adapted from [43].

A.1 Root and coroot spaces

Let $R \subset V_R$ be a set of roots in the root space V_R, and let $V_R^\vee$ be the coroot space dual to V_R. A subset $S \subset R$ is called a system of *simple roots* if all elements $e \in S$ are linearly independent and every root $e' \in R$ belongs to the nonnegative or nonpositive integer linear span of S. A *positive root* is a positive linear combination of elements of S, and similarly for *negative roots*. As suggested by this definition, there exists a partition $R = R_+ \cup R_- \cup R_0$, where R_+ is the set of positive roots, $R_- = -R_+$ and R_0 is the set of zero roots. To every choice of S, one can associate a *distinguished Weyl chamber* $\mathcal{C}(S)$, where

$$\mathcal{C}(S) = \{\phi \in V_R^\vee \mid \langle \phi, e \rangle \geq 0 \quad , \quad e \in S\}. \tag{A.1}$$

We define *simple coroots* by

$$\alpha_i^\vee = 2\frac{\alpha_i}{\langle \alpha_i, \alpha_i \rangle}, \tag{A.2}$$

where above $\langle , \rangle$ is the Euclidean inner product. The *Cartan matrix* is defined as:

$$A_{ij} = \langle \alpha_i, \alpha_j^\vee \rangle = 2\frac{\langle \alpha_i, \alpha_j \rangle}{\langle \alpha_j, \alpha_j \rangle} \equiv D_j^{-1} \langle \alpha_i, \alpha_j \rangle. \tag{A.3}$$

In practice, we expand the real vector multiplet scalar vev ϕ in a basis of simple coroots:

$$\phi = \sum_i \phi_i \alpha_i^\vee \tag{A.4}$$

For some computations, we will find it convenient to expand the simple roots in the *Dynkin basis*[7], or the basis of fundamental weights, as fundamental weights are canonically dual to simple coroots. To illustrate this point, consider the inner product

$$\langle \phi, \alpha_i \rangle = \sum_{j,k} \phi_j A_{ik} \langle \alpha_j^\vee, w_k \rangle = \sum_{j,k} \phi_j A_{ik} \delta_{jk} = \sum_k A_{ik} \phi_k. \tag{A.5}$$

We can apply the same logic above to the scalar product as applied to two coroots:

$$\langle \phi, \phi \rangle = \sum_{i,j} \phi_i \phi_j \langle \alpha_i^\vee, \alpha_j^\vee \rangle = \sum_{i,j} \phi_j D_j^{-1} A_{ji} \phi_i \equiv \sum_{i,j} \phi_j h_{ji} \phi_i, \tag{A.6}$$

where in the above equation we have defined the metric tensor

$$(h^{-1})_{ij} = (A^{-1})_{ij} D_j. \tag{A.7}$$

Therefore, the vector multiplet scalars for the classical kinetic term can be said to be in the (canonical dual of the) Dynkin basis when the quadratic form is given by the inverse of the Lie algebra metric tensor (A.7).

[7]Note that the rows of the Cartan matrix A are the simple roots in the Dynkin basis.

A.2 Changing from Dynkin to orthogonal basis

In some cases, we find it more convenient to work in the orthogonal basis. Therefore, for reference we derive the linear transformation necessary to express the coroot ϕ in the orthogonal basis, given an expansion of ϕ in terms of simple coroots $\alpha_i^\vee$.

To begin, recall that the Dynkin basis is canonically dual to the basis of simple coroots in the following sense

$$\langle \alpha_i^\vee, w_j \rangle = \delta_{ij}, \tag{A.8}$$

In matrix form, the above equation reads

$$A\Omega^t = I, \tag{A.9}$$

where we define Ω through the following relation:

$$\Omega = (AA^t)^{-1}A. \tag{A.10}$$

Note that the rows of the above matrix Ω are the fundamental weights, where Ω can be viewed as a change of basis matrix from the orthogonal basis to the Dynkin basis:

$$w_i = \sum_j \Omega_{ij}\hat{e}_j. \tag{A.11}$$

The matrix Ω will be useful in the following derivation.

In order to determine the correct change of basis for ϕ, we will first convert the simple roots α_i to the orthogonal basis, using the Dynkin basis as an intermediate step. Expanding α_i, we find

$$\alpha_i = \sum_j A_{ij}w_j = \sum_{j,k} A_{ij}\Omega_{jk}e_k, \tag{A.12}$$

where $\hat{e}_k$ is a standard basis vector. By inverting Ω and exploiting the canonical pairing between simple coroots and fundamental weights, we notice that we may write:

$$\langle \phi, \hat{e}_k \rangle = \sum_{i,l} (\Omega^{-1})_{kl} \langle \phi_i \alpha_i^\vee, w_l \rangle = \sum_i (\Omega^{-1})_{ki}\phi_i, \tag{A.13}$$

where Ω^{-1} is the pseudo-inverse of Ω. Therefore, the inner product between ϕ and a simple root must satisfy the following equation:

$$\langle \phi, \alpha_i \rangle = \sum_k \left(\sum_j A_{ij}\Omega_{jk} \right) \left(\sum_l (\Omega^{-1})_{kl}\phi_l \right) = \sum_j A_{ij}\phi_j. \tag{A.14}$$

In the above equation, we identify

$$\widetilde{A}_{ik} = \sum_j A_{ij}\Omega_{jk} \tag{A.15}$$

as the components of the matrix whose rows are the simple roots in the orthogonal basis. Therefore, it must be the case that the coroot is expressed in an orthogonal basis as

$$\phi_i = \sum_j \Omega_{ij}\widetilde{\phi}_j. \tag{A.16}$$

In practice, we adopt the notation

$$a_i \equiv \widetilde{\phi}_i \tag{A.17}$$

to be consistent with commonly used notation in the literature.

A.3 Lengths of weights, index of a representation

In this section, we expand roots and weights in a basis of simple roots $\alpha_{i=1,\ldots,r_G}$ (this basis is referred to as the α-basis in [43]). The *length*[8] $l(e)$ of a root $e = \sum_i e_i\alpha_i$ is defined as follows:

$$l(e) = \sum_i e_i. \tag{A.18}$$

By linearity, we can extend this notion to weights $w = \sum_i w_i\alpha_i$:

$$l(w) = \sum_i w_i. \tag{A.19}$$

The lengths of the weights of an irreducible representation $\mathbf{R}(w^+)$ with highest weight w^+ are related to the *quadratic Dynkin index* $c^{(2)}_{\mathbf{R}(w^+)}$ (also referred to as simply 'the index' of the representation $\mathbf{R}(w^+)$) [44]:

$$c^{(2)}_{\mathbf{R}(w^+)} = \frac{\dim(\mathbf{R}(w^+))}{\dim(G)}\langle w^+, w^+ + 2\delta\rangle = C(G)\sum_{w\in\mathbf{R}(w^+)} l(w)^2, \tag{A.20}$$

where in the above expression

$$\delta = \frac{1}{2}\sum_{e\in R_+} e. \tag{A.21}$$

[8]In [43], the 'length' of a root or weight is referred to as the 'height'.

For classical Lie algebras G, the normalization constant $C(G)$ is chosen so that the index of the fundamental representation is equal to 1:

$$C(G) = \frac{1}{\sum_{w \in \mathbf{F}} l(w)^2}. \tag{A.22}$$

However, a different normalization is chosen for the exceptional Lie algebras.

B Bound on Matter Representation Dimension

In our classification, we assume that the dimension of the largest matter representation (or half-dimension, in the case of pseudoreal representations) is no larger than the dimension of the adjoint representation. In this section, we explain why this assumption is implied by Conjecture 3, which asserts that the prepotential must be positive on the entire fundamental Weyl chamber.

There exists a point ϕ^* in the fundamental Weyl chamber where the inner products $e \cdot \phi, w \cdot \phi$ are equal to the lengths of the corresponding root or weight. This can be understood as follows. In a basis of simple roots, the inner product $e \cdot \phi$ may be expressed as:

$$e \cdot \phi = \sum_{i,j} e_i \phi_j \langle \alpha_i, \alpha_j^\vee \rangle = \sum_{i,j} e_i \phi_j A_{ij}, \tag{B.1}$$

and a similar expression holds for $w \cdot \phi$. The conditions placed on ϕ parametrizing the fundamental Weyl chamber $\mathcal{C}(S)$ thus translate to the following inequalities:

$$\sum_j A_{ij} \phi_j \geq 0. \tag{B.2}$$

Evidently, it is always possible to find a solution ϕ^* to the equation

$$\sum_j A_{ij} \phi_j = 1 \quad \text{for all } i, \tag{B.3}$$

since the only constraint on the coefficients $\sum_j A_{ij} \phi_j$ is that they be non-negative, and a Cartan matrix is by definition nonsingular. At this point ϕ^*, we find

$$e \cdot \phi^* = \sum_j e_j = l(e), \qquad w \cdot \phi^* = \sum_j w_j = l(w). \tag{B.4}$$

Therefore, at infinite coupling $1/g_0^2 = 0$, the prepotential evaluated at this point ϕ^* is proportional to

$$6\mathcal{F}(\phi^*) = \sum_{e \in \text{roots}} |l(e)|^3 - \sum_{w \in \mathbf{R}_f} |l(w)|^3 \tag{B.5}$$

and the classical CS term

$$\sum_{w \in \mathbf{F}} (w \cdot \phi^*)^3 = \sum_{w \in \mathbf{F}} l(w)^3 = 0. \tag{B.6}$$

We claim that the difference of sums (B.5) is negative if

$$c^{(2)}_{\mathbf{adj}} < c^{(2)}_{\mathbf{R}_f}. \tag{B.7}$$

(In the case of pseudoreal representations, we replace $c^{(2)}_{\mathbf{R}_f}$ with $\frac{1}{2} c^{(2)}_{\mathbf{R}_f}$.) To see this, assume that the above inequality holds, and observe that $l(w) \in \frac{1}{2}\mathbb{Z}$ for any weight w, and therefore up to an overall constant, the quadratic indices

$$c^{(2)}_{\mathbf{R}_f} = \sum_{w \in \mathbf{R}_f} n_w^2, \qquad c^{(2)}_{\mathbf{adj}} = \sum_{e \in \mathbf{adj}} n_e^2, \tag{B.8}$$

where $n_w \in \mathbb{Z}_{\geq 0}$. We therefore find that the quadratic indices are proportional to sums of squares of positive integers. If the above sums satisfy the inequality (B.7), then it must also be true that the sums of cubes n_w^3, n_e^3 satisfy the same inequality. But the sums of the cubes of these positive integers are proportional to the sums of the cubes of the lengths. Therefore, it follows that (B.5) must be negative, which violates the condition imposed by Conjecture 3 at the point ϕ^*.

One can verify that $\dim(\mathbf{R}_f) > \dim(\mathbf{adj})$ implies that $c^{(2)}_{\mathbf{R}_f} > c^{(2)}_{\mathbf{adj}}$, which justifies the exclusion of matter representations with dimension greater than that of the adjoint from our classification.

C Convergence of S^5 partition function

In this appendix we collect several formulas for the expression of the S^5 partition function evaluated using localization. The main result here is that the convergence of the perturbative contribution to the S^5 partition function is equal to the demand that the perturbative prepotential be positive on the entire Coulomb branch. We can use this to give another criterion for the UV completeness of 5d gauge theories, which appears to coincide with the other criteria presented in this article, at least in all examples we have checked. This is summarized in the conjectures in section 3.2, particularly conjecture 3.

C.1 The 5d partition function

The partition function can be represented by the path integral on S^5, which in turn can be evaluated using localization; this partition function receives contributions from a perturbative part and a non-perturbative part, where some aspects regarding the latter are still conjectural [45–52]. The general form is suspected to be:

$$Z^{S^5} = \int Z_{\text{pert}} Z_{\text{inst}}^3, \tag{C.1}$$

where Z_{pert} is the perturbative part and Z_{inst} is the non-perturbative contribution. The latter arises from contact instantons [46, 52], which fill the S^1 in the Hopf-fibration realization of S^5 as an S^1 fibered over $\mathbb{CP}^2$. They are localized at three points on $\mathbb{CP}^2$ hence the power in the integral. In general they can be expanded in a power series in $\mathbf{q} = e^{-\frac{16\pi^3 r}{g_{YM}^2}}$:

$$Z_{\text{inst}} = 1 + O\left(e^{-\frac{16\pi^3 r}{g_{\text{YM}}^2}}\right), \tag{C.2}$$

where r/g_{YM}^2 is the ratio of the radius of S^5 to the coupling constant.

Let us first ignore the instanton contribution, and consider only the perturbative part. We shall use the expression for it given in [46, 47]. The full expression is then:

$$\begin{aligned} Z = & \frac{1}{|W|}\int_{\text{Cartan}} d\sigma e^{-\frac{4\pi^3 r}{g_{\text{YM}}^2}\text{tr}_{\mathbf{F}}\sigma^2 + \frac{\pi\kappa}{3}\text{tr}_{\mathbf{F}}\sigma^3} \det{}_{\mathbf{adj}}\left(\sin(i\pi\sigma)e^{\frac{1}{2}f(i\sigma)}\right) \\ & \times \prod_I \det{}_{\mathbf{R}_I}\left((\cos(i\pi\sigma))^{\frac{1}{4}} e^{-\frac{1}{4}f(\frac{1}{2}-i\sigma)-\frac{1}{4}f(\frac{1}{2}+i\sigma)}\right) + \text{instanton contributions}, \end{aligned} \tag{C.3}$$

where $|W|$ is the size of the Weyl group. Also, κ is the Chern-Simons level (if present), and f is a function defined by:

$$f(y) \equiv \frac{i\pi y^3}{3} + y^2\log(1-e^{-2\pi i y}) + \frac{iy}{\pi}\text{Li}_2(e^{-2\pi i y}) + \frac{1}{2\pi^2}\text{Li}_3(e^{-2\pi i y}) - \frac{\zeta(3)}{2\pi^2} \tag{C.4}$$

The integral is done over the Cartan subalgebra and the notation $\text{tr}_{\mathbf{R}}, \det_{\mathbf{R}}$ stands for the trace and determinant in the representation $\mathbf{R}$, where $\mathbf{F}$ denote the fundamental represetnation and **adj** denotes the adjoint representation.

Ignoring the instanton contributions, the above integral can be recast in the following form [53]:

$$Z = \frac{1}{|W|}\int_{\text{Cartan}} d\sigma e^{-F(\sigma)} \tag{C.5}$$

where:

$$F(\sigma) = \frac{4\pi^3 r}{g_{\text{YM}}^2}\text{tr}_{\mathbf{F}}\sigma^2 + \frac{\pi k}{3}\text{tr}_{\mathbf{F}}\sigma^3 + \text{tr}_{\mathbf{adj}}F_V(\sigma) + \sum_I \text{tr}_{\mathbf{R}_I}F_H(\sigma) \tag{C.6}$$

We will be concerned with the conditions needed for the convergence of the integral (C.5), for which we will need the asymptotic expansion of $F(\sigma)$, which is:

$$F_V(\sigma) \approx \frac{\pi}{6}|\sigma|^3 - \pi|\sigma| \tag{C.7}$$

$$F_H(\sigma) \approx -\frac{\pi}{6}|\sigma|^3 - \frac{\pi}{8}|\sigma| \tag{C.8}$$

One can see that the leading contributions are of order σ^3, where the contribution of the gauge multiplets generally makes the integral converge while the ones from matter and Chern-Simons terms make it diverge. Thus, the convergence of the integral constrains the number and representations of matter fields and the Chern-Simons level. Hence, it is tempting to conjecture that convergence of the integral may be related to the existence of a non-trivial fixed point.

In the $\sigma \to \infty$ limit the resulting expression for $F(\sigma)$ can be identified with the gauge theory prepotential [54]. This allows us to recast the condition as follows:

$$\sigma \to \infty \Rightarrow F(\sigma) \to \infty \tag{C.9}$$

where F is now the prepotential.

Thus we see that the convergence of the perturbative part of the partition function is equivalent to the demand that the perturbative prepotential be everywhere positive. We stress here that the above (piecewise) expression F for the prepotential is naive because in general a different prepotential is needed for each effective description of the theory valid in a given subset of the naive Coulomb branch. In the absence of instanton corrections, we expect that F will not have a well-defined global expression valid on all of $\mathcal{C}$. In fact, we have encountered numerous examples in our classification program where the prepotential associated to some gauge theory description is only valid on a particular subset of the naive Coulomb branch. Nevertheless, this criterion (i.e. Conjecture 3) leads to physically sensible results consistent with the predictions of our other conjectures.

An interesting case is when the prepotential vanishes along one direction but is positive along all others. In that case the perturbative part of the partition function may diverges by the linear term when $g_{\mathrm{YM}} \to \infty$, but should converge for every other value. These cases are then marginal, and in all examples we have checked correspond to 6d lifting theories.

Thus we see that examining the perturbative part of the partition function, we are naturally led to a criterion for the existence of a UV fixed point for a 5d gauge theories. In all the examples we have checked, this criterion gives identical results as the other criteria introduced in this article.

Before ending we wish to discuss the physical aspects of this criterion as well as possible generalizations. A physical argument for this criterion is that the partition function is a characteristic of the theory and must be a finite number so it seems strange for it to diverge. It is known that in some cases partition functions diverges. For instance the index of some 3d theories, the so called 'bad' by [55], diverges. In that case it is due to monopole operators going below the unitary bound, and is believed to signal the appearance of singlets. When the S^5 partition function diverges it is expected that likewise there should be a physical explanation for this.

A natural physical explanation then is that the theory needs a UV completion and thus additional degrees of freedom that could curve the divergence. This is also supported as this divergence is of UV type, that is in the limit of infinite Coulomb vev.

There are however several arguments one can raise against this. One such argument is that we only look at part of the expression since we ignored the instanton corrections. So, first, it is possible that even if the perturbative part converges, the instanton contribution diverges. This just means that this condition is not sufficient, but that might be so even when the full partition function converges. It is still reasonable that this is a necessary condition.

However, it is possible that both the perturbative part and some of the instanton contributions diverges, but their sum converges. This seems extremely unlikely since the perturbative part and instanton contributions have different dependence on the coupling constant, which is a mass parameter in 5d controlling the instanton masses. So even if such a cancellation occurs changing the value of the coupling constant should destroy it and leads to a divergence. Since the partition function must converge for every value of g_{YM}, it still seems to be a good necessary condition.

Special attention should be given to the marginal case when the coefficient of the σ^3 term vanishes exactly along some direction. In that case the partition function only diverges when $g_{\mathrm{YM}} \to \infty$ so one cannot rule out that the full partition function also converges for $g_{\mathrm{YM}} \to \infty$ where the divergence is canceled by instanton contributions.

Another issue that can be raised is how well can we trust the result for the S^5 partition function particularly in the $g_{\mathrm{YM}} \to \infty$ limit. In other words, how well does the gauge theory partition function captures properties of the underlying SCFT when it exists. It is natural to expect that the 5d SCFT should have a physical object that can be identified as its S^5 partition functions. This will be a function of various mass deformation, identified with flavor masses and coupling constants in low-energy gauge theory descriptions. The masses in turn can be defined as central charges in the SUSY algebra. Physically we expect this object to be finite for any value of the masses. If we identify this object with the gauge theory partition function then a physical argument for its convergence naturally arises. In that lights, the agreement of this criterion with the others seem to imply that the localized partition function of the gauge theory captures some aspects of the partition function of the underlying SCFT.

Finally we comment on possible generalizations of this criterion. The most obvious one is to generalize to the complete partition function by including the non-perturbative part. As we explained when we discussed the exotic cases, it is expected that there will be some non-perturbative corrections to the perturbative prepotential. Given the identity of the large value behavior of the exponent of the integrand with the perturbative prepotential, and the existence of the non-perturbative instanton corrections, it is tempting to suspect that the latter may give as a window into non-perturbative corrections to the perturbative prepotential. We also only considered the round sphere, while there are generalizations of all the expressions also to the squashed sphere. It might be interesting to explore the generalization to the squashed sphere. It may also be interesting to better understand the relation between the gauge theory partition function and that of the underlying SCFT. We reserve further study of all these issues to future work.

References

[1] E. Witten, *Some comments on string dynamics*, in *Future perspectives in string theory. Proceedings, Conference, Strings'95, Los Angeles, USA, March 13-18, 1995*, pp. 501–523, 1995. hep-th/9507121.

[2] J. J. Heckman, D. R. Morrison, and C. Vafa, *On the Classification of 6D SCFTs and Generalized ADE Orbifolds*, *JHEP* **05** (2014) 028, [arXiv:1312.5746]. [Erratum: JHEP06,017(2015)].

[3] J. J. Heckman, D. R. Morrison, T. Rudelius, and C. Vafa, *Atomic Classification of 6D SCFTs*, *Fortsch. Phys.* **63** (2015) 468–530, [arXiv:1502.05405].

[4] L. Bhardwaj, *Classification of 6d $\mathcal{N} = (1, 0)$ gauge theories*, *JHEP* **11** (2015) 002, [arXiv:1502.06594].

[5] D. Xie and S.-T. Yau, *Three dimensional canonical singularity and five dimensional N=1 SCFT*, arXiv:1704.00799.

[6] N. Seiberg, *Five-dimensional SUSY field theories, nontrivial fixed points and string dynamics*, *Phys. Lett.* **B388** (1996) 753–760, [hep-th/9608111].

[7] D. R. Morrison and N. Seiberg, *Extremal transitions and five-dimensional supersymmetric field theories*, *Nucl. Phys.* **B483** (1997) 229–247, [hep-th/9609070].

[8] K. A. Intriligator, D. R. Morrison, and N. Seiberg, *Five-dimensional supersymmetric gauge theories and degenerations of Calabi-Yau spaces*, *Nucl. Phys.* **B497** (1997) 56–100, [hep-th/9702198].

[9] S. H. Katz, A. Klemm, and C. Vafa, *Geometric engineering of quantum field theories*, *Nucl. Phys.* **B497** (1997) 173–195, [hep-th/9609239].

[10] S. Katz, P. Mayr, and C. Vafa, *Mirror symmetry and exact solution of 4-D N=2 gauge theories: 1.*, *Adv. Theor. Math. Phys.* **1** (1998) 53–114, [hep-th/9706110].

[11] M. R. Douglas, S. H. Katz, and C. Vafa, *Small instantons, Del Pezzo surfaces and type I-prime theory*, *Nucl. Phys.* **B497** (1997) 155–172, [hep-th/9609071].

[12] O. Aharony and A. Hanany, *Branes, superpotentials and superconformal fixed points*, *Nucl. Phys.* **B504** (1997) 239–271, [hep-th/9704170].

[13] O. Bergman and G. Zafrir, *Lifting 4d dualities to 5d*, *JHEP* **04** (2015) 141, [arXiv:1410.2806].

[14] H. Hayashi, S.-S. Kim, K. Lee, M. Taki, and F. Yagi, *A new 5d description of 6d D-type minimal conformal matter*, *JHEP* **08** (2015) 097, [arXiv:1505.04439].

[15] K. Yonekura, *Instanton operators and symmetry enhancement in 5d supersymmetric quiver gauge theories*, *JHEP* **07** (2015) 167, [arXiv:1505.04743].

[16] D. Gaiotto and H.-C. Kim, *Duality walls and defects in 5d $\mathcal{N}=1$ theories*, *JHEP* **01** (2017) 019, [arXiv:1506.03871].

[17] O. Bergman and G. Zafrir, *5d fixed points from brane webs and O7-planes*, *JHEP* **12** (2015) 163, [arXiv:1507.03860].

[18] O. Aharony, A. Hanany, and B. Kol, *Webs of (p,q) five-branes, five-dimensional field theories and grid diagrams*, *JHEP* **01** (1998) 002, [hep-th/9710116].

[19] N. C. Leung and C. Vafa, *Branes and toric geometry*, *Adv. Theor. Math. Phys.* **2** (1998) 91–118, [hep-th/9711013].

[20] E. Witten, *Phase transitions in M theory and F theory*, *Nucl. Phys.* **B471** (1996) 195–216, [hep-th/9603150].

[21] G. Zafrir, *Brane webs, 5d gauge theories and 6d $\mathcal{N}=(1,0)$ SCFT's*, *JHEP* **12** (2015) 157, [arXiv:1509.02016].

[22] H. Hayashi, S.-S. Kim, K. Lee, M. Taki, and F. Yagi, *More on 5d descriptions of 6d SCFTs*, arXiv:1512.08239.

[23] M. Del Zotto, C. Vafa, and D. Xie, *Geometric engineering, mirror symmetry and* $6\mathrm{d}_{(1,0)} \to 4\mathrm{d}_{(\mathcal{N}=2)}$, *JHEP* **11** (2015) 123, [arXiv:1504.08348].

[24] H. Hayashi and K. Ohmori, *5d/6d DE instantons from trivalent gluing of web diagrams*, arXiv:1702.07263.

[25] M. Del Zotto, J. J. Heckman, and D. R. Morrison, *6D SCFTs and Phases of 5D Theories*, arXiv:1703.02981.

[26] G. Zafrir, *Instanton operators and symmetry enhancement in 5d supersymmetric USp, SO and exceptional gauge theories*, *JHEP* **07** (2015) 087, [arXiv:1503.08136].

[27] O. Bergman, D. Rodrguez-Gmez, and G. Zafrir, *5-Brane Webs, Symmetry Enhancement, and Duality in 5d Supersymmetric Gauge Theory*, *JHEP* **03** (2014) 112, [arXiv:1311.4199].

[28] S. H. Katz, D. R. Morrison, and M. R. Plesser, *Enhanced gauge symmetry in type II string theory*, *Nucl. Phys.* **B477** (1996) 105–140, [hep-th/9601108].

[29] Y. Tachikawa, *On S-duality of 5d super Yang-Mills on S1*, *JHEP* **11** (2011) 123, [arXiv:1110.0531].

[30] Y. Tachikawa, *Instanton operators and symmetry enhancement in 5d supersymmetric gauge theories*, *PTEP* **2015** (2015), no. 4 043B06, [arXiv:1501.01031].

[31] H. Hayashi, S.-S. Kim, K. Lee, and F. Yagi, *6d SCFTs, 5d Dualities and Tao Web Diagrams*, arXiv:1509.03300.

[32] E. Witten, *An SU(2) Anomaly*, *Phys. Lett.* **B117** (1982) 324–328.

[33] K. Ohmori and H. Shimizu, *S^1/T^2 compactifications of 6d $\mathcal{N} = (1, 0)$ theories and brane webs*, *JHEP* **03** (2016) 024, [arXiv:1509.03195].

[34] S.-S. Kim, M. Taki, and F. Yagi, *Tao Probing the End of the World*, *PTEP* **2015** (2015), no. 8 083B02, [arXiv:1504.03672].

[35] M. Del Zotto, J. J. Heckman, A. Tomasiello, and C. Vafa, *6d Conformal Matter*, *JHEP* **02** (2015) 054, [arXiv:1407.6359].

[36] O. J. Ganor, D. R. Morrison, and N. Seiberg, *Branes, Calabi-Yau spaces, and toroidal compactification of the N=1 six-dimensional E(8) theory*, *Nucl. Phys.* **B487** (1997) 93–127, [hep-th/9610251].

[37] N. A. Nekrasov, *Seiberg-Witten prepotential from instanton counting*, *Adv. Theor. Math. Phys.* **7** (2003), no. 5 831–864, [hep-th/0206161].

[38] N. Nekrasov and A. Okounkov, *Seiberg-Witten theory and random partitions*, *Prog. Math.* **244** (2006) 525–596, [hep-th/0306238].

[39] R. Gopakumar and C. Vafa, *M theory and topological strings. 1.*, hep-th/9809187.

[40] R. Gopakumar and C. Vafa, *M theory and topological strings. 2.*, hep-th/9812127.

[41] H.-C. Kim, S. Kim, E. Koh, K. Lee, and S. Lee, *On instantons as Kaluza-Klein modes of M5-branes*, *JHEP* **12** (2011) 031, [arXiv:1110.2175].

[42] C. Hwang, J. Kim, S. Kim, and J. Park, *General instanton counting and 5d SCFT*, *JHEP* **07** (2015) 063, [arXiv:1406.6793]. [Addendum: JHEP04,094(2016)].

[43] R. Feger and T. W. Kephart, *LieART?A Mathematica application for Lie algebras and*

representation theory, *Comput. Phys. Commun.* **192** (2015) 166–195, [arXiv:1206.6379].

[44] J. Patera and R. T. Sharp, *On the Triangle Anomaly Number of SU(N) Representations*, *J. Math. Phys.* **22** (1981) 2352.

[45] K. Hosomichi, R.-K. Seong, and S. Terashima, *Supersymmetric Gauge Theories on the Five-Sphere*, *Nucl. Phys.* **B865** (2012) 376–396, [arXiv:1203.0371].

[46] J. Klln and M. Zabzine, *Twisted supersymmetric 5D Yang-Mills theory and contact geometry*, *JHEP* **05** (2012) 125, [arXiv:1202.1956].

[47] J. Klln, J. Qiu, and M. Zabzine, *The perturbative partition function of supersymmetric 5D Yang-Mills theory with matter on the five-sphere*, *JHEP* **08** (2012) 157, [arXiv:1206.6008].

[48] H.-C. Kim and S. Kim, *M5-branes from gauge theories on the 5-sphere*, *JHEP* **05** (2013) 144, [arXiv:1206.6339].

[49] Y. Imamura, *Perturbative partition function for squashed S5*, *PTEP* **2013** (2013), no. 7 073B01, [arXiv:1210.6308].

[50] G. Lockhart and C. Vafa, *Superconformal Partition Functions and Non-perturbative Topological Strings*, arXiv:1210.5909.

[51] Y. Imamura, *Supersymmetric theories on squashed five-sphere*, *PTEP* **2013** (2013) 013B04, [arXiv:1209.0561].

[52] H.-C. Kim, J. Kim, and S. Kim, *Instantons on the 5-sphere and M5-branes*, arXiv:1211.0144.

[53] D. L. Jafferis and S. S. Pufu, *Exact results for five-dimensional superconformal field theories with gravity duals*, *JHEP* **05** (2014) 032, [arXiv:1207.4359].

[54] J. Kallen, J. A. Minahan, A. Nedelin, and M. Zabzine, *N^3-behavior from 5D Yang-Mills theory*, *JHEP* **10** (2012) 184, [arXiv:1207.3763].

[55] D. Gaiotto and E. Witten, *Supersymmetric Boundary Conditions in N=4 Super Yang-Mills Theory*, *J. Statist. Phys.* **135** (2009) 789–855, [arXiv:0804.2902].

Published for SISSA by Springer

Received: *February 15, 2018*
Accepted: *April 12, 2018*
Published: *April 17, 2018*

On geometric classification of 5d SCFTs

Patrick Jefferson,[a] Sheldon Katz,[b] Hee-Cheol Kim[a,c] and Cumrun Vafa[a]

[a] *Jefferson Physical Laboratory, Harvard University, Cambridge, MA 02138, U.S.A.*
[b] *Department of Mathematics, University of Illinois at Urbana-Champaign, Urbana, IL 61801, U.S.A.*
[c] *Department of Physics, POSTECH, 77 Cheongam-Ro Nam-Gu, Pohang 37673, Korea*

E-mail: patrickjefferson@fas.harvard.edu, katzs@illinois.edu, heecheol1@gmail.com, vafa@physics.harvard.edu

Abstract: We formulate geometric conditions necessary for engineering 5d superconformal field theories (SCFTs) via M-theory compactification on a local Calabi-Yau 3-fold. Extending the classification of the rank 1 cases, which are realized geometrically as shrinking del Pezzo surfaces embedded in a 3-fold, we propose an exhaustive classification of local 3-folds engineering rank 2 SCFTs in 5d. This systematic classification confirms that all rank 2 SCFTs predicted using gauge theoretic arguments can be realized as consistent theories, with the exception of one family which is shown to be non-perturbatively inconsistent and thereby ruled out by geometric considerations. We find that all rank 2 SCFTs descend from 6d (1,0) SCFTs compactified on a circle possibly twisted with an automorphism together with holonomies for global symmetries around the Kaluza-Klein circle. These results support our conjecture that every 5d SCFT can be obtained from the circle compactification of some parent 6d (1,0) SCFT.

Keywords: Conformal Field Models in String Theory, Differential and Algebraic Geometry, Field Theories in Higher Dimensions, Supersymmetry and Duality

ArXiv ePrint: 1801.04036

Article funded by SCOAP[3].

https://doi.org/10.1007/JHEP04(2018)103

Contents

1 Introduction

The discovery of superconformal theories (SCFTs) in six and five dimensions has been one of the most surprising results emerging from string theory in the past few decades. There are two types of 6d SCFTs, both of which are classified in terms of singular geometries: $\mathcal{N} =$

$(2,0)$ theories [1] and $\mathcal{N}=(1,0)$ theories [2–4]. Given the surprising effectiveness of geometry in describing 6d SCFTs, a natural next step is to attempt to classify 5d SCFTs in terms of singular geometries. In some ways, 5d SCFTs are more rigid as there is only a single type of 5d SCFT corresponding to the 5d $\mathcal{N}=1$ (i.e. eight supercharges) superconformal algebra. Many examples of 5d SCFTs have been realized in string theory using brane probes [5], M-theory on local Calabi-Yau 3-folds [6–8], and type IIB (p,q) 5-brane webs [9–12].

The classification of 6d $\mathcal{N}=(1,0)$ theories led to a picture involving generalized 'quiver-like' theories whose structures could by and large be anticipated from field theoretic reasoning. There are of course exceptions to this idea and explicit geometric constructions in F-theory clarified which possible exceptions arise that evade field theoretic analysis [2, 3]. Similarly, in the 5d case, one might expect field theoretic reasoning to be a powerful, albeit incomplete guide. Indeed, as spearheaded in [8] it has been clear for a long time that field theoretic tools combined with the constraints of supersymmetry provide an unexpectedly powerful method for deducing the existence of interacting UV fixed points. More recently it was found in [13] that relaxing some of the constraints in [8] can resolve the conflict between the necessity of assumptions in [8] with some known stringy constructions. However, it is unclear whether or not there are additional conditions needed to guarantee the existence of gauge theories as consistent 5d SCFTs. Moreover, there are known cases in which a 5d SCFT is not a gauge theory (for example, M-theory on a local $\mathbb{P}^2$ embedded in a Calabi-Yau 3-fold).[1] A reasonable follow-up to the field theoretic approach, then, is to try to check if the necessary gauge theoretic consistency conditions described in [13] are in fact also sufficient, by using other string constructions to engineer the same theories. The main aim of this paper is to use geometric constructions of 5d SCFTs, realized as M-theory compactified on local Calabi-Yau (CY) 3-fold (and cross checked with dual constructions involving (p,q) 5-brane webs), to devise a classification scheme for 5d SCFTs. As a byproduct of our efforts, we are led to either validate or exclude various candidate 5d SCFTs predicted by the perturbative gauge theoretic analysis.

The basic mathematical setup leading to 5d SCFTs from M-theory on CY 3-folds involves studying how all compact 4-cycles (compact complex surfaces) inside a non-compact 3-fold can be shrunk to a point at a finite distance in moduli space; we call CY 3-folds engineering 5d SCFTs in this manner 'shrinkable' 3-folds. This geometric picture can be schematically represented by a graph whose nodes are 4-cycles (surfaces) and whose edges denote the resulting intersecting 2-cycles (curves). We note that a systematic study of the consistency conditions needed to construct such geometries has not been undertaken in the mathematics literature. Starting from a collapsed set of 4-cycles, the condition that one can resolve the singularities and thereby bring the 4-cycles to finite volume restricts the admissible types of Kähler surfaces (i.e. the nodes of the graph). We call the number of nodes of such a graph the *rank* of the 5d SCFT. In particular, we show that the nodes of the graph must be rational or ruled surfaces (possibly blown up at a positive number of

[1] Despite the fact that these cases do not admit a Lagrangian description, they can nevertheless be obtained from a gauge theory by passing through phases where some non-perturbative degrees of freedom become massless.

JHEP04(2018)103

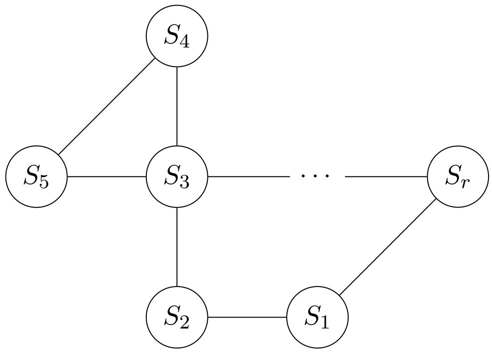

Figure 1. Graphical representation of a rank r Kähler surface $S = \cup S_i \subset X$ embedded in local Calabi-Yau 3-fold X. The nodes of the graph correspond to 4-cycles S_i, while the edges $C_{i,i+1} = S_i \cap S_{i+1}$ correspond to 2-cycles along which the nodes intersect.

points)[2] in the rank 2 case, and further conjecture this to be true for arbitrary rank. The Calabi-Yau condition and the requirement of positive volumes place further restrictions on the allowed intersections of the surfaces (i.e. the edges of the graph; see figure 1). We thus devise a set of necessary critieria which must be satisfied for a 3-fold to engineer a 5d SCFT and conjecture that these criteria are sufficient to guarantee the existence of a 5d SCFT; this conjecture is supported by various cross checks using (p, q) 5-brane webs. Furthermore, we conjecture that all 5d SCFTs can be realized in M-theory on CY 3-folds satisfying these criteria. Similar to the 6d case, where F-theory compactified on elliptic 3-folds was used to classify $\mathcal{N} = (1, 0)$ theories and it was subsequently found that for a few exotic cases frozen singularities are necessary to realize $O7^+$ planes in F-theory [14, 15], we find that in the M-theory case it is also necessary to include frozen singularities to obtain a complete classification of 5d SCFTs.

A complete classification of such CY 3-folds appears to be a rather daunting task. For example, it is unknown whether or not the list of possible 5d SCFTs is finite for a given rank. Luckily, it turns out that the rank 2 case is finite, permitting an exhaustive classification of physically distinct SCFTs.

By classifying rank 2 SCFTs in terms of Calabi-Yau geometry, we learn that all rank 2 gauge theories predicted in [13], except for one family, are realized.[3] Additionally, we are also able to pinpoint the non-perturbative physics missing in the gauge theoretic approach of [13] responsible for excluding this family of SCFTs. Furthermore, the geometric approach allows us to identify additional non-Lagrangian SCFTs whose existence motivates the existence of dual (p, q) 5-brane web configurations.

[2]Rational and ruled surfaces are equivalent to (respectively) $\mathbb{P}^2$ and ruled surfaces over genus g curves (which we argue can be restricted to $g = 0$)—see section 3.5.1 for additional details.

[3]We conjecture that all SCFTs admit at least one Coulomb branch parameter at the CFT point. The missing family which is represented by SU(3) at Chern-Simons level $k = 8$ has no Coulomb branch parameter at the would-be CFT point and that is why we rule it out. This family would have led to a putative CFT which allows a Coulomb branch deformation only after a mass deformation (i.e. turning on $1/g^2$).

JHEP04(2018)103

Given the significant practical challenges presented by this classification program, it is natural to ask if the insight we have gained from the rank 2 case can be used to streamline the classification of higher rank cases. Indeed, a careful examination of the list of rank 2 theories reveals a beautifully simple picture: rank 2 SCFTs in 5d can be organized into four distinct families, related and interconnected by RG flows triggered by mass deformations — see figure 16. Each family of 5d SCFTs has a parent 6d SCFT, where the parent 6d SCFT is related to a 5d descendant by circle compactification, up to a choice of automorphism twist (see [16] for work on classifying such automorphism twists, and see [17] for a discussion of additional discrete data characterizing circle compactifications of 6d SCFTs.) Thus the rank 2 classification could have been anticipated entirely from the 6d perspective! This result echoes a well-known property of rank 1 SCFTs: rank 1 5d SCFTs belong to a single family which descends from the 6d E-string theory via circle compactification.

We thus conjecture that *all 5d SCFTs arise from 6d SCFTs compactified on a circle, possibly up to an automorphism twist.* More precisely, we anticipate that all 5d SCFTs can be organized into distinct families, each of which arises from a 6d theory. For a fixed rank in 5d, the possible 6d SCFT parents are rather limited. For example (ignoring the possible automorphism twist), the 6d SCFTs leading to rank r 5d SCFTs will have $r-k$ dimensional tensor branches with rank k gauge algebra. This suggests a practical method to classify 5d SCFT families starting with the 6d classification: compactifying a 6d SCFT on a circle produces a 5d theory with a Kaluza Klein (KK) tower of states. We call such theories '5d KK theories'; these theories are in some sense analogous to 6d little string theories. To obtain non-trivial 5d SCFTs from 5d KK theories we need to turn on holonomies suitably tuned to trigger an RG flow to a nontrivial 5d SCFT in the infrared. Aspects of the phase structure of 5d theories arising from circle compactifications of 6d SCFTs were analyzed in [18].

The organization of this paper is as follows. In section 2 we discuss the preliminaries of 5d SCFTs, their effective gauge theory descriptions on the Coulomb branch, and their realizations in M-theory. In section 3 we discuss the mathematics of shrinkable 3-folds and explain the basic approach of our geometric classification program. In section 4 we repeat the classification of rank 1 5d SCFTs and extend the same methods to the rank 2 case. We also discuss the connection to 6d $\mathcal{N} = (1, 0)$ SCFTs. Some mathematical results essential for the rank 2 classification are collected in the appendices: appendix A contains an explicit description of the Mori cones of blowups of Hirzebruch surfaces; appendix B contains some numerical bounds constraining rank 2 shrinkable 3-folds; finally, appendix C contains a detailed discussion of some smoothness assumptions which simplify the classification program.

2 Effective description of 5d SCFTs

In this section we discuss some of the preliminaries that set the stage for the classification of 5d SCFTs later in this paper. The following discussion involves two perspectives on 5d $\mathcal{N} = 1$ theories: the gauge theoretic perspective, and the geometric perspective of M-theory compactified on a Calabi-Yau 3-fold.

5d superconformal field theories (SCFTs) are strongly interacting systems with no marginal deformations [19] and no known Lagrangian description at the CFT fixed point.

In order to study the physics of these conformal theories, one needs to use rather indirect approaches. 5d SCFTs admit supersymmetric relevant deformations which lead to several weakly interacting effective descriptions while preserving some amount of supersymmetry. Surprisingly, these effective descriptions can be powerful tools for studying the dynamics of the conformal point. There exist some CFT observables which are rigidly protected under the renormalization group (RG) flow triggered by these deformations. Many BPS quantities are such observables: for example, the spectrum of BPS operators, supersymmetric partition functions, effective Lagrangians on the Coulomb branch, the Coulomb branch of moduli space, etc. In particular, BPS observables are protected by supersymmetry and thus we expect BPS quantities appearing in the effective theories to be a reliable description of the corresponding observables at the CFT fixed point.

String theory provides many effective descriptions of 5d SCFTs. Multiple D4-brane systems in Type IIA string theory and (p, q) 5-brane webs in Type IIB string theory can engineer various 5d SCFTs as singularities. Away from the singularity, when mass parameters and gauge couplings are turned on, these brane systems often permit a gauge theory description of the corresponding 5d theories.

5d SCFTs can also be engineered in M-theory: M-theory on a singular non-compact Calabi-Yau 3-fold is described at long distances by an SCFT living on the five-dimensional spacetime transverse to the 3-fold. In familiar cases, the Calabi-Yau singularity can be resolved by means of various Kähler deformations, which correspond to mass and Coulomb branch deformations in the corresponding gauge theory.

2.1 Gauge theory description

Gauge theories in five dimensions are non-renormalizable and flow to free fixed points at low energy. As a result, these theories are typically believed to be 'trivial' theories. However, a large class of 5d gauge theories, mostly engineered in string theory, turn out to have interacting CFT fixed points in the UV [5]. In such cases, 5d gauge theories are rather interesting since they can provide low energy effective descriptions of the CFT.

In this paper, we focus primarily on gauge theories which have 5d SCFTs as their UV completions. These theories preserve $\mathcal{N} = 1$ supersymmetry, and their massless field content consists of vector multiplets with gauge algebra G and hypermultiplets in a representation $\mathbf{R} = \oplus \mathbf{R}_j$ of G. These gauge theories might be further specified by topological data k corresponding to classical Chern-Simons level, as in the case of $G = \mathrm{SU}(N \geq 3)$, or discrete θ-angle as in the cases $G = \mathrm{Sp}(N)$. We can also consider the cases with product gauge algebra $G = \prod_i G_i$. Once the data $G, \mathbf{R}, k$ is fixed, the low energy gauge theory Lagrangian is uniquely determined by supersymmetry. Our notation for describing 5d gauge theories is

$$G_k + \sum_j N_{\mathbf{R}_j} \mathbf{R}_j, \tag{2.1}$$

where $\mathbf{R}_j$ is the representation under which the j-th matter hypermultiplet is charged, $N_{\mathbf{R}_j}$ is the number of hypermultiplets in the representation $\mathbf{R}_j$.

5d $\mathcal{N} = 1$ gauge theories possesses a rich vacuum structure. The moduli space of vacua is parametrized by expectation values of various local operators. In particular, we are interested in the Coulomb branch of vacua parametrized by vacuum expectation values of scalar fields ϕ in the vector multiplets. Here the scalar field ϕ takes values in the Cartan subalgebra of the gauge group G. So the dimension of the moduli space of the Coulomb branch is given by the rank of group G, $r = \text{rank}(G)$. By abuse of notation, we will denote both a scalar field in the vector multiplet and its expectation value by ϕ from now on.

There are global symmetries acting on the hypermultiplets. The classical Lagrangian has global symmetry algebra F rotating the perturbative hypermultiplets and also a topological $\mathrm{U}(1)_I$ symmetry for each gauge group. The objects charged under the $\mathrm{U}(1)_I$ are non-perturbative particles called 'instantons'. Surprisingly, this classical global symmetry is often enhanced in the CFT fixed point by non-perturbative instanton dynamics [5, 7]. The flavor symmetry of the perturbative hypermultiplets can combine with the topological $\mathrm{U}(1)_I$ instanton symmetry and enhance to an even larger symmetry algebra in the UV CFT. One can turn on mass parameters m_i associated to the global symmetry. Doing so breaks some of the global symmetry. In particular, the mass deformation with parameter g^{-2} along the $\mathrm{U}(1)_I$ instanton symmetry leads to a gauge theory description with gauge coupling g at low energy.

At a generic point in the Coulomb branch, the gauge symmetry G is broken to the maximal torus $\mathrm{U}(1)^r$. Thus the low energy dynamics on the Coulomb branch can be effectively described by abelian gauge theories. The low energy abelian action is determined by a prepotential $\mathcal{F}$. The prepotential is 1-loop exact and the full quantum result is a cubic polynomial of the vector multiplet scalar ϕ and mass parameters m_j, given by [8, 20]:

$$\mathcal{F} = \frac{1}{2g^2}h_{ij}\phi_i\phi_j + \frac{k}{6}d_{ijk}\phi_i\phi_j\phi_k + \frac{1}{12}\left(\sum_{e\in\text{root}}|e\cdot\phi|^2 - \sum_j\sum_{w\in\mathbf{R}_j}|w\cdot\phi + m_i|^3\right), \tag{2.2}$$

where by abuse of notation $\mathbf{R}_j$ denotes the set of weights of the j-th hypermultiplet representation of G, $h_{ij} = \text{Tr}(T_iT_j)$, and $d_{ijk} = \frac{1}{2}\text{Tr}_{\mathbf{F}}(T_i\{T_j, T_k\})$ with $\mathbf{F}$ in the fundamental representation. The first two terms in the prepotential are from the classical Lagrangian and the last two terms are 1-loop corrections coming from integrating out charged fermions in the Coulomb branch. We remark that the prepotential may have different values in the different sub-chambers (or phases) of the Coulomb branch due to the absolute values in the 1-loop contributions.

The 1-loop correction to the prepotential renormalizes the gauge coupling. The effective coupling in the Coulomb branch is simply given by a second derivative of the quantum prepotential which also fixes the exact metric on the Coulomb branch:

$$(\tau_{\text{eff}})_{ij} = (g_{\text{eff}}^{-2})_{ij} = \partial_i\partial_j\mathcal{F}, \qquad ds^2 = (\tau_{\text{eff}})_{ij}d\phi_i d\phi_j . \tag{2.3}$$

Interestingly, the exact spectrum of magnetic monopoles on the Coulomb branch can be easily obtained from the quantum prepotential. Since monopoles are magnetically dual to electric gauge bosons, tensions of magnetic monopole strings can be computed as

$$\phi_{Di} = \partial_i\mathcal{F}, \quad i = 1, \cdots r . \tag{2.4}$$

JHEP04(2018)103

One can also compute Chern-Simons couplings:

$$k_{ijk} = \partial_i \partial_j \partial_k \mathcal{F}. \tag{2.5}$$

Therefore, we can use $\mathcal{F}$ to exactly compute some quantum observables such as the Coulomb branch metric and monopole spectrum.

In [8, 13], the above supersymmetry protected data is used to attempt a classification of possible 5d SCFTs admitting low energy gauge theory descriptions. The main idea in these classification programs is that the quantum metric on the Coulomb branch should be positive semi-definite in the CFT limit, as required by unitarity. In [8], the positivity condition of the metric was imposed throughout the 'perturbative' Coulomb branch and all sensible gauge theories were subsequently identified using this constraint. In this classification, the 'perturbative' Coulomb branch is determined by forcing only *perturbative* particles to have positive masses. Under this condition, the number and type of hypermultiplets are strictly constrained and quiver type gauge theories are ruled out; see [8] for details. We refer to this classification as the 'IMS classification'.

However, it was pointed out later works [10, 12, 21–23] that string theory can engineer many 5d gauge theories with non-trivial CFT fixed points not included among the theories in the IMS classification. It turns out that the condition of metric positivity throughout the entire perturbative Coulomb branch is too strong [13] and unnecessarily excludes many non-trivial 5d gauge theories. This suggests that the IMS classification is incomplete, and the gauge theories exceeding the IMS bounds lead us to revisit the problem of classifying 5d SCFTs.

Let us briefly review the classification of [13]. One of the main results of this analysis is the observation that the 'perturbative' Coulomb branch receives quantum corrections by light non-perturbative states [10]. It is possible that some of non-perturbative states can become massless somewhere in the perturbative Coulomb branch. These hyperplanes in the Coulomb branch where these light states become massless can be thought of as 'non-perturbative' walls. Beyond such walls, the perturbative Coulomb branch breaks down. One way to see this is to note that the signature of the quantum metric on the Coulomb branch changes beyond these non-perturbative walls, which implies the metric cannot be trusted in these regions. However, the classification in [8] imposes metric positivity on the whole perturbative Coulomb branch, even beyond non-perturbative walls. The result is that some theories are excluded because of the unreliability of the metric in these regions, and this leads to an incomplete classification. In order to obtain a complete classification, metric positivity should be applied only on the 'physical' Coulomb branch, which can be computed by accounting for restrictions introduced by non-perturbative states.

In general, it is difficult to identify the correct physical Coulomb branch after taking into account non-perturbative effects since this necessarily involves studying the full non-perturbative spectrum. In particular, it is not easy to analyze the spectrum of gauge theory instantons. Only when we know a precise UV completion of the instanton moduli space, such as the ADHM construction, can we compute the exact spectrum using localization. For most gauge theories, such a convenient construction of the instanton moduli space is lacking.

JHEP04(2018)103

Fortunately, the perturbative prepotential contains part of the exact spectrum of non-perturbative states. As noted in (2.4), the full monopole spectrum can be obtained from the prepotential. We can use this information to identify some of the non-perturbative walls in the perturbative Coulomb branch. By relaxing the metric positivity constraint to apply only to the region interior to such non-perturbative walls, it was conjectured in [13] that all gauge theories having interacting CFT fixed points satisfy the metric positivity condition in the sub-locus of Coulomb branch where perturbative particles and monopole strings have positive masses. In [13], it was also shown that a large class of known 5d gauge theories satisfy this criterion. It may be true that all the known 5d gauge theories having 5d SCFT fixed points satisfy this refined condition.

In addition, there are two more conjectures in [13] used to carry out the classification of 5d gauge theories with simple gauge algebras. The first conjecture is that if all perturbative particles and monopoles have positive masses *somewhere* in the Coulomb branch, the gauge theory has a UV CFT fixed point. The second conjecture is that perturbative prepotentials of all gauge theories with UV CFT fixed points are positive *everywhere* in the perturbative Coulomb branch. Note that the first conjecture is not sufficient to guarantee that all instanton particles have positive mass and also that the metric is positive in the same region. So this is simply a necessary condition. We will see later that certain theories predicted by this approach must be excluded because some non-perturbative particles acquire negative masses in the CFT limit. The second conjecture is based on the convergence of the 1-loop sphere partition function of 5d CFTs, but there is neither physical nor mathematical motivation for this conjecture beyond its practical implications. Using these two conjectures, non-trivial gauge theories with single gauge node were fully classified in [13]. This classification includes all known single gauge node theories and additionally predicts a large number of new gauge theories.

In this paper, we construct rank 1 and rank 2 CFTs using Calabi-Yau geometry. Rank 1 gauge theories arising from SCFTs were classified in [5, 6, 8, 24]; these theories have gauge algebra SU(2) with $N_{\mathbf{F}} \leq 7$. Geometrically, the rank 1 SCFTs can be engineered by del Pezzo surfaces embedded in a non-compact 3-fold. The families of rank 2 gauge theories predicted by the classification of [13] are displayed in table 1. The UV completions of the theories shown in table 1 are all expected to be 6d theories, rather than 5d SCFTs; on the other hand, their descendants obtained by mass deformations are expected to have 5d CFT fixed points. Many of these theories in table 1 are new theories, for example SU(3) with $(N_{\mathbf{F}}, |k|) = (6,4), (3, \frac{13}{2}), (0,9)$ in (a).

One of the purposes of this paper is to check if the new rank 2 CFTs predicted in [13] (or descendants of theories in table 1) can be constructed geometrically. We will see that, surprisingly, almost all new theories in table 1 admit geometric constructions, therefore their descendants indeed have interacting CFT fixed points. However, some theories do not correspond to geometries in their conformal limits due to subtle non-perturbative effects. Therefore, the geometric constructions of this paper indicate that the criteria described in [13] require additional non-perturbative corrections in order to be complete. We hope to revisit the field theoretic approach of [13] in the near future with the benefit of our improved understanding.

JHEP04(2018)103

$N_{\mathbf{Sym}}$	$N_{\mathbf{F}}$	$\lvert k\rvert$
1	0	$\frac{3}{2}$
1	1	0
0	10	0
0	9	$\frac{3}{2}$
0	6	4
0	3	$\frac{13}{2}$
0	0	9

(a) Marginal SU(3) theories with CS level k, $N_{\mathbf{Sym}}$ symmetric and $N_{\mathbf{F}}$ fundamental hypermultiplets.

$N_{\mathbf{AS}}$	$N_{\mathbf{F}}$
3	0
2	4
1	8
0	10

(b) Marginal Sp(2) gauge theories with $N_{\mathbf{AS}}$ anti-symmetric, $N_{\mathbf{F}}$ fundamental hypermultiplets. The theory with $N_{\mathbf{AS}} = 3$ can have $\theta = 0, \pi$.

$N_{\mathbf{F}}$
6

(c) A marginal G_2 gauge theory with $N_{\mathbf{F}}$ fundamental matters.

Table 1. Rank 2 gauge theories.

2.2 M-theory compactifications

String compactifications are an extraordinarily useful tool for realizing local, non-perturbative models of gauge sector physics in terms of brane dynamics. Consider in particular M-theory on a non-compact singular Calabi Yau variety Y, which is conjectured to be described at low energies by a 5d $\mathcal{N} = 1$ SCFT. We are specifically interested in studying the Coulomb branch deformations of these 5d SCFTs. The heart of this analysis is the correspondence between the Coulomb branch $\mathcal{C}$ and the extended Kähler cone $\mathcal{K}(Y)$ of the singular threefold Y [20]:

$$\mathcal{C} = \mathcal{K}(Y). \tag{2.6}$$

The above correspondence is made more precise by establishing a dictionary between the geometry of the threefold and the BPS spectrum of the associated 5d theory, which we now describe in detail. Consider a smooth non-compact 3-fold X. The Kähler metric of X depends on $h^{1,1}(X)$ moduli controlling the sizes of complex p cycles in X. In order to decouple gravitational interactions, it is necessary to scale the volume of X to be infinitely large while keeping the volumes of all 2- and 4-cycles at finite size; this has the effect of sending the 5d Planck mass to infinity. Given a basis $D_i \in H^{1,1}(X)$, one may therefore express the Kähler form J as the linear combination

$$J = \phi_i D_i, \quad i = 1, \ldots, h^{1,1}(X), \tag{2.7}$$

where the Kähler moduli $\phi_{i=1,\ldots,r}$ associated to (cohomology classes dual to) compact 4-cycles $D_i = S_i$ are identified with Coulomb branch moduli, while the Kähler moduli $\phi_{r+j,\ldots,r+M} = m_{j=1,\ldots,M}$ associated to non-compact 4-cycles $D_{r+j} = N_j$ are interpreted as mass parameters of the 5d theory. To align the discussion with the 5d field theoretic

JHEP04(2018)103

interpretation, we find it useful to partition the Kähler moduli into r Coulomb branch parameters and M mass parameters:

$$h^{1,1}(X) = r + M. \tag{2.8}$$

Note that when the associated 5d field theory admits a description as a gauge theory, r coincides with the rank of the gauge group.

The BPS states of the 5d theory include electric particles and (dual) magnetic strings. Geometrically these states correspond to M2 branes wrapping holomorphic 2-cycles and magnetic dual M5 branes wrapping holomorphic 4-cycles, and the masses and tensions of these BPS degrees of freedom are proportional to the volumes of the corresponding holomorphic cycles. At a generic point $\phi \in \mathcal{C}$ the spectrum of BPS states is massive, and this is reflected by the fact that the 2- and 4-cycles of Y have finite volume. Since the conformal point $\phi = 0$ is characterized by the appearance of interacting massless and tensionless degrees of freedom, we interpret the threefold Y as a singular limit of the smooth threefold X in which some collection of compact 4-cycles have collapsed to a point. Said differently, X is a desingularization of Y.

The above discussion suggests that the data of the massive BPS spectrum is encoded in the geometry of X. Indeed this is the case, the main connection to geometry being the interpretation of the 5d prepotential (2.2) as the cubic polynomial of triple intersection numbers of 4-cycles in X:

$$\mathcal{F} = \mathrm{vol}(X) = \frac{1}{3!}\int_X J^3 = \frac{1}{3!}\phi_i\phi_j\phi_k \int_X D_i \wedge D_j \wedge D_k. \tag{2.9}$$

In the previous section, we saw that various data characterizing the massive BPS spectrum can be expressed as derivatives of $\mathcal{F}$. This data equivalently characterizes the geometry of X. In particular, the tensions (2.3) of elementary monopole strings are the volumes of the compact 4-cycles S_i:

$$\phi_{Di} = \partial_i \mathcal{F} = \mathrm{vol}(S_i) = \frac{1}{2!}\int_X J^2 \wedge S_i, \quad 1 \leq i \leq r, \tag{2.10}$$

the matrix of effective couplings has as its components the volumes of various 2-cycles:

$$\tau_{ij} = \partial_i\partial_j \mathcal{F} = \mathrm{vol}(S_i \cap S_j) = \int_X J \wedge S_i \wedge S_j, \quad 1 \leq i, j \leq r, \tag{2.11}$$

and the effective Chern-Simons couplings k_{ijk} are triple intersection numbers:

$$k_{ijk} = \partial_i\partial_j\partial_k \mathcal{F} = \int_X D_i \wedge D_j \wedge D_k. \tag{2.12}$$

The Kähler cone $\mathcal{K}$ of the singularity Y can also be specified quite easily; $\mathcal{K}$ is simply the set of all positive Kähler forms (parametrized by the moduli ϕ):

$$\mathcal{K}(X \backslash Y) = \left\{ J = \phi_i D_i \;\middle|\; \int_C J > 0 \;\text{ for all holomorphic curves } C \subset X \right\}. \tag{2.13}$$

Thus, it is possible to study Coulomb branch deformations of 5d SCFTs purely in terms of the geometry of a smooth 3-fold X. Generically there are multiple smooth 3-folds X_i which share a common singular limit Y, so the extended Kähler cone is simply the closure of the union of Kähler cones,

$$\mathcal{K}(Y) = \overline{\cup \mathcal{K}(X_i \backslash Y)}. \tag{2.14}$$

The extended Kähler cone has the structure of a fan, with pairs of cones separated by hypersurfaces in the interior of $\mathcal{K}(Y)$. The boundaries of $\mathcal{K}(X_i \backslash Y)$ correspond to loci where the 3-fold X_i develops a singularity. The interior boundaries are regions where a holomorphic curve collapses to zero volume and formally develops negative volume in the adjacent Kähler cone, signaling a flop transition (see section (3.5.1) for further discussion.) By contrast, the boundaries of $\mathcal{K}(Y)$ are loci where one of the 4-cycles can collapse to a 2-cycle or a point. The SCFT point is the origin of $\mathcal{K}(Y)$, and corresponds to the singularity Y which is characterized by a connected union of 4-cycles shrinking to a point.

In some cases the 5d theory associated to a 3-fold X admits a description as a gauge theory. In such cases, the abelian gauge algebra is $H^2(X, \mathbb{R})/H^2(X, \mathbb{Z})$ and enhances to a non-abelian gauge algebra in the singularity Y. The simple coroots of the gauge algebra correspond to the classes $S_i \in H^2(X, \mathbb{Z})$, whereas the simple roots are generic fibers f_j contained in $H_2(X, \mathbb{Z})$. More precisely, the W-bosons of the 5d theory correspond to M2-branes wrapping holomorphic curves f_j, and so the Cartan matrix A_{ij} is the matrix of charges

$$A_{ij} = -\int_{f_j} S_i. \tag{2.15}$$

In practice, we work in an algebro-geometric setting in which volumes of holomorphic cycles can be computed as intersection products. Thus the volumes of 2-cycles $C_i \subset H_2(X, \mathbb{Z})$ and 4-cycles $S_i \subset H_4(X, \mathbb{Z})$ are expressed in terms of the intersection products of numerical classes of (resp.) complex curves $[C]$ and surfaces $[D]$. That is, $\mathrm{vol}(C) = (J \cdot [C])_X$ and $\mathrm{vol}(S) = (J \cdot J \cdot S_i)_X$. We abuse notation and use the same symbols to denote p-cycles, their homology classes, and their numerical equivalence classes whenever the context is clear.

3 Classification program

3.1 Physical equivalence classes of 3-folds

In this section we propose a classification of CY 3-folds defining 5d SCFTs via M-theory compactification. One way to approach this problem is to study singular 3-folds for which there exist desingularizations that preserve the Calabi-Yau condition (i.e. *crepant resolutions.*) However, the problem of classifying singular 3-folds admitting crepant resolutions is notoriously difficult. Rather than attempting to classify singularities, we instead classify *physical equivalence classes* of singularities. We define a pair of 3-folds to be physically equivalent (i.e. leading to the same SCFT, up to decoupled sectors) if they are related by a finite change in Kähler and complex parameters. There is a conjectural aspect to this definition which we now clarify.

It is immediate from the above definition that normalizable Kähler and complex deformations do not change the physical equivalence class of a 3-fold, since these deformations do not change the singular limit (and hence do not change the SCFT). However, we also find it useful to identify 3-folds that differ by non-dynamical large complex deformations. While the singular limits of such 3-folds are not identical, we claim they are nevertheless closely related in that their SCFTs differ at most by decoupled free states. As we will see, the notion of physical equivalence dramatically simplifies the problem of classification.

3.2 Shrinkable 3-folds

In this section we specify the necessary criteria a smooth 3-fold must satisfy in order to define a 5d SCFT. Note that we assume all 5d SCFTs have a *maximal* Coulomb branch, meaning that there exists a phase in which the 5d theory has no dynamical massless hypermultiplets, possibly after turning on some mass parameters. Geometrically this means that we assume there exists a smooth 3-fold which has no normalizable (dynamical) complex structure deformations. The geometry of such a 3-fold is thus controlled by three types of parameters: normalizable Kähler (i.e. Coulomb branch) parameters, non-normalizable Kähler (i.e. mass) parameters, and non-dynamical non-normalizable complex structure deformation parameters (see section 3.5 for an example).

Before spelling out the necessary criteria, we recall the key features of the geometries which are the subject of our analysis. We are interested in smooth, non-compact CY 3-folds X containing a finite number of compact 4-cycles S_i and non-compact 4-cycles N_j. As discussed in the previous section the number of independent compact 4-cycles is equal to the number of Coulomb branch parameters, while the number of mass parameters is identified with the number of non-normalizable Kähler deformations. The 4-cycles $S_i \subset X$ are irreducible projective algebraic surfaces, hence Kähler. Moreover, X also contains compact 2-cycles which can either be isolated or part of a family of compact 2-cycles belonging to one of the 4-cycles.

From the physics perspective the natural condition for CY 3-folds to lead to SCFTs is that we can tune non-normalizable Kähler parameters (mass parameters) so that at a finite distance in normalizable Kähler moduli space we can reach a singular CY 3-fold which has no finite volume cycles or surfaces. However, formulating this in algebro-geometric terms is not simple. Instead we formulate it in a somewhat different way which we believe is equivalent to this. Namely, in order for a 3-fold X to define a 5d SCFT, X must satisfy the property of being *shrinkable*, which we define below:

Definition. Let X be a smooth CY 3-fold modeled locally as the neighborhood of a connected union of compact Kähler surfaces $S = \cup S_i$. We say X is *shrinkable* if there exists an intersecting (possibly empty) union of non-compact surfaces $N = \cup N_j$ and a limit Y of Kähler metrics such that:

1. S (and all curves $C \subset S$) have zero volume in Y;

2. Y is at finite distance from a metric X_0 for which N has zero volume while S has positive volume.

By abuse of terminology, we say the surface S is shrinkable if S is contained in a shrinkable 3-fold X as a maximal compact algebraic surface.

Let us now translate the above definition of shrinkability into a set of necessary geometric conditions. We consider first the limit where all non-normalizable Kähler moduli have been set to zero. In this limit we may have a singular 3-fold which is described by the Kähler class $J = \phi_i S_i$. Our convention is to assume $\phi_i \geq 0$ and compute volumes with respect to $-J$; thus, the volume of a curve C is given by $\mathrm{vol}(C) = -J \cdot C$ and the volume of a divisor D is $\mathrm{vol}(D) = J^2 \cdot D$.[4] Since we require $-J$ to define a Kähler metric which assigns postive volumes to complex p-cycles in X, a necessary condition for shrinkablity is

$$\mathrm{vol}(C) = -J \cdot C \geq 0, \quad \forall C \subset S. \tag{3.1}$$

What happens when the inequality (3.1) is saturated? Suppose there exists a curve C, with $\mathrm{vol}(C) = 0$. So far, we have only considered the case in which all non-normalizable Kähler moduli are set to zero. To give finite volume to C requires a non-normalizable Kähler deformation, which in turn implies the existence of a non-compact 4-cycle N attached to S along C. Notice that since C belongs to N, there may also be other compact curves C' which are homologous to C in N; in particular, the full set of curves homologous to C can fiber over N. For each of these curves C' it must be that $\mathrm{vol}(C') = 0$, and thus N can be said to have degenerated to a non-compact 2-cycle along its fibers.[5] By making a non-normalizable Kähler deformation, we can bring the curve $C = S \cap N$ to finite volume, and we expect that we are again in a situation where the surface S is contractible.

We believe that the above necessary criteria are in fact sufficient to define a shrinkable 3-fold:

Conjecture. Let X be a smooth CY 3-fold modeled locally as the neighborhood of a connected union of compact Kähler surfaces $S = \cup S_i$. Then S is shrinkable provided that $-J \cdot C \geq 0$ for all curves $C \subset S$ and that there is one S_i with positive volume and the rest should have non-negative (possibly zero) volume.

Elliptic Calabi-Yau 3-folds are immediately ruled out by these criteria. F-theory on an elliptic 3-fold engineers a 6d theory. In a 6d theory, cubic terms in the prepotential $\mathcal{F}$ are trivial; they are non-trivial only when we compactify the 6d theory on a circle and turn on holonomies for gauge symmetries where the circle size is inversely proportional to a mass parameter (or a non-compact Kähler parameter). This means that the volumes of all 4-cycles in the associated 3-fold are zero when we turn off mass parameters (or equivalently, in the 6d limit). Therefore elliptic 3-folds are not shrinkable.

[4] This choice of sign is consistent with the description of Kähler classes J on compact CY 3-folds, as the expansion of J (or any other ample divisor class) in terms of S_i will have non-positive coefficients. A simple example illustrating this point is the rank 1 case, for which S is a del Pezzo surface. Since $J \cdot C = \phi K_S \cdot C$, it follows that J has non-positive intersection with all curves $C \in S$. We therefore have to change the sign in order for J to be a limit of Kähler classes on X.

[5] It would interesting to compare this defintion of shrinkability with the conjecture of [25] that canonical 3-fold singularities give 5d SCFTs, since it is known that the only noncompact 4-cycles in a Calabi-Yau (crepant) resolution of a canonical 3-fold singularity are ADE fibrations. However, we do not need this for the description in our classification.

3.3 Building blocks for shrinkable 3-folds

We now argue in favor of a series of simplifying assumptions we make concerning the surfaces S which are instrumental for our proposed classification of shrinkable rank 2 surfaces modulo physical equivalence. Observe that when the inequalities of (3.1) are all strict, then S is *contractible* [26], so that S can be contracted to an isolated singular point p of a singular 3-fold Y. In more precise mathematical terms, this means there exists a holomorphic map $f : X \to Y$ with $f(S) = p$ such that f restricts to an isomorphism away from S, i.e. $f|_{X-S} : X - S \cong Y - p$. Since X is at finite distance from Y in moduli space, it is evident that contractibility of $S \subset X$ implies shrinkability of X. When a curve has zero volume, we expect that we can obtain a contractible surface by means of a non-normalizable Kähler deformation which involves bringing non-compact 4-cycles to finite volume. Hence, we conjecture that a holomorphic map f exists when S is shrinkable, as well:

Conjecture. Let X be a shrinkable CY 3-fold modeled locally as a neighborhood of a connected union of compact Kähler surfaces $S = \cup S_i$ meeting a (possibly empty) collection of non-compact surfaces $N = \cup N_j$. Then there exists a holomorphic map $f : X \to Y$ sending S to a point p and N to a collection of curves C such that $f|_{X-S-N} : X - S - N \to Y - C$ is an isomorphism.

The existence of a holomorphic map f as described above permits a number of simplifying assumptions for the following reasons. Replacing the singular 3-fold Y by its normalization if necessary, we can assume that the singularities of Y are normal. It follows that Y has "canonical singularities", and moreover that X is a crepant resolution of Y. But it is known the components of the resolutions of canonical threefold singularities Y are rational or ruled [27].

We next argue that we can further restrict the types of possible building blocks by exploiting physical equivalence:

Conjecture. Shrinkable surfaces are physically equivalent to a shrinkable surface $S = \cup S_i$, where the irreducible components S_i are either equal to $\mathbb{P}^2$ or a blowup $\mathrm{Bl}_p\mathbb{F}_n$ of a Hirzebruch surface at p points intersecting one another (or self-intersecting) transversally. Moreover, there exist non-negative integers $p_{\max}(n)$ such that $p \leq p_{\max}(n)$.

We briefly discuss the content of the above conjecture, deferring a more detailed discussion of the first two points to section 3.5. In that section, we describe the rank 2 case only. For higher rank, we have to also consider the situation where three surfaces can intersect transversally.[6] At such a point of intersection, called a triple point, the three intersecting surfaces have local equation $xyz = 0$. As part of the argument in section 3.5, we blow up a point where two surfaces intersect, at which the intersecting surfaces have local equation $xy = 0$, so our construction will not apply at a triple point. To handle triple points, we simply supplement the argument in section 3.5.1 by noting that a complex structure deformation will keep a point to be blown up distinct from any of the triple points.

[6] Since four or more surfaces in a threefold cannot intersect nontrivially and transversally, we only need to consider intersections of three surfaces at a time.

JHEP04(2018)103

1. Using a combination of complex structure and Kähler deformations, it is possible to map a 3-fold containing a ruled surface over a genus g to a 3-fold containing a Hirzebruch surface. We defer a detailed discussion to section 3.5.

2. In all examples that we have investigated, we have been able to bypass non-transverse intersections in one of two ways: either by a complex structure deformation, or by a Kähler deformation in the form of a flop. The idea is that when we flop a curve (in S_1, say) which passes through a point of non-transversal intersection, the result is to blow up S_2 at that point, simplifying the singularity of the intersection curve and rendering it more transverse. We therefore assume that a combination of complex and Kähler deformations will always suffice to produce a 3-fold containing transversally intersecting surfaces S_i.

3. We prove in appendix A.2 that if $p > p_{\max}(n)$ there are infinitely many generators for rational curves. The presence of infinitely many generators is expected to indicate the presence of an infinite dimensional global symmetry group. An example of this is dP_9 (note $p_{\max}(1) = 7$), in which case the symmetry group permuting these generators is the affine E_8 Weyl group. In such a case, the Weyl group is infinite dimensional, and can be interpreted as a finite symmetry group of a 6d theory viewed from the 5d perspective. As we discussed above, geometries associated to 6d theories are not shrinkable. Since a CFT should not have an infinite dimensional global symmetry group, we claim that surfaces S_i with an infinite number of Mori cone generators cannot be building blocks for 5d SCFTs and are thus excluded.

3.4 Consistency conditions for shrinkable 3-folds

The condition that S is contained in a CY 3-fold imposes constraints on the curves of intersection of the components of S, which will be exploited in a crucial way in our classification program.

Let S_1 and S_2 be two smooth surfaces glued along a curve $C = S_1 \cap S_2$. Now suppose that $S_1 \cup S_2$ is contained in a 3-fold X, and that the intersection of S_1 and S_2 is transverse in X. Then the normal bundle of C in X is given by $N_{C,X} = N_{C,S_1} \oplus N_{C,S_2}$. The Calabi-Yau condition then implies

$$C^2_{S_1} \oplus C^2_{S_2} = 2g - 2, \tag{3.2}$$

where g is the genus of C and the subscripts on the right-hand side denote the irreducible surface in which the self-intersection takes place. The gluing curves must satisfy the adjunction formula for each surface S_i:

$$(K \cdot C)_{S_i} + C^2_{S_i} = 2g - 2, \tag{3.3}$$

where K_{S_i} is the canonical class of the surface S_i. For the rank 2 case, which is the primary focus of this paper, we argue in section 4.2 that it suffices for our classification to assume that $g = 0$.

Suppose a compact connected holomorphic surface S satisfies the above constraints on its curves of intersection. These constraints immediately imply that a CY 3-fold can be found containing a neighborhood in S of the curves of intersection (for example, the total space of the normal bundle of $S_1 \cap S_2$ in X works, as the complement of $S_1 \cap S_2 \subset S$ is smooth). Moreover, we can also find local CY 3-folds containing the complement of the intersection curves $S_1 \cap S_2$ in S (for example, just take the total space of the canonical bundle as before). Therefore, it seems reasonable to expect that above two types of local models can be glued to form a local model of a CY 3-fold. In other words, given smooth holomorphic surfaces S_1 and S_2 glued along a smooth curve C and satisfying (3.2), a smooth CY 3-fold X can be found containing $S = S_1 \cup S_2$. While we have not proven that such an X can always be found if (3.2) and (3.3) are satisfied, these conditions are consistent with all known examples and it is presumably not too difficult to rigorously prove this.

We emphasize here that the above gluing condition is a local condition that has no bearing on the overall topology of the surface S, and therefore permits a variety of interesting configurations. In principle there is nothing preventing, for example, gluing two surfaces together along multiple irreducible curves. Another interesting configuration involves two curves belonging to a single surface S_i being glued together. However, we will see that the only gluing configurations which play a role in the rank 2 classification are pairwise transverse intersections between the irreducible components S_1 and S_2.

The above discussion plays an essential role in our classification because we do not need to actually construct X to proceed; rather, we only require the existence of X and the existence of a surface S can be used as a proxy for the existence of a local 3-fold. Thus the problem of classifying shrinkable 3-folds can be reduced to the problem of classifying embeddable, shrinkable surfaces S.

A simple example: $S = \mathbb{F}_0 \cup \mathbb{F}_2$. An illustrative example of this construction is a simple complex surface $S = S_1 \cup S_2$ with $S_1 = \mathbb{F}_0, S_2 = \mathbb{F}_2$ as depicted in figure 2. Our rank 2 ansatz gives us

$$J^3 = S_1^3\phi_1^3 + S_2^3\phi_2^3 + 3\phi_1\phi_2(J \cdot S_1 \cdot S_2) = K_{S_1}^2\phi_1^3 + K_{S_2}^2\phi_2^3 - 3\phi_1\phi_2 \mathrm{vol}(S_1 \cap S_2). \tag{3.4}$$

The first order of business is to determine an appropriate gluing. Gluing these two surfaces together requires us to identify an irreducible, smooth curve $C = S_1 \cap S_2$ belonging to the Mori cone of both surfaces, satisfying (3.2). In the case of Hirzebruch surfaces $\mathbb{F}_{n_i}$, the Mori cones are the positive linear spans $\langle E_i, F_i \rangle$, where the curve classes satisfy the intersections $F_i^2 = 0, E_i \cdot F_i = 1, E_i^2 = -n_i$, so the range of possibilities is severely restricted. The gluing condition (3.2) implies that the self intersection of one of the two gluing curves must be negative. Since the curve E is the unique rational curve with negative self intersection [28], it therefore follows that we must select $C_{S_i} = E_i$ for one of the two surfaces, say $C_{S_2} = E_2$. The other curve must then satisfy

$$C_{S_1}^2 = 0. \tag{3.5}$$

As a trial solution let us take $C_{S_1} = aF_1 + bE_1$, so that $C_{S_1}^2 = 2ab = 0$. Therefore, either $a = 0$ or $b = 0$. From the adjunction formula (3.3), we know that $(C \cdot E_1 + C \cdot F_1)_{S_1} = a + b = 1$, and therefore the remaining nonzero coefficient must be set equal to unity. To

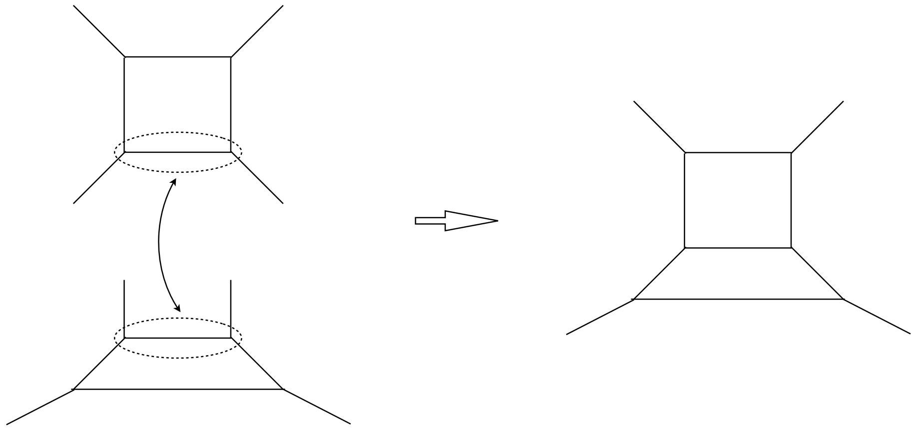

Figure 2. Example of a gluing construction of the Kähler surface $S = \mathbb{F}_0 \cup \mathbb{F}_2$. The gluing curves in both surfaces, C_1, C_2, are encircled by dashed lines in the left figure. The final geometry (on the right) is the result of identifying these two curves subject to the conditions described in section 3.

be concrete, we choose

$$C_{S_1} = F_1, \quad C_{S_2} = E_2. \tag{3.6}$$

Now that we have constructed the surface S, we must check that the local 3-fold X associated to this surface is shrinkable. We parametrize a Kähler class J as follows:

$$J = \phi_1[\mathbb{F}_0] + \phi_2[\mathbb{F}_2], \tag{3.7}$$

where $[\mathbb{F}]$ is the class associated to the 4-cycle $\mathbb{F} \subset X$. The Mori cone of X is the union of the Mori cones of the component surfaces S_i, namely the positive span $\langle E_1, E_2, F_2 \rangle$ (we omit F_1 because the gluing identifies F_1 and E_2.) Therefore, the shrinkability condition (3.1) implies

$$(\mathrm{vol}(E_1), \mathrm{vol}(E_2), \mathrm{vol}(F_2)) = (2\phi_1 - \phi_2, 2\phi_1, -\phi_1 + 2\phi_2) \geq 0. \tag{3.8}$$

Since that the above conditions can be satisfied for a nontrivial set of Coulomb branch parameters ϕ_i, we conclude that the geometry X corresponds to a 5d SCFT on the Coulomb branch.

3.5 Geometry of physical equivalences

In this section we discuss some important types of physical equivalences upon which our classification relies. Many of these equivalences identify 3-folds related by geometric transitions, i.e. maps between smooth geometries which involve passing through an intermediate singularity. Another type of physical equivalence identifies 3-folds related by a "large" change in the complex structure of non-dynamical modes, which interpolates between two singular geometries — this is a Hanany-Witten transition [29]. We illustrate these two types of maps in turn.

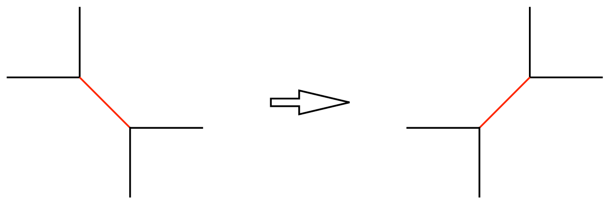

Figure 3. A local illustration of a flop transition $X \to X'$ between two CY 3-folds. The red lines in both diagrams correspond to the -1 curves in (respectively) X and X'.

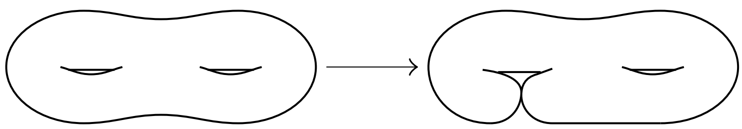

Figure 4. A genus $g = 2$ Riemann surface degenerating into a $g = 1$ Riemann surface with a nodal singularity as the result of identifying two points. By identifying g pairs of points in this manner, it is possible for a smooth curve of genus g to degenerate into a rational curve with g nodal singularities.

3.5.1 Geometric transitions

Flop transitions. One of the simplest and most thoroughly studied types of geometric transitions is a *flop transition*, which is a topology-changing transition $X \to X'$ between two 3-folds X, X' that is in practice typically realized by blowing down a -1 curve $C \subset X$ and blowing up a different -1 curve $C' \subset X'$ (see figure 3). A flop is a birational map $X \dashrightarrow X'$ which is an isomorphism away from curves C, C', with $K_X \cdot C = K_{X'} \cdot C' = 0$. If C and C' are both isomorphic to $\mathbb{P}^1$, the flop is called a simple flop. Simple flops were classified in [30].

In field theoretic terms, a flop transition corresponds to a continuous change of the mass of a particular state in the matter hypermultiplet from positive to negative values; this change corresponds to a singular phase transition on the Coulomb branch.

Genus reduction. We saw in section 3.3 that the S_i can be ruled surfaces over higher genus curves as well as genus 0. Here we argue that by our notion of physical equivalences we can restrict to $g = 0$ using geometric transitions. This can be obtained by composing a complex structure deformation of a surface S_i with a flop transition. This provides a map from a ruled surface over a curve of genus g to a self-glued Hirzebruch surface.

This type of geometric transition is particularly important because it exhibits the non-normalizable Kähler moduli of the local 3-fold defined by a ruled surface over a curve of genus g as blowup parameters of the 3-fold defined by a self-glued surface $\mathrm{Bl}_{2g}\mathbb{F}_n$. While we have not proven that the transition can always be achieved in the higher rank case due to the requirement that additional compact surfaces remain glued throughout the transition, we nevertheless believe this construction can be extended to higher rank surfaces with at most minor modifications.

Before giving a detailed description of this geometric transition, we recall that by the irreducibility of the moduli space $\overline{M}_g$ of stable curves of genus g the complex structure of

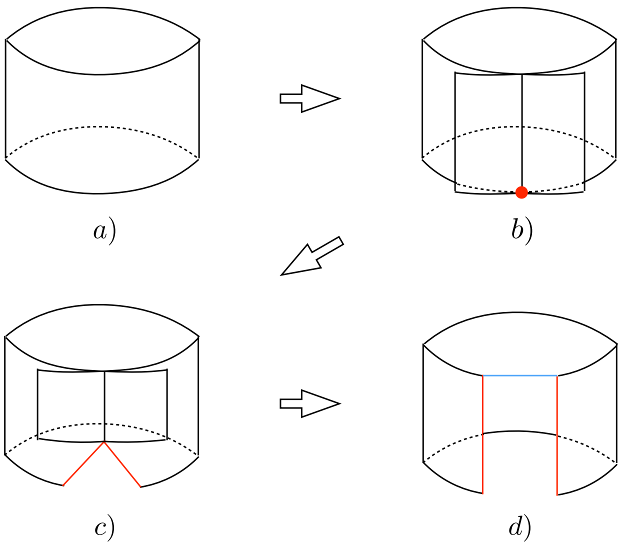

Figure 5. A transition from a ruled surface over a $g = 1$ curve to a Hirzebruch surface. The red point in the second figure is a blowup point on a nodal curve and the red lines in the third figure are the exceptional curves. Two proper transforms of the fiber F in a blown up Hirzebruch surface are glued together along the nodal curve.

a smooth curve C of genus g can be degenerated to a rational curve C_0 with g nodes (see figure 4.) The curve C_0 can be constructed directly by identifying g pairs of points of $\mathbb{P}^1$. Note that this construction immediately extends to give a degeneration of a ruled surface S over C to a ruled surface S_0 over the singular curve C_0. Conversely, the degeneration of the ruled surface can be described by starting with $\mathbb{P}^1$-bundle over $\mathbb{P}^1$ (i.e. a Hirzebruch surface $\mathbb{F}_n$) and identifying g pairs of fibers $F \subset \mathbb{F}_n$.

However, this description of S_0 is not completely satisfactory, as S_0 cannot be embedded into a CY 3-fold for the following reason. Let $F \subset S_0$ be one of the singular fibers obtained by identifying g pairs of fibers. Locally, S_0 has two branches near F with equation $xy = 0$ (pulled back from the local equation $xy = 0$ of a node of C_0). Being a fiber, F has self-intersection 0 in each branch, So if S_0 were contained in a smooth threefold, the normal bundle of F would be $\mathcal{O}_F \oplus \mathcal{O}_F$. Fortunately, the geometric transition naturally rectifies this problem by introducing blowups, in a manner which we describe below.

Consider again the degeneration point of view, which can be described by a holomorphic map $\pi : \mathcal{S} \to \Delta$. Here $\mathcal{S}$ is a smooth[7] threefold, Δ is a disk, $\pi^{-1}(0) \simeq S_0$, and $\pi^{-1}(t)$ is diffeomorphic to S for $t \neq 0$. We now pick a point $p \in F \subset S_0 \subset \mathcal{S}$ and blow up p to get $\phi : \widetilde{\mathcal{S}} \to \mathcal{S}$. Via $\pi \circ \phi$ we can view $\widetilde{\mathcal{S}}$ as a family over Δ. However, $\widetilde{\mathcal{S}}$ and $\mathcal{S}$ are isomorphic over $\Delta - 0$, so this gives another degeneration of S. The singular limit is $(\pi \circ \phi)^{-1}(0)$, which we now describe.

[7] Requiring $\mathcal{S}$ to be smooth is not a problem; its local equation near a point of F can be taken as $xy = t$, which is smooth. This is the same local calculation which shows that $\overline{M}_g$ is smooth at the nodal curves (in the orbifold sense).

JHEP04(2018)103

Blowing up a point p in a smooth threefold creates an exceptional divisor E isomorphic to $\mathbb{P}^2$, and blows up S_0 to a surface $\widetilde{S_0}$. We have $(\pi \circ \phi)^{-1}(0) = \widetilde{S}_0 \cup \mathbb{P}^2$. It remains to describe $\widetilde{S}_0$ and how $\mathbb{P}^2$ is attached to it.

Since S_0 has local equation $xy = 0$ at p, the exceptional curve of $\widetilde{S}_0 \to S_0$ has $xy = 0$ as its equation. In this latter instance, the equation $xy = 0$ is understood as a homogeneous equation in the exceptional $\mathbb{P}^2$ of the blown-up threefold. In other words, $\mathbb{P}^2$ meets $\widetilde{S_0}$ in two intersecting projective lines L, L'; each of these $\mathbb{P}^1$'s can be thought of as arising from the blowup of p in a corresponding branch of S_0 near p.

The point of intersection $q = L \cap L'$ also intersects the proper transform $\widetilde{F}$ of the original singular fiber F. The curve $\widetilde{F}$ is still singular in $\widetilde{S_0}$ and still has two branches in a local description, but now the blowup has reduced the self-intersection from 0 to $\widetilde{F}^2 = -1$ in each branch. So if $\widetilde{S_0}$ is contained in a smooth threefold, then the normal bundle of $\widetilde{F}$ is $\mathcal{O}_F(-1) \oplus \mathcal{O}_F(-1)$ and the threefold can be Calabi-Yau!

We can apply this construction to all of the g singular fibers. Since $\widetilde{F}$ has self-intersection -1 in each branch, we can view it as the gluing of a pair of exceptional $\mathbb{P}^1$'s. Therefore the resulting $\widetilde{S}_0$ is a blown up Hirzebruch surface with g pairs of exceptional curves identified. Each singular fiber consists of a double curve with self-intersection -1 in each branch, glued at a common point q to curves L, L' of self-intersection -1 in each of the respective local branches (the surface $\widetilde{S}_0$ is smooth along $L \cup L' - \{q\}$).

In the degeneration described above, we also need to attach g copies of $\mathbb{P}^2$. However, we are only concerned with the rank 2 case, so in our examples these $\mathbb{P}^2$'s can replaced by noncompact cycles containing $L \cup L'$ and safely ignored.

The final step is to flop the g curves $\widetilde{F}_1, \dots \widetilde{F}_g$, where we have added a subscript to $\widetilde{F}$ to distinguish these curves. Let us investigate the birational transform of $\widetilde{S_0}$ after the flops. When the curves $\widetilde{F}_i$ are contracted, the points of intersection $q_i = L_i \cap L'_i$ become conifolds. When we complete the flops, new $\mathbb{P}^1$'s appear in place of the q_i and the curves L_i, L'_i get separated. These curves become identified with fibers of a ruled surface over the desingularization $\widetilde{C}_0$ of C_0, the fibers over the pairs of points of $\widetilde{C}_0$ which get identified to form a node of C_0. Since $\widetilde{C}_0$ is isomorphic to $\mathbb{P}^1$, the result is a Hirzebruch surface in general with blowups.

An example of genus reduction: $G_2 + N_{\mathbf{F}}\mathbf{F}$. An illustrative example of complex deformations that exchange ruled surfaces over a curve of genus $g > 0$ for self-glued Hirzebruch surfaces blown up at $2g$ points is the family of shrinkable 3-folds engineering $G_2 + N_{\mathbf{F}}\mathbf{F}$, as described in [31].

We begin by recalling the form of the gauge theoretic 1-loop prepotential for $G_2 + N_{\mathbf{F}}\mathbf{F} + N_{\mathbf{adj}}\mathbf{adj}$:

$$\begin{aligned} 6\mathcal{F}_{\text{1-loop}} &= (8 - 8N_{\mathbf{F}} - 8N_{\mathbf{adj}})\phi_1^3 + (8 - 8N_{\mathbf{adj}})\phi_2^3 \\ &\quad + 3\phi_1\phi_2[(6 + 3N_{\mathbf{F}} - 6N_{\mathbf{adj}})\phi_1 + (8N_{\mathbf{adj}} - N_{\mathbf{F}} - 8)\phi_2]. \end{aligned} \tag{3.9}$$

We set $N_{\mathbf{adj}} = 0$ to be consistent with $\mathcal{N} = 1$ supersymmetry. By giving a nonzero value to mass parameters in the hypermultiplet contributions to the prepotential, one can study the RG flow from $N_{\mathbf{F}}$ to $N_{\mathbf{F}} - 1$ flavors. In order to decouple a massive hypermultiplet, the

g	a	(n_1, n_2)
0	1	$(8, 0)$
1	0	$(9, 1)$
2	2	$(10, 0)$
3	1	$(11, 1)$
4	0	$(12, 2)$
4	3	$(12, 0)$
5	2	$(13, 1)$
6	4	$(14, 0)$

Table 2. Shrinkable surfaces $S = \mathbb{F}^g_{n_1} \cup \mathbb{F}_{n_2}$ engineering $G_2 + N_{\mathbf{F}}\mathbf{F}$ gauge theories. The surface $\mathbb{F}^g_{n_1}$ is a ruled surface over a curve E with $g(E) = N_{\mathbf{F}}$ and satisfying $E^2 = -n_1$. The gluing curve $C = S_1 \cap S_2$ is given by $C_{S_1} = E$ and $C_{S_2} = aF + 3H$. The fiber classes are given by are $f_i = F_i$.

theory must pass through three phase transitions. These four phases have the following prepotentials (we omit mass parameter terms for brevity):

$$
\begin{aligned}
6\mathcal{F}^{(1)} &= (8 - 8N_{\mathbf{F}})\phi_1^3 + 8\phi_2^3 + 3\phi_1\phi_2[\phi_1 (3N_{\mathbf{F}} + 6) - \phi_2 (N_{\mathbf{F}} + 8)] \\
6\mathcal{F}^{(2)} &= (16 - 8N_{\mathbf{F}})\phi_1^3 + 7\phi_2^3 + 3\phi_1\phi_2[\phi_1 (3N_{\mathbf{F}} + 2) - \phi_2 (N_{\mathbf{F}} + 6)] \\
6\mathcal{F}^{(3)} &= (15 - 8N_{\mathbf{F}})\phi_1^3 + 8\phi_2^3 + 3\phi_1\phi_2[\phi_1 (3N_{\mathbf{F}} + 3) - \phi_2 (N_{\mathbf{F}} + 7)] \\
6\mathcal{F}^{(4)} &= 6\mathcal{F}^{(1)}_{N_{\mathbf{F}}-1}.
\end{aligned}
\tag{3.10}
$$

We determine a shrinkable Kähler surface S that engineers this theory by setting the triple intersection polynomial (3.4) equal to prepotential (3.9) and demanding that there exist an intersection matrix $f_i \cdot S_j = (A_{G_2})_{ij}$ for some choice of fiber classes $f_i \subset S_i$. Restricting the possible building blocks to be blowups of rational and ruled surfaces *without self-gluing*, the only solutions to these conditions are the geometries shown in table 2. For all of these surfaces we have $9n_2 + 6a = 2g - 2 + n_1$, as required by (3.2). A key point here is that the surface S_1 must be a ruled surface of a curve of genus $g = N_{\mathbf{F}}$. This is precisely the geometric setup described in [31].

We now demonstrate that we can engineer the same family of theories described above by replacing S_1 with the surface $S_1' = \mathrm{Bl}_{2g}\mathbb{F}^{(g)}_{n_1}$, where again $g = N_{\mathbf{F}}$ and the superscript notation indicates S_1' is obtained by identifying g pairs of exceptional curves in $\mathrm{Bl}_{2g}\mathbb{F}_{n_1}$ (i.e. self-gluing; see appendix A.1 for some mathematical background.) This shrinkable surface not only reproduces the prepotential (3.9) and G_2 Cartan matrix, but also has the merit of exhibiting the RG flow (3.10) in a very natural manner. The four phases, related by flops, have the following geometries:

1. $\mathrm{Bl}_{2g}\mathbb{F}^{(g)}_{8-g} \cup \mathbb{F}_{n_2}$, where the blowups are all at special points[8] $F \cap E$.

[8] Note that while we consider blowups at special points $F \cap E \subset \mathbb{F}_n$ here for convenience, since we do not introduce any additional irreducible curves with self intersection less than -1, we can without loss of

2. $\mathrm{Bl}_{2g-2}\mathbb{F}_{8-g}^{(g-1)} \cup \mathrm{Bl}_1\mathbb{F}_{n_2}$.

3. $\mathrm{Bl}_{2g-1}\mathbb{F}_{8-g}^{(g-1)} \cup \mathbb{F}_{n_2\pm 1}$.

4. $\mathrm{Bl}_{2g-2}\mathbb{F}_{9-g}^{(g-1)} \cup \mathbb{F}_{n_2\pm 1}$.

The first phase is $\mathrm{Bl}_{2g}\mathbb{F}_{8-g}^{(g)} \cup \mathbb{F}_{n_2}$, where we introduce g self-gluings of $\mathrm{Bl}_{2g}\mathbb{F}_p$ along the pairs of exceptional divisors $X_{2i}, X_{2i-1}, i = 1, \ldots, g$,[9] the where the gluing curve is defined by $C_{S_1} = E - \sum_{i=1}^{2g} X_i$ and $C_{S_2} = F + 3H$, so that $a = 1$ in the notation adopted in the caption of table 2. Since the canonical class[10] is given by $K_{\mathbb{F}_{8-g}} + 2\sum_{i=1}^{N_\mathbf{F}}(X_{2i-1} + X_{2i})$, we find a perfect match with the first line of (3.10), using the adjunction relation $9n_2 + 6 - (8+g) = 2g-2$.

We now describe the flop to the second phase. The matter curve with volume $2\phi_1 - \phi_2$ which shrinks is one of the self-gluing exceptional divisors, say X_1. Blowing down X_1 forces us to also blow down X_2. We can blow up $\mathbb{F}_{n_2}$ at a generic point $F_2 \cap H_2$ if we eventually want to decrease n_2 to $n_2 - 1$, or at a special point $F_2 \cap E_2$ if we want to increase n_2 to $n_2 + 1$ in the third phase.

The geometry of the second phase is $\mathrm{Bl}_{2g-2}\mathbb{F}_{8-g}^{(g-1)} \cup \mathrm{Bl}_1\mathbb{F}_{n_2}$, where $C_{S_1} = E - \sum_{i=1}^{2g-2} X_i$ and $C_{S_2} = aF + 3H - 2Y_1$. Since the blowup of $\mathbb{F}_{n_2}$ is at the double point of E introduced by gluing X_{2g-1} to X_{2g}, the coefficient of Y in C_{S_2} is -2.

The matter curve with volume $\phi_2 - \phi_1$ which we blow down is $F_2 - Y_1 \subset \mathrm{Bl}_1\mathbb{F}_{n_2}$. Because $F - Y_1$ meets C in one point, we must introduce an exceptional divisor Y_2 in the surface S_1, leading us to the third phase.

The geometry of the third phase is $\mathrm{Bl}_{2g-1}\mathbb{F}_{8-g}^{(g-1)} \cup \mathbb{F}_{n_2\pm 1}$, where $C_{S_1} = E - \sum_{i=1}^{2g-2} X_i - Y_2$. Concerning the gluing curve class $C \subset \mathbb{F}_{n_2\pm 1}$, there are two possible cases. In the case of a generic blowup, the proper transforms of $H, F \subset S_2$ are $H - Y_1, Y_1$, so we set $C_{S_2} = (a+1)F + 3H$, where now $H_{S_2}^2 = n_2 - 1$. It follows that $C_{S_2}^2 = ((a+1)F + 3H)_{S_2}^2 = 6(a+1) + 9(n_2 - 1) = 3g + 3$, which is a nontrivial check that this geometry is consistent with the phase structure of the G_2 theory. On the other hand, in the case of a special blowup, the difference is that the proper transform of $H \subset S_2$ is H, so that $C_{S_2} = H + (a-2)F$, where now $H_{S_2}^2 = n_2 + 1$. We again confirm that $C_{S_2}^2 = ((a-2)F + 3H)_{S_2}^2 = 6(a-2) + 9(n_2+1) = 3g+3$.

In order to reach the fourth and final phase, the matter curve with volume ϕ_1 which we blow down is $F - Y_2 \subset S_1$. The geometry of the fourth phase is $\mathrm{Bl}_{2g-2}\mathbb{F}_{9-g}^{(g-1)} \cup \mathbb{F}_{n_2\pm 1}$. Keeping in mind the previous identity $n_1 = 8 - g$ along with the fact that we blow down

generality view a blowup of $\mathbb{F}_n$ at p special points as a blowup of $\mathbb{F}_{n+p}$ at p general points. We explore the distinction between special and general points in more depth in section 4.2.

[9]Here and in the sequel, we use the notation X_i to denote the exceptional divisor of the i-th blowup, since we reserve the more standard notation E_i for sections of Hirzebruch surfaces.

[10]More precisely, the dualizing sheaf of the singular surface $\mathrm{Bl}_{2g}\mathbb{F}_{8-g}^{(g)}$, pulled back to its natural desingularization $\mathrm{Bl}_{2g}\mathbb{F}_{8-g}$.

JHEP04(2018)103

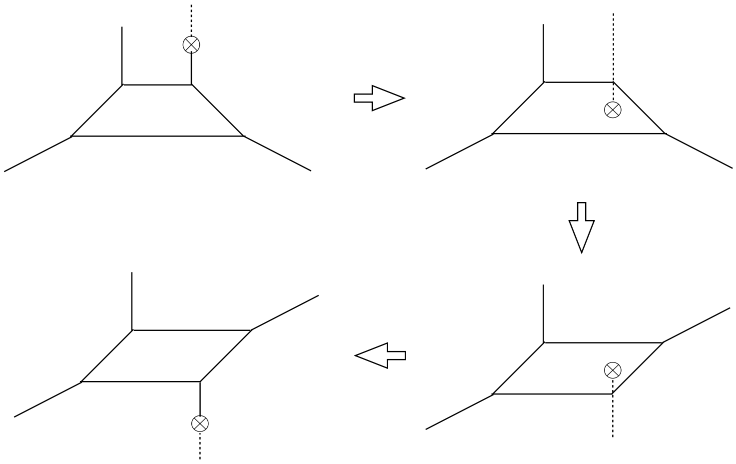

Figure 6. Hanany-Witten transition from $\mathbb{F}_2$ to $\mathbb{F}_0$. The $\otimes$ symbol denotes the location of a transverse $(0,1)$ 7-brane, and the dashed line denotes the location of the 7-brane monodromy cut.

the curve $F - Y_2 \subset S_1$, we compute the canonical class:

$$\begin{aligned} K_{S_1} &= -2H + (n_1 - 2)F + 2\sum_{i=1}^{g-1}(X_{2i-1} + X_{2i}) + Y_2 \\ &= -2H + ((n_1+1) - 2)F + 2\sum_{i=1}^{g-1}(X_{2i-1} + X_{2i}). \end{aligned} \tag{3.11}$$

Note also that the self-intersection of $H \subset S_1$ shifts from $8-g$ to $9-g$.

3.5.2 Hanany-Witten transitions and complex deformations

The next type of transition we will discuss is a *complex structure deformation.* In particular, we concern ourselves with two types of complex structure deformations that preserve the rank of the 3-fold. The first type of complex structure deformation is a Hanany-Witten (HW) transition [29]. This type of transition is most easily understood in the setting of (p,q) 5-brane webs, and involves interchanging the relative position of a (p,q) 7-brane and a (p,q) 5-brane. After the transition, despite the fact that the brane webs look different, in the low-energy decoupling limit the corresponding SCFTs describe the same physics up to decoupled free sectors. The example displayed in figure 6 describes a geometric (or HW) transition from a local 3-fold X with $S = \mathbb{F}_2$ to another 3-fold X' with $S' = \mathbb{F}_0$. Therefore, X and X' are physically equivalent.

This example can be geometrically described as follows: $\mathbb{F}_2$ is physically equivalent to $\mathbb{F}_0$ by a (non-normalizable) complex structure deformation. One way to see this is to first contract the curve E in $\mathbb{F}_2$ (with $E^2 = -2$) to an A_1 singularity, which can be identified with the quadric cone $x^2+y^2+z^2 = 0$ in $\mathbb{P}^3$. A complex structure deformation takes this to a smooth quadric surface (e.g. $w^2+x^2+y^2+z^2 = 0$), which is isomorphic to $\mathbb{P}^1 \times \mathbb{P}^1 = \mathbb{F}_0$.

Another type of complex structure deformation involves changing special type blow ups (i.e. blow ups on top of blow ups) to generic blow ups, where the blow up points are

JHEP04(2018)103

$S = S_1 \cup S_2$	G
$(\mathbb{F}_6 \cup \mathrm{dP}_4)^*$	$\mathrm{Sp}(2)_{\theta=0} + 3\mathbf{AS}$
$(\mathbb{F}_2 \cup \mathrm{dP}_7)^*$	$\mathrm{SU}(3)_4 + 6\mathbf{F}$ $\mathrm{Sp}(2) + 4\mathbf{F} + 2\mathbf{AS}$ $G_2 + 6\mathbf{F}$
$(\mathrm{Bl}_9\mathbb{F}_4 \cup \mathbb{F}_0)^*$	$\mathrm{SU}(3)_{\frac{3}{2}} + 9\mathbf{F}$ $\mathrm{Sp}(2) + 8\mathbf{F} + \mathbf{AS}$
$(\mathrm{Bl}_{10}\mathbb{F}_6 \cup \mathbb{F}_0)^*$	$\mathrm{SU}(3)_0 + 10\mathbf{F}$ $\mathrm{Sp}(2) + 10\mathbf{F}$

Table 3. Rank 2 geometries with maximal M. In the above table, S is the rank 2 Kähler surface, while G is the corresponding gauge theory description. These geometries denoted as $(\cdot)^*$ are not shrinkable and correspond to 5d KK theories.

not on top of one another, unless the blow up curve is part of the identification between S_i's. We will show that in the rank 2 case this can be avoided and we can always assume general point blow ups.

4 Classifications

Let $S = \cup S_i$ be a connected union of surfaces contained in a CY 3-fold X. We classify all shrinkable S for rank 1 and rank 2 according to the conjectures and algorithm described in section 3. We first summarize the rank 1 and rank 2 classification results and in the next two subsections we present details of the classification.

All rank 1 and rank 2 shrinkable geometries (or SCFTs) belong to one or more families of geometric RG-flows, and the geometries in each RG-flow family are related by rank-preserving mass deformations (or blowdowns of -1 curves in geometric terminology), up to physical equivalence. The ideas of geometric RG-flow and rank-preserving mass deformations will be discussed later. Based on these ideas, we can start from a "top" geometry, which corresponds to a 5d CFT or a 6d CFT on a circle (equivalently, a 5d Kaluza-Klein (KK) theory), and obtain all other geometries in the same family by a finite sequence of geometric transitions or mass deformations. This UV geometry is at the top of the RG-flow in a given family and can therefore be a representative of the entire RG-flow family. We conjecture that all descendants of the top UV geometry engineer 5d SCFTs. When shrinkable, the top UV geometry itself also engineers a 5d SCFT.

For rank 1 geometries, we have only one RG-flow family corresponding to a local elliptic 3-fold defined by the del Pezzo surface dP_9. All other rank 1 geometries are obtained by blowing down exceptional curves. The RG-flow family of dP_9 involves other del Pezzo surfaces dP_n with $n \leq 8$ and a Hirzebruch surface $\mathbb{F}_0$; it is believed that these are the complete set of geometries leading to rank 1 5d SCFTs.

JHEP04(2018)103

Similarly, the top rank 2 geometries are summarized in table 3. We have identified four geometric RG-flow families represented by these top geometries. These geometries are not shrinkable; rather, we expect that these geometries have 6d UV completions and thus they engineer 5d KK theories. However, their descendants, obtained by blowing down -1 curves, are shrinkable and therefore give rise to 5d SCFTs. For example, the geometry $\mathrm{Bl}_9\mathbb{F}_4 \cup \mathbb{F}_0$ is ruled out from our CFT classification because its building block $\mathrm{Bl}_9\mathbb{F}_4$ has an infinite number of Mori cone generators as explained in appendix A.2.1, violating our criterion in section 3.3. However, a geometric RG-flow from this geometry by blowing down an exceptional curve as well as a number of flop transitions leads to the geometry $\mathrm{Bl}_8\mathbb{F}_3 \cup \mathrm{dP}_1$ which is now shrinkable and engineers a 5d SCFT. Similarly, other geometries in table 3 are associated to KK theories, but their descendants are shrinkable. Therefore, we find that all rank 1 and 2 smooth 3-fold geometries engineering 5d SCFTs are mass deformations of 5d KK theories. See section 4.2 for further discussion.

This result confirms the existence of many new rank 2 SCFTs predicted in [13] which are listed in table 1. For example, the $\mathrm{SU}(3)_7$ gauge theory is predicted to exist in table 1a. This theory turns out to have a geometric realization as $\mathbb{F}_0 \cup \mathbb{F}_8$ which is a descendant of $\mathbb{F}_2 \cup \mathrm{dP}_7$. This implies that the gauge theory approach in [13], which analyzes the magnetic monopole and perturbative BPS spectrum, is quite powerful and capable of predicting new interacting 5d SCFTs.

Our study also reveals that there are no smooth 3-fold geometries associated to the following gauge theories:

$$\begin{aligned} &\mathrm{SU}(3)_{\frac{1}{2}} + 1\mathbf{Sym}\,, \\ &\mathrm{SU}(3)_7 + 2\mathbf{F} \;\to\; \mathrm{SU}(3)_{\frac{15}{2}} + 1\mathbf{F} \;\to\; \mathrm{SU}(3)_8\,. \end{aligned} \tag{4.1}$$

These theories are expected to have interacting CFT fixed points by the perturbative gauge theory analysis in [13]. See table 1a. The SCFT of the first gauge theory indeed exists — this theory is a mass deformation of the $\mathrm{SU}(3)_0$ theory with $N_{\mathbf{Sym}} = 1, N_{\mathbf{F}} = 1$ whose brane construction is given in [32, 33]. Our study of smooth 3-folds fails to capture this theory. The reason for this failure is because the corresponding geometry involves a 'frozen' singularity. For example, the brane construction in [32, 33] contains $\mathrm{O7}^+$-planes; indeed, constructions involving $\mathrm{O7}^+$ planes are dual to frozen singularities involving non-geometric monodromies and a fractional M-theory 3-form background as discussed in [14]. Therefore, we do not expect that our analysis can capture this type of singularity, and hence the geometric classification in this paper is incomplete in this sense. We nevertheless conjecture that our classification includes all 5d SCFTs coming from *smooth* Calabi-Yau threefolds which do not involve frozen singularities dual to brane constructions involving $\mathrm{O7}^+$ planes. In the following sections, we classify smooth rank 1 and rank 2 3-fold geometries engineering 5d SCFTs in their singular limits.

On the other hand, we predict that there are no SCFTs corresponding to three gauge theories belonging to the RG flow in the second line of (4.1). As we discuss in section 4.2, despite the fact that these gauge theories can be realized geometrically using our algorithm, they are shrinkable only when we attach a number of non-degenerate non-compact 4-cycles to the compact surface S. Introducing these non-compact 4-cycles entails non-normalizable Kähler deformations which in the field theory setting corresponds to introducing nonzero mass parameters. We find that these mass parameters cannot be set to zero in the CFT limit — at small nonzero values, the corresponding geometries develop at least one 2-cycle with negative volume and therefore their singular limits do not engineer well-defined CFT fixed points. This computation excludes the three gauge theories in the second line of (4.1) as possible candidates for interacting 5d SCFTs. This is also an indication that the classification criteria described in [13] are necessary, but not sufficient to identify 5d SCFT fixed points. The criteria of [13] must be modified to account for non-perturbative BPS states (such as instantons in gauge theories) in order to be both necessary and sufficient.

We also remark that a single 3-fold X can admit multiple gauge theory descriptions. This is possible because some geometries admit more than one distinct choice of fiber class associated to charged gauge bosons. The existence of multiple gauge theoretic descriptions corresponding to a single geometry suggests that the gauge descriptions are dual to one another. Starting with the "top" UV geometries in table 3, we predict the following dualities:

$$\begin{aligned}
&\mathrm{SU}(3)_{5-\frac{N_{\mathbf{F}}}{2}} + N_{\mathbf{F}}\mathbf{F} \cong \mathrm{Sp}(2) + N_{\mathbf{F}}\mathbf{F}\,, && N_{\mathbf{F}} \leq 10\\
&\mathrm{SU}(3)_{6-\frac{N_{\mathbf{F}}}{2}} + N_{\mathbf{F}}\mathbf{F} \cong \mathrm{Sp}(2) + 1\mathbf{AS} + (N_{\mathbf{F}}-1)\mathbf{F}\,, && 1 \leq N_{\mathbf{F}} \leq 9\\
&\mathrm{SU}(3)_{7-\frac{N_{\mathbf{F}}}{2}} + N_{\mathbf{F}}\mathbf{F} \cong G_2 + N_{\mathbf{F}}\mathbf{F} \overset{2\leq N_{\mathbf{F}}}{\cong} \mathrm{Sp}(2) + 2\mathbf{AS} + (N_{\mathbf{F}}-2)\mathbf{F}\,, && N_{\mathbf{F}} \leq 6
\end{aligned} \tag{4.2}$$

The first and the second dualities in (4.2) were conjectured already in [22] and in [13], respectively. So our construction provides concrete geometric evidence for these duality conjectures. On the other hand, the third duality is a new duality discovered by an explicit geometric construction in this section.

4.1 Rank 1 classification

We warm up by starting with rank 1, recovering the result that all rank 1 5d SCFTs are geometrically engineered by local 3-folds containing a del Pezzo surface. More precisely, our algorithm identifies del Pezzo surfaces as shrinkable, but also identifies additional shrinkable surfaces; however, each of these turns out to be physically equivalent to a del Pezzo surface.

Recall that a del Pezzo surface S is defined to be a smooth algebraic surface whose anticanonical bundle $-K_S$ is ample — this means that $-K_S \cdot C > 0$ for all effective curves $C \subset S$. The classification of del Pezzo surfaces is well known: S is either dP_n for $0 \leq n \leq 8$ or $\mathbb{P}^1 \times \mathbb{P}^1 = \mathbb{F}_0$. Such a surface satisfies (3.1) as well as $K_S^2 > 0$, so is shrinkable. We now set out to systematically classify rank 1 shrinkable surfaces up to physical equivalence.

To apply (3.1), we need to know K_S, the generators of the Mori cone of curves on S, and the intersection numbers of the curves in S. Our algorithm leads us to consider $\mathbb{P}^2$, $\mathbb{F}_n$, and their generic blowups.

$\mathbb{P}^2$ is del Pezzo, but it is instructive to check shrinkability anyway. For $\mathbb{P}^2$, the Mori cone is generated by the class ℓ of a line, $\ell^2 = 1$, and $K_{\mathbb{P}^2} = -3\ell$. So $K_{\mathbb{P}^2}^2 = 9 > 0$ and $K_{\mathbb{P}^2}\ell = -3 < 0$, so $\mathbb{P}^2$ is shrinkable.

JHEP04(2018)103

Next, we consider $\mathbb{F}_0$, $\mathbb{F}_1$ and $\mathbb{F}_{n\geq 2}$ separately. Since $\mathbb{F}_1$ is the blowup of $\mathbb{P}^2$ at a point, $\mathbb{F}_1$ and its generic blowups are just the generic blowups of $\mathbb{P}^2$. Similarly, $\mathbb{F}_0$ is del Pezzo, and the blowup of $\mathbb{F}_0$ at a point is isomorphic to the blowup of $\mathbb{P}^2$ at two points [28]. So the possibilities for S can be reduced to either generic blowups of $\mathbb{P}^2$, or $\mathbb{F}_{n\geq 2}$.

As usual, we denote by dP_n the blowup of $\mathbb{P}^2$ at general points $p_1, \ldots, p_n$. Let $X_1, \ldots, X_n$ denote the corresponding exceptional $\mathbb{P}^1$'s,[11] and we let ℓ denote the class of the total transform in dP_n of a line in $\mathbb{P}^2$. The intersection numbers are

$$\ell^2 = 1, \quad X_i \cdot X_j = -\delta_{ij}, \quad \ell \cdot X_i = 0 \tag{4.3}$$

and $K_{\mathrm{dP}_n} = -3\ell + \sum_{i=1}^n X_i$. Then $K^2_{\mathrm{dP}_n} = 9 - n > 0$ for $n \leq 8$.

We first observe that dP_n is not shrinkable for $n \geq 9$. To see this, we simply observe that $K^2_{\mathrm{dP}_n} \leq 0$ for $n \geq 9$ which implies that the string tensions are not positive.

Again, we can cite known results simply say that dP_n is shrinkable for $n \leq 8$, but it is instructive to work out details without assuming this fact. We adopt a convenient shorthand to describe the generators of the Mori cone: any curve $C \subset \mathrm{dP}_n$ other than the X_i will project to a curve $D \subset \mathbb{P}^2$ of some degree $d > 0$. Let m_i be the multiplicity of D at p_i, so that $m_i = 0$ if $p_i \notin D$, $m_i = 1$ if p is a nonsingular point of D, $m_i = 2$ if p is a node or cusp of D, etc. Then the class of C is $d\ell - \sum_{i=1}^n a_i X_i$. It is customary to abbreviate this class as $(d; m_1, \ldots, m_n)$, as well as to omit any m_i which are zero. Then the Mori cone of dP_n is generated by the classes[12]

$$X_i,\ (1;1^2),\ (2,1^5),\ (3,2,1^6),\ (4,2^3,1^5),\ (5,2^6,1^2),\ (6;3,2^7) \tag{4.4}$$

up to permuting the order of the p_i. It follows from the adjunction formula (3.3) that each of the curve classes C in (4.4) satisfies $K_{\mathrm{dP}_n} \cdot C = -1$,[13] so dP_n is shrinkable.

Next, consider the Hirzebruch surfaces $S = \mathbb{F}_n$. Using the notation in appendix A.2, there are two disjoint toric sections E, H and the fiber class F. These classes satisfy

$$H^2 = n,\ E^2 = -n,\ H \cdot E = 0,\ H \cdot F = E \cdot F = 1,\ F^2 = 0,\ H = E + nF. \tag{4.5}$$

The canonical bundle of $\mathbb{F}_n$ is $K_{\mathbb{F}_n} = -2H + (n-2)F$ and so $K^2_{\mathbb{F}_n} = 8 > 0$. Furthermore, the Mori cone of effective curves is generated by E and F. While $K_{\mathbb{F}_n} \cdot F = -2 < 0$, we also have $K_{\mathbb{F}_n} \cdot E = n - 2$, which is strictly negative for $n < 2$, zero for $n = 2$, but strictly positive for $n > 2$. Thus $\mathbb{F}_2$ is shrinkable. However, as discussed in section 3, this is physically equivalent to $\mathbb{F}_0$. The same reasoning combined with the earlier observation that $\mathrm{Bl}_1\mathbb{F}_0 \simeq \mathrm{dP}_2$ shows that $\mathrm{Bl}_p\mathbb{F}_2$ is physically equivalent to dP_{p+1}.

In conclusion, all rank 1 shrinkable surfaces are physically equivalent to dP_n for some n or $\mathbb{F}_0$.

---

[11] As noted earlier, we reserve the more customary notation E for the curves on Hirzebruch surfaces described in appendix A.2.

[12] Strictly speaking, we have only written the Mori generators for $n = 8$. For $n < 8$, we modify (4.4) by removing those generators which need more than n exceptional divisors to define them. In addition, for $n = 1$, we include $(1; 1)$ as a generator.

[13] For $n = 1$, we also check that $K_{\mathrm{dP}_1} \cdot (\ell - X_1) = -2$.

4.2 Rank 2 classification

The main result of this paper is a full classification of shrinkable rank 2 geometries up to physical equivalence. We preface our result by arguing some further simplifying assumptions we make about the surface S in order to make the classification into a manageable problem.

Three simplifications. In this section we show that we can utilize the following three simplifying assumptions for classifying shrinkable rank 2 surfaces:

- $S_1 \cap S_2$ is an irreducible curve.
- $S_1 \cap S_2$ is a rational curve.
- The surfaces S_i are equal to $\mathbb{P}^2$ or Hirzebruch surfaces and their blowups at general points.

We now discuss these three simplifications in order.

First, we argue that in the case of a rank 2 surface $S = S_1 \cup S_2$, we can assume that S_1 is not glued to S_2 along multiple curves. Namely, there exists a single edge between two nodes. Suppose we glue two surfaces along C_1, C_2 with appropriate identifications. Since S_1 and S_2 should intersect transversally, we have $(C_1 \cdot C_2)_{S_1} = (C_1 \cdot C_2)_{S_2} = 0$. This means that C_1, C_2 do not intersect. We claim there always exists an effective curve $D = d_1 + d_2$ such that $\mathrm{vol}(D) \leq 0$. If $\mathrm{vol}(D) < 0$, then S is not shrinkable, so it suffices to consider the situation where $\mathrm{vol}(D) = 0$. But in that case, we will further show below that we can arrange for the curve D to be elliptic (i.e. $g(D) = 1$), which would contradict our conjectures. Therefore, the full surface is not shrinkable implying that we cannot glue two surfaces along two or more curves.

In order to show this, we first prove that there always exist curves $d_i \subset S_i$ with $K_{S_i} \cdot d_i \geq -2$ that intersect both C_1 and C_2. These classes d_1 and d_2 are identified as follows. First, if both C_1 and C_2 are not fiber classes, we can always find a curve d_1 satisfying these conditions among $\{F,\, F - X_i,\, H - X_i - X_j\}$[14] in $\mathrm{Bl}_p\mathbb{F}_n$, where X_i are exceptional curves associated to the blowups of $\mathbb{F}_n$ at p general points. When $n > 2$, $C_1 = E$, otherwise the volume of the curve E will be negative. Next, suppose C_1 or C_2 is a fiber class. This is possible only when $S_1 = \mathrm{Bl}_p\mathbb{F}_1$ or dP_n, otherwise the class E, which has $E \cdot C_1 \neq 0$ or $E \cdot C_2 \neq 0$, will have negative volume thus preventing the surface S from being shrinkable. In the case that $S_1 = \mathrm{Bl}_p\mathbb{F}_1$, when C_1 is a fiber class F_1, C_2 must be one of X_i's, due to the assumption of transversal intersection. Then we can take $d_1 = H - X_i$ with $H^2 = 1$. With any choice of d_1 given here, we find that $\mathrm{vol}(d_1) = m\phi_1 - n\phi_2$ with $m = 1, 2$ and $n \geq 2$ where $\phi_i \geq 0$. We can choose $d_2 \subset S_2$ in the same manner and then show that $\mathrm{vol}(d_2) = m'\phi_1 - n'\phi_2$ with $m' = 1, 2$ and $n' \geq 2$.

This proves $\mathrm{vol}(D) \leq 0$ for an effective curve $D = d_1 + d_2$. Now we will assume $\mathrm{vol}(C_i) \geq 0$ for all other curves C_i because otherise the surface is not shrinkable and already

[14]For general n we choose $d_1 = F - X_i$ if $C_1 = X_i$ or $C_2 = X_i$, otherwise $d_1 = F$. When $n = 2$ and $C_1 = X_1, C_2 = X_2$, we choose $d_1 = H - X_1 - X_2$.

ruled out. As already noted above, it is clear that the total surface is not shrinkable when $\mathrm{vol}(D) < 0$. Moreover, when $\mathrm{vol}(D) = 0$, i.e. when $m = m' = n = n' = 0$, the curves d_1 and d_2 are both fiber classes $F_i \subset S_i$. In this case, the curve F_1 and F_2 can be deformed so that $F_1 \cap C_i = F_2 \cap C_i$ for $i = 1, 2$. Then the curve $D = F_1 + F_2$ is the union of two rational curves intersecting in two points, hence elliptic. By further complex structure deformation if necessary, we can arrange that all fibers F_1 of S_1 meet all fibers F_2 of S_2 in two points, or in other words, that $S = S_1 \cup S_2$ is elliptically fibered.

We argue that we can deform the complex structure of X if necessary so that X is also elliptically fibered. To see this, let E be an elliptic fiber of S. Since E is part of an elliptic fibration of S, we have that $N_{E/S} \simeq \mathcal{O}_E$. Furthermore, $\det(N_{E/X})$ is trivial by the Calabi-Yau condition and the ellipticity of E. Then the normal bundle sequence

$$0 \to N_{E/S} \to N_{E/X} \to N_{S/X}|_E \to 0 \tag{4.6}$$

is identified with

$$0 \to \mathcal{O}_E \to N_{E/X} \to \mathcal{O}_E \to 0. \tag{4.7}$$

However, since $H^1(\mathcal{O}_E) \neq 0$, (4.7) generically does not split[15] and dim $H^0(N_{E/X}) = 1$. The uniqueness of a normal direction says that E moves in a 1-parameter family, enough deformations to fiber S but not enough to fiber X.

However, we can choose a complex structure deformation of X so that (4.7) splits, and then $N_{E/X} \simeq \mathcal{O}_E^2$. In this situation, E moves in two independent directions and fibers X.

This justifies our claim, hence S is not shrinkable. The same argument holds for cases with more than two edges (i.e. gluing curves) between S_1 and S_2. Therefore rank 2 geometries formed by two surfaces glued along two or more different curves are not shrinkable.

Second, we claim that the gluing curves must be rational. Suppose $C = S_1 \cap S_2$ has $g > 0$. In appendix A.2 we explain that we must have finitely many Mori cone generators in each S_i (which implies a bound on the number of blowups), hence we have finitely many Mori cone generators in $X \supset S = S_1 \cup S_2$. We argue that this implies $C^2_{S_i} \geq 0$ as follows. We assume $C^2_{S_i} < 0$ and derive a contradiction. Since $C^2_{S_i} + C \cdot K_{S_i} = 2g - 2 \geq 0$, we have $C \cdot K_{S_i} > 0$. Anticipating the next bulleted claim that the building blocks are generic blowups of Hirzebruch surfaces at a bounded number of points, we show in appendix A.2 that $C_{S_i} \cdot K_{S_i} > 0$ implies $C_{S_i} = E$. This is a contradiction, since $g > 0$. Although this argument is slightly circular in its current form depending as it does on the next bulleted claim, we believe that with further care we can independently justify $C^2_{S_i} \geq 0$. Furthermore, an extensive computer search has revealed no counterexamples.

Let us now return to the claim that the gluing curves are rational. Recalling equations (3.2) and (3.3), we have

$$C^2_{S_1} + C^2_{S_2} = C^2_{S_i} + K_{S_i} \cdot C = 2g - 2\,. \tag{4.8}$$

These conditions tell us that $K_{S_i} \cdot C \geq 0$. This implies that the volume of the intersection curve, $\mathrm{vol}(C) = -\phi_1 K_{S_1} \cdot C - \phi_2 K_{S_2} \cdot C$, is negative unless $C^2_{S_1} = C^2_{S_2} = 0$ and $g = 1$, i.e.

[15] The non-splitting of (4.7) identifies $N_{E/X}$ as the Atiyah bundle on E.

unless C is an elliptic curve. This proves that rank 2 geometries containing two surfaces meeting in a curve with genus $g > 0$ are not shrinkable.

Third, we observe that many of the building blocks in our classification program are related to one another by maps (for instance, isomorphisms and complex deformations) which at the level of 5d SCFT physics constitute physical equivalences. Therefore, we observe that the full number of rank 2 surfaces that can be constructed from our list of building blocks dramatically overcounts the number of unique CFT fixed points, and hence we can reduce the complexity of the problem at the outset by restricting our attention to a minimal representative set of configurations capturing the full list of physical equivalence classes. We will argue in particular that we need only consider configurations $S = S_1 \cup S_2$ for which S_1 is a blowup of $\mathbb{F}_{n>0}$ at p generic points[16] and S_2 is dP_m or $\mathbb{F}_0$. We summarize our simplifications by stating that *every rank 2 shrinkable CY 3-fold can be realized locally as a neighborhood of $S = S_1 \cup S_2$, for which $S_1 = \mathrm{Bl}_p\mathbb{F}_{n_1>0}$ and $S_2 = \mathrm{dP}_{n_2}$ or $\mathbb{F}_0$. Moreover, the surfaces S_1, S_2 are glued along a single smooth rational curve $C = S_1 \cap S_2$.*

We argue the third simplification as follows. First, observe that all of the curves C' with self intersection $C'^2 < -2$ which do not intersect the gluing curve C have negative volume. Therefore, the only curves $C' \neq C$ with negative self-intersection should have $C'^2 \geq -2$. Suppose $C'^2 = -2$ and the surface S is shrinkable. Then, it should follow that such a geometry is related via complex deformation to a physically-equivalent surface for which the only curves C' of negative self-intersection have $C'^2 = -1$. The idea is essentially identical to the description of a transitions already described in section 3.5: we perform a conifold transition. Strictly speaking, this is only true up to physical equivalence, but that is good enough for us. Hence, we may assume that the only component surfaces S_i appearing in our representative classes are those for which all curves $C' \neq C$ satisfy $C'^2 \geq -1$. This already places a significant constraint on the possible configurations $S_1 \cup S_2$.

Next, recall that our list of possible building blocks includes $\mathbb{P}^2$ and $\mathrm{Bl}_p\mathbb{F}_n$, where the configuration of p points can be special or generic. The gluing condition (3.2) implies that one of the two gluing curves C_{S_1} or C_{S_2} must have negative self-intersection. Therefore, we are forced to fix one of the two surfaces, say $S_1 = \mathrm{Bl}_p\mathbb{F}_{n_1}$. Observe that any blowup of $\mathbb{F}_n$ at p points $F \cap E$ is always isomorphic to the blowup of $\mathbb{F}_{n+p}$ at p generic points, so (redefining n) we can always assume that S_1 is a blowup of $\mathbb{F}_{n_1}$ at p points away from the curve E with self intersection $E^2 = -n_1$.

Assume that $n \geq 2$ and suppose we take such a surface S_1 and glue it to S_2 along some curve $C_{S_1} \neq E$. Then this violates the condition that all curves $C' \neq C_1$ satisfy $C'^2 \geq -1$, in particular for $C' = E$. Hence, we are forced to set $C_{S_1} = E$, and moreover we are confined to surfaces $S_1 = \mathrm{Bl}_p\mathbb{F}_{n_1}$ for which the configuration of points p is a generic configuration (a special configuration of points would produce curves with self-intersection less than -1).

Let us focus on S_2. If $n_1 \geq 2$, then S_2 must be glued to S_1 along a curve C_{S_2} with non-negative self intersection, $C_{S_2}^2 \geq 0$. Since we may again assume that all $C' \neq C_{S_2}$ satisfy $C'^2 \geq -1$, it follows that $S_2 = \mathrm{dP}_{n_2}$ or $S_2 = \mathbb{F}_0$. Returning to the remaining cases

[16] By "generic point", we mean a point not contained in any exceptional divisors, i.e. rational curves with self intersection -1.

$n_1 < 2$, we find these cases consist of gluing configurations for which $S_i = \mathrm{dP}_{n_i}$ glued along curves C_{S_i} with $C_{S_i}^2 = -1$. However, $\mathrm{dP}_n \cong \mathrm{Bl}_{n-1}\mathbb{F}_1$, and therefore in order to avoid overcounting we assume that our configuration is again of the form conjectured above.

Finally, we turn our attention to the case where one of the component surfaces S_i is a ruled surface over a curve of genus $g > 0$. As explained in section 3.5, a ruled surface over a curve with genus $g > 0$ is physically equivalent to a blowup of $\mathbb{F}_n$ at $2g$ generic points with g self-gluings. Notice that when S_1 is the $\mathrm{Bl}_{2g}\mathbb{F}_n$ with g self-gluings, the gluing curve C_{S_1} should be the section E (with $E^2 = -n$) since otherwise E has negative volume or leads to an elliptic fiber class. This implies due to the shrinkability condition that the second surface S_2 is again dP_m or $\mathbb{F}_0$. The self-gluing curves must always be exceptional curves, and hence we perform a flop transition in which we blow these curves down at the expense of blowing up another curve inside the surface S_2. Provided we always perform enough blow downs to completely eliminate the self-glued curves, we can always exchange a configuration involving a self-glued blowup of $\mathbb{F}_n$ with one of the configurations described in the above conjecture. This completes our argument concerning the representative configurations for rank 2 surfaces $S = S_1 \cup S_2$.

Endpoint classification: 0 and 1 mass parameters. In this section we show that we can first classify geometries which are blown down 'as much as possible'; we refer to these as 'endpoint geometries'. The general classification then follows by classifying endpoints and subsequently classifying their possible blowups.

Suppose a SCFT admits mass deformations for its global symmetry. Then we can take a large mass limit and integrate out all the heavy degrees of freedom. This triggers an RG flow and it is expected that the SCFT below energy scales set by the masses flows to another SCFT with a lower rank global symmetry group commuting with the mass deformations of the UV SCFT. In general, such mass deformations can reduce the rank of the resulting theory. Another possibility is for the IR theory to be a trivial free theory.

We pay attention to a particular class of mass deformations which leads to interacting SCFTs while preserving the rank of the UV SCFT. Equivalently, we restrict our attention to mass deformations which do not change the dimension of the Coulomb branch. One can typically obtain a new interacting SCFT with the same rank by means of such 'rank-preserving mass deformations'. We expect that RG flows of the UV SCFT triggered by such mass deformations can generate a family of SCFTs with the same rank but different global symmetries. SCFTs in the family are distinguished by their global symmetries (i.e. the number of mass parameters), as well as topological data such as the classical Chern-Simons level k or $\mathbb{Z}_2$-valued θ angle.

These types of RG flows terminate in a class of interacting SCFTs which we will call 'endpoint SCFTs'. An endpoint SCFT is defined to be a theory which does not admit any rank-preserving mass deformations. Thus these theories are 'endpoints' of RG flows and they cannot flow to other SCFTs via rank-preserving deformations. Endpoint geometries engineer endpoint SCFTs.

Rank-preserving mass deformations and endpoint geometries are mathematically well-defined notions. We define distinct endpoint geometries to be surfaces which cannot be

JHEP04(2018)103

related to another smooth surface of the same rank via a large mass deformation. Rank-preserving mass deformations are defined as follows: suppose S is shrinkable and $C \subset S_j$ is a -1 curve which does not intersect any S_k for $k \neq j$. Then S can be blown down to a surface $S' = \cup S'_i$ with S'_j the blowdown of the -1 curve of S_j and $S'_k \simeq S_k$ for $k \neq j$. This type of blowdown is the geometric realization of a rank-preserving mass deformation.

We will now show that *if S is shrinkable, then its endpoint geometry S' is also shrinkable.* If $C' \subset S'_i$, let $C \subset S_i$ be its proper transform. We have $K^2_{S'_i} = K^2_{S_i} + 1$. If $i \neq j$ we have $K_{S_j} \cdot C = K_{S'_j} \cdot C'$, so we need only consider the case $i = j$. Let $p \in S'_j$ be the point that the -1 curve in S_j blows down to, and suppose that C' has multiplicity m at p. Then $K_{S'_i} \cdot C' = K_{S_i} \cdot C - m$. The desired conclusion follows immediately.

Endpoint SCFTs are interesting due to the following reasons. First, these theories are the simplest theories in their family of RG flows. Their parameter spaces are smaller, so they are comparatively easier to understand than other theories belonging to the same family. The classification of endpoint SCFTs is therefore a much easier problem than the full classification, as we will see below. We can thus regard the endpoint classification as a tutorial on our classification algorithm. Second, all other SCFTs in the family of RG flows in principle can be obtained from endpoint theories by increasing the number of mass parameters. Namely, we can undo mass deformations, and retrace the RG flow to obtain an entire family of UV SCFTs. This could sound puzzling: we know that RG flow is irreversible. So it may be hard to accept the idea that we can restore UV theories starting from an IR theory. However, this turns out to be the case among 5d supersymmetric theories. Since 5d $\mathcal{N} = 1$ SCFTs are so strongly constrained by supersymmetry, one can control their RG flows by tuning discrete data such as (for theories with gauge theory descriptions) gauge algebra, matter representations, classical CS level, and discrete θ angle. We expect that this allows us to build a family of SCFTs starting from an endpoint theory.

From the geometric standpoint, these constraints can be understood as arising from the Calabi-Yau condition. Mass deformations of a 3-fold correspond to blowups or blowdowns of exceptional curves. As discussed above, a large mass deformation corresponds to blowing down a -1 curve which is isolated from gluing curves and is in fact a reversible geometric transition — one can just as easily blow up the same curve to recover the original 3-fold. This means that by starting from an endpoint geometry, it is possible to obtain a family of local (smooth) 3-folds by blowing up all possible exceptional curves. In this sense, the study of endpoint geometries is a good starting point for the classification of 5d SCFTs.

Let us now classify all rank 2 endpoint geometries by employing our classification algorithm. We learned above that rank 2 geometries are constructed by gluing $S_1 = \mathrm{Bl}_p\mathbb{F}_{m_1}$ and $S_2 = \mathrm{dP}_{m_2}$ or $\mathbb{F}_0$. This implies that endpoint geometries will take the form $\mathbb{P}^2 \cup \mathbb{F}_n$ or $\mathbb{F}_{n_1} \cup \mathbb{F}_{n_2}$. Therefore the endpoint classification reduces to a simple classification of these two types of geometries.

We first classify geometries of the type $\mathbb{P}^2 \cup \mathbb{F}_n$. We can choose a curve class $C_{S_1} = C_1 = a\ell$ in $\mathbb{P}^2$ with a positive integer a and $C_{S_2} = C_2 = E$ in $\mathbb{F}_n$ satisfying the gluing condition (3.2). Since C should be rational, the integer in C_1 is fixed to be either $a = 1$ or $a = 2$. Accordingly, the second surface is fixed to be $\mathbb{F}_3$ or $\mathbb{F}_6$ respectively. Hence we find

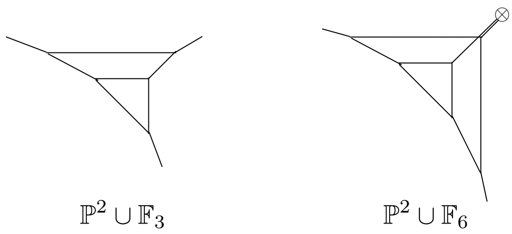

Figure 7. Brane configurations of rank 2 SCFTs with zero mass.

only two geometries of this type:

$$\begin{aligned} &\mathbb{P}^2 \cup \mathbb{F}_3 \quad \text{with} \quad C_1 = \ell\,, \quad C_2 = E_3\,, \\ &\mathbb{P}^2 \cup \mathbb{F}_6 \quad \text{with} \quad C_1 = 2\ell\,, \quad C_2 = E_6\,. \end{aligned} \tag{4.9}$$

These two geometries have brane constructions as depicted in figure 7. These geometries have no mass parameter. Therefore we do not expect any gauge theory descriptions associated to these CFTs.

The second type of endpoint geometry can be classified in the same manner. Due to the gluing condition (3.2), a gluing curve in one of two Hirzebruch surfaces should have negative self-intersection. We choose $C_2 = E_2$ in the second surface $\mathbb{F}_{n_2}$. Then the gluing curve C_1 in the first surface $\mathbb{F}_{n_1}$ needs to be a rational irreducible curve with self-intersection $n_2 - 2$. The curve C_1 takes the form of $C_1 = aF_1 + bH_1$ with $a, b \geq 0$ or $C_1 = E_1$, and must satisfy

$$C_1^2 = n_2 - 2\,, \quad C_1 \cdot S_1 = -n_2\,. \tag{4.10}$$

We now need to check shrinkability conditions. In both irreducible components $S_i = \mathbb{F}_{n_i}$, the curve classes generating Mori cone are E_i, F_i. When these curve classes have non-negative volumes with respect to the Kähler class $-J = -\phi_1 S_1 - \phi_2 S_2$, the local 3-fold defined by S is shrinkable and thus engineers a 5d SCFT. In this case, the criteria for shrinkability are

$$\begin{aligned} &\mathrm{vol}(E_1) = (2-n_1)\phi_1 - a\phi_2 \geq 0\,, && \mathrm{vol}(F_1) = 2\phi_1 - b\phi_2 \geq 0\,, \\ &\mathrm{vol}(E_2) = (2a + 2b - bn)\phi_1 + (2-n)\phi_2 \geq 0\,, && \mathrm{vol}(F_2) = -\phi_1 + 2\phi_2 \geq 0\,, \end{aligned} \tag{4.11}$$

with $\phi_1, \phi_2 > 0$. We can easily solve these conditions and the gluing condition (3.2). Each solution will give a shrinkable geometry and thus a SCFT. The full list of shrinkable surfaces $\mathbb{F}_{n_1} \cup \mathbb{F}_{n_2}$ (denoted by (n_1, n_2)) is given in tables 4b and 4c. Some of these geometries have brane constructions given in figure 8. We find that only the six geometries in table 4b are independent endpoint geometries.

In fact, all the endpoint geometries in table 4b have gauge theory descriptions with simple gauge group G. As explained in section 2.2, a distinguished property of geometries corresponding to gauge theories is that the matrix of intersection numbers (2.15) of holomorphic fiber classes f_i with the surfaces S_i is equal to (minus) the Cartan matrix of the gauge algebra. We remark here that the Hirzebruch surface $\mathbb{F}_0$ has a base-fiber duality

$S_1 \cup S_2$	C_{S_1}	C_{S_2}
$\mathbb{P}^2 \cup \mathbb{F}_3$	ℓ	E
$\mathbb{P}^2 \cup \mathbb{F}_6$	2ℓ	E

(a) Endpoint geometries with $M = 0$.

(n_1, n_2)	C_{S_1}	G	(n_1, n_2)	C_{S_1}	G
$(0,2)$	F	$\mathrm{SU}(3)_1$	$(0,8)$	$F+3H$	$\mathrm{SU}(3)_7, G_2$
$(0,4)$	$F+H$	$\mathrm{SU}(3)_3$	$(1,1)$	E	$\mathrm{SU}(3)_0$
$(0,6)$	$F+2H$	$\mathrm{SU}(3)_5, \mathrm{Sp}(2)_\pi$	$(1,7)$	$2F+H$	$\mathrm{SU}(3)_6$

(b) Endpoint geometries with $M = 1$. Here $C_{S_2} = E$. These geometries have gauge theory descriptions with gauge group $G = \mathrm{SU}(3)_k, \mathrm{Sp}(2)_\theta, G_2$ where k is the classical CS level and θ is the $\mathbb{Z}_2$-valued θ angle.

(n_1, n_2)	C_{S_1}	G	Endpoint
$(1,2)$	F	$\mathrm{SU}(2)\hat{\times}\mathrm{SU}(2)$	$\mathbb{P}^2 \cup \mathbb{F}_3$
$(1,3)$	H	$\mathrm{SU}(3)_2$	$\mathbb{P}^2 \cup \mathbb{F}_3$
$(1,5)$	$F+H$	$\mathrm{SU}(3)_4$	$\mathbb{P}^2 \cup \mathbb{F}_6$
$(1,6)$	$2H$	$\mathrm{Sp}(2)_0$	$\mathbb{P}^2 \cup \mathbb{F}_6$
$(2,4)$	H	$\mathrm{SU}(3)_1$	$\cdot$
$(0,10)$	$F+4H$	$\mathrm{SU}(3)_9$	$\cdot$

(c) Other geometries of $\mathbb{F}_{n_1} \cup \mathbb{F}_{n_2}$. The first four are not endpoints and flow to geometries in (a) by mass deformations. $(2,4)$ is an endpoint, but is also equivalent to $(0,4)$ by a HW transition. $(0,10)$ is an endpoint, but not shrinkable.

Table 4. Classification of all rank 2 geometries with $M = 0, 1$.

exchanging the base curve class H and the fiber curve class F. Geometrically, this is an isomorphism between two geometries related by the exchange of H and F. It is possible that the dual geometry often has different gauge theory realization from the gauge theory of the original geometry. In this case, the geometric duality leads to a duality between two different gauge theories.

Aside from studying the Cartan matrices, we can also compare the triple intersection polynomial J^3 to the perturbative expression for the prepotential given in (2.2). For the geometries in table 4b and 4c, the prepotentials are

$$6\mathcal{F} = J^3 = 8\phi_1^3 + 3\phi_1\phi_2(-n_2\phi_1 + (n_2 - 1)\phi_2) + 8\phi_2^3 \,. \tag{4.12}$$

We can compare these prepotentials against known gauge theory prepotentials as a means to identify the corresponding gauge theories.

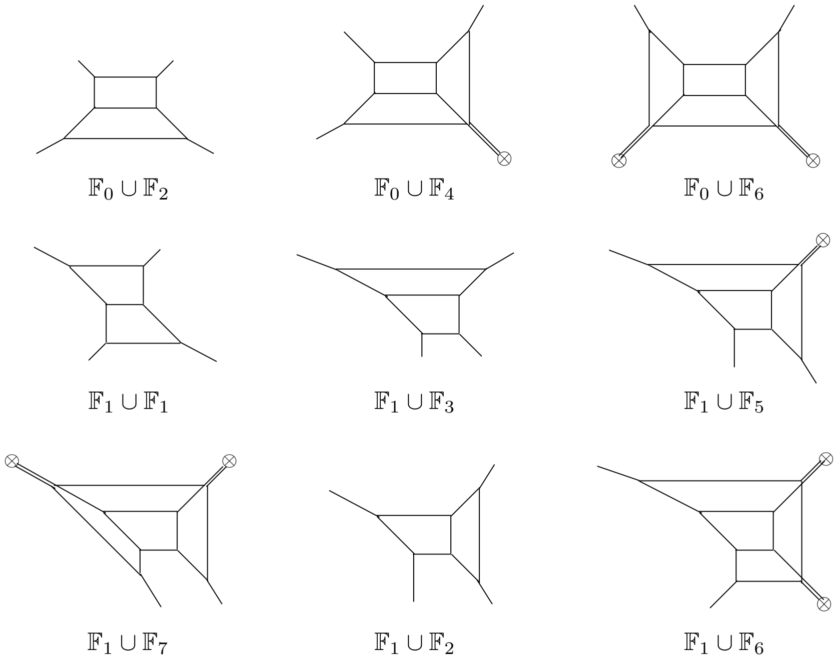

Figure 8. Brane configurations of rank 2 SCFTs with $M = 1$.

Let us first select the respective fibers H, F for $\mathbb{F}_0 \cup \mathbb{F}_{n_2}$, and F, F for $\mathbb{F}_1 \cup \mathbb{F}_{n_2}$. The Cartan matrix A_{ij} of the following geometries computed using these fiber classes is that of the gauge algebra SU(3) as

$$(A_{\mathrm{SU}(3)})_{ij} \;:\; (n_1, n_2) \;=\; (0,2)\,,\; (0,4)\,,\; (0,6)\,,\; (0,8)\,,\; (1,1)\,,\; (1,7)\,, \tag{4.13}$$

for the choices of degrees (n_1, n_2) of $\mathbb{F}_{n_1} \cup \mathbb{F}_{n_2}$. Moreover, their triple intersections agree with gauge theory prepotentials of $\mathrm{SU}(3)_k$ listed in table 4b. Therefore, we expect that these endpoint geometries have $\mathrm{SU}(3)_k$ gauge theory realizations.

The geometries $(0,6)$ and $(0,8)$ are particularly interesting, as they have two different gauge theory descriptions related by the base-fiber exchange of $\mathbb{F}_0$. When we consider the fibers classes to be F, F, the two geometries $(0,6), (0,8)$ exhibit (respectively) $\mathrm{Sp}(2), G_2$ Cartan matrices. On the other hand, if we choose fiber classes H, F, the geometries exhibit the SU(3) Cartan matrix in both cases.

Studying triple intersection numbers gives us a means to narrow down the precise gauge theory that corresponds to these geometries. The triple intersection polynomial J^3 of the geometry $(0,6)$ is identical to the prepotentials of both pure $\mathrm{SU}(3)_5$ gauge theory and also pure $\mathrm{Sp}(2)_\theta$ theory, which can have either $\theta = 0$ or $\theta = \pi$. However, the prepotential cannot distinguish two Sp(2) cases. We can instead determine the θ angle using the known duality between SU(3) and Sp(2). In [22], it was conjectured that $\mathrm{SU}(3)_5$ is dual to $\mathrm{Sp}(2)_\pi$. This suggests that the geometry $(0,6)$ corresponds to $\mathrm{Sp}(2)_\pi$ while $(1,6)$ corresponds to $\mathrm{Sp}(2)_0$. Thus, the geometric construction provides yet additional evidence supporting the duality between the $\mathrm{SU}(3)_5$ and $\mathrm{Sp}(2)_\pi$ gauge theories.

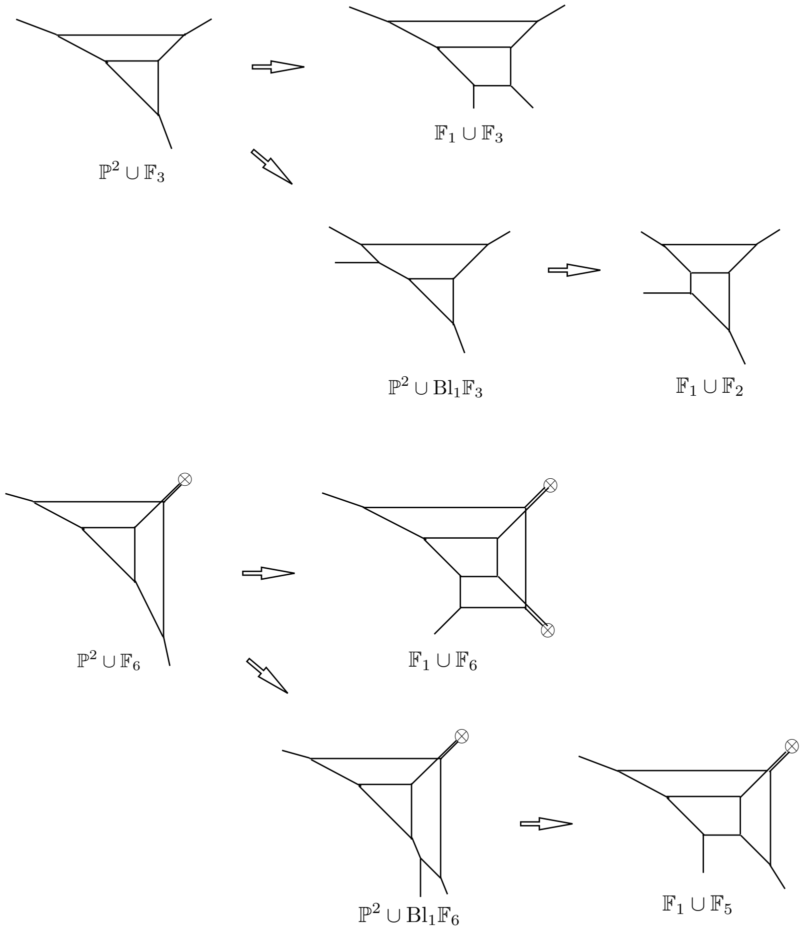

Figure 9. Geometric transitions from $\mathbb{P}^2 \cup \mathbb{F}_3$ and $\mathbb{P}^2 \cup \mathbb{F}_6$ to $\mathbb{F}_1 \cup \mathbb{F}_n$'s with $n = 2, 3, 5, 6$.

JHEP04(2018)103

As another example of a duality between gauge theories, the triple intersections of $(0, 8)$ agree with the prepotentials of $\mathrm{SU}(3)_7$ and G_2 gauge theories. We thus conjecture that $\mathrm{SU}(3)_7$ and G_2 theories are dual and describe the low energy physics of the SCFT corresponding to $\mathbb{F}_0 \cup \mathbb{F}_8$.

Additional (not necessarily endpoint) geometries of type $\mathbb{F}_{n_1} \cup \mathbb{F}_{n_2}$ are displayed in table 4c. The first five geometries in table 4c are shrinkable. However, the first four geometries of these are not endpoints. They all can be obtained from other endpoint geometries, $\mathbb{P}^2 \cup \mathbb{F}_3$ or $\mathbb{P}^2 \cup \mathbb{F}_6$, by blowing up a point and performing flop transitions; see figure 9 for more details. We find that these geometries but $(1, 2)$ have gauge theory descriptions as listed in table 4c. The geometry $(1, 2)$ has gauge algebra $\mathrm{SU}(2)\hat{\times}\mathrm{SU}(2)$ where $\hat{\times}$ denotes that we gauge the $\mathrm{SU}(2)$ global symmetry of another $\mathrm{SU}(2)$ gauge theory which arises from the $\mathrm{U}(1)_I$ instanton symmetry in the IR gauge theory.

The geometry $(2, 4)$ in table 4c is an endpoint geometry admitting no additional rank preserving mass deformations. However, this geometry is equivalent to another endpoint geometry $(0,4)$ by a complex structure deformation, or a Hanany-Witten transition. Thus these two geometries belong to the same physical equivalence class.

Lastly, the geometry $(0,10)$ is not shrinkable. This geometry satisfies all other shrinkablity conditions, but we find that no 4-cycles have nonzero volume at any point in the Kähler cone. Thus $(0,10)$ is not shrinkable unless we make a non-normalizable Kähler deformation. This means the corresponding field theory possesses an intrinsic energy scale set by the Kähler parameter of the non-compact 4-cycle. Therefore, we do not expect that this geometry corresponds to a 5d SCFT. Indeed, in section 4.2, we will argue that this geometry gives a 5d KK theory.

We have finished the full classification of rank 2 endpoint geometries (thus rank 2 endpoint SCFTs), which have $M = 0, 1$. The result is rather surprising — we observe that all rank 2 SCFTs are actually realized by gauge theories and their mass deformations. Note that geometries $\mathbb{P}^2 \cup \mathbb{F}_3$ and $\mathbb{P}^2 \cup \mathbb{F}_6$ corresponding to non-Lagrangian theories can also viewed as deformations of geometries which admit gauge theory descriptions, for example (respectively) $\mathbb{F}_1 \cup \mathbb{F}_2$ and $\mathbb{F}_1 \cup \mathbb{F}_5$. This seems to suggest that gauge theory descriptions are generally quite useful, even for 5d SCFTs of higher rank.

Furthermore, all geometries in table 4 except for $(1,2)$ were already predicted in [13] using perturbative gauge theory analysis. In fact these geometric constructions confirm all predictions with $r = 2$ and $M = 1$ in [13] except for $\mathrm{SU}(3)_8$. It was conjectured in [13] that the $\mathrm{SU}(3)_8$ theory exists and has an interacting UV fixed point. However, the existence of this theory appears to be ruled out by our geometric classification.

Let us briefly discuss the geometry of the $\mathrm{SU}(3)_8$ gauge theory. This theory in fact has a geometric realization as the local 3-fold with Kähler surface $\mathbb{F}_1 \cup \mathbb{F}_9$, where we identify the 2-cycles $C_{S_1} = 3F_1 + H_1$ and $C_{S_2} = E_2$. However, this geometry is not shrinkable because at least one 2-cycle contained in S has negative volume. For example, the volumes

$$\mathrm{vol}(E_1) = \phi_1 - 3\phi_2\,, \quad \mathrm{vol}(F_2) = 2\phi_2 - \phi_1 \tag{4.14}$$

with $\phi_1, \phi_2 > 0$ cannot be both non-negative. Therefore the Coulomb branch of this geometry is trivial and this geometry is not shrinkable. In order to make the geometry shrinkable we need to attach a non-compact 4-cycle with non-zero Kähler parameter corresponding to bare gauge coupling constant $1/g^2$. This Kähler parameter cannot be tuned to zero while maintaining positivity of the Kähler metric. So even though the IR gauge description with $1/g^2 \neq 0$ makes sense geometrically, we cannot take the $1/g^2 = 0$ limit without taking the Coulomb branch parameter to 0. This means that if the point $1/g^2 = 0$ is a CFT point, then it has no Coulomb branch deformation, and thus in conflict with a SCFT from this gauge theory based on our assumptions. Thus we do not expect that this geometry has a CFT limit. The gauge theory analysis in [13] uses only the perturbative spectrum and monopole tensions and thus cannot capture the spectrum of M2-branes wrapping the curve $E_1 \subset \mathbb{F}_1$ (which correspond to instantons in the gauge theory). Missing non-perturbative states such as these are crucial for assessing whether or not a geometry is shrinkable. This again shows that the perturbative constraints used in [13] are necessary but not sufficient to guarantee the existence of CFT fixed points.

Full rank 2 classification. We showed in the previous section that our classification program can be reduced to a classification of the following types of geometric configurations: $\mathrm{Bl}_{p_1}\mathbb{F}_n \cup \mathrm{dP}_{p_2}$ and $\mathrm{Bl}_{p_1}\mathbb{F}_n \cup \mathbb{F}_0$. As already discussed p_2 and p_1 are bounded above by $p_{\max}(n)$, which we note depends upon both the degree n and the type of gluing configuration. However, we are still faced with the problem of restricting the range of (non-negative) integer n for which there exist shrinkable configurations. It turns out that some necessary conditions of shrinkability allows us to derive a crude bound on n. From a physical perspective, the existence of such a bound is not surprising as it is closely tied to the existence of only a finite number of 5d interacting fixed CFT points for a fixed rank.

Appropriate bounds on n can be determined in the two separate cases of $S_2 = \mathrm{dP}_{p_2}$ or $S_2 = \mathbb{F}_0$. For both cases, we need only consider $n \geq 2$, since setting $n = 0, 1$ produces a geometric configuration isomorphic to $\mathrm{dP}_{p_1+1} \cup \mathrm{dP}_{p_2}$. In the case of $S_2 = \mathrm{dP}_2$, we find that $n \leq 7$, while in the case of $S_2 = \mathbb{F}_0$, we find that $n \leq 8$. See appendix B for proofs of these bounds.

We present our classification of rank 2 Kähler surfaces associated to 5d UV interacting fixed points in figures 10–27. These results are organized by the number of mass parameters M, with $0 \leq M \leq 11$. Given $M > 0$ mass parameters, a shrinkable geometry with $M - 1$ mass parameters may be obtained by performing a blowdown of an exceptional divisor (possibly after a sequence of flops) in the surface S; in the associated field theory, blowing down an exceptional curve corresponds to integrating out a massive matter hypermultiplet.

In each figure, we list the Kähler surface $S = S_1 \overset{C_{S_2}}{\cup} S_2$, where $C_{S_2} = (S_1 \cap S_2)_{S_2}$ is the curve along which the two surfaces are glued, restricted to the *second* surface S_2. Geometries marked with $(\cdot)^*$ correspond to 5d KK theories. Beneath each geometry, we also list the associated gauge theory; geometries with no associated gauge system indicated do not admit a known description as a gauge theory.

Our method for identifying gauge theoretic descriptions involves comparing the triple intersection J^3 with the gauge-theoretic prepotential $6\mathcal{F}$ in (2.2) for given gauge group and matter content in the Kähler cone, as well as identifying a geometric realization of the Cartan matrix of associated to the gauge algebra.

The Cartan matrices are determined up to sign by a choice of fibers[17] $f_1 \subset S_1, f_2 \subset S_2$ satisfying

$$(f_i \cdot S_j)_{S_i} = -(A_G)_{ij}. \tag{4.15}$$

Geometrically, these fibers are rational curves over which M2-branes may be wrapped to give rise to charged BPS vectors in the 5d spectrum. In figures 10–27, we indicate to the left of each gauge description a possible choice of fibers giving rise to stated gauge algebra. We merely list all possible gauge theory descriptions and do not attempt to list all possible configurations of fibers. When there is more than one choice of fiber leading to different Cartan matrices (and hence different gauge symmetries), there are dualities between the associated gauge theory descriptions. For $\mathrm{dP}_{p_2<8}$, the possible fibers are (using the same

[17] In the present discussion, a *fiber* is a rational curve f with self intersection $f^2 = 0$.

JHEP04(2018)103

notation as in (4.4))

$$(1;1)\,,\ (2;1^4)\,,\ (3;2,1^6)\,,\ (4;2^3,1^4)\,,\ (5;2^6,1). \tag{4.16}$$

The list of possible fibers in $\mathrm{Bl}_{p_1}\mathbb{F}_n$ is significantly more complicated; see appendix A.2.3.

We also note that the double arrows connecting pairs of different geometries S indicate flop transitions mapping the geometries into one another. Each figure contains several clusters of geometries connected by arrows, with each cluster belonging to the same birational, and thus physical, equivalence class. Arrows decorated with the symbol $\phi_1 \leftrightarrow \phi_2$ indicate that the flop transition requires us to reverse our identifications $S_1 \leftrightarrow S_2$, and flip the sign of the Chern-Simons level, $k \to -k$.

Finally, we remark that the gluing curves $C_{S_2} \in \mathrm{dP}_{p_2 \geq 3}$ are only listed up to the action of the Weyl group $W(E_{p_2})$. Said differently, each choice of gluing curve displayed in the figures is a single element in the Weyl orbit. We now briefly describe the Weyl group action in dP_{p_2} and explain why in most cases we only need to distinguish geometric configurations whose gluing curves belong to the same Weyl orbit in a given surface. Given a simple root $\alpha_i = X_i - X_{i+1}, i = 1, \dots, p_2 - 1$, and an effective curve

$$C = d\ell - m_i X_i, \tag{4.17}$$

the Weyl reflections w_{α_i} act by transposing exceptional divisors, $X_i \leftrightarrow X_{i+1}$, while the reflection $w_{\alpha_{p_2}}$ associated to the root $\alpha_{p_2} = \ell - \sum_{i=1}^{3} X_i$ acts on C as follows:

$$\begin{aligned} w_{\alpha_{p_2}}(C) = (2d - m_1 - m_2 - m_3)\ell - (d - m_2 - m_3)X_1 - (d - m_1 - m_3)X_2 \\ - (d - m_1 - m_2)X_3 - \sum_{i>3} m_i X_i. \end{aligned} \tag{4.18}$$

As was shown in [34], the action of $W(E_{p_2})$ on a rational curve $C \in \mathrm{dP}_{p_2}$ for $p_2 \geq 4$ and degree $d_C \equiv -K \cdot C = C^2 + 2 = n$ in all cases studied in this paper is transitive. Therefore, since the Weyl action $w_\alpha : C \mapsto C + (C \cdot \alpha)C$ preserves intersection products,

$$C \cdot C' = (C + (C \cdot \alpha)\alpha) \cdot (C' + (C' \cdot \alpha)\alpha), \tag{4.19}$$

it is sufficient to set the gluing curve C_{S_2} equal to a single element of the Weyl orbit in order to understand the full intersection structure, as the intersection numbers are identical up to permutation for any two elements belonging to the same Weyl orbit. For $p_2 < 3$, the Weyl group either has multiple orbits (as in the case of $p_2 = 3$) or is otherwise undefined (as in the case of $p_2 < 3$), and so for $p_2 < 4$ we only list gluing curves C_{S_2} up to cyclic permutations of the exceptional divisors X_i.

Upon mass deforming these SCFTs and flowing to the IR we get a tree of relations between these conformal theories which is summarized in the RG flow tree diagram in figure 16. The top theories of the RG families are related to 5d KK theories which are discussed in the next section.

JHEP04(2018)103

$(\mathrm{Bl}_{10}\mathbb{F}_6 \overset{2\ell}{\cup} \mathrm{dP}_1)^*$

$F, \ell - X_1$	$\mathrm{Sp}(2) + 10\mathbf{F}$
$H + 2F - \sum X_i, \ell - X_1$	$\hat{A}_1$

$(\mathrm{Bl}_{10}\mathbb{F}_6 \overset{F+2E}{\cup} \mathbb{F}_0)^*$

F, F	$\mathrm{Sp}(2) + 10\mathbf{F}$
F, E	$\mathrm{SU}(3)_0 + 10\mathbf{F}$
$H + 2F - \sum X_i, F$	$\hat{A}_1$

$(\mathrm{Bl}_9\mathbb{F}_5 \overset{2\ell - X_1}{\cup} \mathrm{dP}_2)^*$

$F, \ell - X_1$	$\mathrm{SU}(3)_0 + 10\mathbf{F}$
$F, \ell - X_2$	$\mathrm{Sp}(2) + 10\mathbf{F}$
$H + 2F - \sum X_i, \ell - X_2$	$\hat{A}_1$

$(\mathrm{Bl}_8\mathbb{F}_4 \overset{2\ell - \sum_{i=1}^2 X_i}{\cup} \mathrm{dP}_3)^*$

$F, \ell - X_1$	$\mathrm{SU}(3)_0 + 10\mathbf{F}$
$F, \ell - X_3$	$\mathrm{Sp}(2) + 10\mathbf{F}$
$H + 2F - \sum X_i, \ell - X_3$	$\hat{A}_1$

$(\mathrm{Bl}_7\mathbb{F}_3 \overset{2\ell - \sum_{i=1}^3 X_i}{\cup} \mathrm{dP}_4)^*$

$F, \ell - X_1$	$\mathrm{SU}(3)_0 + 10\mathbf{F}$
$F, \ell - X_4$	$\mathrm{Sp}(2) + 10\mathbf{F}$
$H + 2F - \sum X_i, \ell - X_4$	$\hat{A}_1$

$(\mathrm{Bl}_6\mathbb{F}_2 \overset{2\ell - \sum_{i=1}^4 X_i}{\cup} \mathrm{dP}_5)^*$

$F, \ell - X_1$	$\mathrm{SU}(3)_0 + 10\mathbf{F}$
$F, \ell - X_5$	$\mathrm{Sp}(2) + 10\mathbf{F}$
$H - X_1 - X_2, 2\ell - \sum_{i=1}^4 X_i$	$[\mathrm{SU}(2) + 4\mathbf{F}] \times [\mathrm{SU}(2) + 4\mathbf{F}]$
$H + 2F - \sum X_i, \ell - X_5$	$\hat{A}_1$

$(\mathrm{Bl}_5\mathbb{F}_1 \overset{2\ell - \sum_{i=1}^5 X_i}{\cup} \mathrm{dP}_6)^*$

$F, \ell - X_1$	$\mathrm{SU}(3)_0 + 10\mathbf{F}$
$F, \ell - X_6$	$\mathrm{Sp}(2) + 10\mathbf{F}$
$f_1 \cdot E = 0, 2\ell - \sum_{i=2}^5 X_i$	$[\mathrm{SU}(2) + 4\mathbf{F}] \times [\mathrm{SU}(2) + 4\mathbf{F}]$
$f_1 \cdot E = 2, \ell - X_6$	$\hat{A}_1$

Figure 10. $M = 11$ geometries.

$(\mathrm{Bl}_9\mathbb{F}_4 \overset{F+E}{\cup} \mathbb{F}_0)^*$

F, E	$\mathrm{SU}(3)_{-\frac{3}{2}} + 9\mathbf{F}$
$H + 2F - \sum_{i=1}^{8} X_i, E$	$\mathrm{Sp}(2) + 8\mathbf{F} + 1\mathbf{AS}$

$\mathrm{Bl}_{10}\mathbb{F}_6 \overset{2\ell}{\cup} \mathbb{P}^2$

$\downarrow\uparrow$

$\mathrm{Bl}_9\mathbb{F}_5 \overset{2\ell-X_1}{\cup} \mathrm{dP}_1$

$F, \ell - X_1$	$\mathrm{SU}(3)_{-\frac{1}{2}} + 9\mathbf{F}$
$H + 2F - \sum X_i, \ell - X_1$	$\mathrm{Sp}(2) + 9\mathbf{F}$

$\downarrow\uparrow$

$\mathrm{Bl}_8\mathbb{F}_4 \overset{2\ell-\sum_{i=1}^{2} X_i}{\cup} \mathrm{dP}_2$

$F, \ell - X_1$	$\mathrm{SU}(3)_{-\frac{1}{2}} + 9\mathbf{F}$
$H + 2F - \sum X_i, \ell - X_1$	$\mathrm{Sp}(2) + 9\mathbf{F}$

$\downarrow\uparrow$

$\mathrm{Bl}_7\mathbb{F}_3 \overset{2\ell-\sum_{i=1}^{3} X_i}{\cup} \mathrm{dP}_3$

$F, \ell - X_1$	$\mathrm{SU}(3)_{-\frac{1}{2}} + 9\mathbf{F}$
$H + 2F - \sum X_i, \ell - X_1$	$\mathrm{Sp}(2) + 9\mathbf{F}$

$\downarrow\uparrow$

$\mathrm{Bl}_6\mathbb{F}_2 \overset{2\ell-\sum_{i=1}^{4} X_i}{\cup} \mathrm{dP}_4$

$F, \ell - X_1$	$\mathrm{SU}(3)_{-\frac{1}{2}} + 9\mathbf{F}$
$H + 2F - \sum X_i, \ell - X_1$	$\mathrm{Sp}(2) + 9\mathbf{F}$
$H - X_1 - X_2, 2\ell - \sum X_i$	$[\mathrm{SU}(2) + 4\mathbf{F}] \times [\mathrm{SU}(2) + 3\mathbf{F}]$

$\downarrow\uparrow \; \phi_1 \leftrightarrow \phi_2$

$\mathrm{Bl}_4\mathbb{F}_1 \overset{2\ell-\sum_{i=1}^{5} X_i}{\cup} \mathrm{dP}_6$

$F, \ell - X_5$	$\mathrm{SU}(3)_{\frac{1}{2}} + 9\mathbf{F}$
$F, \ell - X_6$	$\mathrm{Sp}(2) + 9\mathbf{F}$
$f_1 \cdot E = 0, \ell - X_6$	$[\mathrm{SU}(2) + 3\mathbf{F}] \times [\mathrm{SU}(2) + 4\mathbf{F}]$

$\longleftrightarrow$

$\mathrm{Bl}_9\mathbb{F}_6 \overset{F+2E}{\cup} \mathbb{F}_0$

F, F	$\mathrm{Sp}(2) + 9\mathbf{F}$
F, E	$\mathrm{SU}(3)_{\frac{1}{2}} + 9\mathbf{F}$

$\mathrm{Bl}_9\mathbb{F}_6 \overset{2\ell}{\cup} \mathrm{dP}_1$

$F, \ell - X_1$	$\mathrm{Sp}(2) + 9\mathbf{F}$

$\Leftrightarrow$

$\mathrm{Bl}_8\mathbb{F}_5 \overset{2\ell-X_1}{\cup} \mathrm{dP}_2$

$F, \ell - X_1$	$\mathrm{SU}(3)_{\frac{1}{2}} + 9\mathbf{F}$
$F, \ell - X_2$	$\mathrm{Sp}(2) + 9\mathbf{F}$

$\downarrow\uparrow$

$\mathrm{Bl}_7\mathbb{F}_4 \overset{2\ell-\sum_{i=1}^{2} X_i}{\cup} \mathrm{dP}_3$

$F, \ell - X_1$	$\mathrm{SU}(3)_{\frac{1}{2}} + 9\mathbf{F}$
$F, \ell - X_3$	$\mathrm{Sp}(2) + 9\mathbf{F}$

$\downarrow\uparrow$

$\mathrm{Bl}_6\mathbb{F}_3 \overset{2\ell-\sum_{i=1}^{3} X_i}{\cup} \mathrm{dP}_4$

$F, \ell - X_1$	$\mathrm{SU}(3)_{\frac{1}{2}} + 9\mathbf{F}$
$F, \ell - X_4$	$\mathrm{Sp}(2) + 9\mathbf{F}$

$\downarrow\uparrow$

$\mathrm{Bl}_5\mathbb{F}_2 \overset{2\ell-\sum_{i=1}^{4} X_i}{\cup} \mathrm{dP}_5$

$F, \ell - X_1$	$\mathrm{SU}(3)_{\frac{1}{2}} + 9\mathbf{F}$
$F, \ell - X_5$	$\mathrm{Sp}(2) + 9\mathbf{F}$
$H - X_1 - X_2, 2\ell - \sum_{i=1}^{4} X_i$	$[\mathrm{SU}(2) + 3\mathbf{F}] \times [\mathrm{SU}(2) + 4\mathbf{F}]$

Figure 11. $M = 10$ geometries.

$\mathrm{Bl}_8\mathbb{F}_3 \overset{\ell}{\cup} \mathrm{dP}_1$

$F, \ell - X_1$	$\mathrm{SU}(3)_{-2} + 8\mathbf{F}$
$H + 2F - \sum_{i=1}^{7} X_i, \ell - X_1$	$\mathrm{Sp}(2) + 7\mathbf{F} + 1\mathbf{AS}$

$\mathrm{Bl}_7\mathbb{F}_4 \overset{2\ell-\sum_{i=1}^{2} X_i}{\cup} \mathrm{dP}_2 \longleftrightarrow \mathrm{Bl}_8\mathbb{F}_5 \overset{2\ell-X_1}{\cup} \mathrm{dP}_1 \longleftrightarrow \mathrm{Bl}_9\mathbb{F}_6 \overset{2\ell}{\cup} \mathbb{P}^2$

$\mathrm{Bl}_7\mathbb{F}_4 \overset{2\ell-\sum_{i=1}^{2} X_i}{\cup} \mathrm{dP}_2$

$F, \ell - X_1$	$\mathrm{SU}(3)_0 + 8\mathbf{F}$

$\mathrm{Bl}_8\mathbb{F}_5 \overset{2\ell-X_1}{\cup} \mathrm{dP}_1$

$F, \ell - X_1$	$\mathrm{SU}(3)_0 + 8\mathbf{F}$

$\mathrm{Bl}_6\mathbb{F}_3 \overset{2\ell-\sum_{i=1}^{3} X_i}{\cup} \mathrm{dP}_3$

$F, \ell - X_1$	$\mathrm{SU}(3)_0 + 8\mathbf{F}$

$\mathrm{Bl}_5\mathbb{F}_2 \overset{2\ell-\sum_{i=1}^{4} X_i}{\cup} \mathrm{dP}_4$

$F, \ell - X_1$	$\mathrm{SU}(3)_0 + 8\mathbf{F}$
$H - X_1 - X_2, 2\ell - \sum X_i$	$[\mathrm{SU}(2) + 3\mathbf{F}] \times [\mathrm{SU}(2) + 3\mathbf{F}]$

$\mathrm{Bl}_4\mathbb{F}_1 \overset{2\ell-\sum_{i=1}^{5} X_i}{\cup} \mathrm{dP}_5$

$F, \ell - X_1$	$\mathrm{SU}(3)_0 + 8\mathbf{F}$
$f_1 \cdot E = 0, 2l - \sum_{i=1}^{4} X_i$	$[\mathrm{SU}(2) + 3\mathbf{F}] \times [\mathrm{SU}(2) + 3\mathbf{F}]$

$\mathrm{Bl}_8\mathbb{F}_4 \overset{F+E}{\cup} \mathbb{F}_0$

F, F	$\mathrm{SU}(3)_{-1} + 8\mathbf{F}$
$H + 2F - \sum X_i, F$	$\mathrm{Sp}(2) + 8\mathbf{F}$

$\mathrm{Bl}_6\mathbb{F}_2 \overset{\ell-X_1}{\cup} \mathrm{dP}_3$

$F, \ell - X_1$	$\mathrm{SU}(3)_{-1} + 8\mathbf{F}$
$H + 2F - \sum X_i, \ell - X_2$	$\mathrm{Sp}(2) + 8\mathbf{F}$
$H - X_1 - X_2, \ell - X_1$	$[\mathrm{SU}(2) + 4\mathbf{F}] \times [\mathrm{SU}(2) + 2\mathbf{F}]$

$\mathrm{Bl}_7\mathbb{F}_3 \overset{\ell}{\cup} \mathrm{dP}_2$

$F, \ell - X_1$	$\mathrm{SU}(3)_{-1} + 8\mathbf{F}$
$H + 2F - \sum X_i, \ell - X_1$	$\mathrm{Sp}(2) + 8\mathbf{F}$

$\mathrm{Bl}_8\mathbb{F}_6 \overset{2\ell}{\cup} \mathrm{dP}_1$

$F, \ell - X_1$	$\mathrm{Sp}(2) + 8\mathbf{F}$

$\downarrow\uparrow \phi_1 \leftrightarrow \phi_2$

$\mathrm{Bl}_3\mathbb{F}_1 \overset{2\ell-\sum_{i=1}^{5} X_i}{\cup} \mathrm{dP}_6$

$F, \ell - X_1$	$\mathrm{SU}(3)_1 + 8\mathbf{F}$
$F, \ell - X_6$	$\mathrm{Sp}(2) + 8\mathbf{F}$
$f_1 \cdot E = 0, 2\ell - \sum_{i=1}^{4} X_i$	$[\mathrm{SU}(2) + 2\mathbf{F}] \times [\mathrm{SU}(2) + 4\mathbf{F}]$

$\mathrm{Bl}_6\mathbb{F}_4 \overset{2\ell-\sum_{i=1}^{2} X_i}{\cup} \mathrm{dP}_3$

$F, \ell - X_1$	$\mathrm{SU}(3)_1 + 8\mathbf{F}$
$F, \ell - X_3$	$\mathrm{Sp}(2) + 8\mathbf{F}$

$\mathrm{Bl}_7\mathbb{F}_5 \overset{2\ell-X_1}{\cup} \mathrm{dP}_2$

$F, \ell - X_1$	$\mathrm{SU}(3)_1 + 8\mathbf{F}$
$F, \ell - X_2$	$\mathrm{Sp}(2) + 8\mathbf{F}$

$\mathrm{Bl}_4\mathbb{F}_2 \overset{2\ell-\sum_{i=1}^{4} X_i}{\cup} \mathrm{dP}_5$

$F, \ell - X_1$	$\mathrm{SU}(3)_1 + 8\mathbf{F}$
$F, \ell - X_5$	$\mathrm{Sp}(2) + 8\mathbf{F}$
$H - X_1 - X_2, 2\ell - \sum_{i=1}^{4} X_i$	$[\mathrm{SU}(2) + 2\mathbf{F}] \times [\mathrm{SU}(2) + 4\mathbf{F}]$

$\mathrm{Bl}_5\mathbb{F}_3 \overset{2\ell-\sum_{i=1}^{3} X_i}{\cup} \mathrm{dP}_4$

$F, \ell - X_1$	$\mathrm{SU}(3)_1 + 8\mathbf{F}$
$F, \ell - X_4$	$\mathrm{Sp}(2) + 8\mathbf{F}$

$\mathrm{Bl}_8\mathbb{F}_6 \overset{F+2E}{\cup} \mathbb{F}_0$

F, F	$\mathrm{Sp}(2) + 8\mathbf{F}$
F, E	$\mathrm{SU}(3)_1 + 8\mathbf{F}$

Figure 12. $M = 9$ geometries.

$\mathrm{Bl}_2\mathbb{F}_1 \overset{2\ell-\sum_{i=1}^5 X_i}{\cup} \mathrm{dP}_6$

$F, \ell - X_1$	$\mathrm{SU}(3)_{\frac{3}{2}} + 7\mathbf{F}$
$F, \ell - X_6$	$\mathrm{Sp}(2) + 7\mathbf{F}$
$f_1 \cdot E = 0, 2l - \sum_{i=1}^4 X_i$	$[\mathrm{SU}(2) + 1\mathbf{F}] \times [\mathrm{SU}(2) + 4\mathbf{F}]$

$\phi_1 \leftrightarrow \phi_2$

$\mathrm{Bl}_6\mathbb{F}_2 \overset{\ell - X_1}{\cup} \mathrm{dP}_2$

$F, \ell - X_2$	$\mathrm{SU}(3)_{-\frac{3}{2}} + 7\mathbf{F}$
$H + 2F - \sum X_i, \ell - X_2$	$\mathrm{Sp}(2) + 7\mathbf{F}$
$H - X_1 - X_2, \ell - X_1$	$[\mathrm{SU}(2) + 4\mathbf{F}] \times [\mathrm{SU}(2) + 1\mathbf{F}]$

$\mathrm{Bl}_3\mathbb{F}_2 \overset{2\ell-\sum_{i=1}^4 X_i}{\cup} \mathrm{dP}_5$

$F, \ell - X_1$	$\mathrm{SU}(3)_{\frac{3}{2}} + 7\mathbf{F}$
$F, \ell - X_5$	$\mathrm{Sp}(2) + 7\mathbf{F}$
$H - X_1 - X_2, 2\ell - \sum_{i=1}^4 X_i$	$[\mathrm{SU}(2) + 1\mathbf{F}] \times [\mathrm{SU}(2) + 4\mathbf{F}]$

$\mathrm{Bl}_7\mathbb{F}_3 \overset{\ell}{\cup} \mathrm{dP}_1$

$F, \ell - X_1$	$\mathrm{SU}(3)_{-\frac{3}{2}} + 7\mathbf{F}$
$H + 2F - \sum X_i, \ell - X_1$	$\mathrm{Sp}(2) + 7\mathbf{F}$

$\mathrm{Bl}_7\mathbb{F}_6 \overset{2\ell}{\cup} \mathrm{dP}_1$

$F, \ell - X_1$	$\mathrm{Sp}(2) + 7\mathbf{F}$

$\mathrm{Bl}_4\mathbb{F}_3 \overset{2\ell-\sum_{i=1}^3 X_i}{\cup} \mathrm{dP}_4$

$F, \ell - X_1$	$\mathrm{SU}(3)_{\frac{3}{2}} + 7\mathbf{F}$
$F, \ell - X_4$	$\mathrm{Sp}(2) + 7\mathbf{F}$

$\mathrm{Bl}_7\mathbb{F}_6 \overset{F+2E}{\cup} \mathbb{F}_0$

F, F	$\mathrm{Sp}(2) + 7\mathbf{F}$
F, E	$\mathrm{SU}(3)_{\frac{3}{2}} + 7\mathbf{F}$

$\mathrm{Bl}_6\mathbb{F}_5 \overset{2\ell - X_1}{\cup} \mathrm{dP}_2$

$F, \ell - X_1$	$\mathrm{SU}(3)_{\frac{3}{2}} + 7\mathbf{F}$
$F, \ell - X_2$	$\mathrm{Sp}(2) + 7\mathbf{F}$

$\mathrm{Bl}_5\mathbb{F}_4 \overset{2\ell-\sum_{i=1}^2 X_i}{\cup} \mathrm{dP}_3$

$F, \ell - X_1$	$\mathrm{SU}(3)_{\frac{3}{2}} + 7\mathbf{F}$
$F, \ell - X_3$	$\mathrm{Sp}(2) + 7\mathbf{F}$

$\mathrm{Bl}_7\mathbb{F}_2 \overset{E}{\cup} \mathbb{F}_0$

F, F	$\mathrm{SU}(3)_{-\frac{5}{2}} + 7\mathbf{F}$
$H - X_1 - X_2, E$	$[\mathrm{SU}(2) + 5\mathbf{F}] \times \mathrm{SU}(2)_\pi$
$H + 2F - \sum_{i=1}^6 X_i, F$	$\mathrm{Sp}(2) + 6\mathbf{F} + 1\mathbf{AS}$

$\mathrm{Bl}_8\mathbb{F}_6 \overset{2\ell}{\cup} \mathbb{P}^2$

$\mathrm{Bl}_7\mathbb{F}_5 \overset{2\ell - X_1}{\cup} \mathrm{dP}_1$

$F, \ell - X_1$	$\mathrm{SU}(3)_{\frac{1}{2}} + 7\mathbf{F}$

$\mathrm{Bl}_6\mathbb{F}_4 \overset{2\ell-\sum_{i=1}^2 X_i}{\cup} \mathrm{dP}_2$

$F, \ell - X_1$	$\mathrm{SU}(3)_{\frac{1}{2}} + 7\mathbf{F}$

$\mathrm{Bl}_5\mathbb{F}_3 \overset{2\ell-\sum_{i=1}^3 X_i}{\cup} \mathrm{dP}_3$

$F, \ell - X_1$	$\mathrm{SU}(3)_{\frac{1}{2}} + 7\mathbf{F}$

$\mathrm{Bl}_4\mathbb{F}_2 \overset{2\ell-\sum_{i=1}^4 X_i}{\cup} \mathrm{dP}_4$

$F, \ell - X_1$	$\mathrm{SU}(3)_{\frac{1}{2}} + 7\mathbf{F}$
$H - X_1 - X_2, 2\ell - \sum X_i$	$[\mathrm{SU}(2) + 2\mathbf{F}] \times [\mathrm{SU}(2) + 3\mathbf{F}]$

$\mathrm{Bl}_8\mathbb{F}_3 \overset{\ell}{\cup} \mathbb{P}^2$

$\mathrm{Bl}_7\mathbb{F}_4 \overset{F+E}{\cup} \mathbb{F}_0$

F, F	$\mathrm{SU}(3)_{-\frac{1}{2}} + 7\mathbf{F}$

$\mathrm{Bl}_6\mathbb{F}_3 \overset{\ell}{\cup} \mathrm{dP}_2$

$F, \ell - X_1$	$\mathrm{SU}(3)_{-\frac{1}{2}} + 7\mathbf{F}$

$\mathrm{Bl}_5\mathbb{F}_2 \overset{\ell - X_1}{\cup} \mathrm{dP}_3$

$F, \ell - X_1$	$\mathrm{SU}(3)_{-\frac{1}{2}} + 7\mathbf{F}$
$H - X_1 - X_2, \ell - X_1$	$[\mathrm{SU}(2) + 3\mathbf{F}] \times [\mathrm{SU}(2) + 2\mathbf{F}]$

$\phi_1 \leftrightarrow \phi_2$

$\mathrm{Bl}_3\mathbb{F}_1 \overset{2\ell-\sum_{i=1}^5 X_i}{\cup} \mathrm{dP}_5$

$F, \ell - X_1$	$\mathrm{SU}(3)_{\frac{1}{2}} + 7\mathbf{F}$
$f_1 \cdot E = 0, 2\ell - \sum_{i=1}^4 X_i$	$[\mathrm{SU}(2) + 2\mathbf{F}] \times [\mathrm{SU}(2) + 3\mathbf{F}]$

Figure 13. $M = 8$ geometries. (See footnote 18 for a comment about $\mathrm{Bl}_8\mathbb{F}_3 \cup \mathbb{P}^2$.)

JHEP04(2018)103

$\mathrm{Bl}_5\mathbb{F}_1 \overset{\ell-X_1-X_2}{\cup} \mathrm{dP}_2$

$F, \ell - X_1$	$[\mathrm{SU}(2)+4\mathbf{F}]\times \mathrm{SU}(2)_0$

$\mathrm{Bl}_6\mathbb{F}_2 \overset{\ell-X_1}{\cup} \mathrm{dP}_1$

$H - X_1 - X_2, \ell - X_1$	$[\mathrm{SU}(2)+4\mathbf{F}]\times \mathrm{SU}(2)_0$

$\mathrm{Bl}_7\mathbb{F}_3 \overset{\ell}{\cup} \mathbb{P}^2$

$\mathrm{Bl}_6\mathbb{F}_2 \overset{E}{\cup} \mathbb{F}_0$

F, F	$\mathrm{SU}(3)_{-2}+6\mathbf{F}$
$H+2F-\sum X_i, F$	$\mathrm{Sp}(2)+6\mathbf{F}$
$H - X_1 - X_2, E$	$[\mathrm{SU}(2)+4\mathbf{F}]\times \mathrm{SU}(2)_\pi$

$\phi_1 \leftrightarrow \phi_2$

$\mathrm{Bl}_1\mathbb{F}_1 \overset{2\ell-\sum_{i=1}^5 X_i}{\cup} \mathrm{dP}_6$

$F, \ell - X_1$	$\mathrm{SU}(3)_2+6\mathbf{F}$
$F, \ell - X_6$	$\mathrm{Sp}(2)+6\mathbf{F}$
$f_1 \cdot E = 0, 2\ell - \sum_{i=1}^4 X_i$	$\mathrm{SU}(2)_\pi \times [\mathrm{SU}(2)+4\mathbf{F}]$

$\mathrm{Bl}_2\mathbb{F}_2 \overset{2\ell-\sum_{i=1}^4 X_i}{\cup} \mathrm{dP}_5$

$F, \ell - X_1$	$\mathrm{SU}(3)_2+6\mathbf{F}$
$F, \ell - X_5$	$\mathrm{Sp}(2)+6\mathbf{F}$
$H - X_1 - X_2, 2\ell - \sum_{i=1}^4 X_i$	$\mathrm{SU}(2)_\pi \times [\mathrm{SU}(2)+4\mathbf{F}]$

$\mathrm{Bl}_6\mathbb{F}_6 \overset{2\ell}{\cup} \mathrm{dP}_1$

$F, \ell - X_1$	$\mathrm{Sp}(2)+6\mathbf{F}$

$\mathrm{Bl}_3\mathbb{F}_3 \overset{2\ell-\sum_{i=1}^3 X_i}{\cup} \mathrm{dP}_4$

$F, \ell - X_1$	$\mathrm{SU}(3)_2+6\mathbf{F}$
$F, \ell - X_4$	$\mathrm{Sp}(2)+6\mathbf{F}$

$\mathrm{Bl}_6\mathbb{F}_6 \overset{F+2E}{\cup} \mathbb{F}_0$

F, F	$\mathrm{Sp}(2)+6\mathbf{F}$
F, E	$\mathrm{SU}(3)_2+6\mathbf{F}$

$\mathrm{Bl}_5\mathbb{F}_5 \overset{2\ell-X_1}{\cup} \mathrm{dP}_2$

$F, \ell - X_1$	$\mathrm{SU}(3)_2+6\mathbf{F}$
$F, \ell - X_2$	$\mathrm{Sp}(2)+6\mathbf{F}$

$\mathrm{Bl}_4\mathbb{F}_4 \overset{2\ell-\sum_{i=1}^2 X_i}{\cup} \mathrm{dP}_3$

$F, \ell - X_1$	$\mathrm{SU}(3)_2+6\mathbf{F}$
$F, \ell - X_3$	$\mathrm{Sp}(2)+6\mathbf{F}$

Figure 14. $M = 7$ geometries.

$(\mathbb{F}_2 \overset{\ell-X_1}{\cup} \mathrm{dP}_7)^*$

$F, \ell - X_2$	$\mathrm{SU}(3)_4 + 6\mathbf{F}$
$F, 2\ell - \sum_{i=2}^{5} X_i$	$\mathrm{Sp}(2) + 4\mathbf{F} + 2\mathbf{AS}$
$F, 4\ell - \sum_{i=1}^{4} X_i - 2\sum_{j=5}^{7} X_j$	$G_2 + 6\mathbf{F}$
$F, 5\ell - X_1 - 2\sum_{i=2}^{7} X_i$	$A_2^{(2)}$

$\mathrm{Bl}_6\mathbb{F}_5 \overset{2\ell-X_1}{\cup} \mathrm{dP}_1 \longleftrightarrow \mathrm{Bl}_7\mathbb{F}_6 \overset{2\ell}{\cup} \mathbb{P}^2$

$F, \ell - X_1$	$\mathrm{SU}(3)_1 + 6\mathbf{F}$

$\downarrow\uparrow$

$\mathrm{Bl}_5\mathbb{F}_4 \overset{2\ell-\sum_{i=1}^{2} X_i}{\cup} \mathrm{dP}_2$

$F, \ell - X_1$	$\mathrm{SU}(3)_1 + 6\mathbf{F}$

$\downarrow\uparrow$

$\mathrm{Bl}_4\mathbb{F}_3 \overset{2\ell-\sum_{i=1}^{3} X_i}{\cup} \mathrm{dP}_3$

$F, \ell - X_1$	$\mathrm{SU}(3)_1 + 6\mathbf{F}$

$\downarrow\uparrow$

$\mathrm{Bl}_3\mathbb{F}_2 \overset{2\ell-\sum_{i=1}^{4} X_i}{\cup} \mathrm{dP}_4$

$F, \ell - X_1$	$\mathrm{SU}(3)_1 + 6\mathbf{F}$
$H - X_1 - X_2, 2\ell - \sum X_i$	$[\mathrm{SU}(2) + 1\mathbf{F}] \times [\mathrm{SU}(2) + 3\mathbf{F}]$

$\downarrow\uparrow$

$\mathrm{Bl}_2\mathbb{F}_1 \overset{2\ell-\sum_{i=1}^{5} X_i}{\cup} \mathrm{dP}_5$

$F, \ell - X_1$	$\mathrm{SU}(3)_1 + 6\mathbf{F}$
$f_1 \cdot E = 0, 2\ell - \sum_{i=1}^{4} X_i$	$[\mathrm{SU}(2) + 1\mathbf{F}] \times [\mathrm{SU}(2) \times 3\mathbf{F}]$

$\uparrow\downarrow \phi_1 \leftrightarrow \phi_2$

$\mathrm{Bl}_5\mathbb{F}_2 \overset{\ell-X_1}{\cup} \mathrm{dP}_2$

$F, \ell - X_2$	$\mathrm{SU}(3)_{-1} + 6\mathbf{F}$
$H - X_1 - X_2, \ell - X_1$	$[\mathrm{SU}(2) + 3\mathbf{F}] \times [\mathrm{SU}(2) + 1\mathbf{F}]$

$\downarrow\uparrow$

$\mathrm{Bl}_6\mathbb{F}_3 \overset{\ell}{\cup} \mathrm{dP}_1$

$F, \ell - X_1$	$\mathrm{SU}(3)_{-1} + 6\mathbf{F}$

$\mathbb{F}_1 \overset{X_1}{\cup} \mathrm{dP}_7$

$F, \ell - X_1$	$\mathrm{SU}(3)_3 + 6\mathbf{F}$
$F, \ell - X_2$	$\mathrm{Sp}(2) + 5\mathbf{F} + 1\mathbf{AS}$

$\mathrm{Bl}_6\mathbb{F}_4 \overset{F+E}{\cup} \mathbb{F}_0$

F, E	$\mathrm{SU}(3)_0 + 6\mathbf{F}$

$\uparrow\downarrow$

$\mathrm{Bl}_5\mathbb{F}_3 \overset{\ell}{\cup} \mathrm{dP}_2$

$F, \ell - X_1$	$\mathrm{SU}(3)_0 + 6\mathbf{F}$

$\uparrow\downarrow$

$\mathrm{Bl}_4\mathbb{F}_2 \overset{\ell-X_1}{\cup} \mathrm{dP}_3$

$F, \ell - X_2$	$\mathrm{SU}(3)_0 + 6\mathbf{F}$
$H - X_1 - X_2, \ell - X_1$	$[\mathrm{SU}(2) + 2\mathbf{F}] \times [\mathrm{SU}(2) \times 2\mathbf{F}]$

$\uparrow\downarrow$

$\mathrm{Bl}_3\mathbb{F}_1 \overset{\ell-X_1-X_2}{\cup} \mathrm{dP}_4$

$F, \ell - X_3$	$\mathrm{SU}(3)_0 + 6\mathbf{F}$
$f_1 \cdot E = 0, \ell - X_1$	$[\mathrm{SU}(2) + 2\mathbf{F}] \times [\mathrm{SU}(2) \times 2\mathbf{F}]$

Figure 15. $M = 7$ geometries, cont.

JHEP04(2018)103

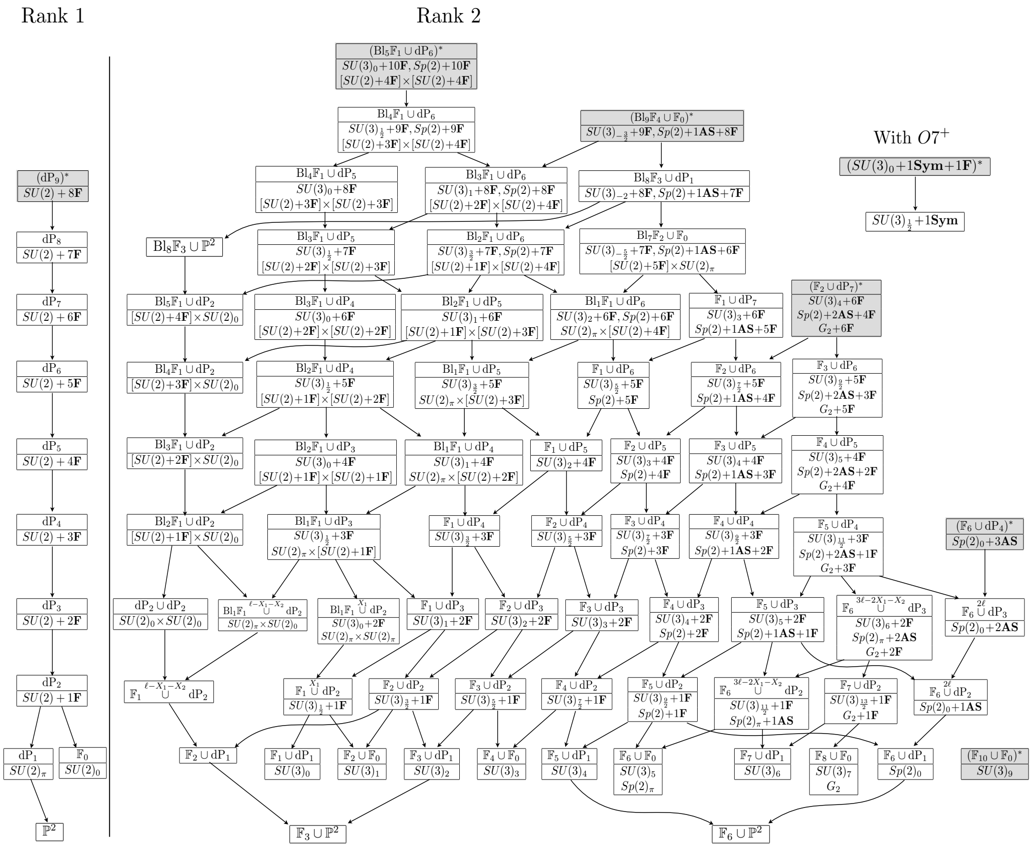

Figure 16. The diagram above shows the RG flow among rank 1 and rank 2 SCFTs obtained by mass deformations. The first and the second rows in each box correspond to the geometric and the gauge theoretic descriptions respectively of a 5d theory.[18] The parent theory in each branch is a 5d KK theory related to a 6d theory on S^1.

JHEP04(2018)103

[18]We note that while $\mathrm{Bl}_8\mathbb{F}_3 \cup \mathbb{P}^2$ has no gauge theory description, it is nonetheless related to $[\mathrm{SU}(2) + 5\mathbf{F}] \times \mathrm{SU}(2)_0$ by a flop transition: a flop of $\mathrm{Bl}_8\mathbb{F}_3 \cup \mathbb{P}^2$ leads to the geometry $\mathrm{Bl}_7\mathbb{F}_2 \overset{\ell-X_1}{\cup} \mathrm{dP}_1$, which has gauge theory description $[\mathrm{SU}(2) + 5\mathbf{F}] \times \mathrm{SU}(2)_0$. However, $\mathrm{Bl}_7\mathbb{F}_2 \overset{\ell-X_1}{\cup} \mathrm{dP}_1$ is not shrinkable, which implies that the BPS spectrum of the gauge theory will develop a negative mass before reaching a CFT fixed point. Nevertheless, this gauge theory makes sense as an effective description of the CFT from $\mathrm{Bl}_8\mathbb{F}_3 \cup \mathbb{P}^2$ through a flop transition to $\mathrm{Bl}_7\mathbb{F}_2 \overset{\ell-X_1}{\cup} \mathrm{dP}_1$ when mass parameters are turned on. We are greatful to Gabi Zafrir for pointing out that the CFT related to the $[\mathrm{SU}(2) + 5\mathbf{F}] \times \mathrm{SU}(2)_0$ gauge theory should exist since an associated (p, q) 5-brane system exists.

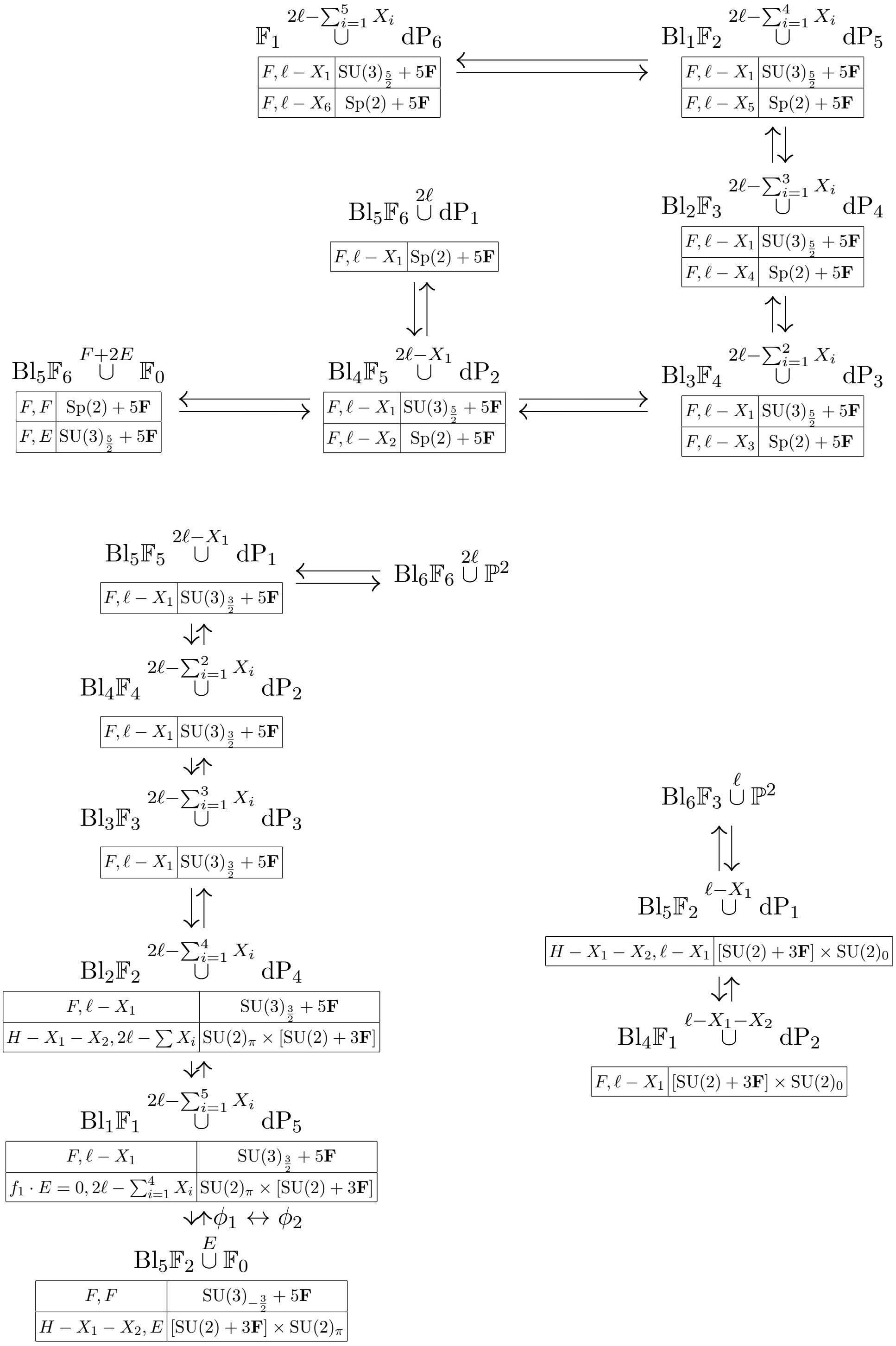

Figure 17. $M = 6$ geometries.

$\mathbb{F}_3 \overset{\ell}{\cup} \mathrm{dP}_6$

$F, \ell - X_6$	$\mathrm{SU}(3)_{\frac{9}{2}} + 5\mathbf{F}$
$F, 2\ell - \sum_{i=3}^{6} X_i$	$\mathrm{Sp}(2) + 3\mathbf{F} + 2\mathbf{AS}$
$F, 3\ell - \sum_{i=1}^{5} X_i - 2X_6$	$G_2 + 5\mathbf{F}$

$\mathbb{F}_2 \overset{\ell - X_1}{\cup} \mathrm{dP}_6$

$F, \ell - X_2$	$\mathrm{SU}(3)_{\frac{7}{2}} + 5\mathbf{F}$
$F, 2\ell - \sum_{i=3}^{6} X_i$	$\mathrm{Sp}(2) + 4\mathbf{F} + 1\mathbf{AS}$

$\mathrm{Bl}_5\mathbb{F}_4 \overset{F+E}{\cup} \mathbb{F}_0$

F, F	$\mathrm{SU}(3)_{\frac{1}{2}} + 5\mathbf{F}$

$\Updownarrow$

$\mathrm{Bl}_4\mathbb{F}_3 \overset{\ell}{\cup} \mathrm{dP}_2$

$F, \ell - X_1$	$\mathrm{SU}(3)_{\frac{1}{2}} + 5\mathbf{F}$

$\Updownarrow$

$\mathrm{Bl}_3\mathbb{F}_2 \overset{\ell - X_1}{\cup} \mathrm{dP}_3$

$F, \ell - X_1$	$\mathrm{SU}(3)_{\frac{1}{2}} + 5\mathbf{F}$
$H - X_1 - X_2, \ell - X_1$	$[\mathrm{SU}(2) + 1\mathbf{F}] \times [\mathrm{SU}(2) + 2\mathbf{F}]$

$\Updownarrow$

$\mathrm{Bl}_2\mathbb{F}_1 \overset{\ell - X_1 - X_2}{\cup} \mathrm{dP}_4$

$F, \ell - X_4$	$\mathrm{SU}(3)_{\frac{1}{2}} + 5\mathbf{F}$
$f_1 \cdot E = 0, \ell - X_1$	$[\mathrm{SU}(2) + 1\mathbf{F}] \times [\mathrm{SU}(2) + 2\mathbf{F}]$

$\Updownarrow \phi_1 \leftrightarrow \phi_2$

$\mathrm{Bl}_4\mathbb{F}_2 \overset{\ell - X_1}{\cup} \mathrm{dP}_2$

$F, \ell - X_1$	$\mathrm{SU}(3)_{-\frac{1}{2}} + 5\mathbf{F}$
$H - X_1 - X_2, \ell - X_1$	$[\mathrm{SU}(2) + 2\mathbf{F}] \times [\mathrm{SU}(2) + 1\mathbf{F}]$

$\Updownarrow$

$\mathrm{Bl}_5\mathbb{F}_3 \overset{\ell}{\cup} \mathrm{dP}_1$

$F, \ell - X_1$	$\mathrm{SU}(3)_{-\frac{1}{2}} + 5\mathbf{F}$

Figure 18. $M = 6$ geometries, cont.

$\mathbb{F}_2 \overset{2\ell-\sum_{i=1}^{4}X_i}{\cup} \mathrm{dP}_5$

$F, \ell - X_1$	$\mathrm{SU}(3)_3 + 4\mathbf{F}$
$F, \ell - X_5$	$\mathrm{Sp}(2) + 4\mathbf{F}$

$\updownarrows$

$\mathrm{Bl}_1\mathbb{F}_3 \overset{2\ell-\sum_{i=1}^{3}X_i}{\cup} \mathrm{dP}_4$

$F, \ell - X_1$	$\mathrm{SU}(3)_3 + 4\mathbf{F}$
$\ell - X_4$	$\mathrm{Sp}(2) + 4\mathbf{F}$

$\updownarrows$

$\mathrm{Bl}_4\mathbb{F}_6 \overset{2\ell}{\cup} \mathrm{dP}_1$

$F, \ell - X_1$	$\mathrm{Sp}(2) + 4\mathbf{F}$

$\downuparrows$

$\mathrm{Bl}_4\mathbb{F}_6 \overset{F+2E}{\cup} \mathbb{F}_0$

F, F	$\mathrm{Sp}(2) + 4\mathbf{F}$
F, E	$\mathrm{SU}(3)_3 + 4\mathbf{F}$

$\leftrightarrows$

$\mathrm{Bl}_3\mathbb{F}_5 \overset{2\ell-X_1}{\cup} \mathrm{dP}_2$

$F, \ell - X_1$	$\mathrm{SU}(3)_3 + 4\mathbf{F}$
$F, \ell - X_2$	$\mathrm{Sp}(2) + 4\mathbf{F}$

$\rightleftarrows$

$\mathrm{Bl}_2\mathbb{F}_4 \overset{2\ell-\sum_{i=1}^{2}X_i}{\cup} \mathrm{dP}_3$

$F, \ell - X_1$	$\mathrm{SU}(3)_3 + 4\mathbf{F}$
$F, \ell - X_3$	$\mathrm{Sp}(2) + 4\mathbf{F}$

$\mathrm{Bl}_5\mathbb{F}_6 \overset{2\ell}{\cup} \mathbb{P}^2$

$\downuparrows$

$\mathrm{Bl}_4\mathbb{F}_5 \overset{2\ell-X_1}{\cup} \mathrm{dP}_1$

$F, \ell - X_1$	$\mathrm{SU}(3)_2 + 4\mathbf{F}$

$\downuparrows$

$\mathrm{Bl}_3\mathbb{F}_4 \overset{2\ell-\sum_{i=1}^{2}X_i}{\cup} \mathrm{dP}_2$

$F, \ell - X_{j=1,2}$	$\mathrm{SU}(3)_2 + 4\mathbf{F}$

$\downuparrows$

$\mathrm{Bl}_2\mathbb{F}_3 \overset{2\ell-\sum_{i=1}^{3}X_i}{\cup} \mathrm{dP}_3$

$F, \ell - X_{j=1,\ldots,3}$	$\mathrm{SU}(3)_2 + 4\mathbf{F}$

$\downuparrows$

$\mathrm{Bl}_1\mathbb{F}_2 \overset{2\ell-\sum_{i=1}^{4}X_i}{\cup} \mathrm{dP}_4$

$F, \ell - X_{j=1,\ldots,4}$	$\mathrm{SU}(3)_2 + 4\mathbf{F}$

$\downuparrows$

$\mathbb{F}_1 \overset{2\ell-\sum_{i=1}^{5}X_i}{\cup} \mathrm{dP}_5$

$F, \ell - X_1$	$\mathrm{SU}(3)_2 + 4\mathbf{F}$

Figure 19. $M = 5$ geometries.

$$\mathrm{Bl}_4\mathbb{F}_4 \overset{F+E}{\cup} \mathbb{F}_0$$

F, F	$\mathrm{SU}(3)_1 + 4\mathbf{F}$

$\uparrow\downarrow$

$$\mathrm{Bl}_3\mathbb{F}_3 \overset{\ell}{\cup} \mathrm{dP}_2$$

$F, \ell - X_1$	$\mathrm{SU}(3)_1 + 4\mathbf{F}$

$$\mathrm{Bl}_2\mathbb{F}_2 \overset{\ell - X_1}{\cup} \mathrm{dP}_3$$

$F, \ell - X_2$	$\mathrm{SU}(3)_1 + 4\mathbf{F}$
$H - X_1 - X_2, \ell - X_1$	$\mathrm{SU}(2)_\pi \times [\mathrm{SU}(2) + 2\mathbf{F}]$

$\uparrow\downarrow$

$$\mathrm{Bl}_1\mathbb{F}_1 \overset{\ell - X_1 - X_2}{\cup} \mathrm{dP}_4$$

$F, \ell - X_3$	$\mathrm{SU}(3)_1 + 4\mathbf{F}$
$f_1 \cdot E = 0, \ell - X_1$	$\mathrm{SU}(2)_\pi \times [\mathrm{SU}(2) + 2\mathbf{F}]$

$\downarrow\uparrow \phi_1 \leftrightarrow \phi_2$

$$\mathrm{Bl}_4\mathbb{F}_2 \overset{E}{\cup} \mathbb{F}_0$$

F, F	$\mathrm{SU}(3)_{-1} + 4\mathbf{F}$
$H - X_1 - X_2, E$	$[\mathrm{SU}(2) + 2\mathbf{F}] \times \mathrm{SU}(2)_\pi$

$$\mathrm{Bl}_5\mathbb{F}_3 \overset{\ell}{\cup} \mathbb{P}^2$$

$\uparrow\downarrow$

$$\mathrm{Bl}_4\mathbb{F}_2 \overset{\ell - X_1}{\cup} \mathrm{dP}_1$$

$H - X_1 - X_2, \ell - X_1$	$[\mathrm{SU}(2) + 2\mathbf{F}] \times \mathrm{SU}(2)_0$

$\downarrow\uparrow$

$$\mathrm{Bl}_3\mathbb{F}_1 \overset{\ell - X_1 - X_2}{\cup} \mathrm{dP}_2$$

$F, \ell - X_1$	$[\mathrm{SU}(2) + 2\mathbf{F}] \times \mathrm{SU}(2)_0$

$$\mathrm{Bl}_2\mathbb{F}_1 \overset{\ell - X_1 - X_2}{\cup} \mathrm{dP}_3$$

$F, \ell - X_3$	$\mathrm{SU}(3)_0 + 4\mathbf{F}$
$f_1 \cdot E = 0, \ell - X_1$	$[\mathrm{SU}(2) + 1\mathbf{F}] \times [\mathrm{SU}(2) + 1\mathbf{F}]$

$\downarrow\uparrow$

$$\mathrm{Bl}_3\mathbb{F}_2 \overset{\ell - X_1}{\cup} \mathrm{dP}_2$$

$F, \ell - X_2$	$\mathrm{SU}(3)_0 + 4\mathbf{F}$
$H - X_1 - X_2, \ell - X_1$	$[\mathrm{SU}(2) + 1\mathbf{F}] \times [\mathrm{SU}(2) + 1\mathbf{F}]$

$\leftrightarrows$

$$\mathrm{Bl}_4\mathbb{F}_3 \overset{\ell}{\cup} \mathrm{dP}_1$$

$F, \ell - X_1$	$\mathrm{SU}(3)_0 + 4\mathbf{F}$

$$\mathbb{F}_4 \overset{2\ell - X_1 - X_2}{\cup} \mathrm{dP}_5$$

$F, \ell - X_1$	$\mathrm{SU}(3)_5 + 4\mathbf{F}$
$F, \ell - X_5$	$\mathrm{Sp}(2) + 2\mathbf{F} + 2\mathbf{AS}$
$F, 2\ell - \sum_{i=2}^5 X_i$	$G_2 + 4\mathbf{F}$

$$\mathbb{F}_3 \overset{\ell}{\cup} \mathrm{dP}_5$$

$F, \ell - X_1$	$\mathrm{SU}(3)_4 + 4\mathbf{F}$
$F, 2\ell - \sum X_i$	$\mathrm{Sp}(2) + 3\mathbf{F} + 1\mathbf{AS}$

Figure 20. $M = 5$ geometries, cont.

$\mathrm{Bl}_3\mathbb{F}_6 \overset{2\ell}{\cup} \mathrm{dP}_1$

$F, \ell - X_1$	$\mathrm{Sp}(2) + 3\mathbf{F}$

$\mathbb{F}_3 \overset{2\ell-\sum_{i=1}^{3} X_i}{\cup} \mathrm{dP}_4$

$F, \ell - X_1$	$\mathrm{SU}(3)_{\frac{7}{2}} + 3\mathbf{F}$
$F, \ell - X_4$	$\mathrm{Sp}(2) + 3\mathbf{F}$

$\downarrow\uparrow$

$\mathrm{Bl}_3\mathbb{F}_6 \overset{F+2E}{\cup} \mathbb{F}_0$

F, F	$\mathrm{Sp}(2) + 3\mathbf{F}$
F, E	$\mathrm{SU}(3)_{\frac{7}{2}} + 3\mathbf{F}$

$\leftrightarrows$

$\mathrm{Bl}_2\mathbb{F}_5 \overset{2\ell-X_1}{\cup} \mathrm{dP}_2$

$F, \ell - X_1$	$\mathrm{SU}(3)_{\frac{7}{2}} + 3\mathbf{F}$
$F, \ell - X_2$	$\mathrm{Sp}(2) + 3\mathbf{F}$

$\leftrightarrows$

$\mathrm{Bl}_1\mathbb{F}_4 \overset{2\ell-\sum_{i=1}^{2} X_i}{\cup} \mathrm{dP}_3$

$F, \ell - X_1$	$\mathrm{SU}(3)_{\frac{7}{2}} + 3\mathbf{F}$
$F, \ell - X_3$	$\mathrm{Sp}(2) + 3\mathbf{F}$

$\mathrm{Bl}_4\mathbb{F}_6 \overset{2\ell}{\cup} \mathbb{P}^2$

$\downarrow\uparrow$

$\mathrm{Bl}_3\mathbb{F}_5 \overset{2\ell-X_1}{\cup} \mathrm{dP}_1$

$F, \ell - X_1$	$\mathrm{SU}(3)_{\frac{5}{2}} + 3\mathbf{F}$

$\downarrow\uparrow$

$\mathrm{Bl}_2\mathbb{F}_4 \overset{2\ell-\sum_{i=1}^{2} X_i}{\cup} \mathrm{dP}_2$

$F, \ell - X_1$	$\mathrm{SU}(3)_{\frac{5}{2}} + 3\mathbf{F}$

$\downarrow\uparrow$

$\mathrm{Bl}_1\mathbb{F}_3 \overset{2\ell-\sum_{i=1}^{3} X_i}{\cup} \mathrm{dP}_3$

$F, \ell - X_1$	$\mathrm{SU}(3)_{\frac{5}{2}} + 3\mathbf{F}$

$\downarrow\uparrow$

$\mathbb{F}_2 \overset{2\ell-\sum_{i=1}^{4} X_i}{\cup} \mathrm{dP}_4$

$F, \ell - X_1$	$\mathrm{SU}(3)_{\frac{5}{2}} + 3\mathbf{F}$

$\mathrm{Bl}_3\mathbb{F}_4 \overset{F+E}{\cup} \mathbb{F}_0$

F, F	$\mathrm{SU}(3)_{\frac{3}{2}} + 3\mathbf{F}$

$\uparrow\downarrow$

$\mathrm{Bl}_2\mathbb{F}_3 \overset{\ell}{\cup} \mathrm{dP}_2$

$F, \ell - X_1$	$\mathrm{SU}(3)_{\frac{3}{2}} + 3\mathbf{F}$

$\uparrow\downarrow$

$\mathrm{Bl}_1\mathbb{F}_2 \overset{\ell-X_1}{\cup} \mathrm{dP}_3$

$F, \ell - X_1$	$\mathrm{SU}(3)_{\frac{3}{2}} + 3\mathbf{F}$

$\uparrow\downarrow$

$\mathbb{F}_1 \overset{\ell-X_1-X_2}{\cup} \mathrm{dP}_4$

$F, \ell - X_3$	$\mathrm{SU}(3)_{\frac{3}{2}} + 3\mathbf{F}$

Figure 21. $M = 4$ geometries.

$(\mathbb{F}_6 \overset{2\ell}{\cup} \mathrm{dP}_4)^*$

$F, \ell - X_1$	$\mathrm{Sp}(2)_0 + 3\mathbf{AS}$
$F, 2\ell - \sum X_i$	$A_2^{(2)}$

$\mathrm{Bl}_4\mathbb{F}_3 \overset{\ell}{\cup} \mathbb{P}^2$

$\upharpoonleft\downharpoonright$

$\mathrm{Bl}_3\mathbb{F}_2 \overset{\ell - X_1}{\cup} \mathrm{dP}_1$

$H - X_1 - X_2, \ell - X_1$	$[\mathrm{SU}(2) + 1\mathbf{F}] \times \mathrm{SU}(2)_0$

$\leftrightarrows$

$\mathrm{Bl}_2\mathbb{F}_1 \overset{\ell - X_1 - X_2}{\cup} \mathrm{dP}_2$

$F, \ell - X_{j=1,2}$	$[\mathrm{SU}(2) + \mathbf{F}] \times \mathrm{SU}(2)_0$

$\mathrm{Bl}_2\mathbb{F}_2 \overset{\ell - X_1}{\cup} \mathrm{dP}_2$

$F, \ell - X_2$	$\mathrm{SU}(3)_{\frac{1}{2}} + 3\mathbf{F}$
$H - X_1 - X_2, \ell - X_1$	$\mathrm{SU}(2)_\pi \times [\mathrm{SU}(2) + 1\mathbf{F}]$

$\leftrightarrows$

$\mathrm{Bl}_1\mathbb{F}_1 \overset{\ell - X_1 - X_2}{\cup} \mathrm{dP}_3$

$F, \ell - X_3$	$\mathrm{SU}(3)_{\frac{1}{2}} + 3\mathbf{F}$
$f_1 \cdot E = 0, \ell - X_1$	$\mathrm{SU}(2)_\pi \times [\mathrm{SU}(2) + 1\mathbf{F}]$

$\downharpoonleft\upharpoonright$

$\mathrm{Bl}_3\mathbb{F}_3 \overset{\ell}{\cup} \mathrm{dP}_1$

$F, \ell - X_1$	$\mathrm{SU}(3)_{\frac{1}{2}} + 3\mathbf{F}$

$\phi_1 \leftrightarrow \phi_2$

$\mathrm{Bl}_3\mathbb{F}_2 \overset{E}{\cup} \mathbb{F}_0$

F, F	$\mathrm{SU}(3)_{-\frac{1}{2}} + 3\mathbf{F}$
$H - X_1 - X_2, E$	$[\mathrm{SU}(2) + 1\mathbf{F}] \times \mathrm{SU}(2)_\pi$

$\mathbb{F}_5 \overset{2\ell - X_1}{\cup} \mathrm{dP}_4$

$F, \ell - X_1$	$\mathrm{SU}(3)_{\frac{11}{2}} + 3\mathbf{F}$
$F, \ell - X_1$	$\mathrm{Sp}(2) + \mathbf{F} + 2\mathbf{AS}$
$F, 2\ell - \sum X_i$	$G_2 + 3\mathbf{F}$

$\mathbb{F}_4 \overset{2\ell - X_1 - X_2}{\cup} \mathrm{dP}_4$

$F, \ell - X_1$	$\mathrm{SU}(3)_{\frac{9}{2}} + 3\mathbf{F}$
$F, \ell - X_3$	$\mathrm{Sp}(2) + 2\mathbf{F} + 1\mathbf{AS}$

Figure 22. $M = 4$ geometries, cont.

$$
\mathrm{Bl}_3\mathbb{F}_6 \overset{2\ell}{\cup} \mathbb{P}^2 \;\rightleftarrows\; \begin{array}{c} \mathrm{Bl}_2\mathbb{F}_5 \overset{2\ell-X_1}{\cup} \mathrm{dP}_1 \\ \begin{array}{|c|c|}\hline F, \ell - X_1 & \mathrm{SU}(3)_3 + 2\mathbf{F} \\ \hline \end{array} \end{array} \;\rightleftarrows\; \begin{array}{c} \mathrm{Bl}_1\mathbb{F}_4 \overset{2\ell-\sum_{i=1}^{2} X_i}{\cup} \mathrm{dP}_2 \\ \begin{array}{|c|c|}\hline F, \ell - X_{j=1,2} & \mathrm{SU}(3)_3 + 2\mathbf{F} \\ \hline \end{array} \\ \downarrow\uparrow \\ \mathbb{F}_3 \overset{2\ell-\sum_{i=1}^{3} X_i}{\cup} \mathrm{dP}_3 \\ \begin{array}{|c|c|}\hline F, \ell - X_1 & \mathrm{SU}(3)_3 + 2\mathbf{F} \\ \hline \end{array} \end{array}
$$

$$
\begin{array}{c} \mathrm{Bl}_2\mathbb{F}_6 \overset{F+2E}{\cup} \mathbb{F}_0 \\ \begin{array}{|c|c|}\hline F, F & \mathrm{Sp}(2) + 2\mathbf{F} \\ \hline F, E & \mathrm{SU}(3)_4 + 2\mathbf{F} \\ \hline \end{array} \end{array} \;\rightleftarrows\; \begin{array}{c} \mathrm{Bl}_2\mathbb{F}_6 \overset{2\ell}{\cup} \mathrm{dP}_1 \\ \begin{array}{|c|c|}\hline F, \ell - X_1 & \mathrm{Sp}(2) + 2\mathbf{F} \\ \hline \end{array} \\ \downarrow\uparrow \\ \mathrm{Bl}_1\mathbb{F}_5 \overset{2\ell-X_1}{\cup} \mathrm{dP}_2 \\ \begin{array}{|c|c|}\hline F, \ell - X_1 & \mathrm{SU}(3)_4 + 2\mathbf{F} \\ \hline F, \ell - X_2 & \mathrm{Sp}(2) + 2\mathbf{F} \\ \hline \end{array} \end{array} \;\rightleftarrows\; \begin{array}{c} \mathbb{F}_4 \overset{2\ell-\sum_{i=1}^{2} X_i}{\cup} \mathrm{dP}_3 \\ \begin{array}{|c|c|}\hline F, \ell - X_1 & \mathrm{SU}(3)_4 + 2\mathbf{F} \\ \hline F, \ell - X_3 & \mathrm{Sp}(2) + 2\mathbf{F} \\ \hline \end{array} \end{array}
$$

$$
\begin{array}{c} \mathrm{Bl}_2\mathbb{F}_4 \overset{F+E}{\cup} \mathbb{F}_0 \\ \begin{array}{|c|c|}\hline F, F & \mathrm{SU}(3)_2 + 2\mathbf{F} \\ \hline \end{array} \end{array} \;\leftrightarrows\; \begin{array}{c} \mathrm{Bl}_1\mathbb{F}_3 \overset{\ell}{\cup} \mathrm{dP}_2 \\ \begin{array}{|c|c|}\hline F, \ell - X_1 & \mathrm{SU}(3)_2 + 2\mathbf{F} \\ \hline \end{array} \end{array} \;\leftrightarrows\; \begin{array}{c} \mathbb{F}_2 \overset{\ell-X_1}{\cup} \mathrm{dP}_3 \\ \begin{array}{|c|c|}\hline F, \ell - X_1 & \mathrm{SU}(3)_2 + 2\mathbf{F} \\ \hline \end{array} \end{array}
$$

Figure 23. $M = 3$ geometries.

$\mathrm{Bl}_3\mathbb{F}_3 \overset{\ell}{\cup} \mathbb{P}^2$

$\updownarrows$

$\mathrm{dP}_2 \overset{\ell-X_1-X_2}{\cup} \mathrm{dP}_2$

$\ell - X_1, \ell - X_1$	$\mathrm{SU}(2)_0 \times \mathrm{SU}(2)_0$

$\mathrm{Bl}_2\mathbb{F}_2 \overset{\ell-X_1}{\cup} \mathrm{dP}_1$

$H - X_1 - X_2, \ell - X_1$	$\mathrm{SU}(2)_\pi \times \mathrm{SU}(2)_0$

$\rightleftarrows$

$\mathrm{Bl}_1\mathbb{F}_1 \overset{\ell-X_1-X_2}{\cup} \mathrm{dP}_2$

$f_1 \cdot E = 0, \ell - X_1$	$\mathrm{SU}(2)_\pi \times \mathrm{SU}(2)_0$

$\mathrm{Bl}_2\mathbb{F}_2 \overset{E}{\cup} \mathbb{F}_0$

F, F	$\mathrm{SU}(3)_0 + 2\mathbf{F}$
$H - X_1 - X_2, E$	$\mathrm{SU}(2)_\pi \times \mathrm{SU}(2)_\pi$

$\leftrightarrows$

$\mathrm{Bl}_1\mathbb{F}_1 \overset{X_1}{\cup} \mathrm{dP}_2$

$F, \ell - X_1$	$\mathrm{SU}(3)_0 + 2\mathbf{F}$
$f_1 \cdot E = 0, \ell - X_2$	$\mathrm{SU}(2)_\pi \times \mathrm{SU}(2)_\pi$

$\mathrm{Bl}_2\mathbb{F}_3 \overset{\ell}{\cup} \mathrm{dP}_1$

$F, \ell - X_1$	$\mathrm{SU}(3)_1 + 2\mathbf{F}$

$\leftrightarrows$

$\mathrm{Bl}_1\mathbb{F}_2 \overset{\ell-X_1}{\cup} \mathrm{dP}_2$

$F, \ell - X_2$	$\mathrm{SU}(3)_1 + 2\mathbf{F}$

$\leftrightarrows$

$\mathbb{F}_1 \overset{\ell-X_1-X_2}{\cup} \mathrm{dP}_3$

$F, \ell - X_3$	$\mathrm{SU}(3)_1 + 2\mathbf{F}$

$\mathbb{F}_5 \overset{2\ell-X_1}{\cup} \mathrm{dP}_3$

$F, \ell - X_1$	$\mathrm{SU}(3)_5 + 2\mathbf{F}$
$F, \ell - X_2$	$\mathrm{Sp}(2) + 1\mathbf{F} + 1\mathbf{AS}$

$\mathbb{F}_6 \overset{2\ell}{\cup} \mathrm{dP}_3$

$F, \ell - X_1$	$\mathrm{Sp}(2)_0 + 2\mathbf{AS}$

$\mathbb{F}_6 \overset{3\ell-2X_1-X_2}{\cup} \mathrm{dP}_3$

$F, \ell - X_2$	$\mathrm{Sp}(2)_\pi + 2\mathbf{AS}$
$F, \ell - X_1$	$\mathrm{SU}(3)_6 + 2\mathbf{F}$
$F, \ell - X_3$	$G_2 + 2\mathbf{F}$

Figure 24. $M = 3$ geometries, cont. Note that for the geometry $\mathrm{dP}_2 \cup \mathrm{dP}_2$ at the top, the gluing curves in *both* surfaces are $C = \ell - X_1 - X_2$, in contrast to the other geometries.

$$\mathrm{Bl}_2\mathbb{F}_6 \overset{2\ell}{\cup} \mathbb{P}^2 \;\rightleftarrows\; \mathrm{Bl}_1\mathbb{F}_5 \overset{2\ell-X_1}{\cup} \mathrm{dP}_1 \;\rightleftarrows\; \mathbb{F}_4 \overset{2\ell-\sum_{i=1}^{2}X_i}{\cup} \mathrm{dP}_2$$

$\mathrm{Bl}_1\mathbb{F}_5 \overset{2\ell-X_1}{\cup} \mathrm{dP}_1$:

$F, \ell - X_1$	$\mathrm{SU}(3)_{\frac{7}{2}} + 1\mathbf{F}$

$\mathbb{F}_4 \overset{2\ell-\sum_{i=1}^{2}X_i}{\cup} \mathrm{dP}_2$:

$F, \ell - X_{j=1,2}$	$\mathrm{SU}(3)_{\frac{7}{2}} + 1\mathbf{F}$

$$\mathrm{Bl}_1\mathbb{F}_6 \overset{F+2E}{\cup} \mathbb{F}_0 \;\leftrightarrows\; \mathbb{F}_5 \overset{2\ell-X_1}{\cup} \mathrm{dP}_2 \;\leftrightarrows\; \mathrm{Bl}_1\mathbb{F}_6 \overset{2\ell}{\cup} \mathrm{dP}_1$$

$\mathrm{Bl}_1\mathbb{F}_6 \overset{F+2E}{\cup} \mathbb{F}_0$:

F, F	$\mathrm{Sp}(2) + 1\mathbf{F}$
F, E	$\mathrm{SU}(3)_{\frac{9}{2}} + 1\mathbf{F}$

$\mathbb{F}_5 \overset{2\ell-X_1}{\cup} \mathrm{dP}_2$:

$F, \ell - X_1$	$\mathrm{SU}(3)_{\frac{9}{2}} + 1\mathbf{F}$
$F, \ell - X_2$	$\mathrm{Sp}(2) + 1\mathbf{F}$

$\mathrm{Bl}_1\mathbb{F}_6 \overset{2\ell}{\cup} \mathrm{dP}_1$:

$F, \ell - X_1$	$\mathrm{Sp}(2) + 1\mathbf{F}$

$$\mathrm{Bl}_1\mathbb{F}_4 \overset{F+E}{\cup} \mathbb{F}_0 \;\leftrightarrows\; \mathbb{F}_3 \overset{\ell}{\cup} \mathrm{dP}_2$$

$\mathrm{Bl}_1\mathbb{F}_4 \overset{F+E}{\cup} \mathbb{F}_0$:

F, F	$\mathrm{SU}(3)_{\frac{5}{2}} + 1\mathbf{F}$

$\mathbb{F}_3 \overset{\ell}{\cup} \mathrm{dP}_2$:

$F, \ell - X_1$	$\mathrm{SU}(3)_{\frac{5}{2}} + 1\mathbf{F}$

$$\mathrm{Bl}_2\mathbb{F}_3 \overset{\ell}{\cup} \mathbb{P}^2 \;\leftrightarrows\; \mathrm{Bl}_1\mathbb{F}_2 \overset{\ell-X_1}{\cup} \mathrm{dP}_1 \;\leftrightarrows\; \mathbb{F}_1 \overset{\ell-X_1-X_2}{\cup} \mathrm{dP}_2$$

$$\mathrm{Bl}_1\mathbb{F}_2 \overset{E}{\cup} \mathbb{F}_0 \;\leftrightarrows\; \mathbb{F}_1 \overset{X_1}{\cup} \mathrm{dP}_2$$

$\mathrm{Bl}_1\mathbb{F}_2 \overset{E}{\cup} \mathbb{F}_0$:

F, F	$\mathrm{SU}(3)_{\frac{1}{2}} + 1\mathbf{F}$

$\mathbb{F}_1 \overset{X_1}{\cup} \mathrm{dP}_2$:

$F, \ell - X_1$	$\mathrm{SU}(3)_{\frac{1}{2}} + 1\mathbf{F}$

$$\mathrm{Bl}_1\mathbb{F}_3 \overset{\ell}{\cup} \mathrm{dP}_1 \;\leftrightarrows\; \mathbb{F}_2 \overset{\ell-X_1}{\cup} \mathrm{dP}_2$$

$\mathrm{Bl}_1\mathbb{F}_3 \overset{\ell}{\cup} \mathrm{dP}_1$:

$F, \ell - X_1$	$\mathrm{SU}(3)_{\frac{3}{2}} + 1\mathbf{F}$

$\mathbb{F}_2 \overset{\ell-X_1}{\cup} \mathrm{dP}_2$:

$F, \ell - X_2$	$\mathrm{SU}(3)_{\frac{3}{2}} + 1\mathbf{F}$

$\mathbb{F}_7 \overset{3\ell-2X_1}{\cup} \mathrm{dP}_2$:

$F, \ell - X_1$	$\mathrm{SU}(3)_{\frac{13}{2}} + 1\mathbf{F}$
$F, \ell - X_2$	$G_2 + 1\mathbf{F}$

$\mathbb{F}_6 \overset{2\ell}{\cup} \mathrm{dP}_2$:

$F, \ell - X_1$	$\mathrm{Sp}(2)_0 + 1\mathbf{AS}$

$\mathbb{F}_6 \overset{3\ell-2X_1-X_2}{\cup} \mathrm{dP}_2$:

$F, \ell - X_1$	$\mathrm{SU}(3)_{\frac{11}{2}} + 1\mathbf{F}$
$F, \ell - X_2$	$\mathrm{Sp}(2)_\pi + 1\mathbf{AS}$

Figure 25. $M = 2$ geometries.

$$\mathbb{F}_{2b} \overset{F+(b-1)E}{\cup} \mathbb{F}_0$$

$b=1$	F, E	$\mathrm{SU}(3)_1$
$b=2$	F, F	$\mathrm{SU}(3)_3$
$b=3$	F, E	$\mathrm{SU}(3)_5$
$b=3$	F, F	$\mathrm{Sp}(2)_\pi$
$b=4$	F, E	$\mathrm{SU}(3)_7$
$b=4$	F, F	G_2
$b=5$	F, E	$\mathrm{SU}(3)_9$
$b=5$	F, F	$A_2^{(2)}$

$$\mathrm{Bl}_1\mathbb{F}_6 \overset{2\ell}{\cup} \mathbb{P}^2 \rightleftarrows \mathbb{F}_5 \overset{2\ell-X_1}{\cup} \mathrm{dP}_1 \qquad \mathrm{Bl}_1\mathbb{F}_3 \overset{\ell}{\cup} \mathbb{P}^2 \rightleftarrows \mathbb{F}_2 \overset{\ell-X_1}{\cup} \mathrm{dP}_1$$

$F, \ell - X_1$	$\mathrm{SU}(3)_4$

$$\mathbb{F}_3 \overset{\ell}{\cup} \mathrm{dP}_1$$

$F, \ell - X_1$	$\mathrm{SU}(3)_2$

$$\mathbb{F}_6 \overset{2\ell}{\cup} \mathrm{dP}_1$$

$F, \ell - X_1$	$\mathrm{Sp}(2)_0$

$$\mathbb{F}_1 \overset{X_1}{\cup} \mathrm{dP}_1$$

$F, \ell - X_1$	$\mathrm{SU}(3)_0$

$$\mathbb{F}_7 \overset{3\ell-2X_1}{\cup} \mathrm{dP}_1$$

$F, \ell - X_1$	$\mathrm{SU}(3)_6$

Figure 26. $M = 1$ geometries.

$$\mathbb{F}_3 \overset{\ell}{\cup} \mathbb{P}^2 \qquad \mathbb{F}_6 \overset{2\ell}{\cup} \mathbb{P}^2$$

Figure 27. $M = 0$ geometries.

6d theories on a circle. In this section we show that the complicated web of theories we have uncovered are actually unified from the perspective of 5d Kaluza-Klein (KK) theories arising from 6d SCFTs compactified on a circle (up to possible automorphism twists and holonomies).

As discussed in section 4.1, shrinkable rank 1 geometries are classified by del Pezzo surfaces $\mathrm{dP}_{n\leq 8}$ and $\mathbb{F}_0$ up to physical equivalence. Interestingly, all of them can be obtained via geometric RG flows from dP_9 (equivalently, $\frac{1}{2}$K3). The local dP_9 model is an elliptic 3-fold engineering the 6d SCFT called the 'E-string theory'. Therefore all rank 1 5d SCFTs are descendants (i.e. related by rank preserving mass deformations) of the 6d E-string theory compactified on a circle.

We also find that all rank 2 5d SCFTs have 6d origin, but the rank 2 case is significantly more elaborate than the rank 1 case. Geometric constructions produce 5d SCFTs belonging to the four distinct families displayed in table 3. The geometries of type $(\cdot)^*$ are not shrinkable but rather 5d KK theories.[19] We expect that these geometries correspond to 6d SCFTs compactified on a circle, possibly with automorphism twists.

[19] These theories are also called *marginal* theories [13].

One distinguished property of geometries corresponding to 5d KK theories is that there must exist an elliptic curve class whose volume is not controlled by normalizable Kähler moduli. The M2-branes wrapping this elliptic class correspond to KK momentum states. For example, the canonical class $-K_{\mathrm{dP}_9} \subset \mathrm{dP}_9$ is an elliptic class with zero volume associated to the KK momenta of the E-string theory compactified on a circle. Another important property is that some KK geometries contain fiber classes forming an affine gauge algebra. Namely, we can find fiber classes f_i such that

$$-f_i \cdot S_j = (A_{\hat{G}})_{ij}, \tag{4.20}$$

where $\hat{G}$ denotes an affine gauge algebra. This signals that the corresponding geometry is an elliptic geometry realizing a 5d KK theory. We will now identify 6d origins of the geometries in table 3 using these properties.

We begin with $\mathrm{Bl}_{10}\mathbb{F}_6 \cup \mathbb{F}_0$. This geometry has two gauge theory descriptions, namely $\mathrm{SU}(3)_0 + 10\mathbf{F}$ and $\mathrm{Sp}(2) + 10\mathbf{F}$. The 6d origin of these gauge theories is discussed in [21–23, 35]. These theories are a circle reduction of the 6d (D_5, D_5) conformal matter theory introduced in [2, 36]. The geometry $\mathrm{Bl}_{10}\mathbb{F}_6 \cup \mathbb{F}_0$ realizes the circle compactification of this 6d theory. This theory has another duality frame in which an affine gauge algebra is manifest. To see this, choose the fiber classes $f_1 = H + 2F - \sum_{i=1}^{10} X_i$ and $f_2 = F$. These fiber classes indeed form the affine $\hat{A}_1$ Cartan matrix:

$$-(f_i \cdot S_j) = \begin{pmatrix} 2 & -2 \\ -2 & 2 \end{pmatrix}. \tag{4.21}$$

Another geometry $\mathbb{F}_2 \cup \mathrm{dP}_7$ is interesting for similar reasons. This geometry admits three different gauge theory descriptions corresponding to the following choices of fiber classes:

$$\begin{aligned} &f_1 = F, \quad f_2 = \ell - X_2 && \to \quad \mathrm{SU}(3)_4 + 6\mathbf{F}\,, \\ &f_1 = F, \quad f_2 = 2\ell - \sum_{i=2}^{5} X_i && \to \quad \mathrm{Sp}(2) + 2\mathbf{AS} + 4\mathbf{F}\,, \\ &f_1 = F, \quad f_2 = 3\ell - \sum_{i=2}^{6} X_i - 2X_7 && \to \quad G_2 + 6\mathbf{F}\,. \end{aligned} \tag{4.22}$$

Here, the two surfaces are glued along the curves $C_{S_1} = E$ and $C_{S_2} = \ell - X_1$. This implies new dualities between these three gauge theories and their descendants obtained by RG-flows induced by relevant mass deformations. In addition, we find another distinct duality frame:

$$f_1 = F\,, \;\; f_2 = 5\ell - X_1 - 2\sum_{i=2}^{7} X_i\,. \tag{4.23}$$

The fiber classes in this last frame form the affine Cartan matrix $A_2^{(2)}$:

$$-(f_i \cdot S_j) = \begin{pmatrix} 2 & -1 \\ -4 & 2 \end{pmatrix}. \tag{4.24}$$

JHEP04(2018)103

This algebra $A_2^{(2)}$ is obtained by an outer automorphism twist of the affine $A_2^{(1)} = \hat{A}_2$ algebra which identifies $\mathbf{3}$ and $\bar{\mathbf{3}}$ representations in $A_2 \subset \hat{A}_2$. Therefore, one can expect that this geometry is also a KK geometry corresponding to a 6d SU(3) gauge theory compactified on a circle with an outer automorphism twist. The unique 6d theory satisfying these properties is the 6d $\mathcal{N} = (1,0)$ SCFT with SU(3) gauge group and $N_{\mathbf{F}} = 12$ fundamental hypermultiplets. Circle compactification of this 6d theory with an outer automorphism twist of the SU(3) gauge algebra leads to a 5d theory with affine $A_2^{(2)}$ gauge algebra and 6 flavors. This interpretation agrees with the geometric model $\mathbb{F}_2 \cup \mathrm{dP}_7$. Therefore, we conclude that $\mathbb{F}_2 \cup \mathrm{dP}_7$ is a 'KK geometry' engineering the circle compactification of the 6d SU(3) theory with $N_{\mathbf{F}} = 12$.

$\mathbb{F}_6 \cup \mathrm{dP}_4$ is also a KK geometry. When one chooses the fiber classes $f_1 = F_1, f_2 = \ell - X_1$ (with the gluing curve $C_{S_2} = 2\ell$), this geometry has a gauge theory description as $\mathrm{Sp}(2)_0 + 3\mathbf{AS}$. However, if we choose the fiber classes $f_1 = F, f_2 = 2\ell - \sum_{i=1}^4 X_i$, their intersections with the irreducible components S_i form the affine $A_2^{(2)}$ Cartan matrix, up to sign. This suggests that $\mathbb{F}_6 \cup \mathrm{dP}_4$ is a KK geometry. Indeed we find that the 6d SU(3) gauge theory with $N_{\mathbf{F}} = 6$ can give rise to the 5d KK theory associated to this geometry upon circle reduction with an outer automorphism twist.

$\mathbb{F}_{10} \cup \mathbb{F}_0$ is yet another KK geometry constructed by our building blocks. This geometry admits two dual descriptions related to the base-fiber exchange symmetry of $\mathbb{F}_0$. One description is $\mathrm{SU}(3)_9$, while the other is the $A_2^{(2)}$ gauge theory description without matter hypermultiplets. We anticipate that this affine $A_2^{(2)}$ gauge theory is the 5d KK theory coming from the 6d theory $\mathcal{O}(-3)$ minimal SCFT with SU(3) gauge group compactified on a circle with an outer automorphism twist of the SU(3) gauge algebra.

Lastly, $\mathrm{Bl}_9\mathbb{F}_4 \cup \mathbb{F}_0$ is a KK geometry. This geometry is formed by gluing two surfaces along $C_{S_1} = E$ in $\mathrm{Bl}_9\mathbb{F}_4$ and $C_{S_2} = F + H$ in $\mathbb{F}_0$. We find that this geometry involves an elliptic fiber class given by $E + 2X$ (with $E^2 = -4, X^2 = -1, E \cdot X = 2$) in $\mathrm{Bl}_9\mathbb{F}_4$ which signals that this geometry is an elliptic CY 3-fold. In the 5d reduction, this geometry has two gauge theory descriptions as predicted in [13]: $\mathrm{SU}(3)_{\frac{3}{2}}$ with $N_{\mathbf{F}} = 9$ and Sp(2) with $N_{\mathbf{AS}} = 1, N_{\mathbf{F}} = 8$. This geometry is associated to the 6d rank 2 E-string theory on a circle. This becomes clearer after a flop transition with respect to the exceptional curve X. The flop transition described in section 3.5 leads to $\mathrm{dP}_9 \cup \mathbb{F}_0^{g=1}$ geometry where we glue the anticanonical class in dP_9 to the elliptic class E (with $E^2 = 0$) in $\mathbb{F}_0^{g=1}$. This is the rank 2 generalization of dP_9 (or the 6d rank 2 E-string theory).

All top geometries in table 3 come from 6d SCFTs. We also claim that all smooth rank 2 3-folds engineering 5d SCFTs belong to one of the RG-flow families exhibited in table 3. Therefore, we deduce the following conclusion: *All rank 2 5d SCFTs realized by smooth non-compact 3-folds have 6d SCFT origins.*

This is one of the most important lessons from our classification of rank 2 5d SCFTs. The same conclusion may hold also for singular geometries involving $\mathrm{O7}^+$-planes. As mentioned earlier, the classification of smooth 3-folds misses a single geometry corresponding to the theory $\mathrm{SU}(3)_{\frac{1}{2}} + 1\mathbf{Sym}$, despite the fact that this theory is known to have a brane construction involving $\mathrm{O7}^+$-planes [33]. This theory may be the only rank 2 SCFT which cannot be engineered by a smooth 3-fold. But, we also know that this theory can be obtained from a KK theory with 6d origin, so we have found no counterexamples to the notion that all rank 2 5d SCFTs come from 6d SCFTs.

The above discussion motivates classifying automorphisms of 6d SCFTs which lead to 5d KK theories, as in [16]. Given the fact that 6d SCFTs are already classified (not counting frozen singularities involving $O7^+$ planes), the possible automorphisms can be deduced from symmetries of the tensor branch diagrams of 6d SCFTs dressed by gauge symmetries which respect the automorphisms.

Acknowledgments

We would like to thank Ron Donagi, Hirotaka Hayashi, Sung-Soo Kim, Kimyeong Lee, Dave Morrison, Kantaro Ohmori and Gabi Zafrir for useful comments and discussions. We also like to thank SCGP summer workshop 2017 for hospitality during part of this work. The research of P.J. and H.K. and C.V. is supported in part by NSF grant PHY-1067976. S.K. is supported by NSF grant DMS-1502170.

A Mathematical background

A.1 Notation, conventions, and formulae

Let S be a smooth projective variety, and let a (real) *1-cycle* be a formal linear combination $C = \sum a_i C_i$ of irreducible, reduced and proper curves C_i with real coefficients a_i. We declare two 1-cycles C, C' to be *numerically equivalent* if $C \cdot D = C' \cdot D$ for all Cartier divisors D on X. Let $N_1(S)$ be the real vector space of 1-cycles modulo numerical equivalence. The *Mori cone* of S is defined to be the closure of the set

$$\mathrm{NE}(S) = \left\{ \sum a_i [C_i] \mid a_i \in \mathbb{R}_{\geq 0} \right\}, \tag{A.1}$$

where $[C_i]$ are the classes of C_i in $N_1(S)$. Since we work exclusively with numerical equivalence classes, we drop the bracket notation.

Given a local 3-fold X defined by a connected Kähler surface $S = \cup S_i$, the Mori cone of X is given by

$$\overline{\mathrm{NE}(X)} = \overline{\cup \mathrm{NE}(S_i)}. \tag{A.2}$$

The *Kähler cone* $\mathcal{K}(X)$ is defined to be the closure of the set of all divisors J such that $J \cdot C > 0$ for all curves C that lie in the span of the Mori cone, where $\cdot$ is the intersection product of the Chow ring of X. Hence, given a basis $J = \phi_i D_i$, we may parametrize $\mathcal{K}(X)$ as

$$\mathcal{K}(X) = \{\phi : -J \cdot C \geq 0\}. \tag{A.3}$$

Note that the Kähler cone is dual to the Mori cone of X in the sense of convex geometry.

The correspondence between 5d field theory and Calabi-Yau geometry described in section 2.2 allows us to identify blowdowns with RG flows triggered by mass deformations. As a consequence, it is necessary to consider not only minimal surfaces but also their blowups as the basic building blocks S_i of shrinkable 3-folds. For this reason, we find it useful to recall a few facts about the proper transform of the canonical class K of a surface S_i with respect to a blowup. Let $\pi : S' \to S$ be a blowup of a collection of points p_i in general position with multiplicities m_i and exceptional divisors X_i. Then the canonical divisor $K_{S'}$ of S' is

$$K_{S'} = \pi^*(K_S) + \sum X_i. \tag{A.4}$$

Moreover, if the points p_i lie on a curve $C \subset S$, then the proper transform $C' \subset S'$ of the curve C is

$$C' = \pi^*(C) - \sum m_i X_i, \tag{A.5}$$

where m_i is the multiplicity of C at p_i [28]. In some situations, one is also forced to consider self-glued surfaces S'. The self-glued surfaces we study can be obtained from non-self-glued surfaces S_i by identifying pairs of curves $C_1, C_2 \subset S_i$, thus leading to a birational map $\rho : S \to S'$. The canonical class of S' is then determined by

$$\rho^*(K_{S'}) = K_S + C_1 + C_2. \tag{A.6}$$

A.2 Blowups of Hirzebruch surfaces, $\mathrm{Bl}_p\mathbb{F}_{n\geq 2}$

In this appendix, we fix notation for Hirzebruch surfaces and their blowups at general points. We also list their fiber classes and explicitly describe the generators of their Mori cones. Significantly, we show that if the number of blowups exceeds $p_{\max}(n)$, then the Mori cone of $\mathrm{Bl}_p\mathbb{F}_n$ is (countably) infinitely generated. In the context of shrinkable 3-folds, this (roughly) implies the existence of an infinite dimensional discrete symmetry, which is not expected for 5d SCFTs and hence excludes these surfaces from the list of building blocks for shrinkable 3-folds.

A *ruled surface* $\mathbb{F}_n^g$ over a curve E of genus g can be realized as the projectivization of a locally free rank 2 sheaf $\mathcal{E}$ with $\deg(\mathcal{E}) = E^2 = -n$, following the notation of [28]. The Mori cone of a ruled surface is spanned by two curve classes, namely the genus g curve E and a fiber class F. The canonical divisor is

$$K_{\mathbb{F}_n^g} = -2E + (2g - 2 - n)F \tag{A.7}$$

up to numerical equivalence. When $g = 0$, $\mathbb{F}_n^0 = \mathbb{F}_n$ is a *Hirzebruch surface* and can be understood as the projectivization of the bundle $\mathcal{O} \oplus \mathcal{O}(n)$ on $\mathbb{P}^1$. After projectivization, the summands $\mathcal{O}$ and $\mathcal{O}(n)$ of $\mathcal{O} \oplus \mathcal{O}(n)$ correspond to sections which we denote by E and H respectively. At the level of cohomology classes, we have $H = E + nF$. The intersection numbers are

$$H^2 = n,\ E^2 = -n,\ F^2 = 0,\ H \cdot E = 0,\ H \cdot F = E \cdot F = 1. \tag{A.8}$$

The Mori cone of $\mathbb{F}_n$ is generated by E and F. The canonical class is given by

$$K_{\mathbb{F}_n} = -2E - (n+2)\,F. \tag{A.9}$$

Writing a curve class on $\mathbb{F}_n$ as $C = aE + bF$, we can use (A.9) to compute the genus of the curve by the adjunction formula:

$$g(aE + bF) = (a-1)(b-1) - \frac{na(a-1)}{2}. \tag{A.10}$$

A.2.1 Mori cones

Below we list the generators of Mori cones in Hirzebruch surfaces with $p > 0$ blowups at generic points which we denote by $\mathrm{Bl}_p\mathbb{F}_n$. These are particular classes spanning the extremal rays in the Mori cone in the surface. These classes can be expressed as $C = dH + sF - \sum_{i=1}^{p} a_i X_i$, which we abbreviate as $(d, s; a_1, a_2, \cdots, a_p)$, where $H^2 = n, F^2 = 0$ and X_i's are exceptional classes of p blowups.

The Mori cone generators in $\mathrm{Bl}_p\mathbb{F}_n$ with $2 \le n \le 7$ are

$$\begin{aligned}
\mathrm{Bl}_p\mathbb{F}_2 \;:\;\; & E\,,\ X_i\,,\ (0,1;1)\,,\ (1,0;1^3)\,,\ (1,1;1^5)\,,\ (2,0;2,1^5)\,,\\
& (1,2;1^7)\,,\ (2,1;2^2,1^5)\,,\ (3,0;2^4,1^3)\,,\ (3,1;2^6,1)\,,\ (4,0;3,2^6) && \text{(A.11)}\\
\mathrm{Bl}_p\mathbb{F}_3 \;:\;\; & E\,,\ X_i\,,\ (0,1;1)\,,\ (1,0;1^4)\,,\ (1,1;1^6)\,,\ (1,2;1^8)\,,\ (2,0;2^2,1^5)\,,\\
& (2,1;2^3,1^5)\,,\ (3,0;2^7)\,,\ (3,0;3,2^4,1^3)\,,\ (3,1;3,2^6,1)\,,\\
& (4,0;3^4,2^3,1)\,,\ (4,0;4,3,2^6)\,,\ (4,1;3^5,2^3)\,,\ (5,0;4^2,3^4,2^2)\,,\\
& (5,1;4^2,3^6)\,,\ (6,0;4^6,3,2)\,,\ (6,0;5,4^3,3^4)\,,\ (6,1;4^7,3)\,,\\
& (7,0;5^3,4^4,3)\,,\ (7,0;6,4^7)\,,\ (8,0;6,5^5,4^2)\,,\ (9,0;6^4,5^4)\,,\\
& (10,0;7,6^7) && \text{(A.12)}\\
\mathrm{Bl}_p\mathbb{F}_4 \;:\;\; & E\,,\ X_i\,,\ (0,1;1)\,,\ (1,0;1^5)\,,\ (1,1;1^7)\,,\ (2,0;2^3,1^5)\,,\\
& (3,0;3,2^7) && \text{(A.13)}\\
\mathrm{Bl}_p\mathbb{F}_5 \;:\;\; & E\,,\ X_i\,,\ (0,1;1)\,,\ (1,0;1^6)\,,\ (1,1;1^8)\,,\ (2,0;2^4,1^5)\,,\\
& (3,0;3^2,2^7)\,,\ (4,0;3^9) && \text{(A.14)}\\
\mathrm{Bl}_p\mathbb{F}_6 \;:\;\; & E\,,\ X_i\,,\ (0,1;1)\,,\ (1,0;1^7)\,,\ (1,1;1^9)\,,\ (2,0;2^5,1^5)\,,\\
& (3,0;3^3,2^7)\,,\ (4,0;4,3^9) && \text{(A.15)}\\
\mathrm{Bl}_p\mathbb{F}_7 \;:\;\; & E\,,\ X_i\,,\ (0,1;1)\,,\ (1,0;1^8)\,,\ (1,1;1^{10})\,,\ (2,0;2^6,1^5)\,,\\
& (3,0;3^4,2^7)\,,\ (4,0;4^2,3^9)\,,\ (5,0;4^{11}) && \text{(A.16)}
\end{aligned}$$

Here the number of blowups is restricted as $p \le p_{\max}$ where $p_{\max} = 7, 8, 8, 9, 10, 11$ for $n = 2, 3, 4, 5, 6, 7$ respectively.

We are using the cone theorem of Mori theory: the Mori cone is generated by curves with $C \cdot K \ge 0$ (this is the 'K-positive' part of the Mori cone) and the extremal rational curves of Mori theory. There are three types of extremal rational curves on surfaces: (i) lines in $\mathbb{P}^2$, (ii) curves F with $F^2 = 0$ forming a $\mathbb{P}^1$-fibration, and (iii) exceptional curves.

Case (i) obviously does not occur. For case (ii), we claim that any rational curve F with $F^2 = 0$ can be written as a sum of two exceptional curves. We conclude that the Mori cone is generated by the curves C with $C \cdot K \ge 0$ and the exceptional curves. To see this, first note that the fibration which F is a part of must contain at least one reducible fiber. Otherwise, we would have a $\mathbb{P}^1$ bundle, implying that $\mathrm{Bl}_p\mathbb{F}_n$ is itself a Hirzebruch surface, which is impossible since we are assuming that $p > 0$. So we can write the class $F = C_1 + C_2$ as a sum of two curve classes. Then $C_1 \cap C_2$ is a single point, otherwise F would have positive genus. Replacing F by a distinct fiber, we see that $C_i \cdot F = 0$, since each C_i is disjoint from the distinct fiber F. We then compute $C_1 \cdot F = C_1 \cdot (C_1 + C_2) = C_1^2 + 1 = 0$, so $C_1^2 = -1$ and C_1 is an exceptional curve. The same argument shows that C_2 is also an exceptional curve, and the claim is proven.

We now claim that for $p \le n+4$, the only curve C with $C \cdot K \ge 0$ is $C = E$. The above table was produced by listing the exceptional curves and prepending E.

To prove the claim, we write $-K$ in the form

$$-K = E + H + 2F - \sum_{i=1}^{p} X_i. \tag{A.17}$$

We compute that $E \cdot (-K) = -n + 2$. Let us first assume that $n > 2$, in which case $E \cdot (-K) < 0$. Now consider any effective curve $C = \cup C_i$ in the class $-K$ (for $p \le p_{\max}$ there exist such curves by a straightforward dimension count). If each C_i were disjoint from E, we would get a contradiction since $C_i \cdot E \ge 0$ is just a (nonnegative) count of intersection points. Thus E must be one of components of any curve in the class $-K$.[20] It follows that every curve in the class $-K$ is the sum of E and a curve in the class of what is left over: $M_n = H + 2F - \sum_{i=1}^{p} X_i$.[21] Curves in the class M_n move in a family by a straightforward dimension count using the bound on p, hence curves in the class M_n cover $\mathrm{Bl}_p\mathbb{F}$. Since $M_n^2 = n + 4 - p \ge 0$, curves in the class M_n must intersect every curve nontrivially, with one possible exception in the case $p = n+4$: a curve in the class M_n will not meet a different curve in the class M_n, since $M_n^2 = 0$.

So if $C \ne E$, and $C \ne M_n$ in the case $p = n+4$, then $C \cdot (-K) = C \cdot (E + M_n) = C \cdot E + C \cdot M_n$. The first term is nonnegative while the second term is positive, hence $C \cdot K < 0$. If $p = n+4$ and $C = M_n$, the we compute $M_n \cdot K = -2$ directly and there is still no problem.

If $n = 2$, then $-K$ moves in a family covering $\mathrm{Bl}_p\mathbb{F}$ and has no fixed component. So this case is handled by a similar but simpler argument.

In conclusion, the only curve C with $C \cdot K \ge 0$ is $C = E$ and the K-negative part of the Mori cone of $\mathrm{Bl}_{p>0}\mathbb{F}_n$ is generated exclusively by exceptional curves.

We checked numerically that, when $p \ge p_{\max}$, there appear infinitely many Mori cone generators for each surface. We now explain that for $p \ge n+6$, $\mathrm{Bl}_p\mathbb{F}_n$ has infinitely exceptional curves and therefore infinitely many Mori cone generators. We give the argument for $n = 2$ for simplicity of exposition and then repeat the argument in the general case.

We now adapt the argument of [37] from $\mathbb{P}^2$ to $\mathbb{F}_n$. We start by blowing up 4 general points of $\mathbb{F}_2$ to obtain a surface $\mathrm{Bl}_4\mathbb{F}_2$. For each $1 \le j \le 4$, consider the curve $Y_j = H_2 - \sum_{i=1, i\ne j}^{4} X_i$. The Y_j are disjoint exceptional curves ($Y_j \cdot Y_k = 0$ for $j \ne k$) and so can be blown down by a map $\pi : \mathrm{Bl}_4\mathbb{F}_2 \to S$ to a smooth surface S. We claim that $S \simeq \mathrm{Bl}_4\mathbb{F}_2$, producing a birational automorphism of $\mathbb{F}_2$ analagous to the quadratic transformation of $\mathbb{P}^2$ used in [37].

To verify the claim, we begin by observing that $E \cdot Y_j = 0$, i.e. E is disjoint from each Y_j, so blowing down the Y_j does not change the self-intersection of E. In other words, if we put $E' = \pi_*(E)$, we have $E'^2 = -2$. Furthermore, the curve class $H + F - \sum_{i=1}^{4} X_i$ (with $\mathbb{P}^1$ moduli space) has self-intersection 0 and is disjoint from the curves Y_j. So by the same

[20] In the standard terminology of algebraic geometry, E is called a *fixed component* of $|-K|$.

[21] In the standard terminology of algebraic geometry, M_n is called the *moving part* of $-K$, as it is straightforward to check that M_n has no fixed component itself.

reasoning, the curve class $F' = \pi_*(H + F - \sum_{i=1}^4 X_i)$ satisfies $(F')^2 = 0$. Furthermore, $E' \cdot F' = 1$, since $E \cdot (H + F - \sum_{i=1}^4 X_i) = 1$. Thus S has $b_2(S) = 2 + 4 - 4 = 2$ and contains a curve of self-intersection -2 which is a section of $\mathbb{P}^1$-fibration. By classification of rational surfaces, we conclude that S is a Hirzebruch surface, and $S \simeq \mathbb{F}_2$ because of the presence of the curve E'.

We now change notation and rewrite π as $\pi : \mathrm{Bl}_4\mathbb{F}_2 \to \mathbb{F}_2$, replacing E' and F' by E and F. We have

$$\pi^*(E) = E, \qquad \pi^*(F) = H + F - \sum_{i=1}^4 X_i, \qquad \pi^*(X_i) = H - \sum_{j=1,\ j\neq i}^4 X_i. \tag{A.18}$$

We now turn to $\mathrm{Bl}_p\mathbb{F}_2$ with $p \geq 8 > 4$. Since the blowups of the points indexed by $5, \dots, p$ are spectators in the map π above, we can reinterpret π as a map $\mathrm{Bl}_p\mathbb{F}_2 \to \mathbb{F}_2$. The pullbacks of E and F are still given by (A.18) (with i still running from 1 to 4).

We now consider an exceptional curve with class $C = aH + bF - \sum_{i=1}^p m_i X_i$. We reorder the points being blown up if necessary so that the m_i are in nondecreasing order. We assume that $C \neq F - X_i$ for any i. Since $C \cdot (F - X_i) \geq 0$, it follows that $a \geq m_i$ for each i. Let $C' = \pi_*(C)$. We now find the class of C' by computing

$$C' \cdot E = C \cdot \pi^*(E) = b,\ C' \cdot F = C \cdot \pi^*(F) = 3a + b - \sum_{i=1}^4 m_i, \tag{A.19}$$

and

$$C' \cdot X_j = C \cdot Y_j = 2a + b - \sum_{i=1,\ i\neq j}^4 m_i\ (j \leq 4), C' \cdot X_j = m_j\ (j > 4). \tag{A.20}$$

It follows that

$$C' = \left(3a + b - \sum_{i=1}^4 m_i\right) H_2 + bF_2 - \sum_{j=1}^4 \left(2a + b - \sum_{i=1,\ i\neq j}^4 m_i\right) X_j - \sum_{j=5}^p m_j X_j. \tag{A.21}$$

We now claim that $3a + b - \sum_{i=1}^4 m_i > a$. This will complete the proof of infinitely many exceptional curves. Starting with one of the allowed exceptional curves from (A.11), we repeatedly apply π and get a sequence of curves whose coefficient of H_2 increases without bound.

The proof of the claim is simple. Since C is exceptional we have the $C \cdot K = -1$, or

$$4a + 2b - \sum_{i=1}^p m_i = 1. \tag{A.22}$$

Since $4 \leq p/2$ and the m_i are nondecreasing, (A.22) implies that

$$2a + b - \sum_{i=1}^4 m_i > 0. \tag{A.23}$$

Adding a to both sides of (A.23) gives the claimed result.

JHEP04(2018)103

For the case of general n, we blow up $\mathbb{F}_n$ at $n+2$ points and blow down the $n+2$ exceptional curves $Y_j = H - \sum_{i=1,i\neq j}^{n+2} X_j$. By an argument analogous to the case $n=2$ above, we identify this blowdown map with a map $\pi : \mathrm{Bl}_{n+2}\mathbb{F}_n \to \mathbb{F}_n$. In place of (A.18) we have in this situation

$$\pi^*(E) = E, \qquad \pi^*(F_2) = H + F - \sum_{i=1}^{n+2} X_i, \qquad \pi^*(X_i) = H - \sum_{j=1,\ j\neq i}^{n+2} X_j. \tag{A.24}$$

As in the case $n=2$, we consider an exceptional curve with class $C = aH + bF - \sum_{i=1}^{p} m_i X_i$. We reorder the points being blown up if necessary so that the m_i are in nondecreasing order. We assume that $C \neq F - X_i$ for any i and conclude that $a \geq m_i$ for each i as before. Let $C' = \pi_*(C)$. We compute

$$C' \cdot E = C \cdot \pi^*(E) = b,\ C' \cdot F = C \cdot \pi^*(F) = (n+1)\,a + b - \sum_{i=1}^{n+2} m_i, \tag{A.25}$$

and

$$C' \cdot X_j = C \cdot Y_j = na + b - \sum_{i=1,\ i\neq j}^{n+2} m_i\ (j \leq n+2), C' \cdot X_j = m_j\ (j > n+2). \tag{A.26}$$

It follows that

$$C' = \left((n+1)\,a + b - \sum_{i=1}^{n+2} m_i \right) H + bF - \sum_{j=1}^{n+2} \left(na + b - \sum_{i=1,\ i\neq j}^{n+2} m_i \right) X_j - \sum_{j=n+3}^{p} m_j X_j. \tag{A.27}$$

We only have to show that $(n+1)a + b - \sum_{i=1}^{n+2} m_i > a$, or $na + b - \sum_{i=1}^{n+2} m_i > 0$. We divide into the cases of even and odd p. Since the even case is easier, we content ourselves with the odd case and write $p = 2k+1$.

Since C is exceptional we have the $C \cdot K = -1$, or

$$(n+2)\,a + 2b - \sum_{i=1}^{p} m_i = 1, \tag{A.28}$$

which implies

$$\left(\frac{n+2}{2}\right) a + b - \sum_{i=1}^{k} m_i - \frac{m_{k+1}}{2} > 0, \tag{A.29}$$

which further implies, since $a \geq m_{k+1}$

$$\left(\frac{n+3}{2}\right) a + b - \sum_{i=1}^{k+1} m_i > 0. \tag{A.30}$$

We have to replace $\sum_{i=1}^{k+1} m_i$ in (A.30) with $\sum_{i=1}^{n+2} m_i$ in verifying the claim, so we compensate and maintain positivity by adding $((n+2) - (k+1))a$ in (A.30). We only have to observe that the resulting coefficient of a is at most n. The difference between this coefficient and n is

$$n - \left(\binom{n+3}{2} + (n+2) - (k+1) \right) = k + 1 - \binom{n+7}{2} \tag{A.31}$$

which is nonnegative since $p \geq n+6$.

However, we are trying to do too much here and can relax the result to $p = n+5$ if $n \geq 4$, by starting with an exceptional curve whose class has $b = 0$. For example, we can consider the curve $H - \sum_{i=5}^{n+5} X_i$.

Now (A.28) simplifies to

$$(n+2)\, a - \sum_{i=1}^{n+5} m_i = 1 \tag{A.32}$$

and we have to show

$$(n+1)\, a - \sum_{i=1}^{n+2} m_i > a, \tag{A.33}$$

or equivalently

$$na - \sum_{i=1}^{n+2} m_i > 0. \tag{A.34}$$

Since the m_i are arranged in nondecreasing order, (A.34) follows from (A.32) by comparing the coefficients of a and the number of m_i terms in these two formulas after noting that $n/(n+2) \geq (n+2)/(n+5)$ for $n \geq 4$. This shows that the number of blowups with finite Mori cone is given by $p_{\max} = 7, 8$ (for $n = 2, 3$ by the $p \geq n+6$ bound) and $p_{\max} = 8, 9, 10, \ldots$ for $n = 4, 5, 6, \ldots$ by the $p \geq n+5$ bound we established).

A.2.2 Weyl groups

In this section, we suggest a more conceptual way to show that there are infinitely many Mori cone generators for $\mathrm{Bl}_p\mathbb{F}_n$ and large p while leaving details for future work. We exhibit a natural action of a group surjecting onto the Weyl group of an infinte Kac-Moody Lie algebra on $H^2(\mathrm{Bl}_p\mathbb{F}_n)$ for $p \geq n+2$. See [38] for background and the notation we will follow about Kac-Moody algebras.

To begin with, a permutation of the p blowup points induces a corresponding action on $H^2(\mathrm{Bl}_p\mathbb{F}_n)$, giving an action of the symmetric group S_p on $H^2(\mathrm{Bl}_p\mathbb{F}_n)$. The symmetric group is a reflection group, generated by transpositions. The induced map on $H^2(\mathrm{Bl}_p\mathbb{F}_n)$ associated with the transposition $(i, i+1)$ is identified with the reflection in the hyperplane orthogonal to $\rho_i = X_i - X_{i+1}$ for $i = 1, \ldots, p-1$. We note that $\rho_i^2 = -2$ and $\rho_i \cdot K = 0$. These reflections and the symmetric group that they generate preserve the Mori cone generators. As usual, by a reflection in a curve class ρ with $\rho^2 = -2$ we mean the automorphism of $H^2(\mathrm{Bl}_p\mathbb{F}_n)$ given by

$$C \mapsto C + (C \cdot \rho)\, \rho. \tag{A.35}$$

A simple calculation shows that (A.24) can be identified with the reflection in $\rho_p = H - \sum_{i=1}^{n+2} X_i$. We also have $\rho_p^2 = -2$ and $\rho_p \cdot K = 0$.

Consider the $p \times p$ matrix A with

$$A_{ij} = -\rho_i \cdot \rho_j, \tag{A.36}$$

where in (A.36) the product on the right-hand side is just the intersection product in $H^2(\mathrm{Bl}_p\mathbb{F}_n)$. Since A is symmetric with diagonal entries equal to 2 and nonpositive off-diagonal entries, it follows immediately that A is a generalized Cartan matrix.

Now let $\mathfrak{g}_A$ be the Kac-Moody algebra associated with A. We proceed to identify $\{\rho_1, \ldots, \rho_p\}$ with a set of roots in the associated root system.

Recall the definition of a realization of a generalized Cartan matrix from [38].

Definition. A *realization* of an $n \times n$ generalized Cartan matrix A is a triple $(\mathfrak{h}, \Pi, \Pi^*)$, where $\mathfrak{h}$ is a complex vector space, $\Pi = \{\alpha_1, \ldots, \alpha_n\} \subset \mathfrak{h}^*$, and $\pi^\vee = \{\alpha_1^\vee, \ldots, \alpha_n^\vee\} \subset \mathfrak{h}$ such that Π and $\Pi^\vee$ are each linearly independent sets, $\langle \alpha_i^\vee, \alpha_j \rangle = A_{ij}$, and $\dim \mathfrak{h} = 2n - \mathrm{rank}(A)$.

Returning to our situation where A is given by (A.36), we see that $\mathrm{rank}(A) \geq p-1$ since A contains the nonsingular Cartan matrix of A_{p-1} as a submatrix. So $\mathrm{rank}(A)$ is either $p-1$ or p.

If $\mathrm{rank}A = p$, then $\dim \mathfrak{h} = p$ and we take $\mathfrak{h} = \mathrm{span}(\rho_1, \ldots, \rho_p) \subset H^2(\mathrm{Bl}_p\mathbb{F}_n)$. If $\mathrm{rank}A = p-1$, then $\dim \mathfrak{h} = p+1$ and we take $\mathfrak{h} = K^\perp \subset H^2(\mathrm{Bl}_p\mathbb{F}_n)$. In either case, we identify $\mathfrak{h}^*$ with $\mathfrak{h}$ via the negative of the intersection pairing. With these identifications, we let $\alpha_i = \alpha_i^\vee = \rho_i$ for $i = 1, \ldots, p$ to obtain a realization of A.

The Weyl group W_A of $\mathfrak{g}_A$ is the subgroup of $\mathrm{Aut}(\mathfrak{h}^*)$ generated by the reflections in the roots, and is infinite if $\mathrm{rank}(A) = p-1$. Consider the subgroup $G \subset \mathrm{Aut}(H^2(\mathrm{Bl}_p\mathbb{F}_n))$ generated by the reflections. We have a surjection $G \to W_A$ obtained by restriction to $\mathfrak{h}^*$, so G is also infinite if $\mathrm{rank}(A) = p-1$. We expect that the action of G on the Mori cone generators is effective, which would prove that there are infinitely many Mori cone generators in this case.

We next show that the finiteness of W_A perfectly matches the finiteness of the Mori cone generators as described in section A.2.1. Consider the Dynkin diagram encoding the Cartan matrix A.

If $p = n+2$, we have an $A_{n+1} \times A_1$ Dynkin diagram with a finite Weyl group.

If $p = n+3$, we have an A_{n+3} Dynkin diagram with a finite Weyl group.

If $p \geq n+4$, the $(n+2)$nd vertex corresponding to $\rho_{n+2} = X_{n+2} - X_{n+3}$ is trivalent, being connected to the vertices corresponding to ρ_{n+1}, ρ_{n+3}, and ρ_p. If $p = n+4$, we have an D_{n+4} Dynkin diagram with a finite Weyl group.

If $p = n+5$, we have E_6, E_7, E_8 for $n = 1, 2, 3$ respectively, with a finite Weyl group. If $n \geq 4$, the Weyl group is infinite.

If $p > n+5$, the Weyl group is infinite.

These results are in perfect agreement with the results of section A.2.1, including the observation that the pattern for $p_{\max}$ is not followed for $n \leq 3$.

As an example, consider $\mathrm{Bl}_9\mathbb{F}_4$. In this case

$$A = \begin{pmatrix} 2 & -1 & 0 & 0 & 0 & 0 & 0 & 0 & 0 \\ -1 & 2 & -1 & 0 & 0 & 0 & 0 & 0 & 0 \\ 0 & -1 & 2 & -1 & 0 & 0 & 0 & 0 & 0 \\ 0 & 0 & -1 & 2 & -1 & 0 & 0 & 0 & 0 \\ 0 & 0 & 0 & -1 & 2 & -1 & 0 & 0 & 0 \\ 0 & 0 & 0 & 0 & -1 & 2 & -1 & 0 & -1 \\ 0 & 0 & 0 & 0 & 0 & -1 & 2 & -1 & 0 \\ 0 & 0 & 0 & 0 & 0 & 0 & -1 & 2 & 0 \\ 0 & 0 & 0 & 0 & 0 & -1 & 0 & 0 & 2 \end{pmatrix} \tag{A.37}$$

This A is singular, so $\mathfrak{g}_A$ and G are infinite. In fact, (A.37) is precisely the Cartan matrix of affine E_8 after reversing the order of the roots, so $\mathfrak{g}_A$ is just affine E_8.

More generally, we list the Dynkin diagrams corresponding to $p = p_{\max} + 1$. For convenience, we adopt the notation $T_{p,q,r}$ from the study of triangle singularities. The corresponding Dynkin diagram has one trivalent vertex and three legs, with the lengths of the respectively legs (including the trivalent vertex in each case) are p, q, r. For example, with this notation $D_n = T_{2,2,n-2}$, $E_6 = T_{2,3,3}$, $E_7 = T_{2,3,4}$, and $E_8 = T_{2,3,5}$.

For $n = 2$, $p_{\max} + 1 = 8$, and we get $T_{2,4,4}$, which is affine E_7.

For $n = 3$, $p_{\max} + 1 = 9$, and we get $T_{2,4,5}$. This has an infinite Weyl group, but is not the affine Weyl group of any classical group.

For $n = 4$, $p_{\max} + 1 = 9$, and we get $T_{2,3,6}$, which is affine E_8 as we have explained above.

For $n > 4$, $p_{\max} + 1 = n + 5$, and we get $T_{2,3,n+2}$. This has an infinite Weyl group, but is not the affine Weyl group of any classical group.

A.2.3 Fiber classes

For the purpose of identifying gauge theory descriptions of shrinkable 3-folds, one also needs to know the fiber classes corresponding to W-bosons in the 5d spectrum. A fiber class $f \subset \mathrm{Bl}_p\mathbb{F}_n$ is a rational curve satisfying $f^2 = 0$. When $p = 0$, as described above, there is only a single fiber class, namely $f = F \subset \mathbb{F}_n$. However, when $p > 0$, additional fiber classes may appear.

We denote fiber classes by $f = dH + sF - \sum_{i=1}^{p} a_i X_i$ (where $F^2 = 0, H^2 = n$, and X_i are exceptional curves) which we abbreviate as $(d, s; a_1, \ldots, a_p)$. Using numerical checks, we believe the full set of fiber classes $f \subset \mathrm{Bl}_p\mathbb{F}_n$ with $2 \leq n \leq 7$ and $p \leq p_{\max}$, organized according to the number $f \cdot E = s$, are as follows:

$$\mathrm{Bl}_p\mathbb{F}_2 \ : \ \left\{ \begin{array}{l} (1,0;1^2)\,,\ (2,0;2,1^4)\,,\ (3,0;2^4,1^2)\,, \\ (3,0;3,2,1^5)\,,\ (4,0;3^2,2^3,1^2)\,,\ (5,0;3^5,2,1)\,, \\ (5,0;4,3^2,2^4)\,,\ (6,0;4^2,3^4,2)\,,\ (7,0;4^5,3^2) \\ \\ F\,,\ (1,1;1^4)\,,\ (2,1;2^2,1^4)\,,\ (3,1;2^6)\,, \\ (3,1;3,2^3,1^3)\,,\ (4,1;3^3,2^3,1)\,,\ (4,1;4,2^6)\,, \\ (5,1;4,3^4,2^2)\,,\ (6,1;4^3,3^4)\,,\ (7,1;4^7) \\ \\ (1,2;1^6)\,,\ (2,2;2^3,1^4)\,,\ (3,2;3,2^5,1)\,, \\ (4,2;3^4,2^3)\,,\ (5,2;4,3^6) \end{array} \right\} \tag{A.38}$$

$$\mathrm{Bl}_p\mathbb{F}_3 \ : \ \left\{ \begin{array}{l} (1,0;1^3)\,,\ (2,0;2^2,1^4)\,,\ (3,0;3,2^4,1^2)\,,\ (3,0;3^2,2,1^5)\,, \\ (4,0;3^4,2^3)\,,\ (4,0;3^5,1^3)\,,\ (4,0;4,3^2,2^3,1^2)\,, \\ (5,0;4^3,3^2,2^2,1)\,,\ (5,0;5,3^5,2,1)\,,\ (5,0;5,4,3^2,2^4)\,, \\ (6,0;5,4^4,3^2,1)\,,\ (6,0;5^2,4^2,3^2,2^2)\,,\ (6,0;6,4^2,3^4,2)\,, \\ (7,0;5^5,3^2,2)\,,\ (7,0;6,5^2,4^3,3,2)\,,\ (7,0;6,5^3,3^4)\,, \\ (7,0;6^2,4^3,3^3)\,,\ (7,0;7,4^5,3^2)\,,\ (8,0;6^2,5^4,4,2)\,, \\ (8,0;6^3,5^2,4,3^2)\,,\ (8,0;7,5^5,3^2)\,,\ (8,0;7,6,5^2,4^3,3)\,, \\ (9,0;7,6^4,5,4,3)\,,\ (9,0;7^2,6,5^4,3)\,,\ (9,0;7^2,6^2,5,4^3)\,, \\ (9,0;8,6^2,5^3,4^2)\,,\ (10,0;7^3,6^4,3)\,,\ (10,0;7^4,6^2,4^2)\,, \\ (10,0;8,7^2,6^2,5^2,4)\,,\ (10,0;8^2,6^2,5^4)\,,\ (10,0;9,6^4,5^3)\,, \\ (11,0;8^2,7^3,6^2,4)\,,\ (11,0;8^3,7,6^2,5^2)\,,\ (11,0;9,7^4,6,5^2)\,, \\ (11,0;9,8,7,6^4,5)\,,\ (12,0;9,8^3,7^2,6,5)\,, \\ (12,0;9^2,7^5,5)\,,\ (12,0;9^2,8,7^2,6^3)\,,\ (13,0;9^2,8^5,5)\,, \\ (13,0;9^3,8^3,6^2)\,,\ (13,0;9^4,7^3,6)\,,\ (18,0;12^2,11^4,10^2)\,, \\ (19,0;12^5,11^3) \\ \\ F\,,\ (1,1;1^5)\,,\ (2,1;2^3,1^4)\,,\ (3,1;3,2^6)\,,\ (4,1;4^2,2^6)\,, \\ (3,1;3^2,2^3,1^3)\,,\ (4,1;4,3^3,2^3,1)\,,\ (5,1;4^3,3^4,1)\,, \\ (5,1;4^4,3,2^3)\,,\ (5,1;5,4,3^4,2^2)\,,\ (6,1;5^2,4^3,3^2,2)\,, \\ (6,1;6,4^3,3^4)\,,\ (7,1;5^5,4^2,2)\,,\ (7,1;6,5^3,4^2,3^2)\,, \\ (7,1;6^2,4^5,3)\,,\ (7,1;7,4^7)\,,\ (8,1;6^3,5^3,4,3)\,, \\ (8,1;6^4,4^4)\,,\ (8,1;7,6,5^3,4^3)\,,\ (9,1;6^7,3)\,, \\ (9,1;7,6^5,4^2)\,,\ (9,1;7^2,6^2,5^3,4)\,,\ (9,1;8,6^2,5^5)\,, \\ (10,1;7^4,6^3,4)\,,\ (10,1;8,7^2,6^3,5^2)\,,\ (11,1;8^2,7^4,6,5)\,, \\ (11,1;8^3,7,6^4)\,,\ (11,1;9,7^4,6^3)\,,\ (12,1;8^6,6^2)\,, \\ (12,1;9,8^3,7^3,6)\,,\ (13,1;9^3,8^3,7^2)\,,\ (16,1;10^8) \\ \\ (1,2;1^7)\,,\ (2,2;2^4,1^4)\,,\ (3,2;3^2,2^5,1)\,, \\ (4,2;3^7,1)\,,\ (4,2;4,3^4,2^3)\,,\ (5,2;4^4,3^3,2)\,, \\ (5,2;5,4,3^6)\,,\ (6,2;5^2,4^4,3^2)\,,\ (7,2;5^6,4,3)\,, \\ (7,2;6,5^3,4^4)\,,\ (8,2;6^3,5^4,4)\,,\ (8,2;7,5^7)\,, \\ (9,2;7,6^5,5^2)\,,\ (10,2;7^4,6^4)\,,\ (11,2;8,7^7) \end{array} \right\} \tag{A.39}$$

$$\mathrm{Bl}_p\mathbb{F}_4 \;:\; \left\{ \begin{array}{l} (1,0;1^4)\,,\ (2,0;2^3,1^4)\,,\ (3,0;3^2,2^4,1^2)\,,\ (4,0;4,3^4,2^3)\,, \\ (5,0;4^4,3^4) \\ \\ F\,,\ (1,1;1^6)\,,\ (2,1;2^4,1^4)\,,\ (3,1;3^2,2^6)\,,\ (4,1;3^8) \\ \\ (1,2;1^8) \end{array} \right\} \tag{A.40}$$

$$\mathrm{Bl}_p\mathbb{F}_5 \;:\; \left\{ \begin{array}{l} (1,0;1^5)\,,\ (2,0;2^4,1^4)\,,\ (3,0;3^3,2^4,1^2)\,, \\ (4,0;4^2,3^4,2^3)\,,\ (5,0;5,4^4,3^4)\,,\ (6,0;5^4,4^5) \\ \\ F\,,\ (1,1;1^7)\,,\ (2,1;2^5,1^4)\,,\ (3,1;3^3,2^6)\,, \\ (4,1;4,3^8) \\ \\ (1,2;1^9) \end{array} \right\} \tag{A.41}$$

$$\mathrm{Bl}_p\mathbb{F}_6 \;:\; \left\{ \begin{array}{l} (1,0;1^6)\,,\ (2,0;2^5,1^4)\,,\ (3,0;3^4,2^4,1^2)\,, \\ (4,0;4^3,3^4,2^3)\,,\ (5,0;5^2,4^4,3^4)\,,\ (6,0;6,5^4,4^5)\,, \\ (7,0;6^4,5^6) \\ \\ F\,,\ (1,1;1^8)\,,\ (2,1;2^6,1^4)\,,\ (3,1;3^4,2^6)\,, \\ (4,1;4^2,3^8)\,,\ (5,1;4^{10}) \\ \\ (1,2;1^{10}) \end{array} \right\} \tag{A.42}$$

$$\mathrm{Bl}_p\mathbb{F}_7 \;:\; \left\{ \begin{array}{l} (1,0;1^7)\,,\ (2,0;2^6,1^4)\,,\ (3,0;3^5,2^4,1^2)\,, \\ (4,0;4^4,3^4,2^3)\,,\ (5,0;5^3,4^4,3^4)\,,\ (6,0;6^2,5^4,4^5) \\ \\ F\,,\ (1,1;1^9)\,,\ (2,1;2^7,1^4)\,,\ (3,1;3^5,2^6)\,, \\ (4,1;4^3,3^8)\,,\ (5,1;5,4^{10}) \\ \\ (1,2;1^{11}) \end{array} \right\}. \tag{A.43}$$

B Numerical bounds

B.1 Bound on n for $\mathbf{Bl}_{p_1}\mathbb{F}_{n\geq 2} \cup \mathbf{dP}_{p_2}$

It is possible to place a crude upper bound on n for the Hirzebruch surfaces $\mathbb{F}_n$ that can appear as irreducible components in the rank 2 surfaces $S = S_1 \cup S_2$:

$$n \leq 8. \tag{B.1}$$

This upper bound can be established by exploiting the Calabi-Yau condition on $C = S_1 \cap S_2$, which requires

$$C^2_{S_2} = n - 2, \tag{B.2}$$

where we take $C = d\ell - \sum m_i X_i \in \mathrm{dP}_{p_2}$. For the sake of argument, we find it useful to work in terms of the ratio $z \equiv \phi_2/\phi_1$. The positivity condition imposed on the volume of the curve $F \in \mathbb{F}$ implies $z \leq 2$. Moreover, the positivity condition on the volumes of exceptional divisors $X_i \in \mathrm{dP}_{p_2}$ implies $z \geq m_i$ for all i, and hence we have the condition

$$m_i \leq z \leq 2 \quad \Longrightarrow \quad m_i \leq 2. \tag{B.3}$$

One can "prove" the bound (B.1) by using a computing tool to attempt to solve the Diophantine equation (B.2) subject to the condition (B.3) assuming $n \geq 8$, and demonstrating that there are no solutions.

Another strategy is to define vectors $\vec{m} = (m_1, \ldots, m_{p_2}), \vec{1} = (1, \ldots, 1)$ so that

$$n = -K \cdot C = 3d - \vec{1} \cdot \vec{m} = d^2 - |\vec{m}|^2 + 2, \tag{B.4}$$

where we take

$$\vec{1} \cdot \vec{m} = \sqrt{p_2} m \cos\theta, \quad \sqrt{p_2} = \sqrt{|\vec{1}|^2}, \quad m \equiv \sqrt{|\vec{m}|^2}. \tag{B.5}$$

Solving this system for n, one can attempt to find values of the parameters (θ, m) for all values of $p_2 \leq 8$ satisfying

$$n = \frac{1}{2}\left(3\sqrt{4m^2 - 4m\sqrt{p_2}\cos\theta + 1} - 2m\sqrt{p_2}\cos\theta + 9\right) \geq 8, \tag{B.6}$$

for which there are no solutions.

B.2 Bound on n for $\mathrm{Bl}_{p_1}\mathbb{F}_n \cup \mathbb{F}_0$

Proposition. Let $S = \mathrm{Bl}_{p_1}\mathbb{F}_n \cup \mathbb{F}_0$, $J = \phi_1[\mathrm{Bl}_{p_1}\mathbb{F}_n] + \phi_2[\mathbb{F}_0]$, and let the gluing curve $C_{\mathbb{F}_0} = aF + bE$.

1. If $p_1 = 0$, then S is not shrinkable for $n > 10$.

2. If $p_1 > 0$, then S is not shrinkable for $n > 6$.

Proof. For the case $p_1 = 0$, requiring that the Mori generators have non-negative volumes straightforwardly leads to the conditions

$$ab + 1 = a + b, \quad 2ab = n - 2, \quad \max\left\{\frac{a}{2}, \frac{b}{2}, \frac{n-2}{n}\right\} \leq 2. \tag{B.7}$$

The first two conditions above have solution

$$a = 1 \quad \text{or} \quad b = 1. \tag{B.8}$$

Since F and E may be interchanged freely in $\mathbb{F}_0$, with no less of generality we set $a = 1$. Simplifying the above constraints, we find $2b = n - 2$, which implies

$$n \leq 10. \tag{B.9}$$

When $p_1 > 0$, one can show (cf. appendix A.2) that the Mori cone of $\mathrm{Bl}_{p_1}\mathbb{F}_n$ contains as a generator a rational curve of self intersection -1 meeting the gluing curve $C_{\mathrm{Bl}_{p_1}\mathbb{F}_n} = E$ at a single point, and hence the third condition in (B.7) must be adjusted to $\max\{a/2, b/2, (n-2)/n\} \leq 1$. Again setting $a = 1$, one finds

$$n \leq 6. \tag{B.10}$$

B.3 Bound on p_1, p_2 for $\mathrm{dP}_{p_1} \cup \mathrm{dP}_{p_2}$

Proposition. Let $S = \mathrm{dP}_{p_1} \cup \mathrm{dP}_{p_2}$, and let $J = \phi_1[\mathrm{dP}_{p_1}] + \phi_2[\mathrm{dP}_{p_2}]$.

1. If $p_1, p_2 \geq 2$, then S is not shrinkable for $p_1 > 6$ or $p_2 > 6$.

2. If $p_1 = 1$, then S is not shrinkable for $p_2 > 7$.

Proof. For the first case, assume let $C_1 \in \mathrm{dP}_{p_1 \geq 2}, C_2 \in \mathrm{dP}_{p_2 \geq 2}$ be Mori generators, and let $D = \mathrm{dP}_{p_1} \cap \mathrm{dP}_{p_2}$. Then, setting $\phi_1 = 1, \phi_2 = z$, we have the following positivity conditions:

$$\mathrm{vol}(C_1) = 1 - C_1 \cdot Dz \geq 0, \quad \mathrm{vol}(C_2) = z - C_2 \cdot D \geq 0. \tag{B.11}$$

Combining the above conditions, one finds

$$(C_2 \cdot D)(C_1 \cdot D) \leq 1, \quad \forall C_1 \in \mathrm{dP}_{p_1}, C_2 \in \mathrm{dP}_{p_2}. \tag{B.12}$$

By explicit computation, one can show that the above condition cannot be satisfied for either $p_1 > 6$ or $p_2 > 6$.

For the second case, let $p_1 = 1$. The Mori generators of dP_1 are $X_1, \ell - X_1$ and have respective volumes $\mathrm{vol}(X_1) = 1, \mathrm{vol}(\ell - X_1) = z - 2$, so the condition (B.12) gets modified to

$$C_2 \cdot D \leq 2, \quad \forall C_2 \in \mathrm{dP}_{p_2}, \tag{B.13}$$

which cannot be satisfied for $p_2 = 8$.

C Smoothness of building blocks

In this appendix, we provide some justification for our conjecture that the S_i can be taken to be smooth. If one of the components S_i is singular, the basic idea is that we should be able to find a complex structure deformation which smooths the singularity while preserving the Calabi-Yau embedding. In section 3.4 we gave another conjecture which makes the condition of a Calabi-Yau embedding quite manageable.

This conjecture is natural from the perspective of web diagrams or toric geometry. Consider for example the case of $S = \mathbb{P}(1,1,2)$. This singular geometry is physically equivalent to $\mathbb{F}_2$ in the zero mass limit. Figure 28 depicts how the section E in $\mathbb{F}_2$ changes to the singular point in $\mathbb{P}(1,1,2)$ in this limit. Physically, when two parallel external 5-branes coincide, there are extra free massless states charged under the enhanced global symmetry associated to this brane configuration.[22] The full transition is achieved by giving a vev to these free states. Switching on a vev for these states prevents one from turning on a mass parameter (proportional to the distance between the external 5-branes) and thus leads to a singular configuration $\mathbb{P}(1,1,2)$ that cannot be resolved.

We can extrapolate from this example to a more general geometric setting. Suppose that S has an A_1 singularity. It is well known in that this singularity is smoothable, either by writing the local equation $x^2 + y^2 + z^2 = t$ with t a deformation parameter, or by

[22] Moreover, because the parallel 5-branes are external, these free states can be excited infinitely far away from the 5d SCFT. However, this does not present a problem as first discussed in [9] because the states are decoupled from the 5d sector; see [39].

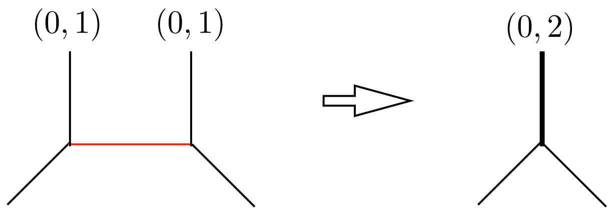

Figure 28. The red line is the curve of self-intersection -2. After the transition $X \to X'$, we see that two vertical external 5-branes are coincident — this configuration describes an isolated singularity in the corresponding 3-fold X'.

first resolving the singularity by a $\mathbb{P}^1$ with self-intersection -2 and then deforming the complex structure so that the -2 curve is no longer holomorphic. It is easy to see that this deformation can take place within a family of Calabi-Yau threefolds. A similar deformation can be provided for any ADE singularity. We treat an ADE singularity when all related masses are turned off and the singularity by associated complex structure deformation in the equal footing.

We can have many more kinds of singularities on surfaces contained in a smooth Calabi-Yau threefold. We content ourselves with providing one example and explaining how the singularity can be avoided up to physical equivalence.

A simple example of a singular rank 1 shrinkable surface S is constructed by letting Y be the singular hypersurface defined by the equation $x^3 + y^3 + z^3 = 0$ in $\mathbb{C}^4$. We can blow up the origin to obtain a Calabi-Yau resolution $f : X \to Y$, and the exceptional divisor is the hypersurface $S \subset \mathbb{P}^3$ defined by $x_1^3 + x_2^3 + x_3^3 = 0$, which is singular at $(x_0, x_1, x_2, x_3) = (1, 0, 0, 0)$. The fact that X is Calabi-Yau is computed by a standard algebro-geometric computation explained for example in [28]. Letting W be the blowup of $\mathbb{C}^4$ at the origin with $E \simeq \mathbb{P}^3$ the exceptional divisor, we have $K_W = 3E$. Since Y is a hypersurface in $\mathbb{C}^4$ with a triple point[23] at the origin, its proper transform X has class $X = -3E$ in W. Then by adjunction $K_X = (K_W + [X])|_X = (3E - 3E)|_X = 0$. This is just a cone in $\mathbb{P}^3$ over a plane curve which is singular at its vertex $(1, 0, 0, 0)$. This singular surface can be checked to be shrinkable.

The notion of physical equivalence allows us to bypass this difficulty. We can identify Y above with Y_0 in the one-parameter family of hypersurfaces Y_t defined by $tw^3+x^3+y^3+z^3 = 0$. Blowing up the origin gives a family $f_t : X_t \to Y_t$ of Calabi-Yau resolutions, with exceptional divisor $S_t = f_t^{-1}(0)$ defined by $tx_0^3 + x_1^3 + x_2^3 + x_3^3 = 0$. However, for $t \neq 0$, S_t is a smooth cubic surface, isomorphic to dP_6 in fact. So the 5d SCFT associated with the singular shrinkable surface S is physically equivalent to the well-known E_6 theory [6]. In other words, we can safely ignore S in our classification. But the only smooth rational or ruled surfaces are $\mathbb{P}^2$ or $\mathrm{Bl}_p\mathbb{P}(\mathcal{E})_g$ (see appendix A). Assuming the above conjecture is true, it is therefore possible to assemble a shrinkable surface S from a concise collection of known "building blocks", whose smooth components S_i are rational or ruled surfaces or their blowups.

[23]The notion of a triple point of hypersurface should not be confused with the notion of the intersection of three surfaces at a triple point which was discussed in section 3.3.

JHEP04(2018)103

References

[1] E. Witten, *Some comments on string dynamics*, in *Future perspectives in string theory. Proceedings, Conference, Strings'95*, Los Angeles U.S.A., 13–18 March 1995, pg. 501 [hep-th/9507121] [INSPIRE].

[2] J.J. Heckman, D.R. Morrison and C. Vafa, *On the classification of 6D SCFTs and generalized ADE orbifolds*, JHEP **05** (2014) 028 [*Erratum ibid.* **06** (2015) 017] [arXiv:1312.5746] [INSPIRE].

[3] J.J. Heckman, D.R. Morrison, T. Rudelius and C. Vafa, *Atomic classification of 6D SCFTs*, Fortsch. Phys. **63** (2015) 468 [arXiv:1502.05405] [INSPIRE].

[4] L. Bhardwaj, *Classification of 6d $N = (1, 0)$ gauge theories*, JHEP **11** (2015) 002 [arXiv:1502.06594] [INSPIRE].

[5] N. Seiberg, *Five-dimensional SUSY field theories, nontrivial fixed points and string dynamics*, Phys. Lett. **B 388** (1996) 753 [hep-th/9608111] [INSPIRE].

[6] D.R. Morrison and N. Seiberg, *Extremal transitions and five-dimensional supersymmetric field theories*, Nucl. Phys. **B 483** (1997) 229 [hep-th/9609070] [INSPIRE].

[7] M.R. Douglas, S.H. Katz and C. Vafa, *Small instantons, del Pezzo surfaces and type-I-prime theory*, Nucl. Phys. **B 497** (1997) 155 [hep-th/9609071] [INSPIRE].

[8] K.A. Intriligator, D.R. Morrison and N. Seiberg, *Five-dimensional supersymmetric gauge theories and degenerations of Calabi-Yau spaces*, Nucl. Phys. **B 497** (1997) 56 [hep-th/9702198] [INSPIRE].

[9] O. Aharony, A. Hanany and B. Kol, *Webs of (p, q) five-branes, five-dimensional field theories and grid diagrams*, JHEP **01** (1998) 002 [hep-th/9710116] [INSPIRE].

[10] O. Aharony and A. Hanany, *Branes, superpotentials and superconformal fixed points*, Nucl. Phys. **B 504** (1997) 239 [hep-th/9704170] [INSPIRE].

[11] N.C. Leung and C. Vafa, *Branes and toric geometry*, Adv. Theor. Math. Phys. **2** (1998) 91 [hep-th/9711013] [INSPIRE].

[12] O. Bergman and G. Zafrir, *Lifting 4d dualities to 5d*, JHEP **04** (2015) 141 [arXiv:1410.2806] [INSPIRE].

[13] P. Jefferson, H.-C. Kim, C. Vafa and G. Zafrir, *Towards classification of 5d SCFTs: single gauge node*, arXiv:1705.05836 [INSPIRE].

[14] Y. Tachikawa, *Frozen singularities in M and F-theory*, JHEP **06** (2016) 128 [arXiv:1508.06679] [INSPIRE].

[15] L. Bhardwaj, D. Morrison, Y. Tachikawa and A. Tomasiello, *The frozen phase of F-theory*, in progress.

[16] F. Apruzzi, J.J. Heckman and T. Rudelius, *Green-Schwarz automorphisms and 6D SCFTs*, JHEP **02** (2018) 157 [arXiv:1707.06242] [INSPIRE].

[17] M. Del Zotto, J.J. Heckman, D.S. Park and T. Rudelius, *On the defect group of a 6D SCFT*, Lett. Math. Phys. **106** (2016) 765 [arXiv:1503.04806] [INSPIRE].

JHEP04(2018)103

[18] M. Del Zotto, J.J. Heckman and D.R. Morrison, *6D SCFTs and phases of 5D theories*, *JHEP* **09** (2017) 147 [arXiv:1703.02981] [INSPIRE].

[19] C. Cordova, T.T. Dumitrescu and K. Intriligator, *Multiplets of superconformal symmetry in diverse dimensions*, arXiv:1612.00809 [INSPIRE].

[20] E. Witten, *Phase transitions in M-theory and F-theory*, *Nucl. Phys.* **B 471** (1996) 195 [hep-th/9603150] [INSPIRE].

[21] H. Hayashi, S.-S. Kim, K. Lee, M. Taki and F. Yagi, *A new 5d description of 6d D-type minimal conformal matter*, *JHEP* **08** (2015) 097 [arXiv:1505.04439] [INSPIRE].

[22] D. Gaiotto and H.-C. Kim, *Duality walls and defects in 5d $N = 1$ theories*, *JHEP* **01** (2017) 019 [arXiv:1506.03871] [INSPIRE].

[23] K. Yonekura, *Instanton operators and symmetry enhancement in 5d supersymmetric quiver gauge theories*, *JHEP* **07** (2015) 167 [arXiv:1505.04743] [INSPIRE].

[24] S.H. Katz, A. Klemm and C. Vafa, *Geometric engineering of quantum field theories*, *Nucl. Phys.* **B 497** (1997) 173 [hep-th/9609239] [INSPIRE].

[25] D. Xie and S.-T. Yau, *Three dimensional canonical singularity and five dimensional $N = 1$ SCFT*, *JHEP* **06** (2017) 134 [arXiv:1704.00799] [INSPIRE].

[26] H. Grauert, *Über Modifikationen und exzeptionelle analytische Mengen* (in German), *Math. Ann.* **146** (1962) 331.

[27] A. Beauville ed., *Canonical 3-folds*, Sijthoff and Noordhoff, The Netherlands, (1979).

[28] P. Griffiths and J. Harris, *Principles of algebraic geometry*, Wiley-Interscience, New York U.S.A., (1978).

[29] A. Hanany and E. Witten, *Type IIB superstrings, BPS monopoles and three-dimensional gauge dynamics*, *Nucl. Phys.* **B 492** (1997) 152 [hep-th/9611230] [INSPIRE].

[30] S. Katz and D.R. Morrison, *Gorenstein threefold singularities with small resolutions via invariant theory for Weyl groups*, *J. Alg. Geom.* **1** (1992) 449 [alg-geom/9202002].

[31] D.-E. Diaconescu and R. Entin, *Calabi-Yau spaces and five-dimensional field theories with exceptional gauge symmetry*, *Nucl. Phys.* **B 538** (1999) 451 [hep-th/9807170] [INSPIRE].

[32] O. Bergman and G. Zafrir, *5d fixed points from brane webs and O7-planes*, *JHEP* **12** (2015) 163 [arXiv:1507.03860] [INSPIRE].

[33] H. Hayashi, S.-S. Kim, K. Lee, M. Taki and F. Yagi, *More on 5d descriptions of 6d SCFTs*, *JHEP* **10** (2016) 126 [arXiv:1512.08239] [INSPIRE].

[34] A. Iqbal, A. Neitzke and C. Vafa, *A mysterious duality*, *Adv. Theor. Math. Phys.* **5** (2002) 769 [hep-th/0111068] [INSPIRE].

[35] H. Hayashi, S.-S. Kim, K. Lee and F. Yagi, *Equivalence of several descriptions for 6d SCFT*, *JHEP* **01** (2017) 093 [arXiv:1607.07786] [INSPIRE].

[36] M. Del Zotto, J.J. Heckman, A. Tomasiello and C. Vafa, *6d conformal matter*, *JHEP* **02** (2015) 054 [arXiv:1407.6359] [INSPIRE].

[37] M. Nagata, *On rational surfaces, II*, *Mem. College Sci. Univ. Kyoto* **A 33** (1960) 271.

[38] V. Kac, *Infinite dimensional Lie algebras*, Cambridge Univ. Press, Cambridge U.K., (1990).

[39] H. Hayashi, H.-C. Kim and T. Nishinaka, *Topological strings and 5d T_N partition functions*, *JHEP* **06** (2014) 014 [arXiv:1310.3854] [INSPIRE].

Published for SISSA by Springer

Received: June 25, 2020
Accepted: November 6, 2020
Published: December 23, 2020

Twisted circle compactifications of $6d$ SCFTs

Lakshya Bhardwaj,[a] Patrick Jefferson,[b] Hee-Cheol Kim,[c] Houri-Christina Tarazi[a] and Cumrun Vafa[a]

[a] *Department of Physics, Harvard University, 17 Oxford St., Cambridge, MA 02138, U.S.A.*

[b] *Center for Theoretical Physics, Department of Physics, Massachusetts Institute of Technology, 77 Massachusetts Avenue, Cambridge, MA 02139, U.S.A.*

[c] *Department of Physics, POSTECH, 77 Cheongam-Ro, Nam-Gu, Pohang 790-784, Korea*

E-mail: bhardwaj@maths.ox.ac.uk, pjeffers@mit.edu, heecheol@postech.ac.kr, h_tarazi@g.harvard.edu, vafa@physics.harvard.edu

Abstract: We study $6d$ superconformal field theories (SCFTs) compactified on a circle with arbitrary twists. The theories obtained after compactification, often referred to as $5d$ Kaluza-Klein (KK) theories, can be viewed as starting points for RG flows to $5d$ SCFTs. According to a conjecture, all $5d$ SCFTs can be obtained in this fashion. We compute the Coulomb branch prepotential for all $5d$ KK theories obtainable in this manner and associate to these theories a smooth local genus one fibered Calabi-Yau threefold in which is encoded information about all possible RG flows to $5d$ SCFTs. These Calabi-Yau threefolds provide hitherto unknown M-theory duals of F-theory configurations compactified on a circle with twists. For certain exceptional KK theories that do not admit a standard geometric description we propose an algebraic description that appears to retain the properties of the local Calabi-Yau threefolds necessary to determine RG flows to $5d$ SCFTs, along with other relevant physical data.

Keywords: Conformal Field Models in String Theory, Field Theories in Higher Dimensions, Conformal Field Theory, M-Theory

ArXiv ePrint: 1909.11666

https://doi.org/10.1007/JHEP12(2020)151

Contents

---

1 Introduction

Recently, there has been a resurgence of interest in the problem of classifying 5*d* superconformal field theories (SCFTs), with a particular emphasis on exploring the relationship between 5*d* UV fixed points and 6*d* UV fixed points [1–11]. The motivation for studying this relationship is the observation that all known 5*d* SCFTs can be organized into families of theories (connected to one another by RG flows) whose "progenitors" are 6*d* SCFTs compactified on a circle [1, 2], and hence every 6*d* SCFT compactified on a circle provides a natural starting point for the systematic identification of a large family of 5*d* SCFTs.

While it has been appreciated in the literature for some time that circle compactifications of 6*d* SCFTs can flow to 5*d* SCFTs, only recently has the existence of a 6*d* UV fixed point been understood in an intrinsically 5*d* setting. To understand this point, let us recall that the most widely used method for identifying 5*d* SCFTs is to construct a candidate effective field theory assumed to be a relevant deformation of a 5*d* UV fixed point, and to verify the effective theory passes a number of consistency checks which are believed to be sufficient to guarantee the existence of a such a non-trivial UV fixed point. This method, which has been used to construct numerous examples of UV complete minimally supersymmetric 5*d* QFTs — both by means of standard gauge theoretic methods [1, 12, 13], as well as string theory constructions such as (p, q) 5-brane configurations in type IIB string theory [14–20] and M-theory compactifications on local Calabi-Yau threefolds [2, 21–23]—has also led to the identification of numerous examples of theories that despite not satisfying the criteria necessary for the existence of a non-trivial 5d UV completion, nonetheless exhibit certain features that suggest they can be UV completed in 6d. All known examples of such theories are characterized by the emergence of an intrinsic length scale that is interpreted as the size of a compactification circle, and it has been argued that each of these theories is a circle compactification of a $6d$ SCFT possibly twisted by the action of a discrete global symmetry;[1] see for example [2–4, 18, 24–28]. These observations have led to the identification of a set of criteria believed sufficient to imply the existence of a $6d$ UV completion for certain 5d theories, and this introduces the possibility of also classifying circle compactifications of $6d$ SCFTs using 5d physics.

It was recently conjectured [2] that all $5d$ SCFTs can be obtained via RG flows starting from $5d$ Kaluza-Klein (KK) theories. The latter are defined as $6d$ SCFTs compactified on a circle (of finite radius) possibly with discrete twists around the circle. Given a 5d KK theory, the RG flows of interest correspond to integrating out BPS particles from the 5d KK theory — thus, if the full BPS spectrum is known then according to the conjecture of [2] it is possible to classify all $5d$ SCFTs by systematically studying all possible RG flows from the $5d$ KK theory.

In this paper, we focus on the geometric approach in which one realizes a $5d$ KK theory via a compactification of M-theory on a genus one fibered Calabi-Yau threefold. The set of holomorphic curves in the threefold completely encode the information about the spectrum of BPS particles required to track all RG flows down to $5d$ SCFTs. Therefore, a precursor to classifying RG flows from 5d KK theories to 5d SCFTs is to geometrically classify all 5d KK theories themselves in terms of Calabi-Yau threefolds. See [10] (also [2]) for explicit application of this geometric procedure to the classification of $5d$ SCFTs up to rank three.

It is believed that all $6d$ SCFTs can be constructed by compactifying F-theory on singular elliptically fibered Calabi-Yau threefolds admitting certain singular limits characterized by the contraction of holomorphic curves in the base of the fibration. Here we should distinguish between two different kinds of compactifications of F-theory depending on whether or not they contain $O7^+$ plane from the point of view of type IIB string theory. If there is no $O7^+$, then the compactification is said to lie in the *unfrozen* phase of F-theory; otherwise it is said to lie in the *frozen* phase [29–31] of F-theory. These two phases are qualitatively different in the following sense: the rules for converting geometry in the unfrozen phase to the corresponding $6d$ physics are far more straightforward than the rules for converting geometry in the frozen phase to the corresponding $6d$ physics [32]. See [33, 34] (see also [35]) for the classification of $6d$ SCFTs arising from the unfrozen phase of F-theory, and [36] for the classification of $6d$ SCFTs arising from the frozen phase of F-theory.

A $5d$ KK theory corresponding to the untwisted compactification of a $6d$ SCFT arising in the unfrozen phase can be constructed by compactifying M-theory on a Calabi-Yau threefold which is a resolution of the Calabi-Yau threefold arising in the F-theory construction. This fact is a special case of the duality between M-theory and (unfrozen phase of) F-theory compactified on a circle (without any twist). Explicit resolution of all Calabi-Yau threefolds associated to $6d$ SCFTs was performed by [3, 4], and hence the Calabi-Yau threefolds associated to corresponding $5d$ KK theories was determined. These threefolds are elliptically fibered since the threefolds associated to $6d$ SCFTs are elliptically fibered to begin with.

[1] Twisting the theory around the circle means that we introduce a holonomy for the background gauge fields associated to discrete global symmetries of the theory.

JHEP12(2020)151

In this paper, we extend the work of [3, 4] and determine a resolved local Calabi-Yau threefold describing every $5d$ KK theory, with the exception of certain examples which do not appear to admit a conventional geometric description.[2] Not only do we include twisted compactifications of $6d$ SCFTs arising in the unfrozen phase, but also the untwisted and twisted compactifications of $6d$ SCFTs arising in the frozen phase. We find that these Calabi-Yau threefolds are in general only genus one fibered and may not be elliptically fibered, which means that the fibration may not admit a zero section.

Our analysis can be divided into two parts. In the first part of the analysis, which is purely field theoretic, we determine the prepotential for each $5d$ KK theory by using the following observations: each $6d$ SCFT admits a $6d$ gauge theory description which can be reduced on a circle with an appropriate twist to obtain a canonical $5d$ gauge theory description of the associated $5d$ KK theory. The Green-Schwarz term in $6d$ reduces to a Chern-Simons term in the $5d$ gauge theory, which induces a tree-level contribution to the prepotential. Combining this contribution with the one-loop contribution coming from the $5d$ gauge theory produces the full prepotential for the $5d$ KK theory. In the second part of the analysis, we interpret the prepotential as describing the triple intersection numbers of 4-cycles inside a yet to be determined Calabi-Yau threefold. Using the data of these triple intersection numbers, along with some other consistency conditions, we are able to determine a description of the Calabi-Yau threefold as a neighborhood of intersecting Kähler surfaces along the lines of the discussion in [2–4], and we verify that each threefold admits the structure of genus one fibration.[3] By construction, compactifying M-theory on this Calabi-Yau threefold leads to the $5d$ KK theory whose prepotential we computed in the first part of the analysis.

One can view these Calabi-Yau threefolds as providing hitherto unknown M-theory duals of general unfrozen and frozen F-theory configurations compactified on a circle possibly with a discrete twist. Even though we have provided explicit results only for F-theory configurations realizing $6d$ SCFTs, our methods should in principle apply to any general F-theory configuration.

Notice that at no step in our analysis do we distinguish between $6d$ SCFTs arising from the unfrozen phase and $6d$ SCFTs arising from the frozen phase. Thus, according to our analysis, the rules for converting geometry into the corresponding $5d$ physics are uniform irrespective of whether the $5d$ KK theory arises from the compactification of a $6d$ SCFT lying in the frozen or the unfrozen phase. In other words, the frozen and unfrozen six-dimensional compactifications of F-theory are given a unified geometric description[4] in M-theory.

[2]For these examples, we propose an algebraic description which mimics certain properties of the Calabi-Yau threefolds associated to other KK theories. This algebraic description can be used to compute RG flows starting from these KK theories to $5d$ SCFTs. In the paper we sometimes abuse terminology and use the word 'geometry' to refer to both theories that admit a conventional geometric description along with those (i.e. "non-geometric" theories) for which only an algebraic description is available.

[3]See for example [37] for a discussion of F-theory compactifications on genus one fibered, in contrast to elliptically fibered, Calabi-Yau varieties.

[4]Some of the frozen theories belong to the class of exceptional KK theories which do not admit a conventional geometric description, and thus to which we only associate an algebraic description.

JHEP12(2020)151

We close the introduction with a brief overview of the structure of Calabi-Yau threefolds that we associate to $5d$ KK theories. By construction, the structure of these threefolds descends from the structure of $6d$ SCFTs. Recall that an important object characterizing a $6d$ SCFT is the matrix of Dirac pairings of "fundamental" BPS strings visible on the tensor branch of the $6d$ SCFT. The matrix of Dirac pairings is a symmetric, positive definite, integer matrix with positive entries on the diagonal and non-positive off-diagonal entries. Thus, the Dirac pairing matrix is analogous to the Cartan matrix of a simply laced Lie algebra, and we can associate to this matrix a graph analogous to a Dynkin graph for a simply laced Lie algebra.

As discussed in more detail later in the paper, the matrix of Dirac pairings descends to a matrix of Chern-Simons terms in the canonical gauge theory associated to the $5d$ KK theory, where the precise map between the two matrices depends on the choice of twist. We find that $5d$ KK theories end up organizing themselves according to this matrix of Chern-Simons terms. Like the matrix of Dirac pairings, the matrix of Chern-Simons terms is in general a positive definite, integer matrix with positive entries on the diagonal and non-positive off-diagonal entries, where off-diagonal entries can only be zero if their transposes are also zero. But, unlike the matrix of Dirac pairings, the matrix of Chern-Simons terms is not necessarily a symmetric matrix. Thus, the matrix of Chern-Simons couplings is analogous to the Cartan matrix of a general (simply or non-simply laced) Lie algebra, and we associate to it a graph analogous to a Dynkin graph for a general Lie algebra.

In this way, $5d$ KK theories are characterized by graphs that generalize Dynkin graphs. The associated Calabi-Yau geometry is assembled according to the structure of this graph:

- To each node in the graph, we associate a collection of Hirzebruch surfaces intersecting with each other. In fact, we associate a family of such collections parametrized by an integer ν, where the collections labeled by different values of ν are related to one another by flop transitions. A key point is that a certain linear combination of the $\mathbb{P}^1$ fibers of these Hirzebruch surfaces has genus one, and an appropriate multiple of the genus one fiber is identified physically with the KK mode of momentum one around the circle.

- To a pair of nodes connected to each other by some edges, we associate certain gluing[5] rules. These gluing rules describe how to glue the collection of surfaces associated to a node to the collection of surfaces associated to another node. These gluing rules capture the data of intersections between the two collections of surfaces. In general, the gluing rules provided in this paper work only for a subset of the values of ν parametrizing the two collections of surfaces being glued together. Our claim is that given a $5d$ KK theory, we can always find at least one value of ν for each node in the associated graph such that the gluing rules for each edge work.

[5]When two Kähler surfaces intersect transversely along a common holomorphic curve inside of a Calabi-Yau threefold, the intersection implies that a holomorphic curve inside one of the two surfaces is identified with a holomorphic curve inside of the other surface. We refer to this identification as a *gluing* together of the two surfaces.

JHEP12(2020)151

By applying these gluing rules, it can be checked that a multiple of the genus one fiber in one collection of surfaces is glued to a multiple of the genus fiber in the other collection of surfaces. These multiples are such that the KK mode associated to one collection is identified with the KK mode associated to the other collection. This must be so since there is only a single KK mode associated to the full KK theory and the genus one fibers inside each collection are merely different geometric manifestations of the same mode.

- Once we are done gluing all the collections of surfaces according to the gluing rules associated to each edge, we obtain a larger collection of surfaces intersecting with each other. The Calabi-Yau threefold associated to the KK theory is by definition a local neighborhood of this larger collection of surfaces. As we have described above, this Calabi-Yau threefold is canonically genus one fibered.

The rest of the paper is organized as follows. In section 2, we review how all $6d$ SCFTs can be neatly encapsulated in terms of graphs that capture the data of the tensor branch of the corresponding $6d$ SCFTs. We list all the possible vertices and edges appearing in such graphs. Our presentation treats unfrozen and frozen cases on an equal footing. Another distinguishing feature of our presentation is that we carefully distinguish different theories having the same gauge algebra content and same Dirac pairing. This includes the theta angle for $\mathfrak{sp}(n)$, different distributions of hypers between the spinor and cospinor representations of $\mathfrak{so}(12)$, as well as some frozen cases.

In section 3, we study all the possible twists of $6d$ SCFTs once they are compactified on a circle. Each twist leads to a different $5d$ KK theory. The different twists of a $6d$ SCFT $\mathfrak{T}$ are characterized by equivalence classes in the group of discrete global symmetries of $\mathfrak{T}$. We show that these equivalence classes can be described by foldings of the graphs $\Sigma_{\mathfrak{T}}$ associated to $\mathfrak{T}$ along with choice of an outer automorphism for each gauge algebra appearing in the low energy theory on the tensor branch of $\mathfrak{T}$. Thus, different $5d$ KK theories are also classified by graphs that generalize the graphs classifying $6d$ SCFTs. We provide a list of all the possible vertices and edges that can appear in the graphs associated to $5d$ KK theories.

In section 4, we provide a prescription to obtain the prepotential of any $5d$ KK theory. This is done by compactifying the low energy gauge theory appearing on the tensor branch of the corresponding $6d$ SCFT on a circle with the corresponding twist. This leads to a $5d$ gauge theory whose prepotential, along with a shift, is identified as the prepotential for the $5d$ KK theory.

In section 5, we associate a genus-one fibered Calabi-Yau threefold to each $5d$ KK theory, except for a few exceptional cases, for which we provide an algebraic description mimicking the essential properties of genus one fibered Calabi-Yau threefolds. The chief ingredient in the determination of the threefold is the prepotential determined in section 4. The prepotential captures the data of the triple intersection numbers of surfaces inside the threefold. Once a description of the threefold as a local neighborhood of a collection of surfaces glued to each other is presented, these triple intersections can be computed in a multitude of different ways. Demanding all of these different computations to give the same result leads to strong consistency constraints on such a description and often uniquely fixes

JHEP12(2020)151

the description (up to isomorphisms). Other consistency conditions playing a crucial role are also discussed in section 5.1.

The description of the geometry is provided in two different steps according to the structure of the graph associated to the $5d$ KK theory under study. First, a part of the geometry is assigned to each vertex in the graph according to results presented in section 5.2. Then, depending on the configuration of edges in the graph, different parts of the geometry corresponding to different vertices in the graph are glued to each other via the gluing rules presented in sections 5.3 and 5.4.

In section 6, we present our conclusions. In appendix A, we review some geometric background relevant for this paper. In appendix B, we address certain exceptional examples of geometries and gluing rules that do not admit a straightforward analysis following the main methods described in this paper. In appendix C, we provide a concrete and non-trivial check of our proposal for computing the prepotential and geometries associated to $5d$ KK theories. We demonstrate that a $5d$ KK theory arising from a non-trivial twist (involving a permutation of tensor multiplets) of a $6d$ SCFT has a $5d$ gauge theory description found in earlier studies by using brane constructions. In appendix D, we provide some more checks of our proposal. Finally, in appendix E we provide instructions for using the Mathematica notebook submitted as supplementary material along with this paper. The Mathematica notebook allows one to compute the prepotential for $5d$ KK theories involving one or two nodes. Combining these results, one can obtain the prepotential for any $5d$ KK theory. The notebook also converts the prepotential into triple intersection numbers for the associated geometry and displays these intersection numbers in a graphical form.

2 Structure of $6d$ SCFTs

In this section, we review the fact that $6d$ SCFTs are characterized by graphs that are analogous to Dynkin graphs associated to simply laced Lie algebras. In the next section, we will show that $5d$ KK theories are also characterized by similar graphs that are instead analogous to Dynkin graphs associated to general (i.e. both simply laced and non-simply laced) Lie algebras.

The low-energy theory on the tensor branch of a $6d$ SCFT $\mathfrak{T}$ can be organized in terms of tensor multiplets B_i. There is a gauge algebra $\mathfrak{g}_i$ associated to each i where $\mathfrak{g}_i$ can either be a simple or a trivial algebra. Each tensor multiplet B_i is also associated to a "fundamental" BPS string excitation S^i such that the charge of S^i under B_j is the Kronecker delta δ^i_j. The Dirac pairing Ω^{ij} between S^i and S^j appears in the Green-Schwarz term in the Lagrangian

$$\Omega^{ij} B_i \wedge \mathrm{tr}(F_j^2) \tag{2.1}$$

where F_j is the field strength for $\mathfrak{g}_j$ if $\mathfrak{g}_j$ is simple and $F_j = 0$ if $\mathfrak{g}_j$ is trivial.

$[\Omega^{ij}]$ is a symmetric, positive definite matrix with all of its entries valued in integers. Thus, it is analogous to the Cartan matrix for a simply laced Lie algebra. The only possible values for off-diagonal entries are $\Omega^{ij} = 0, -1, -2$. We note that $\Omega^{ij} = -2$ is only possible for $6d$ SCFTs arising from the frozen phase of F-theory [32, 36].

JHEP12(2020)151

$\mathfrak{g}_i$ Ω^{ii}	Comments	Hypermultiplet content
$\mathfrak{sp}(n)_\theta$ 1	$\theta = 0, \pi$	$(2n+8)\mathsf{F}$
$\mathfrak{su}(n)$ 1	$n \geq 3$	$(n+8)\mathsf{F} + \Lambda^2$
$\mathfrak{su}(\widehat{n})$ 1	$n \geq 8$; frozen; non-geometric	$(n-8)\mathsf{F} + \mathsf{S}^2$
$\mathfrak{su}(\tilde{6})$ 1		$15\mathsf{F} + \frac{1}{2}\Lambda^3$
$\mathfrak{su}(n)$ 2		$2n\mathsf{F}$
$\mathfrak{su}(3)$ 3		
$\mathfrak{so}(n)$ 4	$n \geq 8$	$(n-8)\mathsf{F}$
$\mathfrak{so}(8)$ k	$1 \leq k \leq 3$	$(4-k)\mathsf{F} + (4-k)\mathsf{S} + (4-k)\mathsf{C}$
$\mathfrak{so}(n)$ k	$1 \leq k \leq 3$; $7 \leq n \leq 12, n \neq 8$	$(n-4-k)\mathsf{F} + 2^{\lceil \frac{9-n}{2} \rceil}(4-k)\mathsf{S}$
$\mathfrak{so}(\widehat{12})$ k	$k = 1, 2$	$(8-k)\mathsf{F} + \frac{1}{2}(3-k)\mathsf{S} + \frac{1}{2}\mathsf{C}$
$\mathfrak{so}(13)$ 2		$7\mathsf{F} + \frac{1}{2}\mathsf{S}$
$\mathfrak{g}_2$ k	$1 \leq k \leq 3$	$(10-3k)\mathsf{F}$
$\mathfrak{f}_4$ k	$1 \leq k \leq 5$	$(5-k)\mathsf{F}$
$\mathfrak{e}_6$ k	$1 \leq k \leq 6$	$(6-k)\mathsf{F}$
$\mathfrak{e}_7$ k	$1 \leq k \leq 8$	$\frac{1}{2}(8-k)\mathsf{F}$
$\mathfrak{e}_8$ 12		

Table 1. List of all the possible nodes with non-trivial $\mathfrak{g}_i$ appearing in graphs associated to $6d$ SCFTs. A hat or a tilde distinguishes different nodes having same values of Ω^{ii} and $\mathfrak{g}_i$.

JHEP12(2020)151

$\mathfrak{g}_i$ Ω^{ii}	Comments	Flavor symmetry algebra, $\mathfrak{f}$
$\mathfrak{sp}(0)_\theta$ 1	$\theta = 0, \pi$	$\mathfrak{e}_8$
$\mathfrak{su}(1)$ 2		$\mathfrak{su}(2)$

Table 2. List of all the possible nodes with trivial $\mathfrak{g}_i$ that can appear in graphs associated to $6d$ SCFTs. If $\Omega^{ii} = 2$, we refer to the trivial gauge algebra as $\mathfrak{su}(1)$ and if $\Omega^{ii} = 1$, we refer to the trivial gauge algebra as $\mathfrak{sp}(0)$. In the latter case, sometimes a $\mathbb{Z}_2$ valued theta angle is physically relevant. We also list the flavor symmetry algebra $\mathfrak{f}$ for each case. The sum of gauge algebras neighboring each such node must be contained inside the corresponding $\mathfrak{f}$.

We can thus display the data of a $6d$ SCFT in terms of an associated graph $\Sigma_{\mathfrak{T}}$ that is constructed as follows:

- **Nodes**: for each tensor multiplet B_i, we place a node i with value $\overset{\mathfrak{g}_i}{\Omega^{ii}}$. All such possibilities are listed in table 1 when $\mathfrak{g}_i$ is non-trivial, and in table 2 when $\mathfrak{g}_i$ is trivial. In the former case, each node contributes hypers charged under a representation $\mathcal{R}_i$ of $\mathfrak{g}_i$ where $\mathcal{R}_i$ is shown in table 1. In the latter case, for the node with $\mathfrak{g}_i = \mathfrak{sp}(0)$, an important role is played by the adjoint representation of $\mathfrak{e}_8$, which is formed by the BPS string excitations associated to this node.

  We note that the node $\overset{\mathfrak{su}(\hat{n})}{1}$ only arises in the frozen phase of F-theory.

  In the case of $\Omega^{ii} = 1$ and $\mathfrak{g}_i = \mathfrak{sp}(n)$, there is a possibility of a $\mathbb{Z}_2$ valued $6d$ theta angle which is physically relevant (in the context of $6d$ SCFTs) only when the $2n+8$ hypers in fundamental are gauged by a neighboring $\mathfrak{su}(2n+8)$ gauge algebra. For $\mathfrak{g}_i = \mathfrak{sp}(0)$, the theta angle is physically relevant (in the context of $6d$ SCFTs) only if there is a neighboring $\mathfrak{su}(8)$ gauge algebra [38]. This can be understood in terms of two different embeddings of $\mathfrak{su}(8)$ into $\mathfrak{e}_8$ (both having embedding index one), so that the adjoint of $\mathfrak{e}_8$ decomposes differently in the two cases, leading to different spectrum of string excitations.

  In the case of $\Omega^{ii} = 1$ and $\mathfrak{g}_i = \mathfrak{su}(6)$, there are two possible choices of matter content. We distinguish the non-standard choice of matter content by denoting the corresponding $\mathfrak{g}_i$ as $\mathfrak{su}(\tilde{6})$.

  In the case of $\mathfrak{g}_i = \mathfrak{so}(12)$, the two spinor representations S and C are not conjugate to each other but have same contributions to the anomaly polynomial. The total number of hypers in the two spinor representations is fixed by the value of Ω^{ii}. But since the two spinor representations are not conjugate, the relative distribution of hypers between the two makes a difference. For $\Omega^{ii} = 1, 2$, we can obtain two inequivalent theories in this way (note that the existence of two inequivalent theories with $\mathfrak{so}(12)$ gauge symmetry was pointed out in [11].) The version containing both S and C is distinguished from the one contataining only S by denoting its $\mathfrak{g}_i$ as $\mathfrak{so}(\widehat{12})$.

JHEP12(2020)151

$\overset{\mathfrak{g}_i}{\Omega^{ii}} \;\text{——}\; \overset{\mathfrak{g}_j}{\Omega^{jj}}$	Comments	Mixed hyper content
$\overset{\mathfrak{sp}(n_i)}{1} \;\text{———}\; \overset{\mathfrak{su}(n_j)}{2}$	$n_i \leq n_j$; $n_j \leq 2n_i + 7$	$\mathsf{F} \otimes \mathsf{F}$
$\overset{\mathfrak{sp}(n_i)_\theta}{1} \;\text{———}\; \overset{\mathfrak{su}(n_j)}{2}$	$n_j = 2n_i + 8$; $\theta = 0, \pi$	$\mathsf{F} \otimes \mathsf{F}$
$\overset{\mathfrak{sp}(n_i)}{1} \;\text{———}\; \overset{\mathfrak{so}(n_j)}{k}$	$n_i \leq n_j - 4 - k$; $n_j \leq 4n_i + 16$; $2 \leq k \leq 4$	$\frac{1}{2}(\mathsf{F} \otimes \mathsf{F})$
$\overset{\mathfrak{sp}(n_i)}{1} \;\text{———}\; \overset{\mathfrak{so}(\widehat{12})}{2}$	$n_i \leq 6$	$\frac{1}{2}(\mathsf{F} \otimes \mathsf{F})$
$\overset{\mathfrak{sp}(n_i)}{1} \;\text{- - - - -}\; \overset{\mathfrak{so}(8)}{k}$	$n_i \leq 4 - k$; $k \leq 3$	$\frac{1}{2}(\mathsf{F} \otimes \mathsf{S})$
$\overset{\mathfrak{sp}(n_i)}{1} \;\text{- - - - -}\; \overset{\mathfrak{so}(7)}{k}$	$n_i \leq 8 - 2k$; $k = 2, 3$	$\frac{1}{2}(\mathsf{F} \otimes \mathsf{S})$
$\overset{\mathfrak{sp}(n_i)}{1} \;\text{———}\; \overset{\mathfrak{g}_2}{k}$	$n_i \leq 10 - 3k$; $k = 2, 3$	$\frac{1}{2}(\mathsf{F} \otimes \mathsf{F})$
$\overset{\mathfrak{su}(n_i)}{1} \;\text{———}\; \overset{\mathfrak{su}(n_j)}{2}$	$n_i \leq 2n_j$; $n_j \leq n_i + 8$	$\mathsf{F} \otimes \mathsf{F}$
$\overset{\mathfrak{su}(\hat{n}_i)}{1} \;\text{———}\; \overset{\mathfrak{su}(n_j)}{2}$	$n_i \leq 2n_j$; $n_j \leq n_i - 8$	$\mathsf{F} \otimes \mathsf{F}$
$\overset{\mathfrak{su}(\tilde{6})}{1} \;\text{———}\; \overset{\mathfrak{su}(n_j)}{2}$	$3 \leq n_j \leq 15$	$\mathsf{F} \otimes \mathsf{F}$
$\overset{\mathfrak{su}(n_i)}{2} \;\text{———}\; \overset{\mathfrak{su}(n_j)}{2}$	$n_i \leq 2n_j$; $n_j \leq 2n_i$	$\mathsf{F} \otimes \mathsf{F}$
$\overset{\mathfrak{su}(n_i)}{2} \;\text{—}\,{\scriptstyle 2}\,\text{—}\; \overset{\mathfrak{so}(n_j)}{4}$	$n_i \leq n_j - 8$; $n_j \leq 2n_i$; frozen	$\mathsf{F} \otimes \mathsf{F}$
$\overset{\mathfrak{su}(2)}{2} \;\text{- - - - -}\; \overset{\mathfrak{so}(7)}{k}$	$1 \leq k \leq 3$	$\frac{1}{2}(\mathsf{F} \otimes \mathsf{S})$
$\overset{\mathfrak{su}(2)}{2} \;\text{———}\; \overset{\mathfrak{g}_2}{k}$	$1 \leq k \leq 3$	$\frac{1}{2}(\mathsf{F} \otimes \mathsf{F})$

Table 3. List of all the possible edges between two gauge-theoretic nodes that can appear in graphs characterizing $6d$ SCFTs. An edge with 2 in the middle of it denotes the fact that there are two edges between the two asocciated nodes. Solid edges denote matter in bifundamental and dashed edges denote matter in $\mathsf{F} \otimes \mathsf{S}$. The theta angle of $\mathfrak{sp}(n)$ is only displayed when it is physically relevant.

- **Edges**: consider two nodes i and j whose values are $\overset{\mathfrak{g}_i}{\Omega^{ii}}$ and $\overset{\mathfrak{g}_j}{\Omega^{jj}}$ respectively. We place $-\Omega^{ij}$ number of edges between i and j. For instance, if $\Omega^{ij} = -1$, then we display this as

$$\overset{\mathfrak{g}_i}{\Omega^{ii}} \;\text{———}\; \overset{\mathfrak{g}_j}{\Omega^{jj}} \tag{2.2}$$

$\overset{\mathfrak{g}_i}{\Omega^{ii}} \text{ —— } \overset{\mathfrak{g}_j}{\Omega^{jj}}$	Comments	Mixed hyper content
$\overset{\mathfrak{sp}(0)}{1} \text{ ——— } \overset{\mathfrak{su}(n)}{2}$	$n \leq 9, n \neq 8$	
$\overset{\mathfrak{sp}(0)_\theta}{1} \text{ ——— } \overset{\mathfrak{su}(n)}{2}$	$n = 8;\ \theta = 0, \pi$	
$\overset{\mathfrak{sp}(0)}{1} \text{ ——— } \overset{\mathfrak{su}(3)}{3}$		
$\overset{\mathfrak{sp}(0)}{1} \text{ ——— } \overset{\mathfrak{so}(n)}{k}$	$n \leq 16;\ 2 \leq k \leq 4$	
$\overset{\mathfrak{sp}(0)}{1} \text{ ——— } \overset{\mathfrak{so}(\widehat{12})}{2}$		
$\overset{\mathfrak{sp}(0)}{1} \text{ ——— } \overset{\mathfrak{g}_2}{k}$	$k = 2, 3$	
$\overset{\mathfrak{sp}(0)}{1} \text{ ——— } \overset{\mathfrak{f}_4}{k}$	$2 \leq k \leq 5$	
$\overset{\mathfrak{sp}(0)}{1} \text{ ——— } \overset{\mathfrak{e}_6}{k}$	$2 \leq k \leq 6$	
$\overset{\mathfrak{sp}(0)}{1} \text{ ——— } \overset{\mathfrak{e}_7}{k}$	$2 \leq k \leq 8$	
$\overset{\mathfrak{sp}(0)}{1} \text{ ——— } \overset{\mathfrak{e}_8}{12}$		
$\overset{\mathfrak{su}(1)}{2} \text{ ——— } \overset{\mathfrak{sp}(1)}{1}$		$\frac{1}{2}\mathsf{F}$ in $\mathfrak{g}_j = \mathfrak{sp}(1)$
$\overset{\mathfrak{su}(1)}{2} \text{ ——— } \overset{\mathfrak{su}(2)}{2}$		$\frac{1}{2}\mathsf{F}$ in $\mathfrak{g}_j = \mathfrak{su}(2)$

Table 4. List of all the possible edges between a gauge-theoretic and a non-gauge-theoretic node that can appear in graphs characterizing $6d$ SCFTs. The theta angle of $\mathfrak{sp}(0)$ is only displayed when it is physically relevant.

$\overset{\mathfrak{g}_i}{\Omega^{ii}} \text{ —— } \overset{\mathfrak{g}_j}{\Omega^{jj}}$
$\overset{\mathfrak{sp}(0)}{1} \text{ ——— } \overset{\mathfrak{su}(1)}{2}$
$\overset{\mathfrak{su}(1)}{2} \text{ ——— } \overset{\mathfrak{su}(1)}{2}$

Table 5. List of all the possible edges between two non-gauge-theoretic nodes that can appear in graphs characterizing $6d$ SCFTs. The theta angle of $\mathfrak{sp}(0)$ is not displayed since it is not physically relevant.

JHEP12(2020)151

$\begin{array}{ccc} \mathfrak{g}_i & \mathfrak{sp}(0) & \mathfrak{g}_k \\ \Omega^{ii} \text{ —— } & 1 & \text{ —— } \Omega^{kk} \end{array}$	Comments
$\begin{array}{ccc} \mathfrak{su}(2) & \mathfrak{sp}(0) & \mathfrak{g} \\ 2 \text{ —— } & 1 & \text{ —— } k \end{array}$	$k \geq 3$; $\mathfrak{g} = \mathfrak{e}_7, \mathfrak{e}_6, \mathfrak{f}_4, \mathfrak{g}_2, \mathfrak{so}(n \leq 12)$
$\begin{array}{ccc} \mathfrak{su}(3) & \mathfrak{sp}(0) & \mathfrak{g} \\ k \text{ —— } & 1 & \text{ —— } l \end{array}$	$k, l \geq 2$; $k + l \geq 5$; $\mathfrak{g} = \mathfrak{e}_6, \mathfrak{f}_4, \mathfrak{g}_2, \mathfrak{so}(n \leq 10), \mathfrak{su}(n \leq 6)$
$\begin{array}{ccc} \mathfrak{su}(4) & \mathfrak{sp}(0) & \mathfrak{g} \\ 2 \text{ —— } & 1 & \text{ —— } k \end{array}$	$k = 3, 4$; $\mathfrak{g} = \mathfrak{g}_2, \mathfrak{so}(n \leq 10)$
$\begin{array}{ccc} \mathfrak{so}(7) & \mathfrak{sp}(0) & \mathfrak{g} \\ k \text{ —— } & 1 & \text{ —— } l \end{array}$	$k, l \geq 2$; $k + l \geq 5$; $\mathfrak{g} = \mathfrak{g}_2, \mathfrak{so}(n \leq 9)$
$\begin{array}{ccc} \mathfrak{so}(8) & \mathfrak{sp}(0) & \mathfrak{g} \\ k \text{ —— } & 1 & \text{ —— } l \end{array}$	$k, l \geq 2$; $k + l \geq 5$; $\mathfrak{g} = \mathfrak{g}_2, \mathfrak{so}(8)$
$\begin{array}{ccc} \mathfrak{so}(9) & \mathfrak{sp}(0) & \mathfrak{g} \\ k \text{ —— } & 1 & \text{ —— } l \end{array}$	$k, l \geq 2$; $k + l \geq 5$; $\mathfrak{g} = \mathfrak{g}_2$
$\begin{array}{ccc} \mathfrak{g}_2 & \mathfrak{sp}(0) & \mathfrak{g} \\ k \text{ —— } & 1 & \text{ —— } l \end{array}$	$k, l \geq 2$; $k + l \geq 5$; $\mathfrak{g} = \mathfrak{f}_4, \mathfrak{g}_2$

Table 6. List of all the possibilities for multiple neighbors of $\mathfrak{sp}(0)$.

and, if $\Omega^{ij} = -2$, then we display this as

$$\begin{array}{ccc} \mathfrak{g}_i & & \mathfrak{g}_j \\ \Omega^{ii} & \text{— }{\scriptstyle 2}\text{ —} & \Omega^{jj} \end{array} \tag{2.3}$$

There are no edges between nodes i and j if $\Omega^{ij} = 0$. All the possible edges are listed in table 3 when both $\mathfrak{g}_i$ and $\mathfrak{g}_j$ are non-trivial, in table 4 when only one of $\mathfrak{g}_i$ and $\mathfrak{g}_j$ is non-trivial, and in table 5 when both $\mathfrak{g}_i$ and $\mathfrak{g}_j$ are trivial.

Each edge corresponds to a hyper transforming in a mixed representation $\mathcal{R}_{ij} = \mathcal{R}_{ij,i} \otimes \mathcal{R}_{ij,j}$ of $\mathfrak{g}_i \oplus \mathfrak{g}_j$ where $\mathcal{R}_{ij,i}$ is a representation of $\mathfrak{g}_i$ and $\mathcal{R}_{ij,j}$ is a representation of $\mathfrak{g}_j$. The possible $\mathcal{R}_{ij}$ are shown in the third column of table 3. Note that we must have $\oplus_j \mathcal{R}_{ij,i}^{\oplus \dim(\mathcal{R}_{ij,j})} \subseteq \mathcal{R}_i$ as representations of $\mathfrak{g}_i$ for each node i.

In the case of $\Omega^{ii} = 1$, $\mathfrak{g}_i = \mathfrak{sp}(n_i)$, $\Omega^{jj} = k$, $\mathfrak{g}_j = \mathfrak{so}(7, 8)$ and $\Omega^{ij} = -1$, there are two possible mixed representations $\frac{1}{2}(\mathsf{F} \otimes \mathsf{F})$ or $\frac{1}{2}(\mathsf{F} \otimes \mathsf{S})$. We distinguish the case $\frac{1}{2}(\mathsf{F} \otimes \mathsf{S})$ by denoting the corresponding edge as a dashed line. Notice that when $\mathfrak{g}_j = \mathfrak{so}(8)$, the dashed edge is only physically relevant when it is a part of a configuration of form

$$\begin{array}{ccc} \mathfrak{sp}(n_i) & \mathfrak{so}(8) & \mathfrak{sp}(n_k) \\ 1 \text{ - - - - - } & k & \text{ —— } 1 \end{array} \tag{2.4}$$

Otherwise, the dashed edge can be converted to the non-dashed edge by applying an outer-automorphism of $\mathfrak{so}(8)$.

- **Multiple neighbors of $\mathfrak{sp}(0)$**: consider a node i with value $\begin{array}{c} \mathfrak{sp}(0) \\ 1 \end{array}$. Related to the fact that the flavor symmetry algebra associated to this node is $\mathfrak{e}_8$, it can be

JHEP12(2020)151

shown that its neighbors must satisfy $\oplus_j \mathfrak{g}_j \subseteq \mathfrak{e}_8$ where only those j are included in the sum for which $\Omega^{ij} = -1$. In fact all such subalgebras are realized except[6] for $\mathfrak{so}(13) \oplus \mathfrak{su}(2)$.

In the context of $6d$ SCFTs, it is not possible for $\mathfrak{sp}(0)$ to have more than two neighbors. We collect all the possibilities for multiple neighbors of $\mathfrak{sp}(0)$ in table 6.

Notice that the relationship between $\Sigma_{\mathfrak{T}}$ and $[\Omega^{ij}]$ is analogous to the relationship between Dynkin graph and Cartan matrix of a simply laced Lie algebra.

3 Structure of 5d KK theories

3.1 Twists

Consider a QFT $\mathfrak{T}$ that admits a discrete global symmetry group Γ. When we compactify $\mathfrak{T}$ on a circle, we have the option of "twisting" $\mathfrak{T}$ around the circle. This means that we introduce a holonomy $\gamma \in \Gamma$ for the background gauge field corresponding to Γ. Note that the number of distinct twists is not given by the number of elements in Γ, but rather by the number of conjugacy classes in Γ. This is because two holonomies that are conjugate in Γ are physically equivalent and thus lead to the same twist.

In this section, we will explore all the possible twists for $6d$ SCFTs. Each twist leads to a different $5d$ KK theory.

3.2 Discrete symmetries from outer automorphisms

A general discrete symmetry of a $6d$ SCFT $\mathfrak{T}$ is generated by combining two kinds of basic discrete symmetries. We start by discussing the first kind of basic discrete symmetries. These arise from outer automorphisms of gauge algebras $\mathfrak{g}_i$.

$\mathfrak{su}(n)$ for $n \geq 3$, $\mathfrak{so}(2m)$ for $m \geq 4$ and $\mathfrak{e}_6$ admit an order two outer automorphism that we call $\mathcal{O}^{(2)}$. It exchanges the roots in the following fashion

$\mathfrak{su}(2n)$, $\mathcal{O}^{(2)}$:

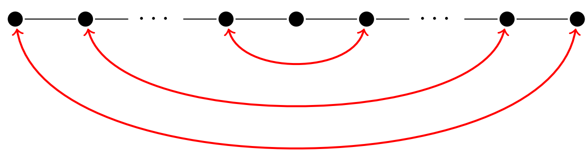

$\mathfrak{su}(2n+1)$, $\mathcal{O}^{(2)}$:

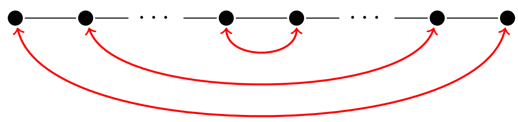

[6]It can be shown that the embedding index of each neighboring $\mathfrak{g}_j$ inside $\mathfrak{e}_8$ must be one. The only possible embedding of $\mathfrak{so}(13) \oplus \mathfrak{su}(2)$ into $\mathfrak{e}_8$ follows from first embedding $\mathfrak{so}(13) \oplus \mathfrak{su}(2)$ into $\mathfrak{so}(16)$ as a special maximal subalgebra and then embedding $\mathfrak{so}(16)$ into $\mathfrak{e}_8$ as a regular maximal subalgebra. The embedding index of the $\mathfrak{su}(2)$ factor under this embedding is two rather than one, thus $\mathfrak{so}(13) \oplus \mathfrak{su}(2)$ cannot be realized as a neighbor of $\mathfrak{sp}(0)$. The absence of $\mathfrak{so}(13) \oplus \mathfrak{su}(2)$ neighbor was first noticed in [39].

$\mathfrak{g}$	$\mathcal{O}^{(q)}$	$\mathcal{O}^{(q)} \cdot \mathcal{R}_{\mathfrak{g}}$
$\mathfrak{su}(m)$	$\mathcal{O}^{(2)}$	$\mathsf{F} \longleftrightarrow \bar{\mathsf{F}}$, $\Lambda^n \longleftrightarrow \bar{\Lambda}^n$, $\mathsf{S}^2 \longleftrightarrow \bar{\mathsf{S}}^2$
$\mathfrak{so}(2m)$	$\mathcal{O}^{(2)}$	$\mathsf{F} \longrightarrow \mathsf{F}$, $\mathsf{S} \longleftrightarrow \mathsf{C}$
$\mathfrak{e}_6$	$\mathcal{O}^{(2)}$	$\mathsf{F} \longleftrightarrow \bar{\mathsf{F}}$
$\mathfrak{so}(8)$	$\mathcal{O}^{(3)}$	$\mathsf{F} \longrightarrow \mathsf{S}$, $\mathsf{S} \longrightarrow \mathsf{C}$, $\mathsf{C} \longrightarrow \mathsf{F}$

Table 7. List of non-trivial outer automorphisms $\mathcal{O}^{(q)}$ of $\mathfrak{g}$ and their actions $\mathcal{O}^{(q)} \cdot \mathcal{R}_{\mathfrak{g}}$ on various irreducible representations $\mathcal{R}_{\mathfrak{g}}$ of $\mathfrak{g}$. F denotes fundamental representation, Λ^n denotes the irreducible n-index antisymmetric representation, S^2 denotes the irreducible 2-index symmetric representation, and S and C denote irreducible spinor and cospinor representations. Bar on top of a representation denotes the complex conjugate of that representation. F of $\mathfrak{so}(2m)$ is left invariant by the action of $\mathcal{O}^{(2)}$.

$\mathfrak{so}(2n)$, $\mathcal{O}^{(2)}$:

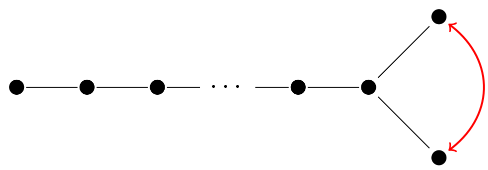

$\mathfrak{e}_6$, $\mathcal{O}^{(2)}$:

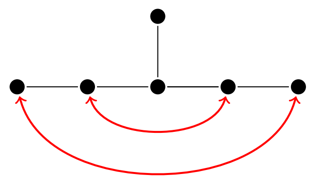

$\mathfrak{so}(8)$ also admits an order three outer automorphism which we call $\mathcal{O}^{(3)}$. It cyclically permutes the roots as shown below

$\mathfrak{so}(8)$, $\mathcal{O}^{(3)}$:

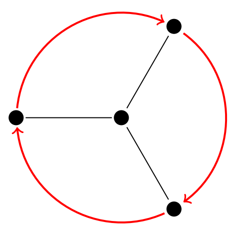

The full group of outer automorphisms of $\mathfrak{so}(8)$ is the symmetric group S_3 which can be generated by combining $\mathcal{O}^{(2)}$ and $\mathcal{O}^{(3)}$. Note that $\mathcal{O}^{(2)}$ and $\mathcal{O}^{(3)}$ are not conjugate to each other (since they have different orders) and hence we need to consider both of them.

The above action of an outer automorphism $\mathcal{O}^{(q)}$ (for $q = 2, 3$) on the roots of $\mathfrak{g}$ translates to an action on the Dynkin coefficients of the weights for representations of $\mathfrak{g}$. In other words, the action of $\mathcal{O}^{(q)}$ can be viewed as an action on representations of $\mathfrak{g}$ — see table 7.

An outer automorphism $\mathcal{O}^{(q_i)}$ of a gauge algebra $\mathfrak{g}_i \in \mathfrak{T}$ is a symmetry of $\mathfrak{T}$ if

$$\mathcal{O}^{(q_i)} \cdot \mathcal{R}_i = \mathcal{R}_i \tag{3.1}$$

$$\mathcal{O}^{(q_i)} \cdot \mathcal{R}_{ij,i} = \mathcal{R}_{ij,i} \quad \forall j \tag{3.2}$$

where $\mathcal{O}^{(q_i)} \cdot \mathcal{R}$ denotes the action of $\mathcal{O}^{(q_i)}$ on $\mathcal{R}$. We should keep in mind that a hyper in a representation $\mathcal{R}$ is the same as a hyper in representation $\bar{\mathcal{R}}$. So, $\mathcal{R}_i$ and $\mathcal{R}_{ij,i}$ are only defined up to complex conjugation on constituent irreps. Thus, whenever $\mathcal{R} \leftrightarrow \bar{\mathcal{R}}$ in table 7, it means that two distinct hypers in $\mathcal{R}$ are interchanged with each other under the action of the outer automorphism.

As an example consider the $6d$ theory given by

$$\begin{array}{c} \mathfrak{su}(n) \\ 2 \end{array} \tag{3.3}$$

The theory includes $2n$ hypers in F. The outer automorphism $\mathcal{O}^{(2)}$ of $\mathfrak{su}(n)$ descends to a discrete symmetry of the theory whose action on the hypermultiplets can be manifested as follows. We divide the $2n$ hypers into two ordered sets such that each set contains n hypers. Then we exchange these two sets with each other.

3.3 Discrete symmetries from permutation of tensor multiplets

Now we turn to a discussion of the second kind of basic discrete symmetries. These arise from permutation of tensor multiplets $i \to S(i)$ such that

$$\mathfrak{g}_{S(i)} = \mathfrak{g}_i \tag{3.4}$$

$$\Omega^{S(i)S(j)} = \Omega^{ij} \tag{3.5}$$

for all i, j. This is a symmetry of $\mathfrak{T}$ if

$$\mathcal{R}_{S(i)} \simeq \mathcal{R}_i \tag{3.6}$$

$$\mathcal{R}_{S(i)S(j)} \simeq \mathcal{R}_{ij} \tag{3.7}$$

for all i, j.

As an example, consider the $6d$ theory given by

$$\begin{tikzcd} \overset{\mathfrak{so}(p)}{4} \arrow[r, dash] & \overset{\mathfrak{sp}(n)}{1} \arrow[r, dash] & \overset{\mathfrak{so}(m)}{4} \arrow[r, dash] & \overset{\mathfrak{sp}(n)}{1} \arrow[r, dash] & \overset{\mathfrak{so}(p)}{4} \end{tikzcd} \tag{3.8}$$

The permutation

$$\begin{tikzcd} \overset{\mathfrak{so}(p)}{4} \arrow[r, dash] \arrow[rrrr, <->, bend right, red] & \overset{\mathfrak{sp}(n)}{1} \arrow[r, dash] \arrow[rr, <->, bend right, red] & \overset{\mathfrak{so}(m)}{4} \arrow[r, dash] & \overset{\mathfrak{sp}(n)}{1} \arrow[r, dash] & \overset{\mathfrak{so}(p)}{4} \end{tikzcd} \tag{3.9}$$

is a symmetry of the theory.

JHEP12(2020)151

As another example, consider the $6d$ theory given by

$$\begin{array}{cccc} \mathfrak{su}(m) & \mathfrak{su}(n) & \mathfrak{su}(n) & \mathfrak{su}(m) \\ 2 & \!\!\text{------}\!\! 2 & \!\!\text{------}\!\! 2 & \!\!\text{------}\!\! 2 \end{array} \tag{3.10}$$

The permutation

$$\begin{tikzcd} \overset{\mathfrak{su}(m)}{2} \arrow[rrr, dash] \arrow[rrr, bend right=50, <->] & \overset{\mathfrak{su}(n)}{2} \arrow[r, bend right=50, <->] & \overset{\mathfrak{su}(n)}{2} & \overset{\mathfrak{su}(m)}{2} \end{tikzcd} \tag{3.11}$$

is a symmetry of the theory.

Now, consider a permutation S that is a symmetry of $\mathfrak{T}$. We can use the data of S to convert $[\Omega^{ij}]$ into another matrix $[\Omega_S^{\alpha\beta}]$. Here α, β etc. parametrize orbits of nodes i under the iterative action of S. To define a particular entry $\Omega_S^{\alpha\beta}$, we pick a node i lying in the orbit α and let

$$\Omega_S^{\alpha\beta} = \sum_{j\in\beta} \Omega^{ij} \tag{3.12}$$

where the sum is over all nodes j lying in the orbit β. Notice that the resulting matrix $[\Omega_S^{\alpha\beta}]$ need not be symmetric but must be positive definite. It turns out for S associated to $6d$ SCFTs that whenever $\Omega_S^{\alpha\beta} \neq \Omega_S^{\beta\alpha}$, then the smaller of the two entries is -1. Thus, $[\Omega_S^{\alpha\beta}]$ is analogous to the Cartan matrix for a general (i.e. either simply laced or non-simply laced) Lie algebra.

Let us compute the matrix $[\Omega_S^{\alpha\beta}]$ for the above example (3.8). To start with, $[\Omega^{ij}]$ is

$$\begin{pmatrix} 4 & -1 & 0 & 0 & 0 \\ -1 & 1 & -1 & 0 & 0 \\ 0 & -1 & 4 & -1 & 0 \\ 0 & 0 & -1 & 1 & -1 \\ 0 & 0 & 0 & -1 & 4 \end{pmatrix}$$

There are three orbits. The third node lies in the first orbit, the second and fourth nodes lie in the second orbit, and the first and fifth nodes lie in the third orbit. Applying our prescription (3.12), we find that $[\Omega_S^{\alpha\beta}]$ is

$$\begin{pmatrix} 4 & -2 & 0 \\ -1 & 1 & -1 \\ 0 & -1 & 4 \end{pmatrix}$$

Similarly, we can compute the matrix $[\Omega_S^{\alpha\beta}]$ for the above example (3.10). $[\Omega^{ij}]$ is

$$\begin{pmatrix} 2 & -1 & 0 & 0 \\ -1 & 2 & -1 & 0 \\ 0 & -1 & 2 & -1 \\ 0 & 0 & -1 & 2 \end{pmatrix}$$

and $[\Omega_S^{\alpha\beta}]$ is

$$\begin{pmatrix} 1 & -1 \\ -1 & 2 \end{pmatrix}.$$

Now, we define a graph $\Sigma_{\mathfrak{T}}^S$ associated to $[\Omega_S^{\alpha\beta}]$:

- **Nodes**: the nodes of $\Sigma_{\mathfrak{T}}^S$ are in one-to-one correspondence with the set of orbits α. The value of node α is $\overset{\mathfrak{g}_i}{\Omega^{ii}}$ where i is a node of $\Sigma_{\mathfrak{T}}$ lying in the orbit α.
- **Edges**: let $\alpha \neq \beta$ and let $\Omega_S^{\alpha\beta} \geq \Omega_S^{\beta\alpha}$. Then we place $-\Omega_S^{\alpha\beta}$ number of edges between nodes α and β. If $\Omega_S^{\alpha\beta} = \Omega_S^{\beta\alpha}$, then the edges are undirected. If $\Omega_S^{\alpha\beta} > \Omega_S^{\beta\alpha}$, then all the edges are directed from α to β.
- **Self-edges**: let $l_\alpha = \Omega^{ii} - \Omega_S^{\alpha\alpha}$ where i is a node of $\Sigma_{\mathfrak{T}}$ lying in the orbit α. Then, we introduce l_α edges such that the source and target of each edge is the same node α.

$\Sigma_{\mathfrak{T}}^S$ can be understood as a folding[7] of $\Sigma_{\mathfrak{T}}$ by the action of S. Observe that the relationship between $\Sigma_{\mathfrak{T}}^S$ and $[\Omega_S^{\alpha\beta}]$ is analogous to the relationship between the Dynkin graph and Cartan matrix for a general (i.e. either simply laced or non-simply laced) Lie algebra.

For our example (3.8), the folded graph $\Sigma_{\mathfrak{T}}^S$ is

$$\begin{tikzcd} \overset{\mathfrak{so}(m)}{4} \arrow[r, "2"] & \overset{\mathfrak{sp}(n)}{1} \arrow[r, no head] & \overset{\mathfrak{so}(p)}{4} \end{tikzcd} \tag{3.13}$$

and for (3.10), the folded graph $\Sigma_{\mathfrak{T}}^S$ is

$$\begin{tikzcd} \overset{\mathfrak{su}(n)}{2} \arrow[r, no head] \arrow[loop below, no head] & \overset{\mathfrak{su}(m)}{2} \end{tikzcd} \tag{3.14}$$

We note that, starting from the data of $\Sigma_{\mathfrak{T}}^S$, we can only reconstruct S up to conjugation. But this is enough to keep track of the twist associated to S. Thus, throughout this paper, we will specify twists via folded graphs $\Sigma_{\mathfrak{T}}^S$ and will not refer to an explicit S inducing the folding.

[7]Notice that, unlike the foldings of Dynkin diagrams, the foldings of graphs $\Sigma_{\mathfrak{T}}$ can lead to self-edges.

3.4 General discrete symmetries

We now discuss twists associated to general discrete symmetries that combine the basic discrete symmetries discussed in sections 3.2 and 3.3. That is, we consider actions of the form

$$\left(\prod_i \mathcal{O}^{(q_i)}\right) S \tag{3.15}$$

where S is a permutation of the tensor multiplets and $\mathcal{O}^{(q_i)}$ is an outer automorphism of order q_i of gauge algebra $\mathfrak{g}_i$, where each $q_i \in \{1,2,3\}$ and $q_i = 1$ denotes the identity automorphism. Eq. (3.15) is a symmetry of the 6d theory $\mathfrak{T}$ only if

$$\mathfrak{g}_{S(i)} \simeq \mathfrak{g}_i \tag{3.16}$$
$$\Omega^{S(i)S(j)} = \Omega^{ij} \tag{3.17}$$

and

$$\mathcal{O}^{(q_{S(i)})} \cdot \mathcal{R}_i = \mathcal{R}_{S(i)} \tag{3.18}$$
$$\mathcal{O}^{(q_{S(i)})} \cdot \mathcal{R}_{S(i)S(j),S(i)} = \mathcal{R}_{ij,i} \tag{3.19}$$

As in section 3.3, we associate the matrix $[\Omega_S^{\alpha\beta}]$ to the twist generated by the action of (3.15).

As an example, consider the 6d SCFT

$$\begin{array}{ccccc} \mathfrak{su}(m) & & \mathfrak{su}(n) & & \mathfrak{su}(m) \\ 2 & \text{———} & 2 & \text{———} & 2 \end{array} \tag{3.20}$$

Suppose we want to perform the outer-automorphism $\mathcal{O}^{(2)}$ for the middle $\mathfrak{su}(n)$ node. Recall from the discussion around (3.3) that the outer automorphism of $\mathfrak{su}(n)$ exchanges the fundamental hypers in pairs. However, the graph in (3.20) indicates that the fundamental hypers of the middle $\mathfrak{su}(n)$ algebra are part of bifundamental representations formed by taking the tensor product with the fundamental representations of the neighboring $\mathfrak{su}(m)$ algebras. Therefore, if we want $\mathcal{O}^{(2)}$ to be a symmetry of the theory, we must permute the two neighboring $\mathfrak{su}(m)$ as well. Thus, $\mathcal{O}^{(2)}$ by itself is not a symmetry of the theory, but its combination with the permutation

$$\begin{tikzcd} \overset{\mathfrak{su}(m)}{2} \arrow[r, dash] \arrow[rr, leftrightarrow, bend right] & \overset{\mathfrak{su}(n)}{2} \arrow[r, dash] & \overset{\mathfrak{su}(m)}{2} \end{tikzcd} \tag{3.21}$$

is a symmetry of the theory. Thus, we see that in general it is not possible to decompose a general symmetry of the form (3.15) into more basic symmetries discussed earlier.

As another illustrative example, consider

$$\begin{array}{ccccc} \mathfrak{so}(2m) & & \mathfrak{sp}(n) & & \mathfrak{so}(2m) \\ 4 & \text{———} & 1 & \text{———} & 4 \end{array} \tag{3.22}$$

Consider sending the left $\mathfrak{so}(2m)$ to the right $\mathfrak{so}(2m)$ with an outer automorphism $\mathcal{O}^{(2)}$, and sending the right $\mathfrak{so}(2m)$ to the left $\mathfrak{so}(2m)$ without any outer automorphism. We can represent this action as

$$\begin{tikzcd} \overset{\mathfrak{so}(2m)}{4} \arrow[r, dash] \arrow[rr, bend right, "\mathcal{O}^{(2)}"'] & \overset{\mathfrak{sp}(n)}{1} \arrow[r, dash] & \overset{\mathfrak{so}(2m)}{4} \arrow[ll, bend right, "\mathcal{O}^{(1)}"'] \end{tikzcd} \tag{3.23}$$

This action is a symmetry of the theory and is represented as

$$\mathcal{O}_1^{(1)}\mathcal{O}_3^{(2)}S \tag{3.24}$$

in the notation of (3.15). Here we have labeled the nodes as $1, 2, 3$ from left to right and the subscript of $\mathcal{O}$ denotes the node it is acting at. We can also consider the action

$$\begin{tikzcd} \overset{\mathfrak{so}(2m)}{4} \arrow[r, dash] \arrow[rr, bend right, "\mathcal{O}^{(2)}"'] & \overset{\mathfrak{sp}(n)}{1} \arrow[r, dash] & \overset{\mathfrak{so}(2m)}{4} \arrow[ll, bend right, "\mathcal{O}^{(2)}"'] \end{tikzcd} \tag{3.25}$$

which is also a symmetry of the theory and is represented as

$$\mathcal{O}_1^{(2)}\mathcal{O}_3^{(2)}S \tag{3.26}$$

in the notation of (3.15).

Now, let $\mathfrak{g}_\alpha = \mathfrak{g}_i$ and $\Omega^{\alpha\alpha} = \Omega^{ii}$ where i is a node of $\Sigma_{\mathfrak{T}}$ lying in the orbit α of S. Then $\mathcal{O}^{(q_i)}$ can be viewed as an outer automorphism of $\mathfrak{g}_\alpha$. Let us define an outer automorphism $\mathcal{O}^{(q_\alpha)}$ of $\mathfrak{g}_\alpha$ by

$$\mathcal{O}^{(q_\alpha)} = \prod_{i\in\alpha} \mathcal{O}^{(q_i)} \tag{3.27}$$

where each $\mathcal{O}^{(q_i)}$ on the right hand side is viewed as an outer automorphism of $\mathfrak{g}_\alpha$ and the $\mathcal{O}^{(q_i)}$ for all i lying in the orbit α are then multiplied with each other to produce the outer automorphism $\mathcal{O}^{(q_\alpha)}$ of $\mathfrak{g}_\alpha$. Notice that we have chosen some ordering of various i while evaluating the product $\prod_{i\in\alpha}\mathcal{O}^{(q_i)}$. Different orderings produce different but conjugate $\mathcal{O}^{(q_\alpha)}$. Thus, we leave the ordering unspecified since we are only interested in the conjugacy class of $\mathcal{O}^{(q_\alpha)}$.

JHEP12(2020)151

$\mathfrak{g}_\alpha$ $\Omega^{\alpha\alpha}$	Comments
$\mathfrak{su}(n)^{(2)}$ 1	$n = 3, 4$
$\mathfrak{su}(n)^{(2)}$ 2	$n \geq 3$
$\mathfrak{su}(3)^{(2)}$ 3	
$\mathfrak{so}(2n)^{(2)}$ 4	$n \geq 5$
$\mathfrak{so}(8)^{(q)}$ k	$1 \leq k \leq 4$; $q = 2, 3$
$\mathfrak{so}(10)^{(2)}$ 2	
$\mathfrak{so}(\widehat{12})^{(2)}$ 2	
$\mathfrak{e}_6^{(2)}$ k	$k = 2, 4, 6$
$\mathfrak{su}(n)^{(1)}$ 2	$n \geq 1$; non-geometric

Table 8. List of all the new nodes that can appear in graphs associated to $5d$ KK theories. We also list all the possibilities where an edge starts and ends on the same node. The comment "non-geometric" for the last entry refers to the fact that there is no completely geometric description of this node. See also a node appearing in table 1. If a KK theory involves either of these two kinds of nodes, then it does not admit a conventional geometric description.

We can now associate a graph $\Sigma_{\mathfrak{T}}^{S,\{q_\alpha\}}$ to the action of (3.15). We start from the graph $\Sigma_{\mathfrak{T}}^{S}$ defined in section 3.3 and modify the values of the node α to $\begin{array}{c}\mathfrak{g}_\alpha^{(q_\alpha)} \\ \Omega_S^{\alpha\alpha}\end{array}$ where i is a node of $\Sigma_{\mathfrak{T}}$ lying in the orbit α. The graph obtained after this simple modification is what we refer to as $\Sigma_{\mathfrak{T}}^{S,\{q_\alpha\}}$.

Note that the data of $\Sigma_{\mathfrak{T}}^{S,\{q_\alpha\}}$ is enough to reconstruct the action (3.15) up to conjugation. Thus, we will capture the twist associated to the action (3.15) by the graph $\Sigma_{\mathfrak{T}}^{S,\{q_\alpha\}}$ and call the resulting $5d$ KK theory as $\mathfrak{T}^{KK}_{S,\{q_\alpha\}}$.

For the example discussed around (3.20), $\Sigma_{\mathfrak{T}}^{S,\{q_\alpha\}}$ is

$$\begin{array}{ccc} \mathfrak{su}(n)^{(2)} & & \mathfrak{su}(m)^{(1)} \\ 2 & \text{---}\, {\scriptstyle 2} \longrightarrow & 2 \end{array} \tag{3.28}$$

$\mathfrak{g}_\alpha^{(q_\alpha)}$ $\mathfrak{g}_\beta^{(q_\beta)}$ $\Omega^{\alpha\alpha}$ ——— $\Omega^{\beta\beta}$	Comments
$\mathfrak{sp}(n_\alpha)^{(1)}$ $\mathfrak{so}(n_\beta)^{(2)}$ 1 ——— k	$n_\alpha \leq n_\beta - 4 - k$; $n_\beta \leq 4n_\alpha + 14$; $2 \leq k \leq 4$
$\mathfrak{sp}(n_\alpha)^{(1)}$ $\mathfrak{so}(\widehat{12})^{(2)}$ 1 ——— 2	$n_\alpha \leq 6$
$\mathfrak{su}(n_\alpha)^{(1)}$ $\mathfrak{so}(n_\beta)^{(2)}$ 2 — $_2$ — 4	$n_\alpha \leq n_\beta - 8$; $n_\beta \leq 2n_\alpha$
$\mathfrak{su}(n_\alpha)^{(1)}$ $\mathfrak{su}(n_\beta)^{(1)}$ 2 ——— 2	$n_\alpha \leq 2n_\beta$; $n_\beta \leq n_\alpha$
$\mathfrak{sp}(0)^{(1)}$ $\mathfrak{su}(n)^{(2)}$ 1 ——— 2	$3 \leq n \leq 9, n \neq 8$
$\mathfrak{sp}(0)_\theta^{(1)}$ $\mathfrak{su}(8)^{(2)}$ 1 ——— 2	$\theta = 0, \pi$
$\mathfrak{sp}(0)^{(1)}$ $\mathfrak{su}(3)^{(2)}$ 1 ——— 3	
$\mathfrak{sp}(0)^{(1)}$ $\mathfrak{so}(8)^{(q)}$ 1 ——— k	$2 \leq k \leq 4$; $q = 2, 3$
$\mathfrak{sp}(0)^{(1)}$ $\mathfrak{so}(10)^{(2)}$ 1 ——— k	$k = 2, 4$
$\mathfrak{sp}(0)^{(1)}$ $\mathfrak{so}(2n)^{(2)}$ 1 ——— 4	$n = 6, 7$
$\mathfrak{sp}(0)^{(1)}$ $\mathfrak{so}(\widehat{12})^{(2)}$ 1 ——— 2	
$\mathfrak{sp}(0)^{(1)}$ $\mathfrak{e}_6^{(2)}$ 1 ——— k	$k = 2, 4, 6$
$\mathfrak{su}(n)^{(1)}$ $\mathfrak{su}(1)^{(1)}$ 2 ——— 2	$n = 1, 2$

Table 9. List of all the new undirected edges that can appear in graphs characterizing $5d$ KK theories.

JHEP12(2020)151

$\mathfrak{g}_\alpha^{(q_\alpha)} \quad \mathfrak{g}_\beta^{(q_\beta)}$ $\Omega^{\alpha\alpha} \xrightarrow{e} \Omega^{\beta\beta}$	Comments
$\mathfrak{sp}(n_\alpha)^{(1)} \quad \mathfrak{so}(n_\beta)^{(q_\beta)}$ $1 \xrightarrow{2} k$	$n_\alpha \leq n_\beta - 4 - k$; $n_\beta \leq 2n_\alpha + 10 - 2q_\beta$; $k = 3, 4$; $q_\beta = 1, 2$
$\mathfrak{sp}(n_\alpha)^{(1)} \quad \mathfrak{so}(7)^{(1)}$ $1 \overset{2}{\dashrightarrow} 3$	$n_\alpha = 1, 2$
$\mathfrak{sp}(1)^{(1)} \quad \mathfrak{g}_2^{(1)}$ $1 \xrightarrow{2} 3$	
$\mathfrak{sp}(n_\alpha)^{(1)} \quad \mathfrak{so}(n_\beta)^{(q_\beta)}$ $1 \xrightarrow{3} 4$	$n_\alpha \leq n_\beta - 8$; $3n_\beta \leq 4n_\alpha + 17 - q_\beta$; $q_\beta = 1, 2$
$\mathfrak{su}(n_\alpha)^{(1)} \quad \mathfrak{su}(n_\beta)^{(1)}$ $2 \xrightarrow{e} 2$	$n_\alpha \leq 2n_\beta$; $en_\beta \leq 2n_\alpha$; $e = 2, 3$
$\mathfrak{su}(n_\alpha)^{(2)} \quad \mathfrak{su}(n_\beta)^{(1)}$ $2 \xrightarrow{2} 2$	$n_\alpha \leq 2n_\beta$; $n_\beta \leq n_\alpha$
$\mathfrak{g}_2^{(1)} \quad \mathfrak{su}(2)^{(1)}$ $2 \xrightarrow{e} 2$	$e = 2, 3$
$\mathfrak{so}(7)^{(1)} \quad \mathfrak{su}(2)^{(1)}$ $2 \overset{e}{\dashrightarrow} 2$	$e = 2, 3$
$\mathfrak{so}(7)^{(1)} \quad \mathfrak{su}(2)^{(1)}$ $3 \overset{2}{\dashrightarrow} 2$	
$\mathfrak{so}(7)^{(1)} \quad \mathfrak{sp}(1)^{(1)}$ $3 \overset{2}{\dashrightarrow} 1$	
$\mathfrak{so}(8)^{(2)} \quad \mathfrak{sp}(1)^{(1)}$ $3 \text{ - - - } 2 \longrightarrow 1$	
$\mathfrak{so}(n_\alpha)^{(q_\alpha)} \quad \mathfrak{sp}(n_\beta)^{(1)}$ $k \xrightarrow{2} 1$	$n_\alpha \leq 4n_\beta + 16$; $2n_\beta \leq n_\alpha - 4 - k$; $k = 3, 4$; $q_\alpha = 1, 2$
$\mathfrak{so}(n_\alpha)^{(q_\alpha)} \quad \mathfrak{sp}(n_\beta)^{(1)}$ $4 \xrightarrow{3} 1$	$n_\alpha \leq 4n_\beta + 16$; $3n_\beta \leq n_\alpha - 8$; $q_\alpha = 1, 2$

Table 10. List of all the possible directed edges between two gauge-theoretic nodes that can appear in graphs characterizing $5d$ KK theories. An arrow with e in the middle of it denotes e edges directed in the direction of arrow. Solid edges arise from foldings of solid edges and dashed edges arise from foldings of dashed edges. A partially dashed and partially solid edge with 2 in the middle of it arises from a folding together of a dashed edge and a solid edge.

$\begin{array}{ccc} \mathfrak{g}_\alpha^{(q_\alpha)} & & \mathfrak{g}_\beta^{(q_\beta)} \\ \Omega^{\alpha\alpha} & \overset{e}{\longrightarrow} & \Omega^{\beta\beta} \end{array}$	Comments
$\begin{array}{ccc} \mathfrak{sp}(0)^{(1)} & & \mathfrak{su}(3)^{(q)} \\ 1 & \overset{2}{\longrightarrow} & 3 \end{array}$	$q = 1, 2$
$\begin{array}{ccc} \mathfrak{sp}(0)^{(1)} & & \mathfrak{so}(7)^{(1)} \\ 1 & \overset{2}{\longrightarrow} & 3 \end{array}$	
$\begin{array}{ccc} \mathfrak{sp}(0)^{(1)} & & \mathfrak{so}(8)^{(1)} \\ 1 & \overset{2}{\longrightarrow} & k \end{array}$	$k = 3, 4$
$\begin{array}{ccc} \mathfrak{sp}(0)^{(1)} & & \mathfrak{g}_2^{(1)} \\ 1 & \overset{2}{\longrightarrow} & 3 \end{array}$	
$\begin{array}{ccc} \mathfrak{su}(3)^{(q)} & & \mathfrak{sp}(0)^{(1)} \\ 3 & \overset{2}{\longrightarrow} & 1 \end{array}$	$q = 1, 2$
$\begin{array}{ccc} \mathfrak{so}(n)^{(q)} & & \mathfrak{sp}(0)^{(1)} \\ k & \overset{e}{\longrightarrow} & 1 \end{array}$	$n \leq 16$; $2 \leq e \leq k-1$; $k = 3, 4$; $q = 1, 2$
$\begin{array}{ccc} \mathfrak{g}_2^{(1)} & & \mathfrak{sp}(0)^{(1)} \\ 3 & \overset{2}{\longrightarrow} & 1 \end{array}$	
$\begin{array}{ccc} \mathfrak{f}_4^{(1)} & & \mathfrak{sp}(0)^{(1)} \\ k & \overset{e}{\longrightarrow} & 1 \end{array}$	$2 \leq e \leq k-1$; $3 \leq k \leq 5$
$\begin{array}{ccc} \mathfrak{e}_6^{(q)} & & \mathfrak{sp}(0)^{(1)} \\ k & \overset{e}{\longrightarrow} & 1 \end{array}$	$2 \leq e \leq k-1$; $3 \leq k \leq 6$; $q = 1, 2$
$\begin{array}{ccc} \mathfrak{e}_7^{(1)} & & \mathfrak{sp}(0)^{(1)} \\ k & \overset{e}{\longrightarrow} & 1 \end{array}$	$2 \leq e \leq k-1$; $3 \leq k \leq 8$
$\begin{array}{ccc} \mathfrak{e}_8^{(1)} & & \mathfrak{sp}(0)^{(1)} \\ 12 & \overset{e}{\longrightarrow} & 1 \end{array}$	$2 \leq e \leq 11$
$\begin{array}{ccc} \mathfrak{su}(n)^{(1)} & & \mathfrak{su}(1)^{(1)} \\ 2 & \overset{e}{\longrightarrow} & 2 \end{array}$	$n = 1, 2$; $e = 2, 3$

Table 11. List of all the possible directed edges involving at least one non-gauge-theoretic node that can appear in graphs characterizing $5d$ KK theories.

Similarly, for (3.23), $\Sigma_{\mathfrak{T}}^{S,\{q_\alpha\}}$ is

$$\begin{array}{ccc} \mathfrak{sp}(n)^{(1)} & & \mathfrak{so}(2m)^{(2)} \\ 1 & \overset{2}{\longrightarrow} & 4 \end{array} \tag{3.29}$$

However, for (3.25), $\Sigma_{\mathfrak{T}}^{S,\{q_\alpha\}}$ is

$$\begin{array}{ccc} \mathfrak{sp}(n)^{(1)} & & \mathfrak{so}(2m)^{(1)} \\ 1 & \overset{2}{\longrightarrow} & 4 \end{array} \tag{3.30}$$

$\overset{\mathfrak{g}_i^{(q_i)}}{\Omega^{ii}} - \overset{\mathfrak{sp}(0)^{(1)}}{1} - \overset{\mathfrak{g}_k^{(q_k)}}{\Omega^{kk}}$	Comments
$\overset{\mathfrak{su}(2)^{(1)}}{2} - \overset{\mathfrak{sp}(0)^{(1)}}{1} - \overset{\mathfrak{g}^{(q)}}{k}$	$k \geq 3$; $\mathfrak{g}^{(q)} = \mathfrak{e}_6^{(2)}, \mathfrak{so}(8,10)^{(2)}, \mathfrak{so}(8)^{(3)}$
$\overset{\mathfrak{su}(3)^{(1)}}{k} - \overset{\mathfrak{sp}(0)^{(1)}}{1} - \overset{\mathfrak{g}^{(q)}}{l}$	$k, l \geq 3$; $k + l \geq 5$; $\mathfrak{g}^{(q)} = \mathfrak{so}(8)^{(2)}, \mathfrak{so}(8)^{(3)}, \mathfrak{su}(n \leq 4)^{(2)}$
$\overset{\mathfrak{su}(3)^{(2)}}{k} - \overset{\mathfrak{sp}(0)^{(1)}}{1} - \overset{\mathfrak{g}^{(1)}}{l}$	$k, l \geq 2$; $k + l \geq 5$; $\mathfrak{g} = \mathfrak{f}_4, \mathfrak{g}_2, \mathfrak{so}(n \leq 9), \mathfrak{su}(4)$
$\overset{\mathfrak{su}(3)^{(2)}}{k} - \overset{\mathfrak{sp}(0)^{(1)}}{1} - \overset{\mathfrak{g}^{(2)}}{l}$	$k, l \geq 2$; $k + l \geq 5$; $\mathfrak{g} = \mathfrak{e}_6, \mathfrak{so}(8,10), \mathfrak{su}(n \leq 6)$
$\overset{\mathfrak{su}(4)^{(2)}}{2} - \overset{\mathfrak{sp}(0)^{(1)}}{1} - \overset{\mathfrak{g}^{(q)}}{k}$	$k = 3, 4$; $\mathfrak{g}^{(q)} = \mathfrak{g}_2^{(1)}, \mathfrak{so}(n \leq 9)^{(1)}, \mathfrak{so}(8,10)^{(2)}$
$\overset{\mathfrak{so}(8)^{(2)}}{k} - \overset{\mathfrak{sp}(0)^{(1)}}{1} - \overset{\mathfrak{g}^{(q)}}{l}$	$k, l \geq 2$; $k + l \geq 5$; $\mathfrak{g}^{(q)} = \mathfrak{g}_2^{(1)}, \mathfrak{su}(4)^{(1)}, \mathfrak{so}(7)^{(1)}, \mathfrak{so}(8)^{(2)}$
$\overset{\mathfrak{so}(8)^{(3)}}{k} - \overset{\mathfrak{sp}(0)^{(1)}}{1} - \overset{\mathfrak{g}^{(q)}}{l}$	$k, l \geq 2$; $k + l \geq 5$; $\mathfrak{g}^{(q)} = \mathfrak{su}(3)^{(2)}, \mathfrak{so}(8)^{(3)}$

Table 12. List of all the new possibilities for multiple neighbors of $\mathfrak{sp}(0)^{(1)}$ connected to it by undirected edges.

which is the same as $\Sigma_{\mathfrak{T}}^{S,\{q_\alpha\}}$ for the symmetry

$$\begin{tikzcd} \overset{\mathfrak{so}(2m)}{4} \arrow[r, dash] \arrow[rr, <->, bend right] & \overset{\mathfrak{sp}(n)}{1} \arrow[r, dash] & \overset{\mathfrak{so}(2m)}{4} \end{tikzcd} \tag{3.31}$$

which does not involve any outer automorphisms. Thus, according to our claim, (3.25) and 3.31) must be in the same conjugacy class. Let us demonstrate it explicitly. Conjugating (3.26) by $\mathcal{O}_1^{(2)}$, we get

$$\mathcal{O}_1^{(2)}(\mathcal{O}_1^{(2)}\mathcal{O}_3^{(2)}S)\mathcal{O}_1^{(2)} \tag{3.32}$$
$$= \mathcal{O}_3^{(2)}S\mathcal{O}_1^{(2)} \tag{3.33}$$
$$= \mathcal{O}_3^{(2)}\mathcal{O}_3^{(2)}S \tag{3.34}$$
$$= S \tag{3.35}$$

Thus, the KK theories corresponding to (3.25) and (3.31) must be the same, and we denote it by the folded graph (3.30).

In a similar fashion, by studying various $6d$ SCFTs and their symmetries, we can isolate all the possible ingredients that can appear in graphs of the form $\Sigma_{\mathfrak{T}}^{S,\{q_\alpha\}}$ associated to $5d$ KK theories:

- First of all, the nodes listed in tables 1 and 2 are all allowed. We simply write each gauge algebra $\mathfrak{g}$ appearing in table 1 as $\mathfrak{g}^{(1)}$.

- Similarly, the edges appearing in tables 3, 4 and 5 are all allowed with each gauge algebra being written as $\mathfrak{g}^{(1)}$.

- The new nodes that can appear in graphs associated to $5d$ KK theories but do not appear in graphs associated to $6d$ SCFTs are listed in table 8.

- The new undirected edges appearing for graphs associated to $5d$ KK theories are listed in table 9.

  The configuration

$$\begin{array}{ccc} \mathfrak{sp}(n_\alpha)^{(1)} & & \mathfrak{so}(n_\beta)^{(2)} \\ 1 & \text{------} & k \end{array} \tag{3.36}$$

  for $n_\beta = 4n_\alpha + 16$ and $n_\alpha \geq 0$ is not allowed since the choice of theta angle for $\mathfrak{sp}(n_\alpha)$ in the associated $6d$ theory is correlated to the choice of a spinor representation of the neighboring $\mathfrak{so}(4n_\alpha + 16)$. Thus, the outer automorphism $\mathcal{O}^{(2)}$ of $\mathfrak{so}(4n_\alpha + 16)$ is not a symmetry of the theory.[8]

- The directed edges between two nodes both carrying a non-trivial gauge algebra are listed in table 10.

  The configuration

$$\begin{array}{ccc} \mathfrak{sp}(n_\alpha)^{(1)} & & \mathfrak{so}(n_\beta)^{(2)} \\ 1 & \text{---}\,{\scriptstyle 2}\,\longrightarrow & k \end{array} \tag{3.37}$$

  with $n_\beta = 2n_\alpha + 8$ is not allowed. This configuration descends from (3.23) with $n = n_\alpha$ and $m = n_\alpha + 4$. Recall that the choice of theta angle of the gauge algebra $\mathfrak{sp}(n_\alpha)$ is equivalent to the choice of a spinor representation of its flavor symmetry algebra $\mathfrak{so}(4n_\alpha + 16)$. But $\mathfrak{so}(2n_\alpha + 8) \oplus \mathfrak{so}(2n_\alpha + 8)$ subalgebra of $\mathfrak{so}(4n_\alpha + 16)$ is gauged. The S of $\mathfrak{so}(4n_\alpha + 16)$ decomposes as $(\mathsf{S} \otimes \mathsf{C}) \oplus (\mathsf{C} \otimes \mathsf{S})$ of $\mathfrak{so}(2n_\alpha + 8) \oplus \mathfrak{so}(2n_\alpha + 8)$ which is sent to $(\mathsf{C} \otimes \mathsf{C}) \oplus (\mathsf{S} \otimes \mathsf{S})$ of $\mathfrak{so}(2n_\alpha + 8) \oplus \mathfrak{so}(2n_\alpha + 8)$ by the action depicted in (3.23). Thus, (3.23) is not a symmetry when $n = n_\alpha$ and $m = n_\alpha + 4$.

  For similar reasons, the configuration

$$\begin{array}{ccc} \mathfrak{sp}(n_\alpha)^{(1)} & & \mathfrak{so}(n_\beta)^{(2)} \\ 1 & \text{---}\,{\scriptstyle 3}\,\longrightarrow & k \end{array} \tag{3.38}$$

  with $3n_\beta = 4n_\alpha + 16$ is not allowed.

  The KK theory

$$\begin{array}{ccc} \mathfrak{so}(8)^{(2)} & & \mathfrak{sp}(1)^{(1)} \\ 3 & \text{- - -}\,{\scriptstyle 2}\,\longrightarrow & 1 \end{array} \tag{3.39}$$

[8] The authors thank Gabi Zafrir for a discussion on this point.

arises from the $6d$ SCFT

$$\begin{array}{ccccc} \mathfrak{sp}(1) & & \mathfrak{so}(8) & & \mathfrak{sp}(1) \\ 1 & \text{--------} & 3 & \text{———} & 1 \end{array} \tag{3.40}$$

by performing the outer automorphism $\mathcal{O}^{(2)}$ of $\mathfrak{so}(8)$ which permutes F and S, and hence induces the exchange of the two $\mathfrak{sp}(1)$.

- Other kinds of directed edges are listed in table 11.

  Due to similar reasons as explained above, the configuration

$$\begin{array}{ccc} \mathfrak{sp}(0)^{(1)} & & \mathfrak{so}(8)^{(2)} \\ 1 & \overset{}{\text{——}}\,{}_2\!\longrightarrow & k \end{array} \tag{3.41}$$

  is not allowed.

- There are various kinds of possibilities for multiple neighbors of $\mathfrak{sp}(0)^{(1)}$. All of the possibilities listed in table 6 are allowed with the substitution of $\mathfrak{g}^{(1)}$ in place of every trivial or non-trivial algebra $\mathfrak{g}$ appearing in that table. New possibilities involving undirected edges are listed in table 12. These are obtained by performing outer automorphisms on the possibilities listed in table 6. However, some of the outer automorphisms do not yield a symmetry of the theory.

  For example, consider the decomposition of the adjoint $\mathbf{248}$ of $\mathfrak{e}_8$ under $\mathfrak{su}(3) \oplus \mathfrak{e}_6$

$$\mathbf{248} \to (\mathbf{8}, \mathbf{1}) \oplus (\mathbf{1}, \mathbf{78}) \oplus (\mathbf{3}, \mathbf{27}) \oplus (\mathbf{3}', \mathbf{27}') \tag{3.42}$$

  It can be seen from the above decomposition that neither the outer automorphism of $\mathfrak{su}(3)$ nor the outer automorphism of $\mathfrak{e}_6$ is a symmetry of the decomposition, implying that neither the configuration

$$\begin{array}{ccccc} \mathfrak{su}(3)^{(2)} & & \mathfrak{sp}(0)^{(1)} & & \mathfrak{e}_6^{(1)} \\ k & \text{———} & 1 & \text{———} & l \end{array} \tag{3.43}$$

  nor the configuration

$$\begin{array}{ccccc} \mathfrak{su}(3)^{(1)} & & \mathfrak{sp}(0)^{(1)} & & \mathfrak{e}_6^{(2)} \\ k & \text{———} & 1 & \text{———} & l \end{array} \tag{3.44}$$

  is an allowed KK theory. However, the configuration

$$\begin{array}{ccccc} \mathfrak{su}(3)^{(2)} & & \mathfrak{sp}(0)^{(1)} & & \mathfrak{e}_6^{(2)} \\ k & \text{———} & 1 & \text{———} & l \end{array} \tag{3.45}$$

  is an allowed KK theory since the combined outer automorphism of $\mathfrak{su}(3)$ and $\mathfrak{e}_6$ is indeed a symmetry of the decomposition (3.42). Correspondingly, neither (3.43) nor (3.44) appears in the table 12, while (3.45) does appear in table 12.

JHEP12(2020)151

Similarly, the reader can check that the following configurations do not give rise to allowed KK theories:

$$\begin{array}{ccccc} \mathfrak{so}(8)^{(2)} & & \mathfrak{sp}(0)^{(1)} & & \mathfrak{so}(8)^{(q)} \\ k & \text{———} & 1 & \text{———} & l \end{array} \tag{3.46}$$

for $q = 1, 3$. However, $q = 2$ is allowed.

$$\begin{array}{ccccc} \mathfrak{su}(4)^{(p)} & & \mathfrak{sp}(0)^{(1)} & & \mathfrak{so}(10)^{(q)} \\ k & \text{———} & 1 & \text{———} & l \end{array} \tag{3.47}$$

for (p, q) equal to $(1, 2)$ and $(2, 1)$. However, $(1, 1)$ and $(2, 2)$ are allowed.

$$\begin{array}{ccccc} \mathfrak{su}(3)^{(p)} & & \mathfrak{sp}(0)^{(1)} & & \mathfrak{so}(10)^{(q)} \\ k & \text{———} & 1 & \text{———} & l \end{array} \tag{3.48}$$

for (p, q) equal to $(1, 2)$ and $(2, 1)$.

$$\begin{array}{ccccc} \mathfrak{su}(3)^{(p)} & & \mathfrak{sp}(0)^{(1)} & & \mathfrak{su}(5,6)^{(q)} \\ k & \text{———} & 1 & \text{———} & l \end{array} \tag{3.49}$$

for (p, q) equal to $(1, 2)$ and $(2, 1)$.

$$\begin{array}{ccccc} \mathfrak{su}(2)^{(1)} & & \mathfrak{sp}(0)^{(1)} & & \mathfrak{so}(12)^{(2)} \\ k & \text{———} & 1 & \text{———} & l \end{array} \tag{3.50}$$

$$\begin{array}{ccccc} \mathfrak{su}(4)^{(p)} & & \mathfrak{sp}(0)^{(1)} & & \mathfrak{so}(8)^{(3)} \\ k & \text{———} & 1 & \text{———} & l \end{array} \tag{3.51}$$

for $p = 1, 2$.

$$\begin{array}{ccccc} \mathfrak{so}(7)^{(1)} & & \mathfrak{sp}(0)^{(1)} & & \mathfrak{so}(8)^{(3)} \\ k & \text{———} & 1 & \text{———} & l \end{array} \tag{3.52}$$

- It is not possible for $\mathfrak{sp}(0)^{(1)}$ to have multiple neighbors when one of the neighbors is connected to it by a directed edge going outwards from $\mathfrak{sp}(0)^{(1)}$. This is simply a consequence of the fact that $\mathfrak{sp}(0)$ cannot have three neighbors in the context of $6d$ SCFTs.

  However, it is possible for $\mathfrak{sp}(0)^{(1)}$ to have multiple neighbors with some neighbors having directed edges pointing inwards towards $\mathfrak{sp}(0)^{(1)}$. These possibilities can be simply obtained by replacing one or more undirected edges appearing in tables 6 and 12 by suitable directed edges (pointing inwards) taken from table 11. One has to ensure that the matrix associated to the resulting configuration is positive definite, which disallows some substitutions. We do not pursue a full classification of such cases since they won't be useful in this paper. Later on, in section 5.4.4, we will provide a general prescription to obtain the gluing rules associated to such directed edges from the gluing rules associated to their "parent" undirected edges.

JHEP12(2020)151

$\mathfrak{g}$	$\mathcal{O}^{(q)}$	$\mathfrak{h}$	$\mathcal{R}_{\mathfrak{g}} \to \mathcal{R}_{\mathfrak{h}}$
$\mathfrak{su}(2m)$	$\mathcal{O}^{(2)}$	$\mathfrak{sp}(m)$	$\mathsf{F} \to \mathsf{F}$, $\bar{\mathsf{F}} \to \mathsf{F}$, $\Lambda^2 \to \Lambda^2 \oplus 1$
$\mathfrak{su}(2m+1)$	$\mathcal{O}^{(2)}$	$\mathfrak{sp}(m)$	$\mathsf{F} \to \mathsf{F} \oplus 1$, $\bar{\mathsf{F}} \to \mathsf{F} \oplus 1$
$\mathfrak{so}(2m)$	$\mathcal{O}^{(2)}$	$\mathfrak{so}(2m-1)$	$\mathsf{F} \to \mathsf{F} \oplus 1$, $\mathsf{S} \to \mathsf{S}$, $\mathsf{C} \to \mathsf{S}$
$\mathfrak{e}_6$	$\mathcal{O}^{(2)}$	$\mathfrak{f}_4$	$\mathsf{F} \to \mathsf{F} \oplus 1$, $\bar{\mathsf{F}} \to \mathsf{F} \oplus 1$
$\mathfrak{so}(8)$	$\mathcal{O}^{(3)}$	$\mathfrak{g}_2$	$\mathsf{F} \to \mathsf{F} \oplus 1$, $\mathsf{S} \to \mathsf{F} \oplus 1$, $\mathsf{C} \to \mathsf{F} \oplus 1$

Table 13. The table displays the invariant algebra $\mathfrak{h}$ when $\mathfrak{g}$ is quotiented by $\mathcal{O}^{(q)}$. An irrep $\mathcal{R}_{\mathfrak{g}}$ of $\mathfrak{g}$ decomposes to an irrep $\mathcal{R}_{\mathfrak{h}}$ of $\mathfrak{h}$ and this decomposition is displayed (for representations relevant in this paper) in the column labeled $\mathcal{R}_{\mathfrak{g}} \to \mathcal{R}_{\mathfrak{h}}$. 1 denotes the singlet representation.

4 Prepotential for 5d KK theories

The goal of this section is to propose a formula for the prepotential of a 5d KK theory $\mathfrak{T}^{KK}_{S,\{q_\alpha\}}$ starting from the tensor branch description of the corresponding 6d SCFT $\mathfrak{T}$.

4.1 Prepotential

Compactify a 6d SCFT $\mathfrak{T}$ on a circle with a twist $S,\{q_\alpha\}$ around the circle. Let us analyze the low energy theory. Every node α in $\Sigma_{\mathfrak{T}}^{S,\{q_\alpha\}}$ gives rise to a low energy 5d gauge algebra $\mathfrak{h}_\alpha = \mathfrak{g}_\alpha/\mathcal{O}^{(q_\alpha)}$ which is the subalgebra of $\mathfrak{g}_\alpha$ left invariant by the action of outer automorphism $\mathcal{O}^{(q_\alpha)}$. In this paper, our choice of outer automorphisms is such that the invariant subalgebras are those listed in table 13. For each node α, we obtain an additional $\mathfrak{u}(1)_\alpha$ gauge algebra in the low energy 5d theory coming from the reduction of a tensor multiplet B_i on the circle where i lies in the orbit α.

Now we determine the spectrum of hypermultiplets charged under $\oplus_\alpha \mathfrak{h}_\alpha$ under the low energy 5d theory. First of all, for every node i in 6d theory, we define $\mathcal{T}_i = \oplus_j \mathcal{R}_{ij,i}^{\oplus \dim(\mathcal{R}_{ij,j})}$. Recall that $\mathcal{T}_i \subseteq \mathcal{R}_i$ and hence the 6d theory contains hypermultiplets charged under representation $\mathcal{S}_i$ of $\mathfrak{g}_i$ where $\mathcal{S}_i$ is defined such that $\mathcal{S}_i \oplus \mathcal{T}_i = \mathcal{R}_i$. $\mathcal{S}_i$ is the representation formed by those hypers that are only charged $\mathfrak{g}_i$ and not under any other gauge algebra $\mathfrak{g}_j$ with $j \neq i$.

As detailed in table 13, irreducible representations $\mathcal{R}_{\mathfrak{g}_\alpha}$ of $\mathfrak{g}_\alpha$ can be viewed as irreducible representations of $\mathcal{R}_{\mathfrak{h}_\alpha}$. We can thus view hypers transforming in representation $\mathcal{S}_i$ of $\mathfrak{g}_i$ as transforming in a representation of $\mathfrak{h}_\alpha$. Let us denote this representation of $\mathfrak{h}_\alpha$ by $\tilde{\mathcal{S}}_\alpha$. The outer automorphism $\mathcal{O}^{(q_\alpha)}$ then permutes constituent irreps inside $\tilde{\mathcal{S}}_\alpha$ and thus acts on $\tilde{\mathcal{S}}_\alpha$ as an automorphism. The low energy 5d theory then contains hypers transforming in the representation

$$\mathcal{S}_\alpha := \tilde{\mathcal{S}}_\alpha/\mathcal{O}^{(q_\alpha)} \tag{4.1}$$

These hypers are only charged under $\mathfrak{h}_\alpha$ and not under any other gauge algebra $\mathfrak{h}_\beta$ with $\beta \neq \alpha$.

Now consider other hypermultiplets that are charged under multiple gauge algebras in the 6d theory. These descend to hypermultiplets charged under multiple gauge algebras in the low energy $5d$ theory plus some hypers only charged under the individual algebras. Consider the mixed representation $\mathcal{R}_{ij} = \mathcal{R}_{ij,i} \otimes \mathcal{R}_{ij,j}$ of $\mathfrak{g}_i \oplus \mathfrak{g}_j$ in the $6d$ theory. Let i and j lie in orbits α and β respectively. Let $\mathcal{R}_{ij,i}$ decompose as $\mathcal{R}_{\alpha\beta,\alpha} \oplus n_{\alpha\beta,\alpha}\mathbf{1}$ when viewed as a representation of $\mathfrak{h}_\alpha$, where $\mathcal{R}_{\alpha\beta,\alpha}$ is the full subrepresentation that is charged non-trivially under $\mathfrak{h}_\alpha$. Similarly, let $\mathcal{R}_{ij,j}$ decompose as $\mathcal{R}_{\alpha\beta,\beta} \oplus n_{\alpha\beta,\beta}\mathbf{1}$ when viewed as a representation of $\mathfrak{h}_\beta$, where $\mathcal{R}_{\alpha\beta,\beta}$ is the full subrepresentation that is charged non-trivially under $\mathfrak{h}_\beta$. Then, under the twist, $\mathcal{R}_{ij}$ descends to a mixed representation $\mathcal{R}_{\alpha\beta}$ of $\mathfrak{h}_\alpha \oplus \mathfrak{h}_\beta$ plus representations $\mathcal{S}_{\alpha\beta,\alpha}$ and $\mathcal{S}_{\alpha\beta,\beta}$ of $\mathfrak{h}_\alpha$ and $\mathfrak{h}_\beta$ respectively. Here $\mathcal{R}_{\alpha\beta} = \mathcal{R}_{\alpha\beta,\alpha} \otimes \mathcal{R}_{\alpha\beta,\beta}$, $\mathsf{S}_{\alpha\beta,\alpha} = n_{\alpha\beta,\beta}\mathcal{R}_{\alpha\beta,\alpha}$, and $\mathsf{S}_{\alpha\beta,\beta} = n_{\alpha\beta,\alpha}\mathcal{R}_{\alpha\beta,\beta}$.

In addition to the above, we also obtain hypers in the symmetric product $\mathrm{Sym}^2(\mathcal{R}_{ij,i})$ for all $j \neq i$ such that both j and i are in the same orbit α. Thus, the full representation $\mathcal{R}_\alpha$ formed by hypers under $\mathfrak{h}_\alpha$ is

$$\mathcal{R}_\alpha = \oplus_{j\in\alpha}\mathrm{Sym}^2(\mathcal{R}_{ij,i})|_{\mathfrak{h}_\alpha} \oplus \mathcal{S}_\alpha \oplus_\beta \left(\mathcal{R}_{\alpha\beta,\alpha}^{\oplus\dim(\mathcal{R}_{\alpha\beta,\beta})} \oplus \mathcal{S}_{\alpha\beta,\alpha}\right) \tag{4.2}$$

where $\mathrm{Sym}^2(\mathcal{R}_{ij,i})|_{\mathfrak{h}_\alpha}$ means that we view $\mathrm{Sym}^2(\mathcal{R}_{ij,i})$ as a representation of $\mathfrak{h}_\alpha$. Note that in the above expression, i is a fixed node in the orbit α, j cannot equal i, and β cannot equal α. There are no hypers charged under $\mathfrak{u}(1)_\alpha$. Just as the representations $\mathcal{R}_i$ and $\mathcal{R}_{ij}$ for all i and j determine the full matter content for $6d$ SCFTs, the representations $\mathcal{R}_\alpha$ and $\mathcal{R}_{\alpha\beta}$ for all α and β determine the full matter content for $5d$ KK theories.

As an example, let us determine the low energy $5d$ theory for (3.23). The $5d$ gauge algebra is $\mathfrak{h} = \mathfrak{sp}(n) \oplus \mathfrak{so}(2m-1)$. A half-bifundamental of $\mathfrak{sp}(n) \oplus \mathfrak{so}(2m)$ decomposes as a half-bifundamental of $\mathfrak{sp}(n) \oplus \mathfrak{so}(2m-1)$ plus a half-fundamental of $\mathfrak{sp}(n)$. Thus, the two half-bifundamentals between the $\mathfrak{sp}(n)$ and the two $\mathfrak{so}(2m)$ in (3.23) descend to a half-bifundamental of $\mathfrak{h}$ plus a half-fundamental of $\mathfrak{sp}(n)$ in the $5d$ theory. There are $2m-8-n$ extra fundamentals of the left $\mathfrak{so}(2m)$ in (3.23) not charged under any other gauge algebra. Similarly, there are $2m-8-n$ extra fundamentals of the right $\mathfrak{so}(2m)$ in (3.23) not charged under any other gauge algebra. These two sets of fundamentals descend to $2m-8-n$ fundamentals of $\mathfrak{so}(2m-1)$ in the $5d$ theory. We also obtain $2m-8-n$ singlets that decouple and so we ignore them. Finally, there are $2n+8-2m$ extra fundamentals of $\mathfrak{sp}(n)$ in (3.23) not charged under any other gauge algebra. These hypers descend to $2n+8-2m$ extra fundamentals of $\mathfrak{sp}(n)$ in the low energy $5d$ theory that are not charged under $\mathfrak{so}(2m-1)$. To recap, the low energy $5d$ theory is an $\mathfrak{sp}(n)\oplus\mathfrak{so}(2m-1)$ gauge theory with a half-bifundamental plus $4n+17-4m$ half-fundamentals of $\mathfrak{sp}(n)$ plus $2m-8-n$ fundamentals of $\mathfrak{so}(2m-1)$.

As another example, let us determine the low energy $5d$ theory for (3.14). The two $\mathfrak{su}(m)$ get identified to a single $\mathfrak{su}(m)$ algebra. Similarly, the two $\mathfrak{su}(n)$ get identified to a single $\mathfrak{su}(n)$ algebra. Thus the $5d$ gauge algebra is $\mathfrak{h} = \mathfrak{su}(n) \oplus \mathfrak{su}(m)$. The bifundamentals of $\mathfrak{su}(m)\oplus\mathfrak{su}(n)$ descend to a single bifundamental of $\mathfrak{h}$. The bifundamental of $\mathfrak{su}(n)\oplus\mathfrak{su}(n)$ descends to S^2 of $\mathfrak{su}(n)$. Furthermore, we obtain $n-m$ extra fundamentals of $\mathfrak{su}(n)$ and $2m-n$ extra fundamentals of $\mathfrak{su}(m)$. Thus, the low energy $5d$ theory is an $\mathfrak{su}(n) \oplus \mathfrak{su}(m)$ gauge theory with a bifundamental plus $(2m-n)\mathsf{F}$ of $\mathfrak{su}(m)$ plus $(n-m)\mathsf{F} \oplus \mathsf{S}^2$ of $\mathfrak{su}(n)$.

The low energy $5d$ gauge theory also contains tree-level Chern-Simons terms that arise from the reduction of (2.1) on the circle. These can be written as

$$\Omega_S^{\alpha\beta} A_{0,\alpha} \wedge \mathrm{tr}(F_\beta^2) \tag{4.3}$$

where $A_{0,\alpha}$ is the gauge field corresponding to the $\mathfrak{u}(1)_\alpha$ obtained by reducing B_α on the circle and F_β is the gauge field strength for $\mathfrak{h}_\beta$. In writing (4.3), we have used the fact that the index of $\mathfrak{h}_\beta$ in $\mathfrak{g}_\beta$ is one which is true for our choice of $\mathfrak{h}$ listed in table 7. Eq. (4.3) contributes the following tree-level term to the prepotential

$$6\mathcal{F}^{\text{tree}}_{S,\{q_\alpha\}} = 6\sum_{\alpha,\beta} \frac{1}{2}\Omega_S^{\alpha\beta}\phi_{0,\alpha}\left(K_\beta^{ab}\phi_{a,\beta}\phi_{b,\beta}\right) \tag{4.4}$$

where $\phi_{0,\alpha}$ is the scalar living in the vector multiplet corresponding to $\mathfrak{u}(1)_\alpha$ and $\phi_{a,\beta}$ are scalars living in the vector multiplets corresponding to $\mathfrak{u}(1)_{a,\beta}$ which parametrize the Cartan of $\mathfrak{h}_\beta$. Here K_β^{ab} is the Killing form on $\mathfrak{h}_\beta$ normalized such that its diagonal entries are minimum positive integers while keeping all the other entries integer valued.

Let $\mathfrak{h} = \oplus_\alpha \mathfrak{h}_\alpha$ be the total gauge algebra visible at low energies. The low energy hypermultiplets form some representation $\mathcal{R}$ of $\mathfrak{h}$ which decomposes into irreducible representations of $\mathfrak{h}$ as $\mathcal{R} = \oplus_f \mathcal{R}_f$. Note that it is possible to have $f \neq f'$ such that $\mathcal{R}_f = \mathcal{R}_{f'}$. In other words, the index f distinguishes multiple copies of representation $\mathcal{R}_f$. Now we can add the one-loop contribution to the prepotential (4.4) to obtain

$$6\mathcal{F}_{S,\{q_\alpha\}} = \sum_{\alpha,\beta} 3\Omega_S^{\alpha\beta}\phi_{0,\alpha}\left(K_\beta^{ab}\phi_{a,\beta}\phi_{b,\beta}\right) + \frac{1}{2}\left(\sum_r |r\cdot\phi|^3 - \sum_f \sum_{w(\mathcal{R}_f)} |w(\mathcal{R}_f)\cdot\phi + m_f|^3\right) \tag{4.5}$$

where r are the roots of $\mathfrak{h} = \oplus_\alpha \mathfrak{h}_\alpha$, $w(\mathcal{R}_f)$ parametrize weights of $\mathcal{R}_f$ and $m_f \in \mathbb{R}$ is a mass term for each full[9] hypermultiplet f. The notation $w \cdot \phi$ denotes the scalar product of the Dynkin coefficients of the weight w with Coulomb branch parameters. Note that similar approaches for computing prepotentials of 5d theories have appeared in the literature — see for example [40–42].

In (4.5) we must impose that mass terms for hypers belonging to $\mathcal{S}_{\alpha\beta,\alpha}$ and $\mathcal{S}_{\alpha\beta,\beta}$ equal the mass term for hypers belonging to $\mathcal{R}_{\alpha\beta}$. This is because $\mathcal{R}_{\alpha\beta}$, $\mathcal{S}_{\alpha\beta,\alpha}$ and $\mathcal{S}_{\alpha\beta,\beta}$ all descend from the same $6d$ representation $\mathcal{R}_{ij}$ which has only a single $\mathfrak{u}(1)$ symmetry rotating it. The Wilson lines for this $\mathfrak{u}(1)$ around the compactification circle gives rise to the mass terms for $\mathcal{R}_{\alpha\beta}$, $\mathcal{S}_{\alpha\beta,\alpha}$ and $\mathcal{S}_{\alpha\beta,\beta}$, and hence all these mass terms must be equal.

We propose that (4.5) is the full exact prepotential for $\mathfrak{T}^{KK}_{S,\{q_\alpha\}}$ where we have ignored the terms involving the mass parameter $\frac{1}{R}$ where R is the radius of compactification. We are justified in doing so since these terms do not play any role in this paper. Moreover, only the part of $6\mathcal{F}_{S,\{q_\alpha\}}$ that is cubic in Coulomb branch parameters $\phi_{a,\alpha}$ is relevant to the discussion in this paper; so, for convenience, we denote the part of the prepotential cubic in Coulomb branch parameters by $6\mathcal{F}^{\phi}_{S,\{q_\alpha\}}$.

[9]Half-hypermultiplets do not admit mass parameters unless completed into a full hypermultiplet.

Notice that fixing the relative values of $\phi_{a,\alpha}$ and m_f fixes the signs of the terms inside absolute values in (4.5). As the relative values of $\phi_{a,\alpha}$ and m_f are changed, the sign of some of the terms in (4.5) changes. This leads to jumps in the coefficients of various terms in the resulting $6\mathcal{F}^{\phi}_{S,\{q_\alpha\}}$. This means that different relative values of $\phi_{a,\alpha}$ and m_f lead to different phases inside the Coulomb branch of the $5d$ KK theory.

Let us illustrate through a simple example of the KK theory specified by the graph

$$\begin{array}{c}\mathfrak{su}(3)^{(1)}\\ 2\end{array} \tag{4.6}$$

This theory has six hypers in fundamental of $\mathfrak{su}(3)$. The Dynkin coefficients of the positive roots of $\mathfrak{su}(3)$ are $(2,-1)$, $(1,1)$ and $(-1,2)$. The Dynkin coefficients for the weights of fundamental are $(1,0)$, $(-1,1)$ and $(0,-1)$. The Killing form is

$$\begin{pmatrix} 2 & -1 \\ -1 & 2 \end{pmatrix}$$

and $\Omega_S^{\alpha\beta}$ is a 1×1 matrix which equals 2. Without loss of generality, we can take $r\cdot\phi$ for positive roots to be positive. This implies that $r\cdot\phi$ for negative roots is negative.

Let us first fix all the mass terms to be zero. Then the first weight $(1,0)$ contributes with a positive sign since the positivity of $r\cdot\phi$ for positive roots implies that ϕ_1 is positive. Similarly, the third weight $(0,-1)$ contributes with a negative sign to the prepotential. However, the sign of second weight $(-1,1)$ cannot be determined uniquely, and hence the theory has two phases when all mass parameters vanish. These two phases are distinguished by the sign s of the contribution due to the weight $(-1,1)$. The prepotential can be written as

$$\begin{aligned}6\mathcal{F}^{\phi} = 6\mathcal{F} = 12\phi_0\left(\phi_1^2+\phi_2^2-\phi_1\phi_2\right) + \left((2\phi_1-\phi_2)^3+(\phi_1+\phi_2)^3+(2\phi_2-\phi_1)^3\right)\\ -3\left(s\left(\phi_2-\phi_1\right)^3+\phi_1^3+\phi_2^3\right)\end{aligned} \tag{4.7}$$

Here $12\phi_0\left(\phi_1^2+\phi_2^2-\phi_1\phi_2\right)$ is the contribution coming from the Green-Schwarz term in $6d$, $(2\phi_1-\phi_2)^3+(\phi_1+\phi_2)^3+(2\phi_2-\phi_1)^3$ is the contribution coming from the positive and negative roots, and $-3\left(s\left(\phi_2-\phi_1\right)^3+\phi_1^3+\phi_2^3\right)$ is the contribution coming from the weights of six hypers in fundamental.

When we turn on mass parameters, the sign of the weights corresponding to different hypers can be changed. For example, consider turning on a mass parameter for one of the fundamentals m_1 while keeping the mass parameters for the other five fundamentals zero. Now we obtain contributions from terms of the form $|m_1+\phi_1|$, $|m_1-\phi_1+\phi_2|$ and $|m_1-\phi_2|$. Depending on the value of m_1, we go through various new phases of the theory which are parametrized by choices of signs of these three terms. For example, suppose that m_1 is positive and very large, so that all the three terms are positive. Moreover, assume that $\phi_2-\phi_1$ is positive, so that $s=+1$. Then the resulting phase is governed by the following prepotential

$$6\mathcal{F} = 12\phi_0\left(\phi_1^2+\phi_2^2-\phi_1\phi_2\right)+\left((2\phi_1-\phi_2)^3+(\phi_1+\phi_2)^3+(2\phi_2-\phi_1)^3\right) \\ -\frac{5}{2}\left((\phi_2-\phi_1)^3+\phi_1^3+\phi_2^3\right)-\frac{1}{2}\left((\phi_2-\phi_1+m_1)^3+(\phi_1+m_1)^3+(-\phi_2+m_1)^3\right) \tag{4.8}$$

which implies that the truncated prepotential is

$$6\mathcal{F}^\phi = 12\phi_0\left(\phi_1^2+\phi_2^2-\phi_1\phi_2\right)+\left((2\phi_1-\phi_2)^3+(\phi_1+\phi_2)^3+(2\phi_2-\phi_1)^3\right) \\ -3\left((\phi_2-\phi_1)^3+\phi_1^3\right)-2\phi_2^3 \tag{4.9}$$

We caution the reader that there can be phases of the KK theory which cannot be traversed by changing the signs of various contributions to the prepotential. In other words, they are not visible to the canonical low energy gauge theory that we associated to the KK theory in the beginning of this subsection. We will refer to such phases as non-gauge theoretic. This terminology does not mean that the low energy theory governing such phases cannot be understood as Coulomb branch of a gauge theory. Rather it simply means that low energy theory governing such phases cannot be understood as part of Coulomb branch of the canonical gauge theory associated to the corresponding KK theory.

4.2 Shifting the prepotential

Consider a $6d$ theory $\mathfrak{T}$ with gauge algebras $\mathfrak{g}_i$ on its tensor branch. Consider further compactifying $\mathfrak{T}$ on a circle of finite size without a twist. On a generic point of the resulting $5d$ Coulomb branch, the massive BPS spectrum includes W-bosons for the corresponding untwisted affine gauge algebras $\mathfrak{g}_i^{(1)}$. In other words, the abelian gauge algebra visible at low energies on the Coulomb branch is $\oplus_a\mathfrak{u}(1)_{a,i}$ parametrizing the Cartan of $\mathfrak{g}_i$ plus a $\mathfrak{u}(1)_{0,i}$ responsible for affinization. The $\mathfrak{u}(1)_i$ arising from the reduction of tensor multiplet B_i is central to $\oplus_a\mathfrak{u}(1)_{a,i}\oplus\mathfrak{u}(1)_{0,i}$. The untwisted Lie algebras are listed in figure 1 along with their Coxeter and dual Coxeter labels.

We now generalize the above statements to the twisted case. Consider compactifying $\mathfrak{T}$ on a circle of finite size with a twist $S,\{q_\alpha\}$. On a generic point of the resulting $5d$ Coulomb branch, the massive BPS spectrum includes W-bosons for the corresponding twisted/untwisted affine gauge algebras $\mathfrak{g}_\alpha^{(q_\alpha)}$. In other words, the abelian gauge algebra visible at low energies on the Coulomb branch is $\oplus_a\mathfrak{u}(1)_{a,\alpha}$ parametrizing the Cartan of $\mathfrak{h}_\alpha$ plus a $\mathfrak{u}(1)_{0,\alpha}$ responsible for affinization. The $\mathfrak{u}(1)_\alpha$ arising from the reduction of tensor multiplet B_i (with i in orbit of α) is central to $\oplus_a\mathfrak{u}(1)_{a,\alpha}\oplus\mathfrak{u}(1)_{0,\alpha}$. The twisted Lie algebras are listed in table 2 along with their Coxeter and dual Coxeter labels.

The charge under $\mathfrak{u}(1)_{b,\alpha}$ (corresponding to a simple co-root $e_b^\vee$) of a W-boson W_a (corresponding to simple root e_a of $\mathfrak{g}_\alpha^{(q_\alpha)}$) is given by the element A_{ab} of the Cartan matrix. Now consider the $\mathfrak{u}(1)$ embedding into $\oplus_{b=0}^{r_\alpha}\mathfrak{u}(1)_{b,\alpha}$ by the map $e^{i\theta}\to\oplus_{b=0}^{r_\alpha}\left(e^{id_b^\vee\theta}\right)_b$ where $\left(e^{id_b^\vee\theta}\right)_b$ is the element $e^{id_b^\vee\theta}$ of $\mathfrak{u}(1)_{b,\alpha}$ and $d_b^\vee$ are dual Coxeter labels of $\mathfrak{g}_\alpha^{(q_\alpha)}$ listed in figures 1 and 2. Since all the W-bosons W_a are uncharged under this $\mathfrak{u}(1)$, it follows that this $\mathfrak{u}(1)$ can be identified with the central $\mathfrak{u}(1)_\alpha$. The charge of a particle n_α under $\mathfrak{u}(1)_\alpha$ can be written as $\sum_{b=0}^{r_\alpha}d_b^\vee n_{b,\alpha}$ where $n_{b,\alpha}$ is the charge of the particle under $\mathfrak{u}(1)_{b,\alpha}$.

JHEP12(2020)151

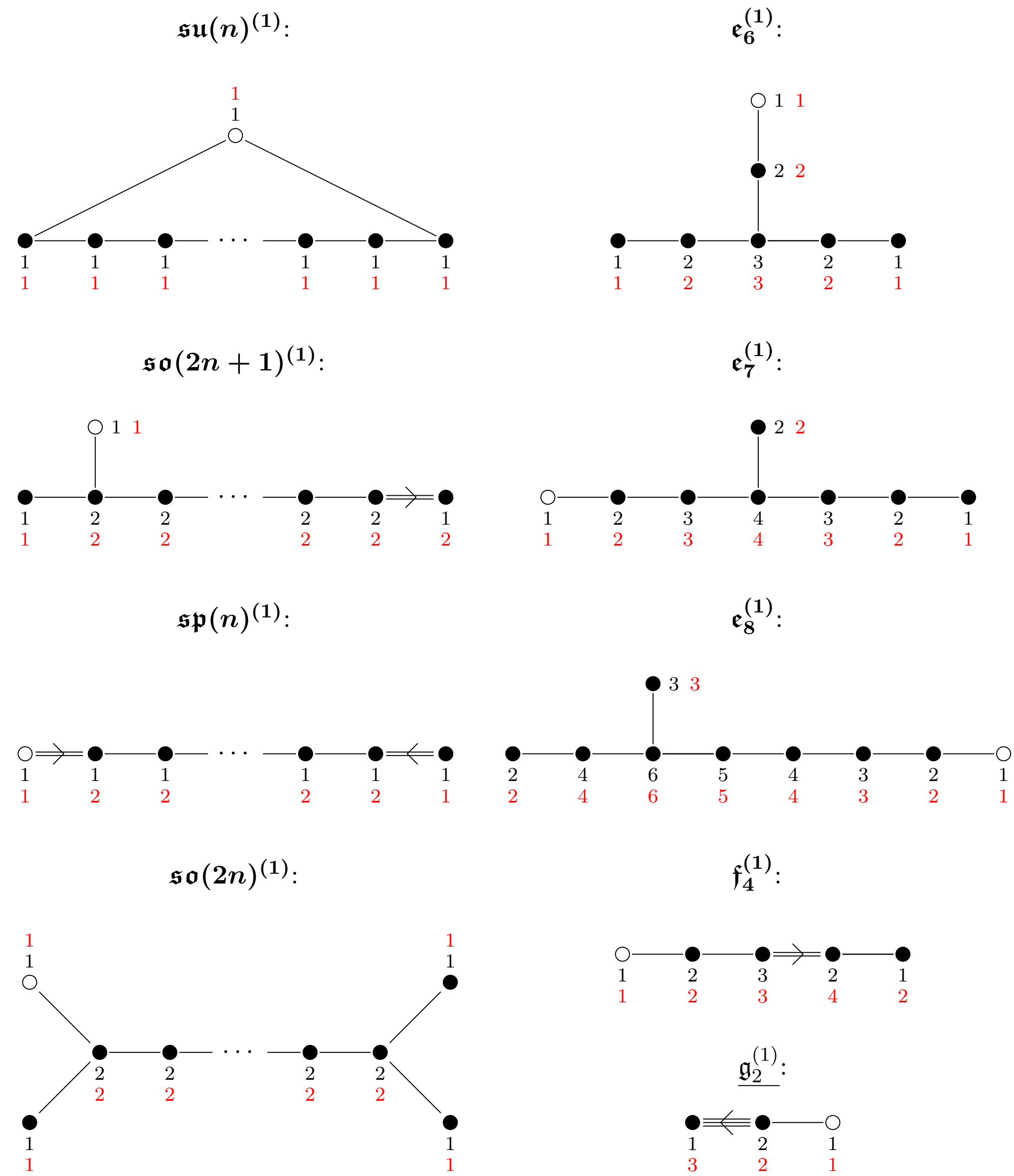

Figure 1. Untwisted affine Lie algebras. The affine node is shown as a hollow circle. The numbers in black $d_a^\vee$ denote the column null vector for the Cartan matrix, popularly known as dual Coxeter labels. The numbers in red d_a denote the row null vector for the Cartan matrix, popularly known as Coxeter labels.

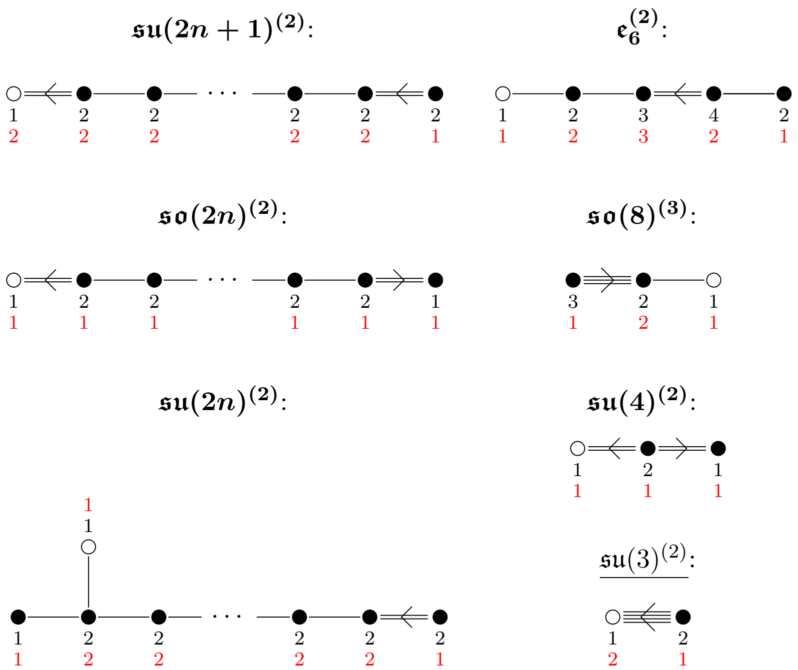

Figure 2. Twisted affine Lie algebras. The affine node is shown as a hollow circle. The numbers in black $d_a^\vee$ denote the column null vector for the Cartan matrix, popularly known as dual Coxeter labels. The numbers in red d_a denote the row null vector for the Cartan matrix, popularly known as Coxeter labels. The total number of nodes for $\mathfrak{su}(2n+1)^{(2)}$ is $n+1$, for $\mathfrak{so}(2n)^{(2)}$ is n, and for $\mathfrak{su}(2n)^{(2)}$ is $n+1$.

The truncated prepotential $6\mathcal{F}^{\phi}_{S,\{q_\alpha\}}$ is written in terms of Coulomb branch parameters $\phi_{b,\alpha}$ (with $1 \leq b \leq r_\alpha$) corresponding to $\mathfrak{u}(1)_{b,\alpha}$ and $\phi_{0,\alpha}$ corresponding to $\mathfrak{u}(1)_\alpha$. To facilitate comparison with geometry, we wish to write the prepotential in terms of Coulomb branch parameters corresponding to $\mathfrak{u}(1)_{b,\alpha}$ for $0 \leq b \leq r_\alpha$. This is achieved by performing the following replacement in $6\mathcal{F}^{\phi}_{S,\{q_\alpha\}}$

$$\phi_{b,\alpha} \to \phi_{b,\alpha} - d_b^\vee \phi_{0,\alpha} \tag{4.10}$$

for all $1 \leq b \leq r_\alpha$ and for all α.[10] We will call the prepotential obtained after this shift as $\tilde{\mathcal{F}}_{S,\{q_\alpha\}}$. The Coulomb branch parameter $\phi_{0,\alpha}$ in $\tilde{\mathcal{F}}_{S,\{q_\alpha\}}$ corresponds to $\mathfrak{u}(1)_{0,\alpha}$ rather than $\mathfrak{u}(1)_\alpha$.

For illustrative purposes, we note that the shift for our example (4.6) is

$$\begin{aligned}\phi_1 &\to \phi_1 - \phi_0\\ \phi_2 &\to \phi_2 - \phi_0\end{aligned}$$

[10]Note that the shift (4.10) has been studied before the in the literature in relation to resolutions of elliptically fibered Calabi-Yau threefolds; in these examples, the effect of the shift is to expand the Kähler form J in basis of primitive divisors — see for example [43].

which means that the shifted prepotential corresponding (4.7) is

$$6\tilde{\mathcal{F}} = 8\phi_0^3 + 8\phi_1^3 + 2\phi_2^3 - 6\phi_1\phi_0^2 + 6\phi_1\phi_2^2 - 6\phi_2\phi_0^2 - 12\phi_2\phi_1^2 \tag{4.11}$$

where we have chosen the phase $s = +1$.

The shifted prepotential for (4.9) is

$$6\tilde{\mathcal{F}} = 7\phi_0^3 + 8\phi_1^3 + 3\phi_2^3 - 6\phi_1\phi_0^2 + 6\phi_1\phi_2^2 - 3\phi_2\phi_0^2 - 3\phi_0\phi_2^2 - 12\phi_2\phi_1^2 \tag{4.12}$$

A Mathematica notebook accompanying the submission of this paper can be used to compute the contribution to $6\tilde{\mathcal{F}}$ (in any gauge-theoretic phase) from a single node or two nodes connected by an edge. Using these two results, one can write the contribution to $6\tilde{\mathcal{F}}$ from two nodes connected by an edge as contributions from the two nodes alone and a contribution from the edge. Thus, we can figure out what is the contribution to $6\tilde{\mathcal{F}}$ by each possible edge. Combining the contributions from the nodes and the edges, one can obtain $6\tilde{\mathcal{F}}_{S,\{q_\alpha\}}$ for any arbitrary graph $\Sigma_{\mathfrak{T}}^{S,\{q_\alpha\}}$. More details and the instructions for using the notebook can be found in appendix E.

5 Geometries associated to 5d KK theories

In this section, we will show that we can associate (at least one) genus-one fibered Calabi-Yau threefold $X_{S,\{q_\alpha\}}$ to every 5d KK theory[11] $\mathfrak{T}^{KK}_{S,\{q_\alpha\}}$. Compactifying M-theory on $X_{S,\{q_\alpha\}}$ produces the Coulomb branch of $\mathfrak{T}^{KK}_{S,\{q_\alpha\}}$. Some of the results appearing below also appeared in [3–5, 44–51]

5.1 General features

In this subsection, we start with a description of general features of the geometric structure of $X_{S,\{q_\alpha\}}$ and the relationship between this geometry and the low energy effective theory governing the Coulomb branch of the KK theory $\mathfrak{T}^{KK}_{S,\{q_\alpha\}}$.

We will show that $X_{S,\{q_\alpha\}}$ can be realized as a local neighborhood of a collection of irreducible compact holomorphic surfaces intersecting with each other pairwise transversely. As we will see, the surfaces fall into families indexed by α. We denote the irreducible surfaces in each family α as $S_{a,\alpha}$ where $0 \leq a \leq r_\alpha$ (where r_α is the rank of $\mathfrak{h}_\alpha$). The Kahler parameters associated to $S_{a,\alpha}$ are identified as the Coulomb branch parameters $\phi_{a,\alpha}$ of the corresponding 5d KK theory discussed in the previous section. Whenever $\mathfrak{h}_\alpha$ is trivial, the rank of $\mathfrak{h}_\alpha$ is zero and hence there is only a single surface $S_{0,\alpha}$ associated to the node α in that case.

5.1.1 Triple intersection numbers and the prepotential

A key role in the relationship between $X_{S,\{q_\alpha\}}$ and $\mathfrak{T}^{KK}_{S,\{q_\alpha\}}$ is played by the shifted prepotential $6\tilde{\mathcal{F}}_{S,\{q_\alpha\}}$. The coefficients $c_{a\alpha,b\beta,c\gamma}$ of $\phi_{a,\alpha}\phi_{b,\beta}\phi_{c,\gamma}$ in $6\tilde{\mathcal{F}}_{S,\{q_\alpha\}}$ capture the triple

[11] We remind the reader that this statement is not completely true for KK theories involving the last node in table 8. For such KK theories, we only propose an algebraic description whose structure closely mimics the structure of genus-one fibered Calabi-Yau threefolds to be discussed in the next subsection 5.1.

JHEP12(2020)151

intersection numbers of surfaces in $X_{S,\{q_\alpha\}}$ as follows:

$$c_{a\alpha,a\alpha,a\alpha} = S_{a,\alpha} \cdot S_{a,\alpha} \cdot S_{a,\alpha} \tag{5.1}$$
$$c_{a\alpha,a\alpha,b\beta} = 3S_{a,\alpha} \cdot S_{a,\alpha} \cdot S_{b,\beta} \tag{5.2}$$
$$c_{a\alpha,b\beta,c\gamma} = 6S_{a,\alpha} \cdot S_{b,\beta} \cdot S_{c,\gamma} \tag{5.3}$$

where $(a,\alpha),(b,\beta),(c,\gamma)$ denote distinct non-equal indices.

A triple intersection product of three surfaces can be computed via intersection numbers inside any one of the three surfaces. To explain it, let us first define the notion of "gluing curves". Consider the intersection locus $\mathcal{L}_{a\alpha,b\beta}$ between two distinct surfaces $S_{a,\alpha}$ and $S_{b,\beta}$ in $X_{S,\{q_\alpha\}}$. $\mathcal{L}_{a\alpha,b\beta}$ splits into geometrically irreducible components as $\sum_i \mathcal{L}^i_{a\alpha,b\beta}$. Each $\mathcal{L}^i_{a\alpha,b\beta}$ appears as an irreducible curve $C^i_{a,\alpha;b,\beta}$ in $S_{a,\alpha}$ and an irreducible curve $C^i_{b,\beta;a,\alpha}$ in $S_{b,\beta}$. In other words, we can manufacture the intersection of $S_{a,\alpha}$ and $S_{b,\beta}$ by identifying the curves

$$C^i_{a,\alpha;b,\beta} \sim C^i_{b,\beta;a,\alpha} \tag{5.4}$$

with each other for all i. Identifying pairs of curves in the above fashion can be thought of as "gluing together" two surfaces along those curves.[12] The reducible curve $C_{a,\alpha;b,\beta} := \sum_i C^i_{a,\alpha;b,\beta}$ is called the "total gluing curve" in $S_{a,\alpha}$ for the intersection of $S_{a,\alpha}$ and $S_{b,\beta}$. Similarly, $C_{b,\beta;a,\alpha} := \sum_i C^i_{b,\beta;a,\alpha}$ is called the total gluing curve in $S_{b,\beta}$ for the intersection of $S_{a,\alpha}$ and $S_{b,\beta}$.

As two distinct surfaces $S_{a,\alpha}$ and $S_{b,\beta}$ can intersect each other, so can a single surface $S_{a,\alpha}$ intersect itself. Much as above for the intersection of two distinct surfaces, the self-intersection of $S_{a,\alpha}$ can be captured in terms of gluings

$$C^i_{a,\alpha} \sim D^i_{a,\alpha} \tag{5.5}$$

where $C^i_{a,\alpha}$ and $D^i_{a,\alpha}$ are irreducible curves in $S_{a,\alpha}$.

Then the triple intersection numbers can be expressed as:

$$S_{a,\alpha} \cdot S_{a,\alpha} \cdot S_{a,\alpha} = K'_{a,\alpha} \cdot K'_{a,\alpha} \tag{5.6}$$
$$S_{a,\alpha} \cdot S_{a,\alpha} \cdot S_{b,\beta} = K'_{a,\alpha} \cdot C_{a,\alpha;b,\beta} = C^2_{b,\beta;a,\alpha} \tag{5.7}$$
$$S_{a,\alpha} \cdot S_{b,\beta} \cdot S_{c,\gamma} = C_{a,\alpha;b,\beta} \cdot C_{a,\alpha;c,\gamma} = C_{b,\beta;c,\gamma} \cdot C_{b,\beta;a,\alpha} = C_{c,\gamma;a,\alpha} \cdot C_{c,\gamma;b,\beta} \tag{5.8}$$

where

$$K'_{a,\alpha} := K_{a,\alpha} + \sum_i \left(C^i_{a,\alpha} + D^i_{a,\alpha} \right) \tag{5.9}$$

and $K_{a,\alpha}$ denotes the canonical class of $S_{a,\alpha}$.

As an illustrative example consider the KK theory (4.6) for which the shifted prepotential in a particular phase is displayed in (4.11). We propose that the associated geometry is as follows. Since there is a single node, we drop the index α and only display the index a. The surfaces are $S_0 = \mathbb{F}_0$, $S_1 = \mathbb{F}_2$, $S_2 = \mathbb{F}_4^6$. The gluing curves between S_0 and S_1 are

[12] On multiple occasions throughout this paper, we abuse the language and denote the identification of two curves as "gluing" of the two curves.

$C_{0;1} = e, C_{1;0} = e$. The gluing curves between S_1 and S_2 are $C_{1;2} = h, C_{2;1} = e$. The gluing curves between S_2 and S_0 are $C_{2;0} = h - \sum x_i, C_{0;2} = e$.

Now we can check that the intersections of these curves indeed give rise to the various coefficients in (4.11):

- First of all, recall from (A.18) that $K^2 = 8 - b$ for $\mathbb{F}_n^b$. Indeed, the coefficients of ϕ_a^3 in (4.11) equal K_a^2.
- One third the coefficient of $\phi_0\phi_1^2$ is zero which matches $C_{0;1}^2 = (e^2)_{S_0}$ where $(e^2)_{S_0}$ denotes that the intersection number e^2 is computed inside S_0 and that in particular the curve e is inside S_0. The coefficient also matches $K_1 \cdot C_{1;0} = (K \cdot e)_{S_1} = 0$. One third of the coefficient of $\phi_2\phi_0^2$ is -2 which indeed matches $C_{2;0}^2 = \left((h - \sum x_i)^2\right)_{S_2} = \left(h^2 - \sum x_i^2\right)_{S_2} = 4 - 6 = -2$ and $K_0 \cdot C_{0;2} = (K \cdot e)_{S_0} = -2$. Similarly, we can check the matching of such intersection numbers with one third the coefficients of other terms of the form $\phi_a\phi_b^2$.
- One sixth the coefficient of $\phi_0\phi_1\phi_2$ is zero which matches $C_{0;1} \cdot C_{0;2} = (e^2)_{S_0} = 0$, $C_{1;2} \cdot C_{1;0} = (h \cdot e)_{S_1} = 0$, and $C_{2,0} \cdot C_{2;1} = \left((h - \sum x_i) \cdot e\right)_{S_2} = 0$.

On the other hand, the geometry associated to (4.12) has $S_0 = \mathbb{F}_0^1$, $S_1 = \mathbb{F}_2$ and $S_2 = \mathbb{F}_4^5$. The gluing curves between S_0 and S_1 are $C_{0;1} = e, C_{1;0} = e$. The gluing curves between S_1 and S_2 are $C_{1;2} = h, C_{2;1} = e$. The gluing curves between S_2 and S_0 are $C_{2;0} = h - \sum x_i, C_{0;2} = e - x$. Here x denotes the exceptional curve of the blowup of S_0 and x_i denote the exceptional curves of the blowups of S_2. One can check that the intersections of these curves indeed give rise to the various coefficients in (4.12).

5.1.2 Consistency of gluings: volume matching, the Calabi-Yau condition, and irreducibility

Not every pair of curves can be identified with one another to form a consistent gluing. First of all, the topology of the two curves must be identical. This implies that a geometrically irreducible curve in one surface can only be identified with a geometrically irreducible curve in another surface, and furthermore that the genera (as defined in appendix A.3) of the two curves must be identical and non-negative. If $C \subset S$ is an irreducible curve, then a necessary condition that must be satisfied by C is that for any other irreducible curve $C' \subset S$ such that $C \neq C$, the intersection product must be non-negative:

$$C \cdot C' \geq 0. \tag{5.10}$$

In this paper, some of the algebraic examples are non-geometric (i.e. do not admit a conventional geometric description satisfying these consistency conditions) because they involve gluings which identify a geometrically *reducible* curve in one surface with a geometrically irreducible curve in another surface. Despite this apparent pathology, these examples nevertheless satisfy the remaining conditions described below.

In addition to the above topological constraints, the volumes of a pair of gluing curves must be the same. The volume of a curve C is computed by intersecting the curve with the Kahler class J via

$$\mathrm{vol}(C) = -J \cdot C \tag{5.11}$$

where

$$J = \sum_{a,\alpha} \phi_{a,\alpha} S_{a,\alpha} + \sum_f m_f N_f \tag{5.12}$$

where m_f are mass parameters and N_f are non-compact surfaces corresponding to those mass parameters. The contribution of mass parameters to the volume will not play a prominent role in this paper, so we define a truncated Kahler class J^ϕ which only keep track of the contribution of Coulomb branch parameters to the volume

$$J^\phi = \sum_{a,\alpha} \phi_{a,\alpha} S_{a,\alpha} \tag{5.13}$$

The volume of C equals the mass of the BPS state obtained by wrapping an M2 brane on C because the intersection number

$$-S_{a,\alpha} \cdot C \tag{5.14}$$

captures the charge under $\mathfrak{u}(1)_{a,\alpha}$ of the BPS state arising from M2 brane wrapping C. If C lies in $S_{a,\alpha}$, then the intersection (5.14) is computed via

$$S_{a,\alpha} \cdot C = K'_{a,\alpha} \cdot C \tag{5.15}$$

If C lies in some other surface $S_{b,\beta}$, then (5.14) is computed via

$$S_{a,\alpha} \cdot C = C_{b,\beta;a,\alpha} \cdot C \tag{5.16}$$

Now, for (5.4) to be consistent we must have

$$J^\phi \cdot C^i_{a,\alpha;b,\beta} = J^\phi \cdot C^i_{b,\beta;a,\alpha} \tag{5.17}$$

which is an important consistency condition for constructing $X_{S,\{q_\alpha\}}$. We have checked that (5.17) is satisfied for all the geometries presented in this paper.

Finally, the gluing curves also have to satisfy the *Calabi-Yau condition* which states that

$$\left(C^i_{a,\alpha;b,\beta}\right)^2 + \left(C^i_{b,\beta;a,\alpha}\right)^2 = 2g-2 \tag{5.18}$$

where g is the genus of $C^i_{a,\alpha;b,\beta}$. See [2, 4] for more details.

Notice that in special situations the Calabi-Yau condition (5.18) is automatically satisfied as long as we satisfy (5.17). This is the situation when there is a single gluing curve $C_{a,\alpha;b,\beta} \sim C_{b,\beta;a,\alpha}$ between two surfaces $S_{a,\alpha}$ and $S_{b,\beta}$ such that neither of them is a self-glued surface. Then, (5.17) implies

$$K \cdot C_{a,\alpha;b,\beta} = C^2_{b,\beta;a,\alpha} \tag{5.19}$$

Adding $C^2_{a,\alpha;b,\beta}$ to both sides of the above equation we get

$$C^2_{a,\alpha;b,\beta} + C^2_{b,\beta;a,\alpha} = 2g-2 \tag{5.20}$$

As an example, in what preceded above we discussed the geometry associated to (4.11). We can check that (5.17) is satisfied for all the gluing curves in the geometry. For instance,

$$J^\phi \cdot C_{0;1} = \phi_0 \left(K_0 \cdot C_{0;1}\right) + \phi_1 C_{0;1}^2 + \phi_2 \left(C_{0;2} \cdot C_{0;1}\right) \tag{5.21}$$

$$= \phi_0 \left(K \cdot e\right)_{S_0} + \phi_1 \left(e^2\right)_{S_0} + \phi_2 \left(e^2\right)_{S_0} \tag{5.22}$$

$$= -2\phi_0 \tag{5.23}$$

and comparing it with

$$J^\phi \cdot C_{1;0} = \phi_0 C_{1;0}^2 + \phi_1 \left(K_1 \cdot C_{1;0}\right) + \phi_2 \left(C_{1;2} \cdot C_{1;0}\right) \tag{5.24}$$

$$= \phi_0 \left(e^2\right)_{S_1} + \phi_1 \left(K \cdot e\right)_{S_1} + \phi_2 \left(e \cdot h\right)_{S_1} \tag{5.25}$$

$$= -2\phi_0 \tag{5.26}$$

we find that indeed the gluing $C_{0;1} \sim C_{1;0}$ is consistent. Similarly, it can be checked that all the other gluings are consistent as well. In a similar fashion, one can also check that all of the gluings in the geometry associated to (4.12) discussed above satisfy (5.17).

5.1.3 Weights, phase transitions and flops

A hypermultiplet transforming in a representation $\mathcal{R}_f$ of the $5d$ gauge algebra $\mathfrak{h} = \oplus_\alpha \mathfrak{h}_\alpha$ appears as a collection of curves inside $X_{S,\{q_\alpha\}}$. These curves are characterized as follows. Let m_f be the mass parameter corresponding to $\mathcal{R}_f$. For each weight $w(\mathcal{R}_f)$ of $\mathcal{R}_f$, define a quantity $\mathrm{vol}\left(w(\mathcal{R}_f)\right)$, which we call the *virtual volume*, by shifting the quantity

$$w(\mathcal{R}_f) \cdot \phi + m_f \tag{5.27}$$

by the shift (4.10) for all α. Then, one can find a holomorphic curve $C_{w(\mathcal{R}_f)}$ in $X_{S,\{q_\alpha\}}$ such that

$$\mathrm{vol}\left(C_{w(\mathcal{R}_f)}\right) = \left|\mathrm{vol}\left(w(\mathcal{R}_f)\right)\right| \tag{5.28}$$

In general, the curve $C_{w(\mathcal{R}_f)}$ can be a positive linear combination of curves living inside various irreducible surfaces. However, some of the curves $C_{w(\mathcal{R}_f)}$ turn out to be living purely inside a single irreducible surface $S_{a,\alpha}$. If such a curve C_w has genus zero and self-intersection -1 inside $S_{a,\alpha}$, then one can perform a *flop transition*[13] on $X_{S,\{q_\alpha\}}$ by flopping C, which corresponds to a phase transition in the Coulomb branch of the $5d$ gauge theory described in previous section. We refer to such a flop transition as a "gauge-theoretic flop transition" to distinguish it from the flop transitions associated to more general -1 curves not associated to any hypermultiplet.

Let the geometry obtained after the flop transition associated to C_w be $X'_{S,\{q_\alpha\}}$. As for $X_{S,\{q_\alpha\}}$, there exist curves $C'_{w(\mathcal{R}_f)}$ in $X'_{S,\{q_\alpha\}}$ associated to weights $w(\mathcal{R}_f)$ such that

$$\mathrm{vol}\left(C'_{w(\mathcal{R}_f)}\right) = \left|\mathrm{vol}'\left(w(\mathcal{R}_f)\right)\right| \tag{5.29}$$

[13]This transition corresponds to blowing down C inside $S_{a,\alpha}$ and performing a blow-up in the neighboring surfaces intersecting C transversally. We will explain such transitions via various illustrations throughout this paper. More detailed background can be found in section 2 of [4].

where $\mathrm{vol}'(w(\mathcal{R}_f))$ is the shift of the quantity (5.27) computed in the new phase. The relationship between the two virtual volumes $\mathrm{vol}'(w(\mathcal{R}_f))$ and $\mathrm{vol}(w(\mathcal{R}_f))$ is

$$\mathrm{vol}'(w(\mathcal{R}_f)) = \mathrm{vol}(w(\mathcal{R}_f)) \tag{5.30}$$

for all $w(\mathcal{R}_f) \neq w$, and

$$\mathrm{vol}'(w) = -\mathrm{vol}(w) \tag{5.31}$$

with a minus sign.

We know from the analysis presented in the last section that the canonical $5d$ gauge theory associated to (4.6) is an $\mathfrak{su}(3)$ gauge theory with six fundamental hypers. The Dynkin coefficients of the weights of fundamental are $(1,0)$, $(-1,1)$ and $(0,-1)$. We call these weights w_1, w_2 and w_3 respectively. We can compute

$$\mathrm{vol}(w_1) = -\phi_0 + \phi_1 \tag{5.32}$$

$$\mathrm{vol}(w_2) = -\phi_1 + \phi_2 \tag{5.33}$$

$$\mathrm{vol}(w_3) = \phi_0 - \phi_2 \tag{5.34}$$

Recall that the phase (4.11) corresponds to $\mathrm{vol}(w_1)$ and $\mathrm{vol}(w_2)$ being positive and $\mathrm{vol}(w_3)$ being negative for all the six fundamentals. Now compute the volume of one of the blowups x_i living in the surface S_2 in the geometry corresponding to (4.11):

$$\mathrm{vol}(x_i) = -\phi_0 + \phi_2 \tag{5.35}$$

Thus we see that C_{w_3} for each fundamental is x_i. The reader can check that $C_{w_2} = f_2 + x_i$ and $C_{w_1} = f_1 + f_2 + x_i$ where f_a denotes the fiber of the Hirzebruch surface S_a.

In fact, the geometries corresponding to (4.11) and (4.12) are related by a flop transition. We first blow down one of the blowups, say x_6, inside S_2. Under this blowdown the identity of S_2 changes from $\mathbb{F}_4^6$ to $\mathbb{F}_4^5$. Since x_6 intersects the gluing curve $h - \sum_{i=1}^{6} x_i$ at one point, the gluing curve after the blowdown becomes $h - \sum_{i=1}^{6} x_i + x_6 = h - \sum_{i=1}^{5} x_i$. The other gluing curve inside S_2 is unaffected since x_6 does not intersect with it. Correspondingly, since the gluing curve for S_1 in S_2 does not intersect x_6, the surface S_1 is unaffected by the flop transition. However, since the gluing curve for S_0 in S_2 intersects x_6, we have to blowup S_0 at a point lying on the gluing curve for S_2 inside S_0. Under the blowup the identity of S_0 changes from $\mathbb{F}_0$ to $\mathbb{F}_0^1$. The gluing curve for S_2 inside S_1 is changed to $e - x$.

Recall that the phase (4.12) corresponds to turning on a large mass m for one of the fundamentals such that

$$\mathrm{vol}(w_3) = \phi_0 - \phi_2 + m \tag{5.36}$$

for this fundamental is positive. Correspondingly, we can compute that

$$\mathrm{vol}(x) = \phi_0 - \phi_2 \tag{5.37}$$

which indeed matches (5.36) up to the contribution from mass parameter, thus verifying (5.31). We are not keeping track of non-compact surfaces in this paper, so we are only able to verify (5.31) up to the contribution from m.

5.1.4 Affine Cartan matrices and intersections of fibers

For each surface $S_{a,\alpha}$ in $X_{S,\{q_\alpha\}}$, we define a canonical fiber $f_{a,\alpha}$ inside it:

- If $\mathfrak{g}_\alpha$ is non-trivial, then $S_{a,\alpha}$ will always be a Hirzebruch surface[14] whose fiber class is the canonical fiber $f_{a,\alpha}$. An M2 brane wrapping this curve gives rise to the W-boson $W_{a,\alpha}$ discussed in last section.

- If the node α is

$$\begin{array}{c}\mathfrak{su}(1)^{(1)}\\ 2\end{array} \tag{5.38}$$

  then it turns out that there is a single corresponding surface $S_{0,\alpha} = F_0^2$ which is self-glued since $e-x$ and $e-y$ are identified with each other where x and y are the exceptional curves corresponding to the two blowups. Due to the self-gluing, the fiber class of $S_{0,\alpha}$ intersects itself inside the threefold $X_{S,\{q_\alpha\}}$ and appears as an elliptic curve with a nodal singularity. It is this fiber class that we refer to as the canonical fiber $f_{0,\alpha}$ in this case.

- If the node α is

$$\begin{array}{c}\mathfrak{sp}(0)^{(1)}_\theta\\ 1\end{array} \tag{5.39}$$

  then it turns out that there is a single corresponding surface $S_{0,\alpha} = dP_9$. The del Pezzo surface[15] dP_9 admits a unique elliptic fiber class $3l - \sum x_i$ which we refer to as the canonical fiber $f_{0,\alpha}$ in this case.

- If the node α is

$$\begin{array}{c}\mathfrak{su}(1)^{(1)}\\ 2\end{array} \tag{5.40}$$

  then it turns out that there is no completely geometric description. We provide an algebraic description in terms of algebraic properties of the curves inside the surface $S_{0,\alpha} = F_1^2$ which is self-glued since x and y are identified with each other. The canonical fiber in this case is $f_{0,\alpha} = 2h + f - 2x - 2y$ which is a genus one curve of self-intersection zero.

For each α we find that

$$f_{a,\alpha} \cdot S_{b,\alpha} = -A_{ab} \tag{5.41}$$

[14] In this paper, by a "Hirzebruch surface", we refer to a Hirzebruch surface possibly with blowups at generic or non-generic locations. Some background on Hirzebruch surfaces can be found in appendix A.

[15] In this paper, by a "del Pezzo surface dP_n", we refer to a surface which is an n point blowup of $\mathbb{P}^2$ but the blowups can be at non-generic locations. Some background on del Pezzo surfaces can be found in appendix A.

JHEP12(2020)151

where A_{ab} is the Cartan matrix of $\mathfrak{g}_\alpha^{(q_\alpha)}$ and $A_{ab} \equiv A_{00} = 0$ whenever $\mathfrak{g}_\alpha$ is trivial. This means that the fibers of Hirzebruch surfaces $S_{a,\alpha}$ for a fixed α intersect in the fashion of Dynkin diagram associated to affine Lie algebra $\mathfrak{g}_\alpha^{(q_\alpha)}$.

Intersection (5.41) is of the form $C \cdot S_{a,\alpha}$ where C is some curve in the threefold $X_{S,\{q_\alpha\}}$ and $S_{a,\alpha}$ is a surface inside the threefold. Like the triple intersection numbers of surfaces inside a threefold, such intersections can also be computed in terms of intersection numbers inside a surface. If C is a curve inside $S_{a,\alpha}$, then

$$C \cdot S_{a,\alpha} = C \cdot K'_{a,\alpha} \tag{5.42}$$

and if C is a curve inside a surface $S_{b,\beta}$ that is distinct from $S_{a,\alpha}$, then

$$C \cdot S_{a,\alpha} = C \cdot C_{b,\beta;a,\alpha} \tag{5.43}$$

Consider the example of (4.11) whose associated geometry was described towards the end of section 5.1.1. We can compute that

$$f_0 \cdot S_0 = (K \cdot f)_{S_0} = -2 \tag{5.44}$$
$$f_1 \cdot S_1 = (K \cdot f)_{S_1} = -2 \tag{5.45}$$
$$f_2 \cdot S_2 = (K \cdot f)_{S_2} = -2 \tag{5.46}$$
$$f_0 \cdot S_1 = C_{0;1} \cdot f_0 = (e \cdot f)_{S_0} = 1 \tag{5.47}$$
$$f_1 \cdot S_2 = C_{1;2} \cdot f_1 = (h \cdot f)_{S_0} = 1 \tag{5.48}$$
$$f_2 \cdot S_0 = C_{2;0} \cdot f_2 = \left(\left(h - \sum x_i\right) \cdot f\right)_{S_0} = 1 \tag{5.49}$$
$$f_1 \cdot S_0 = C_{1;0} \cdot f_1 = (e \cdot f)_{S_1} = 1 \tag{5.50}$$
$$f_2 \cdot S_1 = C_{2;1} \cdot f_2 = (e \cdot f)_{S_2} = 1 \tag{5.51}$$
$$f_0 \cdot S_2 = C_{0;2} \cdot f_0 = (e \cdot f)_{S_0} = 1 \tag{5.52}$$

Thus we see that $f_a \cdot S_b$ indeed reproduces the negative of Cartan matrix of affine Lie algebra $\mathfrak{su}(3)^{(1)}$. We can similarly check that the geometry associated to (4.12) also leads to the Cartan matrix of $\mathfrak{su}(3)^{(1)}$.

5.1.5 The genus one fibration

For each α, combining the fibers $f_{a,\alpha}$, let us define a fiber f_α via

$$f_\alpha = d_a f_{a,\alpha} \tag{5.53}$$

where d_a are Coxeter labels for $\mathfrak{g}_\alpha^{(q_\alpha)}$ listed (in red color) in figures 1 and 2. If $\mathfrak{g}_\alpha$ is trivial, then $d_0 := 1$.

We claim that f_α is a genus one fiber. This means that f_α can be obtained by a degeneration of a torus. It is well-known that torus fibers can degenerate into Kodaira fibers, which are collections of rational curves[16] intersecting in the pattern of untwisted affine Dynkin diagrams of type $\mathfrak{su}(n)^{(1)}$, $\mathfrak{so}(2n)^{(1)}$ and $\mathfrak{e}_n^{(1)}$. The multiplicity of each rational

[16]This means they have genus zero.

component curve is given by the Coxeter label for the corresponding node in the affine Dynkin diagram. The fiber f_α, on the other hand, is composed of rational curves $f_{a,\alpha}$ with their multiplicity given by the Coxeter labels for affine Dynkin diagram $\mathfrak{g}_\alpha^{(q_\alpha)}$. Now, one can notice that every affine Dynkin diagram can be obtained by folding affine Dynkin diagrams of type $\mathfrak{su}(n)^{(1)}$, $\mathfrak{so}(2n)^{(1)}$ and $\mathfrak{e}_n^{(1)}$ as follows:

$$\mathfrak{so}(2n)^{(1)} \to \mathfrak{so}(2n-1)^{(1)} \to \mathfrak{so}(2n-2)^{(2)} \tag{5.54}$$

$$\mathfrak{e}_6^{(1)} \to \mathfrak{f}_4^{(1)} \to \mathfrak{so}(8)^{(3)} \tag{5.55}$$

$$\mathfrak{so}(8)^{(1)} \to \mathfrak{so}(7)^{(1)} \to \mathfrak{g}_2^{(1)} \tag{5.56}$$

$$\mathfrak{so}(4n)^{(1)} \to \mathfrak{su}(2n)^{(2)} \to \mathfrak{su}(2n-1)^{(2)} \tag{5.57}$$

$$\mathfrak{so}(8)^{(1)} \to \mathfrak{so}(7)^{(1)} \to \mathfrak{su}(4)^{(2)} \to \mathfrak{su}(3)^{(2)} \tag{5.58}$$

$$\mathfrak{e}_7^{(1)} \to \mathfrak{e}_6^{(2)} \tag{5.59}$$

Moreover, observe that the Coxeter numbers of two nodes are added if they are identified under gluing. This means that f_α can be obtained by identifying the rational components of the Kodaira fibers according to the above folding rules. This explicitly shows that f_α is a genus one fiber.

Moreover, we find that due to the virtue of gluing rules, f_α is glued to f_β as

$$q_\alpha(-\Omega_{\beta\alpha})f_\alpha \sim q_\beta(-\Omega_{\alpha\beta})f_\beta \tag{5.60}$$

This generalizes the condition in the untwisted unfrozen case [4] where $f_i \sim f_j$ whenever there is an edge between i and j in $\Sigma_\mathfrak{T}$. This shows that certain multiples of genus one fibers are identified with each other as one passes over from one collection of surfaces to another, allowing us to extend the fibration structure consistently throughout the threefold.

More formally, according to a theorem due to Oguiso and Wilson [52, 53], a threefold X admits an genus one fibration structure if and only if there exists an effective divisor S_{T^2} satisfying

$$S_{T^2} \cdot S_{T^2} \cdot S_{T^2} = 0, \quad S_{T^2} \cdot S_{T^2} \neq 0 \tag{5.61}$$

where S_{T^2} lives in the extended Kähler cone, possibly on the boundary. The extended Kähler cone is parameterized by all the Coulomb branch and mass parameters satisfying

$$J \cdot C \geq 0 \tag{5.62}$$

for all holomorphic curves C in X. Physically, the extended Kähler cone corresponds to the Coulomb branch of the (possibly mass deformed) 5d theory corresponding to X.

In all of geometries associated to 5d KK theories, we can find an S_{T^2} which lies in the extended Kähler cone satisfies (5.61). Pick any node α and define

$$S_{T^2} := \sum_{a=0}^{r_\alpha} d_a^\vee S_{a,\alpha} \tag{5.63}$$

where $d_a^\vee$ are dual Coxeter labels for the associated affine algebra $\mathfrak{g}_\alpha^{(q_\alpha)}$ (see figures 1 and 2) and r_α is the rank of invariant subalgebra $\mathfrak{h}_\alpha$. If the node α carries a trivial gauge algebra, then we define $d_0^\vee = 1$ and take (5.63) to be the definition of S_{T^2}.

In the gauge theoretic case, the direction parametrized by (5.63) is special since all the fibers $f_{a,\alpha}$ have zero volume along this direction[17]

$$-S_{T^2}\cdot f_{a,\alpha}=\sum_b A_{ab}d_b^\vee=0 \tag{5.64}$$

Similarly, in the non-gauge theoretic case

$$-S_{T^2}\cdot f_{0,\alpha}=-K'_{0,\alpha}\cdot f_{0,\alpha}=0 \tag{5.65}$$

where the last equality can be checked to be true for every non-gauge theoretic case. Moreover, the reader can check using the explicit description of geometries presented in this paper that

$$S_{T^2}\cdot C\geq 0 \tag{5.66}$$

for all other holomorphic C in the threefold $X_{S,\{q_\alpha\}}$. So, S_{T^2} as defiend in (5.63) lies in the extended Kähler cone of $X_{S,\{q_\alpha\}}$.

Now it can be easily checked for all the geometries presented in this paper that

$$S_{T^2}\cdot S_{T^2}=-q_\alpha\Omega^{\alpha\alpha}\sum_{a=0}^{r_\alpha}(d_af_{a,\alpha})\neq 0 \tag{5.67}$$

where d_a are the Coxeter labels for $\mathfrak{g}_\alpha^{(q_\alpha)}$ with $d_0:=1$ if α is a non-gauge theoretic node. We can now compute

$$S_{T^2}\cdot S_{T^2}\cdot S_{T^2}\propto\sum_{a=0}^{r_\alpha}(d_af_{a,\alpha})\cdot\left(\sum_{b=0}^{r_\alpha}d_b^\vee S_{b,\alpha}\right)=-\sum_{a,b=0}^{r_\alpha}d_aA_{ab}d_b^\vee=0 \tag{5.68}$$

thus verifying both the conditions in (5.61) and establishing the presence of a genus one fibration in $X_{S,\{q_\alpha\}}$.

Let us now discuss the relationship between fibers f_α and the radius of compactification circle R. In general, we can find at least one node μ such that

$$n_\mu f_\mu\sim n_{\mu,\alpha}f_\alpha \tag{5.69}$$

with $n_{\mu,\alpha}\geq n_\mu\geq 1$ for all α . Then the curve

$$f:=l_\mu n_\mu f_\mu \tag{5.70}$$

with l_μ defined in section 3.3 can be identified with the KK mode of unit momentum in $\mathfrak{T}^{KK}_{S,\{q_\alpha\}}$ and has mass $\frac{1}{R}$ where R is the radius of the circle on which the $6d$ theory $\mathfrak{T}$ has been compactified. Thus, all the f_α can be identified as fractional KK modes with mass $\frac{1}{n_\alpha R}$ where $n_\alpha=l_\mu n_{\mu,\alpha}$. This generalizes the condition in the untwisted unfrozen case where the KK mode is identified with

$$f:=f_i \tag{5.71}$$

for any i, which is consistent since $f_i\sim f_j$ for all i,j.

[17]In fact, non-negativity of the volumes of fibers implies that the only directions in the Coulomb branch when mass parameters are turned off are given by $\sum_a d_a^\vee S_{a,\alpha}$ for various α.

Let us now discuss some examples. For the KK theory

$$\begin{array}{ccc} \mathfrak{sp}(n)^{(1)} & & \mathfrak{so}(2m)^{(2)} \\ 1 & \text{———} & 4 \end{array} \tag{5.72}$$

we find that

$$f_{\mathfrak{sp}(n)^{(1)}} \sim 2f_{\mathfrak{so}(2m)^{(2)}} \tag{5.73}$$

and the KK mode is

$$f = f_{\mathfrak{sp}(n)^{(1)}} \tag{5.74}$$

For the KK theory (3.30), we find that

$$f_{\mathfrak{sp}(n)^{(1)}} \sim 2f_{\mathfrak{so}(2m)^{(1)}} \tag{5.75}$$

and the KK mode is

$$f = f_{\mathfrak{sp}(n)^{(1)}} \tag{5.76}$$

For the KK theory (3.28), our gluing rules say that

$$2f_{\mathfrak{su}(n)^{(2)}} \sim 2f_{\mathfrak{su}(m)^{(1)}} \tag{5.77}$$

and the KK mode is

$$f = 2f_{\mathfrak{su}(n)^{(2)}} \tag{5.78}$$

For the KK theory (3.14), our gluing rules say that

$$f_{\mathfrak{su}(n)^{(1)}} \sim f_{\mathfrak{su}(m)^{(1)}} \tag{5.79}$$

and the KK mode is

$$f = 2f_{\mathfrak{su}(n)^{(1)}} \tag{5.80}$$

An interesting example to consider is the KK theory defined by the untwisted compactification of the 6d SCFT

$$\begin{array}{ccccc} \mathfrak{su}(p) & & \mathfrak{so}(m) & & \mathfrak{sp}(n) \\ 2 & \overset{}{—}{\scriptstyle 2}{—} & 4 & \text{———} & 1 \end{array} \tag{5.81}$$

which arises only in the frozen phase. We find that

$$2f_{\mathfrak{su}(p)^{(1)}} \sim 2f_{\mathfrak{so}(m)^{(1)}} \tag{5.82}$$

$$f_{\mathfrak{so}(m)^{(1)}} \sim f_{\mathfrak{sp}(n)^{(1)}} \tag{5.83}$$

and the KK mode is

$$f = 2f_{\mathfrak{su}(p)^{(1)}} \sim 2f_{\mathfrak{so}(m)^{(1)}} \sim 2f_{\mathfrak{sp}(n)^{(1)}} \tag{5.84}$$

If (5.81) arose in the unfrozen phase of F-theory, then we would have obtained

$$f = f_{\mathfrak{su}(p)^{(1)}} \sim f_{\mathfrak{so}(m)^{(1)}} \sim f_{\mathfrak{sp}(n)^{(1)}} \tag{5.85}$$

Thus equation (5.84) is a way to see that (5.81) cannot arise in the unfrozen phase of F-theory.

5.2 Geometry for each node

In this section we will describe the surfaces $S_{a,\alpha}$ along with their intersections associated to a single node α.

5.2.1 Graphical notation

We will capture the data of the surfaces and their intersections by using a graphical notation that would be a simpler version of the graphical notation used in [3, 4]. This subsection is devoted to the explanation of this notation. We find it best to explain the notation with the following example:

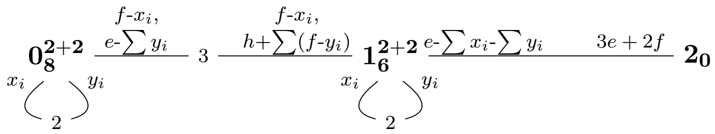

(5.86)

which is a particular phase of the KK theory

$$\begin{array}{c}\mathfrak{so}(8)^{(3)}\\ 2\end{array} \tag{5.87}$$

Since the rank of invariant subalgebra $\mathfrak{h} = \mathfrak{g}_2$ is two, we should have three surfaces in this case labeled by S_a where $0 \leq a \leq 2$. The middle number in the label for each node denotes the index a. Thus the node labeled $\mathbf{0_8^{2+2}}$ denotes the surface S_0, the node labeled $\mathbf{1_6^{2+2}}$ denotes the surface S_1, and the node labeled $\mathbf{2_0}$ denotes the surface S_2.

Every surface S_a is a Hirzebruch surface. The subscript in the label for each node denotes the degree of the corresponding Hirzebruch surface. Thus, S_0 has degree 8, S_1 has degree 6, and S_2 has degree 0. The superscript in the label for each node denotes the number of blowups on the corresponding Hirzebruch surface. Thus, S_0 carries $2+2=4$ blowups and hence $S_0 = \mathbb{F}_8^4$, S_1 carries $2+2=4$ blowups and hence $S_1 = \mathbb{F}_6^4$, and S_2 carries no blowups and hence $S_2 = \mathbb{F}_0$.

The fact that the four blowups on S_0 are displayed as $2+2$ denotes that the four blowups are divided into two sets, with each set containing two blowups. We denote the blowups in the first set as x_i and the blowups in the second set as y_i. The same is true for S_1. In a general graph, the blowups on a surface can be divided into more than two sets, and the number of blowups inside each set can be different. Whatever may be the case, we adopt the notation of denoting the blowups inside the first set as x_i, the blowups inside the second set as y_i, the blowups inside the third set as z_i etc.

The label in the middle of an edge between two nodes denotes the number of irreducible components of the intersection locus between the two surfaces corresponding to the two nodes. As already discussed above, each component of the intersection locus can be viewed as an irreducible gluing curve inside each of the surfaces participating in the intersection. Thus, there is a single gluing curve between S_1 and S_2 in the graph (5.86), but there are three gluing curves between S_0 and S_1. The graph also tells us that the surface S_0 is a self-glued Hirzebruch surface since there are edges which start and end at S_0. Similarly, S_1 is also a self-glued surface. We can see that the number of self-gluings in S_0 are two, and the number of self-gluings in S_1 are also two.

The curves displayed at the ends of edges tell us the identities of various gluing curves. The left end of the edge between $\mathbf{1_6^{2+2}}$ and $\mathbf{2_0}$ reads $e-\sum x_i-\sum y_i$, which means that the corresponding gluing curve inside S_1 is $e-\sum x_i-\sum y_i$. The right end of the edge between $\mathbf{1_6^{2+2}}$ and $\mathbf{2_0}$ reads $3e+2f$, which means that the corresponding gluing curve inside S_2 is $3e+2f$. We note that whenever we write $\sum x_i$ or $\sum y_i$, we mean a sum of all the blowups in the set of blowups denoted by x_i or y_i respectively.

In the above graph, the two self-gluings of S_0 are displayed by writing x_i at one end and y_i at the other end. This tells us that x_i in S_0 is glued to y_i in S_0. Since there is no sum over i, this gluing is supposed to be true for each valued of i. Hence, the two self-gluings are $x_1 \sim y_1$ and $x_2 \sim y_2$. The same is true for self-gluings of S_1.

The gluing curves for the three gluings between S_0 and S_1 are displayed as $f-x_i, e-\sum y_i$ inside S_0 and as $f-x_i, h+\sum(f-y_i)$ inside S_1. These are supposed to be read in the order they are written. Thus, unpacking the notation we learn that the three gluings are

$$(f-x_1)_{S_0} \sim (f-x_1)_{S_1} \tag{5.88}$$

$$(f-x_2)_{S_0} \sim (f-x_2)_{S_1} \tag{5.89}$$

$$(e-y_1-y_2)_{S_0} \sim (h+2f-y_1-y_2)_{S_1} \tag{5.90}$$

We also sometimes suppress multiplicity of a gluing curve. For example, in the geometry

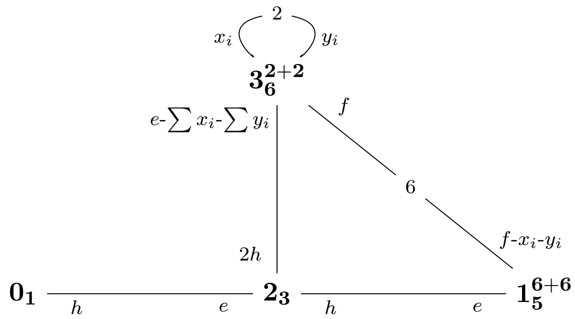

(5.91)

the gluing curve for S_2 in S_3 is displayed simply as f. But the edge between S_2 and S_3 shows that there are six gluing curves involved. This means that the true gluing curve for S_2 in S_3 is actually six copies of the fiber f of S_3.

Now, let us extract the prepotential $6\tilde{\mathcal{F}}$ from the graph (5.86). The coefficient of ϕ_0^3 is

$$(K'^2)_{S_0} = \left(\left(K+\sum x_i+\sum y_i\right)^2\right)_{S_0} = \left(K^2+\sum x_i^2+\sum y_i^2+2\sum K\cdot x_i+2\sum K\cdot y_i\right)_{S_0} \tag{5.92}$$

We have $K^2 = 8-4 = 4$ and $K\cdot x_i = K\cdot y_i = -1$, using which (5.92) reduces to

$$(K'^2)_{S_0} = 4-2-2-4-4 = -8 \tag{5.93}$$

Similarly the coefficient of ϕ_1^3 is -8. The coefficient of ϕ_2^3 is 8. The coefficient of $\phi_2\phi_1^2$ can be computed as

$$\left((3e+2f)^2\right)_{S_2} = 12 \tag{5.94}$$

which coincides with

$$\left(K' \cdot \left(e - \sum x_i - \sum y_i\right)\right)_{S_1} = \left(\left(K + \sum x_i + \sum y_i\right) \cdot \left(e - \sum x_i - \sum y_i\right)\right)_{S_1} = 12 \tag{5.95}$$

as it should for consistency. We can compute the coefficient of $\phi_0\phi_1^2$ to be

$$\left(\left(\left(e - \sum y_i\right) + (f - x_1) + (f - x_2)\right)^2\right)_{S_0} = -8 \tag{5.96}$$

which indeed coincides with

$$\left(K' \cdot ((h + 2f - y_1 - y_2) + (f - x_1) + (f - x_2))\right)_{S_1} = -8 \tag{5.97}$$

Similarly, we can compute coefficients for other terms of the form $\phi_a\phi_b^2$. Finally, the coefficient of $\phi_0\phi_1\phi_2$ must be 0 since there is no edge between S_0 and S_2. But this coefficient can also be computed as an intersection number of gluing curves inside S_1. Thus, the corresponding intersection number better be zero for consistency. Indeed we find that

$$\left(\left(e - \sum x_i - \sum y_i\right) \cdot ((h + 2f - y_1 - y_2) + (f - x_1) + (f - x_2))\right)_{S_1} = 0 \tag{5.98}$$

5.2.2 Untwisted

In this subsection, we collect our results for nodes of the form

$$\begin{array}{c}\mathfrak{g}^{(1)}\\ k\end{array} \tag{5.99}$$

That is, we restrict ourselves to the case where the associated affine Lie algebra is untwisted. All such nodes are displayed in table 1 and table 2. Most such cases were first studied in [3, 4]. We will be able to recover their results. We will associate a collection of geometries parametrized by ν to each node of the form (5.99). Geometries for different values of ν are flop equivalent as long as there are no neighboring nodes, but might cease to be flop equivalent in the presence of neighboring nodes. The geometries associated to (5.99) in [4] are obtained as $\nu = 0, 1$ versions of the geometries associated in this paper.

The geometries associated to nodes of the form (5.99) are presented below. We will display the corresponding node inside a circle placed at top of the geometry:

$$\begin{array}{c}\mathfrak{sp}(n)^{(1)}_{(n+1)\pi}\\ 1\end{array}$$

$$\mathbf{0}_\mathbf{1}^{\mathbf{2n+8-\nu}} \overset{2h\text{-}\sum x_i \qquad h}{\overline{}} \mathbf{1}_{\mathbf{2n+2-\nu}} \overset{e}{\overline{}} \cdots \overset{h}{\overline{}} (\mathbf{n-2})_{\mathbf{8-\nu}} \overset{e \qquad h}{\overline{}} (\mathbf{n-1})_{\mathbf{6-\nu}} \overset{e \qquad 2e+f\text{-}\sum x_i}{\overline{}} \mathbf{n}_\mathbf{0}^{\nu} \tag{5.100}$$

JHEP12(2020)151

where $0 \leq \nu \leq 2n+8$, $n \geq 1$ and the theta angle should be viewed modulo 2π. We can see that $f_a \cdot S_b$ reproduces the negative of Cartan matrix for untwisted affine Lie algebra $\mathfrak{sp}(n)^{(1)}$, where f_a is the canonical fiber of Hirzebruch surface S_a. The same hold true for all the examples discussed below in this subsection. One can check in each example below that $f_a \cdot S_b$ reproduces the negative of Cartan matrix for the associated untwisted affine Lie algebra $\mathfrak{g}^{(1)}$.

$$\begin{array}{c} \mathfrak{sp}(n)^{(1)}_{n\pi} \\ 1 \end{array}$$

$$\mathbf{0_1^{2n+8-\nu}} \overset{2h\text{-}\sum x_i \qquad h}{\text{———}} \mathbf{1_{2n+2-\nu}} \overset{e}{\text{—}} \cdots \overset{h}{\text{—}} \mathbf{(n-2)_{8-\nu}} \overset{e \qquad h}{\text{———}} \mathbf{(n-1)_{6-\nu}} \overset{e \qquad 2h\text{-}\sum x_i}{\text{———}} \mathbf{n_1^{\nu}} \tag{5.101}$$

where $0 \leq \nu \leq 2n+8$, $n \geq 1$ and the theta angle should be viewed modulo 2π. See appendix (B.3) for more discussion on the relationship between theta angle and geometry.

Notice that the two geometries (5.100) and (5.101) are isomorphic by virtue of the isomorphism between $\mathbb{F}_0^1$ and $\mathbb{F}_1^1$ discussed in appendix A.1. Suppose first that $\nu > 0$. Then, the isomorphism applied to S_n sends $2h - x_1$ in $\mathbb{F}_1^{\nu}$ to $2e + f - x_1$ in $\mathbb{F}_0^{\nu}$, thus mapping the gluing curve for S_{n-1} in S_n in (5.101) to the gluing curve for S_{n-1} in S_n in (5.100). Thus the whole geometry (5.101) is mapped to the geometry (5.100) by this isomorphism. For $\nu = 0$, the two geometries (5.101) and (5.100) are flop equivalent due to this isomorphism. This is because they are flop equivalent to $\nu > 0$ versions of the geometries (5.101) and (5.100), and we have already established an isomorphism between the latter geometries.

However, it is possible for this isomorphism to not extend to the full Calabi-Yau threefold when $\mathfrak{sp}(n)$ has other neighbors. The gluing curves inside S_0 and S_n for the surfaces corresponding to these neighbors might not map to each other under the above isomorphism plus flops. Whenever the isomorphism extends to the full threefold, the $\mathfrak{sp}(n)$ theta angle is physically irrelevant. Whenever the isomorphism does not extend to the full threefold, the $\mathfrak{sp}(n)$ theta angle is physically relevant. We will see examples of both situations later when we discuss gluing rules for $\mathfrak{sp}(n)$.

For $n = 0$, we claim that the associated geometry is

$$\begin{array}{c} \mathfrak{sp}(0)^{(1)}_{\theta} \\ 1 \end{array}$$

$$\mathbf{0_1^8} \tag{5.102}$$

One way to see this is to notice that both the geometries (5.100) and (5.101) reduce to (5.102) in the limit $n = 0$. For a more precise way to see that (5.102) is the correct geometry, see the discussion around (B.9).

When $\mathfrak{sp}(0)^{(1)}_\theta$ has no other neighbors, then all the blowups are generic and we can write $S_0 = dP_9$. When $\mathfrak{sp}(0)^{(1)}_\theta$ has neighbors, it turns out that $S_0 = dP_9$ with 9 non-generic blowups is the correct answer, instead of $S_0 = \mathbb{F}_1^8$ with eight non-generic blowups. This is because when the 9 blowups are non-generic, it is not always possible to represent dP_9 as $\mathbb{F}_1^8$ with 8 non-generic blowups. So, $S_0 = \mathbb{F}_1^8$ is not quite the correct answer. See [4] for more discussion on this point. Thus, in this paper, from this point on, we will represent the geometry associated to $\mathfrak{sp}(0)^{(1)}_\theta$ by dP_9.

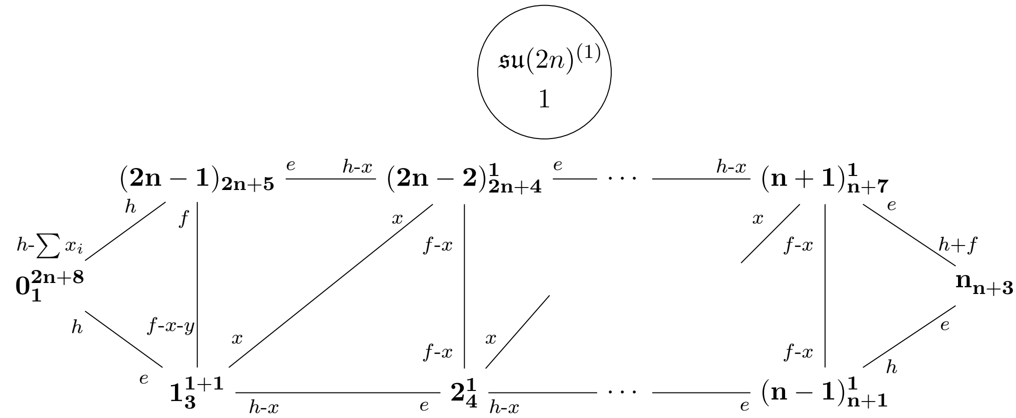

(5.103)

For this geometry, we do not define multiple versions distinguished by the parameter ν. Nevertheless, for uniformity of notation, we denote this geometry with $\nu = 0$. Similarly, we will denote all the following geometries having a single unique version with $\nu = 0$.

For $n = 2$, we have

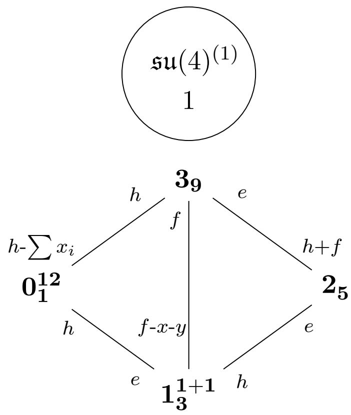

(5.104)

JHEP12(2020)151

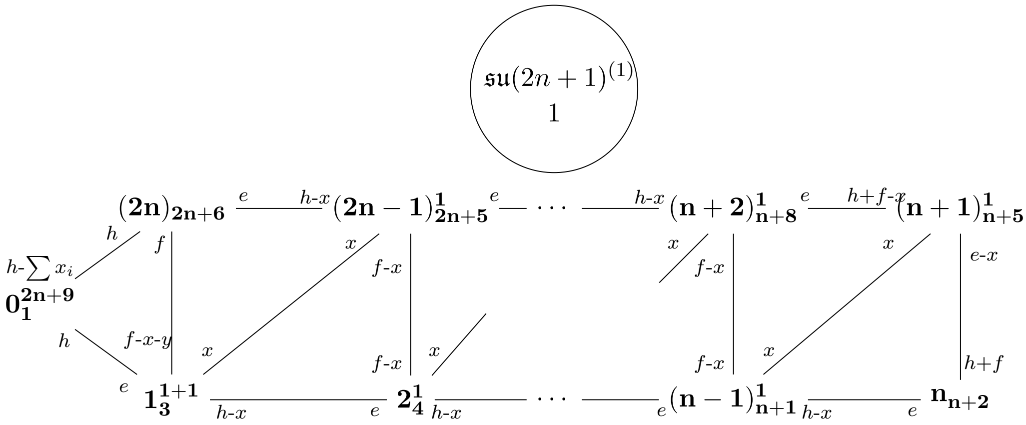

(5.105)

For $n = 1$, we have

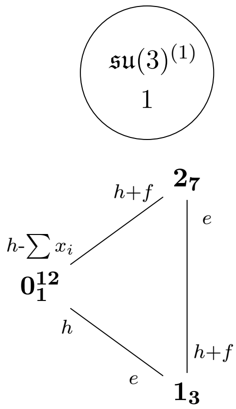

(5.106)

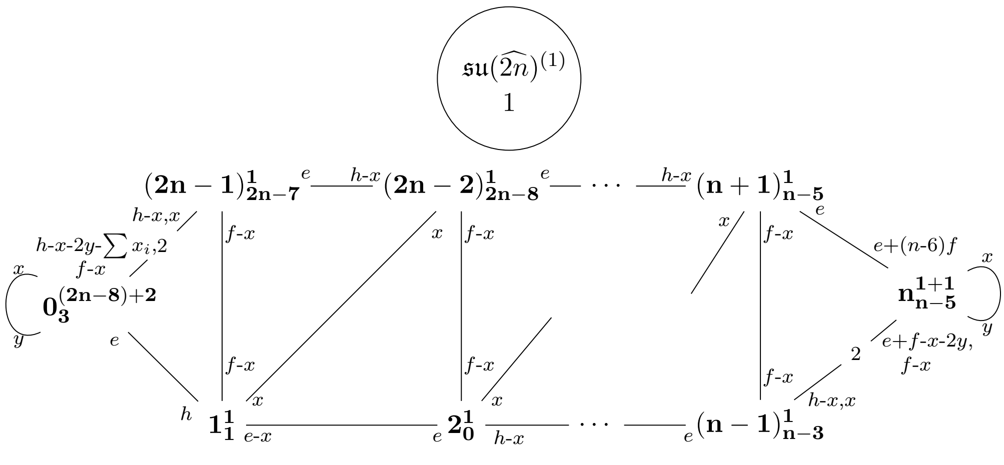

(5.107)

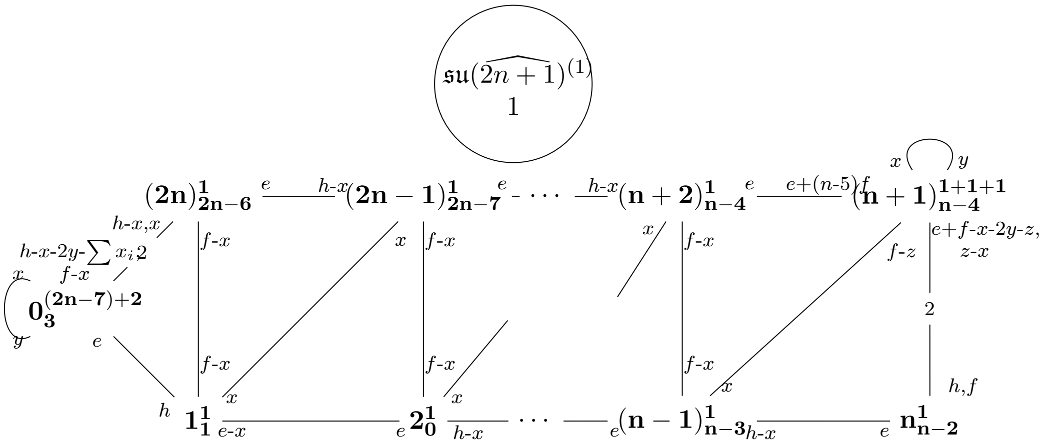

(5.108)

The above two examples are not completely geometric. See the discussion after equation (5.160).

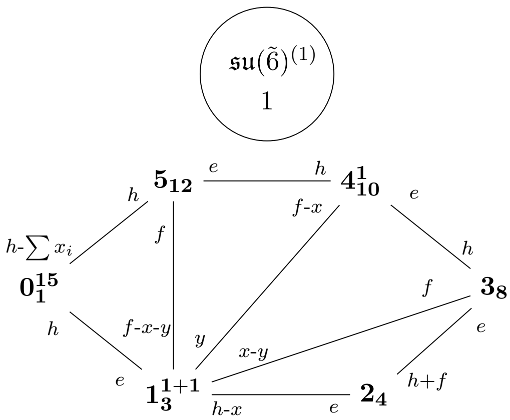

(5.109)

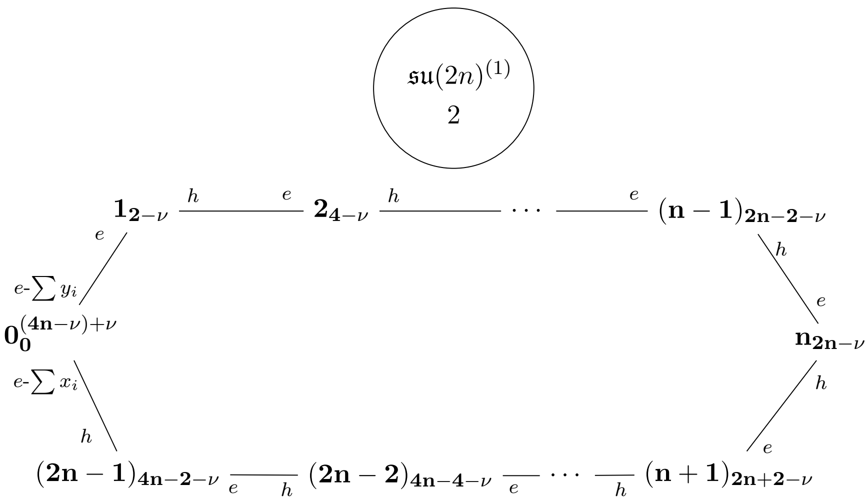

(5.110)

where $0 \leq \nu \leq 4n$ and $n \geq 2$.

For $n = 1$, we have

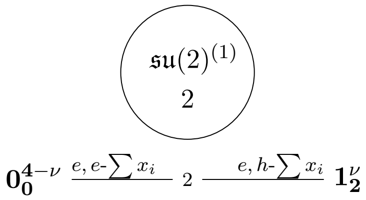

(5.111)

where $0 \leq \nu \leq 4$.

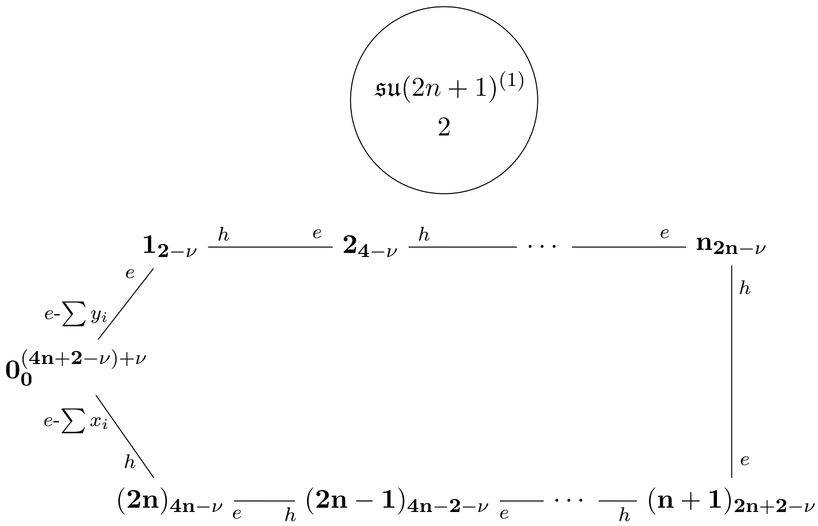

(5.112)

where $0 \leq \nu \leq 4n + 2$ and $n \geq 1$.

For $n = 0$, we claim that the geometry is

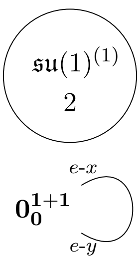

(5.113)

which can be recognized as a limit of $\nu = 1$ phase of (5.112). See appendix B.1 for a

JHEP12(2020)151

derivation that this is the correct answer.

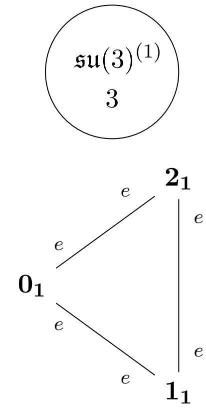

(5.114)

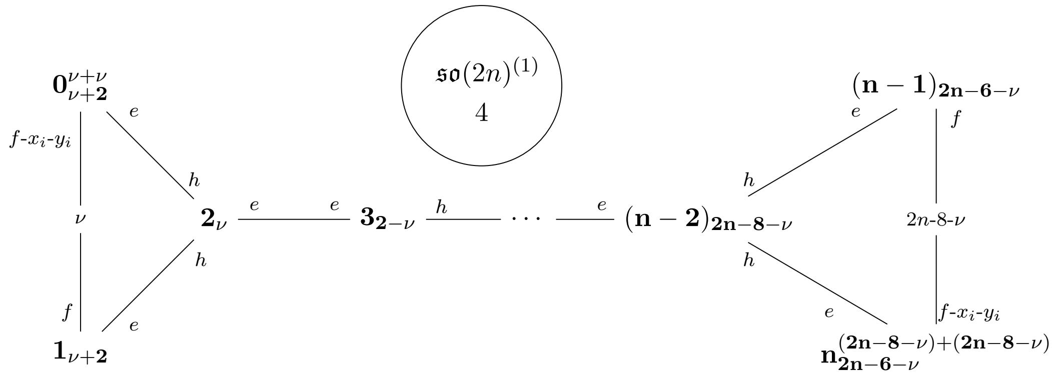

(5.115)

where $0 \leq \nu \leq 2n-8$.

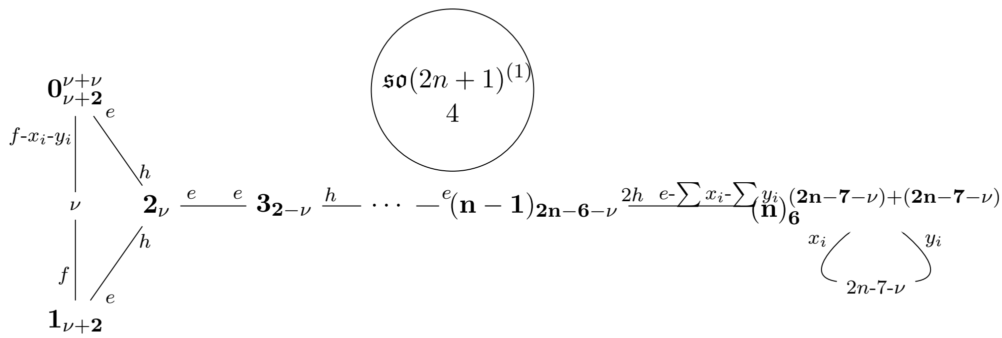

(5.116)

where $0 \leq \nu \leq 2n-7$.

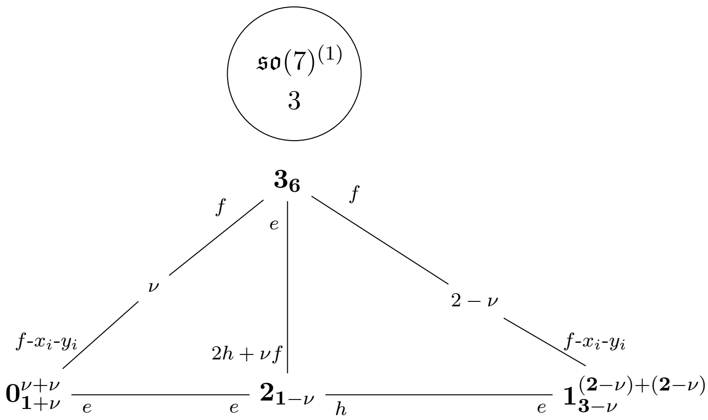

(5.117)

where $0 \leq \nu \leq 1$.

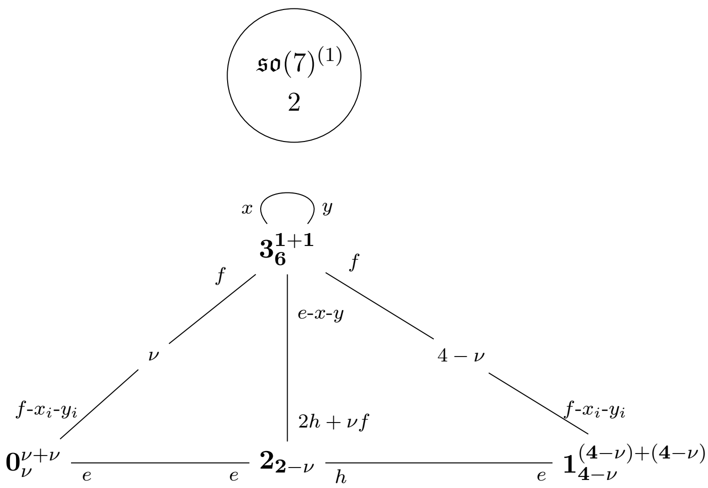

(5.118)

where $0 \leq \nu \leq 2$.

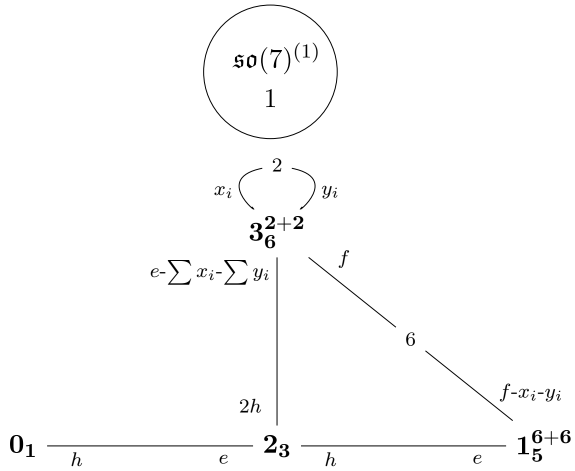

(5.119)

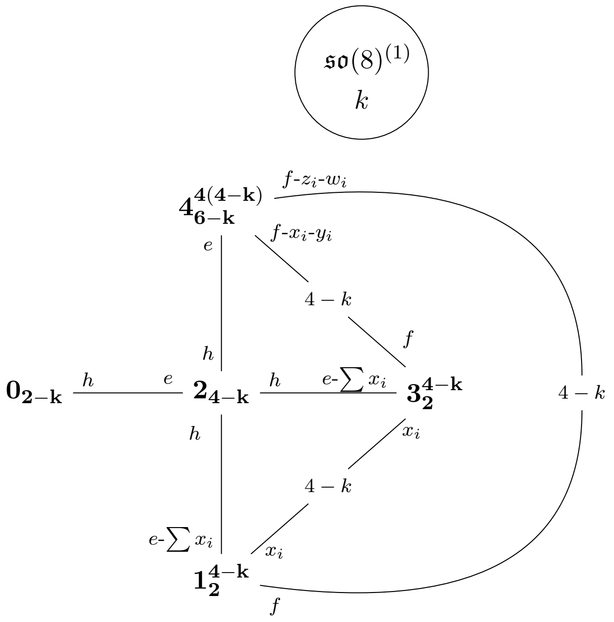

(5.120)

where $1 \leq k \leq 3$ and we have divided the $16-4k$ blowups into four sets of $4-k$ blowups each. We label blowups in the four sets by x_i, y_i, z_i and w_i respectively.

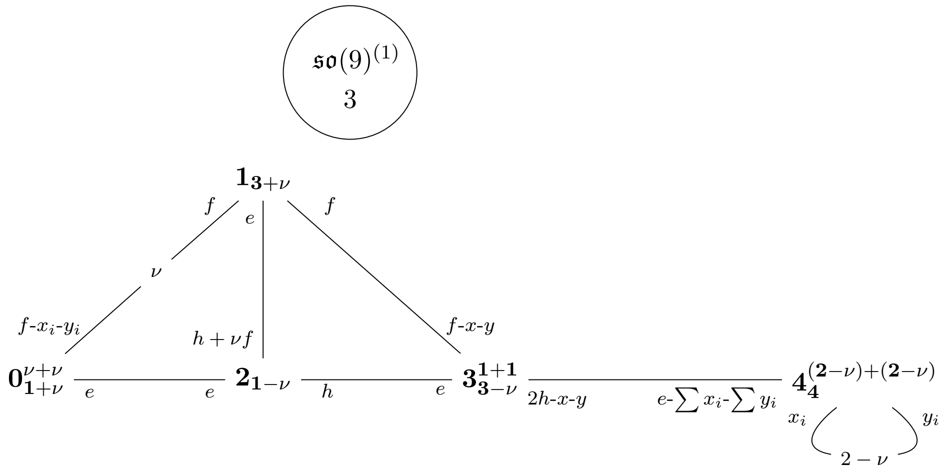

(5.121)

where $0 \leq \nu \leq 1$.

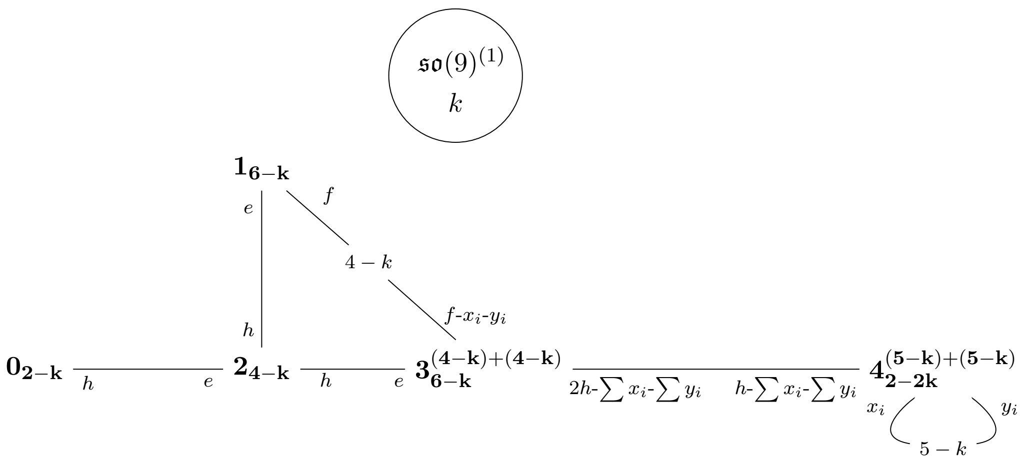

(5.122)

where $1 \leq k \leq 2$.

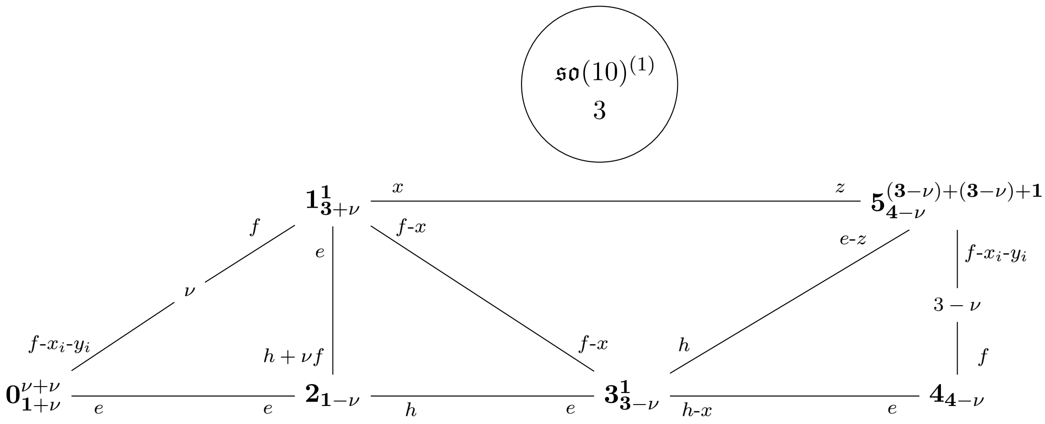

(5.123)

where $0 \leq \nu \leq 1$.

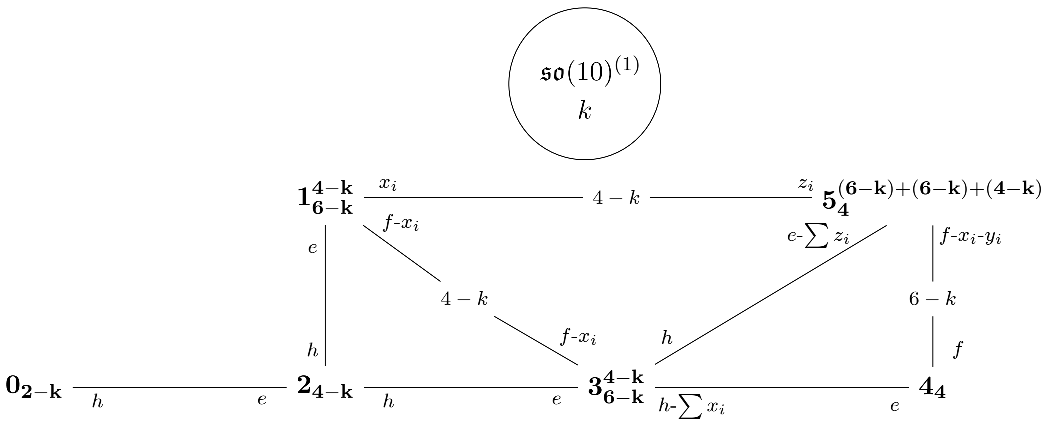

(5.124)

for $1 \leq k \leq 2$.

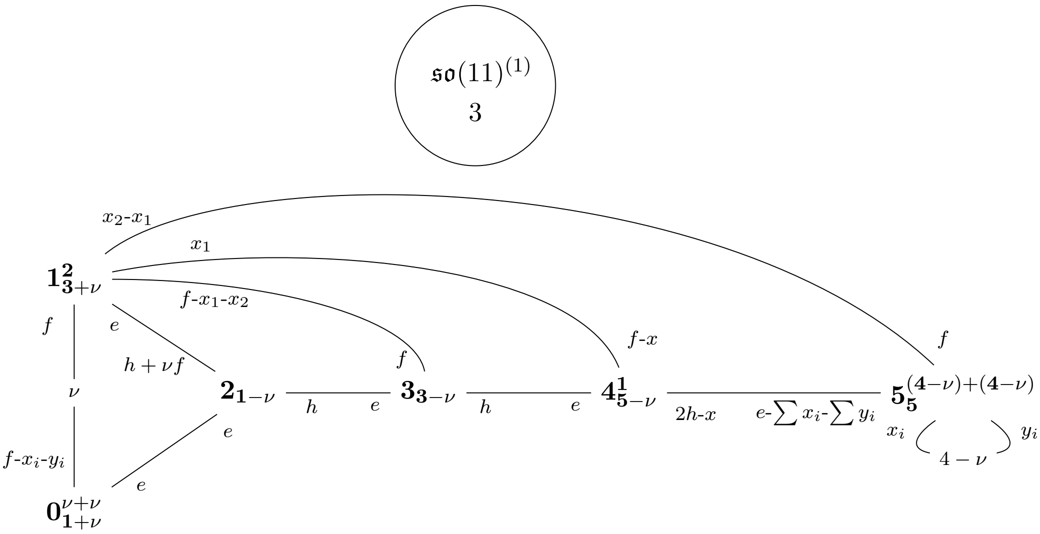

(5.125)

where $0 \leq \nu \leq 2$.

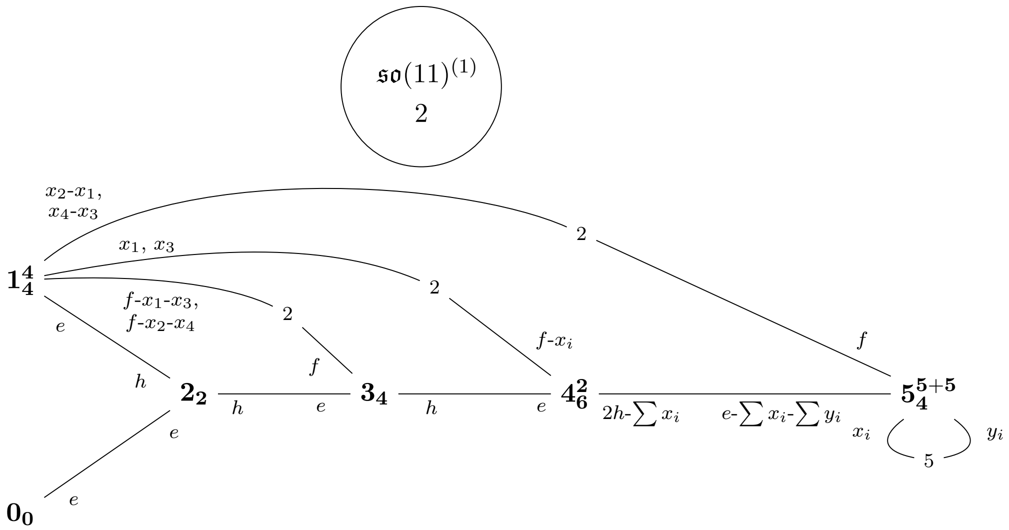

(5.126)

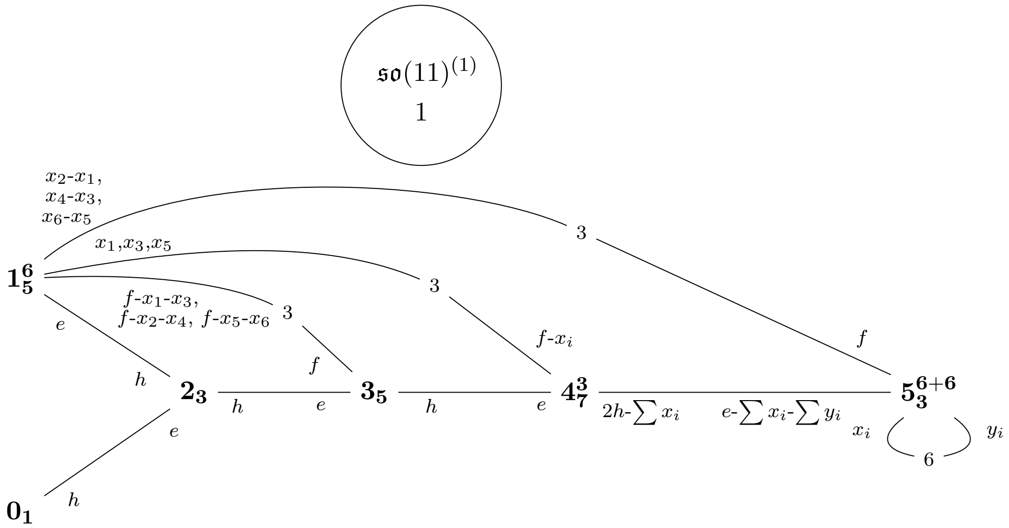

so(11)^(1)
1
x2-x1, x4-x3, x6-x5
x1,x3,x5
f-x1-x3, f-x2-x4, f-x5-x6
f-xi
2h-∑xi
e-∑xi-∑yi
xi
yi

(5.127)

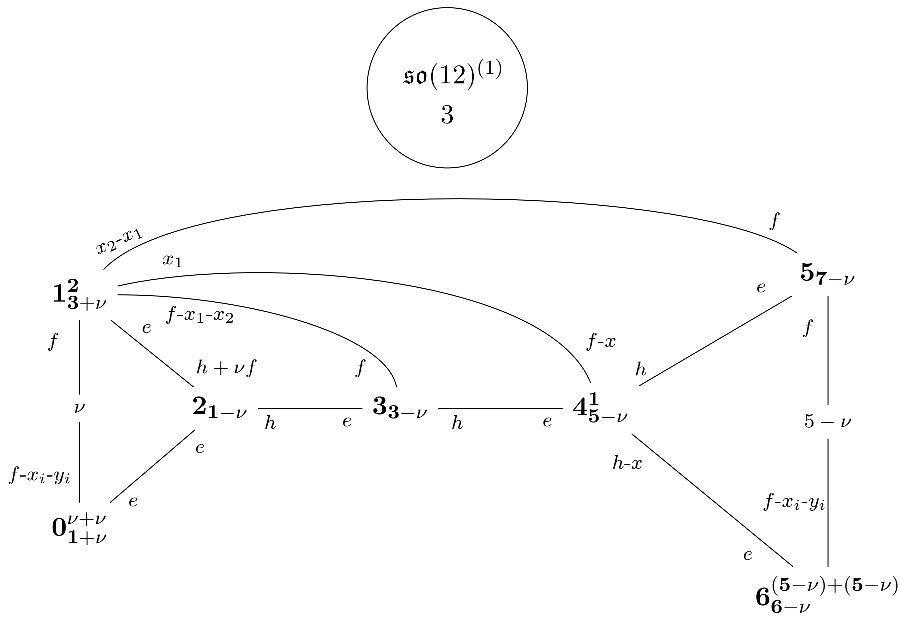

so(12)^(1)
3
x2-x1
x1
f-x1-x2
h + νf
f-x
h-x
f-xi-yi
5 − ν

(5.128)

where $0 \leq \nu \leq 2$.

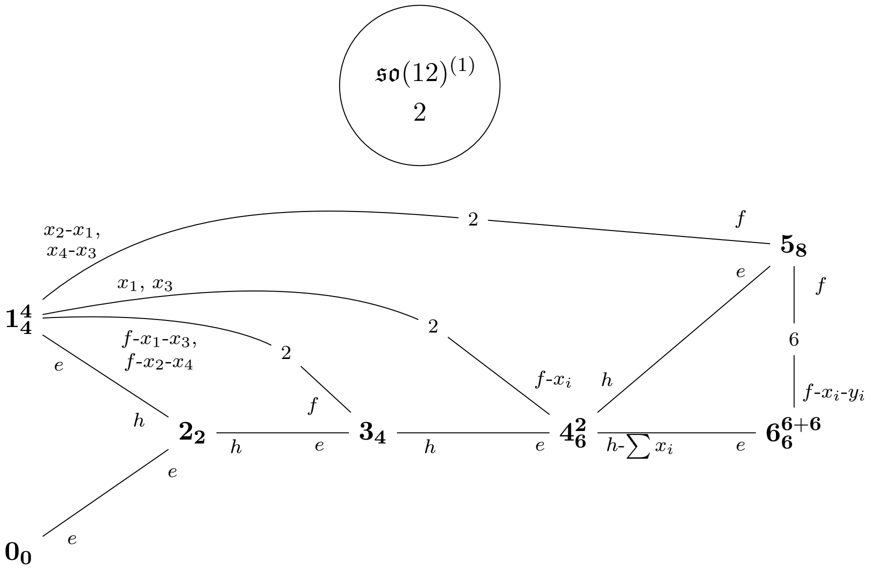

(5.129)

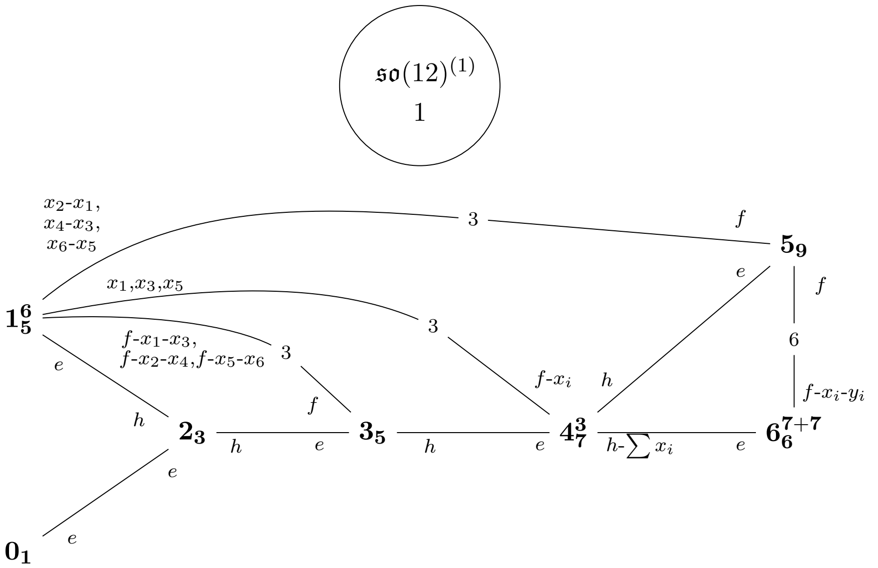

(5.130)

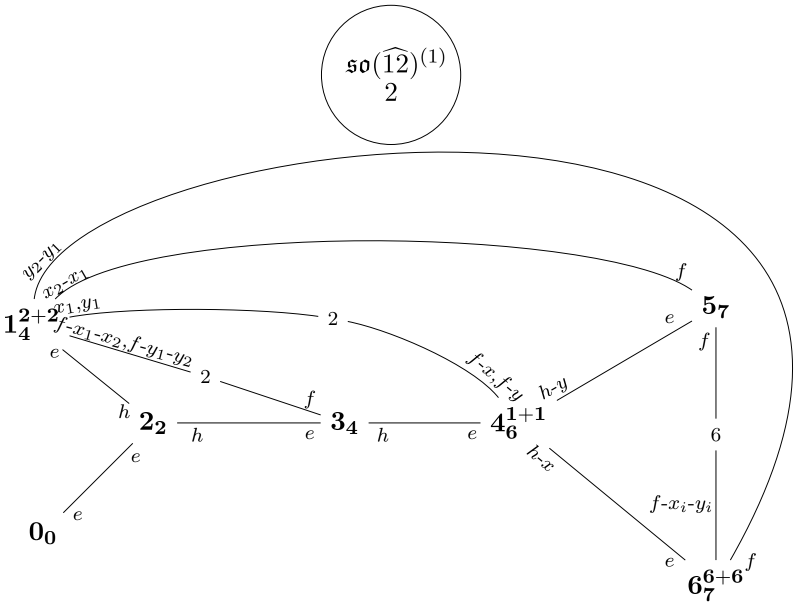
$\mathfrak{so}(\widehat{12})^{(1)}$
2
$\mathbf{1_4^{2+2}}$
$\mathbf{2_2}$
$\mathbf{3_4}$
$\mathbf{4_6^{1+1}}$
$\mathbf{5_7}$
$\mathbf{6_7^{6+6}}$
$\mathbf{0_0}$
y_2-y_1
x_2-x_1
x_1,y_1
f-x_1-x_2,f-y_1-y_2
f-x,f-y
h-y
h-x
f-x_i-y_i
2
2
6

(5.131)

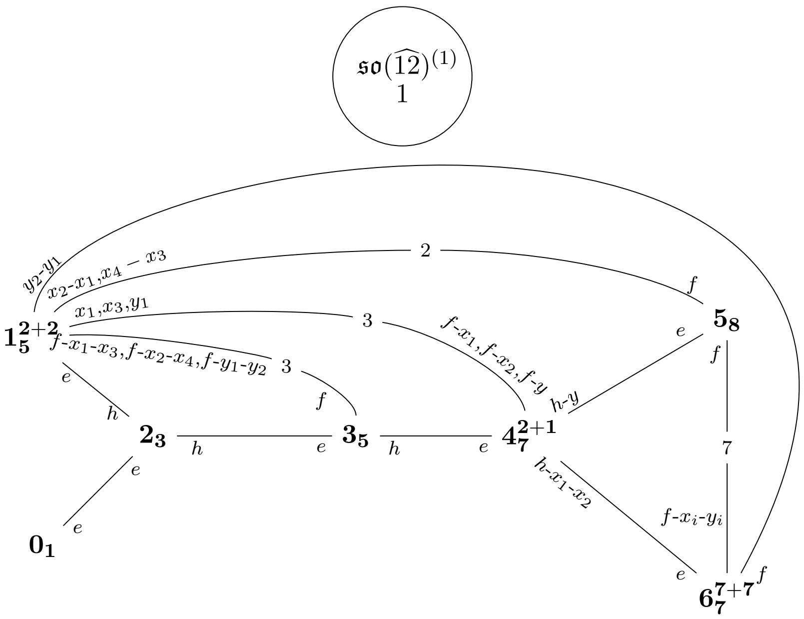
$\mathfrak{so}(\widehat{12})^{(1)}$
1
$\mathbf{1_5^{2+2}}$
$\mathbf{2_3}$
$\mathbf{3_5}$
$\mathbf{4_7^{2+1}}$
$\mathbf{5_8}$
$\mathbf{6_7^{7+7}}$
$\mathbf{0_1}$
y_2-y_1
x_2-x_1,x_4-x_3
x_1,x_3,y_1
f-x_1-x_3,f-x_2-x_4,f-y_1-y_2
f-x_1,f-x_2,f-y
h-y
h-x_1-x_2
f-x_i-y_i
2
3
3
7

(5.132)

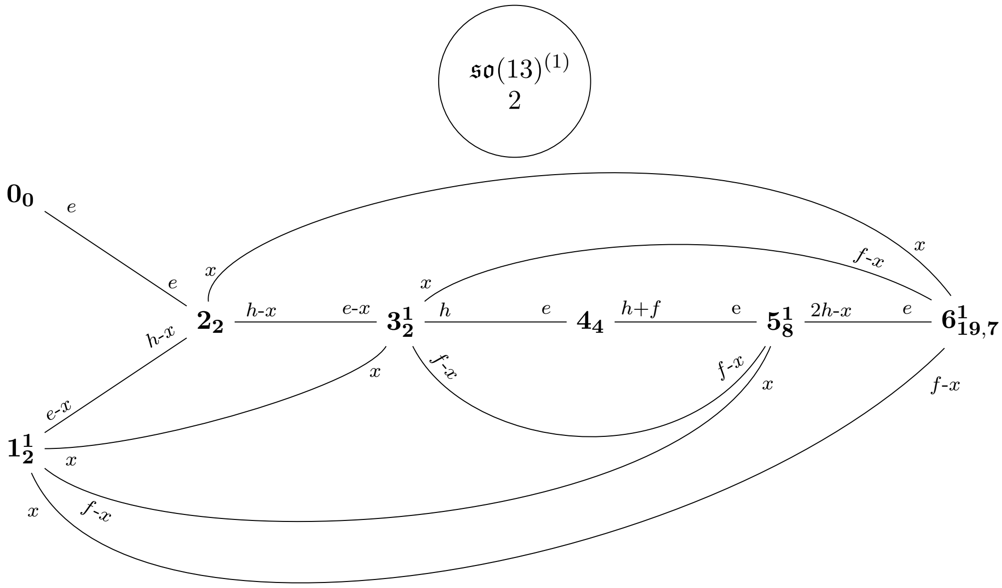

(5.133)

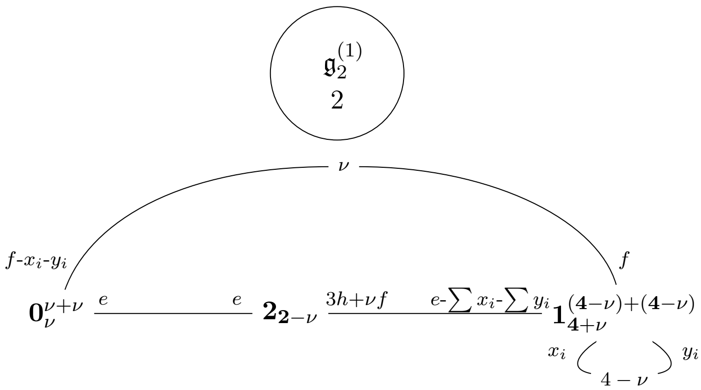

(5.134)

where $0 \leq \nu \leq 2$.

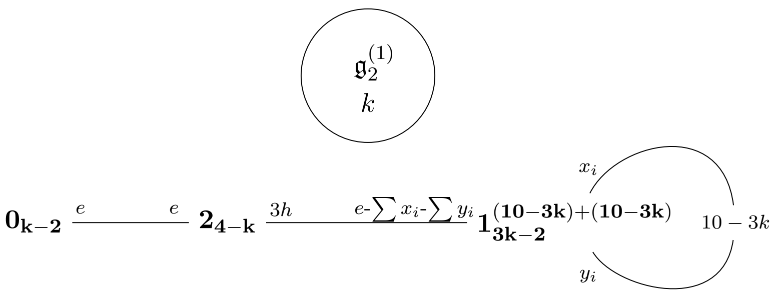

(5.135)

where $k = 1, 3$.

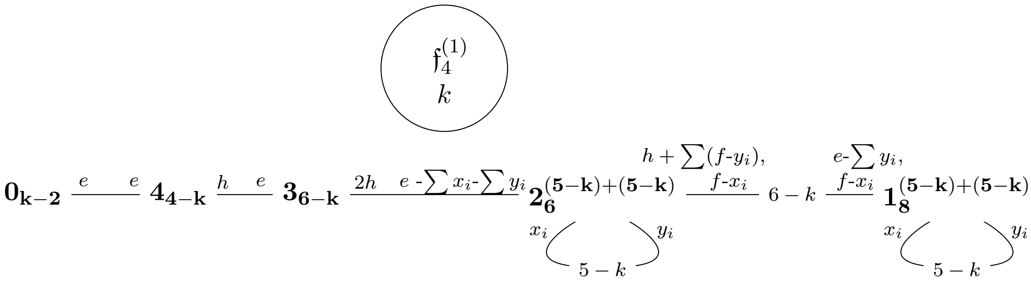

(5.136)

for $1 \le k \le 5$.

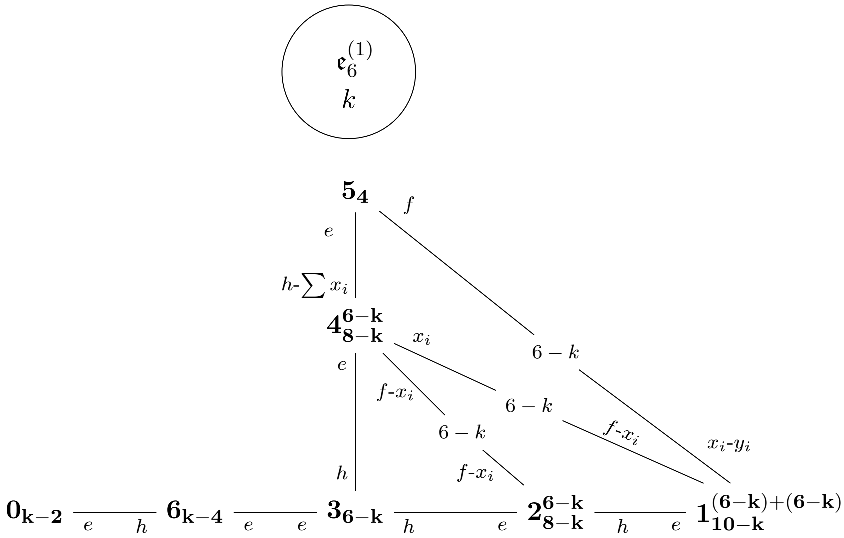

(5.137)

for $1 \le k \le 6$.

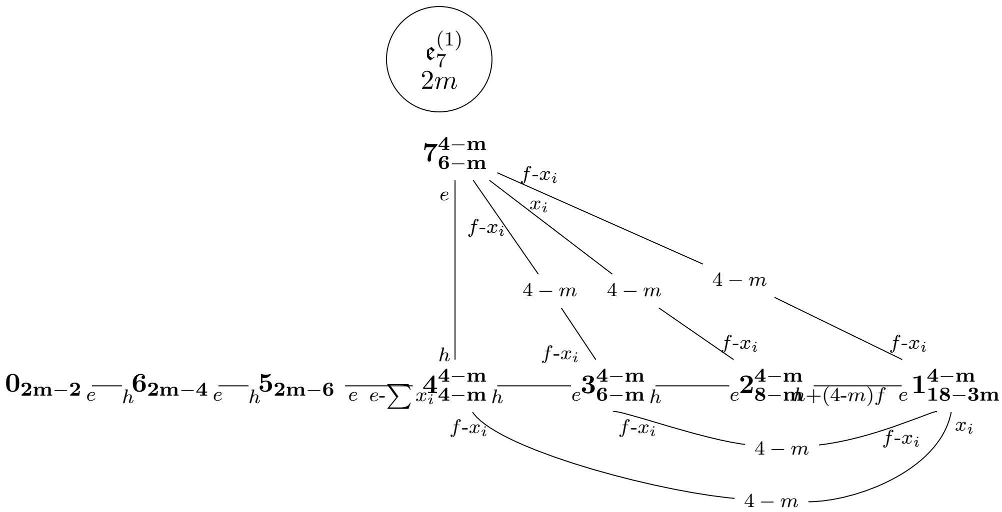

(5.138)

for $1 \leq m \leq 4$.

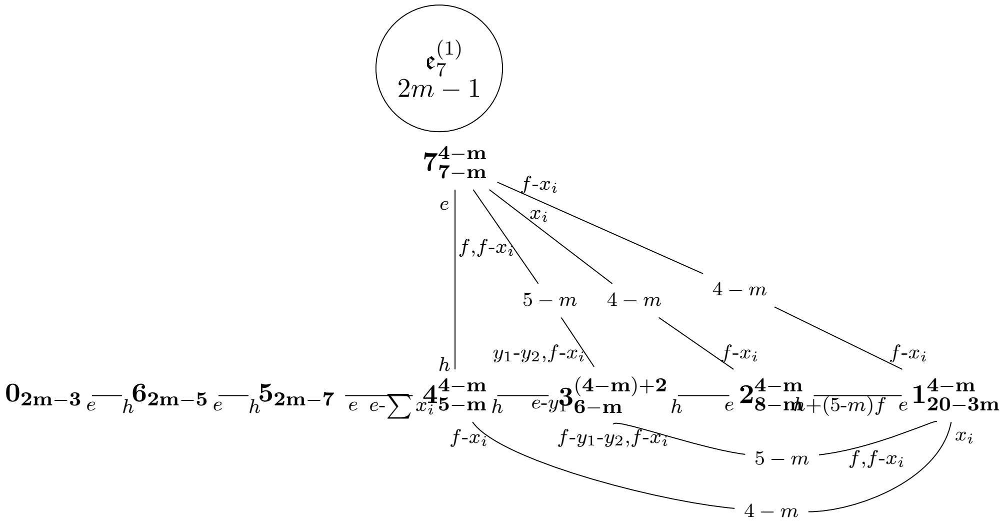

(5.139)

for $1 \leq m \leq 4$.

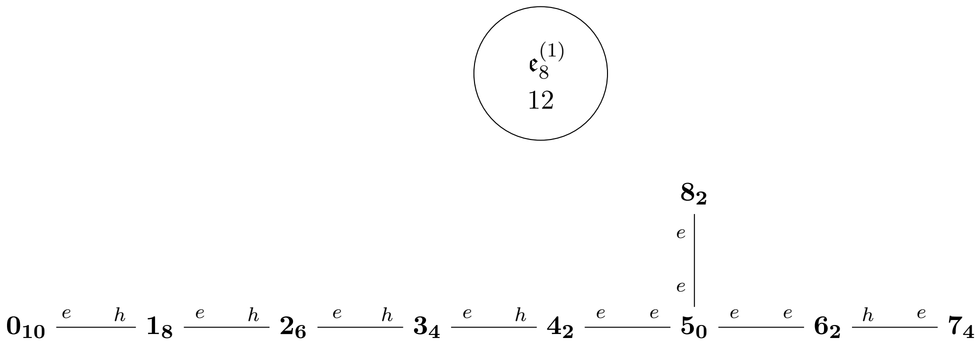

5.2.3 Twisted

In this subsection, we will generalize our results to nodes of the form

$$\begin{array}{c}\mathfrak{g}^{(q)}\\ k\end{array} \tag{5.140}$$

for $q > 1$ and

$$\begin{array}{c}\mathfrak{su}(n)^{(1)}\\ 2\end{array} \tag{5.141}$$

All such nodes are listed in table 8.

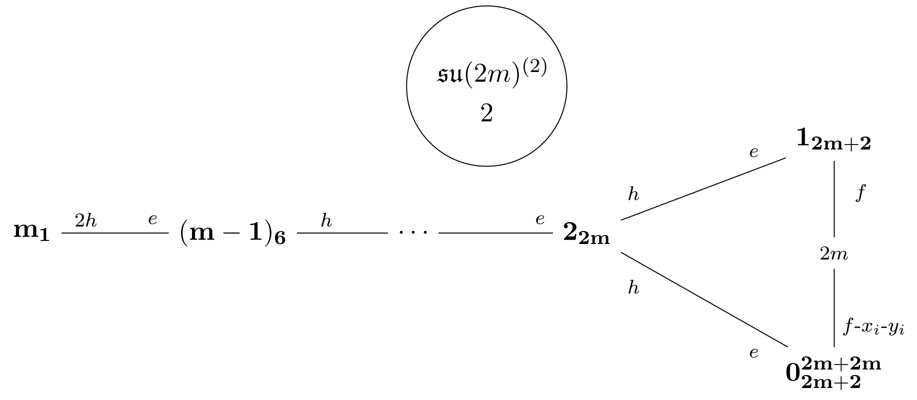

(5.142)

where $m \geq 3$. Notice that the Cartan matrix associated to this geometry is precisely that of $\mathfrak{su}(2m)^{(2)}$. Similar comments hold for all the geometries discussed below in this subsection. For each example below, one can check that $f_a \cdot S_b$ reproduces negative of Cartan matrix of the associated twisted affine algebra $\mathfrak{g}^{(q)}$.

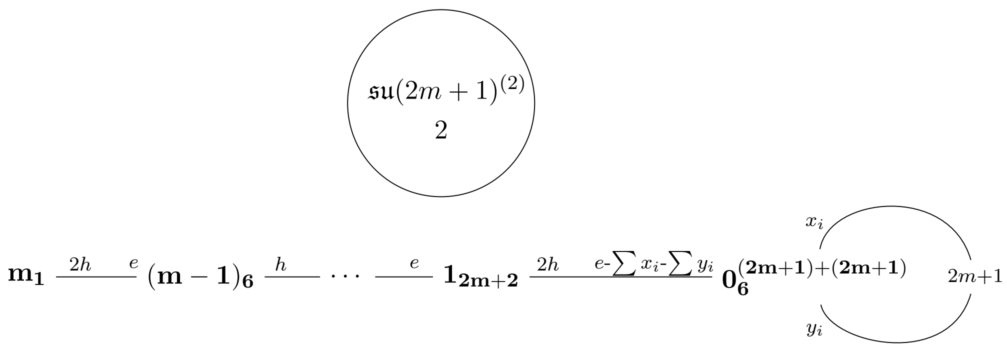

(5.143)

where $m \geq 2$.

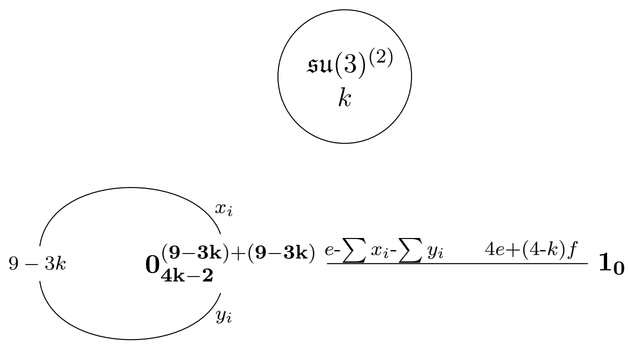

(5.144)

where $1 \leq k \leq 3$.

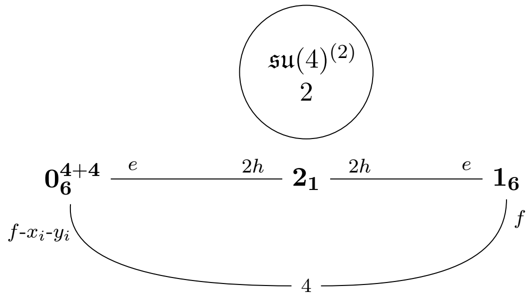

(5.145)

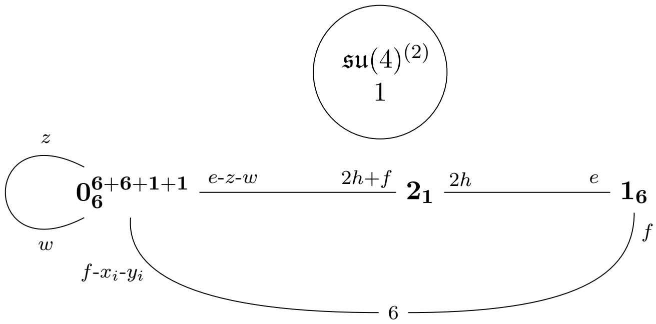

(5.146)

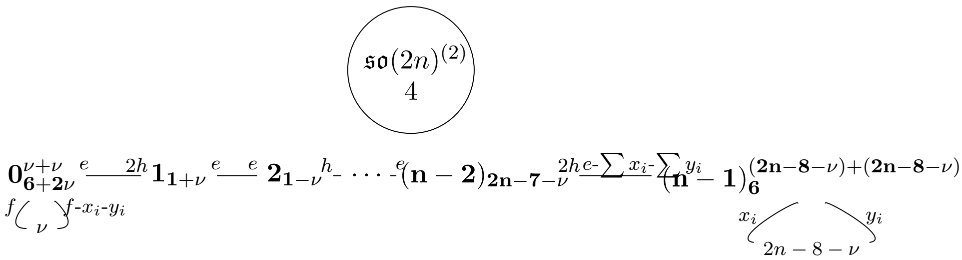

(5.147)

where $0 \leq \nu \leq 2n - 8$.

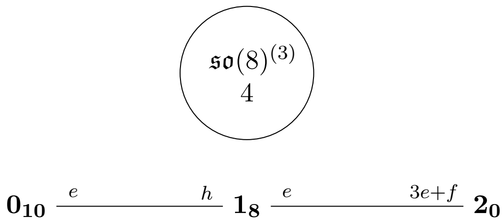

(5.148)

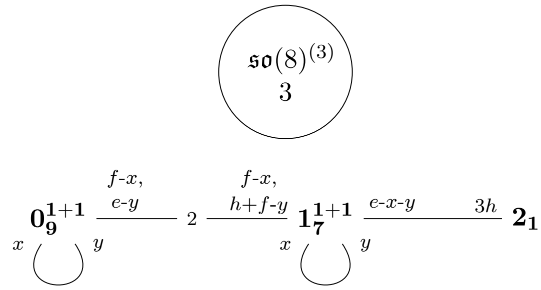

(5.149)

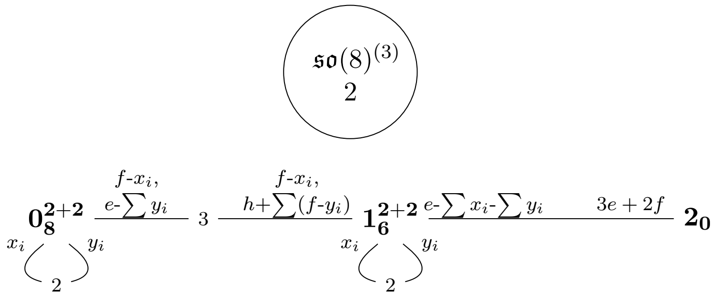

(5.150)

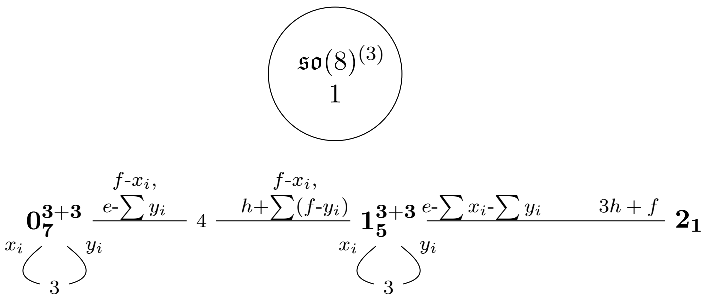

(5.151)

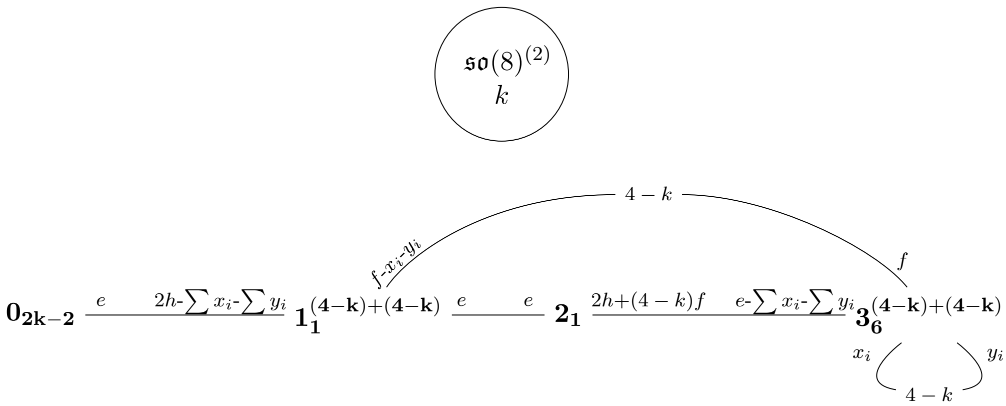

(5.152)

where $1 \leq k \leq 4$.

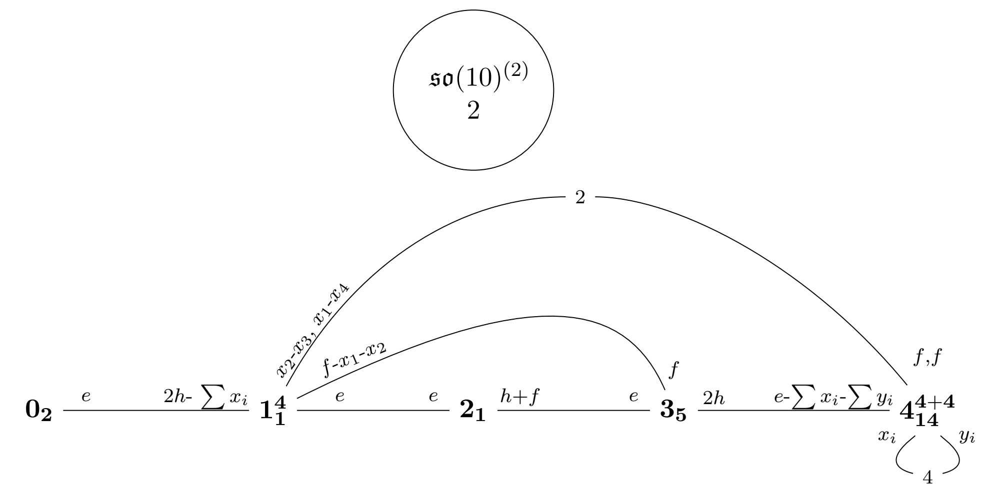

(5.153)

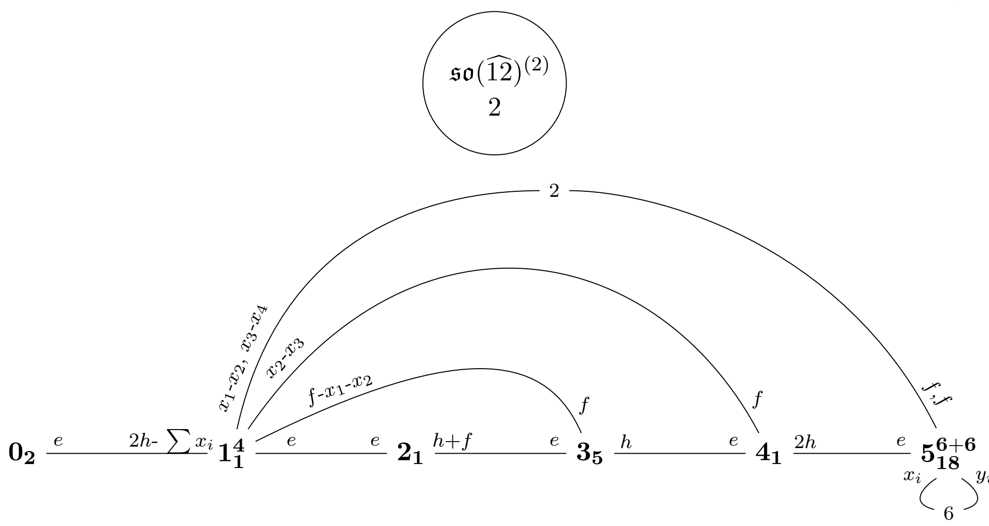

(5.154)

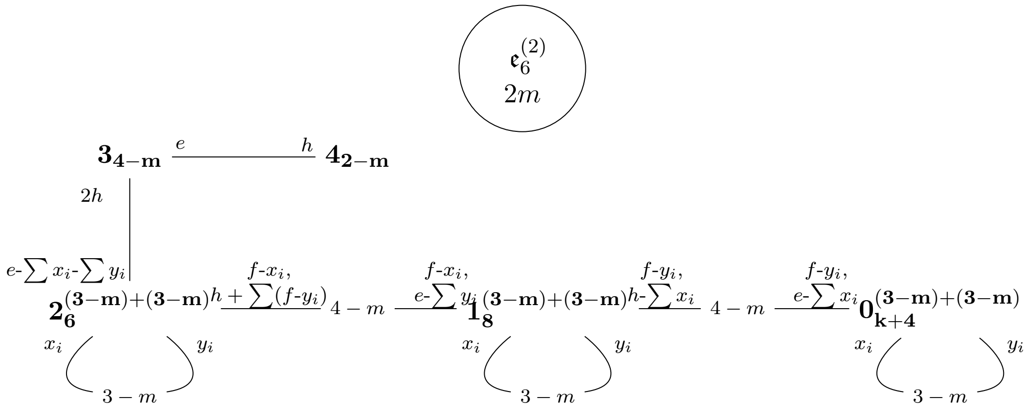

(5.155)

for $1 \leq m \leq 3$.

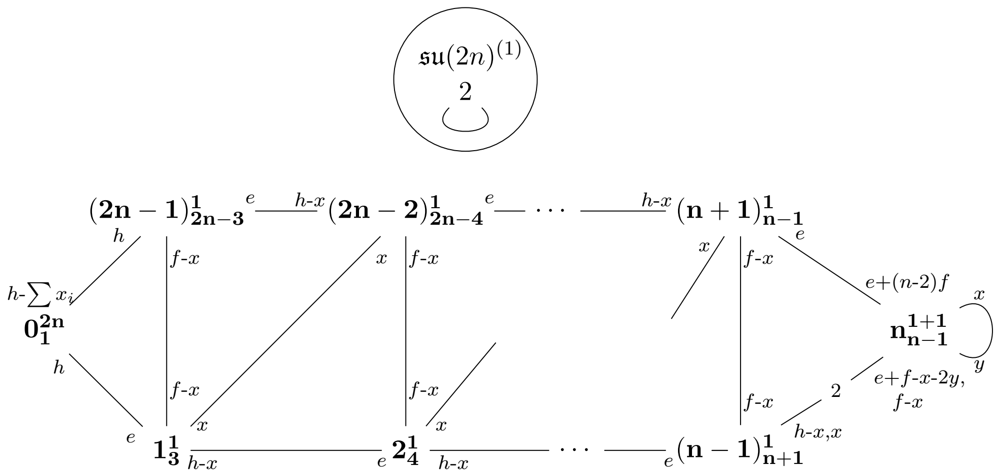

(5.156)

for $n \geq 2$.

For $n = 1$, we have

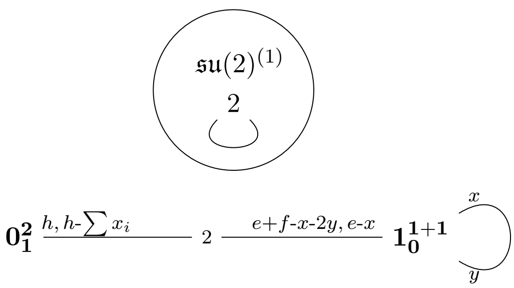

(5.157)

Now we discuss some examples which are not completely geometric:

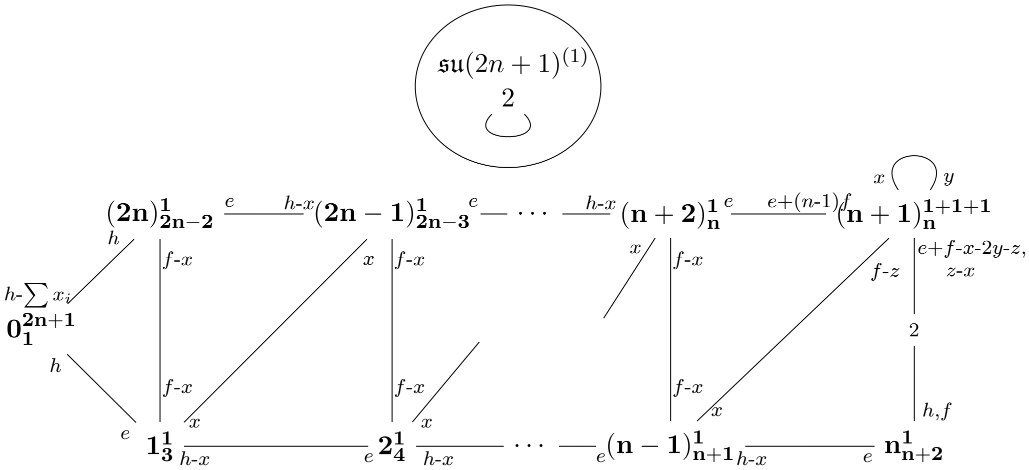

(5.158)

for $n \geq 2$.

For $n = 1$ we have

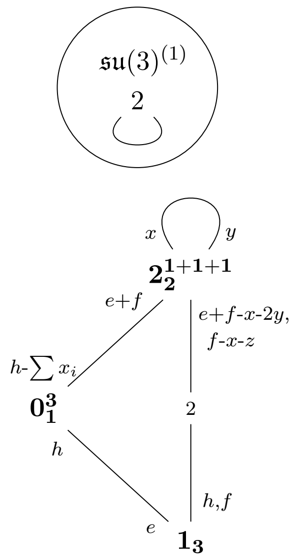

(5.159)

For $n = 0$ we have

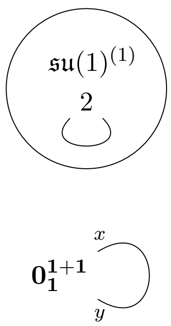

(5.160)

Let us now discuss the reasons why the above five examples are not completely geometric. Let us start with (5.160). The geometry for this example contains the -1 curve $h-x-y$ and hence an M2 brane wrapping this curve should give rise to a BPS particle. However, this BPS particle cannot appear in the associated $5d$ KK theory for the following reason. The existence of a particle associated to $h-x-y$ implies that the KK mode, which is associated to the elliptic curve $2h+f-2x-2y$, decomposes as a bound state of $h-x-y$ and $h+f-x-y$ but this is a contradiction since these two curves do not meet each other and hence there cannot be such a bound state.

Another reasoning is as follows. The volume of f is 2ϕ where ϕ is the Coulomb branch parameter associated to the above surface. On the other hand, the volume of $h-x-y$ is $-\phi$. Requiring non-negative volumes for both curves implies that ϕ must be zero. In other words, there is no direction in the Coulomb branch where all BPS particles have non-negative mass. Thus, this geometry is not *marginal*, in the sense defined by [2], which is a condition that must be satisfied by geometries associated to KK theories.

The precise sense in which the above self-glued $\mathbb{F}_1$ surface is associated to the KK theory

$$\overset{\mathfrak{su}(1)^{(1)}}{2} \tag{5.161}$$

is as follows. The Mori cone of the surface is generated by $h-x-y, f-x, x, e$. However, since the curve $h-x-y$ does not correspond to a BPS particle, the generators of the Mori cone thus do not correspond to the fundamental BPS particles[18] in the associated KK theory (5.161). We propose that the fundamental BPS particles instead correspond to the curves $2h-x-2y, f-x, x, e$. This set of curves satisfies all the properties that must be satisfied by the generators of the Mori cone of a surface. Thus, it is a complete set which can be consistently associated to fundamental BPS particles. The KK mode can be found as a bound state of $2h-x-2y$ and $f-x$. One can check that this set of proposed BPS particles is marginal in the sense that it allows a direction in Coulomb branch with all BPS particles having non-negative volumes. See also appendix B.1 where we verify that this description of the KK theory allows the existence of an RG flow to an $\mathcal{N}=2$ $5d$ SCFT, which is a fact well-known in the literature.

There are two viewpoints one can take on the relationship between self-glued $\mathbb{F}_1$ and the KK theory (5.161). The first is that indeed compactifying M-theory on this surface leads to the KK theory (5.161), but the compactification has some extra ingredients which account for the mismatch between the set of Mori cone generators and the set of fundamental BPS particles.[19] The other viewpoint is that the relationship with self-glued $\mathbb{F}_1$ has no deep meaning and is probably a red herring. At the time of writing of this paper, we do not

[18]We define a fundamental BPS particle to be a BPS particle that cannot arise as a bound state of other BPS particles.

[19]A similar situation occurs in the frozen phase of F-theory [32], where the set of generators of the Mori cone of the base of a threefold used for compactifying F-theory does not match the set of fundamental BPS strings arising in the associated $6d$ theory.

know which of these two viewpoints, or if either of these two viewpoints, is the correct one. We leave this issue for future exploration, and only use the relationship between the two as an algebraic tool to build a formalism for KK theories from which one can explicitly perform RG flows to $5d$ SCFTs.

Now let us discuss the non-geometric nature of the KK theories

$$\begin{array}{c}\mathfrak{su}(m)^{(1)}\\ 2\end{array} \tag{5.162}$$

with $m > 1$. Consider as an example the case of $m = 3$. The surface S_2 contains a gluing curve $e + f - x - 2y$ and hence there must be a BPS particle associated to it. However, notice that it decomposes as $e+f-x-2y = (e-x-y)+(f-y)$ such that the components $e-x-y$ and $f-y$ do not intersect each other. This leads to the same problem as discussed above, and we are forced to hypothesize that the fundamental BPS particles are distinct from the generators of Mori cone due to some non-geometric feature in the M-theory compactification. It is also evident that some of the components of the gluing curves in certain surfaces (which are identified with irreducible curves in adjacent surfaces as part of the gluing construction) fail to satisfy the necessary properties of irreducible curves that are described at the beginning of section 5.1.2.[20] Similar comments apply to each of the $m > 1$ models presented above should be regarded as an algebraic proposal which retains many of the features of the local threefolds that seem to be necessary to compute RG flows to 5d SCFTs.

Similar comments apply to (5.107) and (5.108), and they are also not conventionally geometric.

5.3 Gluing rules between two gauge theoretic nodes

In this section we will describe how to glue the surfaces $S_{a,\alpha}$ corresponding to a node α to the surfaces $S_{b,\beta}$ corresponding to another node β if there is an edge between α and β. The gluing rules are different for different kinds of edges between the two nodes. It turns out that the gluing rules between α and β are insensitive to the values of $\Omega^{\alpha\alpha}$ and $\Omega^{\beta\beta}$. This was also true for all of the cases studied in [4]. For this reason, we will often suppress the data of $\Omega^{\alpha\alpha}$ and $\Omega^{\beta\beta}$ in this subsection.

As a preface to the following subsections, we re-emphasize that the gluing rules must be compatible with the general consistency conditions described in section 5.1.2, and those that do not must again be regarded, most conservatively, as an algebraic proposal that retains certain salient features of conventional smooth threefold geometries. The basic, underlying hypothesis of the gluing rules is that, given a pair of geometries corresponding to circle compactifications of 6d SCFTs, if there exists a consistent gluing of these two

[20]For example, in the case $m = 3$, one can see that the surface $\mathbf{2}_{\mathbf{0}}^{\mathbf{1+1+1}}$ contains a curve class $e+f-x-2y$, which is identified with the curve class h in the surface $\mathbf{1_3}$. Since h is irreducible, this implies that $e+f-x-2y$ must also be irreducible, but this leads to a contradiction (with smoothness) if the usual class $f-y$ remains among the generators of the Mori cone of $\mathbf{2}_{\mathbf{0}}^{\mathbf{1+1+1}}$.

nodes along their respective genus one fibers, then there must also exist a mutual gauging of the respective global symmetries of the parent 6d SCFTs that allows the two theories to be coupled together in the sense described in section 2.

5.3.1 Undirected edges between untwisted algebras

Such edges are displayed in table 3. The gluing rules for all of these cases except for $\mathfrak{su}(n_\alpha)^{(1)} \overset{2}{—} \mathfrak{so}(n_\beta)^{(1)}$ were first studied in [4]. We are able to reproduce their results using our methods.

Gluing rules for $\boldsymbol{\mathfrak{sp}(n_\alpha)^{(1)}_\theta}$ —— $\boldsymbol{\mathfrak{su}(n_\beta)^{(1)}}$: we can take any geometry with $0 \le \nu \le 2n_\alpha + 8 - n_\beta$ for $\mathfrak{sp}(n_\alpha)^{(1)}_\theta$, and any geometry with $0 \le \nu \le 2n_\beta - 2n_\alpha$ for $\mathfrak{su}(n_\beta)^{(1)}$. The gluing rules below work irrespective of the value of θ. The gluing rules are:

- $f - x_1, x_{n_\beta}$ in $S_{0,\alpha}$ are glued to $f - x_1, x_{2n_\alpha}$ in $S_{0,\beta}$.
- $x_i - x_{i+1}$ in $S_{0,\alpha}$ is glued to f in $S_{i,\beta}$ for $i = 1, \cdots, n_\beta - 1$.
- $x_i - x_{i+1}, x_{2n_\alpha - i} - x_{2n_\alpha - i+1}$ in $S_{0,\beta}$ are glued to f, f in $S_{i,\alpha}$ for $i = 1, \cdots, n_\alpha - 1$.
- $x_{n_\alpha} - x_{n_\alpha+1}$ in $S_{0,\beta}$ is glued to f in $S_{n_\alpha,\alpha}$.

By convention, the first item in the above list of gluing rules displays the gluings in an order. That is, $f - x_1$ in $S_{0,\alpha}$ is glued to $f - x_1$ in $S_{0,\beta}$ and x_{n_β} in $S_{0,\alpha}$ is glued to x_{2n_α} in $S_{0,\beta}$. We will adopt this convention in what follows. All the gluings should be read in the order in which they are written.

Let us label the fiber of the Hirzebruch surface $S_{a,\alpha}$ as $f_{a,\alpha}$ and the fiber of the Hirzebruch surface $S_{b,\beta}$ as $f_{b,\beta}$. According the above gluing rules, $f_{0,\alpha}$ is glued to $f_{0,\beta} - x_1 + x_{2n_\alpha} + \sum_{i=1}^{n_\beta - 1} f_{i,\beta}$ where x_1 and x_{2n_α} are blowups in $S_{0,\beta}$, and $2\sum_{i=1}^{n_\alpha - 1} f_{i,\alpha} + f_{n_\alpha,\alpha}$ is glued to $x_1 - x_{2n_\alpha}$ in $S_{0,\beta}$. Combining these two we see that

$$f_{0,\alpha} + 2\sum_{i=1}^{n_\alpha - 1} f_{i,\alpha} + f_{n_\alpha,\alpha} \sim \sum_{i=0}^{n_\beta - 1} f_{i,\beta} \tag{5.163}$$

thus confirming the gluing rule (5.60) for the torus fibers. In a similar fashion, the reader can verify that (5.60) is satisfied for all the gluing rules that follow.

The theta angle of $\mathfrak{sp}(n_\alpha)$ is physically irrelevant if $n_\beta < 2n_\alpha + 8$ and physically relevant if $n_\beta = 2n_\alpha + 8$. Thus the above gluing rules should allow the isomorphism between (5.100) and (5.101) to extend to the combined geometry for

$$\mathfrak{sp}(n_\alpha)^{(1)}_\theta \text{ ——— } \mathfrak{su}(n_\beta)^{(1)} \tag{5.164}$$

in the case $n_\beta < 2n_\alpha + 8$, but not in the case of $n_\beta = 2n_\alpha + 8$.

To see this for $n_\beta < 2n_\alpha + 8$, we can go to the flop frame $\nu = 1$ for $\mathfrak{sp}(n_\alpha)^{(1)}_\theta$ without changing the above gluing rules. Then we can implement the map that formed the isomorphism between (5.100) and (5.101). Since the above gluing rules do not interact with blowups living on $S_{n_\alpha,\alpha}$, the map trivially extends to an isomorphism of the combined geometry associated to (5.164). For $n_\beta = 2n_\alpha + 8$, we cannot reach $\nu > 0$ frame without changing the above gluing rules. Thus the map implementing isomorphism between (5.100) and (5.101) does not extend to an isomorphism of the combined geometry associated to (5.164).

Gluing rules for $\mathfrak{sp}(n_\alpha)^{(1)}_\theta$ —— $\mathfrak{so}(2n_\beta)^{(1)}$: here we allow $2n_\beta = \widehat{12}$. We can take any geometry with $0 \le \nu \le 2n_\alpha + 8 - n_\beta$ for $\mathfrak{sp}(n_\alpha)^{(1)}_\theta$, and any geometry with $0 \le \nu \le 2n_\beta - 4 - \Omega^{\beta\beta} - n_\alpha$ for $\mathfrak{so}(2n_\beta)^{(1)}$. The gluing rules below work for both values of θ. In the future, if the value of θ is unspecified, then the gluing rules work for both the values. In our present case, the gluing rules are:

- $f - x_1 - x_2$ in $S_{0,\alpha}$ is glued to f in $S_{0,\beta}$.
- $x_i - x_{i+1}$ in $S_{0,\alpha}$ is glued to f in $S_{i,\beta}$ for $i = 1, \cdots, n_\beta - 1$.
- $x_{n_{\beta-1}}, x_{n_\beta}$ in $S_{0,\alpha}$ are glued to $f - x_1, y_1$ in $S_{n_\beta,\beta}$.
- $x_i - x_{i+1}, y_{i+1} - y_i$ in $S_{n_\beta,\beta}$ are glued to f, f in $S_{i,\alpha}$ for $i = 1, \cdots, n_\alpha - 1$.
- $x_{n_\alpha} - y_{n_\alpha}$ in $S_{n_\beta,\beta}$ is glued to f in $S_{n_\alpha,\alpha}$.

To show that the theta angle is irrelevant for $n_\beta < 2n_\alpha + 8$, we first notice that we can go to the flop frame $\nu = 1$ for $\mathfrak{sp}(n_\alpha)^{(1)}_\theta$ without changing the above gluing rules. Then the isomorphism between (5.100) and (5.101) extends to an isomorphism of the combined geometry for

$$\mathfrak{sp}(n_\alpha)^{(1)}_\theta \text{ ——— } \mathfrak{so}(2n_\beta)^{(1)} \tag{5.165}$$

For $n_\beta = 2n_\alpha + 8$, the above argument does not work since going to $\nu = 1$ frame changes the gluing rules. However, it turns out that the combined geometries for different θ are flop equivalent up to an outer automorphism of $\mathfrak{so}(2n_\beta)$. To see this, notice that the combined geometry for (5.165) is flop equivalent to the following geometry. We pick the frame $\nu = 2n_\alpha + 8$ for $\mathfrak{sp}(n_\alpha)^{(1)}_\theta$ and $\nu = 2n_\beta - 8$ for $\mathfrak{so}(2n_\beta)^{(1)}$ with the gluing rules being:

- $f - x_1 - x_2$ in $S_{n_\alpha,\alpha}$ is glued to f in $S_{n_\beta,\beta}$.
- $x_i - x_{i+1}$ in $S_{n_\alpha,\alpha}$ is glued to f in $S_{n_\beta-i,\beta}$ for $i = 1, \cdots, n_\beta - 1$.
- $x_{n_{\beta-1}}, x_{n_\beta}$ in $S_{n_\alpha,\alpha}$ are glued to $f - x_1, y_1$ in $S_{0,\beta}$.
- $x_i - x_{i+1}, y_{i+1} - y_i$ in $S_{0,\beta}$ are glued to f, f in $S_{n_\alpha-i,\alpha}$ for $i = 1, \cdots, n_\alpha - 1$.
- $x_{n_\alpha} - y_{n_\alpha}$ in $S_{0,\beta}$ is glued to f in $S_{0,\alpha}$.

Now it is clear that exchanging $f - x_1$ and x_1 interchanges $S_{n_\beta,\beta}$ and $S_{n_\beta-1,\beta}$. Thus the choice of theta angle for $\mathfrak{sp}(n_\alpha)^{(1)}$ is correlated to the choice of an outer automorphism frame of $\mathfrak{so}(2n_\beta)^{(1)}$ for $n_\beta = 2n_\alpha + 8$.

The gluing rules for a configuration having multiple edges are simply obtained by combining the gluing rules mentioned above. We have to just make sure that we never use the same blowup twice. For example, consider the configuration

$$\mathfrak{su}(n_\gamma)^{(1)} \text{------} \mathfrak{sp}(n_\alpha)_\theta^{(1)} \text{------} \mathfrak{so}(2n_\beta)^{(1)} \tag{5.166}$$

Then we can use any geometry with $0 \leq \nu \leq 2n_\alpha + 8 - n_\beta - n_\gamma$ for $\mathfrak{sp}(n_\alpha)_\theta^{(1)}$, any geometry with $0 \leq \nu \leq 2n_\beta - 4 - \Omega^{\beta\beta} - n_\alpha$ for $\mathfrak{so}(2n_\beta)^{(1)}$, and any geometry with $0 \leq \nu \leq 2n_\gamma - 2n_\alpha$ for $\mathfrak{su}(n_\gamma)^{(1)}$. The gluing rules for the sub-configuration

$$\mathfrak{sp}(n_\alpha)_\theta^{(1)} \text{------} \mathfrak{so}(2n_\beta)^{(1)} \tag{5.167}$$

are the same as the ones listed above, while the gluing rules for the sub-configuration

$$\mathfrak{sp}(n_\alpha)_\theta^{(1)} \text{------} \mathfrak{su}(n_\gamma)^{(1)} \tag{5.168}$$

are as follows:

- $f - x_{n_\beta+1}, x_{n_\beta+n_\gamma}$ in $S_{0,\alpha}$ are glued to $f - x_1, x_{2n_\alpha}$ in $S_{0,\gamma}$.
- $x_{n_\beta+i} - x_{n_\beta+i+1}$ in $S_{0,\alpha}$ is glued to f in $S_{i,\gamma}$ for $i = 1, \cdots, n_\gamma - 1$.
- $x_i - x_{i+1}, x_{2n_\alpha-i} - x_{2n_\alpha-i+1}$ in $S_{0,\gamma}$ are glued to f, f in $S_{i,\alpha}$ for $i = 1, \cdots, n_\alpha - 1$.
- $x_{n_\alpha} - x_{n_\alpha+1}$ in $S_{0,\gamma}$ is glued to f in $S_{n_\alpha,\alpha}$.

In a similar way, by choosing mutually exclusive sets of blowups, we can combine the gluing rules to obtain geometries for graphs with multiple algebras and edges between them. Sometimes some of the blowups are allowed to appear in more than one gluing rules. In such cases, we will explicitly mention such blowups and the configurations in which they can appear in multiple gluing rules.

Gluing rules for $\boldsymbol{\mathfrak{sp}(n_\alpha)_\theta^{(1)}}$ —— $\boldsymbol{\mathfrak{so}(2n_\beta+1)^{(1)}}$: we can take any geometry with $1 \leq \nu \leq 2n_\alpha + 8 - n_\beta$ for $\mathfrak{sp}(n_\alpha)_\theta^{(1)}$, and any geometry with $0 \leq \nu \leq 2n_\beta - 3 - \Omega^{\beta\beta} - n_\alpha$ for $\mathfrak{so}(2n_\beta + 1)^{(1)}$. The gluing rules are:

- $f - x_1 - x_2$ in $S_{0,\alpha}$ is glued to f in $S_{0,\beta}$.
- $x_i - x_{i+1}$ in $S_{0,\alpha}$ is glued to f in $S_{i,\beta}$ for $i = 1, \cdots, n_\beta - 1$.
- x_{n_β}, x_{n_β} in $S_{0,\alpha}$ are glued to x_1, y_1 in $S_{n_\beta,\beta}$.
- $x_{i+1} - x_i, y_{i+1} - y_i$ in $S_{n_\beta,\beta}$ are glued to f, f in $S_{i,\alpha}$ for $i = 1, \cdots, n_\alpha - 1$.
- $f - x_{n_\alpha}, f - y_{n_\alpha}$ in $S_{n_\beta,\beta}$ are glued to $f - x_1, x_1$ in $S_{n_\alpha,\alpha}$.

To show that the theta angle is irrelevant, use the map that exchanges x_1 and $f - x_1$ in $S_{n_\alpha,\alpha}$. If this is accompanied by $x_i \leftrightarrow y_i$ in $S_{n_\beta,\beta}$, then the gluing rules remain unchanged.

Consider a configuration of the form

$$\mathfrak{so}(2n_\gamma+1)^{(1)} \text{ ——— } \mathfrak{sp}(n_\alpha)_\theta^{(1)} \text{ ——— } \mathfrak{so}(2n_\beta+1)^{(1)} \tag{5.169}$$

We wish to emphasize that we use the same blowup x_1 on $S_{n_\alpha,\alpha}$ in the gluing rules associated to both

$$\mathfrak{sp}(n_\alpha)_\theta^{(1)} \text{ ——— } \mathfrak{so}(2n_\beta+1)^{(1)} \tag{5.170}$$

and

$$\mathfrak{sp}(n_\alpha)_\theta^{(1)} \text{ ——— } \mathfrak{so}(2n_\gamma+1)^{(1)} \tag{5.171}$$

More explicitly, to obtain gluing rules for (5.169), we can take any geometry with $1 \leq \nu \leq 2n_\alpha + 8 - n_\beta - n_\gamma$ for $\mathfrak{sp}(n_\alpha)_\theta^{(1)}$, any geometry with $0 \leq \nu \leq 2n_\beta - 3 - \Omega^{\beta\beta} - n_\alpha$ for $\mathfrak{so}(2n_\beta+1)^{(1)}$, and any geometry with $0 \leq \nu \leq 2n_\gamma - 3 - \Omega^{\gamma\gamma} - n_\alpha$ for $\mathfrak{so}(2n_\gamma+1)^{(1)}$. The gluing rules for (5.170) are those listed above, and the gluing rules for (5.171) are:

- $f - x_{n_\beta+1} - x_{n_\beta+2}$ in $S_{0,\alpha}$ is glued to f in $S_{0,\gamma}$.
- $x_{n_\beta+i} - x_{n_\beta+i+1}$ in $S_{0,\alpha}$ is glued to f in $S_{i,\gamma}$ for $i = 1, \cdots, n_\gamma - 1$.
- $x_{n_{\beta+\gamma}}, x_{n_{\beta+\gamma}}$ in $S_{0,\alpha}$ are glued to x_1, y_1 in $S_{n_\gamma,\gamma}$.
- $x_{i+1} - x_i, y_{i+1} - y_i$ in $S_{n_\gamma,\gamma}$ are glued to f, f in $S_{i,\alpha}$ for $i = 1, \cdots, n_\alpha - 1$.
- $f - x_{n_\alpha}, f - y_{n_\alpha}$ in $S_{n_\gamma,\gamma}$ are glued to $f - x_1, x_1$ in $S_{n_\alpha,\alpha}$.

with the x_1 in $S_{n_\alpha,\alpha}$ being the same blowup as used in the gluing rules above for (5.170).

However, if we have a third neighbor $\mathfrak{so}(2n_\delta+1)^{(1)}$ of $\mathfrak{sp}(n_\alpha)_\theta^{(1)}$, then we must use a second blowup x_2 on $S_{n_\alpha,\alpha}$. As a consequence, we must choose a geometry with $2 \leq \nu \leq 2n_\alpha + 8 - n_\beta + n_\gamma + n_\delta$ for $\mathfrak{sp}(n_\alpha)_\theta^{(1)}$ to obtain the combined geometry for the configuration

$$\begin{array}{ccccc} & & \mathfrak{so}(2n_\delta+1)^{(1)} & & \\ & & | & & \\ \mathfrak{so}(2n_\gamma+1)^{(1)} & \text{———} & \mathfrak{sp}(n_\alpha)_\theta^{(1)} & \text{———} & \mathfrak{so}(2n_\beta+1)^{(1)} \end{array} \tag{5.172}$$

Gluing rules for $\mathfrak{sp}(n_\alpha)_\theta^{(1)}$ - - - - - - $\mathfrak{so}(8)^{(1)}$: we can take any geometry with $0 \leq \nu \leq 2n_\alpha + 4$ for $\mathfrak{sp}(n_\alpha)_\theta^{(1)}$, and any geometry with $0 \leq \nu \leq 4 - \Omega^{\beta\beta} - n_\alpha$ for $\mathfrak{so}(8)^{(1)}$. The gluing rules are:

- $f - x_1 - x_2$ in $S_{0,\alpha}$ is glued to f in $S_{0,\beta}$.
- $x_1 - x_2$ in $S_{0,\alpha}$ is glued to f in $S_{3,\beta}$.

- $x_2 - x_3$ in $S_{0,\alpha}$ is glued to f in $S_{2,\beta}$.
- $x_3 - x_4$ in $S_{0,\alpha}$ is glued to f in $S_{1,\beta}$.
- x_3, x_4 in $S_{0,\alpha}$ are glued to $f - z_1, w_1$ in $S_{4,\beta}$.
- $z_i - z_{i+1}, w_{i+1} - w_i$ in $S_{4,\beta}$ are glued to f, f in $S_{i,\alpha}$ for $i = 1, \cdots, n_\alpha - 1$.
- $z_{n_\alpha} - w_{n_\alpha}$ in $S_{4,\beta}$ is glued to f in $S_{n_\alpha,\alpha}$.

The theta angle is irrelevant as can be seen in the $\nu = 1$ frame of $\mathfrak{sp}(n_\alpha)^{(1)}_\theta$.

Gluing rules for $\boldsymbol{\mathfrak{sp}(n_\alpha)^{(1)}_\theta}$ - - - - - - $\boldsymbol{\mathfrak{so}(7)^{(1)}}$: we can take any geometry with $0 \le \nu \le 2n_\alpha + 4$ for $\mathfrak{sp}(n_\alpha)^{(1)}_\theta$, and any geometry with $0 \le \nu \le 8 - 2\Omega^{\beta\beta} - n_\alpha$ for $\mathfrak{so}(7)^{(1)}$. The gluing rules are:

- $f - x_1 - x_2$ in $S_{0,\alpha}$ is glued to f in $S_{0,\beta}$.
- $x_2 - x_3$ in $S_{0,\alpha}$ is glued to f in $S_{2,\beta}$.
- $x_1 - x_2, x_3 - x_4$ in $S_{0,\alpha}$ is glued to f in $S_{3,\beta}$.
- x_3, x_4 in $S_{0,\alpha}$ are glued to $f - x_1, y_1$ in $S_{1,\beta}$.
- $x_i - x_{i+1}, y_{i+1} - y_i$ in $S_{1,\beta}$ are glued to f, f in $S_{i,\alpha}$ for $i = 1, \cdots, n_\alpha - 1$.
- $x_{n_\alpha} - y_{n_\alpha}$ in $S_{1,\beta}$ is glued to f in $S_{n_\alpha,\alpha}$.

The theta angle is irrelevant as in the last case.

Gluing rules for $\boldsymbol{\mathfrak{sp}(n_\alpha)^{(1)}_\theta}$ ——— $\boldsymbol{\mathfrak{g}_2^{(1)}}$: we can take any geometry with $1 \le \nu \le 2n_\alpha + 5$ for $\mathfrak{sp}(n_\alpha)^{(1)}_\theta$, and any geometry with $0 \le \nu \le 10 - 3\Omega^{\beta\beta} - n_\alpha$ for $\mathfrak{g}_2^{(1)}$. The gluing rules are:

- $f - x_1 - x_2$ in $S_{0,\alpha}$ is glued to f in $S_{0,\beta}$.
- $x_2 - x_3$ in $S_{0,\alpha}$ is glued to f in $S_{2,\beta}$.
- $x_1 - x_2, x_3, x_3$ in $S_{0,\alpha}$ are glued to f, x_1, y_1 in $S_{1,\beta}$.
- $x_{i+1} - x_i, y_{i+1} - y_i$ in $S_{1,\beta}$ are glued to f, f in $S_{i,\alpha}$ for $i = 1, \cdots, n_\alpha - 1$.
- $f - x_{n_\alpha}, f - y_{n_\alpha}$ in $S_{1,\beta}$ are glued to $f - x_1, x_1$ in $S_{n_\alpha,\alpha}$.

The theta angle is irrelevant.

The blowup x_1 in $S_{n_\alpha,\alpha}$ can be repeated once more if there is another $\mathfrak{g}_2^{(1)}$ neighbor or an $\mathfrak{so}(2n_\gamma+1)^{(1)}$ neighbor of $\mathfrak{sp}(n_\alpha)^{(1)}_\theta$. That is, when we consider configurations of the form

$$\mathfrak{g}_2^{(1)} \text{ ——— } \mathfrak{sp}(n_\alpha)^{(1)}_\theta \text{ ——— } \mathfrak{g}_2^{(1)} \tag{5.173}$$

or of the form

$$\mathfrak{so}(2n_\gamma+1)^{(1)} \;\text{———}\; \mathfrak{sp}(n_\alpha)^{(1)}_\theta \;\text{———}\; \mathfrak{g}_2^{(1)} \tag{5.174}$$

As before, if there is a third $\mathfrak{g}_2$ or $\mathfrak{so}(2n_\delta+1)^{(1)}$ neighbor of $\mathfrak{sp}(n_\alpha)^{(1)}_\theta$, then we must use another blowup x_2 on $S_{n_\alpha,\alpha}$ for the gluing rules corresponding to this neighbor.

Gluing rules for $\mathfrak{su}(n_\alpha)^{(1)}$ ——— $\mathfrak{su}(n_\beta)^{(1)}$: here we allow $n_\alpha = \widehat{n}_\alpha$ and $n_\alpha = \tilde{6}$. We can take any geometry with $0 \le \nu \le 2n_\alpha - n_\beta$ for $\mathfrak{su}(n_\alpha)^{(1)}$, and any geometry with $0 \le \nu \le 2n_\beta - n_\alpha$ for $\mathfrak{su}(n_\beta)^{(1)}$. The gluing rules are:

- $f-x_1, x_{n_\beta}$ in $S_{0,\alpha}$ are glued to $f-x_1, x_{n_\alpha}$ in $S_{0,\beta}$.
- $x_i - x_{i+1}$ in $S_{0,\alpha}$ is glued to f in $S_{i,\beta}$ for $i=1,\cdots,n_\beta-1$.
- $x_i - x_{i+1}$ in $S_{0,\beta}$ is glued to f in $S_{i,\alpha}$ for $i=1,\cdots,n_\alpha-1$.

Gluing rules for $\mathfrak{su}(n_\alpha)^{(1)} - 2 - \mathfrak{so}(2n_\beta)^{(1)}$: we can take any geometry with $n_\beta \le \nu \le 2n_\alpha - n_\beta$ for $\mathfrak{su}(n_\alpha)^{(1)}$, and any geometry with $0 \le \nu \le 2n_\beta - 8 - n_\alpha$ for $\mathfrak{so}(2n_\beta)^{(1)}$. The gluing rules are:

- $f-x_1-x_2, f-y_1-y_2$ in $S_{0,\alpha}$ are glued to f,f in $S_{0,\beta}$.
- $x_i - x_{i+1}, y_i - y_{i+1}$ in $S_{0,\alpha}$ are glued to f,f in $S_{i,\beta}$ for $i=1,\cdots,n_\beta-1$.
- $x_{n_\beta-1}, x_{n_\beta}, y_{n_\beta-1}, y_{n_\beta}$ in $S_{0,\alpha}$ are glued to $f-x_1, y_1, f-y_{n_\alpha}, x_{n_\alpha}$ in $S_{n_\beta,\beta}$.
- $x_i - x_{i+1}, y_{i+1} - y_i$ in $S_{n_\beta,\beta}$ are glued to f,f in $S_{i,\alpha}$ for $i=1,\cdots,n_\alpha-1$.

Gluing rules for $\mathfrak{su}(n_\alpha)^{(1)} - 2 - \mathfrak{so}(2n_\beta+1)^{(1)}$: we can take any geometry with $n_\beta \le \nu \le 2n_\alpha - n_\beta - 1$ for $\mathfrak{su}(n_\alpha)^{(1)}$, and any geometry with $0 \le \nu \le 2n_\beta - 7 - n_\alpha$ for $\mathfrak{so}(2n_\beta)^{(1)}$. The (non-geometric) gluing rules are:

- $f-x_1-x_2, f-y_1-y_2$ in $S_{0,\alpha}$ are glued to f,f in $S_{0,\beta}$.
- $x_i - x_{i+1}, y_i - y_{i+1}$ in $S_{0,\alpha}$ are glued to f,f in $S_{i,\beta}$ for $i=1,\cdots,n_\beta-1$.
- $x_{n_\beta} - x_{n_\beta+1}, x_{n_\beta} - x_{n_\beta+1}, y_{n_\beta}, y_{n_\beta}, x_{n_\beta+1}, x_{n_\beta+1}$ in $S_{0,\alpha}$ are glued to $f, f, x_1, y_1, f - x_{n_\alpha}, f - y_{n_\alpha}$ in $S_{n_\beta,\beta}$.
- $x_{i+1} - x_i, y_{i+1} - y_i$ in $S_{n_\beta,\beta}$ are glued to f,f in $S_{i,\alpha}$ for $i=1,\cdots,n_\alpha-1$.

Gluing rules for $\mathfrak{su}(2)^{(1)}$ - - - - - - $\mathfrak{so}(7)^{(1)}$: we must take the geometry with $\nu=0$ for $\mathfrak{su}(2)^{(1)}$, and we can take any geometry with $0 \le \nu \le 7 - 2\Omega^{\beta\beta}$ for $\mathfrak{so}(7)^{(1)}$. The gluing rules are:

- $f-x_1-x_2$ in $S_{0,\alpha}$ is glued to f in $S_{0,\beta}$.
- $x_2 - x_3$ in $S_{0,\alpha}$ is glued to f in $S_{2,\beta}$.

- $x_1 - x_2, x_3 - x_4$ in $S_{0,\alpha}$ is glued to f in $S_{3,\beta}$.
- x_3, x_4 in $S_{0,\alpha}$ are glued to $f - x_1, y_1$ in $S_{1,\beta}$.
- $x_1 - y_1$ in $S_{1,\beta}$ is glued to f in $S_{1,\alpha}$.

Gluing rules for $\mathfrak{su}(2)^{(1)}$ ——— $\mathfrak{g}_2^{(1)}$: we must take the geometry with $\nu = 1$ for $\mathfrak{su}(2)^{(1)}$, and any geometry with $0 \leq \nu \leq 9 - 3\Omega^{\beta\beta}$ for $\mathfrak{g}_2^{(1)}$. The gluing rules are:

- $f - x_1 - x_2$ in $S_{0,\alpha}$ is glued to f in $S_{0,\beta}$.
- $x_2 - x_3$ in $S_{0,\alpha}$ is glued to f in $S_{2,\beta}$.
- $x_1 - x_2, x_3, x_3$ in $S_{0,\alpha}$ are glued to f, x_1, y_1 in $S_{1,\beta}$.
- $f - x_1, f - y_1$ in $S_{1,\beta}$ are glued to $f - x_1, x_1$ in $S_{1,\alpha}$.

There is another possibility appearing in the twisted case that involves an undirected edge between two untwisted algebras. This possibility is

$$\begin{array}{ccc} \mathfrak{su}(n_\alpha)^{(1)} & & \mathfrak{su}(n_\beta)^{(1)} \\ 2 & \text{———} & 2 \end{array} \tag{5.175}$$

and it is displayed in table 9. The gluing rules for this case are the same as the gluing rules for

$$\mathfrak{su}(n_\alpha)^{(1)} \text{ ——— } \mathfrak{su}(n_\beta)^{(1)} \tag{5.176}$$

presented above.

5.3.2 Undirected edges between a twisted algebra and an untwisted algebra

Now let us provide gluing rules for those cases in table 9 in which both the nodes have non-trivial gauge algebras associated to them, such that at least one of the gauge algebras is twisted.

Gluing rules for $\mathfrak{sp}(n_\alpha)_\theta^{(1)}$ ——— $\mathfrak{so}(2n_\beta)^{(2)}$: here we allow $2n_\beta = \widehat{12}$. We can take any geometry with $1 \leq \nu \leq 2n_\alpha + 8 - n_\beta$ for $\mathfrak{sp}(n_\alpha)_\theta^{(1)}$, and any geometry with $0 \leq \nu \leq 2n_\beta - 4 - \Omega^{\beta\beta} - n_\alpha$ for $\mathfrak{so}(2n_\beta)^{(2)}$. The gluing rules are:

- $f - x_1 - x_2, x_1 - x_2$ in $S_{0,\alpha}$ are glued to f, f in $S_{0,\beta}$.
- $x_i - x_{i+1}$ in $S_{0,\alpha}$ is glued to f in $S_{i-1,\beta}$ for $i = 2, \cdots, n_\beta - 1$.
- x_{n_β}, x_{n_β} in $S_{0,\alpha}$ are glued to x_1, y_1 in $S_{n_\beta-1,\beta}$.
- $x_{i+1} - x_i, y_{i+1} - y_i$ in $S_{n_\beta-1,\beta}$ are glued to f, f in $S_{i,\alpha}$ for $i = 1, \cdots, n_\alpha - 1$.
- $f - x_{n_\alpha}, f - y_{n_\alpha}$ in $S_{n_\beta-1,\beta}$ are glued to $f - x_1, x_1$ in $S_{n_\alpha,\alpha}$.

The theta angle can be seen to be irrelevant by using the blowup x_1 on $S_{n_\alpha,\alpha}$.

JHEP12(2020)151

The blowup x_1 in $S_{n_\alpha,\alpha}$ can be used in gluing rules corresponding to one more neighbor of the form $\mathfrak{so}(2n_\gamma+1)^{(1)}$, $\mathfrak{g}_2^{(1)}$ or $\mathfrak{so}(2n_\gamma)^{(2)}$ of $\mathfrak{sp}(n_\alpha)_\theta^{(1)}$.

The fact that $n_\beta = 2n_\alpha + 8$ is not allowed manifests in the above gluing rules. The total number of blowups carried by $S_{0,\alpha}$ is at max $2n_\alpha + 7$ but the gluing rules require the presence of $2n_\alpha + 8$ blowups on $S_{0,\alpha}$. See the discussion around (3.36) for an explanation of this restriction.

Gluing rules for $\mathfrak{su}(n_\alpha)^{(1)} - 2 - \mathfrak{so}(2n_\beta)^{(2)}$: we can take any geometry with $n_\beta - 1 \leq \nu \leq 2n_\alpha - n_\beta - 1$ for $\mathfrak{su}(n_\alpha)^{(1)}$, and any geometry with $0 \leq \nu \leq 2n_\beta - 8 - n_\alpha$ for $\mathfrak{so}(2n_\beta)^{(1)}$. The (non-geometric) gluing rules are:

- $f - x_1 - x_2, x_1 - x_2, f - x_1 - y_1, x_1 - y_1$ in $S_{0,\alpha}$ are glued to f, f, f, f in $S_{0,\beta}$.
- $x_{i+1} - x_{i+2}, y_i - y_{i+1}$ in $S_{0,\alpha}$ are glued to f, f in $S_{i,\beta}$ for $i = 1, \cdots, n_\beta - 2$.
- $x_{n_\beta} - x_{n_\beta+1}, x_{n_\beta} - x_{n_\beta+1}, y_{n_\beta}, y_{n_\beta}, x_{n_\beta+1}, x_{n_\beta+1}$ in $S_{0,\alpha}$ are glued to $f, f, x_1, y_1, f - x_{n_\alpha}, f - y_{n_\alpha}$ in $S_{n_\beta,\beta}$.
- $x_i - x_{i+1}, y_{i+1} - y_i$ in $S_{n_\beta,\beta}$ are glued to f, f in $S_{i,\alpha}$ for $i = 1, \cdots, n_\alpha - 1$.

5.3.3 Directed edges

Now we move onto gluing rules for edges listed in table 10.

Gluing rules for $\mathfrak{sp}(n_\alpha)^{(1)} - 2 \rightarrow \mathfrak{so}(2n_\beta)^{(1)}$: we can take any geometry with $0 \leq \nu \leq 2n_\alpha + 8 - 2n_\beta$ for $\mathfrak{sp}(n_\alpha)^{(1)}$, and any geometry with $0 \leq \nu \leq 2n_\beta - 4 - \Omega^{\beta\beta} - n_\alpha$ for $\mathfrak{so}(2n_\beta)^{(1)}$. The gluing rules are:

- $x_{n_\beta-1} - x_{n_\beta+1}, x_{n_\beta} - x_{n_\beta+2}$ in $S_{0,\alpha}$ are glued to f, f in $S_{0,\beta}$.
- $x_{n_\beta-i} - x_{n_\beta-i+1}, x_{n_\beta+i} - x_{n_\beta+i+1}$ in $S_{0,\alpha}$ are glued to f, f in $S_{i,\beta}$ for $i = 1, \cdots, n_\beta - 1$.
- $f - x_1 - x_2$ in $S_{0,\alpha}$ is glued to f in $S_{n_\beta,\beta}$. $x_{2n_\beta-1}$ in $S_{0,\alpha}$ is glued to $f - x_1$ in $S_{n_\beta,\beta}$. x_{2n_β} in $S_{0,\alpha}$ is glued to y_1 in $S_{n_\beta,\beta}$.
- $x_i - x_{i+1}, y_{i+1} - y_i$ in $S_{n_\beta,\beta}$ are glued to f, f in $S_{i,\alpha}$ for $i = 1, \cdots, n_\alpha - 1$.
- $x_{n_\alpha} - y_{n_\alpha}$ in $S_{n_\beta,\beta}$ is glued to f in $S_{n_\alpha,\alpha}$.

From this case onward, we are dropping the subscript θ on $\mathfrak{sp}(n)^{(1)}$ whenever theta angle is not physically relevant. In such cases, the gluing rules will work uniformly for both values of θ and using arguments used earlier in the paper, the reader can easily check that the combined geometries descending from different values of theta angle are indeed isomorphic.

Gluing rules for $\mathfrak{sp}(n_\alpha)^{(1)} - 2 \rightarrow \mathfrak{so}(2n_\beta+1)^{(1)}$: we can take any geometry with $1 \leq \nu \leq 2n_\alpha + 7 - 2n_\beta$ for $\mathfrak{sp}(n_\alpha)^{(1)}$, and any geometry with $0 \leq \nu \leq 2n_\beta - 3 - \Omega^{\beta\beta} - n_\alpha$ for $\mathfrak{so}(2n_\beta+1)^{(1)}$. The (non-geometric) gluing rules are:

- $x_{n_\beta} - x_{n_\beta+2}, x_{n_\beta+1} - x_{n_\beta+3}$ in $S_{0,\alpha}$ are glued to f, f in $S_{0,\beta}$.

- $x_{n_\beta-i+1}-x_{n_\beta-i+2}, x_{n_\beta+i+1}-x_{n_\beta+i+2}$ in $S_{0,\alpha}$ are glued to f, f in $S_{i,\beta}$ for $i = 1, \cdots, n_\beta - 1$.

- $f - x_1 - x_2, x_1 - x_2$ in $S_{0,\alpha}$ are glued to f, f in $S_{n_\beta,\beta}$. $x_{2n_\beta+1}$ in $S_{0,\alpha}$ is glued to x_1 in $S_{n_\beta,\beta}$. $x_{2n_\beta+1}$ in $S_{0,\alpha}$ is glued to y_1 in $S_{n_\beta,\beta}$.

- $x_{i+1} - x_i, y_{i+1} - y_i$ in $S_{n_\beta,\beta}$ are glued to f, f in $S_{i,\alpha}$ for $i = 1, \cdots, n_\alpha - 1$.

- $f - x_{n_\alpha}$ in $S_{n_\beta,\beta}$ is glued to x_1 in $S_{n_\alpha,\alpha}$. $f - y_{n_\alpha}$ in $S_{n_\beta,\beta}$ is glued to $f - x_1$ in $S_{n_\alpha,\alpha}$.

Notice that the blowup x_1 in $S_{n_\alpha,\alpha}$ can be used for gluing $\mathfrak{sp}(n_\alpha)^{(1)}$ to one more neighbor, that is in configurations of the following form

$$\mathfrak{so}(2n_\gamma+1)^{(1)} \;\text{———}\; \mathfrak{sp}(n_\alpha)^{(1)} \;\text{—}\; 2 \longrightarrow \mathfrak{so}(2n_\beta+1)^{(1)} \tag{5.177}$$

$$\mathfrak{g}_2^{(1)} \;\text{————}\; \mathfrak{sp}(n_\alpha)^{(1)} \;\text{—}\; 2 \longrightarrow \mathfrak{so}(2n_\beta+1)^{(1)} \tag{5.178}$$

$$\mathfrak{so}(2n_\gamma)^{(2)} \;\text{———}\; \mathfrak{sp}(n_\alpha)^{(1)} \;\text{—}\; 2 \longrightarrow \mathfrak{so}(2n_\beta+1)^{(1)} \tag{5.179}$$

but cannot be used for gluing $\mathfrak{sp}(n_\alpha)^{(1)}$ to two more neighbors.

Gluing rules for $\mathfrak{sp}(n_\alpha)^{(1)} - 2 \rightarrow \mathfrak{so}(2n_\beta)^{(2)}$: we can take any geometry with $1 \leq \nu \leq 2n_\alpha + 7 - 2n_\beta$ for $\mathfrak{sp}(n_\alpha)^{(1)}$, and any geometry with $0 \leq \nu \leq 2n_\beta - 8 - n_\alpha$ for $\mathfrak{so}(2n_\beta)^{(2)}$. The (non-geometric) gluing rules are:

- $x_{n_\beta} - x_{n_\beta+2}, x_{n_\beta+1} - x_{n_\beta+3}, x_{n_\beta} - x_{n_\beta+1}, x_{n_\beta+2} - x_{n_\beta+3}$ in $S_{0,\alpha}$ are glued to f, f, f, f in $S_{0,\beta}$.

- $x_{n_\beta-i}-x_{n_\beta-i+1}, x_{n_\beta+i+2}-x_{n_\beta+i+3}$ in $S_{0,\alpha}$ are glued to f, f in $S_{i,\beta}$ for $i = 1, \cdots, n_\beta - 2$.

- $f - x_1 - x_2, x_1 - x_2$ in $S_{0,\alpha}$ are glued to f, f in $S_{n_\beta-1,\beta}$. $x_{2n_\beta+1}$ in $S_{0,\alpha}$ is glued to x_1 in $S_{n_\beta-1,\beta}$. $x_{2n_\beta+1}$ in $S_{0,\alpha}$ is glued to y_1 in $S_{n_\beta-1,\beta}$.

- $x_{i+1} - x_i, y_{i+1} - y_i$ in $S_{n_\beta-1,\beta}$ are glued to f, f in $S_{i,\alpha}$ for $i = 1, \cdots, n_\alpha - 1$.

- $f - x_{n_\alpha}$ in $S_{n_\beta-1,\beta}$ is glued to x_1 in $S_{n_\alpha,\alpha}$. $f - y_{n_\alpha}$ in $S_{n_\beta,\beta}$ is glued to $f - x_1$ in $S_{n_\alpha,\alpha}$.

The blowup x_1 in $S_{n_\alpha,\alpha}$ can be used to glue $\mathfrak{sp}(n_\alpha)^{(1)}$ to exactly one more neighboring node connected to it by an undirected edge. The neighboring node can carry $\mathfrak{so}(2n_\gamma+1)^{(1)}$, $\mathfrak{g}_2^{(1)}$ or $\mathfrak{so}(2n_\gamma)^{(2)}$.

The fact that $n_\beta = n_\alpha + 4$ is not allowed manifests in the above gluing rules. The total number of blowups carried by $S_{0,\alpha}$ is at max $2n_\alpha + 7$ but the gluing rules require the presence of $2n_\alpha + 9$ blowups on $S_{0,\alpha}$. See the discussion around (3.37) for an explanation of this restriction.

Gluing rules for $\mathfrak{sp}(n_\alpha)^{(1)} \dashrightarrow 2 \dashrightarrow \mathfrak{so}(7)^{(1)}$: we can take any geometry with $0 \leq \nu \leq 2n_\alpha$ for $\mathfrak{sp}(n_\alpha)^{(1)}$, and any geometry with $0 \leq \nu \leq 2 - n_\alpha$ for $\mathfrak{so}(7)^{(1)}$. The gluing rules are:

- $x_3 - x_5, x_4 - x_6$ in $S_{0,\alpha}$ are glued to f, f in $S_{0,\beta}$.

- $f - x_1 - x_2, x_7, x_8$ in $S_{0,\alpha}$ are glued to $f, f - x_1, y_1$ in $S_{1,\beta}$.
- $x_2 - x_3, x_6 - x_7$ in $S_{0,\alpha}$ are glued to f, f in $S_{2,\beta}$.
- $x_1 - x_2, x_3 - x_4, x_5 - x_6, x_7 - x_8$ in $S_{0,\alpha}$ are glued to f, f, f, f in $S_{3,\beta}$.
- $x_i - x_{i+1}, y_{i+1} - y_i$ in $S_{1,\beta}$ are glued to f, f in $S_{i,\alpha}$ for $i = 1, \cdots, n_\alpha - 1$.
- $x_{n_\alpha} - y_{n_\alpha}$ in $S_{1,\beta}$ is glued to f in $S_{n_\alpha,\alpha}$.

Gluing rules for $\mathfrak{sp}(1)^{(1)} \overset{2}{\longrightarrow} \mathfrak{g}_2^{(1)}$: we can take any geometry with $1 \leq \nu \leq 3$ for $\mathfrak{sp}(1)^{(1)}$. The (non-geometric) gluing rules are:

- $x_3 - x_5, x_4 - x_6$ in $S_{0,\alpha}$ are glued to f, f in $S_{0,\beta}$.
- $x_2 - x_3, x_6 - x_7$ in $S_{0,\alpha}$ are glued to f, f in $S_{2,\beta}$.
- $f - x_1 - x_2, x_1 - x_2, x_3 - x_4, x_5 - x_6, x_7, x_7$ in $S_{0,\alpha}$ are glued to f, f, f, f, x_1, y_1 in $S_{1,\beta}$.
- $f - x_1, x_1$ in $S_{1,\alpha}$ are glued to $f - x_1, f - y_1$ in $S_{1,\beta}$.

Notice that the blowup x_1 in $S_{1,\alpha}$ can be used in gluing rules corresponding to exactly one more neighbor of $\mathfrak{sp}(1)^{(1)}$ carrying algebra $\mathfrak{so}(2n_\gamma + 1)^{(1)}$ or $\mathfrak{so}(2n_\gamma)^{(2)}$.

Gluing rules for $\mathfrak{sp}(n_\alpha)^{(1)} \overset{3}{-\!\!\rightarrow} \mathfrak{so}(2n_\beta)^{(1)}$: we can take any geometry with $0 \leq \nu \leq 2n_\alpha + 8 - 3n_\beta$ for $\mathfrak{sp}(n_\alpha)^{(1)}$, and any geometry with $0 \leq \nu \leq 2n_\beta - 8 - n_\alpha$ for $\mathfrak{so}(2n_\beta)^{(1)}$. The gluing rules are:

- $f - x_1 - x_2, x_{2n_\beta-1} - x_{2n_\beta+1}, x_{2n_\beta} - x_{2n_\beta+2}$ in $S_{0,\alpha}$ are glued to f, f, f in $S_{0,\beta}$.
- $x_i - x_{i+1}, x_{2n_\beta-i} - x_{2n_\beta-i+1}, x_{2n_\beta+i} - x_{2n_\beta+i+1}$ in $S_{0,\alpha}$ are glued to f, f, f in $S_{i,\beta}$ for $i = 1, \cdots, n_\beta - 1$.
- $x_{n_\beta-1} - x_{n_\beta+1}, x_{n_\beta} - x_{n_\beta+2}, x_{3n_\beta-1}, x_{3n_\beta}$ in $S_{0,\alpha}$ are glued to $f, f, f - x_1, y_1$ in $S_{n_\beta,\beta}$.
- $x_i - x_{i+1}, y_{i+1} - y_i$ in $S_{n_\beta,\beta}$ are glued to f, f in $S_{i,\alpha}$ for $i = 1, \cdots, n_\alpha - 1$.
- $x_{n_\alpha} - y_{n_\alpha}$ in $S_{n_\beta,\beta}$ is glued to f in $S_{n_\alpha,\alpha}$.

Gluing rules for $\mathfrak{sp}(n_\alpha)^{(1)} \overset{3}{-\!\!\rightarrow} \mathfrak{so}(2n_\beta + 1)^{(1)}$: we can take any geometry with $1 \leq \nu \leq 2n_\alpha + 7 - 3n_\beta$ for $\mathfrak{sp}(n_\alpha)^{(1)}$, and any geometry with $0 \leq \nu \leq 2n_\beta - 7 - n_\alpha$ for $\mathfrak{so}(2n_\beta + 1)^{(1)}$. The (non-geometric) gluing rules are:

- $f - x_1 - x_2, x_{2n_\beta} - x_{2n_\beta+2}, x_{2n_\beta+1} - x_{2n_\beta+3}$ in $S_{0,\alpha}$ are glued to f, f, f in $S_{0,\beta}$.
- $x_i - x_{i+1}, x_{2n_\beta-i+1} - x_{2n_\beta-i+2}, x_{2n_\beta+i+1} - x_{2n_\beta+i+2}$ in $S_{0,\alpha}$ are glued to f, f, f in $S_{i,\beta}$ for $i = 1, \cdots, n_\beta - 1$.
- $x_{n_\beta} - x_{n_\beta+1}, x_{n_\beta} - x_{n_\beta+1}, x_{n_\beta+1} - x_{n_\beta+2}, x_{n_\beta+1} - x_{n_\beta+2}, x_{3n_\beta+1}, x_{3n_\beta+1}$ in $S_{0,\alpha}$ are glued to f, f, f, f, x_1, y_1 in $S_{n_\beta,\beta}$.

- $x_{i+1} - x_i, y_{i+1} - y_i$ in $S_{n_\beta,\beta}$ are glued to f, f in $S_{i,\alpha}$ for $i = 1, \cdots, n_\alpha - 1$.
- $f - x_{n_\alpha}, f - y_{n_\alpha}$ in $S_{n_\beta,\beta}$ are glued to $f - x_1, x_1$ in $S_{n_\alpha,\alpha}$.

Gluing rules for $\mathfrak{sp}(n_\alpha)^{(1)} \overset{3}{-} \mathfrak{so}(2n_\beta)^{(2)}$: we can take any geometry with $1 \leq \nu \leq 2n_\alpha + 7 - 3n_\beta$ for $\mathfrak{sp}(n_\alpha)^{(1)}$, and any geometry with $0 \leq \nu \leq 2n_\beta - 8 - n_\alpha$ for $\mathfrak{so}(2n_\beta)^{(2)}$. The (non-geometric) gluing rules are:

- $f - x_1 - x_2, x_1 - x_2, x_{2n_\beta} - x_{2n_\beta+2}, x_{2n_\beta} - x_{2n_\beta+1}, x_{2n_\beta+1} - x_{2n_\beta+3}, x_{2n_\beta+2} - x_{2n_\beta+3}$ in $S_{0,\alpha}$ are glued to f, f, f, f, f, f in $S_{0,\beta}$.
- $x_{i+1} - x_{i+2}, x_{2n_\beta-i} - x_{2n_\beta-i+1}, x_{2n_\beta+i+2} - x_{2n_\beta+i+3}$ in $S_{0,\alpha}$ are glued to f, f, f in $S_{i,\beta}$ for $i = 1, \cdots, n_\beta - 2$.
- $x_{n_\beta} - x_{n_\beta+1}, x_{n_\beta} - x_{n_\beta+1}, x_{n_\beta+1} - x_{n_\beta+2}, x_{n_\beta+1} - x_{n_\beta+2}, x_{3n_\beta+1}, x_{3n_\beta+1}$ in $S_{0,\alpha}$ are glued to f, f, f, f, x_1, y_1 in $S_{n_\beta-1,\beta}$.
- $x_{i+1} - x_i, y_{i+1} - y_i$ in $S_{n_\beta-1,\beta}$ are glued to f, f in $S_{i,\alpha}$ for $i = 1, \cdots, n_\alpha - 1$.
- $f - x_{n_\alpha}, f - y_{n_\alpha}$ in $S_{n_\beta-1,\beta}$ are glued to $f - x_1, x_1$ in $S_{n_\alpha,\alpha}$.

Again, the fact that $3n_\beta = 2n_\alpha + 8$ is not allowed manifests in the above gluing rules. The total number of blowups carried by $S_{0,\alpha}$ is at max $2n_\alpha + 7$ but the gluing rules require the presence of $2n_\alpha + 9$ blowups on $S_{0,\alpha}$. See the discussion around (3.38) for an explanation of this restriction.

Gluing rules for $\mathfrak{su}(n_\alpha)^{(1)} \overset{2}{-} \to \mathfrak{su}(n_\beta)^{(1)}$: we can take any geometry with $0 \leq \nu \leq 2n_\alpha - 2n_\beta$ for $\mathfrak{su}(n_\alpha)^{(1)}$, and any geometry with $0 \leq \nu \leq 2n_\beta - n_\alpha$ for $\mathfrak{su}(n_\beta)^{(1)}$. The gluing rules are:

- $f - x_1, x_{n_\beta} - x_{n_\beta+1}, x_{2n_\beta}$ in $S_{0,\alpha}$ are glued to $f - x_1, f, x_{n_\alpha}$ in $S_{0,\beta}$.
- $x_i - x_{i+1}, x_{n_\beta+i} - x_{n_\beta+i+1}$ in $S_{0,\alpha}$ are glued to f, f in $S_{i,\beta}$ for $i = 1, \cdots, n_\beta - 1$.
- $x_i - x_{i+1}$ in $S_{0,\beta}$ is glued to f in $S_{i,\alpha}$ for $i = 1, \cdots, n_\alpha - 1$.

Gluing rules for $\mathfrak{su}(n_\alpha)^{(1)} \overset{3}{-} \to \mathfrak{su}(n_\beta)^{(1)}$: we can take any geometry with $0 \leq \nu \leq 2n_\alpha - 3n_\beta$ for $\mathfrak{su}(n_\alpha)^{(1)}$, and any geometry with $0 \leq \nu \leq 2n_\beta - n_\alpha$ for $\mathfrak{su}(n_\beta)^{(1)}$. The gluing rules are:

- $f - x_1, x_{n_\beta} - x_{n_\beta+1}, x_{2n_\beta} - x_{2n_\beta+1}, x_{3n_\beta}$ in $S_{0,\alpha}$ are glued to $f - x_1, f, f, x_{n_\alpha}$ in $S_{0,\beta}$.
- $x_i - x_{i+1}, x_{n_\beta+i} - x_{n_\beta+i+1}, x_{2n_\beta+i} - x_{2n_\beta+i+1}$ in $S_{0,\alpha}$ are glued to f, f, f in $S_{i,\beta}$ for $i = 1, \cdots, n_\beta - 1$.
- $x_i - x_{i+1}$ in $S_{0,\beta}$ is glued to f in $S_{i,\alpha}$ for $i = 1, \cdots, n_\alpha - 1$.

Gluing rules for $\mathfrak{su}(2n_\alpha)^{(2)} \overset{2}{-} \to \mathfrak{su}(n_\beta)^{(1)}$: we can take any geometry with $0 \leq \nu \leq 2n_\beta - 2n_\alpha$ for $\mathfrak{su}(n_\beta)^{(1)}$. The gluing rules are:

- $f-y_{n_\beta}, x_{n_\beta}, f-x_1, y_1$ in $S_{0,\alpha}$ are glued to $x_{2n_\alpha-1}, x_{2n_\alpha}, f-x_2, f-x_1$ in $S_{0,\beta}$.
- $x_i-x_{i+1}, y_{i+1}-y_i$ in $S_{0,\alpha}$ are glued to f, f in $S_{i,\beta}$ for $i=1,\cdots,n_\beta-1$.
- $x_i-x_{i+1}, x_{2n_\alpha-i}-x_{2n_\alpha-i+1}$ in $S_{0,\beta}$ are glued to f, f in $S_{i,\alpha}$ for $i=1,\cdots,n_\alpha-1$.
- $x_{n_\alpha}-x_{n_\alpha+1}$ in $S_{0,\beta}$ is glued to f in $S_{n_\alpha,\alpha}$.

Gluing rules for $\mathfrak{su}(2n_\alpha-1)^{(2)} - {\scriptstyle 2} \rightarrow \mathfrak{su}(n_\beta)^{(1)}$: we can take any geometry with $1\le\nu\le 2n_\beta-2n_\alpha+1$ for $\mathfrak{su}(n_\beta)^{(1)}$. The (non-geometric) gluing rules are:

- $y_{n_\beta}, x_{n_\beta}, f-x_1, f-y_1, f, f$ in $S_{0,\alpha}$ are glued to $x_{2n_\alpha-1}, x_{2n_\alpha-1}, y_1, f-x_1, x_1-x_2, f-x_2-y_1$ in $S_{0,\beta}$.
- x_i-x_{i+1}, y_i-y_{i+1} in $S_{0,\alpha}$ are glued to f, f in $S_{i,\beta}$ for $i=1,\cdots,n_\beta-1$.
- $x_{i+1}-x_{i+2}, x_{2n_\alpha-i-1}-x_{2n_\alpha-i}$ in $S_{0,\beta}$ are glued to f, f in $S_{i,\alpha}$ for $i=1,\cdots,n_\alpha-2$.
- $x_{n_\alpha}-x_{n_\alpha+1}$ in $S_{0,\beta}$ is glued to f in $S_{n_\alpha-1,\alpha}$.

Gluing rules for $\mathfrak{g}_2^{(1)} \;\text{——}\; {\scriptstyle 2} \longrightarrow \mathfrak{su}(2)^{(1)}$: we can take any geometry with $1\le\nu\le 3$ for $\mathfrak{g}_2^{(1)}$, and we must use the geometry with $\nu=1$ for $\mathfrak{su}(2)^{(1)}$. The (non-geometric) gluing rules are:

- $f-x_1, y_1$ in $S_{0,\alpha}$ are glued to $f-x_2, f-x_1$ in $S_{0,\beta}$.
- x_1-y_1 in $S_{0,\alpha}$ is glued to f in $S_{1,\beta}$.
- x_2-x_3 in $S_{0,\beta}$ is glued to f in $S_{2,\alpha}$.
- x_1-x_2, x_3, x_3 in $S_{0,\beta}$ are glued to f, x_1, y_1 in $S_{1,\alpha}$.
- $f-x_1, f-y_1$ in $S_{1,\alpha}$ are glued to $f-x_1, x_1$ in $S_{1,\beta}$.

Gluing rules for $\mathfrak{g}_2^{(1)} \;\text{——}\; {\scriptstyle 3} \longrightarrow \mathfrak{su}(2)^{(1)}$: we can take any geometry with $2\le\nu\le 3$ for $\mathfrak{g}_2^{(1)}$, and we must use the geometry with $\nu=1$ for $\mathfrak{su}(2)^{(1)}$. The (non-geometric) gluing rules are:

- $f-x_1, y_1, x_2-y_2$ in $S_{0,\alpha}$ are glued to $f-x_2, f-x_1, f$ in $S_{0,\beta}$.
- x_1-x_2, y_2-y_1 in $S_{0,\alpha}$ are glued to f, f in $S_{1,\beta}$.
- x_2-x_3 in $S_{0,\beta}$ is glued to f in $S_{2,\alpha}$.
- x_1-x_2, x_3, x_3 in $S_{0,\beta}$ are glued to f, x_1, y_1 in $S_{1,\alpha}$.
- $f-x_1, f-y_1$ in $S_{1,\alpha}$ are glued to $f-x_1, x_1$ in $S_{1,\beta}$.

Gluing rules for $\mathfrak{so}(7)^{(1)} \;\text{-}\,\text{-}\; \mathbf{2} \;\text{-}\,\text{-}\!\!\rightarrow \mathfrak{sp}(1)^{(1)}$ and $\mathfrak{so}(7)^{(1)} \;\text{-}\,\text{-}\; \mathbf{2} \;\text{-}\,\text{-}\!\!\rightarrow \mathfrak{su}(2)^{(1)}$: we can take any geometry with $1 \leq \nu \leq 7 - 2\Omega^{\alpha\alpha}$ for $\mathfrak{so}(7)^{(1)}$, any geometry with $0 \leq \nu \leq 6$ for $\mathfrak{sp}(1)^{(1)}$, and we must use the geometry with $\nu = 0$ for $\mathfrak{su}(2)^{(1)}$. The gluing rules are:

- $f - x_1, y_1$ in $S_{0,\alpha}$ are glued to $f - x_2, f - x_1$ in $S_{0,\beta}$.
- $x_1 - y_1$ in $S_{0,\alpha}$ is glued to f in $S_{1,\beta}$.
- x_3, x_4 in $S_{0,\beta}$ are glued to $f - x_1, y_1$ in $S_{1,\alpha}$.
- $x_2 - x_3$ in $S_{0,\beta}$ is glued to f in $S_{2,\alpha}$.
- $x_1 - x_2, x_3 - x_4$ in $S_{0,\beta}$ are glued to f, f in $S_{3,\alpha}$.
- $x_1 - y_1$ in $S_{1,\alpha}$ is glued to f in $S_{1,\beta}$.

Gluing rules for $\mathfrak{so}(7)^{(1)} \;\text{-}\,\text{-}\; \mathbf{3} \;\text{-}\,\text{-}\!\!\rightarrow \mathfrak{su}(2)^{(1)}$: we can take any geometry with $2 \leq \nu \leq 3$ for $\mathfrak{so}(7)^{(1)}$, and we must use the geometry with $\nu = 0$ for $\mathfrak{su}(2)^{(1)}$. The gluing rules are:

- $f - x_1, y_1, x_2 - y_2$ in $S_{0,\alpha}$ are glued to $f - x_2, f - x_1, f$ in $S_{0,\beta}$.
- $x_1 - x_2, y_2 - y_1$ in $S_{0,\alpha}$ are glued to f, f in $S_{1,\beta}$.
- x_3, x_4 in $S_{0,\beta}$ are glued to $f - x_1, y_1$ in $S_{1,\alpha}$.
- $x_2 - x_3$ in $S_{0,\beta}$ is glued to f in $S_{2,\alpha}$.
- $x_1 - x_2, x_3 - x_4$ in $S_{0,\beta}$ are glued to f, f in $S_{3,\alpha}$.
- $x_1 - y_1$ in $S_{1,\alpha}$ is glued to f in $S_{1,\beta}$.

Gluing rules for $\mathfrak{so}(8)^{(2)} \;\text{-}\,\text{-}\; \mathbf{2} \longrightarrow \mathfrak{sp}(1)^{(1)}$: we can take any geometry with $0 \leq \nu \leq 6$ for $\mathfrak{sp}(1)^{(1)}$. The gluing rules are:

- $f - x_1, y_1$ in $S_{1,\alpha}$ are glued to x_3, x_4 in $S_{0,\beta}$.
- $x_1 - y_1$ in $S_{1,\alpha}$ is glued to f in $S_{1,\beta}$.
- $f - x_1 - x_4, f - x_2 - x_3$ in $S_{0,\beta}$ are glued to f, f in $S_{0,\alpha}$.
- $x_2 - x_3$ in $S_{0,\beta}$ is glued to f in $S_{2,\alpha}$.
- $x_1 - x_2, x_3 - x_4$ in $S_{0,\beta}$ are glued to f, f in $S_{3,\alpha}$.

Gluing rules for $\mathfrak{so}(2n_\alpha)^{(1)} - \mathbf{2} \longrightarrow \mathfrak{sp}(n_\beta)^{(1)}$: we can take any geometry with $n_\beta \leq \nu \leq 2n_\alpha - 4 - \Omega^{\alpha\alpha} - n_\beta$ for $\mathfrak{so}(2n_\alpha)^{(1)}$, and any geometry with $0 \leq \nu \leq 2n_\beta + 8 - n_\alpha$ for $\mathfrak{sp}(n_\beta)^{(1)}$. The gluing rules are:

- $f - x_1, y_1$ in $S_{0,\alpha}$ are glued to $f - x_2, f - x_1$ in $S_{0,\beta}$.

- $x_i - x_{i+1}, y_{i+1} - y_i$ in $S_{0,\alpha}$ are glued to f, f in $S_{i,\beta}$ for $i = 1, \cdots, n_\beta - 1$.
- $x_{n_\beta} - y_{n_\beta}$ in $S_{0,\alpha}$ is glued to f in $S_{n_\beta,\beta}$.
- $x_i - x_{i+1}$ in $S_{0,\beta}$ is glued to f in $S_{i,\alpha}$ for $i = 1, \cdots, n_\alpha - 1$.
- $x_{n_\alpha - 1}, x_{n_\alpha}$ in $S_{0,\beta}$ are glued to $f - x_1, y_1$ in $S_{n_\alpha,\alpha}$.
- $x_i - x_{i+1}, y_{i+1} - y_i$ in $S_{n_\alpha,\alpha}$ are glued to f, f in $S_{i,\beta}$ for $i = 1, \cdots, n_\beta - 1$.
- $x_{n_\beta} - y_{n_\beta}$ in $S_{n_\alpha,\alpha}$ is glued to f in $S_{n_\beta,\beta}$.

Gluing rules for $\mathfrak{so}(2n_\alpha + 1)^{(1)}$ - 2 $\rightarrow \mathfrak{sp}(n_\beta)^{(1)}$: we can take any geometry with $n_\beta \leq \nu \leq 2n_\alpha - 3 - \Omega^{\alpha\alpha} - n_\beta$ for $\mathfrak{so}(2n_\alpha+1)^{(1)}$, and any geometry with $1 \leq \nu \leq 2n_\beta + 8 - n_\alpha$ for $\mathfrak{sp}(n_\beta)^{(1)}$. The gluing rules are:

- $f - x_1, y_1$ in $S_{0,\alpha}$ are glued to $f - x_2, f - x_1$ in $S_{0,\beta}$.
- $x_i - x_{i+1}, y_{i+1} - y_i$ in $S_{0,\alpha}$ are glued to f, f in $S_{i,\beta}$ for $i = 1, \cdots, n_\beta - 1$.
- $x_{n_\beta} - y_{n_\beta}$ in $S_{0,\alpha}$ is glued to f in $S_{n_\beta,\beta}$.
- $x_i - x_{i+1}$ in $S_{0,\beta}$ is glued to f in $S_{i,\alpha}$ for $i = 1, \cdots, n_\alpha - 1$.
- $x_{n_\alpha}, x_{n_\alpha}$ in $S_{0,\beta}$ are glued to x_1, y_1 in $S_{n_\alpha,\alpha}$.
- $x_{i+1} - x_i, y_{i+1} - y_i$ in $S_{n_\alpha,\alpha}$ are glued to f, f in $S_{i,\beta}$ for $i = 1, \cdots, n_\beta - 1$.
- $f - x_{n_\beta}, f - y_{n_\beta}$ in $S_{n_\alpha,\alpha}$ are glued to $f - x_1, x_1$ in $S_{n_\beta,\beta}$.

The blowup x_1 in $S_{n_\beta,\beta}$ can be used to glue $\mathfrak{sp}(n_\beta)^{(1)}$ to exactly one more neighboring node connected to it by an undirected edge. The neighboring node can carry $\mathfrak{so}(2n_\gamma + 1)^{(1)}$, $\mathfrak{g}_2^{(1)}$ or $\mathfrak{so}(2n_\gamma)^{(2)}$.

Gluing rules for $\mathfrak{so}(2n_\alpha)^{(2)}$ — 2 $\rightarrow \mathfrak{sp}(n_\beta)^{(1)}$: we can take any geometry with $n_\beta \leq \nu \leq 2n_\alpha - 8 - n_\beta$ for $\mathfrak{so}(2n_\alpha)^{(2)}$, and any geometry with $1 \leq \nu \leq 2n_\beta + 8 - n_\alpha$ for $\mathfrak{sp}(n_\beta)^{(1)}$. The gluing rules are:

- $f - x_1, y_1, f$ in $S_{0,\alpha}$ are glued to $f - x_2, f - x_1, x_1 - x_2$ in $S_{0,\beta}$.
- $x_i - x_{i+1}, y_{i+1} - y_i$ in $S_{0,\alpha}$ are glued to f, f in $S_{i,\beta}$ for $i = 1, \cdots, n_\beta - 1$.
- $x_{n_\beta} - y_{n_\beta}$ in $S_{0,\alpha}$ is glued to f in $S_{n_\beta,\beta}$.
- $x_{i+1} - x_{i+2}$ in $S_{0,\beta}$ is glued to f in $S_{i,\alpha}$ for $i = 1, \cdots, n_\alpha - 2$.
- $x_{n_\alpha}, x_{n_\alpha}$ in $S_{0,\beta}$ are glued to x_1, y_1 in $S_{n_\alpha - 1,\alpha}$.
- $x_{i+1} - x_i, y_{i+1} - y_i$ in $S_{n_\alpha - 1,\alpha}$ are glued to f, f in $S_{i,\beta}$ for $i = 1, \cdots, n_\beta - 1$.
- $f - x_{n_\beta}, f - y_{n_\beta}$ in $S_{n_\alpha - 1,\alpha}$ are glued to $f - x_1, x_1$ in $S_{n_\beta,\beta}$.

Again, the blowup x_1 in $S_{n_\beta,\beta}$ can be used to glue $\mathfrak{sp}(n_\beta)^{(1)}$ to exactly one more neighboring node carrying $\mathfrak{so}(2n_\gamma+1)^{(1)}$, $\mathfrak{g}_2^{(1)}$ or $\mathfrak{so}(2n_\gamma)^{(2)}$.

Gluing rules for $\mathfrak{so}(2n_\alpha)^{(1)}$ – 3 $\rightarrow$ $\mathfrak{sp}(n_\beta)^{(1)}$: we can take any geometry with $2n_\beta \leq \nu \leq 2n_\alpha - 8 - n_\beta$ for $\mathfrak{so}(2n_\alpha)^{(1)}$, and any geometry with $0 \leq \nu \leq 2n_\beta + 8 - n_\alpha$ for $\mathfrak{sp}(n_\beta)^{(1)}$. The gluing rules are:

- $f - x_1, x_{2n_\beta} - y_{2n_\beta}, y_1$ in $S_{0,\alpha}$ are glued to $f - x_2, f, f - x_1$ in $S_{0,\beta}$.
- $x_i - x_{i+1}, y_{i+1} - y_i, x_{2n_\beta-i} - x_{2n_\beta-i+1}, y_{2n_\beta-i+1} - y_{2n_\beta-i}$ in $S_{0,\alpha}$ are glued to f, f, f, f in $S_{i,\beta}$ for $i = 1, \cdots, n_\beta - 1$.
- $x_{n_\beta} - x_{n_\beta+1}, y_{n_\beta+1} - y_{n_\beta}$ in $S_{0,\alpha}$ are glued to f, f in $S_{n_\beta,\beta}$.
- $x_i - x_{i+1}$ in $S_{0,\beta}$ is glued to f in $S_{i,\alpha}$ for $i = 1, \cdots, n_\alpha - 1$.
- $x_{n_\alpha-1}, x_{n_\alpha}$ in $S_{0,\beta}$ are glued to $f - x_1, y_1$ in $S_{n_\alpha,\alpha}$.
- $x_i - x_{i+1}, y_{i+1} - y_i$ in $S_{n_\alpha,\alpha}$ are glued to f, f in $S_{i,\beta}$ for $i = 1, \cdots, n_\beta - 1$.
- $x_{n_\beta} - y_{n_\beta}$ in $S_{n_\alpha,\alpha}$ is glued to f in $S_{n_\beta,\beta}$.

Gluing rules for $\mathfrak{so}(2n_\alpha+1)^{(1)}$ - 3 $\rightarrow$ $\mathfrak{sp}(n_\beta)^{(1)}$: we can take any geometry with $2n_\beta \leq \nu \leq 2n_\alpha - 7 - n_\beta$ for $\mathfrak{so}(2n_\alpha+1)^{(1)}$, and any geometry with $1 \leq \nu \leq 2n_\beta + 8 - n_\alpha$ for $\mathfrak{sp}(n_\beta)^{(1)}$. The (non-geometric) gluing rules are:

- $f - x_1, x_{2n_\beta} - y_{2n_\beta}, y_1$ in $S_{0,\alpha}$ are glued to $f - x_2, f, f - x_1$ in $S_{0,\beta}$.
- $x_i - x_{i+1}, y_{i+1} - y_i, x_{2n_\beta-i} - x_{2n_\beta-i+1}, y_{2n_\beta-i+1} - y_{2n_\beta-i}$ in $S_{0,\alpha}$ are glued to f, f, f, f in $S_{i,\beta}$ for $i = 1, \cdots, n_\beta - 1$.
- $x_{n_\beta} - x_{n_\beta+1}, y_{n_\beta+1} - y_{n_\beta}$ in $S_{0,\alpha}$ are glued to f, f in $S_{n_\beta,\beta}$.
- $x_i - x_{i+1}$ in $S_{0,\beta}$ is glued to f in $S_{i,\alpha}$ for $i = 1, \cdots, n_\alpha - 1$.
- $x_{n_\alpha}, x_{n_\alpha}$ in $S_{0,\beta}$ are glued to x_1, y_1 in $S_{n_\alpha,\alpha}$.
- $x_{i+1} - x_i, y_{i+1} - y_i$ in $S_{n_\alpha,\alpha}$ are glued to f, f in $S_{i,\beta}$ for $i = 1, \cdots, n_\beta - 1$.
- $f - x_{n_\beta}, f - y_{n_\beta}$ in $S_{n_\alpha,\alpha}$ are glued to $f - x_1, x_1$ in $S_{n_\beta,\beta}$.

Gluing rules for $\mathfrak{so}(2n_\alpha)^{(2)}$ – 3 $\rightarrow$ $\mathfrak{sp}(n_\beta)^{(1)}$: we can take any geometry with $2n_\beta \leq \nu \leq 2n_\alpha - 8 - n_\beta$ for $\mathfrak{so}(2n_\alpha)^{(2)}$, and any geometry with $1 \leq \nu \leq 2n_\beta + 8 - n_\alpha$ for $\mathfrak{sp}(n_\beta)^{(1)}$. The (non-geometric) gluing rules are:

- $f - x_1, x_{2n_\beta} - y_{2n_\beta}, y_1, f$ in $S_{0,\alpha}$ are glued to $f - x_2, f, f - x_1, x_1 - x_2$ in $S_{0,\beta}$.
- $x_i - x_{i+1}, y_{i+1} - y_i, x_{2n_\beta-i} - x_{2n_\beta-i+1}, y_{2n_\beta-i+1} - y_{2n_\beta-i}$ in $S_{0,\alpha}$ are glued to f, f, f, f in $S_{i,\beta}$ for $i = 1, \cdots, n_\beta - 1$.

- $x_{n_\beta} - x_{n_\beta+1}, y_{n_\beta+1} - y_{n_\beta}$ in $S_{0,\alpha}$ are glued to f, f in $S_{n_\beta,\beta}$.
- $x_{i+1} - x_{i+2}$ in $S_{0,\beta}$ is glued to f in $S_{i,\alpha}$ for $i = 1, \cdots, n_\alpha - 2$.
- $x_{n_\alpha}, x_{n_\alpha}$ in $S_{0,\beta}$ are glued to x_1, y_1 in $S_{n_\alpha-1,\alpha}$.
- $x_{i+1} - x_i, y_{i+1} - y_i$ in $S_{n_\alpha-1,\alpha}$ are glued to f, f in $S_{i,\beta}$ for $i = 1, \cdots, n_\beta - 1$.
- $f - x_{n_\beta}, f - y_{n_\beta}$ in $S_{n_\alpha-1,\alpha}$ are glued to $f - x_1, x_1$ in $S_{n_\beta,\beta}$.

5.4 Gluing rules involving non-gauge-theoretic nodes

There are only three such nodes which are listed below

$$\begin{array}{c}\mathfrak{sp}(0)^{(1)}_\theta\\ 1\end{array} \tag{5.180}$$

$$\begin{array}{c}\mathfrak{su}(1)^{(1)}\\ 2\end{array} \tag{5.181}$$

$$\begin{array}{c}\mathfrak{su}(1)^{(1)}\\ 2\end{array} \tag{5.182}$$

The theta angle for $\mathfrak{sp}(0)^{(1)}$ is physically irrelevant as long as there is no neighboring $\mathfrak{su}(8)$.

First consider the edges shown as last two entries of table 4. The gluing rules for these cases are as follows.

Gluing rules for $\begin{array}{ccc}\mathfrak{su}(1)^{(1)} & & \mathfrak{sp}(1)^{(1)}\\ \mathbf{2} & \text{———} & \mathbf{1}\end{array}$ **and** $\begin{array}{ccc}\mathfrak{su}(1)^{(1)} & & \mathfrak{su}(2)^{(1)}\\ \mathbf{2} & \text{———} & \mathbf{2}\end{array}$: we can choose any geometry with $1 \leq \nu \leq 10$ for $\mathfrak{sp}(1)^{(1)}$ and any geometry with $1 \leq \nu \leq 4$ for $\mathfrak{su}(2)^{(1)}$. The (non-geometric) gluing rules are:

- $f - x - y$ in $S_{0,\alpha}$ is glued to f in $S_{0,\beta}$.
- x, y in $S_{0,\alpha}$ are glued to $f - x_1, x_1$ in $S_{1,\beta}$.

As in cases discussed in last subsection, the blowup x_1 in $S_{1,\beta}$ can be used for gluing $\mathfrak{sp}(1)^{(1)}$ or $\mathfrak{su}(2)^{(1)}$ with another neighbor such that the gluing rules for $\mathfrak{sp}(1)^{(1)}$ or $\mathfrak{su}(2)^{(1)}$ with that neighbor allow a blowup on $S_{1,\beta}$ to be used for more than once.

The gluing rules for the edges shown in table 5 are as follows.

Gluing rules for $\begin{array}{ccc}\mathfrak{sp}(0)^{(1)} & & \mathfrak{su}(1)^{(1)}\\ \mathbf{1} & \text{———} & \mathbf{2}\end{array}$:

- $3l - \sum x_i$ in $S_{0,\alpha}$ is glued to f in $S_{0,\beta}$.

See appendix (B.2) for a derivation of the above gluing rules.

JHEP12(2020)151

Gluing rules for $\begin{array}{ccc}\mathfrak{su}(1)^{(1)} & & \mathfrak{su}(1)^{(1)} \\ \mathbf{2} & \frac{\qquad}{} & \mathbf{2}\end{array}$:

- $f-x, x$ in $S_{0,\alpha}$ are glued to $f-x, x$ in $S_{0,\beta}$.

The blowups x in $S_{0,\alpha}$ and x in $S_{0,\beta}$ can be used for gluing to other $\mathfrak{su}(1)^{(1)}$ neighbors. See appendix (B.2) for a derivation of the above gluing rules.

Now consider the edges shown in the last entry of table 9:

Gluing rules for $\begin{array}{ccc}\mathfrak{su}(2)^{(1)} & & \mathfrak{su}(1)^{(1)} \\ \mathbf{2} & \frac{\qquad}{} & \mathbf{2}\end{array}$:

- $f-x_1, x_1$ in $S_{0,\alpha}$ are glued to x, y in $S_{0,\beta}$.
- f in $S_{1,\alpha}$ is glued to $f-x-y$ in $S_{0,\beta}$.

Gluing rules for $\begin{array}{ccc}\mathfrak{su}(1)^{(1)} & & \mathfrak{su}(1)^{(1)} \\ \mathbf{2} & \frac{\qquad}{} & \mathbf{2}\end{array}$:

- $2h-x-2y, f-x$ in $S_{0,\alpha}$ are glued to $f-x, x$ in $S_{0,\beta}$.

The blowup x in $S_{0,\beta}$ can be used for gluing to other $\mathfrak{su}(1)^{(1)}$ neighbors. See appendix (B.2) for a derivation of the above gluing rules. We remind the reader that this gluing rule involves the non-geometric node (5.161) and hence the above gluing rules should be viewed only as an algebraic description and not as a geometric description. See the discussion after equation (5.160) for more details.

Now consider the last entry of table 11:

Gluing rules for $\begin{array}{ccc}\mathfrak{su}(2)^{(1)} & & \mathfrak{su}(1)^{(1)} \\ \mathbf{2} & \overset{2}{\longrightarrow} & \mathbf{2}\end{array}$: we can use any geometry with $1 \leq \nu \leq 3$ for $\mathfrak{su}(2)^{(1)}$. The gluing rules are:

- $f-x_1, x_1$ in $S_{0,\alpha}$ are glued to x, y in $S_{0,\beta}$.
- $f-x_1, x_1$ in $S_{1,\alpha}$ are glued to $f-x, f-y$ in $S_{0,\beta}$.

The blowups x_1 in $S_{0,\alpha}$ and x_1 in $S_{1,\alpha}$ can also be used for gluing to other neighboring nodes of $\mathfrak{su}(2)^{(1)}$ that carry some $\mathfrak{su}(n)^{(1)}$.

Gluing rules for $\begin{array}{ccc}\mathfrak{su}(2)^{(1)} & & \mathfrak{su}(1)^{(1)} \\ \mathbf{2} & \overset{3}{\longrightarrow} & \mathbf{2}\end{array}$: we can use any geometry with $1 \leq \nu \leq 3$ for $\mathfrak{su}(2)^{(1)}$. The gluing rules are:

- $f-x_1, x_1$ in $S_{0,\alpha}$ are glued to x, y in $S_{0,\beta}$.
- $f-x_1, x_1$ in $S_{1,\alpha}$ are glued to $2f-x, f-y$ in $S_{0,\beta}$.

JHEP12(2020)151

The blowups x_1 in $S_{0,\alpha}$ and x_1 in $S_{1,\alpha}$ can also be used for gluing to other neighboring nodes of $\mathfrak{su}(2)^{(1)}$ that carry some $\mathfrak{su}(n)^{(1)}$.

Gluing rules for $\overset{\mathfrak{su}(1)^{(1)}}{\mathbf{2}} \overset{}{\underset{2}{\longrightarrow}} \overset{\mathfrak{su}(1)^{(1)}}{\mathbf{2}}$:

- $f-x, x$ in $S_{0,\alpha}$ are glued to $2f-x, x$ in $S_{0,\beta}$.

(Note that the gluing rules proposed above are non-geometric.) The blowups x in $S_{0,\alpha}$ and x in $S_{0,\beta}$ can be used to further glue to other neighboring $\mathfrak{su}(1)^{(1)}$. See appendix (B.2) for a derivation of the above gluing rules.

Gluing rules for $\overset{\mathfrak{su}(1)^{(1)}}{\mathbf{2}} \overset{}{\underset{3}{\longrightarrow}} \overset{\mathfrak{su}(1)^{(1)}}{\mathbf{2}}$:

- $f-x, x$ in $S_{0,\alpha}$ are glued to $3f-x, x$ in $S_{0,\beta}$.

(Note that the gluing rules proposed above are non-geometric.) The blowups x in $S_{0,\alpha}$ and x in $S_{0,\beta}$ can be used to further glue to other neighboring $\mathfrak{su}(1)^{(1)}$.

5.4.1 $\mathfrak{sp}(0)^{(1)}$ gluings: untwisted, without non-simply-laced

At this point, we are only left with gluings of $\mathfrak{sp}(0)^{(1)}$ to other nodes carrying non-trivial gauge algebras. In this case, we also have to provide gluing rules for two neighbors at a time. This is because the torus fiber for dP_9 is $3l - \sum x_i$ which involves all of the blowups. So all of the blowups must appear in the gluing rules associated to each edge. This is in stark contrast to the gluing rules for non-trivial algebras $\mathfrak{g}^{(q)}$ where (typically) the blowups used for gluing rules associated to different edges are different. Thus in the case of $\mathfrak{g}^{(q)}$, the gluing rules for different edges naturally decouple. However, in the case of $\mathfrak{sp}(0)^{(1)}$, we have to provide gluing rules for multiple neighbors at a time and show explicitly that the curves inside dP_9 involved in gluing rules for different edges do not intersect. It turns out that in the context of $6d$ SCFTs, $\mathfrak{sp}(0)^{(1)}$ can only have a maximum of two neighbors carrying non-trivial algebras.

In the case when all the neighbors are untwisted, $\mathfrak{sp}(0)^{(1)}$ gluings were first studied in [4]. For the completeness of our presentation, we reproduce their results in this subsection (providing enhanced explanations while we do so) before moving onto $\mathfrak{sp}(0)^{(1)}$ gluings arising in the twisted case. Following [4], we will represent these $\mathfrak{sp}(0)^{(1)}$ gluing rules in a graphical notation that we review as we review the results of [4].

To start with, let us consider the gluing rules for

$$\mathfrak{sp}(0)^{(1)} \text{ —— } \mathfrak{e}_8^{(1)} \tag{5.183}$$

which are displayed below

$$\boxed{\mathfrak{sp}(0)^{(1)} \text{ ——— } \mathfrak{e}_8^{(1)}}$$

$$\begin{array}{ccccccccccccccc} & & & & & & & & & & l-x_1-x_2-x_3 & & & & \\ & & & & & & & & & & | & & & & \\ x_8-x_9 & — & x_7-x_8 & — & x_6-x_7 & — & x_5-x_6 & — & x_4-x_5 & — & x_1-x_4 & — & x_2-x_1 & — & x_3-x_2 \end{array} \tag{5.184}$$

where each node denotes a curve in dP_9 whose genus is zero and self-intersection is -2. If there are n edges between two nodes, it denotes that the two corresponding curves intersect in n number of points. Each curve C_a shown above is glued to the fiber f of a Hirzebruch surface S_a in the geometry associated to $\mathfrak{e}_8^{(1)}$. Which curve glues to the fiber of which S_a can be figured out from the position of the curve in the graph above, because the graph takes the form of the corresponding Dynkin diagram, which in this case is $\mathfrak{e}_8^{(1)}$. Notice that

$$\begin{aligned} \sum_a d_a C_a &= (x_8-x_9)+2(x_7-x_8)+3(x_6-x_7)+4(x_5-x_6)+5(x_4-x_5)+6(x_1-x_4) \\ &\quad +4(x_2-x_1)+2(x_3-x_2)+3(l-x_1-x_2-x_3) \\ &= 3l-\sum x_i \end{aligned} \tag{5.185}$$

and thus the torus fibers on both nodes are glued to each other, satisfying (5.60) for the untwisted case.

Now, we can use the above gluing rules to obtain gluing rules for regular maximal subalgebras of $\mathfrak{e}_8$ as follows. For example, to obtain the gluing rules for

$$\mathfrak{su}(2)^{(1)} \text{ ——— } \mathfrak{sp}(0)^{(1)} \text{ ——— } \mathfrak{e}_7^{(1)} \tag{5.186}$$

we first delete the second curve from the left x_7-x_8 in (5.184). After this deletion, the graph takes the form of Dynkin diagram for finite algebra $\mathfrak{su}(2)\oplus\mathfrak{e}_7$. To obtain the gluing rules for (5.186), we simply need to add two extra -2 curves to the graph such that the finite Dynkin diagram of $\mathfrak{su}(2)$ is converted to the affine Dynkin diagram of $\mathfrak{su}(2)^{(1)}$ and similarly the finite Dynkin diagram of $\mathfrak{e}_7$ is converted to the affine Dynkin diagram of $\mathfrak{e}_7^{(1)}$. This is easy to do since we know that a weighted sum of the -2 curves participating in gluing to each affine Dynkin diagram must be $3l-\sum x_i$. This requirement uniquely fixes the extra -2 curves that need to be added. We thus obtain

$$\mathfrak{e}_7^{(1)} \text{ --- } \mathfrak{sp}(0)^{(1)} \text{ --- } \mathfrak{su}(2)^{(1)}$$

$$\begin{array}{ccccccccccccc} & & & & & & l-x_1-x_2-x_3 & & & & & & \\ & & & & & & | & & & & & & \\ x_6-x_7 & - & x_5-x_6 & - & x_4-x_5 & - & x_1-x_4 & - & x_2-x_1 & - & x_3-x_2 & - & l-x_3-x_8-x_9 \end{array}$$

$$x_8-x_9 \;=\!=\!=\; 3l-x_1-x_2-x_3-x_4-x_5-x_6-x_7-2x_8 \tag{5.187}$$

as the gluing rules for (5.186). $l-x_3-x_8-x_9$ glues to the fiber of affine surface for $\mathfrak{e}_7^{(1)}$ and x_8-x_9 glues to the fiber of affine surface for $\mathfrak{su}(2)^{(1)}$. Notice that the curves in each sub-Dynkin diagram sum up to $3l-\sum x_i$ if the sum is weighted by the Coxeter labels of the corresponding affine Dynkin diagram. Also notice that the curves forming the Dynkin diagram for $\mathfrak{e}_7^{(1)}$ do not intersect the curves forming the Dynkin diagram for $\mathfrak{su}(2)^{(1)}$, which explicitly shows that the gluing rules for the two neighbors of $\mathfrak{sp}(0)^{(1)}$ decouple from each other as required.

Incidentally, (5.187) allows us to determined gluing rules for

$$\mathfrak{sp}(0)^{(1)} \text{ --- } \mathfrak{e}_7^{(1)} \tag{5.188}$$

and

$$\mathfrak{sp}(0)^{(1)} \text{ --- } \mathfrak{su}(2)^{(1)} \tag{5.189}$$

without any other second neighbor for $\mathfrak{sp}(0)^{(1)}$. This is done by only keeping the curves spanning the Dynkin diagram of $\mathfrak{e}_7^{(1)}$ or the Dynkin diagram of $\mathfrak{su}(2)^{(1)}$, while omitting the rest of the curves from (5.187). Thus, we obtain

$$\mathfrak{sp}(0)^{(1)} \text{ --- } \mathfrak{e}_7^{(1)}$$

$$\begin{array}{ccccccccccccc} & & & & & & l-x_1-x_2-x_3 & & & & & & \\ & & & & & & | & & & & & & \\ x_6-x_7 & - & x_5-x_6 & - & x_4-x_5 & - & x_1-x_4 & - & x_2-x_1 & - & x_3-x_2 & - & l-x_3-x_8-x_9 \end{array} \tag{5.190}$$

with the fiber in affine surface glued to $l-x_3-x_8-x_9$ and

$$\mathfrak{sp}(0)^{(1)} \text{ --- } \mathfrak{su}(2)^{(1)}$$

$$x_8-x_9 \;=\!=\!=\; 3l-x_1-x_2-x_3-x_4-x_5-x_6-x_7-2x_8 \tag{5.191}$$

with the fiber in affine surface glued to x_8-x_9.

Deleting other nodes from (5.184), we can obtain the following gluing rules

$$
\begin{tikzcd}
\mathfrak{sp}(0)^{(1)} \arrow[r, dash] & \mathfrak{so}(16)^{(1)}
\end{tikzcd}
$$

$$
\begin{tikzcd}[column sep=small]
& 2l-x_1-x_2-x_4-x_5-x_6-x_7 \arrow[d, dash] & & & & l-x_1-x_2-x_3 \arrow[d, dash] & \\
x_8-x_9 \arrow[r, dash] & x_7-x_8 \arrow[r, dash] & x_6-x_7 \arrow[r, dash] & x_5-x_6 \arrow[r, dash] & x_4-x_5 \arrow[r, dash] & x_1-x_4 \arrow[r, dash] & x_2-x_1
\end{tikzcd}
\tag{5.192}
$$

where $x_8 - x_9$ glues to the fiber of affine surface for $\mathfrak{so}(16)^{(1)}$.

$$
\begin{tikzcd}
\mathfrak{sp}(0)^{(1)} \arrow[r, dash] & \mathfrak{su}(9)^{(1)}
\end{tikzcd}
$$

$$
\begin{tikzcd}[column sep=small]
& & & & 3l-x_1-x_2-2x_3-x_4-x_5-x_6-x_7-x_8 \arrow[dllll, dash] \arrow[drrrr, dash] & & & & \\
x_8-x_9 \arrow[r, dash] & x_7-x_8 \arrow[r, dash] & x_6-x_7 \arrow[r, dash] & x_5-x_6 \arrow[r, dash] & x_4-x_5 \arrow[r, dash] & x_1-x_4 \arrow[r, dash] & x_2-x_1 \arrow[r, dash] & x_3-x_2
\end{tikzcd}
\tag{5.193}
$$

where $x_8 - x_9$ glues to the fiber of affine surface for $\mathfrak{su}(9)^{(1)}$.

$$
\begin{tikzcd}
\mathfrak{e}_6^{(1)} \arrow[r, dash] & \mathfrak{sp}(0)^{(1)} \arrow[r, dash] & \mathfrak{su}(3)^{(1)}
\end{tikzcd}
$$

$$
\begin{tikzcd}[column sep=small]
& & l-x_7-x_8-x_9 \arrow[d, dash] & & \\
& & l-x_1-x_2-x_3 \arrow[d, dash] & & \\
x_5-x_6 \arrow[r, dash] & x_4-x_5 \arrow[r, dash] & x_1-x_4 \arrow[r, dash] & x_2-x_1 \arrow[r, dash] & x_3-x_2 \\
& & 3l-x_1-x_2-x_3-x_4-x_5-x_6-2x_7-x_8 \arrow[dl, dash] \arrow[dr, dash] & & \\
& x_8-x_9 \arrow[rr, dash] & & x_7-x_8 &
\end{tikzcd}
\tag{5.194}
$$

where $l - x_7 - x_8 - x_9$ glues to the fiber of affine surface for $\mathfrak{e}_6^{(1)}$ and $x_8 - x_9$ glues to the fiber of affine surface for $\mathfrak{su}(3)^{(1)}$. Incidentally, this also allows us to obtain the following individual gluing rules

$$
\begin{tikzcd}[column sep=small]
\mathfrak{sp}(0)^{(1)} \arrow[r, dash] & \mathfrak{e}_6^{(1)}
\end{tikzcd}
$$

$$
\begin{tikzcd}[column sep=small]
& & l-x_7-x_8-x_9 \arrow[d, dash] & & \\
& & l-x_1-x_2-x_3 \arrow[d, dash] & & \\
x_5-x_6 \arrow[r, dash] & x_4-x_5 \arrow[r, dash] & x_1-x_4 \arrow[r, dash] & x_2-x_1 \arrow[r, dash] & x_3-x_2
\end{tikzcd}
\tag{5.195}
$$

with the fiber in affine surface glued to $l-x_7-x_8-x_9$, and

$$
\begin{tikzcd}[column sep=small]
\mathfrak{sp}(0)^{(1)} \arrow[r, dash] & \mathfrak{su}(3)^{(1)}
\end{tikzcd}
$$

$$
\begin{tikzcd}[column sep=small]
& 3l-x_1-x_2-x_3-x_4-x_5-x_6-2x_7-x_8 \arrow[dl, dash] \arrow[dr, dash] & \\
x_8-x_9 \arrow[rr, dash] & & x_7-x_8
\end{tikzcd}
\tag{5.196}
$$

with the fiber in affine surface glued to x_8-x_9.

Now we can delete some nodes from the above set of gluing rules to obtain gluing rules for other algebras that arise as regular maximal subalgebras of the above algebras. For example, by deleting nodes from (5.192), we can obtain the gluing rules for

$$
\begin{tikzcd}
\mathfrak{so}(8)^{(1)} \arrow[r, dash] & \mathfrak{sp}(0)^{(1)} \arrow[r, dash] & \mathfrak{so}(8)^{(1)}
\end{tikzcd}
\tag{5.197}
$$

since $\mathfrak{so}(8)\oplus\mathfrak{so}(8)$ is a regular maximal subalgebra of $\mathfrak{so}(16)$. The gluing rules are

$$
\begin{array}{c}
\boxed{\mathfrak{so}(8)^{(1)} - \mathfrak{sp}(0)^{(1)} - \mathfrak{so}(8)^{(1)}}\\[1em]
\begin{array}{ccccc}
 & & 2l-x_1-x_2-x_4-x_5-x_6-x_7 & & \\
 & & | & & \\
x_8-x_9 & — & x_7-x_8 & — & x_6-x_7\\
 & & | & & \\
 & & l-x_3-x_6-x_7 & &
\end{array}\\[1em]
\begin{array}{ccccc}
 & & l-x_1-x_2-x_3 & & \\
 & & | & & \\
x_4-x_5 & — & x_1-x_4 & — & x_2-x_1\\
 & & | & & \\
 & & 2l-x_1-x_2-x_6-x_7-x_8-x_9 & &
\end{array}
\end{array}
\tag{5.198}
$$

where the fibers in affine surfaces glue to x_8-x_9 and $2l-x_1-x_2-x_6-x_7-x_8-x_9$. Tha bove gluing rules imply that the gluing rules for a single $\mathfrak{so}(8)^{(1)}$ are obtained by amputating one of the $\mathfrak{so}(8)^{(1)}$ sub-graph from (5.198).

$$
\begin{array}{c}
\boxed{\mathfrak{sp}(0)^{(1)} - \mathfrak{so}(8)^{(1)}}\\[1em]
\begin{array}{ccccc}
 & & 2l-x_1-x_2-x_4-x_5-x_6-x_7 & & \\
 & & | & & \\
x_8-x_9 & — & x_7-x_8 & — & x_6-x_7\\
 & & | & & \\
 & & l-x_3-x_6-x_7 & &
\end{array}
\end{array}
\tag{5.199}
$$

with the fiber in affine surface glued to x_8-x_9. The reader might wonder what happens if amputate the other $\mathfrak{so}(8)^{(1)}$ sub-graph from (5.198) to obtain the gluing rules as

$$\begin{tikzcd} & l-x_1-x_2-x_3 \arrow[d, dash] & \\ x_4-x_5 \arrow[r, dash] & x_1-x_4 \arrow[r, dash] \arrow[d, dash] & x_2-x_1 \\ & 2l-x_1-x_2-x_6-x_7-x_8-x_9 & \end{tikzcd} \tag{5.200}$$

It turns out that (5.199) and (5.200) are related by an automorphism of dP_9. To see this, let's first relabel the blowups as

$$x_1 \leftrightarrow x_7 \tag{5.201}$$

$$x_2 \leftrightarrow x_6 \tag{5.202}$$

$$x_3 \leftrightarrow x_5 \tag{5.203}$$

$$x_4 \leftrightarrow x_8 \tag{5.204}$$

so that (5.199) is converted to

$$\begin{tikzcd} & 2l-x_1-x_2-x_3-x_6-x_7-x_8 \arrow[d, dash] & \\ x_4-x_9 \arrow[r, dash] & x_1-x_4 \arrow[r, dash] \arrow[d, dash] & x_2-x_1 \\ & l-x_1-x_2-x_5 & \end{tikzcd} \tag{5.205}$$

Now we perform two basic automorphisms of dP_9. The basic automorphisms are described in appendix A.2 and involve a choice of three blowups. For the first basic automorphism we choose the blowups x_1, x_2 and x_4, and after performing this operation the gluing rules (5.205) are transformed to

$$\begin{tikzcd} & 2l-x_1-x_2-x_3-x_6-x_7-x_8 \arrow[d, dash] & \\ l-x_1-x_2-x_9 \arrow[r, dash] & x_1-x_4 \arrow[r, dash] \arrow[d, dash] & x_2-x_1 \\ & x_4-x_5 & \end{tikzcd} \tag{5.206}$$

JHEP12(2020)151

For the second basic automorphism we choose x_6, x_7 and x_8 thus transforming (5.206) to

$$\begin{tikzcd}
 & l-x_1-x_2-x_3 \arrow[d, dash] & \\
2l-x_1-x_2-x_6-x_7-x_8-x_9 \arrow[r, dash] & x_1-x_4 \arrow[r, dash] \arrow[d, dash] & x_2-x_1 \\
 & x_4-x_5 &
\end{tikzcd} \tag{5.207}$$

which precisely matches (5.200), thus demonstrating that (5.199) and (5.200) are isomorphic gluing rules.

This will hold true in general in what follows. Whenever we will find two seemingly different gluing rules, they will always turn out to be related by an automorphism, except for two cases. These two cases are the gluing rules for $\mathfrak{su}(8)^{(1)}$ and $\mathfrak{su}(8)^{(2)}$, where we find two possible gluing rules in each case. The two possibilities correspond to different choices of theta angle for $\mathfrak{sp}(0)$ in the $6d$ theory.

Let us collect all of the remaining gluing rules below

$$\mathfrak{so}(10)^{(1)} \text{ --- } \mathfrak{sp}(0)^{(1)} \text{ --- } \mathfrak{su}(4)^{(1)}$$

$$\begin{tikzcd}
 & l-x_1-x_2-x_3 \arrow[d, dash] & 2l-x_2-x_3-x_6-x_7-x_8-x_9 \arrow[d, dash] & \\
x_4-x_5 \arrow[r, dash] & x_1-x_4 \arrow[r, dash] & x_2-x_1 \arrow[r, dash] & x_3-x_2
\end{tikzcd}$$

$$\begin{tikzcd}
 & 3l-x_1-x_2-x_3-x_4-x_5-2x_6-x_7-x_8 \arrow[dl, dash] \arrow[dr, dash] & \\
x_8-x_9 \arrow[dr, dash] & & x_6-x_7 \arrow[dl, dash] \\
 & x_7-x_8 &
\end{tikzcd} \tag{5.208}$$

where the fibers in affine surfaces glue to $x_8 - x_9$ and $2l - x_2 - x_3 - x_6 - x_7 - x_8 - x_9$.

$$\mathfrak{sp}(0)^{(1)} \text{ --- } \mathfrak{so}(14)^{(1)}$$

$$\begin{tikzcd}
 & 2l-x_1-x_2-x_4-x_5-x_6-x_7 \arrow[d, dash] & & & l-x_1-x_3-x_4 \arrow[d, dash] & \\
x_8-x_9 \arrow[r, dash] & x_7-x_8 \arrow[r, dash] & x_6-x_7 \arrow[r, dash] & x_5-x_6 \arrow[r, dash] & x_4-x_5 \arrow[r, dash] & x_1-x_4
\end{tikzcd} \tag{5.209}$$

where the fiber in affine surface glues to $x_8 - x_9$.

$$\mathfrak{e}_6^{(1)} \;\text{———}\; \mathfrak{sp}(0)^{(1)} \;\text{———}\; \mathfrak{su}(2)^{(1)}$$

$$\begin{tikzcd}
 & & l-x_7-x_8-x_9 \arrow[d, dash] & & \\
 & & l-x_1-x_2-x_3 \arrow[d, dash] & & \\
x_5-x_6 \arrow[r, dash] & x_4-x_5 \arrow[r, dash] & x_1-x_4 \arrow[r, dash] & x_2-x_1 \arrow[r, dash] & x_3-x_2 \\
 & x_8-x_9 \arrow[r, equal] & 3l-x_1-x_2-x_3-x_4-x_5-x_6-x_7-2x_8 & &
\end{tikzcd} \tag{5.210}$$

where the fibers in affine surfaces glue to $x_8 - x_9$ and $l - x_7 - x_8 - x_9$.

$$\mathfrak{so}(12)^{(1)} \;\text{———}\; \mathfrak{sp}(0)^{(1)} \;\text{———}\; \mathfrak{su}(2)^{(1)}$$

$$\begin{tikzcd}
 & 2l-x_1-x_2-x_4-x_5-x_8-x_9 \arrow[d, dash] & & l-x_1-x_2-x_3 \arrow[d, dash] & \\
x_6-x_7 \arrow[r, dash] & x_5-x_6 \arrow[r, dash] & x_4-x_5 \arrow[r, dash] & x_1-x_4 \arrow[r, dash] & x_2-x_1 \\
 & x_8-x_9 \arrow[r, equal] & 3l-x_1-x_2-x_3-x_4-x_5-x_6-x_7-2x_8 & &
\end{tikzcd} \tag{5.211}$$

where the fibers in affine surfaces glue to $x_8 - x_9$ and $2l - x_1 - x_2 - x_4 - x_5 - x_8 - x_9$.

$$\mathfrak{so}(10)^{(1)} \;\text{———}\; \mathfrak{sp}(0)^{(1)} \;\text{———}\; \mathfrak{su}(3)^{(1)}$$

$$\begin{tikzcd}
 & l-x_1-x_2-x_3 \arrow[d, dash] & & 2l-x_2-x_3-x_6-x_7-x_8-x_9 \arrow[d, dash] & \\
x_4-x_5 \arrow[r, dash] & x_1-x_4 \arrow[rr, dash] & & x_2-x_1 \arrow[r, dash] & x_3-x_2 \\
 & & 3l-x_1-x_2-x_3-x_4-x_5-x_6-2x_7-x_8 \arrow[dl, dash] \arrow[dr, dash] & & \\
 & x_8-x_9 \arrow[rr, dash] & & x_7-x_8 &
\end{tikzcd} \tag{5.212}$$

where the fibers in affine surfaces glue to $x_8 - x_9$ and $2l - x_2 - x_3 - x_6 - x_7 - x_8 - x_9$.

$$
\begin{tikzcd}
\mathfrak{so}(8)^{(1)} \arrow[r, dash] & \mathfrak{sp}(0)^{(1)} \arrow[r, dash] & \mathfrak{su}(4)^{(1)}
\end{tikzcd}
$$

$$
\begin{tikzcd}
& 2l - x_2 - x_3 - x_6 - x_7 - x_8 - x_9 \arrow[d, dash] & \\
x_1 - x_4 \arrow[r, dash] & x_2 - x_1 \arrow[r, dash] \arrow[d, dash] & x_3 - x_2 \\
& l - x_2 - x_3 - x_5 &
\end{tikzcd}
$$

$$
\begin{tikzcd}
& 3l - x_1 - x_2 - x_3 - x_4 - x_5 - 2x_6 - x_7 - x_8 \arrow[dl, dash] \arrow[dr, dash] & \\
x_8 - x_9 \arrow[dr, dash] & & x_6 - x_7 \arrow[dl, dash] \\
& x_7 - x_8 &
\end{tikzcd}
\tag{5.213}
$$

where the fibers in affine surfaces glue to $x_8 - x_9$ and $2l - x_2 - x_3 - x_6 - x_7 - x_8 - x_9$.

$$
\begin{tikzcd}
\mathfrak{sp}(0)^{(1)} \arrow[r, dash] & \mathfrak{so}(12)^{(1)}
\end{tikzcd}
$$

$$
\begin{tikzcd}
& 2l - x_1 - x_2 - x_4 - x_5 - x_8 - x_9 \arrow[d, dash] & & l - x_1 - x_2 - x_3 \arrow[d, dash] & \\
x_6 - x_7 \arrow[r, dash] & x_5 - x_6 \arrow[r, dash] & x_4 - x_5 \arrow[r, dash] & x_1 - x_4 \arrow[r, dash] & x_2 - x_1
\end{tikzcd}
\tag{5.214}
$$

where the fiber in affine surface glues to $2l - x_1 - x_2 - x_4 - x_5 - x_8 - x_9$.

$$
\begin{tikzcd}
\mathfrak{sp}(0)^{(1)} \arrow[r, dash] & \mathfrak{su}(7)^{(1)}
\end{tikzcd}
$$

$$
\begin{tikzcd}
& & 3l - 2x_1 - x_2 - x_3 - x_4 - x_5 - x_6 - x_7 - x_8 \arrow[dll, dash] \arrow[drrr, dash] & & & \\
x_8 - x_9 \arrow[r, dash] & x_7 - x_8 \arrow[r, dash] & x_6 - x_7 \arrow[r, dash] & x_5 - x_6 \arrow[r, dash] & x_4 - x_5 \arrow[r, dash] & x_1 - x_4
\end{tikzcd}
\tag{5.215}
$$

where the fiber in affine surface glues to $x_8 - x_9$.

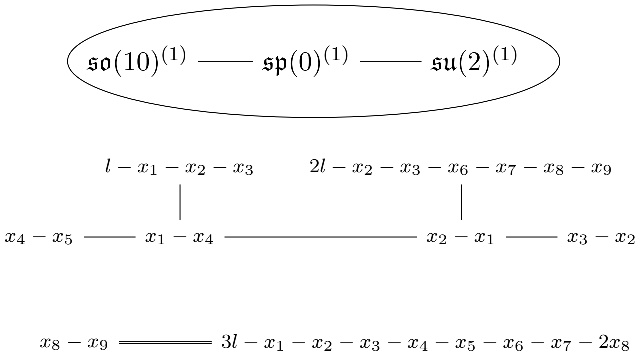

(5.216)

where the fibers in affine surfaces glue to $x_8 - x_9$ and $2l - x_2 - x_3 - x_6 - x_7 - x_8 - x_9$.

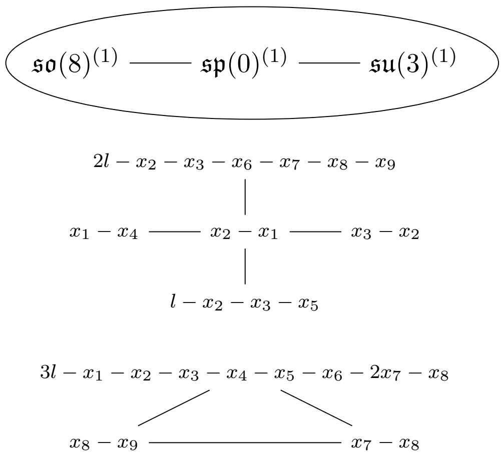

(5.217)

where the fibers in affine surfaces glue to $x_8 - x_9$ and $2l - x_2 - x_3 - x_6 - x_7 - x_8 - x_9$.

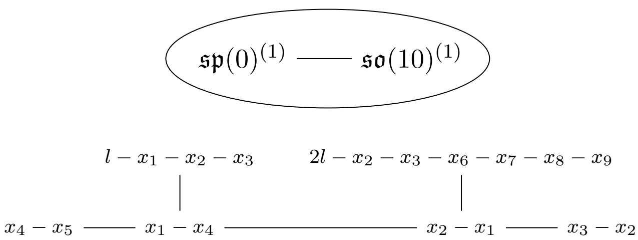

(5.218)

where the fiber in affine surface glues to $2l - x_2 - x_3 - x_6 - x_7 - x_8 - x_9$.

$$\begin{tikzcd}[arrows=dash]
\mathfrak{sp}(0)^{(1)} \arrow[r] & \mathfrak{su}(6)^{(1)}
\end{tikzcd}$$

$$\begin{tikzcd}[arrows=dash, column sep=small]
 & & 3l - x_1 - x_2 - x_3 - 2x_4 - x_5 - x_6 - x_7 - x_8 \arrow[dll] \arrow[drr] & & \\
x_8 - x_9 \arrow[r] & x_7 - x_8 \arrow[r] & x_6 - x_7 \arrow[r] & x_5 - x_6 \arrow[r] & x_4 - x_5
\end{tikzcd} \tag{5.219}$$

where the fiber in affine surface glues to $x_8 - x_9$.

$$\begin{tikzcd}[arrows=dash]
\mathfrak{so}(8)^{(1)} \arrow[r] & \mathfrak{sp}(0)^{(1)} \arrow[r] & \mathfrak{su}(2)^{(1)}
\end{tikzcd}$$

$$\begin{tikzcd}[arrows=dash, column sep=small]
 & 2l - x_2 - x_3 - x_6 - x_7 - x_8 - x_9 \arrow[d] & \\
x_1 - x_4 \arrow[r] & x_2 - x_1 \arrow[r] \arrow[d] & x_3 - x_2 \\
 & l - x_2 - x_3 - x_5 &
\end{tikzcd}$$

$$\begin{tikzcd}[arrows=dash]
x_8 - x_9 \arrow[r, equal] & 3l - x_1 - x_2 - x_3 - x_4 - x_5 - x_6 - x_7 - 2x_8
\end{tikzcd} \tag{5.220}$$

where the fibers in affine surfaces glue to $x_8 - x_9$ and $2l - x_2 - x_3 - x_6 - x_7 - x_8 - x_9$.

$$\begin{tikzcd}[arrows=dash]
\mathfrak{su}(6)^{(1)} \arrow[r] & \mathfrak{sp}(0)^{(1)} \arrow[r] & \mathfrak{su}(3)^{(1)}
\end{tikzcd}$$

$$\begin{tikzcd}[arrows=dash, column sep=small]
 & & 3l - x_1 - x_2 - 2x_3 - x_4 - x_5 - x_7 - x_8 - x_9 \arrow[dll] \arrow[drr] & & \\
x_5 - x_6 \arrow[r] & x_4 - x_5 \arrow[r] & x_1 - x_4 \arrow[r] & x_2 - x_1 \arrow[r] & x_3 - x_2
\end{tikzcd}$$

$$\begin{tikzcd}[arrows=dash, column sep=small]
 & 3l - x_1 - x_2 - x_3 - x_4 - x_5 - x_6 - 2x_7 - x_8 \arrow[dl] \arrow[dr] & \\
x_8 - x_9 \arrow[rr] & & x_7 - x_8
\end{tikzcd} \tag{5.221}$$

where the fibers in affine surfaces glue to $x_8 - x_9$ and $3l - x_1 - x_2 - 2x_3 - x_4 - x_5 - x_7 - x_8 - x_9$.

$$\mathfrak{su}(5)^{(1)} \text{ --- } \mathfrak{sp}(0)^{(1)} \text{ --- } \mathfrak{su}(3)^{(1)}$$

$$\begin{array}{ccccccc} & & & 3l - x_1 - x_2 - 2x_3 - x_4 - x_5 - x_7 - x_8 - x_9 & & & \\ x_4 - x_6 & \text{---} & x_1 - x_4 & \text{---} & x_2 - x_1 & \text{---} & x_3 - x_2 \end{array}$$

$$\begin{array}{ccc} & 3l - x_1 - x_2 - x_3 - x_4 - x_5 - x_6 - 2x_7 - x_8 & \\ x_8 - x_9 & \text{---} & x_7 - x_8 \end{array} \tag{5.222}$$

where the fibers in affine surfaces glue to $x_8 - x_9$ and $3l - x_1 - x_2 - 2x_3 - x_4 - x_5 - x_7 - x_8 - x_9$.

$$\mathfrak{su}(4)^{(1)} \text{ --- } \mathfrak{sp}(0)^{(1)} \text{ --- } \mathfrak{su}(3)^{(1)}$$

$$\begin{array}{ccccc} & & 3l - x_1 - x_2 - 2x_3 - x_4 - x_5 - x_7 - x_8 - x_9 & & \\ x_1 - x_6 & \text{---} & x_2 - x_1 & \text{---} & x_3 - x_2 \end{array}$$

$$\begin{array}{ccc} & 3l - x_1 - x_2 - x_3 - x_4 - x_5 - x_6 - 2x_7 - x_8 & \\ x_8 - x_9 & \text{---} & x_7 - x_8 \end{array} \tag{5.223}$$

where the fibers in affine surfaces glue to x_8-x_9 and $3l-x_1-x_2-2x_3-x_4-x_5-x_7-x_8-x_9$.

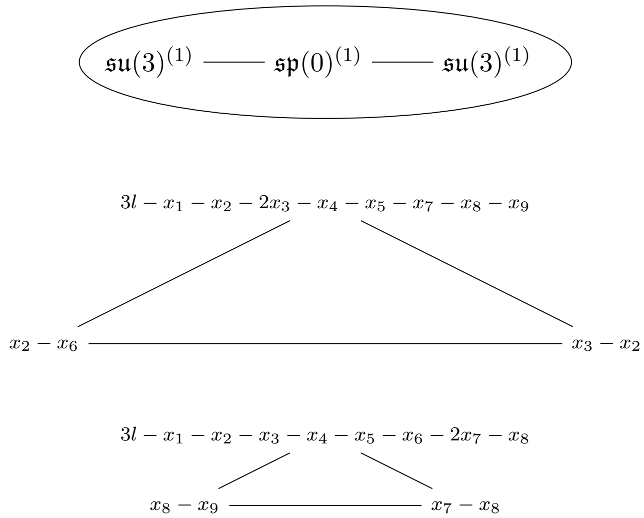

(5.224)

where the fibers in affine surfaces glue to x_8-x_9 and $3l-x_1-x_2-2x_3-x_4-x_5-x_7-x_8-x_9$.

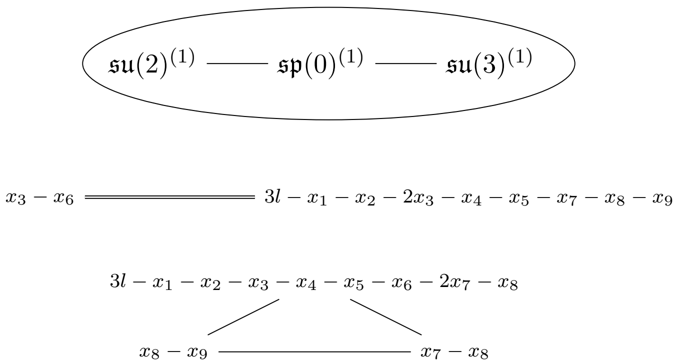

(5.225)

where the fibers in affine surfaces glue to x_8-x_9 and $3l-x_1-x_2-2x_3-x_4-x_5-x_7-x_8-x_9$.

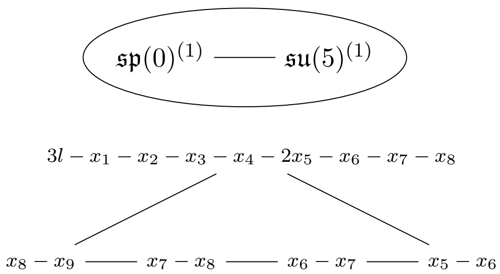

(5.226)

where the fiber in affine surface glues to $x_8 - x_9$.

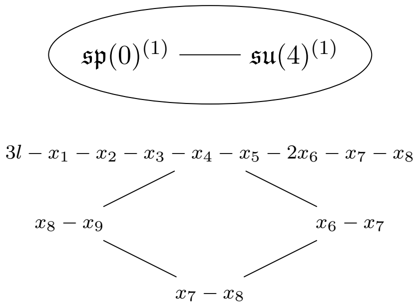

(5.227)

where the fiber in affine surface glues to $x_8 - x_9$.

Finally, we come to the gluing rules for $\mathfrak{su}(8)^{(1)}$ for which we have two versions depending on the choice of theta angle for $\mathfrak{sp}(0)$. The adjoint of $\mathfrak{e}_8$ decomposes into the adjoint plus an irreducible spinor of $\mathfrak{so}(16)$. In our study, this spinor corresponds to the node of $\mathfrak{so}(16)$ Dynkin diagram whose corresponding fiber is glued to $x_2 - x_1$ in (5.192). This is visible from the gluing rules (5.184) for $\mathfrak{e}_8^{(1)}$ since the extra particles in adjoint of $\mathfrak{e}_8$ come from the curve $x_3 - x_2$ which indeed transform in the spinor of $\mathfrak{so}(16)$ associated to $x_2 - x_1$ since $x_3 - x_2$ intersects $x_2 - x_1$.

Now, to obtain the gluing rules for $\mathfrak{su}(8)^{(1)}$, we delete $2l - x_1 - x_2 - x_4 - x_5 - x_6 - x_7$ from (5.192), and we have the choice to either delete $l - x_1 - x_2 - x_3$ or $x_2 - x_1$. This latter choice leads to another choice of spinor of $\mathfrak{so}(16)$. If we delete $x_2 - x_1$, then this matches the previous choice of spinor we had, and leads to the gluing rules for $\theta = 0$. If we delete $l - x_1 - x_2 - x_3$, then this does not match the previous choice of spinor we had, and leads to the gluing rules for $\theta = \pi$. In the latter case, $\mathfrak{su}(8)$ gauges the spinor of $\mathfrak{so}(16)$ in the adjoint of $\mathfrak{e}_8$, and in the former case it does not. Thus the latter case has less global symmetry compared to former. We refer the reader to [38] for more details. The two gluing rules are thus as follows:

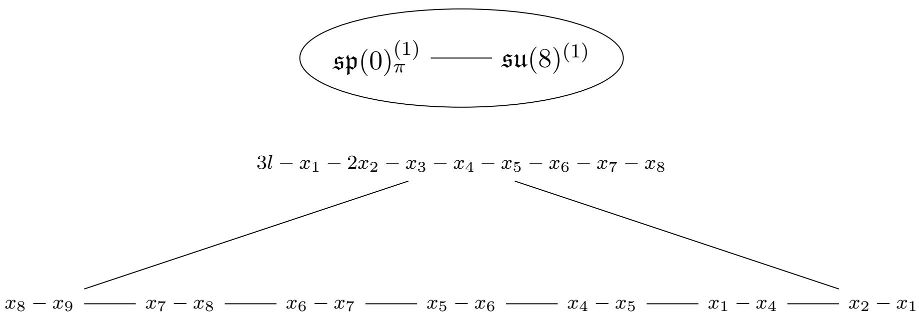

(5.228)

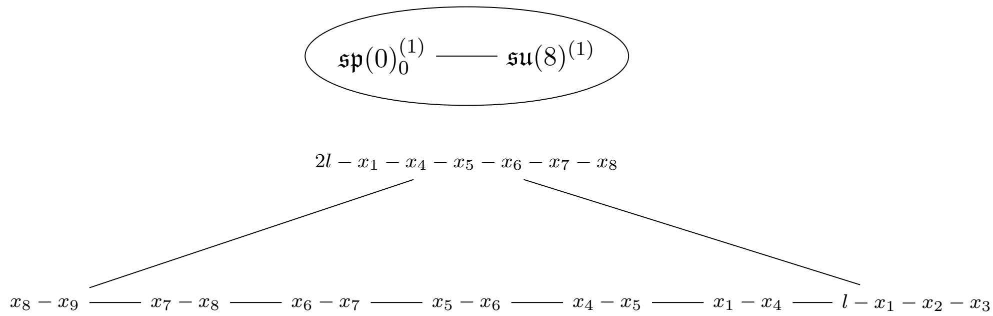

(5.229)

In both the cases, the fiber in affine surface glues to $x_8 - x_9$.

5.4.2 $\mathfrak{sp}(0)^{(1)}$ gluings: untwisted, with non-simply-laced

Until now, we have only considered simply laced subalgebras of $\mathfrak{e}_8$. To generalize our gluing rules to non-simply laced subalgebras of $\mathfrak{e}_8$, we use the folding of Dynkin diagrams. The Dynkin diagrams for untwisted affine non-simply laced algebras can be produced by folding the Dynkin diagrams for untwisted affine simply laced algebras. The foldings relevant in our analysis are:

$$\mathfrak{so}(2n)^{(1)} \to \mathfrak{so}(2n-1)^{(1)} \tag{5.230}$$

$$\mathfrak{e}_6^{(1)} \to \mathfrak{f}_4^{(1)} \tag{5.231}$$

$$\mathfrak{so}(8)^{(1)} \to \mathfrak{so}(7)^{(1)} \to \mathfrak{g}_2^{(1)} \tag{5.232}$$

For example, to obtain the gluing rules for

$$\mathfrak{sp}(0)^{(1)} \;\text{———}\; \mathfrak{so}(15)^{(1)} \tag{5.233}$$

we simply fold the graph (5.192) to obtain

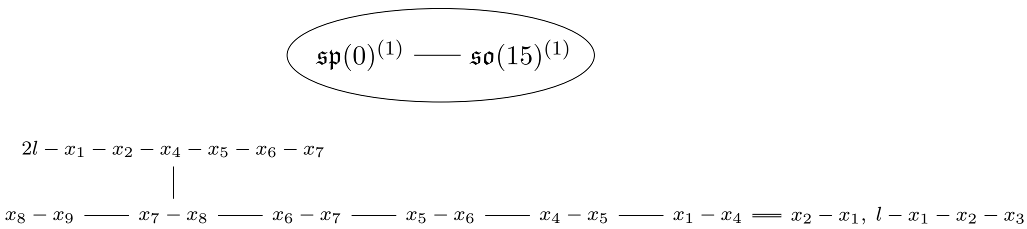

(5.234)

where the fiber in affine surface glues to $x_8 - x_9$ and the rightmost node denotes two -2 curves $x_2 - x_1$ and $l - x_1 - x_2 - x_3$. Both of these curves glue to a copy of the fiber of the corresponding surface in the geometry for $\mathfrak{so}(15)^{(1)}$. We can check that the weighted sum of fibers equals $3l - \sum x_i$.

Since we can now have multiple gluing curves associated to the gluing of dP_9 to some other surface, we have to make sure that all of the gluing curves are on an equal footing. More precisely, we have to make sure that the condition (5.17) is satisfied, which translates

JHEP12(2020)151

to the following condition. Let S_a be the different surfaces dP_9 is glued to, and let C_a^i be the different gluing curves in dP_9 for the gluing to S_a. The *total* gluing curve for the gluing to S_a is

$$C_a := \sum_i C_a^i \tag{5.235}$$

Then (5.17) translates to the condition that

$$C_a^i \cdot C_b = C_a^j \cdot C_b \tag{5.236}$$

for all i, j, a, b. It can be easily verified that (5.234) satisfies this condition. This condition (5.236) will be an important consistency condition in what follows and the reader can verify that all of the geometries that follow satisfy (5.236).

By folding other gluing rules presented above, we can obtain the following gluing rules

$$\mathfrak{so}(9)^{(1)} - \mathfrak{sp}(0)^{(1)} - \mathfrak{su}(4)^{(1)}$$

$$\begin{array}{ccccccc}
 & & & & 2l - x_2 - x_3 - x_6 - x_7 - x_8 - x_9 & & \\
 & & & & | & & \\
l - x_1 - x_2 - x_3,\ x_4 - x_5 & = & x_1 - x_4 & - & x_2 - x_1 & - & x_3 - x_2
\end{array}$$

$$\begin{array}{ccc}
 & 3l - x_1 - x_2 - x_3 - x_4 - x_5 - 2x_6 - x_7 - x_8 & \\
x_8 - x_9 & & x_6 - x_7 \\
 & x_7 - x_8 &
\end{array} \tag{5.237}$$

where the fibers in affine surfaces glue to $x_8 - x_9$ and $2l - x_2 - x_3 - x_6 - x_7 - x_8 - x_9$.

$$\mathfrak{sp}(0)^{(1)} - \mathfrak{so}(13)^{(1)}$$

$$\begin{array}{ccccccccccc}
 & & 2l - x_1 - x_2 - x_4 - x_5 - x_6 - x_7 & & & & & & & & \\
 & & | & & & & & & & & \\
x_8 - x_9 & - & x_7 - x_8 & - & x_6 - x_7 & - & x_5 - x_6 & - & x_4 - x_5 & = & x_1 - x_4,\ l - x_1 - x_3 - x_4
\end{array} \tag{5.238}$$

where the fiber in affine surface glues to $x_8 - x_9$.

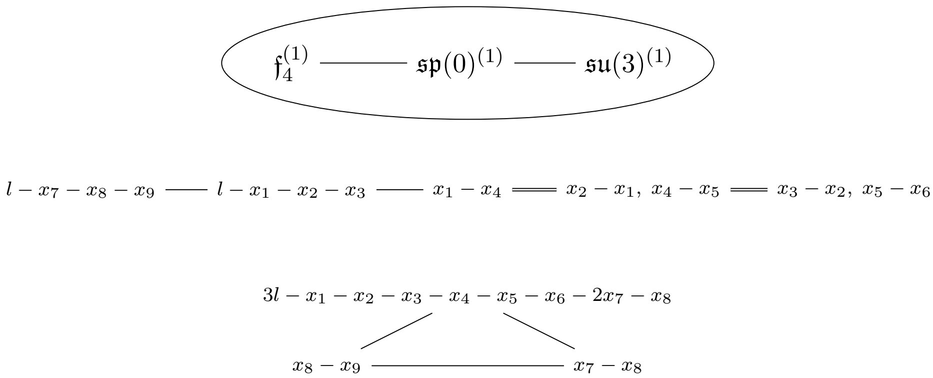

(5.239)

where the fibers in affine surfaces glue to $x_8 - x_9$ and $l - x_7 - x_8 - x_9$.

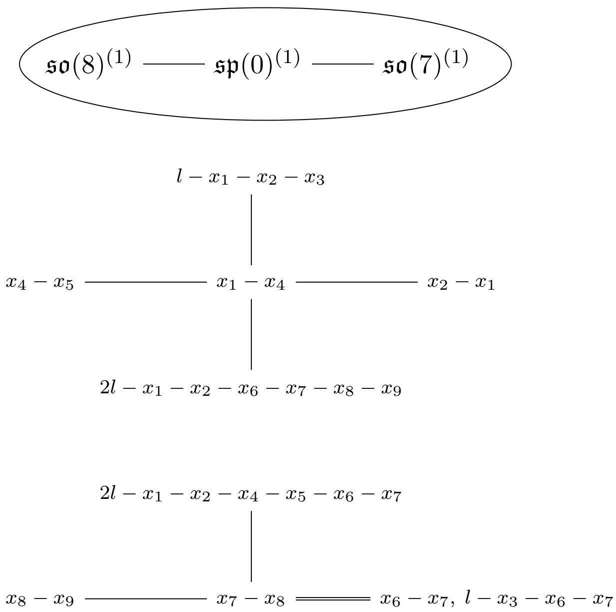

(5.240)

where the fibers in affine surfaces glue to $x_8 - x_9$ and $2l - x_1 - x_2 - x_6 - x_7 - x_8 - x_9$.

$$\mathfrak{so}(7)^{(1)} \;\text{———}\; \mathfrak{sp}(0)^{(1)} \;\text{———}\; \mathfrak{so}(7)^{(1)}$$

$$\begin{tikzcd}
 & 2l-x_1-x_2-x_4-x_5-x_6-x_7 \arrow[d, dash] & \\
x_8-x_9 \arrow[r, dash] & x_7-x_8 \arrow[r, Rightarrow, no head] & x_6-x_7,\ l-x_3-x_6-x_7
\end{tikzcd}$$

$$\begin{tikzcd}
 & 2l-x_1-x_2-x_6-x_7-x_8-x_9 \arrow[d, dash] & \\
x_4-x_5 \arrow[r, dash] & x_1-x_4 \arrow[r, Rightarrow, no head] & x_2-x_1,\ l-x_1-x_2-x_3
\end{tikzcd} \tag{5.241}$$

where the fibers in affine surfaces glue to $x_8 - x_9$ and $2l - x_1 - x_2 - x_6 - x_7 - x_8 - x_9$.

$$\mathfrak{g}_2^{(1)} \;\text{———}\; \mathfrak{sp}(0)^{(1)} \;\text{———}\; \mathfrak{so}(8)^{(1)}$$

$$\begin{tikzcd}
 & l-x_1-x_2-x_3 \arrow[d, dash] & \\
x_4-x_5 \arrow[r, dash] & x_1-x_4 \arrow[r, dash] \arrow[d, dash] & x_2-x_1 \\
 & 2l-x_1-x_2-x_6-x_7-x_8-x_9 &
\end{tikzcd}$$

$$\begin{tikzcd}
x_8-x_9 \arrow[r, dash] & x_7-x_8 \arrow[r, Rightarrow, no head] & x_6-x_7,\ l-x_3-x_6-x_7,\ 2l-x_1-x_2-x_4-x_5-x_6-x_7
\end{tikzcd} \tag{5.242}$$

where the fibers in affine surfaces glue to $x_8 - x_9$ and $2l - x_1 - x_2 - x_6 - x_7 - x_8 - x_9$.

$$\mathfrak{su}(2)^{(1)} \text{ --- } \mathfrak{sp}(0)^{(1)} \text{ --- } \mathfrak{so}(11)^{(1)}$$

$$\begin{tikzcd}
 & 2l-x_1-x_2-x_4-x_5-x_8-x_9 \arrow[d, dash] & & & \\
x_6-x_7 \arrow[r, dash] & x_5-x_6 \arrow[r, dash] & x_4-x_5 \arrow[r, dash] & x_1-x_4 \arrow[r, equal] & x_2-x_1,\ l-x_1-x_2-x_3
\end{tikzcd}$$

$$\begin{tikzcd}
x_8-x_9 \arrow[r, equal] & 3l-x_1-x_2-x_3-x_4-x_5-x_6-x_7-2x_8
\end{tikzcd} \tag{5.243}$$

where the fibers in affine surfaces glue to $x_8 - x_9$ and $2l - x_1 - x_2 - x_4 - x_5 - x_8 - x_9$.

$$\mathfrak{su}(3)^{(1)} \text{ --- } \mathfrak{sp}(0)^{(1)} \text{ --- } \mathfrak{so}(9)^{(1)}$$

$$\begin{tikzcd}
 & & 2l-x_2-x_3-x_6-x_7-x_8-x_9 \arrow[d, dash] & \\
l-x_1-x_2-x_3,\ x_4-x_5 \arrow[r, equal] & x_1-x_4 \arrow[r, dash] & x_2-x_1 \arrow[r, dash] & x_3-x_2
\end{tikzcd}$$

$$\begin{tikzcd}
 & 3l-x_1-x_2-x_3-x_4-x_5-x_6-2x_7-x_8 \arrow[dl, dash] \arrow[dr, dash] & \\
x_8-x_9 \arrow[rr, dash] & & x_7-x_8
\end{tikzcd} \tag{5.244}$$

where the fibers in affine surfaces glue to $x_8 - x_9$ and $2l - x_2 - x_3 - x_6 - x_7 - x_8 - x_9$.

$$\mathfrak{su}(4)^{(1)} \text{ --- } \mathfrak{sp}(0)^{(1)} \text{ --- } \mathfrak{so}(7)^{(1)}$$

$$\begin{tikzcd}
 & 2l-x_2-x_3-x_6-x_7-x_8-x_9 \arrow[d, dash] & \\
x_1-x_4 \arrow[r, dash] & x_2-x_1 \arrow[r, equal] & x_3-x_2,\ l-x_2-x_3-x_5
\end{tikzcd}$$

$$\begin{tikzcd}
 & 3l-x_1-x_2-x_3-x_4-x_5-2x_6-x_7-x_8 \arrow[dl, dash] \arrow[dr, dash] & \\
x_8-x_9 \arrow[dr, dash] & & x_6-x_7 \arrow[dl, dash] \\
 & x_7-x_8 &
\end{tikzcd} \tag{5.245}$$

where the fibers in affine surfaces glue to $x_8 - x_9$ and $2l - x_2 - x_3 - x_6 - x_7 - x_8 - x_9$.

$$
\mathfrak{sp}(0)^{(1)} \;\text{——}\; \mathfrak{so}(11)^{(1)}
$$

$$
\begin{array}{ccccccccc}
 & & 2l - x_1 - x_2 - x_4 - x_5 - x_8 - x_9 & & & & & & \\
 & & | & & & & & & \\
x_6 - x_7 & \text{——} & x_5 - x_6 & \text{——} & x_4 - x_5 & \text{——} & x_1 - x_4 & = & x_2 - x_1,\ l - x_1 - x_2 - x_3
\end{array}
\tag{5.246}
$$

where the fiber in affine surface glues to $2l - x_1 - x_2 - x_4 - x_5 - x_8 - x_9$.

$$
\mathfrak{f}_4^{(1)} \;\text{——}\; \mathfrak{sp}(0)^{(1)} \;\text{——}\; \mathfrak{su}(2)^{(1)}
$$

$$
\begin{array}{c}
l - x_7 - x_8 - x_9 \;\text{——}\; l - x_1 - x_2 - x_3 \;\text{——}\; x_1 - x_4 = x_2 - x_1,\ x_4 - x_5 = x_3 - x_2,\ x_5 - x_6 \\[2ex]
x_8 - x_9 = 3l - x_1 - x_2 - x_3 - x_4 - x_5 - x_6 - x_7 - 2x_8
\end{array}
\tag{5.247}
$$

where the fibers in affine surfaces glue to $x_8 - x_9$ and $l - x_7 - x_8 - x_9$.

$$
\mathfrak{g}_2^{(1)} \;\text{——}\; \mathfrak{sp}(0)^{(1)} \;\text{——}\; \mathfrak{so}(7)^{(1)}
$$

$$
\begin{array}{c}
\begin{array}{ccccc}
 & & 2l - x_1 - x_2 - x_6 - x_7 - x_8 - x_9 & & \\
 & & | & & \\
x_4 - x_5 & \text{——} & x_1 - x_4 & = & x_2 - x_1,\ l - x_1 - x_2 - x_3
\end{array} \\[3ex]
x_8 - x_9 \;\text{——}\; x_7 - x_8 \equiv x_6 - x_7,\ l - x_3 - x_6 - x_7,\ 2l - x_1 - x_2 - x_4 - x_5 - x_6 - x_7
\end{array}
\tag{5.248}
$$

where the fibers in affine surfaces glue to x_8-x_9 and $2l-x_1-x_2-x_6-x_7-x_8-x_9$.

$$
\begin{tikzcd}
\mathfrak{g}_2^{(1)} \arrow[r, dash] & \mathfrak{sp}(0)^{(1)} \arrow[r, dash] & \mathfrak{su}(4)^{(1)}
\end{tikzcd}
$$

$$
\begin{tikzcd}[column sep=small]
& 3l-x_1-2x_2-x_3-x_4-x_6-x_7-x_8-x_9 \arrow[dl, dash] \arrow[dr, dash] & \\
x_4-x_5 \arrow[dr, dash] & & x_2-x_1 \arrow[dl, dash] \\
& x_1-x_4 &
\end{tikzcd}
$$

$$
x_8-x_9 \;\text{———}\; x_7-x_8 \equiv x_6-x_7,\ l-x_3-x_6-x_7,\ 2l-x_1-x_2-x_4-x_5-x_6-x_7 \tag{5.249}
$$

where the fibers in affine surfaces glue to x_8-x_9 and $3l-x_1-2x_2-x_3-x_4-x_6-x_7-x_8-x_9$.

$$
\begin{tikzcd}
\mathfrak{su}(2)^{(1)} \arrow[r, dash] & \mathfrak{sp}(0)^{(1)} \arrow[r, dash] & \mathfrak{so}(9)^{(1)}
\end{tikzcd}
$$

$$
\begin{tikzcd}
& & 2l-x_2-x_3-x_6-x_7-x_8-x_9 \arrow[d, dash] & \\
l-x_1-x_2-x_3,\ x_4-x_5 \arrow[r, Rightarrow, no head] & x_1-x_4 \arrow[r, dash] & x_2-x_1 \arrow[r, dash] & x_3-x_2
\end{tikzcd}
$$

$$
x_8-x_9 = 3l-x_1-x_2-x_3-x_4-x_5-x_6-x_7-2x_8 \tag{5.250}
$$

where the fibers in affine surfaces glue to x_8-x_9 and $2l-x_2-x_3-x_6-x_7-x_8-x_9$.

$$
\begin{tikzcd}
\mathfrak{su}(3)^{(1)} \arrow[r, dash] & \mathfrak{sp}(0)^{(1)} \arrow[r, dash] & \mathfrak{so}(7)^{(1)}
\end{tikzcd}
$$

$$
\begin{tikzcd}
& 2l-x_2-x_3-x_6-x_7-x_8-x_9 \arrow[d, dash] & \\
x_1-x_4 \arrow[r, dash] & x_2-x_1 \arrow[r, Rightarrow, no head] & x_3-x_2,\ l-x_2-x_3-x_5
\end{tikzcd}
$$

$$
\begin{tikzcd}[column sep=small]
& 3l-x_1-x_2-x_3-x_4-x_5-x_6-2x_7-x_8 \arrow[dl, dash] \arrow[dr, dash] & \\
x_8-x_9 \arrow[rr, dash] & & x_7-x_8
\end{tikzcd} \tag{5.251}
$$

where the fibers in affine surfaces glue to $x_8 - x_9$ and $2l - x_2 - x_3 - x_6 - x_7 - x_8 - x_9$.

$$\mathfrak{sp}(0)^{(1)} \text{ —— } \mathfrak{so}(9)^{(1)}$$

$$\begin{array}{ccccccc} & & & & 2l - x_2 - x_3 - x_6 - x_7 - x_8 - x_9 & & \\ & & & & | & & \\ l - x_1 - x_2 - x_3,\ x_4 - x_5 & = & x_1 - x_4 & \text{——} & x_2 - x_1 & \text{——} & x_3 - x_2 \end{array} \tag{5.252}$$

where the fiber in affine surface glues to $2l - x_2 - x_3 - x_6 - x_7 - x_8 - x_9$.

$$\mathfrak{sp}(0)^{(1)} \text{ —— } \mathfrak{f}_4^{(1)}$$

$$l - x_7 - x_8 - x_9 \text{ —— } l - x_1 - x_2 - x_3 \text{ —— } x_1 - x_4 = x_2 - x_1,\ x_4 - x_5 = x_3 - x_2,\ x_5 - x_6 \tag{5.253}$$

where the fiber in affine surface glues to $l - x_7 - x_8 - x_9$.

$$\mathfrak{g}_2^{(1)} \text{ —— } \mathfrak{sp}(0)^{(1)} \text{ —— } \mathfrak{g}_2^{(1)}$$

$$\begin{gathered} 2l - x_1 - x_2 - x_6 - x_7 - x_8 - x_9 \text{ —— } x_1 - x_4 \equiv x_2 - x_1,\ x_4 - x_5,\ l - x_1 - x_2 - x_3 \\ x_8 - x_9 \text{ —— } x_7 - x_8 \equiv x_6 - x_7,\ l - x_3 - x_6 - x_7,\ 2l - x_1 - x_2 - x_4 - x_5 - x_6 - x_7 \end{gathered} \tag{5.254}$$

where the fibers in affine surfaces glue to $x_8 - x_9$ and $2l - x_1 - x_2 - x_6 - x_7 - x_8 - x_9$.

$$\mathfrak{su}(3)^{(1)} \text{ —— } \mathfrak{sp}(0)^{(1)} \text{ —— } \mathfrak{g}_2^{(1)}$$

$$\begin{tikzcd} & 3l - 2x_1 - x_2 - x_3 - x_4 - x_6 - x_7 - x_8 - x_9 \arrow[dl, dash] \arrow[dr, dash] & \\ x_4 - x_5 \arrow[rr, dash] & & x_1 - x_4 \end{tikzcd}$$

$$x_8 - x_9 \text{ —— } x_7 - x_8 \equiv x_6 - x_7,\ l - x_3 - x_6 - x_7,\ 2l - x_1 - x_2 - x_4 - x_5 - x_6 - x_7 \tag{5.255}$$

where the fibers in affine surfaces glue to x_8-x_9 and $3l-2x_1-x_2-x_3-x_4-x_6-x_7-x_8-x_9$.

$$\mathfrak{so}(7)^{(1)} \;—\; \mathfrak{sp}(0)^{(1)} \;—\; \mathfrak{su}(2)^{(1)}$$

$$\begin{array}{c} 2l-x_2-x_3-x_6-x_7-x_8-x_9 \\ | \\ x_1-x_4 \;—\; x_2-x_1 \;=\; x_3-x_2,\; l-x_2-x_3-x_5 \end{array}$$

$$x_8-x_9 \;\equiv\; 3l-x_1-x_2-x_3-x_4-x_5-x_6-x_7-2x_8 \tag{5.256}$$

where the fibers in affine surfaces glue to x_8-x_9 and $2l-x_2-x_3-x_6-x_7-x_8-x_9$.

$$\mathfrak{sp}(0)^{(1)} \;—\; \mathfrak{so}(7)^{(1)}$$

$$\begin{array}{c} 2l-x_2-x_3-x_6-x_7-x_8-x_9 \\ | \\ x_1-x_4 \;—\; x_2-x_1 \;=\; x_3-x_2,\; l-x_2-x_3-x_5 \end{array} \tag{5.257}$$

where the fiber in affine surface glues to $2l-x_2-x3-x_6-x_7-x_8-x_9$.

$$\mathfrak{su}(2)^{(1)} \;—\; \mathfrak{sp}(0)^{(1)} \;—\; \mathfrak{g}_2^{(1)}$$

$$x_4-x_5 \;\equiv\; 3l-x_1-x_2-x_3-2x_4-x_6-x_7-x_8-x_9$$

$$x_8-x_9 \;—\; x_7-x_8 \;\equiv\; x_6-x_7,\; l-x_3-x_6-x_7,\; 2l-x_1-x_2-x_4-x_5-x_6-x_7 \tag{5.258}$$

where the fibers in affine surfaces glue to x_8-x_9 and $3l-x_1-x_2-x_3-2x_4-x_6-x_7-x_8-x_9$.

$$\mathfrak{sp}(0)^{(1)} \;—\; \mathfrak{g}_2^{(1)}$$

$$x_8-x_9 \;—\; x_7-x_8 \;\equiv\; x_6-x_7,\; l-x_3-x_6-x_7,\; 2l-x_1-x_2-x_4-x_5-x_6-x_7 \tag{5.259}$$

where the fiber in affine surface glues to x_8-x_9.

The above cases do not completely exhaust all the possible non-simply laced subalgebras of $\mathfrak{e}_8$. Some of these subalgebras cannot be thought of as foldings of simply laced subalgebras of $\mathfrak{e}_8$. One such example is $\mathfrak{f}_4 \oplus \mathfrak{g}_2$. Notice that unfolding $\mathfrak{f}_4^{(1)} \oplus \mathfrak{g}_2^{(1)}$ leads to $\mathfrak{e}_6^{(1)} \oplus \mathfrak{so}(8)^{(1)}$, but $\mathfrak{e}_6 \oplus \mathfrak{so}(8)$ is not a subalgebra of $\mathfrak{e}_8$. To obtain the gluing rules for this example, we find a collection of curves giving rise to $\mathfrak{g}_2^{(1)}$ not intersecting (5.253) and satisfying (5.236):

$$\mathfrak{f}_4^{(1)} \;\text{———}\; \mathfrak{sp}(0)^{(1)} \;\text{———}\; \mathfrak{g}_2^{(1)}$$

$$l-x_7-x_8-x_9 \;\text{——}\; l-x_1-x_2-x_3 \;\text{——}\; x_1-x_4 \;=\!=\; x_2-x_1,\ x_4-x_5 \;=\!=\; x_3-x_2,\ x_5-x_6$$

$$x_8-x_9 \;\text{——}\; x_7-x_8 \equiv l-x_1-x_4-x_7,\ l-x_2-x_5-x_7,\ l-x_3-x_6-x_7 \tag{5.260}$$

where the fibers in affine surfaces glue to x_8-x_9 and $l-x_7-x_8-x_9$. Notice that even though, by the virtue of (5.236), the total gluing curves see different component gluing curves equally, the different components do not. For example, even though the gluing curve x_3-x_2 has different intersections with the gluing curves $l-x_2-x_5-x_7$ and $l-x_1-x_4-x_7$, the total gluing curve $(x_3-x_2)+(x_5-x_6)$ equal intersections with the two gluing curves $l-x_2-x_5-x_7$ and $l-x_1-x_4-x_7$, as required by (5.236). Similar remarks apply to many of the gluing rules that follow.

To obtain the gluing rules for $\mathfrak{so}(9)\oplus\mathfrak{so}(7)$, we start from (5.241) and extend the chains for one of the $\mathfrak{so}(7)$:

$$\mathfrak{so}(9)^{(1)} \;\text{———}\; \mathfrak{sp}(0)^{(1)} \;\text{———}\; \mathfrak{so}(7)^{(1)}$$

$$\begin{array}{ccccccc} & & 2l-x_1-x_2-x_4-x_5-x_6-x_7 & & & & \\ & & | & & & & \\ x_8-x_9 & \text{———} & x_7-x_8 & \text{———} & x_6-x_7 & =\!= & x_2-x_6,\ l-x_2-x_3-x_6 \end{array}$$

$$\begin{array}{ccccc} & & 2l-x_1-x_2-x_6-x_7-x_8-x_9 & & \\ & & | & & \\ x_4-x_5 & \text{———} & x_1-x_4 & =\!= & x_2-x_1,\ l-x_1-x_2-x_3 \end{array} \tag{5.261}$$

where the fibers in affine surfaces glue to x_8-x_9 and $2l-x_1-x_2-x_6-x_7-x_8-x_9$.

JHEP12(2020)151

By folding $\mathfrak{so}(7)^{(1)}$ we can obtain $\mathfrak{g}_2^{(1)}$, so folding the above gluing rules we obtain the following gluing rules

$$\mathfrak{so}(9)^{(1)} \;\text{——}\; \mathfrak{sp}(0)^{(1)} \;\text{——}\; \mathfrak{g}_2^{(1)}$$

$$\begin{tikzcd}
 & 2l-x_1-x_2-x_4-x_5-x_6-x_7 \arrow[d, no head] & & \\
x_8-x_9 \arrow[r, no head] & x_7-x_8 \arrow[r, no head] & x_6-x_7 \arrow[r, equal] & x_2-x_6,\ l-x_2-x_3-x_6
\end{tikzcd}$$

$$\begin{tikzcd}
2l-x_1-x_2-x_6-x_7-x_8-x_9 \arrow[r, no head] & x_1-x_4 \arrow[r, no head, "\equiv"] & x_2-x_1,\ l-x_1-x_2-x_3,\ x_4-x_5
\end{tikzcd} \tag{5.262}$$

where the fibers in affine surfaces glue to x_8-x_9 and $2l-x_1-x_2-x_6-x_7-x_8-x_9$.

5.4.3 $\mathfrak{sp}(0)^{(1)}$ gluings: twisted algebras, undirected edges

Now we provide gluing rules for the cases involving twisted gauge algebras and undirected edges, that is gluing rules of the form

$$\mathfrak{g}_\alpha^{(q_\alpha)} \;\text{——}\; \mathfrak{sp}(0)^{(1)} \;\text{——}\; \mathfrak{g}_\gamma^{(q_\gamma)} \tag{5.263}$$

Most of these gluing rules can be understood as foldings of gluing rules of the form

$$\mathfrak{g}_\alpha^{(1)} \;\text{——}\; \mathfrak{sp}(0)^{(1)} \;\text{——}\; \mathfrak{g}_\gamma^{(1)} \tag{5.264}$$

provided above. The relevant foldings are

$$\mathfrak{so}(4n)^{(1)} \to \mathfrak{su}(2n)^{(2)} \to \mathfrak{su}(2n-1)^{(2)} \tag{5.265}$$

$$\mathfrak{so}(7)^{(1)} \to \mathfrak{su}(4)^{(2)} \to \mathfrak{su}(3)^{(2)} \tag{5.266}$$

$$\mathfrak{so}(2n+1)^{(1)} \to \mathfrak{so}(2n)^{(2)} \tag{5.267}$$

$$\mathfrak{g}_2^{(1)} \to \mathfrak{su}(3)^{(2)} \tag{5.268}$$

$$\mathfrak{e}_7^{(1)} \to \mathfrak{e}_6^{(2)} \tag{5.269}$$

$$\mathfrak{f}_4^{(1)} \to \mathfrak{so}(8)^{(3)} \tag{5.270}$$

For example, for $\mathfrak{so}(14)^{(2)}$, we fold (5.234) to obtain

$$\mathfrak{sp}(0)^{(1)} \;\text{——}\; \mathfrak{so}(14)^{(2)}$$

$$\begin{tikzcd}[column sep=small]
\begin{array}{c} x_8-x_9, \\ 2l-x_1-x_2-x_4 \\ -x_5-x_6-x_7 \end{array} \arrow[r, equal] & x_7-x_8 \arrow[r, no head] & x_6-x_7 \arrow[r, no head] & x_5-x_6 \arrow[r, no head] & x_4-x_5 \arrow[r, no head] & x_1-x_4 \arrow[r, equal] & \begin{array}{c} x_2-x_1, \\ l-x_1-x_2-x_3 \end{array}
\end{tikzcd} \tag{5.271}$$

where two copies of fibers in affine surface glue to x_8-x_9, $2l-x_1-x_2-x_4-x_5-x_6-x_7$. Let d_a be the dual Coxeter labels for $\mathfrak{so}(14)^{(2)}$ and f_a be the fibers in the Hirzebruch surfaces corresponding to $\mathfrak{so}(14)^{(2)}$. Then,

$$\begin{aligned}2d_af_a =& (x_8-x_9)+(2l-x_1-x_2-x_4-x_5-x_6-x_7)+2(x_7-x_8)+2(x_6-x_7)+2(x_5-x_6)\\&+2(x_4-x_5)+2(x_1-x_4)+(x_2-x_1)+(l-x_1-x_2-x_3)\\=& 3l-\sum x_i\end{aligned}\tag{5.272}$$

Thus, (5.60) holds true in this case. Same holds true for all the following examples in this subsection, as the reader can verify.

To obtain other $\mathfrak{so}(2n)^{(2)}$ of lower rank, we add the curves lying in the middle of the chain in (5.271). Adding x_4-x_5 to $x_1`-x_4$, we obtain the gluing rules for $\mathfrak{so}(12)^{(2)}$:

$$\mathfrak{sp}(0)^{(1)} \;—\; \mathfrak{so}(12)^{(2)}$$

$$\begin{array}{c}x_8-x_9,\\ 2l-x_1-x_2-x_4\\ -x_5-x_6-x_7\end{array} = x_7-x_8 - x_6-x_7 - x_5-x_6 - x_1-x_5 = \begin{array}{c}x_2-x_1,\\ l-x_1-x_2-x_3\end{array}\tag{5.273}$$

where x_8-x_9, $2l-x_1-x_2-x_4-x_5-x_6-x_7$ glue to fibers in affine surface.

Continuing in this fashion, we obtain

$$\mathfrak{sp}(0)^{(1)} \;—\; \mathfrak{so}(10)^{(2)}$$

$$\begin{array}{c}x_8-x_9,\\ 2l-x_1-x_2-x_4-x_5-x_6-x_7\end{array} = x_7-x_8 - x_6-x_7 - x_1-x_6 = \begin{array}{c}x_2-x_1,\\ l-x_1-x_2-x_3\end{array}\tag{5.274}$$

where x_8-x_9, $2l-x_1-x_2-x_4-x_5-x_6-x_7$ glue to fibers in affine surface.

$$\mathfrak{sp}(0)^{(1)} \;—\; \mathfrak{so}(8)^{(2)}$$

$$\begin{array}{c}x_8-x_9,\\ 2l-x_1-x_2-x_4-x_5-x_6-x_7\end{array} = x_7-x_8 - x_1-x_7 = \begin{array}{c}x_2-x_1,\\ l-x_1-x_2-x_3\end{array}\tag{5.275}$$

where x_8-x_9, $2l-x_1-x_2-x_4-x_5-x_6-x_7$ glue to fibers in affine surface.

$$\mathfrak{sp}(0)^{(1)} \;—\; \mathfrak{su}(4)^{(2)}$$

$$\begin{array}{c}x_8-x_9,\\ 2l-x_1-x_2-x_4-x_5-x_6-x_7\end{array} = x_1-x_8 = \begin{array}{c}x_2-x_1,\\ l-x_1-x_2-x_3\end{array}\tag{5.276}$$

where x_8-x_9, $2l-x_1-x_2-x_4-x_5-x_6-x_7$ glue to fibers in affine surface.

By folding (5.192), we obtain the following two gluing rules

$$\mathfrak{sp}(0)_0^{(1)} \;\text{———}\; \mathfrak{su}(8)^{(2)}$$

$$\begin{array}{ccccccc}
 & & 2l-x_1-x_2-x_4-x_5-x_6-x_7,\; l-x_1-x_2-x_3 & & & & \\
 & & \| & & & & \\
\begin{array}{c} x_8-x_9, \\ x_2-x_1 \end{array} & = & \begin{array}{c} x_7-x_8, \\ x_1-x_4 \end{array} & = & \begin{array}{c} x_6-x_7, \\ x_4-x_5 \end{array} & = & x_5-x_6
\end{array} \tag{5.277}$$

where x_8-x_9, x_2-x_1 glue to fibers in the affine surface.

$$\mathfrak{sp}(0)_\pi^{(1)} \;\text{———}\; \mathfrak{su}(8)^{(2)}$$

$$\begin{array}{ccccccc}
 & & 2l-x_1-x_2-x_4-x_5-x_6-x_7,\; x_2-x_1 & & & & \\
 & & \| & & & & \\
\begin{array}{c} x_8-x_9, \\ l-x_1-x_2-x_3 \end{array} & = & \begin{array}{c} x_7-x_8, \\ x_1-x_4 \end{array} & = & \begin{array}{c} x_6-x_7, \\ x_4-x_5 \end{array} & = & x_5-x_6
\end{array} \tag{5.278}$$

where x_8-x_9, $l-x_1-x_2-x_3$ glue to fibers in the affine surface.

Combining x_6-x_7, x_5-x_6 and x_4-x_5 in (5.277), we obtain the gluing rules for $\mathfrak{su}(6)^{(2)}$:

$$\mathfrak{sp}(0)^{(1)} \;\text{———}\; \mathfrak{su}(6)^{(2)}$$

$$\begin{array}{ccccc}
 & & 2l-x_1-x_2-x_4-x_5-x_6-x_7,\; l-x_1-x_2-x_3 & & \\
 & & \| & & \\
\begin{array}{c} x_8-x_9, \\ x_2-x_1 \end{array} & = & \begin{array}{c} x_7-x_8, \\ x_1-x_4 \end{array} & = & x_4-x_7
\end{array} \tag{5.279}$$

where x_8-x_9, x_2-x_1 glue to fibers in the affine surface.

Folding (5.277), we obtain

$$\mathfrak{sp}(0)^{(1)} \;\text{———}\; \mathfrak{su}(7)^{(2)}$$

$$\begin{array}{ccccccc}
\begin{array}{c} x_8-x_9, \\ x_2-x_1, \\ l-x_1-x_2-x_3, \\ 2l-x_1-x_2-x_4-x_5-x_6-x_7 \end{array} & \equiv & \begin{array}{c} x_7-x_8, \\ x_1-x_4 \end{array} & = & \begin{array}{c} x_6-x_7, \\ x_4-x_5 \end{array} & = & x_5-x_6
\end{array} \tag{5.280}$$

where x_8-x_9, x_2-x_1, $l-x_1-x_2-x_3$ and$2l-x_1-x_2-x_4-x_5-x_6-x_7$ glue to four copies of fiber in the affine surface.

JHEP12(2020)151

By adding the curves in the previous configuration, we obtain the following two:

$$\mathfrak{sp}(0)^{(1)} \;—\; \mathfrak{su}(5)^{(2)}$$

$$\begin{array}{ccccc} x_8-x_9, & \equiv & x_7-x_8, & = & x_4-x_7 \\ x_2-x_1, & & x_1-x_4 & & \\ l-x_1-x_2-x_3, & & & & \\ 2l-x_1-x_2-x_4-x_5-x_6-x_7 & & & & \end{array} \tag{5.281}$$

where x_8-x_9, x_2-x_1, $l-x_1-x_2-x_3$ and $2l-x_1-x_2-x_4-x_5-x_6-x_7$ glue to four copies of fiber in the affine surface.

$$\mathfrak{sp}(0)^{(1)} \;—\; \mathfrak{su}(3)^{(2)}$$

$$\begin{array}{ccc} x_8-x_9, & \equiv & x_1-x_8 \\ x_2-x_1, & & \\ l-x_1-x_2-x_3, & & \\ 2l-x_1-x_2-x_4-x_5-x_6-x_7 & & \end{array} \tag{5.282}$$

where x_8-x_9, x_2-x_1, $l-x_1-x_2-x_3$ and $2l-x_1-x_2-x_4-x_5-x_6-x_7$ glue to four copies of fiber in the affine surface.

Folding (5.253), we obtain

$$\mathfrak{sp}(0)^{(1)} \;—\; \mathfrak{so}(8)^{(3)}$$

$$\begin{array}{ccccc} x_1-x_4 & \equiv & x_2-x_1, & \equiv & x_3-x_2, \\ & & x_4-x_5, & & x_5-x_6, \\ & & l-x_1-x_2-x_3 & & l-x_7-x_8-x_9 \end{array} \tag{5.283}$$

where x_3-x_2, x_5-x_6 and $l-x_7-x_8-x_9$ glue to three copies of fiber in the affine surface.

By folding (5.190) and (5.187) we obtain:

$$\mathfrak{sp}(0)^{(1)} \;—\; \mathfrak{e}_6^{(2)}$$

$$\begin{array}{ccccccccc} x_6-x_7, & = & x_5-x_6, & = & x_4-x_5, & = & x_1-x_4 & — & l-x_1-x_2-x_3 \\ l-x_3-x_8-x_9 & & x_3-x_2 & & x_2-x_1 & & & & \end{array} \tag{5.284}$$

where $l-x_3-x_8-x_9$ and x_6-x_7 glue to two copies of fiber in the affine surface.

$$\mathfrak{e}_6^{(2)} \;\text{———}\; \mathfrak{sp}(0)^{(1)} \;\text{———}\; \mathfrak{su}(2)^{(1)}$$

$$\begin{tikzcd}[column sep=small]
\begin{array}{c} x_6-x_7, \\ l-x_3-x_8-x_9 \end{array} \arrow[r, equal] & \begin{array}{c} x_5-x_6, \\ x_3-x_2 \end{array} \arrow[r, equal] & \begin{array}{c} x_4-x_5, \\ x_2-x_1 \end{array} \arrow[r, equal] & x_1-x_4 \arrow[r, dash] & l-x_1-x_2-x_3
\end{tikzcd}$$

$$\begin{tikzcd}
x_8-x_9 \arrow[r, equal] & 3l-x_1-x_2-x_3-x_4-x_5-x_6-x_7-2x_8
\end{tikzcd} \tag{5.285}$$

where x_8-x_9, $l-x_3-x_8-x_9$ and x_6-x_7 glue to fibers inside corresponding affine surfaces.

In a similar fashion, by folding other configurations and sometimes adding some of the curves in them, we can obtain the following configurations:

$$\mathfrak{so}(8)^{(2)} \;\text{———}\; \mathfrak{sp}(0)^{(1)} \;\text{———}\; \mathfrak{su}(4)^{(1)}$$

$$\begin{tikzcd}[column sep=small]
\begin{array}{c} x_3-x_2, \\ 2l-x_2-x_3-x_6-x_7-x_8-x_9 \end{array} \arrow[r, equal] & x_2-x_1 \arrow[r, dash] & x_1-x_4 \arrow[r, equal] & \begin{array}{c} x_4-x_5, \\ l-x_1-x_2-x_3 \end{array}
\end{tikzcd}$$

$$\begin{tikzcd}[column sep=small]
 & 3l-x_1-x_2-x_3-x_4-x_5-2x_6-x_7-x_8 \arrow[dl, dash] \arrow[dr, dash] & \\
x_8-x_9 \arrow[dr, dash] & & x_6-x_7 \arrow[dl, dash] \\
 & x_7-x_8 &
\end{tikzcd} \tag{5.286}$$

where x_8-x_9, $2l-x_2-x_3-x_6-x_7-x_8-x_9$ and x_3-x_2 glue to fibers inside corresponding affine surfaces.

$$\mathfrak{so}(8)^{(2)} \;\text{———}\; \mathfrak{sp}(0)^{(1)} \;\text{———}\; \mathfrak{su}(3)^{(1)}$$

$$\begin{tikzcd}[column sep=small]
\begin{array}{c} x_3-x_2, \\ 2l-x_2-x_3-x_6-x_7-x_8-x_9 \end{array} \arrow[r, equal] & x_2-x_1 \arrow[r, dash] & x_1-x_4 \arrow[r, equal] & \begin{array}{c} x_4-x_5, \\ l-x_1-x_2-x_3 \end{array}
\end{tikzcd}$$

$$\begin{tikzcd}[column sep=small]
 & 3l-x_1-x_2-x_3-x_4-x_5-2x_6-x_7-x_8 \arrow[dl, dash] \arrow[dr, dash] & \\
x_8-x_9 \arrow[rr, dash] & & x_6-x_8
\end{tikzcd} \tag{5.287}$$

where x_8-x_9, $2l-x_2-x_3-x_6-x_7-x_8-x_9$ and x_3-x_2 glue to fibers inside corresponding affine surfaces.

$$\mathfrak{so}(8)^{(1)} \text{ --- } \mathfrak{sp}(0)^{(1)} \text{ --- } \mathfrak{su}(4)^{(2)}$$

$$\begin{tikzcd}
 & 2l-x_1-x_2-x_4-x_5-x_6-x_7 \arrow[d, dash] & \\
x_8-x_9 \arrow[r, dash] & x_7-x_8 \arrow[r, dash] \arrow[d, dash] & x_6-x_7 \\
 & l-x_3-x_6-x_7 &
\end{tikzcd}$$

$$\begin{tikzcd}
x_1-x_4 \arrow[r, equal] \arrow[d, equal] & x_2-x_1,\ x_4-x_5 \\
2l-x_1-x_2-x_6-x_7-x_8-x_9,\ l-x_1-x_2-x_3 &
\end{tikzcd} \tag{5.288}$$

where x_8-x_9, $2l-x_1-x_2-x_6-x_7-x_8-x_9$ and $l-x_1-x_2-x_3$ glue to fibers inside corresponding affine surfaces.

$$\mathfrak{so}(8)^{(1)} \text{ --- } \mathfrak{sp}(0)^{(1)} \text{ --- } \mathfrak{su}(3)^{(2)}$$

$$\begin{tikzcd}
 & 2l-x_1-x_2-x_4-x_5-x_6-x_7 \arrow[d, dash] & \\
x_8-x_9 \arrow[r, dash] & x_7-x_8 \arrow[r, dash] \arrow[d, dash] & x_6-x_7 \\
 & l-x_3-x_6-x_7 &
\end{tikzcd}$$

$$\begin{tikzcd}
\begin{array}{c} x_4-x_5, \\ x_2-x_1, \\ l-x_1-x_2-x_3, \\ 2l-x_1-x_2-x_6-x_7-x_8-x_9 \end{array} \arrow[r, equal] & x_1-x_4
\end{tikzcd} \tag{5.289}$$

where x_8-x_9, $2l-x_1-x_2-x_6-x_7-x_8-x_9$, x_2-x_1, x_4-x_5 and $l-x_1-x_2-x_3$ glue

to fibers inside corresponding affine surfaces.

$$\mathfrak{so}(7)^{(1)} \text{ --- } \mathfrak{sp}(0)^{(1)} \text{ --- } \mathfrak{su}(4)^{(2)}$$

$$\begin{tikzcd}
 & 2l-x_1-x_2-x_4-x_5-x_6-x_7 \arrow[d, dash] & \\
x_8-x_9 \arrow[r, dash] & x_7-x_8 \arrow[r, equal] & x_6-x_7,\ l-x_3-x_6-x_7 \\
 & x_1-x_4 \arrow[r, equal] \arrow[d, equal] & x_2-x_1,\ x_4-x_5 \\
 & 2l-x_1-x_2-x_6-x_7-x_8-x_9,\ l-x_1-x_2-x_3 &
\end{tikzcd} \tag{5.290}$$

where x_8-x_9, $2l-x_1-x_2-x_6-x_7-x_8-x_9$ and $l-x_1-x_2-x_3$ glue to fibers inside corresponding affine surfaces.

$$\mathfrak{so}(7)^{(1)} \text{ --- } \mathfrak{sp}(0)^{(1)} \text{ --- } \mathfrak{su}(3)^{(2)}$$

$$\begin{tikzcd}
 & 2l-x_1-x_2-x_4-x_5-x_6-x_7 \arrow[d, dash] & \\
x_8-x_9 \arrow[r, dash] & x_7-x_8 \arrow[r, equal] & x_6-x_7,\ l-x_3-x_6-x_7 \\
\begin{array}{r} x_4-x_5, \\ x_2-x_1, \\ l-x_1-x_2-x_3, \\ 2l-x_1-x_2-x_6-x_7-x_8-x_9 \end{array} \arrow[r, equal] & x_1-x_4 &
\end{tikzcd} \tag{5.291}$$

where x_8-x_9, $2l-x_1-x_2-x_6-x_7-x_8-x_9$, x_2-x_1, x_4-x_5 and $l-x_1-x_2-x_3$ glue

to fibers inside corresponding affine surfaces.

$$\mathfrak{g}_2^{(1)} \text{ ——— } \mathfrak{sp}(0)^{(1)} \text{ ——— } \mathfrak{su}(4)^{(2)}$$

$$\begin{array}{c}
x_8-x_9 \text{ ——— } x_7-x_8 \equiv\!\equiv\!\equiv x_6-x_7,\ l-x_3-x_6-x_7,\ 2l-x_1-x_2-x_4-x_5-x_6-x_7 \\[2em]
\begin{array}{ccc}
 & x_1-x_4 = \!=\!=\!= & x_2-x_1,\ \ x_4-x_5 \\
 & \Vert & \\
 2l-x_1-x_2-x_6-x_7-x_8-x_9, & l-x_1-x_2-x_3 &
\end{array}
\end{array} \tag{5.292}$$

where x_8-x_9, $2l-x_1-x_2-x_6-x_7-x_8-x_9$ and $l-x_1-x_2-x_3$ glue to fibers inside corresponding affine surfaces.

$$\mathfrak{g}_2^{(1)} \text{ ——— } \mathfrak{sp}(0)^{(1)} \text{ ——— } \mathfrak{su}(3)^{(2)}$$

$$\begin{array}{c}
x_8-x_9 \text{ ——— } x_7-x_8 \equiv\!\equiv\!\equiv x_6-x_7,\ l-x_3-x_6-x_7,\ 2l-x_1-x_2-x_4-x_5-x_6-x_7 \\[2em]
\begin{array}{c}
x_4-x_5, \equiv\!\equiv\!\equiv\ x_1-x_4 \\
x_2-x_1, \\
l-x_1-x_2-x_3, \\
2l-x_1-x_2-x_6-x_7-x_8-x_9
\end{array}
\end{array} \tag{5.293}$$

where x_8-x_9, $2l-x_1-x_2-x_6-x_7-x_8-x_9$, x_2-x_1, x_4-x_5 and $l-x_1-x_2-x_3$ glue to fibers inside corresponding affine surfaces.

$$\mathfrak{so}(10)^{(2)} \text{ ——— } \mathfrak{sp}(0)^{(1)} \text{ ——— } \mathfrak{su}(2)^{(1)}$$

$$\begin{array}{c}
\begin{array}{c} x_6-x_7, \\ 2l-x_1-x_2-x_4-x_5-x_8-x_9 \end{array} = \!=\!= x_5-x_6 \text{ ——— } x_4-x_5 \text{ ——— } x_1-x_4 = \!=\!= \begin{array}{c} x_2-x_1, \\ l-x_1-x_2-x_3 \end{array} \\[2em]
3l-x_1-x_2-x_3-x_4-x_5-x_6-x_7-2x_8 = \!=\!=\!=\!=\!= x_8-x_9
\end{array} \tag{5.294}$$

where x_8-x_9 and $2l-x_1-x_2-x_4-x_5-x_8-x_9$, x_6-x_7 glue to fibers inside corresponding affine surfaces.

$$\mathfrak{so}(8)^{(2)} \;\text{———}\; \mathfrak{sp}(0)^{(1)} \;\text{———}\; \mathfrak{su}(2)^{(1)}$$

$$\begin{array}{c}
\begin{matrix} x_6-x_7, \\ 2l-x_1-x_2-x_4-x_5-x_8-x_9 \end{matrix} \;=\!=\!=\; x_5-x_6 \;\text{———}\; x_1-x_5 \;=\!=\!=\; \begin{matrix} x_2-x_1, \\ l-x_1-x_2-x_3 \end{matrix} \\[2em]
3l-x_1-x_2-x_3-x_4-x_5-x_6-x_7-2x_8 \;=\!=\!=\!=\!=\!=\; x_8-x_9
\end{array} \tag{5.295}$$

where x_8-x_9, $2l-x_1-x_2-x_4-x_5-x_6-x_7$ and x_5-x_9 glue to fibers inside corresponding affine surfaces.

$$\mathfrak{so}(8)^{(2)} \;\text{———}\; \mathfrak{sp}(0)^{(1)} \;\text{———}\; \mathfrak{so}(7)^{(1)}$$

$$\begin{array}{c}
\begin{matrix} x_8-x_9, \\ 2l-x_1-x_2-x_4-x_5-x_6-x_7 \end{matrix} \;=\!=\!=\; x_7-x_8 \;\text{———}\; x_6-x_7 \;=\!=\!=\; \begin{matrix} x_2-x_6, \\ l-x_2-x_3-x_6 \end{matrix} \\[2em]
2l-x_1-x_2-x_6-x_7-x_8-x_9 \\
\Big| \\
x_4-x_5 \;\text{————}\; x_1-x_4 \;=\!=\!=\; x_2-x_1,\; l-x_1-x_2-x_3
\end{array} \tag{5.296}$$

where x_8-x_9, $2l-x_1-x_2-x_4-x_5-x_6-x_7$ and $2l-x_1-x_2-x_6-x_7-x_8-x_9$ glue to fibers inside corresponding affine surfaces.

$$\mathfrak{so}(8)^{(2)} \;\text{———}\; \mathfrak{sp}(0)^{(1)} \;\text{———}\; \mathfrak{g}_2^{(1)}$$

$$\begin{array}{c}
\begin{matrix} x_8-x_9, \\ 2l-x_1-x_2-x_4-x_5-x_6-x_7 \end{matrix} \;=\!=\!=\; x_7-x_8 \;\text{———}\; x_6-x_7 \;=\!=\!=\; \begin{matrix} x_2-x_6, \\ l-x_2-x_3-x_6 \end{matrix} \\[2em]
2l-x_1-x_2-x_6-x_7-x_8-x_9 \;\text{———}\; x_1-x_4 \equiv x_4-x_5,\; l-x_1-x_2-x_3,\; x_2-x_1
\end{array} \tag{5.297}$$

where x_8-x_9, $2l-x_1-x_2-x_4-x_5-x_6-x_7$ and $2l-x_1-x_2-x_6-x_7-x_8-x_9$ glue

to fibers inside corresponding affine surfaces.

$$\mathfrak{so}(8)^{(2)} \text{ --- } \mathfrak{sp}(0)^{(1)} \text{ --- } \mathfrak{su}(4)^{(2)}$$

$$\begin{array}{c}
\begin{array}{c} x_8 - x_9, \\ 2l - x_1 - x_2 - x_4 - x_5 - x_6 - x_7 \end{array} = x_7 - x_8 \text{ --- } x_6 - x_7 = \begin{array}{c} x_2 - x_6, \\ l - x_2 - x_3 - x_6 \end{array} \\[2em]
\begin{array}{c} x_4 - x_5, \\ 2l - x_1 - x_2 - x_6 - x_7 - x_8 - x_9 \end{array} = x_1 - x_4 = x_2 - x_1,\ l - x_1 - x_2 - x_3
\end{array} \tag{5.298}$$

where $x_8 - x_9$, $2l - x_1 - x_2 - x_4 - x_5 - x_6 - x_7$, $x_4 - x_5$ and $2l - x_1 - x_2 - x_6 - x_7 - x_8 - x_9$ glue to fibers inside corresponding affine surfaces.

$$\mathfrak{so}(8)^{(2)} \text{ --- } \mathfrak{sp}(0)^{(1)} \text{ --- } \mathfrak{su}(3)^{(2)}$$

$$\begin{array}{c}
\begin{array}{c} x_8 - x_9, \\ 2l - x_1 - x_2 - x_4 - x_5 - x_6 - x_7 \end{array} = x_7 - x_8 \text{ --- } x_6 - x_7 = \begin{array}{c} x_2 - x_6, \\ l - x_2 - x_3 - x_6 \end{array} \\[2em]
\begin{array}{c} x_4 - x_5, \\ x_2 - x_1, \\ l - x_1 - x_2 - x_3, \\ 2l - x_1 - x_2 - x_6 - x_7 - x_8 - x_9 \end{array} \equiv x_1 - x_4
\end{array} \tag{5.299}$$

where $2l - x_1 - x_2 - x_4 - x_5 - x_6 - x_7$, $x_8 - x_9$, $x_4 - x_5$, $x_2 - x_1$, $l - x_1 - x_2 - x_3$ and $2l - x_1 - x_2 - x_6 - x_7 - x_8 - x_9$ glue to fibers inside corresponding affine surfaces.

$$\mathfrak{su}(4)^{(2)} \text{ --- } \mathfrak{sp}(0)^{(1)} \text{ --- } \mathfrak{su}(3)^{(2)}$$

$$\begin{array}{c}
\begin{array}{c} x_8 - x_9, \\ 2l - x_1 - x_2 - x_4 - x_5 - x_6 - x_7 \end{array} = x_6 - x_8 = \begin{array}{c} x_2 - x_6, \\ l - x_2 - x_3 - x_6 \end{array} \\[2em]
\begin{array}{c} x_4 - x_5, \\ x_2 - x_1, \\ l - x_1 - x_2 - x_3, \\ 2l - x_1 - x_2 - x_6 - x_7 - x_8 - x_9 \end{array} \equiv x_1 - x_4
\end{array} \tag{5.300}$$

where $2l - x_1 - x_2 - x_4 - x_5 - x_6 - x_7$, $x_8 - x_9$, $x_4 - x_5$, $x_2 - x_1$, $l - x_1 - x_2 - x_3$ and

$2l - x_1 - x_2 - x_6 - x_7 - x_8 - x_9$ glue to fibers inside corresponding affine surfaces.

$$\mathfrak{su}(3)^{(2)} \text{———} \mathfrak{sp}(0)^{(1)} \text{———} \mathfrak{su}(3)^{(2)}$$

$$\begin{array}{r}
x_8 - x_9, \equiv x_6 - x_8 \\
x_2 - x_6, \\
l - x_2 - x_3 - x_6, \\
2l - x_1 - x_2 - x_4 - x_5 - x_6 - x_7
\end{array}$$

$$\begin{array}{r}
x_4 - x_5, \equiv x_1 - x_4 \\
x_2 - x_1, \\
l - x_1 - x_2 - x_3, \\
2l - x_1 - x_2 - x_6 - x_7 - x_8 - x_9
\end{array} \tag{5.301}$$

where $2l - x_1 - x_2 - x_4 - x_5 - x_6 - x_7$, $x_8 - x_9$, $x_2 - x_6$, $l - x_2 - x_3 - x_6$, $x_4 - x_5$, $x_2 - x_1$, $l - x_1 - x_2 - x_3$ and $2l - x_1 - x_2 - x_6 - x_7 - x_8 - x_9$ glue to fibers inside corresponding affine surfaces.

$$\mathfrak{f}_4^{(1)} \text{———} \mathfrak{sp}(0)^{(1)} \text{———} \mathfrak{su}(3)^{(2)}$$

$$l - x_7 - x_8 - x_9 \text{ —— } l - x_1 - x_2 - x_3 \text{ —— } x_1 - x_4 = x_2 - x_1,\ x_4 - x_5 = x_3 - x_2,\ x_5 - x_6$$

$$\begin{array}{l}
x_8 - x_9, \equiv x_7 - x_8 \\
l - x_1 - x_4 - x_7, \\
l - x_2 - x_5 - x_7, \\
l - x_3 - x_6 - x_7
\end{array} \tag{5.302}$$

where $x_8 - x_9$, $l - x_1 - x_4 - x_7$, $l - x_2 - x_5 - x_7$, $l - x_3 - x_6 - x_7$ and $l - x_7 - x_8 - x_9$ glue to fibers inside corresponding affine surfaces.

$$\mathfrak{so}(8)^{(3)} \text{———} \mathfrak{sp}(0)^{(1)} \text{———} \mathfrak{su}(3)^{(2)}$$

$$\begin{array}{ccccc}
x_1 - x_4 & \equiv & x_2 - x_1, & \equiv & x_3 - x_2, \\
 & & x_4 - x_5, & & x_5 - x_6, \\
 & & l - x_1 - x_2 - x_3 & & l - x_7 - x_8 - x_9
\end{array}$$

$$\begin{array}{l}
x_8 - x_9, \equiv x_7 - x_8 \\
l - x_1 - x_4 - x_7, \\
l - x_2 - x_5 - x_7, \\
l - x_3 - x_6 - x_7
\end{array} \tag{5.303}$$

where $x_8 - x_9$, $l - x_1 - x_4 - x_7$, $l - x_2 - x_5 - x_7$, $l - x_3 - x_6 - x_7$, $x_3 - x_2$, $x_5 - x_6$, and $l - x_7 - x_8 - x_9$ glue to fibers inside corresponding affine surfaces.

$$\mathfrak{so}(8)^{(3)} \text{ --- } \mathfrak{sp}(0)^{(1)} \text{ --- } \mathfrak{su}(3)^{(1)}$$

$$\begin{array}{ccccc} x_1 - x_4 & \equiv & x_2 - x_1, & \equiv & x_3 - x_2, \\ & & x_4 - x_5, & & x_5 - x_6, \\ & & l - x_1 - x_2 - x_3 & & l - x_7 - x_8 - x_9 \end{array}$$

$$\begin{array}{ccc} & 3l - x_1 - x_2 - x_3 - x_4 - x_5 - x_6 - 2x_7 - x_8 & \\ \diagup & & \diagdown \\ x_8 - x_9 & \text{------} & x_7 - x_8 \end{array} \tag{5.304}$$

where $x_8 - x_9$, $x_3 - x_2$, $x_5 - x_6$, and $l - x_7 - x_8 - x_9$ glue to fibers inside corresponding affine surfaces.

$$\mathfrak{so}(8)^{(3)} \text{ --- } \mathfrak{sp}(0)^{(1)} \text{ --- } \mathfrak{su}(2)^{(1)}$$

$$\begin{array}{ccccc} x_1 - x_4 & \equiv & x_2 - x_1, & \equiv & x_3 - x_2, \\ & & x_4 - x_5, & & x_5 - x_6, \\ & & l - x_1 - x_2 - x_3 & & l - x_7 - x_8 - x_9 \end{array}$$

$$x_8 - x_9 \equiv 3l - x_1 - x_2 - x_3 - x_4 - x_5 - x_6 - x_7 - 2x_8 \tag{5.305}$$

where $x_8 - x_9$, $x_3 - x_2$, $x_5 - x_6$, and $l - x_7 - x_8 - x_9$ glue to fibers inside corresponding affine surfaces.

$$\mathfrak{su}(3)^{(1)} \text{ --- } \mathfrak{sp}(0)^{(1)} \text{ --- } \mathfrak{su}(4)^{(2)}$$

$$\begin{array}{ccccc} x_1 - x_4, & = & x_2 - x_1 & = & x_3 - x_2, \\ l - x_2 - x_3 - x_5 & & & & 2l - x_2 - x_3 - x_6 - x_7 - x_8 - x_9 \end{array}$$

$$\begin{array}{ccc} & 3l - x_1 - x_2 - x_3 - x_4 - x_5 - x_6 - 2x_7 - x_8 & \\ \diagup & & \diagdown \\ x_8 - x_9 & \text{------} & x_7 - x_8 \end{array} \tag{5.306}$$

where $x_8 - x_9$, $x_3 - x_2$ and $2l - x_2 - x_3 - x_6 - x_7 - x_8 - x_9$ glue to fibers inside corresponding affine surfaces.

$$\mathfrak{su}(4)^{(1)} \text{ --- } \mathfrak{sp}(0)^{(1)} \text{ --- } \mathfrak{su}(3)^{(2)}$$

$$\begin{array}{ccc}
 & \begin{array}{c} x_1 - x_4, \equiv x_2 - x_1 \\ x_3 - x_2, \\ l - x_2 - x_3 - x_5, \\ 2l - x_2 - x_3 - x_6 - x_7 - x_8 - x_9 \end{array} & \\
 & 3l - x_1 - x_2 - x_3 - x_4 - x_5 - 2x_6 - x_7 - x_8 & \\
x_8 - x_9 & & x_6 - x_7 \\
 & x_7 - x_8 &
\end{array} \tag{5.307}$$

where $x_8 - x_9$, $x_3 - x_2$, $x_1 - x_4$, $l - x_2 - x_3 - x_5$ and $2l - x_2 - x_3 - x_6 - x_7 - x_8 - x_9$ glue to fibers inside corresponding affine surfaces.

$$\mathfrak{su}(3)^{(1)} \text{ --- } \mathfrak{sp}(0)^{(1)} \text{ --- } \mathfrak{su}(3)^{(2)}$$

$$\begin{array}{ccc}
 & \begin{array}{c} x_1 - x_4, \equiv x_2 - x_1 \\ x_3 - x_2, \\ l - x_2 - x_3 - x_5, \\ 2l - x_2 - x_3 - x_6 - x_7 - x_8 - x_9 \end{array} & \\
 & 3l - x_1 - x_2 - x_3 - x_4 - x_5 - x_6 - 2x_7 - x_8 & \\
x_8 - x_9 & \text{———} & x_7 - x_8
\end{array} \tag{5.308}$$

where $x_8 - x_9$, $x_3 - x_2$, $x_1 - x_4$, $l - x_2 - x_3 - x_5$ and $2l - x_2 - x_3 - x_6 - x_7 - x_8 - x_9$ glue to fibers inside corresponding affine surfaces.

$$\mathfrak{so}(9)^{(1)} \text{ --- } \mathfrak{sp}(0)^{(1)} \text{ --- } \mathfrak{su}(4)^{(2)}$$

$$\begin{array}{c}
2l - x_1 - x_2 - x_4 - x_5 - x_6 - x_7 \\
| \\
x_8 - x_9 \text{ --- } x_7 - x_8 \text{ --- } x_6 - x_7 = x_2 - x_6,\ l - x_2 - x_3 - x_6 \\
\\
x_4 - x_5, = x_1 - x_4 = x_2 - x_1,\ l - x_1 - x_2 - x_3 \\
2l - x_1 - x_2 - x_6 - x_7 - x_8 - x_9
\end{array} \tag{5.309}$$

where x_8-x_9, x_4-x_5 and $2l-x_1-x_2-x_6-x_7-x_8-x_9$ glue to fibers inside corresponding affine surfaces.

$$\mathfrak{so}(9)^{(1)} - \mathfrak{sp}(0)^{(1)} - \mathfrak{su}(3)^{(2)}$$

$$\begin{array}{c} x_2-x_1, \\ x_4-x_5, \\ l-x_1-x_2-x_3, \\ 2l-x_1-x_2-x_6-x_7-x_8-x_9 \end{array} \equiv x_1-x_4$$

$$\begin{array}{ccccccc} & & 2l-x_1-x_2-x_4-x_5-x_6-x_7 & & & & \\ & & | & & & & \\ x_8-x_9 & - & x_7-x_8 & - & x_6-x_7 & = & x_2-x_6,\ l-x_2-x_3-x_6 \end{array} \tag{5.310}$$

where x_8-x_9, x_2-x_1, x_4-x_5, $l-x_1-x_2-x_3$ and $2l-x_1-x_2-x_6-x_7-x_8-x_9$ glue to fibers inside corresponding affine surfaces.

Now, we are left with some possibilities that do not arise as foldings. For example, the unfolding of $\mathfrak{e}_6^{(2)} \oplus \mathfrak{su}(3)^{(1)}$ is $\mathfrak{e}_7^{(1)} \oplus \mathfrak{su}(3)^{(1)}$ which cannot be embedded into $\mathfrak{e}_8^{(1)}$. To obtain the gluing rules for this case, we notice that folding of (5.190) has zero mutual intersection with (5.196).

$$\mathfrak{e}_6^{(2)} - \mathfrak{sp}(0)^{(1)} - \mathfrak{su}(3)^{(2)}$$

$$\begin{array}{ccccccc} & & & & & & l-x_1-x_2-x_3 \\ & & & & & & | \\ \begin{array}{c} x_6-x_7, \\ l-x_3-x_8-x_9 \end{array} & = & \begin{array}{c} x_5-x_6, \\ x_3-x_2 \end{array} & = & \begin{array}{c} x_4-x_5, \\ x_2-x_1 \end{array} & = & x_1-x_4 \end{array}$$

$$\begin{array}{c} x_8-x_9, \\ x_6-x_7, \\ l-x_3-x_6-x_7, \\ 2l-x_1-x_2-x_4-x_5-x_6-x_7 \end{array} \equiv x_7-x_8 \tag{5.311}$$

where x_8-x_9, x_6-x_7, $l-x_3-x_6-x_7$, $2l-x_1-x_2-x_4-x_5-x_6-x_7$, x_6-x_7 and $l-x_7-x_8-x_9$ glue to fibers inside corresponding affine surfaces.

In a similar fashion, by folding, adding curves or by guessing a correct configuration of curves, we can obtain all the other following gluing rules:

$$\mathfrak{sp}(0)^{(1)} \text{ —— } \mathfrak{su}(9)^{(2)}$$

$$\begin{array}{c} x_8-x_9, \\ l-x_1-x_4-x_5, \\ l-x_1-x_3-x_6, \\ l-x_1-x_2-x_7 \end{array} \equiv\!\equiv \begin{array}{c} x_7-x_8, \\ x_1-x_2 \end{array} = \begin{array}{c} x_6-x_7, \\ x_2-x_3 \end{array} = \begin{array}{c} x_5-x_6, \\ x_3-x_4 \end{array} = x_4-x_5 \tag{5.312}$$

where x_8-x_9, $l-x_1-x_4-x_5$, $l-x_1-x_3-x_6$ and $l-x_1-x_2-x_7$ glue to four copies of fiber in the affine surface.

$$\mathfrak{so}(8)^{(2)} \text{ —— } \mathfrak{sp}(0)^{(1)} \text{ —— } \mathfrak{so}(8)^{(2)}$$

$$\begin{array}{c}
\begin{array}{c} x_5-x_2, \\ l-x_2-x_3-x_5 \end{array} = x_2-x_1 \text{ —— } x_1-x_4 = \begin{array}{c} x_4-x_5, \\ 2l-x_1-x_2-x_6-x_7-x_8-x_9 \end{array} \\[2ex]
\begin{array}{c} x_5-x_6, \\ l-x_3-x_5-x_6 \end{array} = x_6-x_7 \text{ —— } x_7-x_8 = \begin{array}{c} x_8-x_9, \\ 2l-x_1-x_2-x_4-x_5-x_6-x_7 \end{array}
\end{array} \tag{5.313}$$

where x_8-x_9, $2l-x_1-x_2-x_4-x_5-x_6-x_7$, x_4-x_5 and $2l-x_1-x_2-x_6-x_7-x_8-x_9$ glue to fibers inside corresponding affine surfaces.

$$\mathfrak{so}(10)^{(2)} \text{ —— } \mathfrak{sp}(0)^{(1)} \text{ —— } \mathfrak{su}(4)^{(2)}$$

$$\begin{array}{c}
\begin{array}{c} x_4-x_5, \\ 2l-x_1-x_2-x_6-x_7-x_8-x_9 \end{array} = x_1-x_4 \text{ —— } x_2-x_1 \text{ —— } x_7-x_2 = \begin{array}{c} x_5-x_7, \\ l-x_3-x_5-x_7 \end{array} \\[2ex]
\begin{array}{c} x_8-x_9, \\ 2l-x_1-x_2-x_4-x_5-x_6-x_7 \end{array} = x_6-x_8 = \begin{array}{c} x_5-x_6, \\ l-x_3-x_5-x_6 \end{array}
\end{array} \tag{5.314}$$

where x_8-x_9, $2l-x_1-x_2-x_4-x_5-x_6-x_7$, x_4-x_5 and $2l-x_1-x_2-x_6-x_7-x_8-x_9$

glue to fibers inside corresponding affine surfaces.

$$\mathfrak{so}(10)^{(2)} \text{ --- } \mathfrak{sp}(0)^{(1)} \text{ --- } \mathfrak{su}(3)^{(2)}$$

$$\begin{tikzcd}[column sep=small]
\begin{array}{c} x_4-x_5, \\ 2l-x_1-x_2-x_6-x_7-x_8-x_9 \end{array} \arrow[r, no head, double] & x_1-x_4 \arrow[r, no head] & x_2-x_1 \arrow[r, no head] & x_7-x_2 \arrow[r, no head, double] & \begin{array}{c} x_5-x_7, \\ l-x_3-x_5-x_7 \end{array}
\end{tikzcd}$$

$$\begin{tikzcd}[column sep=small]
\begin{array}{c} x_8-x_9, \\ x_5-x_6, \\ l-x_3-x_5-x_6, \\ 2l-x_1-x_2-x_4-x_5-x_6-x_7 \end{array} \arrow[r, no head, double] & x_6-x_8
\end{tikzcd} \tag{5.315}$$

where x_8-x_9, x_5-x_6, $l-x_3-x_5-x_6$, $2l-x_1-x_2-x_4-x_5-x_6-x_7$, x_4-x_5 and $2l-x_1-x_2-x_6-x_7-x_8-x_9$ glue to fibers inside corresponding affine surfaces.

$$\mathfrak{su}(6)^{(2)} \text{ --- } \mathfrak{sp}(0)^{(1)} \text{ --- } \mathfrak{su}(3)^{(2)}$$

$$\begin{tikzcd}[column sep=small]
 & x_1-x_4 \arrow[d, no head, double] & \\
\begin{array}{c} l-x_1-x_2-x_4, \\ l-x_2-x_3-x_6 \end{array} \arrow[r, no head, double] & \begin{array}{c} x_4-x_5, \\ x_2-x_1 \end{array} \arrow[r, no head, double] & \begin{array}{c} x_5-x_9, \\ l-x_2-x_7-x_8 \end{array}
\end{tikzcd}$$

$$\begin{tikzcd}[column sep=small]
\begin{array}{c} x_8-x_9, \\ l-x_1-x_4-x_7, \\ l-x_2-x_5-x_7, \\ l-x_3-x_6-x_7 \end{array} \arrow[r, no head, double] & x_7-x_8
\end{tikzcd} \tag{5.316}$$

where x_8-x_9, $l-x_1-x_4-x_7$, $l-x_2-x_5-x_7$, $l-x_3-x_6-x_7$, x_5-x_9 and $l-x_2-x_7-x_8$ glue to fibers inside corresponding affine surfaces.

$$\mathfrak{su}(5)^{(2)} \text{ --- } \mathfrak{sp}(0)^{(1)} \text{ --- } \mathfrak{su}(3)^{(2)}$$

$$\begin{tikzcd}[column sep=small]
\begin{array}{c} l-x_1-x_2-x_4, \\ l-x_2-x_3-x_6, \\ l-x_2-x_7-x_8, \\ x_5-x_9 \end{array} \arrow[r, no head, double] & \begin{array}{c} x_4-x_5, \\ x_2-x_1 \end{array} \arrow[r, no head, double] & x_1-x_4
\end{tikzcd}$$

$$\begin{tikzcd}[column sep=small]
\begin{array}{c} x_8-x_9, \\ l-x_1-x_4-x_7, \\ l-x_2-x_5-x_7, \\ l-x_3-x_6-x_7 \end{array} \arrow[r, no head, double] & x_7-x_8
\end{tikzcd} \tag{5.317}$$

where $x_8 - x_9$, $l - x_1 - x_4 - x_7$, $l - x_2 - x_5 - x_7$, $l - x_3 - x_6 - x_7$, $x_5 - x_9$, $l - x_2 - x_3 - x_6$, $l - x_1 - x_2 - x_4$ and $l - x_2 - x_7 - x_8$ glue to fibers inside corresponding affine surfaces.

$$\mathfrak{so}(8)^{(3)} \;\text{———}\; \mathfrak{sp}(0)^{(1)} \;\text{———}\; \mathfrak{so}(8)^{(3)}$$

$$\begin{array}{ccccc} l - x_1 - x_2 - x_3 & \equiv\equiv & x_1 - x_4, & \equiv\equiv & x_4 - x_7, \\ & & x_2 - x_5, & & x_5 - x_8, \\ & & x_3 - x_6 & & x_6 - x_9 \\ \\ l - x_1 - x_4 - x_7 & \equiv\equiv & x_1 - x_2, & \equiv\equiv & x_2 - x_3, \\ & & x_4 - x_5, & & x_5 - x_6, \\ & & x_7 - x_8 & & x_8 - x_9 \end{array} \tag{5.318}$$

where $x_8 - x_9$, $x_5 - x_6$, $x_2 - x_3$, $x_6 - x_9$, $x_5 - x8$ and $x_4 - x_7$ glue to fibers inside corresponding affine surfaces.

5.4.4 $\mathfrak{sp}(0)^{(1)}$ gluings: directed edges

Finally we consider cases in which one or both the neighbors of $\mathfrak{sp}(0)^{(1)}$ are connected to it via directed edges. Our main constraint comes from (5.60) which states that the torus fibers must be glued appropriately. Let us define $C_{0,\alpha}$ be a -2 curve in dP_9 which glues to the affine surface for $\mathfrak{g}_\alpha^{(q_\alpha)}$ in the gluing rule associated to an undirected edge, that is gluing rule for

$$\mathfrak{sp}(0)^{(1)} \;\text{————}\; \mathfrak{g}_\alpha^{(q_\alpha)} \tag{5.319}$$

If $q_\alpha = 1$, then there is a unique $C_{0,\alpha}$. If $q_\alpha > 1$, then there can be multiple such -2 curves. In this case, we pick the curve containing the blowup x_9 as $C_{0,\alpha}$. This uniquely fixes the -2 curve $C_{0,\alpha}$. The reason for the prominence of the blowup x_9 in this definition is that the KK mass $\frac{1}{R}$ enters into the volume of x_9, and the volume of any other curve in dP_9 that does not involve x_9 is independent of $\frac{1}{R}$. We refer the reader to [4] for more details.

To obtain the gluing rules for

$$\mathfrak{g}_\alpha^{(q_\alpha)} \;\text{————}\; \mathfrak{sp}(0)^{(1)} \xleftarrow{\quad} e_\gamma \;\text{—}\; \mathfrak{g}_\gamma^{(q_\gamma)} \tag{5.320}$$

we start from the gluing rules for

$$\mathfrak{g}_\alpha^{(q_\alpha)} \;\text{————}\; \mathfrak{sp}(0)^{(1)} \;\text{————}\; \mathfrak{g}_\gamma^{(q_\gamma)} \tag{5.321}$$

and simply replace the curve $C_{0,\gamma}$ in dP_9 by the curve $C_{0,\gamma} + e_\gamma\,(3l - \sum x_i)$. Similarly, to obtain the gluing rules for

$$\mathfrak{g}_\alpha^{(q_\alpha)} \;\text{—}\; e_\alpha \longrightarrow \mathfrak{sp}(0)^{(1)} \longleftarrow e_\gamma \;\text{—}\; \mathfrak{g}_\gamma^{(q_\gamma)} \tag{5.322}$$

JHEP12(2020)151

we start from the gluing rules for

$$\mathfrak{g}_\alpha^{(q_\alpha)} \text{ ———— } \mathfrak{sp}(0)^{(1)} \text{ ———— } \mathfrak{g}_\gamma^{(q_\gamma)} \tag{5.323}$$

and simply replace the curves $C_{0,\gamma}$ and $C_{0,\alpha}$ in dP_9 by the curves $C_{0,\gamma} + e_\gamma\,(3l - \sum x_i)$ and $C_{0,\alpha} + e_\alpha\,(3l - \sum x_i)$ respectively. It is trivial to see that this replacement satisfies (5.60).

Now we only need to consider gluing rules of the form

$$\mathfrak{sp}(0)^{(1)} \text{ —— } e_\gamma \longrightarrow \mathfrak{g}_\gamma^{(q_\gamma)} \tag{5.324}$$

since in the context of $6d$ SCFTs, it is not possible for any other node to attach to $\mathfrak{sp}(0)^{(1)}$ in (5.324).

We first work out the following gluing rules by hand:

$$\mathfrak{sp}(0)^{(1)} \text{ —— } 2 \longrightarrow \mathfrak{so}(8)^{(1)}$$

$$\begin{array}{ccccc}
 & & \begin{array}{c} l-x_1-x_2-x_3, \\ 2l-x_1-x_2-x_4-x_5-x_6-x_7 \end{array} & & \\
 & & \Vert & & \\
\begin{array}{c} x_8-x_9, \\ x_2-x_1 \end{array} & = & \begin{array}{c} x_7-x_8, \\ x_1-x_4 \end{array} & = & \begin{array}{c} x_4-x_5, \\ x_6-x_7 \end{array} \\
 & & \Vert & & \\
 & & \begin{array}{c} x_4-x_6, \\ x_5-x_7 \end{array} & &
\end{array} \tag{5.325}$$

where $x_8 - x_9$, $x_2 - x_1$ glue to two copies of fiber in the affine surface. Indeed we can check that twice the torus fiber for $\mathfrak{so}(8)^{(1)}$ is glued to $3l - \sum x_i$.

By folding the above gluing rules, we obtain:

$$\mathfrak{sp}(0)^{(1)} \text{ —— } 2 \longrightarrow \mathfrak{so}(7)^{(1)}$$

$$\begin{array}{ccccc}
 & & \begin{array}{c} l-x_1-x_2-x_3, \\ 2l-x_1-x_2-x_4-x_5-x_6-x_7 \end{array} & & \\
 & & \Vert & & \\
\begin{array}{c} x_4-x_6, \\ x_5-x_7 \end{array} & = & \begin{array}{c} x_7-x_8, \\ x_1-x_4 \end{array} & \equiv & \begin{array}{c} x_4-x_5, \\ x_6-x_7, \\ x_2-x_1, \\ x_8-x_9 \end{array}
\end{array} \tag{5.326}$$

where $x_8 - x_9$, $x_2 - x_1$, $x_6 - x_7$, $x_4 - x_5$ glue to four copies of fiber in the affine surface.

JHEP12(2020)151

Treating $\mathfrak{su}(3)^{(1)}$ as a subalgebra of $\mathfrak{so}(7)^{(1)}$, we can obtain the following gluing rules

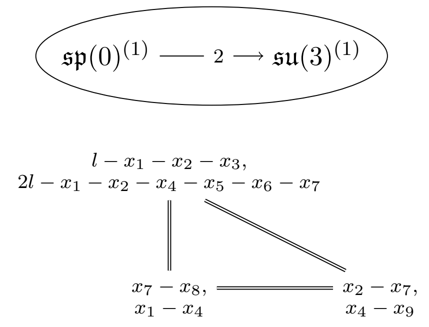

(5.327)

where x_4-x_9, x_2-x_7 glue to two copies of fiber in the affine surface.

Finally, folding (5.326), we obtain

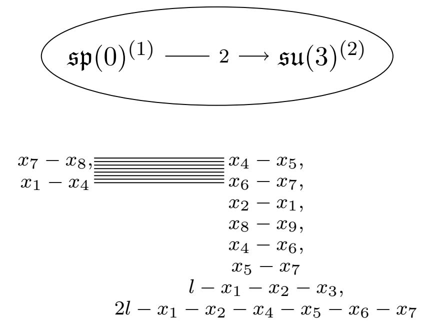

(5.328)

where x_8-x_9, x_2-x_1, x_6-x_7, x_4-x_5, x_4-x_6, x_5-x_7, $l-x_1-x_2-x_3$, $2l-x_1-x_2-x_4-x_5-x_6-x_7$ glue to eight copies of fiber in the affine surface.

6 Conclusions and future directions

In this paper, we have associated a genus-one fibered Calabi-Yau threefold to every $5d$ KK theory, except a few cases for which we provide an algebraic description mimicking the properties of genus-one fibered Calabi-Yau threefolds. Compactifying M-theory on the threefold constructs the KK theory on its Coulomb branch. The threefold is presented as a local neighborhood of a collection of surfaces intersecting with each other. We explicitly identify all the surfaces and their intersections for every KK theory. Such a description of the threefold allows an easy determination of the set of all compact holomorphic curves (known as the Mori cone) inside the threefold along with their intersection numbers with other cycles in the threefold. The Mori cone encodes crucial non-perturbative data needed to perform RG flows on the KK theory which lead to $5d$ SCFTs. For the cases without a completely geometric description we propose an analog of Mori cone using which one can perform RG flows on these outlying KK theories as well.

According to a conjecture (see [2–4]) for which substantial evidence was provided in [2], all the $5d$ SCFTs sit at the end points of such RG flows emanating from $5d$ KK

JHEP12(2020)151

theories. Thus, this work can be viewed as providing a preliminary step towards an explicit classification of $5d$ SCFTs. In principle, the Coulomb branch data of all $5d$ SCFTs is encoded in the properties of Calabi-Yau threefolds presented in this paper (see section 5). Explicitly, such RG flows are performed by performing sequences of flops and blowdowns on the Calabi-Yau threefolds associated to $5d$ KK theories. See [2–4] for a general discussion and [10] for the explicit classification of $5d$ SCFTs up to rank three using the results of this paper. Extending the classification to higher ranks, perhaps using a computer program, would be of significant interest.

The Calabi-Yau threefold associated to a $5d$ KK theory is determined by combining the data of the prepotential of the KK theory with certain geometric consistency conditions. We provide a concrete proposal for the computation of this prepotential based on the definition of the $5d$ KK theory in terms of a $6d$ SCFT on a circle and twisted by a discrete global symmetry around the circle. See section 4 for more details.

Along the way, we provide a graphical classification scheme for $5d$ KK theories which mimics the graphical classification scheme used to classify $6d$ SCFTs. In fact the graphs associated to $5d$ KK theories generalize the graphs associated to $6d$ SCFTs just as Dynkin graphs associated to general Lie algebras generalize the Dynkin graphs associated to simply laced Lie algebras. We provide a full list of all the possible vertices and edges that can appear in graphs associated to $5d$ KK theories. See section 3 for more details. We leave an explicit classification of $5d$ KK theories to a future work. Such a classification can be performed in a straightforward fashion starting from the explicit classification of $6d$ SCFTs presented in [33, 36] and applying the folding operations discussed in section 3.

A noteworthy point deserving a special mention is that our work applies uniformly to all $6d$ SCFTs irrespective of whether they are constructed in the frozen phase of F-theory or in the unfrozen phase of F-theory. In other words, the dictionary relating M-theory and $5d$ KK theories applies uniformly to all $5d$ KK theories irrespective of the F-theory origin of the associated $6d$ SCFT. This is in stark contrast with the case of $6d$ SCFTs for which the dictionary relating F-theory and the resulting $6d$ theory is modified depending on the presence (called the frozen phase) or absence (called the unfrozen phase) of $O7^+$ planes in the base of the elliptic Calabi-Yau threefold used for compactification of F-theory. See [32] for more details.

In the future, it will be interesting to use the geometries presented in this paper to derive $5d$ gauge theory descriptions associated to $6d$ SCFTs compactified on a circle (possibly with a twist). This can be done by performing local S-dualities on the geometries associated to $5d$ KK theories. See the recent work [54] for more details on the methodology.

Acknowledgments

The authors thank Sheldon Katz, Sung Soo Kim, and Gabi Zafrir for valuable discussions, as well as the members of the Simons Center for Geometry and Physics for their hospitality during the 2018 and 2019 Simons Summer Workshop(s) while part of this work was being completed. HK also thanks the members of Harvard University for their hospitality while this work was being completed. The research of CV is supported in part by the

NSF grant PHY-1719924 and by a grant from the Simons Foundation (602883, CV). The research of LB and HCT is supported by the NSF grant PHY-1719924, and HCT also acknowledges partial support from the Greek America Foundation through the Mavroyannis Scholarship. The research of HK is supported by the POSCO Science Fellowship of POSCO TJ Park Foundation and the National Research Foundation of Korea (NRF) Grant 2018R1D1A1B07042934. The research of PJ is supported by the U.S. Department of Energy, Office of Science, Office of High Energy Physics of U.S. Department of Energy under grant Contract Numbers DE-SC0012567 and DE-SC0019127.

A Geometric background

In this section, we recall some background useful for this paper. We refer the reader to section 2 of [4] for a more detailed background on various points discussed below in this appendix.

A.1 Hirzebruch surfaces

A Hirzebruch surface is a $\mathbb{P}^1$ fibration over $\mathbb{P}^1$. We denote a Hirzebruch surface with a degree $-n$ fibration as $\mathbb{F}_n$. We refer to the fiber $\mathbb{P}^1$ as f and the base $\mathbb{P}^1$ as e. Their intersection numbers are

$$e^2 = -n \tag{A.1}$$

$$f^2 = 0 \tag{A.2}$$

$$e \cdot f = 1 \tag{A.3}$$

Another very important curve in $\mathbb{F}_n$ is

$$h := e + nf \tag{A.4}$$

whose genus is zero and intersection numbers are

$$h^2 = n \tag{A.5}$$

$$h \cdot e = 0 \tag{A.6}$$

$$h \cdot f = 1 \tag{A.7}$$

Note that $e = h$ for $\mathbb{F}_0$. The set of holomorphic curves, often referred to as *Mori cone*, for $\mathbb{F}_n$ with $n \geq 0$ is generated by e and f. For $\mathbb{F}_n$ with $n \leq 0$, the Mori cone is generated by h and f.

The canonical class K of $\mathbb{F}_n$ is an antiholomorphic curve which can be determined by the virtue of adjunction formula which states that for a surface S and a curve C inside S, the canonical class K_S of S satisfies

$$(K_S + C) \cdot C = 2g(C) - 2 \tag{A.8}$$

where $g(C)$ is the genus of C. Demanding that K satisfies (A.8) for e, f determines it to be

$$K = -(e + h + 2f) \tag{A.9}$$

from which we can compute that

$$K^2 = 8 \tag{A.10}$$

Notice that $\mathbb{F}_n$ and $\mathbb{F}_{-n}$ are isomorphic to each other via the map

$$e \leftrightarrow h \tag{A.11}$$

$$f \leftrightarrow f \tag{A.12}$$

$$h \leftrightarrow e \tag{A.13}$$

Thus, we will restrict our attention to Hirzebruch surfaces with $n \geq 0$ in what follows. However, at various points in the main body of the paper we find it useful to include Hirzebruch surfaces with negative degrees since they allow us to express answers in a more uniform way.

We also deal with surfaces which arise by performing b number of blowups on $\mathbb{F}_n$. The blowups will often be non-generic. We can obtain different surfaces by performing b blowups in different fashions on $\mathbb{F}_n$. In this paper, we refer to all the different surfaces arising via b blowups of $\mathbb{F}_n$ as $\mathbb{F}_n^b$. The curves inside $\mathbb{F}_n^b$ can be described by adding the curves x_i with $i = 1, \cdots, b$ which are the exceptional divisors created by the blowups. We will use the convention that the total transforms[21] of the curves e, f and h are denoted by the same names e, f and h in $\mathbb{F}_n^b$. Thus, the intersection numbers between e, f and h are those mentioned above, and their intersections with x_i are

$$x_i \cdot x_j = -\delta_{ij} \tag{A.14}$$

$$e \cdot x_i = 0 \tag{A.15}$$

$$f \cdot x_i = 0 \tag{A.16}$$

$$h \cdot x_i = 0 \tag{A.17}$$

The blowup procedure creates curves that can be written as

$$\alpha e + \beta f - \sum \gamma_i x_i \tag{A.18}$$

with $\alpha, \beta, \gamma_i \geq 0$. The important point is that the blowups x_i can appear with negative sign.

Again, using the adjunction formula (A.8) we can find the canonical class K for $\mathbb{F}_n^b$ to be

$$K = -(e + h + 2f) + \sum x_i \tag{A.19}$$

from which we compute

$$K^2 = 8 - b \tag{A.20}$$

An important isomorphism exists between $\mathbb{F}_0^1$ and $\mathbb{F}_1^1$ with the blowup on both surfaces being performed at a generic point. In fact, a single blowup of $\mathbb{F}_0$ is always generic. The

[21] If $B : \tilde{S} \to S$ is a blowup of a surface S, then the total transform of a curve C in S is the curve $B^{-1}(C)$ in $\tilde{S}$.

map from $\mathbb{F}_1^1$ to $\mathbb{F}_0^1$ is

$$e \to e - x \tag{A.21}$$

$$f - x \to x \tag{A.22}$$

$$x \to f - x \tag{A.23}$$

It is easy to see that the above isomorphism only works when the blowups are generic. For, the non-generic one point blowup of $\mathbb{F}_1$ contains the curve $e - x$, which would be sent to $e - f$ inside $\mathbb{F}_0^1$. But $e - f$ is not a holomorphic curve in $\mathbb{F}_0^1$. The above isomorphism is responsible for the equivalence of geometries corresponding to

$$\underset{1}{\mathfrak{sp}(n)^{(1)}_{(n+1)\pi}} \tag{A.24}$$

and

$$\underset{1}{\mathfrak{sp}(n)^{(1)}_{n\pi}} \tag{A.25}$$

whenever the theta angle is physically irrelevant. In the situations where theta angle is physically relevant, the above isomorphism is broken by the presence of neighboring surfaces.

To differentiate between the different surfaces $\mathbb{F}_n^b$ for fixed n and b, we have to track the data of their Mori cone. One important point is that the gluing curves inside the surfaces must be the generators of Mori cone. In the paper, we find many instances in which a surface $\mathbb{F}_n^b$ appearing in different contexts carries different kinds of gluing curves, thus demonstrating that the two $\mathbb{F}_n^b$ are different surfaces. For example, the geometry with $\nu = 0$ for

$$\underset{2}{\mathfrak{su}(n+4)^{(1)}} \tag{A.26}$$

and the geometry with $\nu = 0$ for

$$\underset{1}{\mathfrak{sp}(n)^{(1)}_{(n+1)\pi}} \tag{A.27}$$

both contain a surface $\mathbb{F}_0^{2n+8}$ with different gluing curves $e - \sum x_i$ and $2e + f - \sum x_i$ respectively. Thus the $\mathbb{F}_0^{2n+8}$ appearing in the two theories are different blowups of $\mathbb{F}_0$.

The final point we want to address is that $\mathbb{F}_2$ and $\mathbb{F}_0$ are same up to decoupled states. This can be seen by noticing that the Mori cone of latter embeds into the Mori cone of former. This embedding $\mathbb{F}_0 \to \mathbb{F}_2$ is

$$e \to e + f \tag{A.28}$$

$$f \to f \tag{A.29}$$

This means that $\mathbb{F}_2$ equals $\mathbb{F}_0$ plus some decoupled states. Decoupling these states corresponds to performing a complex structure deformation $\mathbb{F}_2 \to \mathbb{F}_0$. When $\mathbb{F}_0$ and $\mathbb{F}_2$ carry blowups, this conclusion might be changed or unchanged depending on how the blowups are done. See the discussion after (B.17) for an example where this conclusion still holds true even in the presence of blowups.

A.2 Del Pezzo surfaces

The discussion of del Pezzo surfaces starts with the discussion of complex projective plane $\mathbb{P}^2$ which contains a single curve l whose genus is zero and intersection number is

$$l^2 = 1 \tag{A.30}$$

(A.8) determines the canonical class to be

$$K = -3l \tag{A.31}$$

from which we compute

$$K^2 = 9 \tag{A.32}$$

Performing n blowups on $\mathbb{P}^2$ at generic locations leads to the del Pezzo surface dP_n. It can be described in terms of curve l and x_i with intersection numbers

$$x_i \cdot x_j = -\delta_{ij} \tag{A.33}$$

$$l \cdot x_i = 0 \tag{A.34}$$

Again, the blowups create new holomorphic curves which can be written as

$$\alpha l - \sum \gamma_i x_i \tag{A.35}$$

with $\alpha, \gamma_i \geq 0$. In the paper, we abuse the notation and call a non-generic n point blowup of $\mathbb{P}^2$ as dP_n too. The canonical class for dP_n is

$$K = -3l + \sum x_i \tag{A.36}$$

with

$$K^2 = 9 - n \tag{A.37}$$

del Pezzo surfaces and Hirzebruch surfaces are related to each other by virtue of an isomorphism $dP_1 \to \mathbb{F}_1$ which acts as

$$x \to e \tag{A.38}$$

$$l - x \to f \tag{A.39}$$

$$l \to h \tag{A.40}$$

A one point blowup of $\mathbb{P}^2$ is always generic and thus there is a unique dP_1 which appears in the above isomorphism.

A special example of del Pezzo surfaces for us in this paper will be dP_9 which is the geometry associated to

$$\begin{array}{c}\mathfrak{sp}(0)^{(1)}\\ 1\end{array} \tag{A.41}$$

The curve

$$F = 3l - \sum x_i \tag{A.42}$$

has the properties that

$$F^2 = 0 \tag{A.43}$$

and

$$K \cdot F = 0 \tag{A.44}$$

Thus, F is a fiber of genus one, or in other words a torus fiber inside dP_9.

dP_n for $n \geq 3$ admits the following basic automorphism. We first choose three distinct blowups x_i, x_j and x_k, and then implement

$$x_i \to l - x_j - x_k \tag{A.45}$$

$$x_j \to l - x_i - x_k \tag{A.46}$$

$$x_k \to l - x_i - x_j \tag{A.47}$$

$$l \to 2l - x_i - x_j - x_k \tag{A.48}$$

Combining this automorphism with permutations of blowups, we can obtain more general automorphisms of dP_n (with $n \geq 3$) which can be decomposed as a sequence comprising of above mentioned basic automorphisms and permutations of blowups. Notice that for dP_9, any such automorphism leaves the torus fiber (A.42) invariant.

A.3 Arithmetic genus for curves in a self-glued surface

When a surface has no self-gluings, then the arithmetic genus[22] of curves living inside the surface can be computed using the adjunction formula (A.8).

However, when the surface has self-gluings, the genus of the curve is modified. For example, consider gluing the exceptional curves x and y in a generic two point blowup of $\mathbb{F}_1$. The curve $h - x - y$ (which is a rational curve before gluing) looks like an elliptic fiber with nodal singularity after the gluing, so its arithmetic genus should be one instead of zero, which is what would be suggested by (A.8). This example suggests that the intersection numbers of a curve C with the curves C_1 and C_2 participating in a self-gluing should be used to modify (A.8) in order to obtain the correct arithmetic genus. However, not all such intersection numbers participate in such a modification. To see this, consider the curve $f - x$ in the above example. This curve remains rational even after gluing. Thus, even though it intersects x, its genus is correctly captured by (A.8).

The examples of $h - x - y$ and $f - x$ above suggest that the genus of a curve C should only be modified whenever an intersection with C_1 has a partner intersection with C_2. Thus our proposal for the computation of genus of an arbitrary curve C is as follows: let n_1 and n_2 be the intersections of C with C_1 and C_2 respectively, and let $n = \min(n_1, n_2)$. Then, our proposal for computation of genus is

$$2g(C) - 2 = (K_S + C) \cdot C + 2n \tag{A.49}$$

(A.49) allows certain curves to have a non-negative genus even though they did not have a non-negative genus before self-gluing. For example, consider

[22] Throughout this paper, we never use the geometric genus. Whenever the word "genus" appears in this paper, it always refers to arithmetic genus.

- A surface $\mathbb{F}_m^2$ with x glued to y. The curve $e-x-2y$ has $g=0$ according to (A.49) while it has $g=-1$ according to (A.8) which is the formula we would use in the absence of self-gluing. $e-x-2y$ appears as a gluing curve in some of our geometries, for example (5.107), (5.108), (5.156) and (5.158).

- A surface $\mathbb{F}_0^2$ with $e-x$ glued to $e-y$. The curve $2f-x$ has $g=0$ according to (A.49) while it has $g=-1$ according to (A.8). $2f-x$ appears as a gluing curve in the gluing rules for

$$\begin{array}{ccc} \mathfrak{su}(1)^{(1)} & & \mathfrak{su}(1)^{(1)} \\ 2 & \overset{}{\text{---}}\,{\scriptstyle 2}\!\longrightarrow & 2 \end{array} \tag{A.50}$$

B Exceptional cases

In this appendix we study some of the exceptional cases where the methods used in the paper are not applicable in a straightforward manner.

B.1 Geometries for non-gauge theoretic nodes

The following non-gauge theoretic nodes arise in our analysis

$$\begin{array}{c} \mathfrak{sp}(0)^{(1)} \\ 1 \end{array} \tag{B.1}$$

$$\begin{array}{c} \mathfrak{su}(1)^{(1)} \\ 2 \end{array} \tag{B.2}$$

$$\begin{array}{c} \mathfrak{su}(1)^{(1)} \\ 2 \\ \circlearrowleft \end{array} \tag{B.3}$$

According to our proposal the prepotential $6\tilde{\mathcal{F}}$ for each case must be zero. So the geometry cannot be directly guessed from the prepotential. One can try to take corresponding limits of the geometries for the following gauge theoretic nodes

$$\begin{array}{c} \mathfrak{sp}(n)^{(1)} \\ 1 \end{array} \tag{B.4}$$

$$\begin{array}{c} \mathfrak{su}(n)^{(1)} \\ 2 \end{array} \tag{B.5}$$

$$\begin{array}{c} \mathfrak{su}(n)^{(1)} \\ 2 \\ \circlearrowleft \end{array} \tag{B.6}$$

But this procedure is unreliable. For example, taking the limit of the geometry (5.112) would suggest that there should exist a phase of (B.2) governed by the geometry

$$\mathbf{0}_{\mathbf{0}}^{\mathbf{1+1}} \circlearrowleft^{e\text{-}x\text{-}y}_{e} \tag{B.7}$$

However, even though the self-gluing here satisfies the Calabi-Yau condition (5.18), it does not satisfy the condition (5.17). So, this is not a consistent geometry, and there should be no such phase for (B.2).

Fortunately, a gauge theory description of the KK theories (B.1), (B.2) and (B.3) is known, which allows us to reliably compute the corresponding geometries. In terms of the language used throughout this paper, this gauge theory description is a "non-canonical" gauge theory description of these KK theories, since it does not correspond to the 6d gauge theory description on the tensor branch of the corresponding 6d SCFT.

To start with, it is known that (B.1) can be described by the gauge theory $\mathfrak{su}(2)$ with eight fundamental hypers. We can compute the prepotential via

$$6\mathcal{F} = \frac{1}{2}\left(\sum_r |r\cdot\phi|^3 - \sum_f \sum_{w(\mathcal{R}_f)} |w(\mathcal{R}_f)\cdot\phi + m_f|^3\right) \tag{B.8}$$

and convert it into a geometry as described in section 5.1. When all mass parameters are turned off, we obtain the geometry

$$\mathbf{0}_{\mathbf{1}}^{\mathbf{8}} \tag{B.9}$$

which equals dP_9. See the discussion that follows (5.102).

Next, it is known that (B.2) can be described by the gauge theory $\mathfrak{sp}(1)$ with an adjoint hyper and $\theta = 0$. Moreover, it is known that upon integrating out the adjoint matter of $\mathfrak{sp}(n)$, the theta angle remains unchanged. We know that the geometry corresponding to pure $\mathfrak{sp}(1)$ with $\theta = 0$ is

$$\mathbf{0}_{\mathbf{0}} \tag{B.10}$$

where we adopt the convention that f is the W-boson of $\mathfrak{sp}(1)$ and e is an instanton. So, we just have to integrate the adjoint matter into (B.10) to figure out the geometry for (B.2). We can write the weights of the adjoint as $w_1 = (2)$, $w_2 = (0)$ and $w_3 = (-2)$ in terms of their Dynkin coefficient. When mass parameter for adjoint is very large, then according to the discussion in section 5.1, we should be able to find a -1 curve C living inside a non-compact surface N such that C intersects $S_0 = \mathbb{F}_0$ transversely at two points. We can consistently choose the gluing curve for N inside S_0 to be f since $N \cdot f$ must be zero as the mass of the W-boson must be independent of the mass parameter associated to N which is the mass parameter associated to adjoint hyper. As we bring the mass of adjoint to zero, C undergoes a flop transition. If a -1 curve living outside a surface S intersects S at two points transversely, then flopping the -1 curve leads to the emergence of self-gluing on the surface S. Thus, the geometry for (B.2) is

$$\begin{array}{cc} & x \\ \mathbf{0}_{\mathbf{0}}^{\mathbf{1+1}} & \\ & y \end{array} \tag{B.11}$$

with the gluing curve to N being the genus one curve $f-x-y$. We can write the geometry in an isomorphic way by first exchanging e with f, which keeps the description (B.11) while changing the gluing curve to N as $e-x-y$. Now we perform the isomorphism $\mathbb{F}_0^2 \to \mathbb{F}_2^2$ such that

$$e-x-y \to e \tag{B.12}$$
$$f-x \to x \tag{B.13}$$
$$f-y \to y \tag{B.14}$$
$$x \to f-x \tag{B.15}$$
$$y \to f-y \tag{B.16}$$

which changes (B.11) to

$$\begin{array}{cc} & f\text{-}x \\ \mathbf{0}_{\mathbf{2}}^{\mathbf{1+1}} & \\ & f\text{-}y \end{array} \tag{B.17}$$

with the gluing curve to N being e. As discussed at the end of appendix A.1, this geometry gives rise to some decoupled states which can be decoupled by doing a complex structure deformation to

$$\begin{array}{cc} & f\text{-}x \\ \mathbf{0}_{\mathbf{0}}^{\mathbf{1+1}} & \\ & f\text{-}y \end{array} \tag{B.18}$$

Performing an exchange of e and f again leads to the geometry

$$\begin{array}{cc} & e\text{-}x \\ \mathbf{0}_{\mathbf{0}}^{\mathbf{1+1}} & \\ & e\text{-}y \end{array} \tag{B.19}$$

which is what is displayed in (5.113) because the fiber f becomes an elliptic fiber in this frame (with a nodal singularity). This is as we would expect from the fact that (B.2) arises from an untwisted unfrozen $6d$ SCFT and hence it must be possible to feed the geometry (B.19) into F-theory, which requires the presence of an elliptic fibration. The gluing curves for the non-compact surface responsible for mass parameter of adjoint are x and y in this frame.

JHEP12(2020)151

Finally, it is known that (B.3) can be described by the gauge theory $\mathfrak{sp}(1)$ with an adjoint hyper and $\theta = \pi$. The geometry corresponding to pure $\mathfrak{sp}(1)$ with $\theta = \pi$ is

$$\mathbf{0_1} \tag{B.20}$$

In a similar fashion as above, integrating in the adjoint leads to

$$\begin{tikzcd} \mathbf{0_1^{1+1}} \arrow[loop right, dash, "x" near start, "y"' near end] \end{tikzcd} \tag{B.21}$$

which is indeed the "geometry" presented in (5.160). We write the word geometry in quotation marks because it is only to be understood as an algebraic description mimicking the properties of the geometric description available for other KK theories. See the discussion after equation (5.160) for more details.

B.2 Gluing rules between non-gauge theoretic nodes

As we combine non-gauge theoretic nodes via edges, the prepotential $6\tilde{\mathcal{F}}$ still remains zero. Thus, another method to compute the gluing rules presented in the main body of this paper is desirable. The goal of this section is to provide this alternative derivation.

Gluing rules for $\overset{\mathfrak{su}(1)^{(1)}}{\mathbf{2}}\!-\!\!-\!\!-\!\!\overset{\mathfrak{sp}(0)^{(1)}}{\mathbf{1}}$: it is known that this KK theory is equivalent to a $5d$ $\mathfrak{sp}(2)$ gauge theory with eight fundamentals and an antisymmetric. The theta angle for $\mathfrak{sp}(2)$ is irrelevant due to the presence of fundamentals. So we can start with geometry corresponding to any theta angle for pure $\mathfrak{sp}(2)$ and then integrate in the matter. The geometry with theta angle zero is

$$\mathbf{1_6}\ \overset{e}{-}\!\!-\!\!-\!\!-\!\!\overset{2h}{-}\ \mathbf{2_1} \tag{B.22}$$

where we have labeled the surfaces according to the labeling of the corresponding simple co-roots of $\mathfrak{sp}(2)$. Notice that this is different than a similar labeling of the surfaces in terms of simple co-roots of affine algebras used in the main body of the text. The weights for fundamental are

$$\begin{gathered}(1,0)^+\\(-1,1)^+\\(1,-1)^+\\(-1,0)^+\end{gathered}$$

where we have arranged the weights in a spindle shape according to their level and the superscripts on top of the weights denotes the sign of virtual volume of the weights in the totally integrated out phase (B.22). The last weight $(-1,0)$ can be recognized as a -1 curve living in a non-compact surface and intersecting S_1 once. Since there are eight

JHEP12(2020)151

fundamentals, there are eight copies of the above weight system. Making the virtual volume of $(-1,0)$ negative for all eight copies leads to the phase

$$\mathbf{1}_{\mathbf{6}}^{\mathbf{8}} \overset{e \qquad\qquad 2h}{\rule{4cm}{0.4pt}} \mathbf{2}_{\mathbf{1}} \tag{B.23}$$

The weight system in this phase can be written as eight copies of

$$\begin{gathered}(1,0)^+\\(-1,1)^+\\(1,-1)^+\\(-1,0)^-\end{gathered}$$

The blowups x_i correspond to eight copies of the weight $(-1,0)$. Indeed, the volume of x_i is ϕ_1 which is negative of the virtual volume of the weight $(-1,0)$ in this phase. The other weights are obtained by adding the fibers f_i of the two surfaces S_i. For example, $f_1 - x_i$ are eight copies of the weight $(1,-1)$ and indeed $\mathrm{vol}(f_1 - x_i) = \phi_1 - \phi_2$ which matches the virtual volume of $(1,-1)$. Now making the virtual volume of all the eight copies of the weight $(1,-1)$ negative corresponds to flopping the curves $f_1 - x_i$ in (B.23) where f_1 is the fiber of S_1. The resulting geometry is

$$\mathbf{1}_{\mathbf{2}} \overset{h \qquad\qquad 2h\text{-}\sum x_i}{\rule{4cm}{0.4pt}} \mathbf{2}_{\mathbf{1}}^{\mathbf{8}} \tag{B.24}$$

with the weight system being eight copies of

$$\begin{gathered}(1,0)^+\\(-1,1)^+\\(1,-1)^-\\(-1,0)^-\end{gathered}$$

The curves x_i in the phase (B.24) correspond to eight copies of the weight $(1,-1)$. Notice that we can take mass parameter for all eight fundamentals to be zero in this phase since weights which are negatives of each other have virtual volumes of opposite signs. Thus, we have completely integrated in the eight fundamentals. Now we move onto the integration of antisymmetric.

The weight system for antisymmetric of $\mathfrak{sp}(2)$ in phase (B.24) is

$$\begin{gathered}(0,1)^+\\(2,-1)^+\\(0,0)^+\\(-2,1)^+\\(0,-1)^+\end{gathered}$$

Flipping the sign for $(0,-1)$, we obtain

$$\mathbf{1_2} \overset{e \qquad\qquad 2h\text{-}\sum x_i}{\rule{3cm}{0.4pt}} \mathbf{2_1^{8+1}} \tag{B.25}$$

with the ninth blowup y on S_2 not participating in the gluing curve for S_1 inside S_2. Now, flipping the sign for $(-2,1)$ corresponds to flopping $f_2 - y$. Since it intersects the gluing curve $2h - \sum x_i$ twice, this results in a self-gluing on S_1

$$\underset{y}{\overset{x}{\subset}}\ \mathbf{1_2^{1+1}} \overset{h\text{-}x\text{-}y \qquad 2h+f\text{-}\sum x_i}{\rule{3cm}{0.4pt}} \mathbf{2_1^{8}} \tag{B.26}$$

The reader can check that both (5.17) and (5.18) are satisfied here. The weight system of antisymmetric corresponding to this phase is

$$\begin{gathered}(0,1)^+\\(2,-1)^+\\(0,0)^+\\(-2,1)^-\\(0,-1)^-\end{gathered}$$

with $x \sim y$ being identified with the weight $(-2,1)$. After performing an isomorphism on S_1 can be rewritten as

$$\underset{e\text{-}y}{\overset{e\text{-}x}{\subset}}\ \mathbf{1_0^{1+1}} \overset{f \qquad\qquad 2h+f\text{-}\sum x_i}{\rule{3cm}{0.4pt}} \mathbf{2_1^{8}} \tag{B.27}$$

leading to the same gluing rules as those presented in the main text.

Gluing rules for $\overset{\mathfrak{su}(1)^{(1)}}{\mathbf{2}} \rule{1.5cm}{0.4pt} \overset{\mathfrak{su}(1)^{(1)}}{\mathbf{2}}$: it is known that this KK theory is equivalent to a $5d$ $\mathfrak{su}(3)$ gauge theory with an adjoint and Chern-Simons level zero. The geometry for $\mathfrak{su}(3)$ with CS level zero is

$$\mathbf{1_1} \overset{e \qquad\qquad e}{\rule{2cm}{0.4pt}} \mathbf{2_1} \tag{B.28}$$

The weight system for adjoint in this phase is

$$\begin{gathered}(1,1)^+\\(-1,2)^+\ (2,-1)^+\\(0,0)^+\ (0,0)^+\\(1,-2)^+\ (-2,1)^+\\(-1,-1)^+\end{gathered}$$

The weight $(-1,-1)$ can be identified with a -1 curve living in a non-compact surface and intersecting both S_1 and S_2 at one point each. Flipping the sign of this weight leads to the appearance of a blowup on both S_1 and S_2

$$\mathbf{1}_{\mathbf{1}}^{\mathbf{1}} \overset{e,x}{\text{———}} {\scriptstyle 2} \overset{e,x}{\text{———}} \mathbf{2}_{\mathbf{1}}^{\mathbf{1}} \tag{B.29}$$

Notice that both the blowups are glued to each other. This can be understood as a consequence of the fact that they both correspond to the same weight i.e. $(-1,-1)^-$, but since there is a single such weight, these two curves must be identified with each other. In this flop frame, the weight system is

$$\begin{array}{c} (1,1)^+ \\ (-1,2)^+ \; (2,-1)^+ \\ (0,0)^+ \; (0,0)^+ \\ (1,-2)^+ \; (-2,1)^+ \\ (-1,-1)^- \end{array}$$

and the curves corresponding $(-1,2)^+$ and $(-2,1)^+$ can be identified as $(f-x)_{S_1}$ and $(f-x)_{S_2}$ respectively. Flopping both of these, flips the sign of both the weights $(-1,2)$ and $(-2,1)$ and leads to the geometry

$$\overset{x}{\underset{y}{\bigcirc}}\; \mathbf{1}_{\mathbf{0}}^{\mathbf{1+1}} \overset{e\text{-}y,\ f\text{-}x}{\text{————}} {\scriptstyle 2} \overset{e\text{-}y,\ f\text{-}x}{\text{————}} \mathbf{2}_{\mathbf{0}}^{\mathbf{1+1}}\; \overset{x}{\underset{y}{\bigcirc}} \tag{B.30}$$

which after performing an isomorphism of both the surfaces can be written as

$$\overset{e\text{-}x}{\underset{e\text{-}y}{\bigcirc}}\; \mathbf{1}_{\mathbf{0}}^{\mathbf{1+1}} \overset{f\text{-}x,x}{\text{————}} {\scriptstyle 2} \overset{f\text{-}x,x}{\text{————}} \mathbf{2}_{\mathbf{0}}^{\mathbf{1+1}}\; \overset{e\text{-}x}{\underset{e\text{-}y}{\bigcirc}} \tag{B.31}$$

leading to the same gluing rules as those presented in the main text.

Gluing rules for $\overset{\mathfrak{su}(1)^{(1)}}{\mathbf{2}} \text{—} {\scriptstyle 2} \longrightarrow \overset{\mathfrak{su}(1)^{(1)}}{\mathbf{2}}$: it is known that this KK theory is equivalent to a $5d$ $\mathfrak{sp}(2)$ gauge theory with an adjoint and theta angle zero. The geometry for pure $\mathfrak{sp}(2)$ with zero theta angle is known to be

$$\mathbf{1}_{\mathbf{6}} \overset{e \qquad 2h}{\text{————}} \mathbf{2}_{\mathbf{1}} \tag{B.32}$$

The weight system for adjoint in this phase is

$$
\begin{gathered}
(2,0)^+\\
(0,1)^+\\
(-2,2)^+\ (2,-1)^+\\
(0,0)^+\ (0,0)^+\\
(2,-2)^+\ (-2,1)^+\\
(0,-1)^+\\
(-2,0)^+
\end{gathered}
$$

Flipping the sign for $(-2,0)$ leads to the geometry

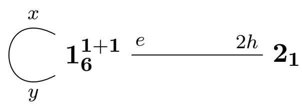

(B.33)

In this phase, the weight $(0,-1)^+$ can be identified with curves f_1-x and f_1-y, along with a -1 curve z living in a non-compact surface and intersecting S_2 at one point. z is glued to f_1-x but not to f_1-y. Since if it glues also to f_1-y, then it would mean that f_1-x is glued to f_1-y resulting in another self-gluing of S_1, namely $f_1-x\sim f_1-y$. After this self-gluing, the volumes of f_1-x and f_1-y will be $\phi_1-\phi_2$ leading to a contradiction with our starting step that their volume is $-\phi_2$.

Now, to flip the sign of the weight $(0,-1)$, we have to flop $f_1-x\sim z$ which automatically flops f_1-y since its volume is same. The flop of f_1-x creates a new blowup on S_1 that we call x'. Similarly, the flop of f_1-y creates a new blowup on S_1 that we call y'. Moreover the flop of z creates a blowup on S_2 that we call z'.

After the flop $S_1=\mathbb{F}_4^2$ with f_1-x' glued to f_1-y' and $S_2=\mathbb{F}_2^1$. The total gluing curve for S_2 in S_1 is $e_1+x'+y'$, and the total gluing curve for S_1 in S_2 is $2h$. The gluing $f_1-x\sim z$ transforms into the gluing $x'\sim z'$ in the new frame. Thus, the total gluing curve splits into two gluing curves:

$$e_1+y'\sim 2h-z' \tag{B.34}$$

$$x'\sim z' \tag{B.35}$$

The reader can check that the curves involved on both sides in both of these gluings have same genus, and moreover (5.17) and (5.18) are satisfied for both gluings. Notice that if we would have tried to split the total gluing curve into three gluing curves e_1,x',y' glued respectively to $2h-2z',z',z'$, we would have run into two problems. First is the same problem that we noted before the flop was performed, that this would imply a second self gluing $x'\sim y'$ of S_1 and the weight system won't match with the system of curves in the geometry anymore. Second, the genus of $2h_2-2z'$ is -1 and the genus of e_1 is $+1$, so the first gluing curve wouldn't make sense.

JHEP12(2020)151

Thus at this step of the integration process, the geometry is

$$\overset{f\text{-}x}{\underset{f\text{-}y}{\bigcirc}}\ \mathbf{1_4^{1+1}}\ \overset{e+y,\ x}{\rule{2.5cm}{0.4pt}}\ {\scriptstyle 2}\ \overset{2h\text{-}z,\ z}{\rule{2.5cm}{0.4pt}}\ \mathbf{2_1^1} \tag{B.36}$$

where we have dropped the primes on the blowups. The corresponding weight system is

$$\begin{array}{c}
(2,0)^+ \\
(0,1)^+ \\
(-2,2)^+\ (2,-1)^+ \\
(0,0)^+\ (0,0)^+ \\
(2,-2)^+\ (-2,1)^+ \\
(0,-1)^- \\
(-2,0)^-
\end{array}$$

By performing an isomorphism, we can write the geometry as

$$\overset{x}{\underset{y}{\bigcirc}}\ \mathbf{1_2^{1+1}}\ \overset{e+f\text{-}x\text{-}2y,\ f\text{-}x}{\rule{3cm}{0.4pt}}\ {\scriptstyle 2}\ \overset{2h\text{-}z,\ z}{\rule{3cm}{0.4pt}}\ \mathbf{2_1^1} \tag{B.37}$$

The weight $(2,-2)^+$ corresponds to the curve $x \sim y$, and the weight $(-2,1)^+$ corresponds to the curve $f_2 - z$. Upon flopping them, we obtain the geometry with adjoint matter completely integrated in

$$\overset{x}{\underset{y}{\bigcirc}}\ \mathbf{1_2^{1+1}}\ \overset{e+f\text{-}y,\ f\text{-}x}{\rule{3cm}{0.4pt}}\ {\scriptstyle 2}\ \overset{2e+f\text{-}x\text{-}2y,\ f\text{-}x}{\rule{3cm}{0.4pt}}\ \mathbf{2_0^{1+1}}\ \overset{x}{\underset{y}{\bigcirc}} \tag{B.38}$$

After an isomorphism, we obtain

$$\overset{e\text{-}x}{\underset{e\text{-}y}{\bigcirc}}\ \mathbf{1_0^{1+1}}\ \overset{f\text{-}x,\ x}{\rule{2.5cm}{0.4pt}}\ {\scriptstyle 2}\ \overset{2f\text{-}x,\ x}{\rule{2.5cm}{0.4pt}}\ \mathbf{2_0^{1+1}}\ \overset{e\text{-}x}{\underset{e\text{-}y}{\bigcirc}} \tag{B.39}$$

which shows that gluing rules are precisely those quoted in the main text.

Gluing rules for $\overset{\mathfrak{su}(1)^{(1)}}{\mathbf{2}}\ \rule{1.5cm}{0.4pt}\ \underset{\bigcirc}{\overset{\mathfrak{su}(1)^{(1)}}{\mathbf{2}}}$: it is known that this KK theory is equivalent to a 5d $\mathfrak{sp}(2)$ gauge theory with an adjoint and theta angle π. Thus, the analysis for this case is similar to that of the last case which was

$$\overset{\mathfrak{su}(1)^{(1)}}{2}\ \text{---}\ {\scriptstyle 2}\ \overset{\mathfrak{su}(1)^{(1)}}{\longrightarrow 2} \tag{B.40}$$

since only the theta angle is different for these two cases. Following similar steps as above, the final "geometry"[23] analogous to (B.38) is found to be

$$\overset{x}{\underset{y}{\circlearrowleft}}\ \mathbf{1}_{\mathbf{2}}^{\mathbf{1+1}} \overset{e+f\text{-}y,\ f\text{-}x}{\rule[0.5ex]{6em}{0.4pt}}\ 2\ \overset{2h\text{-}x\text{-}2y,\ f\text{-}x}{\rule[0.5ex]{7em}{0.4pt}}\ \mathbf{2}_{\mathbf{1}}^{\mathbf{1+1}}\ \overset{x}{\underset{y}{\circlearrowright}} \tag{B.41}$$

which after an isomorphism becomes

$$\overset{e\text{-}x}{\underset{e\text{-}y}{\circlearrowleft}}\ \mathbf{1}_{\mathbf{0}}^{\mathbf{1+1}} \overset{f\text{-}x,\ x}{\rule[0.5ex]{5em}{0.4pt}}\ 2\ \overset{2h\text{-}x\text{-}2y,\ f\text{-}x}{\rule[0.5ex]{6em}{0.4pt}}\ \mathbf{2}_{\mathbf{1}}^{\mathbf{1+1}}\ \overset{x}{\underset{y}{\circlearrowright}} \tag{B.42}$$

which matches the gluing rules claimed in the text.

B.3 Theta angle for $\mathfrak{sp}(n)$

Notice that there are two inequivalent geometries which give rise to a $5d$ pure $\mathfrak{sp}(n)$ gauge theory:

$$\mathbf{1_{2n+2}} \overset{e}{\text{——}} \cdots \overset{h}{\text{——}} \mathbf{(n-2)_8} \overset{e\qquad h}{\text{————}} \mathbf{(n-1)_6} \overset{e\qquad\quad 2e+f}{\text{——————}} \mathbf{n_0} \tag{B.43}$$

and

$$\mathbf{1_{2n+2}} \overset{e}{\text{——}} \cdots \overset{h}{\text{——}} \mathbf{(n-2)_8} \overset{e\qquad h}{\text{————}} \mathbf{(n-1)_6} \overset{e\qquad\quad 2h}{\text{——————}} \mathbf{n_1} \tag{B.44}$$

These two geometries correspond to two different possible values of theta angle. The only difference between (B.43) and (B.44) is whether $S_n = \mathbb{F}_0$ or $S_n = \mathbb{F}_1$. It is well-known that (see for instance [2]) for $\mathfrak{sp}(1)$, $\theta = 0$ has $S_1 = \mathbb{F}_0$ and $\theta = \pi$ has $S_1 = \mathbb{F}_1$, while for $\mathfrak{sp}(2)$, $\theta = 0$ has $S_2 = \mathbb{F}_1$ and $\theta = \pi$ has $S_2 = \mathbb{F}_0$.

We claim that for higher n, the same pattern continues to hold and the theta angle corresponding to $\mathbb{F}_0$ (or $\mathbb{F}_1$) changes by π (mod 2π) every time one increases the rank n by one unit. To see this, one can start from the statement [55] that the KK theory

$$\overset{\mathfrak{su}(1)^{(1)}}{2} \text{——} \cdots \text{——} \overset{\mathfrak{su}(1)^{(1)}}{2} \text{———} \overset{\mathfrak{su}(1)^{(1)}}{2} \text{———} \overset{\mathfrak{su}(1)^{(1)}}{\underset{\circlearrowleft}{2}} \tag{B.45}$$

with a total of n nodes is equivalent to a $5d$ $\mathfrak{sp}(n)$ gauge theory with an adjoint hyper and $\theta = \pi$. We can build the geometry corresponding to (B.45) by using the data presented in this paper and derived in appendix (B.2). Now the key point is that integrating out the adjoint matter does not change the theta angle. So, we can simply integrate out the adjoint matter from the geometry corresponding to (B.45) to land on to pure $\mathfrak{sp}(n)$ theory with $\theta = \pi$. This process is inverse of the process of integrating in of matter discussed

[23]We remind the reader that it should only be viewed as an algebraic description since the KK theory involves the non-geometric node.

in appendices (B.1) and (B.2) and corresponds to making the virtual volumes of all the weights of adjoint of $\mathfrak{sp}(n)$ to have the same sign. Once this is done, it is found that the geometry for $\theta = \pi$ is (B.43) whenever n is even, and the geometry (B.44) whenever n is odd. From this we conclude that the geometry (B.43) corresponds to $\theta = \theta_0$ and the geometry (B.44) corresponds to $\theta = \theta_1$ where

$$\theta_1 = n\pi \pmod{2\pi} \tag{B.46}$$

$$\theta_0 = \theta_1 + \pi \pmod{2\pi} \tag{B.47}$$

C A concrete non-trivial check of our proposal

We devote this section to a concrete and non-trivial check of our proposal. It is known that [24] the KK theory

$$\begin{array}{ccc} \mathfrak{su}(2)^{(1)} & & \mathfrak{su}(2)^{(1)} \\ 2 & \overset{}{\text{——}}\ {\scriptstyle 2} \longrightarrow & 2 \end{array} \tag{C.1}$$

is equivalent to the $5d$ gauge theory with gauge algebra $\mathfrak{su}(2) \oplus \mathfrak{su}(4)$ with a hyper transforming in $\mathsf{F} \otimes \Lambda^2$. More precisely, the gauge-theoretic phase diagram for the $\mathfrak{su}(2) \oplus \mathfrak{su}(4)$ embeds into the phase diagram for the KK theory (C.1). In this section we will show this explicitly.

Let us start with the geometry assigned to (C.1) in the paper with ν chosen to be zero for both $\mathfrak{su}(2)^{(1)}$:

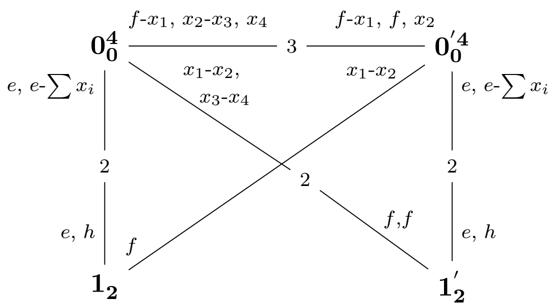

(C.2)

where the surfaces S_0 and S_1 correspond to the left $\mathfrak{su}(2)^{(1)}$ in (C.1), and the surfaces S'_0 and S'_1 correspond to the right $\mathfrak{su}(2)^{(1)}$ in (C.1). As visible in the above diagram, x_4 in S_0 is glued to x_2 in S'_0. Flopping this curve, we obtain

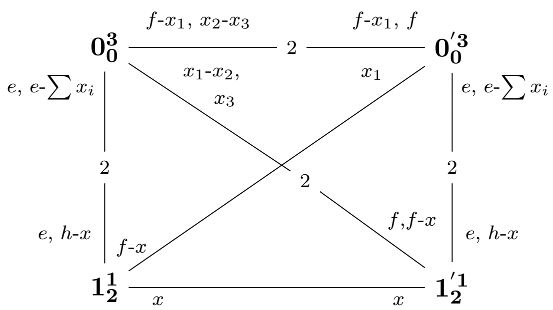

(C.3)

Now flopping $f-x$ in S_1 which is glued to x_1 in S'_0, we obtain

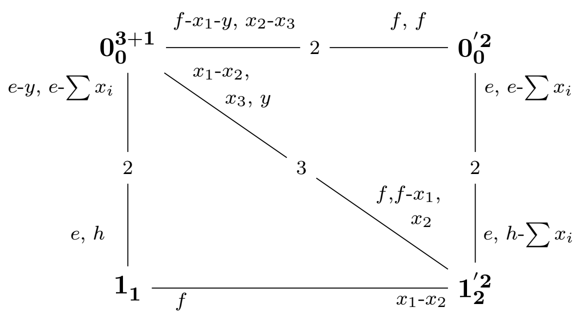

(C.4)

which after performing an isomorphism on S_0 can be written as

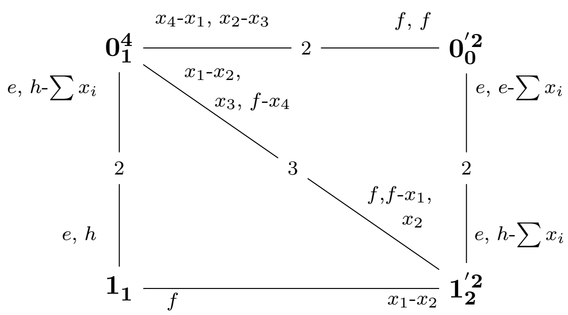

(C.5)

Now, flopping the e curves inside S_0 and S_1 (which are glued to each other), we obtain

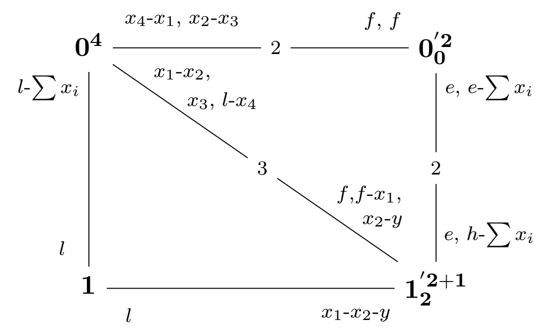

(C.6)

where a surface without a subscript denotes that the surface is a del Pezzo surface rather than a Hirzebruch surface. That is, $S_0 = dP_4$ and $S_1 = \mathbb{P}^2 = dP_0$. Let us use the blowup

x_4 on S_0 to write S_0 in terms of the Hirzebruch surface $\mathbb{F}_1$

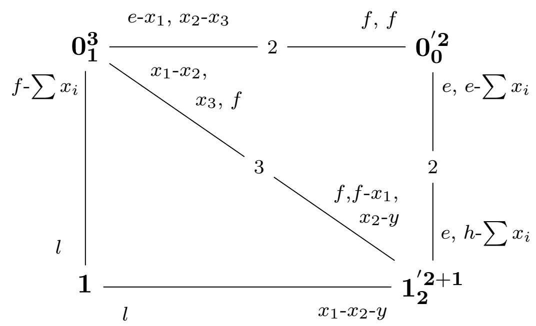

(C.7)

Flopping x_3 in S_0 glued to $f-x_1$ in S_1' gives rise to

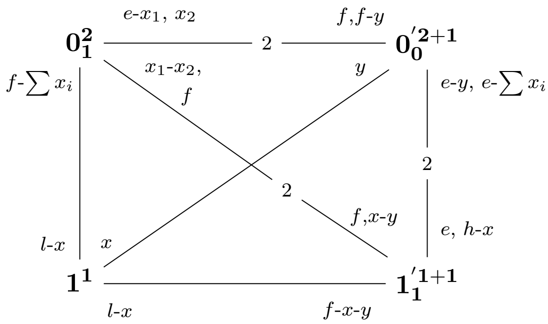

(C.8)

We use x in S_1 to write S_1 in terms of Hirzebruch surface $\mathbb{F}_1$

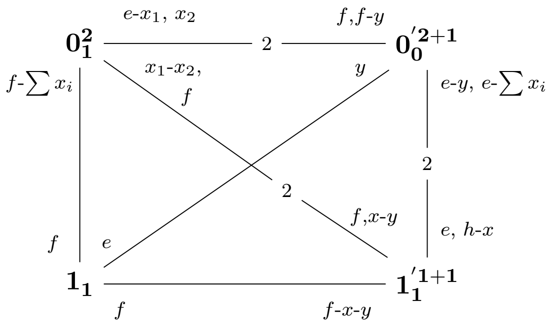

(C.9)

Flop x_2 in S_0 glued to $f-y$ in S_0' to obtain

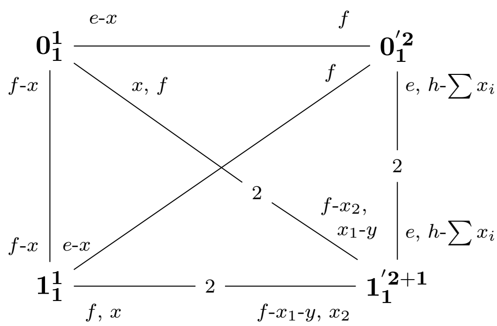

(C.10)

Now flopping $f - x$ in S_0 glued to $f - x$ in S_1, we obtain

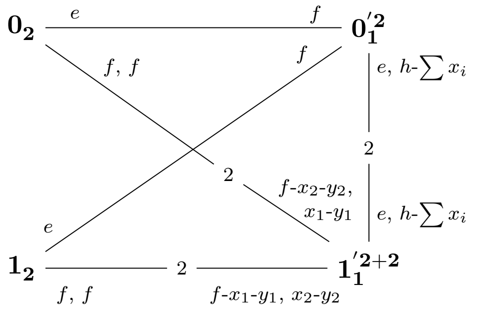

(C.11)

Flopping $f - x_2$ in S_0' we obtain

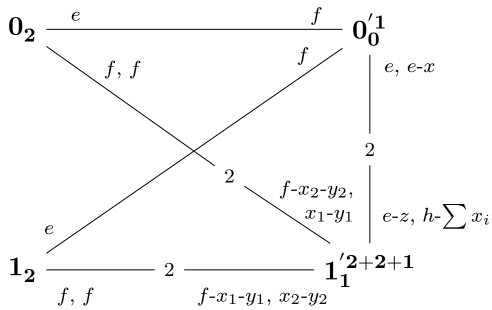

(C.12)

Now flopping x in S_0' we get

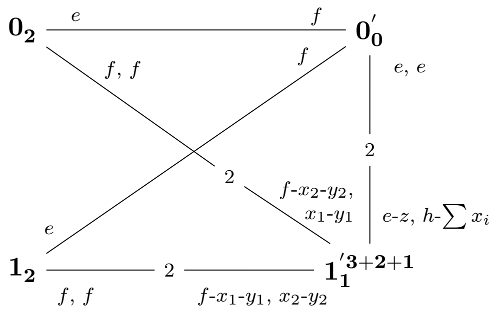

(C.13)

Performing the automorphism on S_0' that exchanges e and f, we obtain

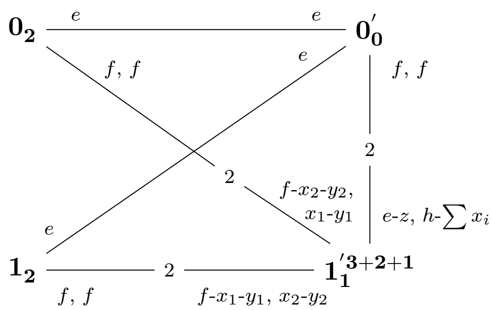

(C.14)

Now let us write S_1' as a del Pezzo surface. This rewrites the e curve as a blowup which we denote by w

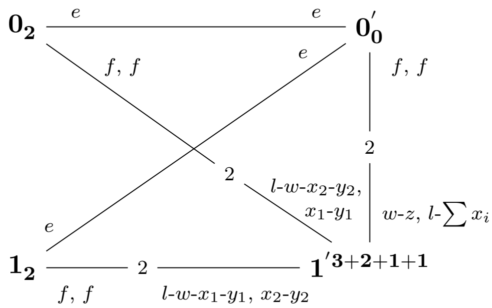

(C.15)

We can now perform a basic automorphism (of del Pezzo surfaces) on S_1' involving the three blowups x_1, x_2 and y_1 to obtain

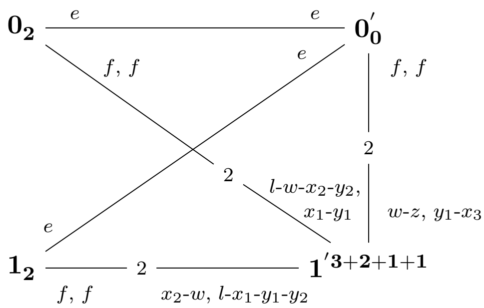

(C.16)

Converting S_1' back into $\mathbb{F}_1$ using the blowup y_2, we obtain

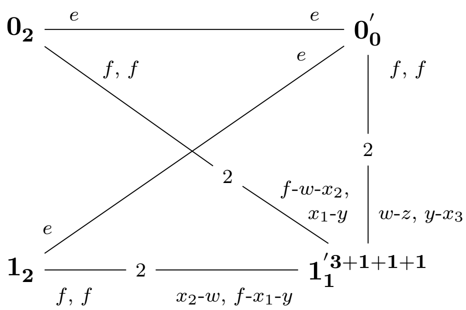

(C.17)

This is the final form of the geometry that we wanted to obtain.

It is clear that S_0, S_0' and S_1 describe an $\mathfrak{su}(4)$ and S_1' describes an $\mathfrak{su}(2)$ in (C.17). This can be checked by intersecting the fibers of the corresponding Hirzebruch surfaces with these surfaces. The intersection matrix yields the Cartan matrix for $\mathfrak{su}(4) \oplus \mathfrak{su}(2)$. Now, let us show that the configuration of blowups indeed describes $\Lambda^2 \otimes \mathsf{F}$ of $\mathfrak{su}(4) \oplus \mathfrak{su}(2)$. For this we relabel the surfaces as

$$S_0 \to S_1 \tag{C.18}$$

$$S_0' \to S_2 \tag{C.19}$$

$$S_1 \to S_3 \tag{C.20}$$

thus rewriting the geometry as

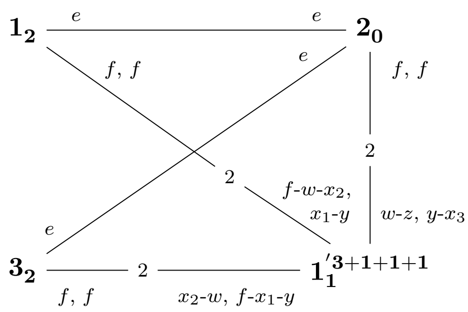

(C.21)

The weight system for $\Lambda^2 \otimes \mathsf{F}$ can be written as

$$
\begin{gathered}
(0,1,0|1) \\
(1,-1,1|1)\ (0,1,0|-1) \\
(-1,0,1|1)\ (1,0,-1|1)\ (1,-1,1|-1) \\
(-1,1,-1|1)\ (-1,0,1|-1)\ (1,0,-1|-1) \\
(0,-1,0|1)\ (-1,1,-1|-1) \\
(0,-1,0|-1)
\end{gathered}
$$

where the three entries on the left hand side of slash denote the weights with respect to $\mathfrak{su}(4)$ comprised by S_1, S_2 and S_3, and the entry on the right hand side of slash denotes the weight with respect to $\mathfrak{su}(2)$ comprised by S'_1.

From the geometry (C.21) we see that the holomorphic curves

$$\mathrm{vol}(x_1) = (1,0,-1|1) \tag{C.22}$$
$$\mathrm{vol}(x_2) = (-1,0,1|1) \tag{C.23}$$
$$\mathrm{vol}(x_3) = (0,-1,0|1) \tag{C.24}$$
$$\mathrm{vol}(y) = (-1,1,-1|1) \tag{C.25}$$
$$\mathrm{vol}(f-z) = (0,1,0|1) \tag{C.26}$$
$$\mathrm{vol}(f-w) = (1,-1,1|1) \tag{C.27}$$

match weights of the form $(x,y,z|1)$, and the antiholomorphic curves $x_1-f, x_2-f, x_3-f, y-f, -z, -w$ match weights of the form $(x,y,z|-1)$, where f denotes the fiber of Hirzebruch surface $S'_1 = \mathbb{F}_1^6$. Thus we have reproduced the full weight system for $\Lambda^2 \otimes \mathsf{F}$, justifying our claim. More precisely, the geometry (C.21) describes the $\mathfrak{su}(4) \oplus \mathfrak{su}(2)$ gauge theory in the gauge-theoretic phase given by the following virtual volumes

$$\begin{gathered}(0,1,0|1)^{+}\\ (1,-1,1|1)^{+}\ (0,1,0|-1)^{-}\\ (-1,0,1|1)^{+}\ (1,0,-1|1)^{+}\ (1,-1,1|-1)^{-}\\ (-1,1,-1|1)^{+}\ (-1,0,1|-1)^{-}\ (1,0,-1|-1)^{-}\\ (0,-1,0|1)^{+}\ (-1,1,-1|-1)^{-}\\ (0,-1,0|-1)^{-}\end{gathered}$$

D Comparisons with known cases in the literature

In this section we provide a comparison with some $5d$ KK theories known in the literature via other methods. In particular, we show that the geometries we obtain for these $5d$ KK theories allow us to see the $5d$ gauge theory descriptions of these $5d$ KK theories that have been proposed in the literature.

D.1 Untwisted

Let us start with an example of untwisted compactification. It has been proposed [28] that

$$\begin{array}{c}\mathfrak{sp}(n)^{(1)}\\ 1\end{array} \tag{D.1}$$

can be described by the $5d$ gauge theory having gauge algebra $\mathfrak{su}(n+2)$ with $2n+8$ hypers in fundamental. To see this consider the $\nu=1$ phase of (5.101)

$$\mathbf{0_1^{2n+7}} \overset{2h\text{-}\sum x_i \qquad\quad h}{\text{———————}} \mathbf{1_{2n+1}} \overset{e}{\text{——}} \cdots \overset{h}{\text{——}} \mathbf{(n-2)_7} \overset{e \qquad\quad h}{\text{————}} \mathbf{(n-1)_5} \overset{e \qquad\quad 2h\text{-}x}{\text{——————}} \mathbf{n_1^1} \tag{D.2}$$

which after an isomorphism can be written as

$$\mathbf{0_{2n+3}^{2n+7}} \overset{e \qquad\qquad h}{\text{———————}} \mathbf{1_{2n+1}} \overset{e}{\text{——}} \cdots \overset{h}{\text{——}} \mathbf{(n-2)_7} \overset{e \qquad\quad h}{\text{————}} \mathbf{(n-1)_5} \overset{e \qquad e+2f\text{-}x}{\text{——————}} \mathbf{n_1^1} \tag{D.3}$$

Now flopping the blowup sitting on S_n back to S_0, we obtain

$$\mathbf{0_{2n+4}^{2n+8}} \overset{e \qquad\qquad h}{\text{———————}} \mathbf{1_{2n+2}} \overset{e}{\text{——}} \cdots \overset{h}{\text{——}} \mathbf{(n-2)_8} \overset{e \qquad\quad h}{\text{————}} \mathbf{(n-1)_6} \overset{e \qquad\quad e+2f}{\text{——————}} \mathbf{n_0} \tag{D.4}$$

where we can see that the associated Cartan matrix is that of $\mathfrak{su}(n+2)$ and the $2n+8$ blowups sitting on S_0 can be identified with the fundamentals. This identification is done by noticing that the volume for a blowup matches the absolute value of virtual volume of a weight for the fundamental of $\mathfrak{su}(n+2)$.

D.2 Twisted

Now, let us consider an example when we twist by an outer automorphism. It has been proposed in [24] that

$$\begin{array}{c}\mathfrak{su}(n)^{(2)}\\ 2\end{array} \tag{D.5}$$

can be described by $5d$ gauge theory with gauge algebra $\mathfrak{so}(n+2)$ and n fundamental hypers. First let us consider the case when $n = 2m$. In this case the geometry is displayed in (5.142). Flopping all the y_i, we obtain

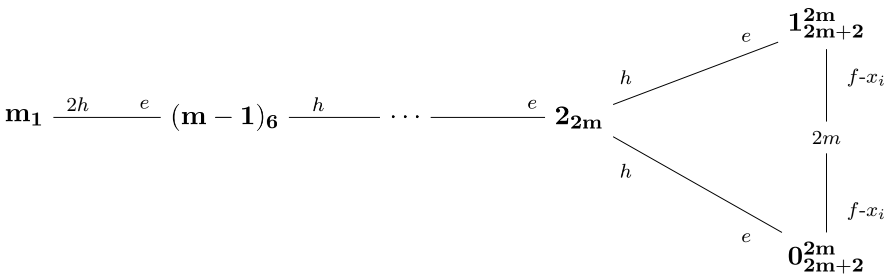

(D.6)

Now flopping all the $f - x_i$, we obtain

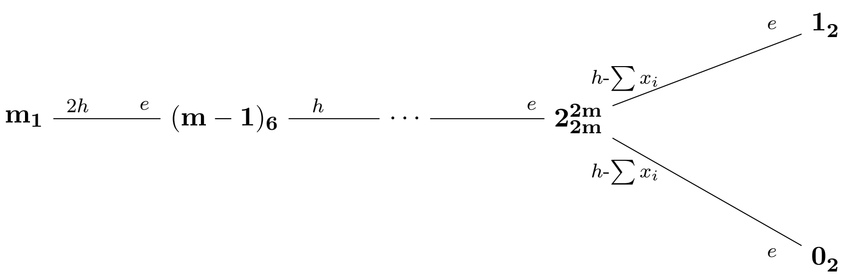

(D.7)

Now we can carry the $2m$ blowups onto S_m to obtain the geometry

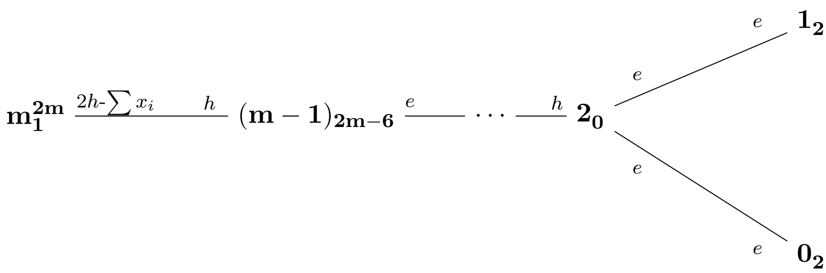

(D.8)

JHEP12(2020)151

which after an isomorphism on S_m can be rewritten as

$$\begin{tikzcd} & & & & \mathbf{1_2} \\ \mathbf{m^{2m}_{2m-4}} \arrow[r, dash, "e \qquad h"] & \mathbf{(m-1)_{2m-6}} \arrow[r, dash, "e"] & \cdots \arrow[r, dash, "h"] & \mathbf{2_0} \arrow[ur, dash, "e \qquad e"] \arrow[dr, dash, "e \qquad e"'] & \\ & & & & \mathbf{0_2} \end{tikzcd} \tag{D.9}$$

The Cartan matrix associated to this geometry is indeed that for $\mathfrak{so}(2m+2)$ and the $2m$ blowups can be identified as $2m$ hypers in fundamental of $\mathfrak{so}(2m+2)$.

Similarly, the geometry for $n = 2m+1$ is given in (5.143). Flopping $x_i \sim y_i$ living on S_0, we obtain

$$\mathbf{m_1} \overset{2h \qquad e}{\text{————}} \mathbf{(m-1)_6} \overset{h}{\text{——}} \cdots \overset{e}{\text{——}} \mathbf{1^{2m+1}_{2m+2}} \overset{2h\text{-}2\sum x_i \qquad\qquad e}{\text{————————}} \mathbf{0_6} \tag{D.10}$$

After performing an isomorphism we can write the above geometry as

$$\mathbf{m_1} \overset{2h \qquad\quad e}{\text{————}} \mathbf{(m-1)_6} \overset{h}{\text{——}} \cdots \overset{e\text{-}\sum x_i}{\text{———}} \mathbf{1^{2m+1}_1} \overset{2h \qquad\quad e}{\text{————}} \mathbf{0_6} \tag{D.11}$$

Now moving the blowups onto S_m we obtain

$$\mathbf{m^{2m+1}_1} \overset{2h\text{-}\sum x_i \quad e}{\text{————}} \mathbf{(m-1)_{2m-5}} \overset{h}{\text{——}} \cdots \overset{e}{\text{——}} \mathbf{1_1} \overset{2h \qquad\quad e}{\text{————}} \mathbf{0_6} \tag{D.12}$$

which can be rewritten as

$$\mathbf{m^{2m+1}_{2m-3}} \overset{e \qquad h}{\text{————}} \mathbf{(m-1)_{2m-5}} \overset{e}{\text{——}} \cdots \overset{e}{\text{——}} \mathbf{1_1} \overset{2h \qquad\quad e}{\text{————}} \mathbf{0_6} \tag{D.13}$$

which precisely describes $\mathfrak{so}(2m+3)$ with $2m+1$ hypers in fundamental of $\mathfrak{so}(2m+3)$.

E Instructions for using the attached Mathematica notebook

A Mathematica notebook is included as supplementary material along with this paper. The use of this notebook requires installation of the Mathematica package LieArt.nb which can be found online at. In particular, the notebook provides the evaluation of two functions Geometry5dKK and SignsKK. The former can be used to compute the shifted prepotential $6\tilde{\mathcal{F}}$ (defined in section 4.2) for $5d$ KK theories whose associated graph contains either one or two nodes; see tables 1–5 and tables 8–11. The latter function can be used for the evaluation of all possible signs associated to different phases of the above prepotential.

The Mathematica notebook is built around the use of the function

```
Geometry5dKK[...]
```

The above function outputs a graphical representation of the shifted prepotential $6\tilde{\mathcal{F}}$ associated to the input $5d$ KK theory. The graphical output is naturally organized in the form of triple intersection numbers for the associated geometry. See section 5.1.1 for the map between triple intersection numbers and the shifted prepotential.

Input. Let us now describe possible inputs for the function Geometry5dKK:

- For a single node

$$\begin{array}{c}\mathfrak{g}^{(q)}\\ k\end{array} \tag{E.1}$$

  the first input is the number k as shown below

```
Geometry5dKK[{k,...}]
```

- For two nodes α and β, the first input is the matrix $\Omega = \begin{pmatrix}\Omega_S^{\alpha\alpha} & \Omega_S^{\alpha\beta}\\ \Omega_S^{\beta\alpha} & \Omega_S^{\beta\beta}\end{pmatrix}$:

```
Geometry5dKK[{Ω,...}]
```

  See section 3.3 for the definition of $\Omega_S^{\alpha\beta}$ etc.

- When there is a single node, the second and final input captures the data of $\mathfrak{g}^{(q)}$. When there are two nodes, the second input captures the data of $\mathfrak{g}_\alpha^{(q_\alpha)}$, and the third and final input captures the data of $\mathfrak{g}_\beta^{(q_\beta)}$. The data of an affine algebra is captured by dividing it into the "algebra part" and the "twist part". For example, the algebra part of $\mathfrak{g}^{(q)}$ is $\mathfrak{g}$ which is a finite Lie algebra, and the twist part of $\mathfrak{g}^{(q)}$ is q. The algebra part can be inserted in LieArt format. For example, A-type can be inserted as

```
A1, A2, ..., An
```

  B-type can be inserted as

```
B2, B3, ..., Bn
```

  C-type can be inserted as

```
C2, C3, ..., Cn
```

  D-type can be inserted as

```
D3, D4, ..., Dn
```

  E-type can be inserted as

```
E6, E7, E8
```

And other types can be inserted as

```
G2, F4
```

The twist part can be inserted as

```
U, T2, T3
```

where U means 'untwisted' (corresponding to $q = 1$), T2 means '$\mathbb{Z}_2$ twisted (corresponding to $q = 2$) and T3 means '$\mathbb{Z}_3$ twisted' (corresponding to $q = 3$).

The full input thus is as follows:

- For a single node, the following format is used:

```
Geometry5dKK[{k,{Algebra,Twist}}]
```

  For example,

```
Geometry5dKK[{2,{A4,T2}}]
```

- For two nodes, the format is:

```
Geometry5dKK[{Ω,{Algebra1,Twist1},{Algebra2,Twist2}}]
```

  For example,

```
Geometry5dKK[{Ω,{C3,U},{D6,T2}}]
```

  In order to consider trivial gauge algebras of type $\mathfrak{su}(1)$, $\mathfrak{sp}(0)$, one needs to insert a zero in the place of the algebra and twist input: that is we perform the replacement $\{Algebra, Twist\} \rightarrow 0$. For example, if $\mathfrak{g}_\alpha$ is trivial, but $\mathfrak{g}_\beta$ is not, then the input takes the form

```
Geometry5dKK[{Ω,0,{Algebra2,Twist2}}]
```

Some of the nodes contain extra decorations. Such nodes can be inserted by using extra identifiers as follows:

- $\overset{\mathfrak{su}(n)^{(1)}}{1}$ vs. $\overset{\mathfrak{su}(\widehat{n})^{(1)}}{1}$

  To incorporate the second case, we replace $Twist$ with $\{Twist, Frozen\}$. For example,

```
Geometry5dKK[{1,{A8,U}}]
```

  becomes

```
Geometry5dKK[{1,{A8,{U,Frozen}}}]
```

- $\overset{\mathfrak{su}(6)^{(1)}}{1}$ vs. $\overset{\mathfrak{su}(\tilde{6})^{(1)}}{1}$

  To incorporate the second case, we replace *Twist* with $\{Twist, Three\}$, so that

  ```
  Geometry5dKK[{1,{A5,U}}]
  ```

  becomes

  ```
  Geometry5dKK[{1,{A5,{U,Three}}}]
  ```

- $\overset{\mathfrak{su}(n)^{(1)}}{2}$ vs $\overset{\mathfrak{su}(n)^{(1)}}{2}$

  To incorporate the second case, we replace *Twist* with $\{Twist, Loop\}$, so that

  ```
  Geometry5dKK[{2,{A5,U}}]
  ```

  becomes

  ```
  Geometry5dKK[{2,{A5,{U,Loop}}}]
  ```

- $\overset{\mathfrak{so}(12)^{(q)}}{k}$ vs $\overset{\mathfrak{so}(\widehat{12})^{(q)}}{1}$

  To incorporate the second case, we replace *Twist* with $\{Twist, Cospinor\}$, so that

  ```
  Geometry5dKK[{1,{D6,U}}]
  ```

  becomes

  ```
  Geometry5dKK[{1,{D6,{U,Cospinor}}}]
  ```

- $\overset{\mathfrak{so}(8)^{(2)}}{3} \dashrightarrow {}_2\!\longrightarrow \overset{\mathfrak{sp}(1)^{(1)}}{1}$

  To incorporate this case we use the usual input without any extra identifiers.

  ```
  Geometry5dKK[{Ω,{D4,T2},{A1,U}}]
  ```

- $\overset{\mathfrak{sp}(n_i)^{(1)}}{1} \;\text{———}\; \overset{\mathfrak{so}(7)^{(1)}}{k}$ vs. $\overset{\mathfrak{sp}(n_i)^{(1)}}{1} \;\text{- - - -}\; \overset{\mathfrak{so}(7)^{(1)}}{k}$ and
  $\overset{\mathfrak{sp}(n_i)^{(1)}}{1} \;\text{———}\; \overset{\mathfrak{so}(8)^{(q)}}{k}$ vs. $\overset{\mathfrak{sp}(n_i)^{(1)}}{1} \;\text{- - - -}\; \overset{\mathfrak{so}(8)^{(q)}}{k}$

JHEP12(2020)151

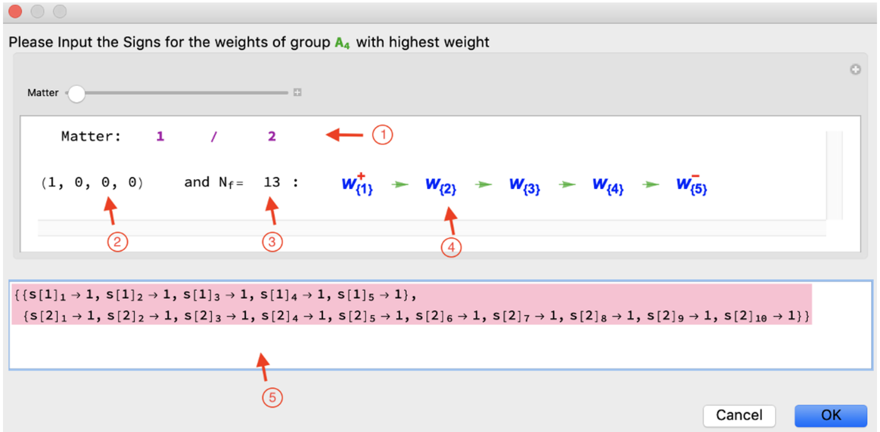

Figure 3. An illustration of the various features of the initial (sign input) pop-up window of the function Geometry5dKK. The various aspects, numbered 1 through 5, are explained in the body of this appendix.

To incorporate these cases, we replace $Twist$ with $\{Twist, S\}$. For example, one would use the following formats:

```
Geometry5dKK[{Ω,{C2,U},{B3,{U,S}}}]
```

and

```
Geometry5dKK[{Ω,{C2,U},{D4,{U,S}}}]
```

Choice of phase. For each input, the output (i.e. the prepotential) depends on a particular choice of gauge-theoretic phase for the theory. The different gauge-theoretic phases correspond to different choices of signs for the virtual volumes of the weights of the representations associated to the matter content for the input KK theory. See sections 4 and 5.1.3 along with appendix B for more details.

After the input is inserted, the notebook will request as additional input the signs of virtual volumes for all the weights corresponding to matter hypermultiplets. A pop-up window appears containing the information needed to make a consistent choice of signs. For example, consider $\mathfrak{su}(5)^{(1)}_1$. After inputting the correct data associated to this theory, a window appears as depicted in figure 3. The information indicated in the window can be understood as follows:

1 This labels the difference choices of irreducible representaitons of the invariant subalgebra (under the twist) in which the hypers of the canonical 5d gauge theory associated to the KK theory transform. In this particular case we have two distinct representations, namely the fundamental and the antisymmetric representations of $\mathfrak{su}(5)$, as can be seen from table 1. The slider on top can be used to slide between the two irreps. For example in figure 3, we see data associated to fundamental representation and in 4 we see the data associated to antisymmetric representation.

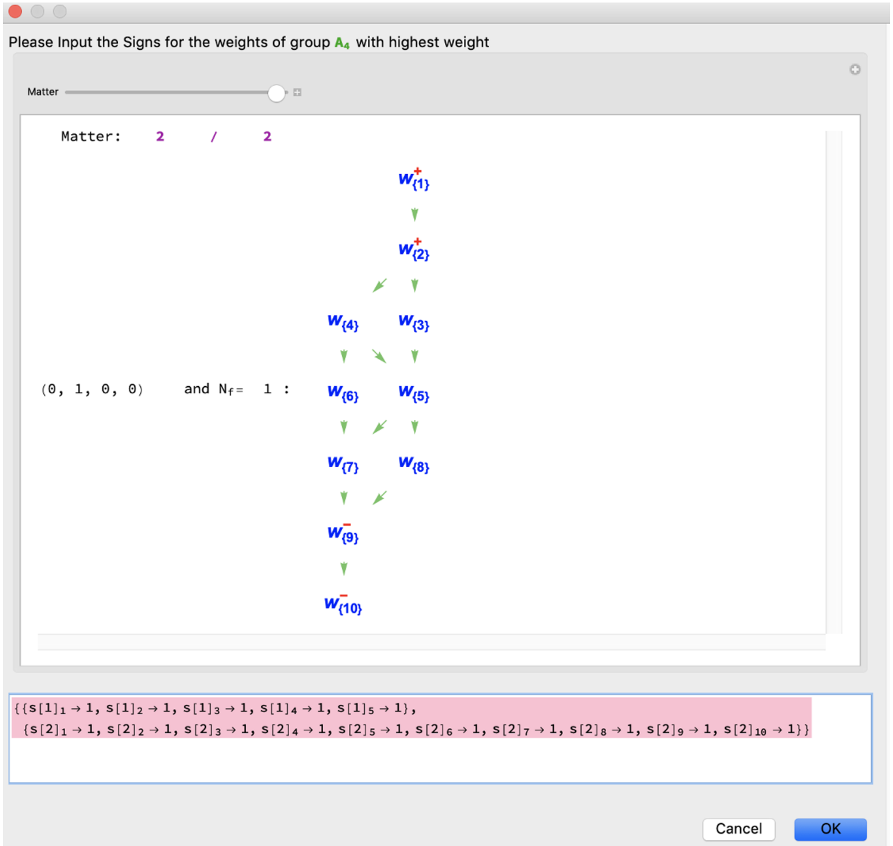

Figure 4. The slider moves between different representations; in the example depicted above, the slider moves from the first to the second representation.

② This indicates the highest weight of the representation.

③ Here, N_f represents the number full hypermultiplets transforming in the given representation. In figure 3 there are 13 hypermultiplets transforming in the fundamental representation, while in figure 4 there is one hypermultiplet transforming in the antisymmetric representation.

④ shows the Hasse diagram of the weight system of the representation. The Hasse diagram is a graphical representation of the partial order of the weight system. Recall, that given a highest weight w_1 one can construct the entire weight system by subtracting positive simple roots, $w_i = w_{i-1} - n_i\alpha_i$ (α_i denote the simple roots). For example, the fundamental representation of $\mathfrak{su}(5)$, which is comprised of weights $w_{i=1,\ldots,5}$, is characterized by the partial order $w_1 \geq w_2 \geq \cdots \geq w_5$, where $w_i \geq w_j$ means that $w_i - w_j = n_i\alpha_i$ where $n_i \geq 0$. This information is important when determining the possible choices of signs for the virtual volumes of weights lying in this weight system. For example, if we choose w_3 to be have a positive virtual volume, then w_2 needs to also have a positive virtual volume since $w_2 \geq w_3$ according to the Hasse diagram.

JHEP12(2020)151

The red superscript indicates whether a weight is positive or negative. A positive (resp. negative) weight is defined as the positive (resp. negative) linear combination of simple roots. When no mass parameters are turned on, then the signs of virtual volumes for positive and negative weights are fixed to be positive and negative, respectively (assuming the dual of the irreducible Weyl chamber is defined as the region in which the virtual volumes of all positive simple roots are positive.) The signs of the rest of the weights are undetermined by the signs of simple roots and hence can be chosen freely as long as the ordering described by the Hasse diagram is satisfied. When mass parameters are turned on, then it is possible for positive weights to have negative virtual volume and negative weights to have positive virtual volume, for some values of the mass parameters. For a generic choice of mass parameters, the only constraint for any of the signs of the weights is that the ordering provided by the Hasse diagram is respected.

⑤ This is the area in which a choice of signs should be specified.A default input is given where all the signs are positive, that is "+1". The notation $s[i]_j$ is explained as follows: i labels each different representation (in this case, i runs over two representations) and j labels the different of weights (in this case, for the fundamental representation, j runs from 1 to 5, while for the antisymmetric representation, j runs from 1 to 10). For example, based on the Hasse diagram presented in figure 3 and assuming we do not turn on any mass parameters, we can make a list of all the allowed choices of signs for the fundamental representation of $\mathfrak{su}(5)$:

$$\begin{aligned} &s(1)_1 \to 1, s(1)_2 \to 1, s(1)_3 \to 1, s(1)_4 \to 1, s(1)_5 \to -1 \\ &s(1)_1 \to 1, s(1)_2 \to 1, s(1)_3 \to 1, s(1)_4 \to -1, s(1)_5 \to -1 \\ &s(1)_1 \to 1, s(1)_2 \to 1, s(1)_3 \to -1, s(1)_4 \to -1, s(1)_5 \to -1 \\ &s(1)_1 \to 1, s(1)_2 \to -1, s(1)_3 \to -1, s(1)_4 \to -1, s(1)_5 \to -1. \end{aligned} \tag{E.2}$$

If we choose to turn mass parameters on then we can also have the following sign choices:

$$\begin{aligned} &s(1)_1 \to 1, s(1)_2 \to 1, s(1)_3 \to 1, s(1)_4 \to 1, s(1)_5 \to 1 \\ &s(1)_1 \to -1, s(1)_2 \to -1, s(1)_3 \to -1, s(1)_4 \to -1, s(1)_5 \to -1. \end{aligned} \tag{E.3}$$

In the case of two nodes, the code first asks for the signs of the weights associated to the first algebra. The pop-up window is exactly as discussed above, with the sole difference being that the notation for the signs is modified to $s[i]_{j,1}$, where in addition to the subscripts i, j that respectively label the different representations and weights, there is another subscript 1 that indicates the representation is charged under the first algebra. After the signs associated to the representations of the first algebra have been specified, a second window appears requesting the signs associated to the second algebra. The format is identical, with the distinction that the signs are denoted by $s[i]_{j,2}$, with the subscript 2 labeling the second algebra. Finally, a third window appears requesting signs for the weights of tensor product representations charged under both the first and second algebras.

JHEP12(2020)151

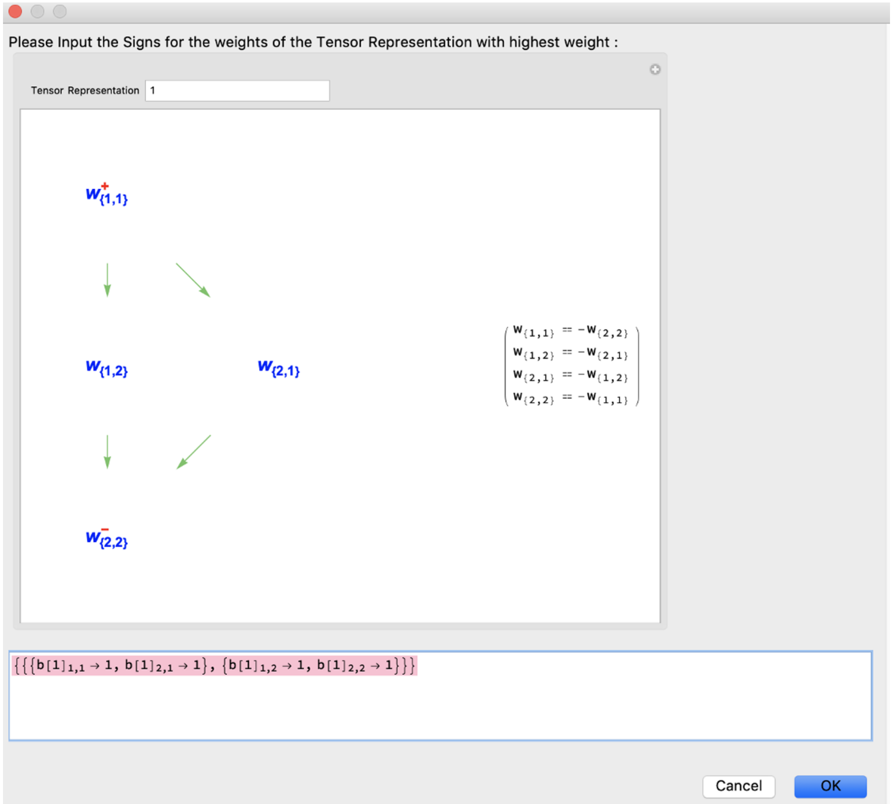

Figure 5. Signs for the tensor product representation.

For example consider $\overset{\mathfrak{su}(2)}{2} \text{———} \overset{\mathfrak{su}(2)}{2}$, for which the input is:

```
Geometry5dKK[{{{2,-1},{-1,2}},{A1,U},{A1,U}}]
```

An example of the third window is displayed in figure 5. In this case, on the upper left side of the window instead of a slider one can find the number of hypermultiplets transforming in a mixed representation. In figure 5 there is one such hypermultiplet, but in other cases there can be a half-integer number of hypermultiplets. This information is necessary to determine a consistent choice of signs, since for example mass parameters cannot be switched on for half-hypermultiplets. The Hasse diagram in this case is that of the tensor product representation $R_1 \otimes R_2$, where $R_1 = R_2 = \mathbf{2}$ of $\mathfrak{su}(2)$. Let v_i denote the weights associated to the first $\mathfrak{su}(2)$ and let ω_i denote the weights associated to the second $\mathfrak{su}(2)$. The weight system of the tensor product of these two representations is

$$w_{\{i,j\}} = v_i \oplus \omega_j. \tag{E.4}$$

The Hasse diagram of this weight system can now be determined based on the ordering of the weights v_i and ω_j. For example,

$$w_{\{1,1\}} = v_1 + \omega_1 \geq v_2 + \omega_1 = w_{\{2,1\}} \tag{E.5}$$

The Hasse diagram and the number of hypermultiplets is enough to determine a consistent choice of signs. The signs follow a similar notation as above, namely

$$b[1]_{i,j} \tag{E.6}$$

where the bracketed '1' indicates that there is only one mixed representation and the subscripts i, j are the same as the subscripts for $w_{\{i,j\}}$, referring to weights of the first and second algebras respectively.

Allowed signs for the representations. As mentioned above the choice of signs depends on the Hasse diagrams, the values of mass parameters, and on which combinations of representations are chosen. The function

```
SignsKK[]
```

determines all the possible allowed signs for each hypermultiplet of a specific theory. A word of caution: the computational cost of this function increases very quickly with the dimensions of the representations.

The input of for this function is of the same format described in the previous section:

```
SignsKK[{k,{Algebra,Twist}}]
```

OR

```
SignsKK[{Ω,{Algebra1,Twist1},{Algebra2,Twist2}}]
```

The output of this function is the appropriate number of hypermultiplets and the type of representation, together with the Hasse diagrams of the weight systems. As described above, the Hasse diagram includes superscripts indicating whether a weight is positive, negative, or indeterminate sign. In the absence of mass parameters the only signs that need to be determined are those of the indeterminate weights. Note that zero weights have superscript '0'. The output, namely all consistent gauge-theoretic phases of the theory, is presented both as a collection of Hasse diagrams and as a list of sign choices. The Hasse diagrams for the allowed signs includes superscripts indicating when the signs are taken to be positive (blue) or negative (red). This function is useful for determining all allowed phases and corresponding sign choices when computing the geometry.

It is important to note that in some cases the signs associated to different hypermultiplets are not independent. For example, consider

$$\begin{array}{ccccc} N_f & \mathfrak{sp}(n_\alpha)^{(1)} & & \mathfrak{so}(n_\beta)^{(2)} & N_f \\ \boxed{2n_\alpha + 8 - \frac{n_\beta - 1}{2}} & 1 & \underset{\frac{1}{2}(n_\alpha \otimes (n_\beta - 1))}{\rule{3cm}{0.4pt}} & k & \boxed{n_\beta - 8 - \frac{n_\alpha}{2}} \end{array} \tag{E.7}$$

where the extra labels indicate the number of hypermultiplets included in the theory. In particular, note that there are $2n_\alpha + 8 - \frac{n_\beta}{2}$ full hypermultiplets of $\mathfrak{sp}(n_\alpha)^{(1)}$ and one half-hyper in a mixed representation. This half-hypermultiplet comes from the branching of the bifundamental $n_\alpha \otimes n_\beta \to n_\alpha \otimes ((n_\beta - 1) \oplus 1)$ after performing the twist of $\mathfrak{so}(n_\beta)^{(2)}$, which leaves invariant the algebra $\mathfrak{so}(n_\beta - 1)$. This implies that the signs associated to the half-hypermultiplet are not independent but rather depend on the signs chosen for the

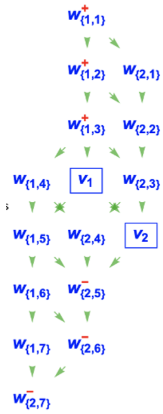

Figure 6. Hasse diagram for the case $n_\alpha = 1, k = 3, n_\beta = 4$ of the theory displayed in (E.7). Note that $w_{\{i,j\}}$ are the weights of the bifundamental and v_1, v_2 are the weights of the half-hypermultiplet.

bifundamental representation. In this case the function SignsKK returns all possible sign choices consistent with these branching rules.

For example, consider $n_\alpha = 1$, $k = 3$ and $n_\beta = 4$. The Hasse diagram for the bifundamental combined with the half-hypermultiplet of $\mathfrak{sp}(1)$ is displayed in figure 6. The possible sign choices are displayed in figure 7.

Output.

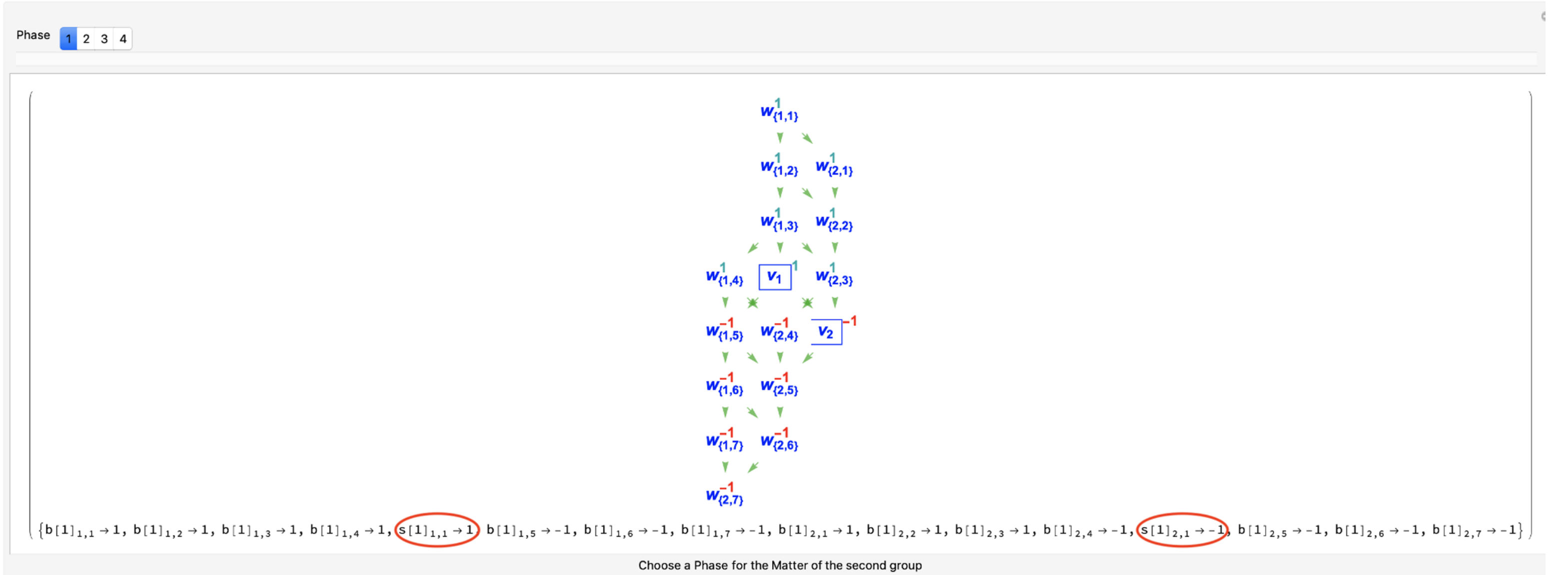

Figure 7. Signs choices for the case $n_\alpha = 1, k = 3, n_\beta = 4$ of the theory displayed in (E.7). The list provides the signs for both the bifundamental and the half hypermultiplet. The signs with the red circles represent those of the half-hypermultiplet.

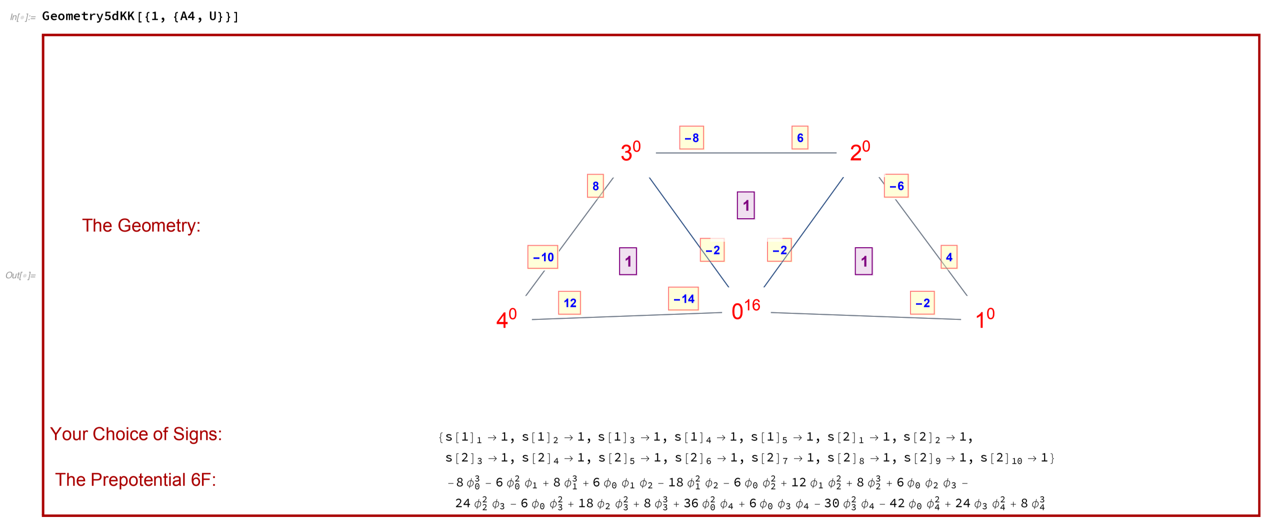

Figure 8. This is the result of the evaluation appearing in figure 3.

Once the signs have been specified in Geometry5dKK, the following output is returned (see an example shown in figure 8), and is comprised of the following elements:

1. The triple intersection numbers for the corresponding geometry are presented in a graphical form similar to the graphs presented in section 5 of this paper. The vertices of the graph are surfaces and edges between the vertices indicate the intersections between the corresponding surfaces. The superscript on a vertex i denotes $8 - S_i^3$. If the superscript is zero, then it is not displayed. Every edge carries two yellow boxes at either ends. Consider an edge going between vertices i and j. The number in the yellow box near the vertex i denotes the triple intersection number $S_i S_j^2$, and the number in the yellow box near the vertex j denotes the triple intersection number $S_i^2 S_j$. If the number carried by some yellow box is zero, then that box is not displayed. There is a purple box placed in the middle of every face formed by three edges joining three vertices, say i, j and k. The number in the purple box denotes the triple intersection number $S_i S_j S_k$. If the number carried by purple box is zero, then it is not displayed.

2. The choice of signs made by the user.

3. The the shifted prepotential $6\tilde{\mathcal{F}}$. In the case of a KK theory with a single node, ϕ_0 is the Coulomb branch parameter associated to the affine node of the Dynkin diagram and ϕ_i with $i = 1, \ldots Rank[Algebra]$ are the Coulomb branch parameters associated to the finite part of the diagram. In the case of a KK theory with two nodes, $\phi_{0,1}, \phi_{i,1}$ are the Coulomb branch parameters associated to the first (affine) algebra and $\phi_{0,2}, \phi_{i,2}$ are the Coulomb branch parameters associated to the second (affine) algebra.

References

[1] P. Jefferson, H.-C. Kim, C. Vafa and G. Zafrir, *Towards classification of* 5d *SCFTs: single gauge node*, arXiv:1705.05836 [INSPIRE].

[2] P. Jefferson, S. Katz, H.-C. Kim and C. Vafa, *On geometric classification of* 5d *SCFTs*, *JHEP* **04** (2018) 103 [arXiv:1801.04036] [INSPIRE].

[3] L. Bhardwaj and P. Jefferson, *Classifying* 5d *SCFTs via* 6d *SCFTs: rank one*, *JHEP* **07** (2019) 178 [*Addendum ibid.* **01** (2020) 153] [arXiv:1809.01650] [INSPIRE].

[4] L. Bhardwaj and P. Jefferson, *Classifying* 5d *SCFTs via* 6d *SCFTs: arbitrary rank*, *JHEP* **10** (2019) 282 [arXiv:1811.10616] [INSPIRE].

[5] M. Del Zotto, J.J. Heckman and D.R. Morrison, 6d *SCFTs and phases of* 5d *theories*, *JHEP* **09** (2017) 147 [arXiv:1703.02981] [INSPIRE].

[6] F. Apruzzi, L. Lin and C. Mayrhofer, *Phases of* 5d *SCFTs from M-/F-theory on non-flat fibrations*, *JHEP* **05** (2019) 187 [arXiv:1811.12400] [INSPIRE].

JHEP12(2020)151

[7] F. Apruzzi, C. Lawrie, L. Lin, S. Schäfer-Nameki and Y.-N. Wang, 5*d superconformal field theories and graphs*, Phys. Lett. B **800** (2020) 135077 [arXiv:1906.11820] [INSPIRE].

[8] F. Apruzzi, C. Lawrie, L. Lin, S. Schäfer-Nameki and Y.-N. Wang, *Fibers add flavor, part I: classification of* 5*d SCFTs, flavor symmetries and BPS states*, JHEP **11** (2019) 068 [arXiv:1907.05404] [INSPIRE].

[9] F. Apruzzi, C. Lawrie, L. Lin, S. Schäfer-Nameki and Y.-N. Wang, *Fibers add flavor, part II:* 5*d SCFTs, gauge theories, and dualities*, JHEP **03** (2020) 052 [arXiv:1909.09128] [INSPIRE].

[10] L. Bhardwaj, *On the classification of* 5*d SCFTs*, JHEP **09** (2020) 007 [arXiv:1909.09635] [INSPIRE].

[11] M. Del Zotto and G. Lockhart, *Universal features of BPS strings in six-dimensional SCFTs*, JHEP **08** (2018) 173 [arXiv:1804.09694] [INSPIRE].

[12] N. Seiberg, *Five-dimensional SUSY field theories, nontrivial fixed points and string dynamics*, Phys. Lett. B **388** (1996) 753 [hep-th/9608111] [INSPIRE].

[13] K.A. Intriligator, D.R. Morrison and N. Seiberg, *Five-dimensional supersymmetric gauge theories and degenerations of Calabi-Yau spaces*, Nucl. Phys. B **497** (1997) 56 [hep-th/9702198] [INSPIRE].

[14] O. Aharony, A. Hanany and B. Kol, *Webs of* (p, q) *five-branes, five-dimensional field theories and grid diagrams*, JHEP **01** (1998) 002 [hep-th/9710116] [INSPIRE].

[15] O. Aharony and A. Hanany, *Branes, superpotentials and superconformal fixed points*, Nucl. Phys. B **504** (1997) 239 [hep-th/9704170] [INSPIRE].

[16] O. Bergman and G. Zafrir, 5*d fixed points from brane webs and O*7*-planes*, JHEP **12** (2015) 163 [arXiv:1507.03860] [INSPIRE].

[17] G. Zafrir, *Brane webs and O*5*-planes*, JHEP **03** (2016) 109 [arXiv:1512.08114] [INSPIRE].

[18] H. Hayashi, S.-S. Kim, K. Lee and F. Yagi, *Rank-*3 *antisymmetric matter on* 5*-brane webs*, JHEP **05** (2019) 133 [arXiv:1902.04754] [INSPIRE].

[19] H. Hayashi, S.-S. Kim, K. Lee and F. Yagi, *Dualities and* 5*-brane webs for* 5*d rank* 2 *SCFTs*, JHEP **12** (2018) 016 [arXiv:1806.10569] [INSPIRE].

[20] H. Hayashi, S.-S. Kim, K. Lee and F. Yagi, 5*-brane webs for* 5*d* $N = 1$ G_2 *gauge theories*, JHEP **03** (2018) 125 [arXiv:1801.03916] [INSPIRE].

[21] D.R. Morrison and N. Seiberg, *Extremal transitions and five-dimensional supersymmetric field theories*, Nucl. Phys. B **483** (1997) 229 [hep-th/9609070] [INSPIRE].

[22] M.R. Douglas, S.H. Katz and C. Vafa, *Small instantons, del Pezzo surfaces and type-I-prime theory*, Nucl. Phys. B **497** (1997) 155 [hep-th/9609071] [INSPIRE].

[23] C. Closset, M. Del Zotto and V. Saxena, *Five-dimensional SCFTs and gauge theory phases: an M-theory/type IIA perspective*, SciPost Phys. **6** (2019) 052 [arXiv:1812.10451] [INSPIRE].

[24] H. Hayashi, S.-S. Kim, K. Lee, M. Taki and F. Yagi, *More on* 5*d descriptions of* 6*d SCFTs*, JHEP **10** (2016) 126 [arXiv:1512.08239] [INSPIRE].

[25] H. Hayashi, S.-S. Kim, K. Lee and F. Yagi, 6*d SCFTs,* 5*d dualities and Tao web diagrams*, JHEP **05** (2019) 203 [arXiv:1509.03300] [INSPIRE].

JHEP12(2020)151

[26] G. Zafrir, *Brane webs,* 5*d gauge theories and* 6*d* $N = (1, 0)$ *SCFT's*, JHEP **12** (2015) 157 [arXiv:1509.02016] [INSPIRE].

[27] S.-S. Kim, M. Taki and F. Yagi, *Tao probing the end of the world*, PTEP **2015** (2015) 083B02 [arXiv:1504.03672] [INSPIRE].

[28] H. Hayashi, S.-S. Kim, K. Lee, M. Taki and F. Yagi, *A new* 5*d description of* 6*d D-type minimal conformal matter*, JHEP **08** (2015) 097 [arXiv:1505.04439] [INSPIRE].

[29] E. Witten, *Toroidal compactification without vector structure*, JHEP **02** (1998) 006 [hep-th/9712028] [INSPIRE].

[30] J. de Boer et al., *Triples, fluxes, and strings*, Adv. Theor. Math. Phys. **4** (2002) 995 [hep-th/0103170] [INSPIRE].

[31] Y. Tachikawa, *Frozen singularities in M and F-theory*, JHEP **06** (2016) 128 [arXiv:1508.06679] [INSPIRE].

[32] L. Bhardwaj, D.R. Morrison, Y. Tachikawa and A. Tomasiello, *The frozen phase of F-theory*, JHEP **08** (2018) 138 [arXiv:1805.09070] [INSPIRE].

[33] J.J. Heckman, D.R. Morrison, T. Rudelius and C. Vafa, *Atomic classification of* 6*D SCFTs*, Fortsch. Phys. **63** (2015) 468 [arXiv:1502.05405] [INSPIRE].

[34] J.J. Heckman, D.R. Morrison and C. Vafa, *On the classification of* 6*d SCFTs and generalized ADE orbifolds*, JHEP **05** (2014) 028 [*Erratum ibid.* **06** (2015) 017] [arXiv:1312.5746] [INSPIRE].

[35] L. Bhardwaj, *Classification of* 6*d* $N = (1, 0)$ *gauge theories*, JHEP **11** (2015) 002 [arXiv:1502.06594] [INSPIRE].

[36] L. Bhardwaj, *Revisiting the classifications of* 6*d SCFTs and LSTs*, JHEP **03** (2020) 171 [arXiv:1903.10503] [INSPIRE].

[37] D.R. Morrison and W. Taylor, *Sections, multisections, and* U(1) *fields in F-theory*, arXiv:1404.1527 [INSPIRE].

[38] N. Mekareeya, K. Ohmori, Y. Tachikawa and G. Zafrir, E_8 *instantons on type-A ALE spaces and supersymmetric field theories*, JHEP **09** (2017) 144 [arXiv:1707.04370] [INSPIRE].

[39] D.D. Frey and T. Rudelius, 6*d SCFTs and the classification of homomorphisms* $\Gamma_{\mathrm{ADE}} \to E_8$, Adv. Theor. Math. Phys. **24** (2020) 709 [arXiv:1811.04921] [INSPIRE].

[40] F. Bonetti and T.W. Grimm, *Six-dimensional* (1, 0) *effective action of F-theory via M-theory on Calabi-Yau threefolds*, JHEP **05** (2012) 019 [arXiv:1112.1082] [INSPIRE].

[41] F. Bonetti, T.W. Grimm and S. Hohenegger, *Exploring* 6*d origins of* 5*d supergravities with Chern-Simons terms*, JHEP **05** (2013) 124 [arXiv:1303.2661] [INSPIRE].

[42] T.W. Grimm and A. Kapfer, *Anomaly cancelation in field theory and F-theory on a circle*, JHEP **05** (2016) 102 [arXiv:1502.05398] [INSPIRE].

[43] T.W. Grimm, *The* $N = 1$ *effective action of F-theory compactifications*, Nucl. Phys. B **845** (2011) 48 [arXiv:1008.4133] [INSPIRE].

[44] M. Esole, P. Jefferson and M.J. Kang, *Euler characteristics of crepant resolutions of Weierstrass models*, Commun. Math. Phys. **371** (2019) 99 [arXiv:1703.00905] [INSPIRE].

[45] M. Esole and S.-H. Shao, *M-theory on elliptic Calabi-Yau threefolds and* 6*d anomalies*, arXiv:1504.01387 [INSPIRE].

[46] M. Esole and M.J. Kang, *The geometry of the* SU(2) $\times$ G_2*-model*, *JHEP* **02** (2019) 091 [arXiv:1805.03214] [INSPIRE].

[47] M. Esole, R. Jagadeesan and M.J. Kang, *The geometry of* G_2*,* Spin(7)*, and* Spin(8)*-models*, arXiv:1709.04913 [INSPIRE].

[48] M. Esole, P. Jefferson and M.J. Kang, *The geometry of* F_4*-models*, arXiv:1704.08251 [INSPIRE].

[49] M. Esole and S.-T. Yau, *Small resolutions of* SU(5)*-models in F-theory*, *Adv. Theor. Math. Phys.* **17** (2013) 1195 [arXiv:1107.0733] [INSPIRE].

[50] M. Esole, S.-H. Shao and S.-T. Yau, *Singularities and gauge theory phases*, *Adv. Theor. Math. Phys.* **19** (2015) 1183 [arXiv:1402.6331] [INSPIRE].

[51] M. Esole, S.-H. Shao and S.-T. Yau, *Singularities and gauge theory phases II*, *Adv. Theor. Math. Phys.* **20** (2016) 683 [arXiv:1407.1867] [INSPIRE].

[52] K. Oguiso, *On algebraic fiber space structures on a Calabi-Yau* 3*-fold*, *Int. J. Math.* **04** (1993) 439.

[53] P.M.H. Wilson, *The existence of elliptic fibre space structures on Calabi-Yau threefolds*, *Math. Annalen* **300** (1994) 693.

[54] L. Bhardwaj, *Dualities of* 5d *gauge theories from S-duality*, *JHEP* **07** (2020) 012 [arXiv:1909.05250] [INSPIRE].

[55] Y. Tachikawa, *On S-duality of* 5d *super Yang-Mills on* S^1, *JHEP* **11** (2011) 123 [arXiv:1110.0531] [INSPIRE].

JHEP12(2020)151